

# ***SOILS and ROCKS***

An International Journal of Geotechnical and Geoenvironmental Engineering

## **Editor**

Renato Pinto da Cunha

University of Brasília, Brazil

## ***Co-editor***

Ana Vieira

National Laboratory for Civil Engineering, Portugal

## **Associate Editors**

Gilson de F. N. Gtirana Jr.

*Federal University of Goiás, Brazil*

José A. Schiavon

*Aeronautics Institute of Technology, Brazil*

Leandro Neves Duarte

*Federal University of São João del-Rei, Brazil*

Luciano Soares da Cunha

*University of Brasília, Brazil*

Marcio Leão

*Federal University of Viçosa / IBMEC-BH, Brazil*

Nuno Cristelo

*University of Trás-os-Montes and Alto Douro, Portugal*

Paulo J. R. Albuquerque

*Campinas State University, Brazil*

Ricardo Pontes Resende

*University Institute of Lisbon, Portugal*

Rui Carrilho Gomes

*Technical University of Lisbon, Portugal*

Sara Rios

*University of Porto, Portugal*

Silvrano Adonias Dantas Neto

*Federal University of Ceará, Brazil*

Teresa M. Bodas Freitas

*Technical University of Lisbon, Portugal*

## **Advisory Panel**

Alejo O. Sfriso

*University of Buenos Aires, Argentina*

Harry Poulos

*University of Sidney, Australia*

Luis A. Vallejo

*Complutense University of Madrid, Spain*

Emanuel Maranha das Neves

*Technical University of Lisbon, Portugal*

Michele Jamiolkowski

*Studio Geotecnico Italiano, Italy*

Roger Frank

*École des Ponts ParisTech, France*

Willy Lacerda

*Federal University of Rio de Janeiro, Brazil*

## **Editorial Board**

Abdelmalek Bouazza

*Monash University, Australia*

Alessandro Mandolini

*University of Naples Federico II, Italy*

Alessio Ferrari

*École Polytechnique Fédérale de Lausanne, Switzerland*

Antônio Roque

*National Laboratory for Civil Engineering, Portugal*

Antônio Viana da Fonseca

*University of Porto, Portugal*

Armando Antão

*NOVA University Lisbon, Portugal*

Beatrice Baudet

*University College of London, UK*

Catherine O'Sullivan

*Imperial College London, UK*

Cristhian Mendoza

*National University of Colombia, Colombia*

Cristiana Ferreira

*University of Porto, Portugal*

Cristina Tsuha

*University of São Paulo at São Carlos, Brazil*

Daniel Dias

*Antea Group / Grenoble-Alpes University, France*

Debasis Roy

*Indian Institute of Technology Kharagpur, India*

Denis Kalumba

*Cape Town University, South Africa*

Ian Schumann M. Martins

*Federal University of Rio de Janeiro, Brazil*

Jean Rodrigo Garcia

*Federal University of Uberlândia, Brazil*

José Muralha

*National Laboratory for Civil Engineering, Portugal*

Kátia Vanessa Bicalho

*Federal University of Espirito Santo, Brazil*

Krishna R. Reddy

*University of Illinois at Chicago, USA*

Limin Zhang

*The Hong Kong Univ. of Science Technology, China*

Márcio de Souza Soares de Almeida

*Federal University of Rio de Janeiro, Brazil*

Marcelo Javier Sanchez Castilla

*Texas A&M University College Station, USA*

Marco Barla

*Politecnico di Torino, Italy*

Marcos Arroyo

*Polytechnic University of Catalonia, Spain*

Marcos Massao Futai

*University of São Paulo, Brazil*

Maria de Lurdes Lopes

*University of Porto, Portugal*

Mauricio Martinez Sales

*Federal University of Goiás, Brazil*

Nilo Cesar Consoli

*Federal University of Rio Grande do Sul, Brazil*

Olavo Francisco dos Santos Júnior

*Federal University of Rio Grande do Norte, Brazil*

Orianne Jenck

*Grenoble-Alpes University, France*

Paulo Venda Oliveira

*University of Coimbra, Portugal*

Rafaela Cardoso

*Technical University of Lisbon, Portugal*

Roberto Quental Coutinho

*Federal University of Pernambuco, Brazil*

Rui Carrilho Gomes

*Technical University of Lisbon, Portugal*

Sai K. Vanapalli

*University of Ottawa, Canada*

Samir Maghous

*Federal University of Rio Grande do Sul, Brazil*

Satoshi Nishimura

*Hokkaido University, Japan*

Siang Huat Goh

*National University of Singapore, Singapore*

Tácio Mauro Campos

*Pontifical Catholic University of Rio de Janeiro, Brazil*

Tiago Miranda

*University of Minho, Portugal*

Zhen-Yu Yin

*Hong Kong Polytechnic University, China*

Zhongxuan Yang

*Zhejiang University, China*

## **Honorary Members**

André Pacheco de Assis

Clovis Ribeiro de M. Leme (in memoriam)

Delfino L. G. Gambetti

Eduardo Soares de Macedo

Ennio Marques Palmeira

Eraldo Luporini Pastore

Francisco de Rezende Lopes

Francisco Nogueira de Jorge

Jaime de Oliveira Campos

João Augusto M. Pimenta

José Carlos A. Cintra

José Carlos Virgili

José Couto Marques

José Jorge Nader

José Maria de Camargo Barros

Manuel Matos Fernandes

Maurício Abramento

Maurício Erlich

Newton Moreira de Souza

Orencio Monje Villar

Osni José Pejon

Paulo Eduardo Lima de Santa Maria

Paulo Scarano Hemsí

Ricardo Oliveira

Ronaldo Rocha

Rui Taiji Mori (in memoriam)

Susumu Niyama

Vera Cristina Rocha da Silva

Waldemar Coelho Hachich

Willy Lacerda



Soils and Rocks publishes papers in English in the broad fields of Geotechnical Engineering, Engineering Geology, and Geoenvironmental Engineering. The Journal is published quarterly in March, June, September and December. The first issue was released in 1978, under the name *Solos e Rochas*, being originally published by the Graduate School of Engineering of the Federal University of Rio de Janeiro. In 1980, the Brazilian Association for Soil Mechanics and Geotechnical Engineering took over the editorial and publishing responsibilities of *Solos e Rochas*, increasing its reach. In 2007, the journal was renamed Soils and Rocks and acquired the status of an international journal, being published jointly by the Brazilian Association for Soil Mechanics and Geotechnical Engineering, by the Portuguese Geotechnical Society, and until 2010 by the Brazilian Association for Engineering Geology and the Environment.

***Soils and Rocks***

1978,	1 (1, 2)
1979,	1 (3), 2 (1,2)
1980-1983,	3-6 (1, 2, 3)
1984,	7 (single number)
1985-1987,	8-10 (1, 2, 3)
1988-1990,	11-13 (single number)
1991-1992,	14-15 (1, 2)
1993,	16 (1, 2, 3, 4)
1994-2010,	17-33 (1, 2, 3)
2011,	34 (1, 2, 3, 4)
2012-2019,	35-42 (1, 2, 3)
2020,	43 (1, 2, 3, 4)
2021,	44 (1, 2, 3)

ISSN 1980-9743  
ISSN-e 2675-5475

CDU 624.131.1

## ***Soils and Rocks***

An International Journal of Geotechnical and Geoenvironmental Engineering

ISSN 1980-9743 ISSN-e 2675-5475

### **Publication of**

ABMS - Brazilian Association for Soil Mechanics and Geotechnical Engineering

SPG - Portuguese Geotechnical Society

Volume 44, N. 3, July-September 2021

Invited Editors: T.M.P. Campos, F.A.M. Marinho, G.F.N. Gitirana Jr.

### **Table of Contents**

#### ARTICLES

*Myths and misconceptions related to unsaturated soil mechanics*

Delwyn G. Fredlund

*Application of in situ tests in unsaturated soils to analysis of spread footings*

Gerald A. Miller, Rodney W. Collins, Kanthasamy K. Muraleetharan, Tareq Z. Abuawad

*Hydromechanical behavior of unsaturated soils: Interpretation of compression curves in terms of effective stress*

John S. McCartney, Fatemah Behbehani

*An improved framework for volume change of shrink/swell soils subjected to time-varying climatic effects*

Austin H. Olaiz, Mohammad Mosawi, Claudia E. Zapata

*The role of unsaturated soil mechanics in unconventional tailings deposition*

Paul Simms

*Behavior of unsaturated cohesive-frictional soils over a whole range of suction/thermo-controlled stress paths and modes of deformation*

Laureano R. Hoyos, Roya Davoodi-Bilesavar, Ujwalkumar D. Patil, Jairo E. Yepes-Heredia, Diego D. Pérez-Ruiz, José A. Cruz

*The new expertise required for designing safe tailings storage facilities*

Gordon Ward Wilson

*Unsaturated soils in the context of tropical soils*

José Camapum de Carvalho, Gilson de F. N. Gitirana Jr.

#### CASE STUDY

*Unsaturated mine tailings disposal*

Luciano A. Oldecop, Germán J. Rodari

*Brasília municipal solid waste landfill: a case study on flow and slope stability*

José Fernando Thomé Jucá, Alison de Souza Norberto, José Ivan do Santos Júnior, Fernando A. M. Marinho

#### REVIEW ARTICLES

*Review of expansive and collapsible soil volume change models within a unified elastoplastic framework*

Sandra L. Houston, Xiong Zhang

*Analytical and numerical methods for prediction of the bearing capacity of shallow foundations in unsaturated soils*

Sai K. Vanapalli, Won-Taek Oh




## ***ARTICLES***

***Soils and Rocks***  
v. 44, n. 3



## Myths and misconceptions related to unsaturated soil mechanics

Delwyn G. Fredlund<sup>1#</sup> 

Article

### Keywords

Unsaturated soil mechanics  
Soil suction  
Unsaturated soil property functions  
Moisture flux  
Myths

### Abstract

There have been three main pillars associated with the development of an applied engineering science for both saturated and unsaturated soil mechanics; namely, i) the synthesis of continuum mechanics theories of physical behavior, ii) the laboratory measurement of relevant soil properties, and iii) analyses that illustrate the solution of practical example problems. Geotechnical engineers have, however, been relatively slow in adopting unsaturated soil mechanics into geotechnical engineering practice. There have been several so-called “myths or misconceptions” that appear to have hindered the application of unsaturated soil mechanics. This paper attempts to describe and dispel what are deemed to be misconceptions related to the more general implementation of unsaturated soil mechanics into engineering practice. The so-called “myths” come from the acceptance of false information related to unsaturated soil behavior and a hesitancy to embrace changes to existing empirical protocols. Several misconceptions are identified in the paper that are related to: i) complexity of unsaturated soil mechanics theories, ii) inability to readily measure soil suctions *in-situ*, iii) the nonlinearity of unsaturated soil property functions, iv) permanency of soil suctions above the water table, v) difficulties associated with assessing ground surface moisture flux conditions, and vi) difficulties associated with numerical modeling that involves solving nonlinear partial differential equations. Each of the above-mentioned items are dealt with as myths or misconceptions in the sense of being impediments to the application of unsaturated soil mechanics in geotechnical engineering practice.

### 1. Introduction to debunking unsaturated soil mechanics myths and misconceptions

Soil mechanics became recognized as an important applied science following the study of saturated soil behavior near the middle of the 1900s. Soil mechanics became widely accepted through the publication of books such as *Theoretical Soil Mechanics* by Terzaghi (1943), *From Theory to Practice of Soil Mechanics* by Terzaghi & Peck (1967), *Fundamentals of Soil Mechanics* by Taylor (1948), and others. These books synthesized the general behavior of saturated soils for three main phenomenological processes; namely, i) flow of water through porous media, ii) volume change and distortion of soils, and iii) shear strength behavior. In the case of each physical behavior there were three so-called pillars of soil mechanics. These were: i) the synthesis of a theory of physical behavior, ii) the laboratory measurement of relevant soil properties, and iii) the presentation of relevant example problems. The three-pillar paradigm has well served the geotechnical community for over half a century.

Geotechnical engineers have, however, been relatively slow in embracing and implementing a similar consensus involving the three pillars for unsaturated soil mechanics. Unfortunately, geotechnical engineers seem to have “bought into” several misconceptions related to unsaturated soil mechanics. I will attempt to dispel these misconceptions and bring value-added benefits to the implementation of unsaturated soil mechanics in geotechnical engineering practice. The so-called “myths” are deemed to be the result of accepting misconceptions or false information along with a lack of desire to embrace change in existing protocols.

### 2. Describing misconceptions common in “unsaturated soil mechanics”

Along with all the outstanding past research on unsaturated soils, it seems inevitable that there should be a few inaccurate perceptions about unsaturated soil mechanics theory as it pertains to mainstream geotechnical practice. Finding a consensus on fundamental perceptions is important as engineers

<sup>#</sup>Corresponding author. E-mail address: delwyn.fredlund@gmail.com

<sup>1</sup>Unsaturated Soil Technology Ltd., Saskatoon, SK, Canada.

Submitted on January 13, 2021; Final Acceptance on February 18, 2021; Discussion open until November 30, 2021.

<https://doi.org/10.28927/SR.2021.062521>



This is an Open Access article distributed under the terms of the Creative Commons Attribution License, which permits unrestricted use, distribution, and reproduction in any medium, provided the original work is properly cited.



move towards the worldwide application of unsaturated soil mechanics in geotechnical engineering practice.

## 2.1 Myths & misconceptions

The application of unsaturated soil mechanics has been hindered through acceptance of one or more of the following false rationales. For example, it is often rationalized that;

- 1) unsaturated soil mechanics theories are excessively complex and hard to understand,
- 2) soil suctions need to be measured *in-situ*,
- 3) *in-situ* suctions are temporary and disappear following rainfall,
- 4) unsaturated soil properties are too costly and difficult to measure in the laboratory,
- 5) analysis of practical problems involves complex nonlinear mathematics, leading to serious modeling challenges and rendering it impractical,
- 6) ground surface boundary conditions take the form of moisture fluxes that are related to highly variable and random weather conditions, and,
- 7) it is often rationalized that the present protocols are acceptable, “So why change? Aren’t we doing fine?”

I will attempt to dispel each of the above-mentioned concerns as myths (i.e., unsubstantiated, indefensible false perceptions). The hope is that greater benefits might be accrued through bringing unsaturated soil mechanics into the practice of geotechnical engineering. Section 2 of this article describes the context and variables associated with unsaturated soils while the remaining parts of the article are devoted to dispelling myths and misconceptions amongst geotechnical engineers.

## 2.2 Pillars of unsaturated soil mechanics

There have been three so-called pillars associated with the application of saturated soil mechanics. Likewise, there are three pillars for unsaturated soil mechanics (See Figure 1).

The pillars are labelled as: i) theory, ii) laboratory testing, and iii) numerical modeling. The pillar “theory” stands for a synthesis of research findings (and hopefully a consensus) that have been presented at research conference and through journal publications. “Theory” contains a distillation of protocols that appear to be acceptable for prudent geotechnical engineering practice. Protocols constitute a living, ongoing statement that may evolve as new research is published.

The *First International Conference on Unsaturated Soils* was held in Paris, France, in 1995. Since that time there has been a proliferation of regional and international conferences focusing on unsaturated soils research. The result has been the emergence of a theoretical context that treats unsaturated soil mechanics as a continuum mechanics type extension of the framework that has proven to be so successful for saturated soil mechanics.

Geotechnical engineers are known for their practice of retrieving small (undisturbed) soil samples from boreholes and then measuring relevant physical soil properties in the laboratory (e.g., coefficient of permeability, coefficient of volume change, shear strength). This procedure has proven to be acceptable for the application of saturated soil mechanics; however, the cost of using the same approach for testing unsaturated soils has proven to be far too high, being estimated to be in the order of 10 times as expensive as testing for saturated soil properties (Fredlund & Rahardjo, 1993).

The solution to the costly laboratory testing of unsaturated soils dilemma has involved the measurement of one or more alternate soil property functions that can then be used to estimate required unsaturated soil property functions, USPFs. The most common proposed procedure has been to measure the soil-water characteristic curve, SWCC, and the shrinkage curve, SC, in the laboratory. These two USPFs can then be used to calculate all volume-mass versus soil suction relationships for the soil (under drying soil conditions). The USPFs can cover the entire range of possible soil suctions (i.e., from a fraction of 1 kPa to a maximum value of 1,000,000 kPa). The USPFs are then used to estimate the i) unsaturated soils

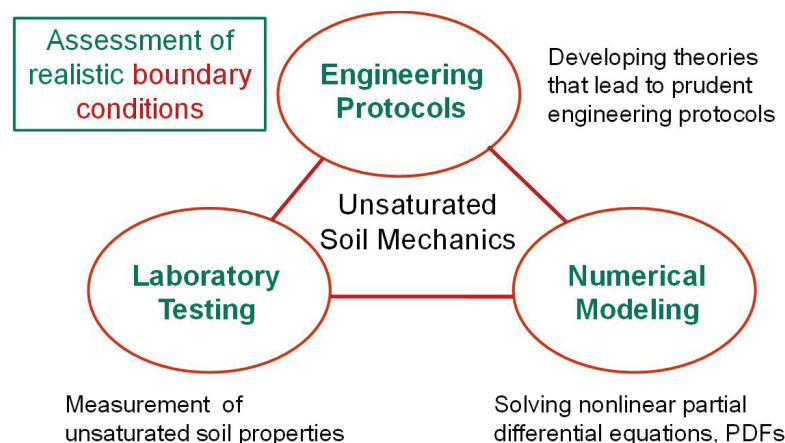


**Figure 1.** Basic pillars for implementation of unsaturated soil mechanics (Fredlund, 2017).

permeability function, ii) water storage function, iii) shear strength function, and iv) other unsaturated soil property functions. The cost of performing the combined SWCC and SC tests in the laboratory is generally less than \$1500 (CAD).

Generally, the cost associated with measuring the SWCC and SC can be shown to yield considerable cost-benefit to the client. The functions are called “estimated” unsaturated soil property functions but are of satisfactory accuracy for most geotechnical engineering applications. Certainly, this approach becomes a significant improvement over not analyzing the unsaturated portion of the soil profile (Fredlund & Houston, 2009).

The third pillar of unsaturated soil mechanics involves the use of numerical modeling techniques for the solution of (nonlinear) partial differential equations that describe the physical behavior of an element of unsaturated soil. The past few decades have seen two disciplines rise to the occasion with valuable resources for solving unsaturated soils numerical modeling solutions. These are the computer software discipline along with high-speed computer hardware and the mathematics discipline. Together, these disciplines have provided practical modeling techniques that ensure the convergence of partial differential equations to a unique solution.

Also shown on Figure 1 is the importance of assessing climatic-dependent moisture flux boundary conditions. With only a few exceptions, most unsaturated soil problems are near ground surface problems. Therefore, soil-atmosphere interaction defines an important boundary condition for the solution of practical problems. Suffice it to say at this point that data from weather stations have become a valuable resource, providing an opportunity for extensive analysis of collected weather information.

### 2.3 Importance of reasonable assumptions

Moving a basic science to an applied science requires invoking a series of assumptions. The effect of various

assumptions is usually studied by researchers and a decision is made on the most acceptable assumptions to invoke.

In the foreword to *Unsaturated Soil Mechanics in Engineering Practice*, Morgenstern (2012, p. xiii) wrote,

A fundamental distinction between saturated and unsaturated soil behavior is the need to express the relationship in the latter between water content and soil suction, i.e., the soil-water characteristic curve. Since 1993, there has been an explosion of studies into the measurement of soil suction and the development of soil-water characteristic curves.

It is fair to say that the use of the soil-water characteristic curve (and shrinkage curve) has opened the way for an increase in the application of unsaturated soil mechanics. The laboratory testing protocols are not perfect but are a vast improvement over the previous omission of the unsaturated soil zone when performing an analysis. Research into the use of the SWCC for the estimation of USPFs has caught the imagination for geotechnical researchers around the world (Fredlund, 2017). Recent research conferences have shown this topic to be the single most popular area of unsaturated soil mechanics’ research.

### 2.4 Boundaries of the unsaturated soil zone

An unsaturated soil profile (i.e., portion of soil above the water table), can be subdivided into three main zones, as shown in Figure 2. The zones are the: i) capillary zone immediately above the groundwater table where the voids are predominantly filled with water, ii) two-phase zone where the soil voids are filled with varying ratios of water and air, iii) dry zone where the voids of the soil mainly contain air (Blight, 2013; Fredlund, 2015; Houston, 2019; Rahardjo et al. 2019; Tarantino & El Mountassir, 2013; Vanapalli & Mohamed, 2006). It is important for geotechnical engineering purposes to recognize that the unsaturated zone commences immediately above the water table where the pore-water pressures become negative. The division between the capillary zone and the two-phase zone designates the air-

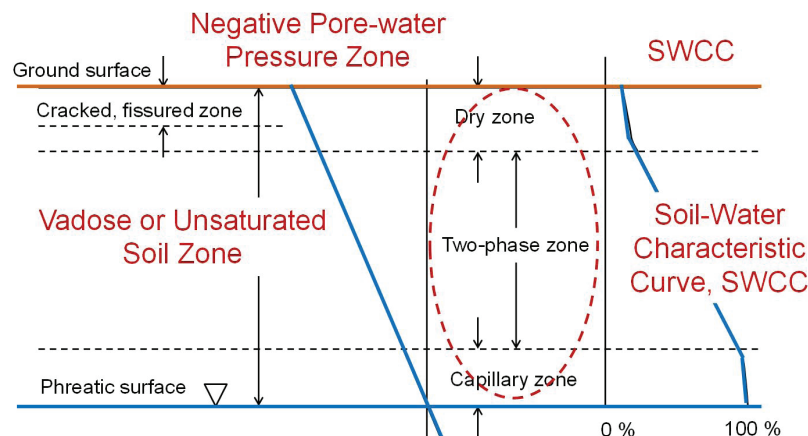


**Figure 2.** Subdivisions of the unsaturated soil zone (Fredlund, 2015).

entry value, AEV, of the soil. The AEV is likely the single most significant piece of soils information required by the geotechnical engineer. The AEV designates the point at which the soil begins to truly behave as an unsaturated soil. In other words, it is the point beyond which the soil properties are no longer constants but rather, take on the form of nonlinear functions of soil suction.

Figure 2 corresponds to hydrostatic conditions of a homogeneous profile, for zero moisture flux at ground surface. Under equilibrium conditions the pore-water pressure is negative and varies linearly above the water table, regardless of the soil type. The equilibrium pore-water pressure line is referred to as the hydrostatic pressure line. While the equilibrium pore-water pressures are linear, the designation of the amount of water in the soil reveals two distinct zones; namely, i) the top of the capillary zone showing the air-entry value and, ii) the start of residual conditions. These two zones are associated with the soil-water characteristic curve, SWCC, and become the primary information that is required by the geotechnical engineer when defining unsaturated soil property functions. It is recognized that the SWCC is stress path dependent (i.e., hysteretic), but it is important to first visualize the broad general relationship that exists between field conditions and laboratory test conditions.

The linear (equilibrium) pore-water pressure line can deviate from hydrostatic conditions as a result of positive moisture fluxes (i.e., precipitation) or negative moisture fluxes (i.e., evaporation) at the ground surface as shown in Figure 3. In other words, the upper portion of the hydrostatic line responds to climatic conditions imposed at the ground surface. Historically, classic soil mechanics has focused mainly on imposing a “hydraulic head” or having a “zero moisture flux” boundary condition. For unsaturated soil conditions, it is necessary to accommodate varying ground surface moisture fluxes applied in a steady state and/or

transient manner. Weather station information can be used to quantify ground surface moisture flux conditions.

The main change in going from saturated soil mechanics to unsaturated soil mechanics lies in the “sign” associated with the pore-water pressure. However, there are other complications that arise when considering negative pore-water pressures. The pressure can become extremely negative, reaching to a limiting value of 1,000,000 kPa under zero water content conditions.

The major difference between saturated and unsaturated soil mechanics lies in the fact that equal changes in total stresses and pore-water pressures do not produce the same physical response in an unsaturated soil (Fredlund & Morgenstern, 1977). Consequently, it becomes necessary to handle total stress changes independent from pore-water pressure changes, as shown in Figure 4. The independence of total stress changes and pore-water pressure changes is fundamental to understanding the difference between saturated and unsaturated soil behavior. Creating an acceptable and accurate theoretical visualization of unsaturated soil behavior constitutes the first step in applying unsaturated soil mechanics.

## 2.5 Myths to be dispelled

Before considering the application of unsaturated soil mechanics, let us address the myth regarding the permanency of *in-situ* soil suction. In other words, logic leads to the conclusion, “Why should geotechnical engineers care about unsaturated soil mechanics if there is no permanency associated with negative pore-water pressures?” This myth is closely related to the belief that it is also necessary to be able to measure suctions *in-situ* before being able to apply unsaturated soil mechanics in engineering practice. An attempt is made herein to show that this rationale cannot be justified or defended. There are significant value-added benefits to be

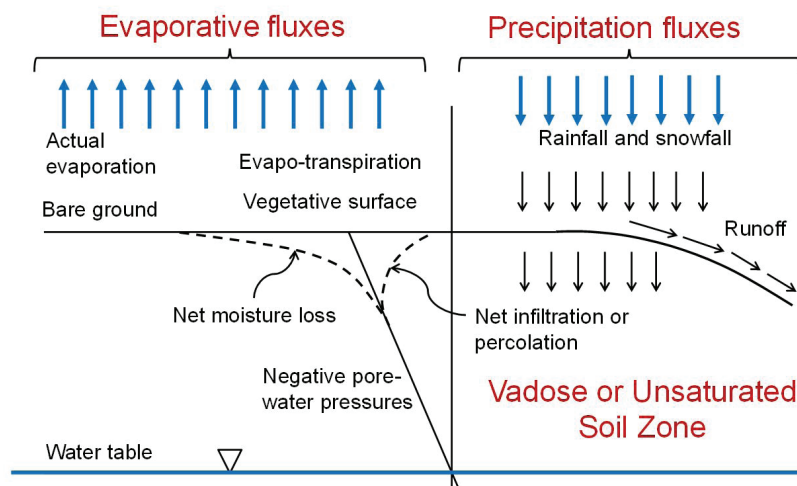


**Figure 3.** Components of moisture movement associated with net moisture flux conditions at ground surface (Fredlund, 2015).

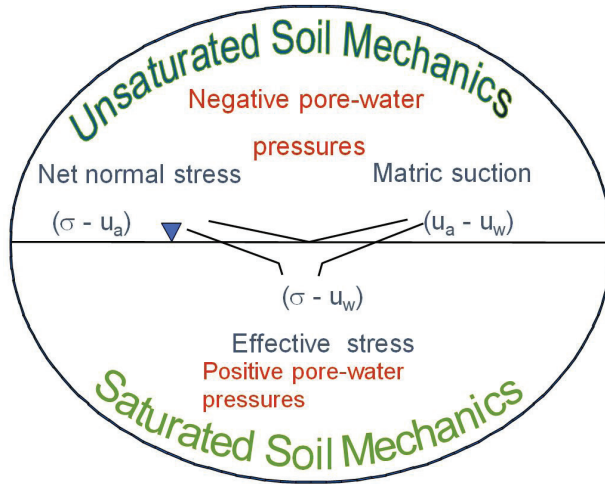


**Figure 4.** Pictorial visualization of the stress state for saturated/unsaturated soil systems.

gained through the application of unsaturated soil mechanics for near ground surface problems.

### 3. Misconceptions surrounding the permanency of soil suctions

There is one question that commonly arises during discussion sessions at unsaturated soils research conferences. The question goes something like this: *“In-situ suction are extremely transient, disappearing as soon as there is a rainfall and moisture infiltrates from the ground surface. Therefore, why are we interested in conditions other than saturated soil conditions?”* This sounds like a reasonable question; however, the answer is not quite that simple. In fact, the opposite conclusion might be more realistic. It might be more realistic to ask, *“What conditions need to be met in order for in-situ soil suctions to disappear following heavy or prolonged rainstorm conditions?”*

Before discussing the issue of soil suction permanency, let us first address concerns related to the measurement of *in-situ* soil suction. Negative aspersions regarding the application of unsaturated soil mechanics are often couched in questions that go something like this, *“Why should we concern ourselves with unsaturated soil mechanics when we have no easy-to-use methods to measure suction in the field?”*

#### 3.1 If only it were possible to measure soil suctions in the field!

Tensiometers were manufactured in the early 1900s as a device that would extend the measurement range of piezometers into the negative pore-water pressure range. Over the years the tensiometers have undergone a series of minor refinements such as those illustrated in Figure 5.

Tensiometers provide a direct measure of negative pore-water pressure but have a measurement range limited to approximately 90% of one atmosphere, sustainable for a limited time (e.g., one day). The major shortcoming of tensiometers is related to possible cavitation of the fluid in the measurement system of the instrument.

Other proposed suction device designs have been proposed but also have limitations. For example, pre-pressurized, high suction range devices are mainly suitable for laboratory usage and thermal conductivity heat-dissipation sensors require calibration and lack desired accuracy. It is fair to say that there has not been a “game-changing” device that fully meets the desired requirements for geotechnical engineering applications.

The concept of axis-translation testing of unsaturated soils has worked well in the laboratory for a wide range of research studies by scaling up the ambient air pressure such that water in the measurement system never gets into the absolute negative pore-water pressure range. While axis-translation has been hailed a success for laboratory testing, the technique cannot be translated to field conditions.

Before despairing over the difficulties related to measuring *in-situ* suction, let us consider the following question, *“Is it necessary to be able to measure suctions in the field?”* The primary purpose for measuring negative pore-water pressures *in-situ* is for verification of proposed theories of unsaturated soil behavior. The ability to undertake field verification studies would enhance confidence in the application of unsaturated soil theories.

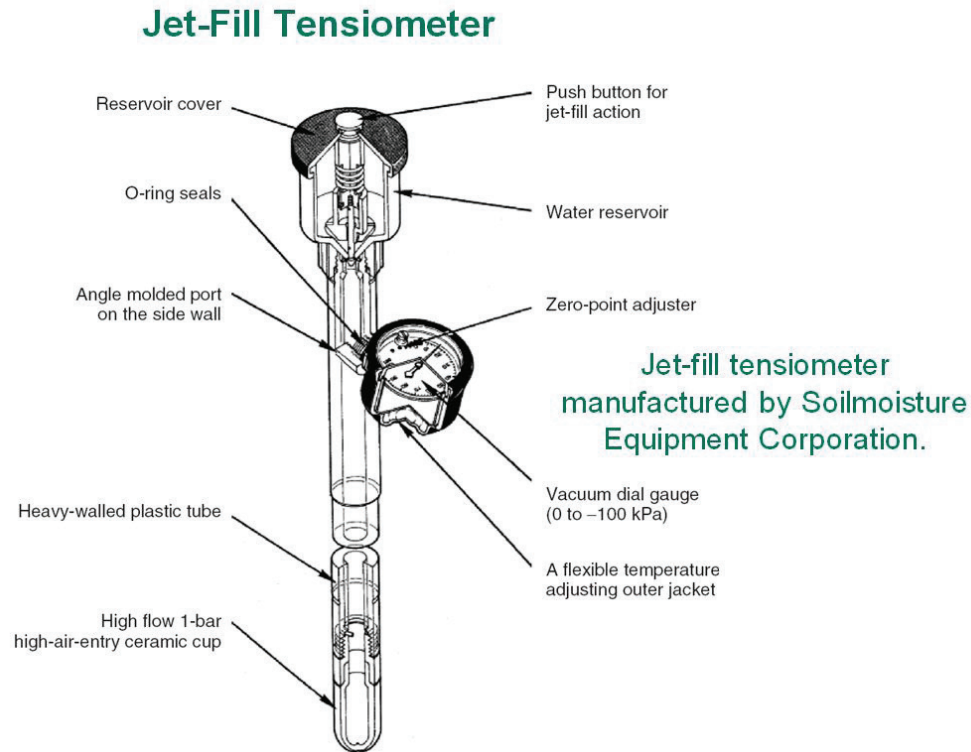
Let us suppose, however, that the physical behavior of unsaturated soils has been adequately verified in the laboratory. Once laboratory verification has been achieved, then the unsaturated soil theories can be assumed to be applicable for use in the field with reasonable confidence. It is fair to say that most unsaturated soil theories have been adequately tested and verified in the laboratory and can therefore be used with confidence in geotechnical engineering practice (Fredlund, 2017).

Let us now further consider the questions related to the permanency of suctions in the field.

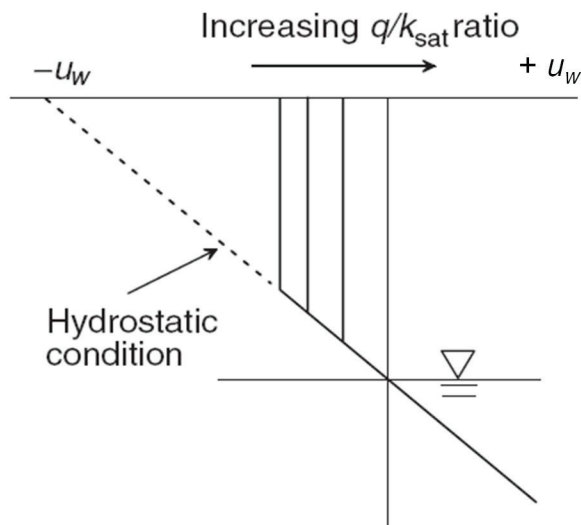
#### 3.2 Is it possible to rely on suctions in the field through wet weather conditions?

Moisture infiltration conditions can be divided into two categories; namely, i) the situation where the average ground surface flux is lower than the saturated coefficient of permeability of the soil near ground surface, and ii) the situation where the ground surface moisture flux is maintained at an intensity equal to or greater than the saturated coefficient of permeability of the soil near ground surface (Kasim et al. 1998; Lu and Griffiths, 2004; Srivastava and Yeh, 1991). Let us consider the case of a homogeneous soil deposit where the moisture flux is low but continues over a long-time.





**Figure 5.** Typical Jet-Filled manufactured by *Soil Moisture Equipment Corporation, California*.



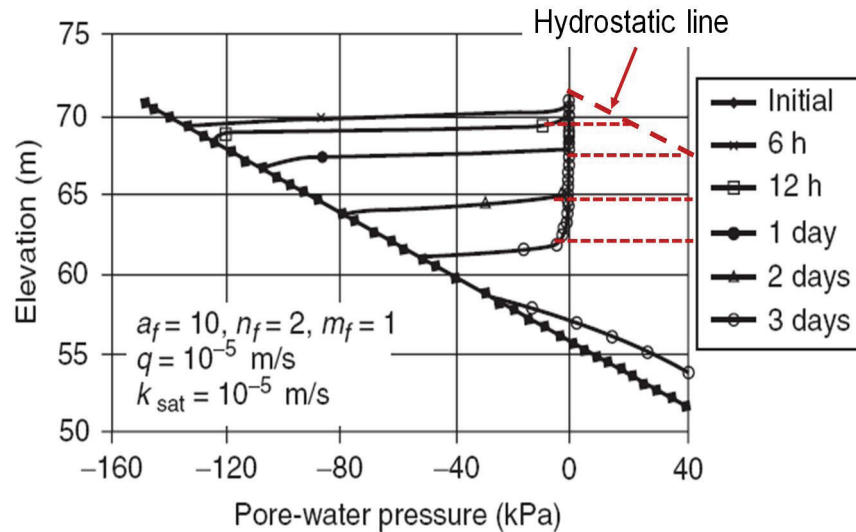
**Figure 6.** Infiltration into an unsaturated soil under steady state conditions with various ground surface moisture fluxes expressed as a ratio of the saturated coefficient of permeability at ground surface.

Figure 6 presents an approximation of pore-water pressures when the average infiltration rate is less than the saturated coefficient of permeability (Kasim et al., 1998). Under steady state conditions, infiltration occurs under a gradient of 1.0 and can be represented by a vertical line until the hydrostatic line is intercepted. The location of the vertical

line is a function of the ratio of the average (ground surface) moisture flux,  $q$ , to the saturated coefficient of permeability of the soil,  $k_{sat}$ . The soil below ground surface remains at a near constant suction value regardless of how long the rain falls. It could rain constantly at the same rate year after year (i.e., steady state) and our verified unsaturated flow theory indicates that a certain amount of suction would always be maintained in the soil. It should be noted that the pore-water pressure profiles shown in Figure 6 are in reality an indication of the maximum pore-water pressures possible because the condition shown takes time to develop. In other words, it takes time for the equilibrium condition shown to develop.

Steady state rainfall can be considered as an extreme condition in the sense that rainfall does continue forever. In reality, rainfalls stop and the pore-water pressures slowly tends towards hydrostatic conditions.

Let us now consider the second possibility where the moisture infiltration rate exceeds the saturated coefficient of permeability of the near ground surface soil as shown in Figure 7. The pore-water pressure at ground surface reduces to zero and a wetting-front forms. Meanwhile, the remainder of the soil profile maintains negative pore-water pressures. If the excessive rainfall continues over a long period of time, the wetting front slowly moves downward. Fortunately, rainfalls stop and the pore-water pressures tend towards the original hydrostatic condition. It can be observed that a positive pressure hydrostatic condition also commences to form at the ground surface and slowly move downward forming a wetting front.



**Figure 7.** Pore-water pressure profiles under transient rainfall conditions that are in excess of the saturated coefficient of permeability of the soil (modified from Zhang et al., 2004).

Negative pore-water pressures throughout the unsaturated soils profile can only disappear under high moisture fluxes conditions over long periods of time. For a slope to fail, the rainfall must be excessive and remain excessive. Under these conditions, the wetting front has time to move downward throughout the unsaturated soil profile. Consequently, it is **not** easy to wipe-out negative pore-water pressures (or suctions) by subjecting a slope to rainfall. There are two distinct questions that should be given consideration by the geotechnical engineer, namely, i.) How long can suctions be maintained? and ii.) What would be an adequate suction value to use for design purposes?

Failure of a natural slope will most likely occur when the slope is subjected to moisture flux conditions that are larger and longer than has ever occurred in the past. The “trigger” that allows a soil mass to become unstable lies in a knowledge of the state of stress in the pore-water phase above the groundwater table. Numerical seepage modeling can provide geotechnical engineers with value-added information regarding the conditions under which a slope might become unstable.

An understanding of moisture flow into an unsaturated soil assists the geotechnical engineer in finding engineered solutions for slope stability concerns. Even so, geotechnical engineers tend to be reluctant to rely upon *in-situ* suction for the stability of a slope. It might be of assistance to rephrase the question that should be addressed. “*Is it possible to significantly increase the stability of a slope by reducing the near-ground-surface coefficient of permeability of the soil by one, two or more orders of magnitude?*” Or, if the near-ground-surface permeability can be reduced, would the



**Figure 8.** Picture of the Po Shan Landslide in Hong Kong in 1972.

stability of the slope be increased by one, two or three orders of magnitude in terms of elapsed time to failure?

The decrease in the coefficient of permeability of the near ground surface material is essentially what was done in Hong Kong following the disastrous slope failure that passed through the mid-levels of Hong Kong Island in 1972 killing 78 persons (Figure 8). The maintenance of slopes in Hong Kong has proven to be extremely effective by covering sloping surfaces with a mixture of “chunam” (i.e., a paste of decomposed granite, flyash and cement). The plastering of chunam over the surface of cut-slopes has been found to reduce moisture infiltration by approximately 90%; thereby largely solving the landslide problem. Figure 9 shows a typical cut-slope in Hong Kong that has been covered with chunam, guiding the surface rainfall water into a drainage system that guides water into the harbour.



### 3.3 Quantifying ground surface moisture flux conditions

All unsaturated soil deposits have a ground surface that is exposed to atmospheric weather conditions. The quantification of moisture flux boundary conditions (i.e., Neumann boundary conditions), has not been a part of historical soil mechanics which was largely restricted to zero moisture flux boundary conditions or a “hydraulic head” boundary condition. The lack of a soil mechanics methodology for quantifying actual net moisture flux boundary conditions has provided an excuse for not analyzing moisture flux boundary condition problems into unsaturated soils.

The moisture flux at ground surface is the net value obtained from the summation of downward moisture flux (i.e., rainfall and snowfall), upward moisture movement (i.e.,



**Figure 9.** Use of chunam in Hong Kong to maintain the stability of slopes.

actual evaporation and evapotranspiration), and surface runoff (Figure 10). The “bad” news is each of these components needs to be independently quantified with respect to time (i.e., often over one or more years). The “good” news is that related disciplines (e.g., surface hydrology and agriculture) have proposed and verified methodologies for the quantification of the components of moisture flux. In addition, weather stations have been installed and programmed to collect moisture flux data all around the world. The data collected in most weather stations (i.e., temperature, wind speed, relative humidity and net solar radiation) provide the necessary input for the calculation of potential evaporation through use of the Penman, Wilson-Penman, or some other method (e.g., Thornthwaite, Monteith, etc.).

Independent methodologies have been proposed and tested for the calculation of water runoff as well as “actual evaporation”. The calculation of net moisture flux constitutes a new “tool” that is available to the geotechnical engineer. The calculation of net moisture flux lends itself well to database technologies (e.g., EXCEL). The primary engineered application making use of net moisture flux calculations has involved the design of soil cover systems (i.e., store-and-release covers).

### 4. Debunking myths related to measurement of unsaturated soil properties

I have attempted to debunk several misconceptions or myths that are often used as excuses for not accepting and applying unsaturated soil mechanics in engineering practice. Let us consider the following verbal exchange in response to an inquiry about an unsaturated soil mechanics problem.

Let us assume that a potential client phones my office and says to me, “*I have a problem that involves unsaturated soils*”. Before listening to my client’s explanation of the problem

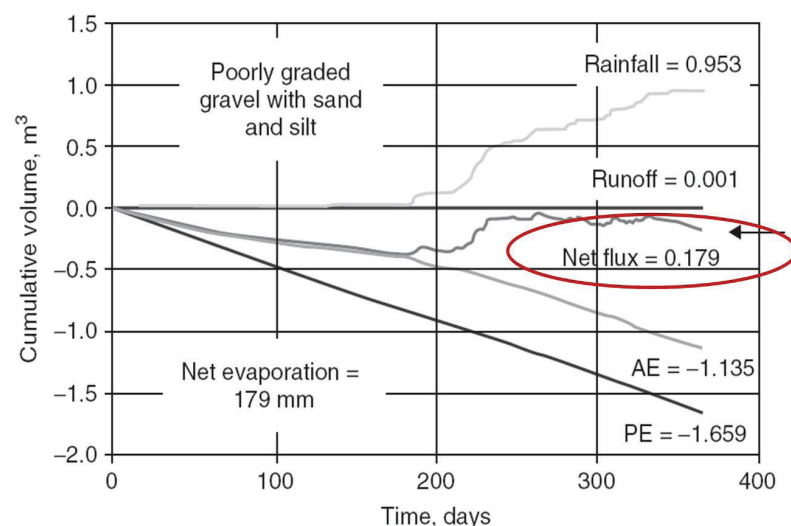


**Figure 10.** Net moisture infiltration at the ground surface calculated from weather station data (Fredlund et al., 2012).

I respond as follows, “We need to measure the soil-water characteristic curve for the soil”. The client might rightfully say, “But I haven’t told you what’s the problem and you are already saying you need to do some laboratory testing”.

My response may have sounded arrogant and extreme; however, there is a point to be made and it can be stated as follows. There is one piece of unsaturated soil property information that stands out as being of paramount importance when addressing virtually any problem involving unsaturated soils. An understanding of the soil-water characteristic curve, SWCC, (along with a simple shrinkage curve test), provides the unsaturated soils information that is required for the geotechnical engineer to extend saturated soil properties into the unsaturated soils range.

#### 4.1 Dispelling myths related to measuring unsaturated soil properties

The cost of measuring the unsaturated permeability function for a soil can be orders of magnitude more costly than measuring the saturated soil properties for the same soil (Fredlund & Rahardjo, 1993). Staying within the historic paradigm for saturated soil mechanics simply provides a cost-based excuse for not becoming involved in unsaturated soil mechanics. In other words, using the old paradigm that involves obtaining undisturbed soil sampling and direct laboratory testing for the physical soil properties of interest invokes costs that are prohibitive. As a result, it is necessary for geotechnical engineers to ask some serious questions regarding the need to consider using a new soil property assessment paradigm that would cost less while still providing sufficient accuracy and reliability for engineering practice.

Figure 11 attempts to show the similar basic soil property requirements between saturated soil mechanics theories and unsaturated soil mechanics theories. Moving from below the

water table (i.e., saturated soil conditions) to above the water table (i.e., unsaturated soil conditions) changes soil mechanics from having soil properties that can be viewed in terms of a series of soil constants to soil properties that are functions of negative pore-water pressures (or soil suction). The change from “soil constants” to “soil property functions” occur at the top of the capillary zone (or at the air-entry value) of the soil.

Above the capillary zone, the soil moves away from saturation and the soil properties can change quite rapidly. The transition in the designation of the soil properties transforms soil mechanics analyses from having linear constitutive relations to having nonlinear constitutive relations. The nonlinearity gives rise to a new challenge when analyzing practical engineering problems. However, on the positive side, research studies have verified that it is possible to “estimate” all unsaturated soil property functions through use of a modestly priced laboratory measurement of the soil-water characteristic curve, SWCC along with the shrinkage curve. In each case, the soil property is anchored to the saturated soil properties with a change in soil properties as the air-entry value of the soil is exceeded.

Figure 11 shows the three basic application areas for soil mechanics (i.e., water flow, shear strength, and volume change). The figure shows the constitutive equation form of the laws governing the behavior of saturated and unsaturated soils. The difference between the treatment of saturated and unsaturated soils lies in the form of the mathematical equations required to describe unsaturated soil constitutive relations.

#### 4.2 Emergence of a new paradigm for unsaturated soil property functions

Colleagues in soil physics and other agriculture-related disciplines have long recognized that a new approach was

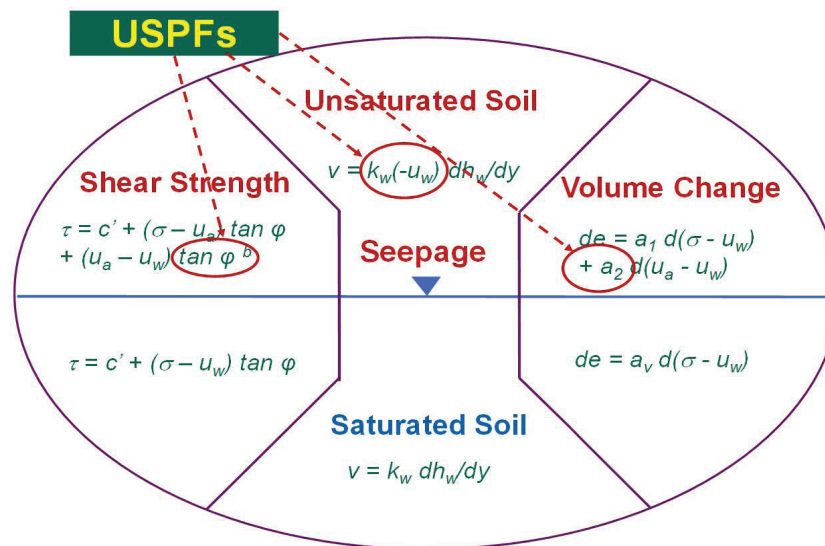


**Figure 11.** Three fundamental unsaturated soil property functions required in saturated/unsaturated soil mechanics.

required for soil property evaluation when dealing with unsaturated soils (van Genuchten, 1980). Initial interest was primarily limited to the evaluation of the unsaturated hydraulic conductivity properties of the soil (Fredlund et al., 1994). The new approach that evolved required the laboratory measurement of “*something other*” than the direct unsaturated soil property functions. That “*something other*” was the soil-water characteristic curve, SWCC, or the relationship between soil suction and the amount of water in the soil (Klute, 1965, 1986) as depicted in Figure 12.

The assumption was made that water flow through a soil was related to the amount of water in the voids. As a result, it was reasoned that the SWCC could be used to calculate a permeability function that would extend from saturated soil conditions to essentially the dry state. However, it was obvious that this approach had its challenges, mainly because there was not a unique relationship between the amount of water in the soil and the stress path adhered to during the test. Rather, there was a family of SWCC curves including scanning curves.

The primary curves were referred to as the *Initial Drying* curve (from 100% saturation), the *Main Drying* curve, and the *Main Wetting* curve. Soil samples were generally tested under zero total stress conditions and the *Main Drying* curve and the *Main Wetting* curves formed bounding or limiting conditions. The laboratory characterization of all branches of the family of SWCC was time consuming and costly.

The *Main Drying* curve was the easiest laboratory relationship to measure and with time became the main SWCC quantified. It became most common practice to control matric suctions using the axis-translation technique in the low suction range (i.e., up to 1500 kPa) and measure total suction in the high suction range (greater than 1500 kPa) using hygrometric means as shown by the raw data in Figure 13. The data was fitted using a regression analysis based on one of the numerous sigmoidal type equations that have been proposed for SWCCs. It is important that the equation selected be applicable over the

entire range of suctions from a fraction of 1 kPa to 1,000,000 kPa (e.g., Fredlund & Xing, 1994).

There are two points on the drying SWCC that are of primary interest to geotechnical engineers; namely, i) the true air-entry value of the soil, and ii) the rate of desaturation of the soil with respect to soil suction. Both variables require the determination of the degree of saturation with respect to changes in soil suction, (*S*-SWCC). However, gravimetric water content SWCC was the easiest to measure in the laboratory. Changes in gravimetric water content as soil suction was changed could possibly signify changes in degree of saturation or might also reflect changes in overall volume. It is important to be able to separate out the effects of volume change from the effects of desaturation of the soil. The separation of volume change and desaturation can be accomplished through measurement of the shrinkage curve for the soil, (*SC*) (Fredlund & Zhang, 2013). By using the drying shrinkage curve, the same stress path is followed during both the SWCC test and the shrinkage curve measurement for the soil (see Figure 14).

#### 4.3 Combining the *w*-SWCC and the shrinkage curve, *SC*, laboratory results

Combining the results of the gravimetric water content SWCC and the shrinkage curve allows the calculation of all volume-mass relationships versus soil suction; that is, the void ratio characteristic curve, *e*-CC, the volumetric water content characteristic curve,  $\theta$ -SWCC, and the degree of saturation characteristic curve, *S*-SWCC. The point of greatest importance along the *S*-SWCC is the true air-entry value of the soil, (i.e., the top of the capillary zone) where unsaturated soil properties come into effect (Shown in Figure 15). It is noted that the true air-entry value for a soil is often more than one order of magnitude greater than the “apparent” air-entry value observed on the gravimetric water content SWCC.

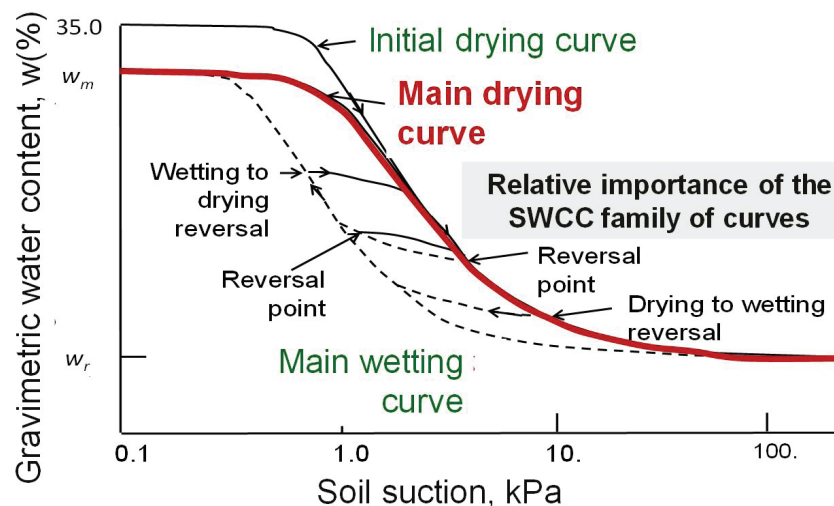


**Figure 12.** Basics of the soil-water characteristic curve, SWCC, family of curves (from Klute, 1965, 1986).

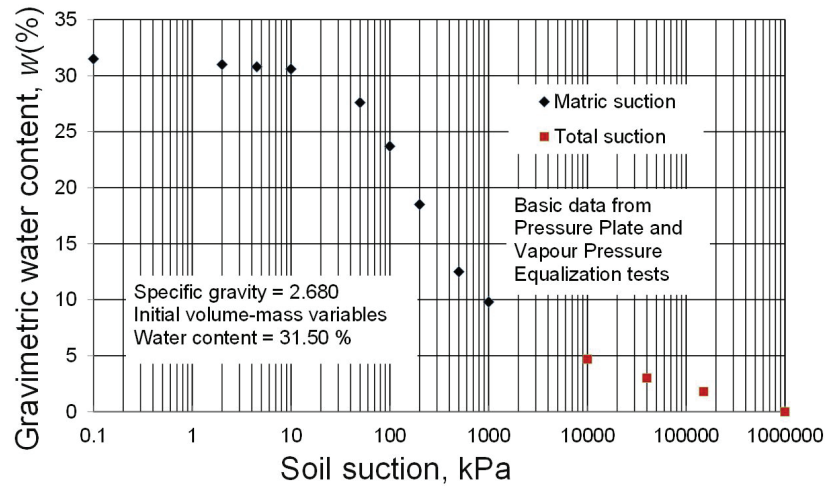


Figure 13. Gravimetric soil-water characteristic curve measurements over the entire range of soil suctions (Fredlund, 2019a).

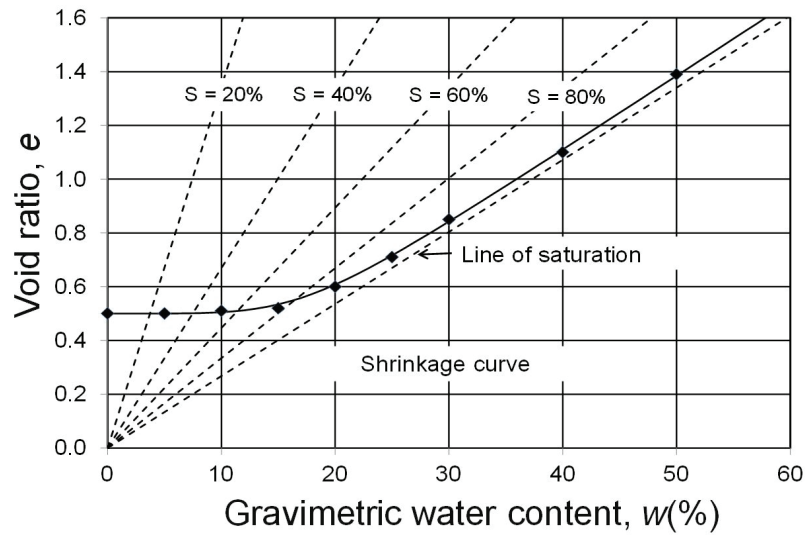


Figure 14. Typical shrinkage curve relating changes in volume to changes in water content (Fredlund, 2019b).

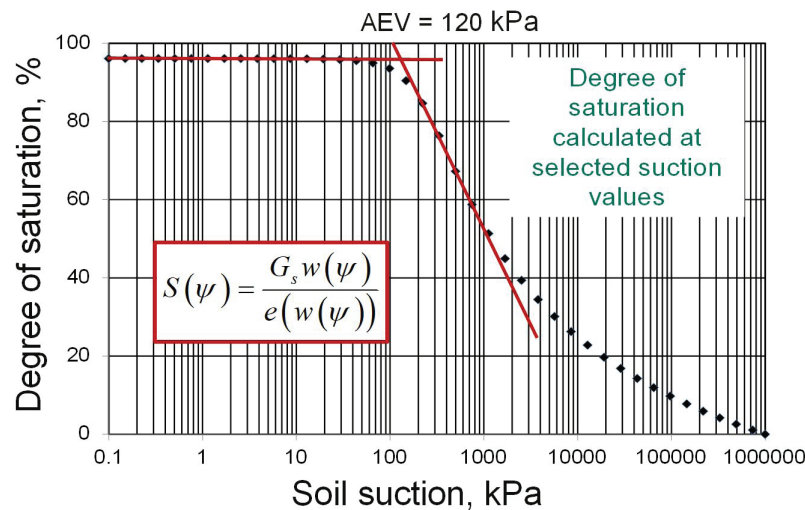


Figure 15. Degree of saturation soil-water characteristic curve,  $S$ -SWCC, calculated over the entire soil suction range using the  $w$ -SWCC and the Shrinkage Curve (Fredlund, 2019b).



#### 4.4 Calculation of unsaturated soil property functions

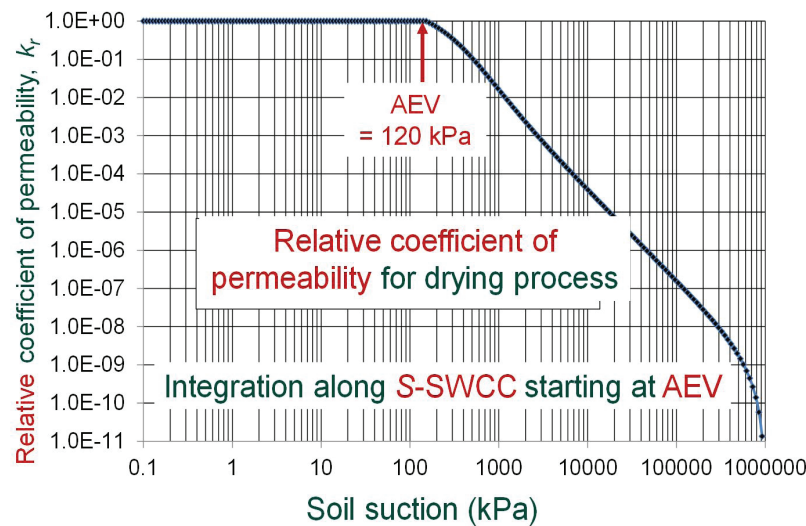
The appropriate volume-mass SWCCs can now be used along with one of the empirical “estimation” procedures proposed in the research literature for calculating the unsaturated soil property functions. An important unsaturated soil property function is the coefficient of permeability function and an example permeability function is shown in Figure 16. The coefficient of permeability is shown to decrease significantly once the air-entry value of the soil is exceeded. Note that the unsaturated soil permeability function can start from a dimensionless value of 1.0 corresponding to saturated soil conditions. The permeability function can then be scaled downward such that under saturated soil conditions the coefficient of permeability corresponds to the actual saturated coefficient of permeability.

The effect of hysteresis in the permeability function can be related back to the difference between the drying and

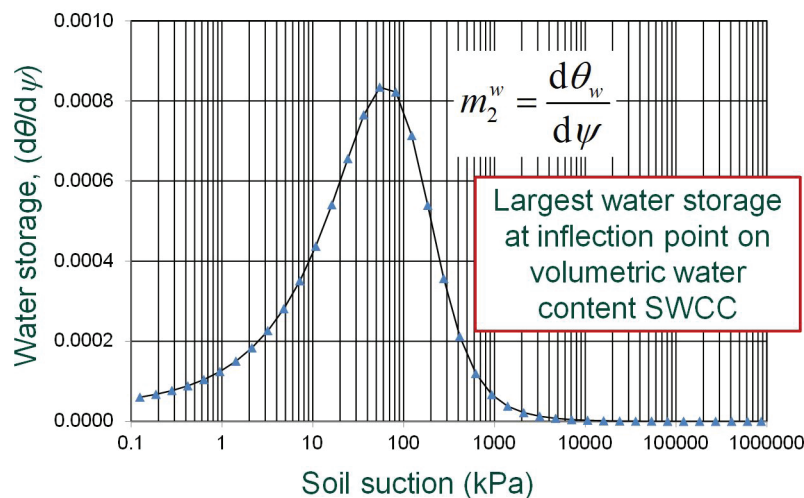
wetting  $S$ -SWCC. In other words, the difference between the drying and wetting  $S$ -SWCCs can be used to provide an estimation of the difference between the drying and wetting permeability functions (Pham et al., 2003).

Figure 17 shows a typical water storage function for an unsaturated soil. The formulation for transient seepage through an unsaturated soil is usually formulated such that the water storage function can be designated as the (arithmetic) slope of the volumetric water content SWCC ( $\theta$ -SWCC). Once again, there is a drying and a wetting water storage function with the maximum water storage value corresponding to the inflection point along the  $\theta$ -SWCC.

It is also possible to calculate other unsaturated soil property functions. For example, a shear strength function or a volume change function may need to be estimated. The assumption is being made that the soil behaves as a stable-structured soil. In each case, the unsaturated soil constitutive relationship can be calculated from an understanding of the



**Figure 16.** Coefficient of permeability unsaturated soil property function corresponding to the drying  $S$ -SWCC (Fredlund & Xing, 1994).



**Figure 17.** Typical water storage function for an unsaturated soil (Fredlund, 2019b).

SWCC and SC. All unsaturated soil property functions are empirical and based on a variety of assumptions. In some cases, the thought processes and proposed application protocols have originated in other disciplines and simply need to be confirmed for geotechnical engineering applications.

#### 4.5 Calculation of unsaturated soil property functions

Practical geotechnical engineering protocols have been distilled from research studies into unsaturated soil mechanics over the past several decades. In all cases, estimations for unsaturated soil property functions are based on a careful evaluation of the volume-mass properties and the response of the soil to changes in soil suction over a large range of suction values. There are assumptions associated with each empirical procedure that have been proposed for the calculation of unsaturated soil property functions. The assessment of each unsaturated soil property function has been approximated but the functions have proven to be extremely useful in providing geotechnical engineers with information on what will likely happen in response to a series of “*What if?*” questions that might be asked.

### 5. Debunking computational challenges

The evolution of a science basis for unsaturated soil mechanics did not start at the origination of the science for saturated soils. It appears that geotechnical engineers lacked understanding as to how best to apply unsaturated soil mechanics in engineering practice. In hindsight it is observed that the basic science principles for unsaturated soil mechanics are similar to the principles accepted for saturated soil mechanics. A significant challenge that needed to be addressed was the quantification of unsaturated soil property functions. The determination of unsaturated soil property functions has largely been resolved through use of “estimation” procedures based on laboratory measured soil-water characteristic curves, SWCCs, in conjunction with a shrinkage curve, SC. The last major question that needed to be addressed was, “*Can unsaturated soil behavior be modeled using nonlinear partial differential equation solvers?*”

There are two disciplines that have played an important role in making it possible to solve highly nonlinear partial differential equations of the type associated with unsaturated soil behavior. Mathematicians have developed a variety of mesh generation and mesh refinement and optimization techniques to provide robust numerical modeling techniques for nonlinear formulations. The computing industry has also increased its computing capability at a rapid pace that has been coincident with the emergence of unsaturated soil mechanics theories.

Unsaturated soil property functions have the form of nonlinear mathematical functions and as a result unsaturated soil mechanics requires significant computational capabilities. Nonlinearity arises because the soil properties are related to an (unknown) variable that was part of the solution. In seepage

problems, for example, the coefficient of permeability of the soil depends on the (negative) pore-water pressure and the pore-water pressure head is a component of the hydraulic head driving flow. Consequently, it is necessary to assume a value for the coefficient of permeability and then solve the seepage problem. Then a check must be made to ascertain whether the assumed value for the coefficient of permeability was correct. The nonlinear nature of the problem leads to a “trial and error” iterative type of solution. Fortunately, computers lend themselves well to this type of a challenge.

#### 5.1 Resistance to change in soil mechanics

Even though solutions for unsaturated soil mechanics problems have been extensively promoted at research conferences, still there appears to have been some resistance to change within the geotechnical engineering community. It is now possible to view soil continua as having an unsaturated soil zone and a saturated zone with a smooth seamless transition between the zones. Unfortunately, it often seemed easier to revert to crude past protocols rather than embrace the benefits of new, more rigorous procedures applicable for unsaturated soil mechanics. There are, however, considerable value-added benefits to be gained through simultaneously modeling of the saturated and unsaturated soil zones of a continua. The development of recent commercial software packages has made it considerably easier to accommodate saturated/unsaturated soil behavior modeling.

The complexities of the mathematical relations associated with unsaturated soil mechanics (e.g., nonlinear partial differential equations) can be largely obscured from the geotechnical engineer through use of recent software developments. Usage of special purpose software packages require: i) a delineation of the ground surface and the underlying soil strata, ii) the entry to the unsaturated soil properties, and iii) the designation of appropriate boundary conditions.

#### 5.2 Example solution of a saturated/unsaturated seepage problem

Steady state and unsteady state (or transient) solutions to a saturated/unsaturated soils problem are used to illustrate the role of numerical modeling solutions. Steady state problems require the input of a coefficient of permeability function. Unsteady state problems require that a water storage function also be input as a second soil property. It is noteworthy that there are similar transmission type properties and storage type properties required when considering virtually any continuum mechanics field problem (e.g., heat flow, air flow, chemical movement, etc.).

#### 5.3 Modeling a steady state problem involving saturated/unsaturated soil zones

Figure 18 shows a typical coefficient of permeability function for an unsaturated soil. A permeability function must



be used to determine the coefficient of permeability once the pore-water pressure becomes negative. However, the soil can be assumed to have a constant coefficient of permeability (i.e.,  $k_{sat}$ ) when the pore-water pressure remains below the air-entry value for the soil (i.e., the capillary zone).

It is possible to hard code into computer software one of several possible mathematical equations for the permeability function. However, it has been found to be just as efficient to input a table of values (e.g., 20 to 40 points) that cover the entire range of possible soil suction values that might be encountered when solving the seepage problem. Interpolation along the soil suction versus permeability should linearize the function because of the logarithmic nature of the suction scale. Different permeability calculation models (or calculation procedures) might be used in various software packages;

however, a table of points along the soil property function seems to be quite acceptable to numerical modellers.

Figure 19 shows the hydraulic head along with the zero-pressure line (i.e., piezometric line) under steady state seepage through a dam with a low permeability clay soil core. Subdivision of the geometry into mesh of finite elements may be either part of the numerical solver or it might be controlled by the modeller. It can be observed that the equipotential lines (or lines of hydraulic head) are seamless through the positive and negative pore-water pressure zones. Numerous numerical software codes in the marketplace simultaneously solve for hydraulic heads in the positive and negative pore-water pressure ranges (e.g., SV/Flow, Seep/W, etc.). Numerical modellers can quickly check and observe the response of the model to a series of “What if-?” queries.

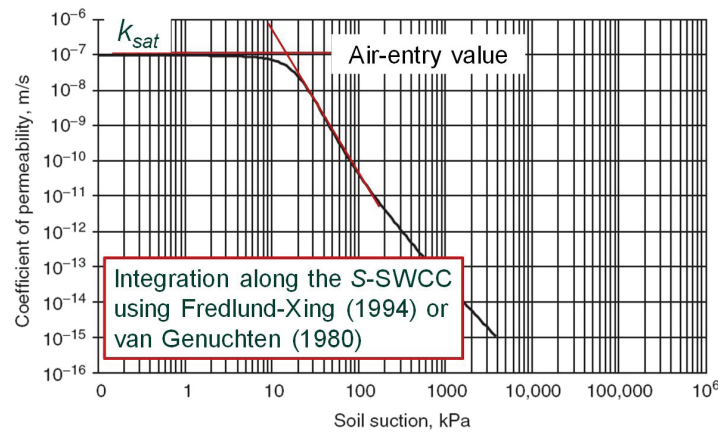
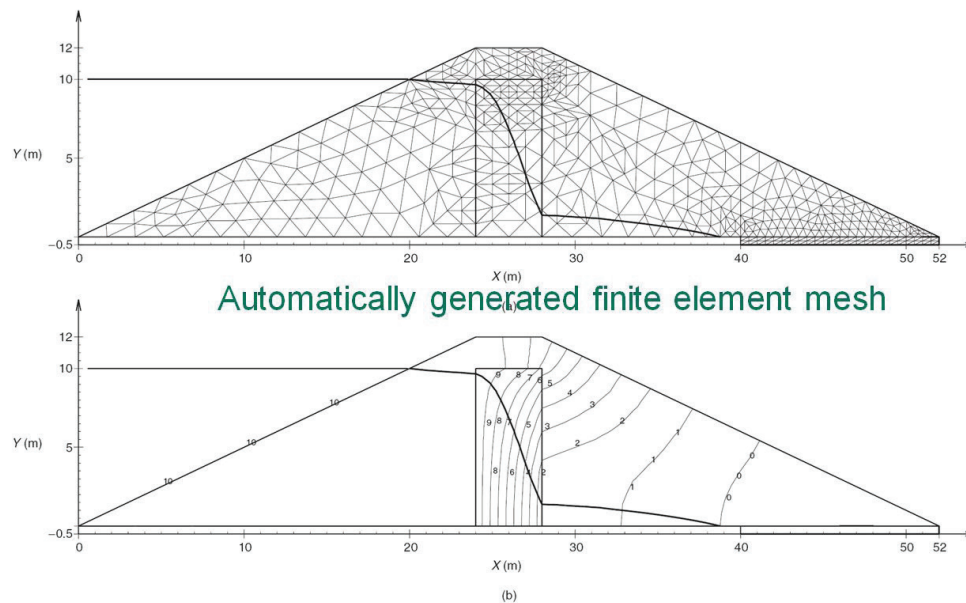


**Figure 18.** Permeability function for analyzing steady state and unsteady state seepage through an unsaturated soil (Fredlund et al., 2012).



Contours of computed hydraulic head or equipotential lines.

**Figure 19.** Contours of hydraulic head and the piezometric line under steady state seepage conditions (Fredlund et al., 2012).

#### 5.4 Modeling an unsteady state problem involving saturated/unsaturated soil zones

Transient (or unsteady state) seepage infers that the modeling process commences at an initial point in time and then a process (i.e., seepage in this case) is followed for a period of elapsed time. Figure 20 shows an example of the water storage function required when performing a transient seepage analysis that involves an unsaturated soil. The water storage function is calculated from the slope of the volumetric water content soil-water characteristic curve. The water storage can be input in a tabular format with interpolation performed on a logarithmic scale.

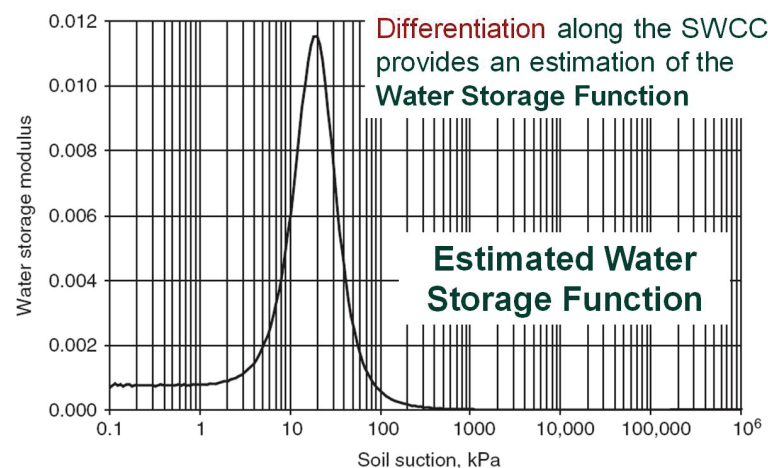
The example problem being considered assumes that water is instantly placed in the reservoir and the process of seepage into the compacted homogeneous earthfill dam is modeled with respect to time. The results at three elapsed times are shown: i) Figure 21 after 25 days, ii) Figure 22 after 60 days, and iii) Figure 23 after 1500 days (Fredlund et al., 2012). The solution reverts to what is essentially a steady state solution after 1500 days.

Figure 21 shows high head gradients as water enters the upstream face of the dam. The line of zero pressure (phreatic line) takes time to develop. Flow goes across the phreatic line as the hydraulic head contours spread out and move towards the downstream portion of the dam.

The phreatic line and the hydraulic head contours take on the form of a steady state solution after an elapsed time of 1500 days.

#### 5.5 Need for the teaching and demonstration of unsaturated soil mechanics at universities

New technologies are not immediately brought into engineering practice as soon as they are proven to be superior and correct. Rather, there commonly appears to be resistance to changing the way things have been done. It is necessary to go through a series of steps to bring about changes in engineering protocols. Usually there is a need to thoroughly understand the new procedures and be assured of the safety or lack of risk associated with putting new protocols into practice. This paper has largely focused on



**Figure 20.** Example of the water storage function required when analyzing transient seepage analysis on an unsaturated soil (Fredlund et al., 2012).

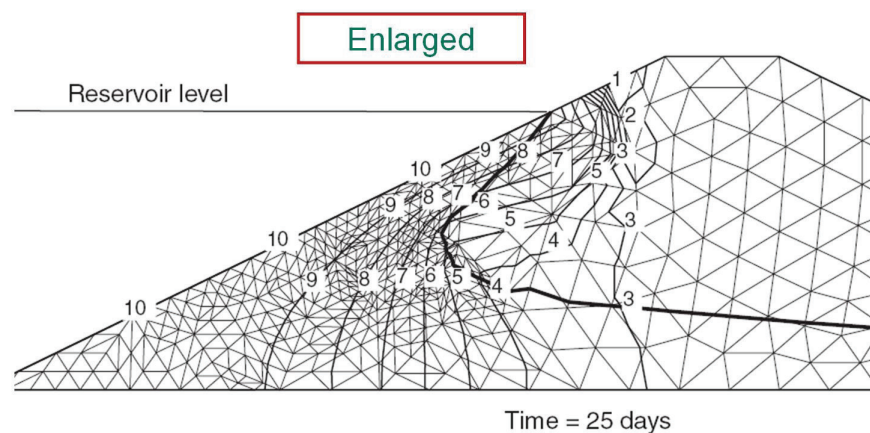


**Figure 21.** Contours of hydraulic head and the piezometric line under unsteady state seepage for 25 days (Fredlund et al., 2012).

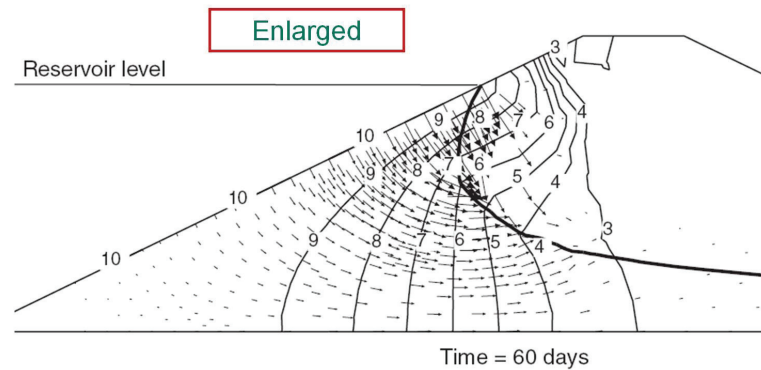


**Figure 22.** Contours of hydraulic head and the piezometric line under unsteady state seepage for 60 days (Fredlund et al., 2012).

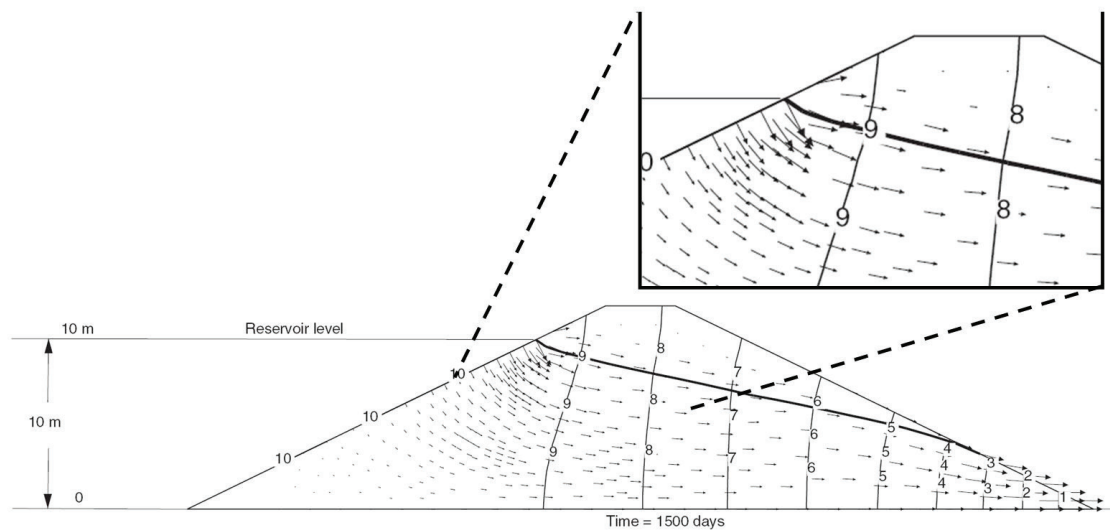


**Figure 23.** Contours of hydraulic head and the piezometric line under unsteady state seepage after 1500 days (Fredlund et al., 2012).

dispelling myths, misconceptions and unjustified challenges that have interfered with the implementation of unsaturated soil mechanics. An attempt has been made to dispel each of the common myths.

The teaching of unsaturated soil mechanics theories, along with examples and case histories, plays another important role in gaining acceptance of unsaturated soil mechanics. To assist in moving forward with implementation, a series of six one-hour lectures have been recorded on *Webinar* for the International Society of Soil Mechanics and Geotechnical Engineering, ISSMGE. The topics presented are shown in Figure 24. The *Webinar* lectures are presently in the library of ISSMGE and can be accessed free of charge. The lecture material has been synthesized largely based on the book *Unsaturated Soil Mechanics in Engineering Practice*, (Fredlund et al., 2012).

There is an ongoing need for the synthesis of other information related to unsaturated soil mechanics. One example is the need for standard (or generally accepted) testing procedures to be described in detail and adopted by regulatory agencies around the world. Several software companies appear to have

been out-in-front with the development of both two-dimensional and three-dimensional software codes that simultaneously model both the saturated and unsaturated soil zones.

## 5.6 Debunking unsaturated soils misconceptions

The teaching of soil mechanics at universities has mainly focused on the behavior of saturated soils. Not surprisingly, geotechnical engineers have inherited some preconceived inhibitions about the application of unsaturated soil mechanics. An attempt is made herein to debunk some misconceptions related to the acceptance and use of unsaturated soil mechanics. Misconceptions discussed can be listed as follows:

- 1) It is a commonly expressed viewpoint that theories related to unsaturated soils are too difficult for practicing geotechnical engineers to comprehend. However, the fundamental principles underlying saturated soil mechanics can be shown to also apply for unsaturated soil mechanics (i.e., both are based on a phenomenological continuum mechanics approach);

## Lecture Series for Introduction to Unsaturated Soil Mechanics

- Lecture 1: Introduction to Unsaturated Soil Mechanics
- Lecture 2: Fundamental State Variables & their Measurement
- Lecture 3: Soil-Water Characteristic Curve, SWCC, & Shrinkage Curve, SC
- Lecture 4: Water Flow & Solutions
- Lecture 5: Shear Strength & Solutions
- Lecture 6: Volume Change & Solutions

Notes are based on “Unsaturated Soil Mechanics in Engineering Practice”, (2012)

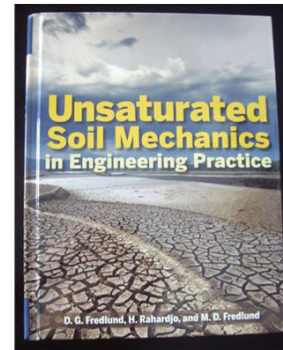


**Figure 24.** Lecture Notes on Unsaturated Soil Mechanics prepared for the International Society for Soil Mechanics and Geotechnical Engineering in 2019.

- 2) It is a misconception to conclude that it is necessary to wait in applying unsaturated soil mechanics principles and analyses until a better *in-situ* soil suction measurement device is discovered. Rather, the laboratory verification of unsaturated soil mechanics' theories provides an adequate framework for applying unsaturated soil mechanics theories that function similarly in the field as in the laboratory;
  - 3) It is a misconception to conclude that soil suctions readily disappear when rain falls on the ground surface. Only under conditions of very heavy rainfall over a long, long period of time can a slope become unstable. *In-situ* suctions do not quickly disappear following intense precipitation conditions. It has been shown that it is not easy to “wipe out” negative pore-water pressures either under low intensity or high intensity rainfall conditions. In other words, the dissipation of negative pore-water pressures is a relatively slow process;
  - 4) While it is difficult and costly to measure unsaturated soil property functions in the laboratory, there has been an increase in methodologies proposed for the estimation of the soil property functions through the measurement of the soil-water characteristic curve, SWCC, (and the shrinkage curve, SC) for a soil. These estimation methodologies have been shown to produce adequate results for most unsaturated soils problems. The SWCC and SC are not too costly and difficult to perform in geotechnical testing laboratories;
  - 5) It is not right to argue that the analyses of practical geotechnical engineering problems are too complex for available numerical modeling solutions. Ground surface boundary conditions can also be accommodated. Moisture fluxes are related to highly variable weather conditions; however, practical methodologies have been provided for geotechnical engineers with assistance from colleagues in surface hydrology. The quantification of net moisture flux at the ground surface has been extensively applied in the design of earth cover systems.
- It is difficult to bring about change in geotechnical engineering protocols, even when there are benefits to be gained in applying improved technologies. It is important to move past present-day inhibitions when the most significant roadblock simply involves the will of the geotechnical engineer.

### Declaration of interest

The author declares that there are no conflicting interests that could inappropriately bias their work.

### List of symbols

AEV	air-entry value
e-CC	void ratio characteristic curve
SC	shrinkage curve
SWCC	soil-water characteristic curve



$\theta$ -SWCC volumetric water content characteristic curve  
S-SWCC degree of saturation characteristic curve  
 $w$ -SWCC gravimetric water content characteristic curve  
USPFs unsaturated soil property functions

## References

- Blight, G.E. (2013). *Unsaturated soil mechanics in geotechnical practice*. Boca Raton: South Africa CRC Press, Taylor & Francis Group.
- Fredlund, D.G., & Houston, S.L. (2009). Protocols for the assessment of unsaturated soil properties in geotechnical engineering practice. *Canadian Geotechnical Journal*, 46(6), 694-707. <http://dx.doi.org/10.1139/T09-010>.
- Fredlund, D.G., & Rahardjo, H. (1993). *Soil Mechanics for Unsaturated Soil*; John Wiley & Sons: New York, NY, USA.
- Fredlund, D.G., Rahardjo, H., & Fredlund, M.D. (2012). *Unsaturated soil mechanics in engineering practice*. New York: John Wiley & Sons.
- Fredlund, D.G. (2015). Relationship between the laboratory soil-water characteristic curves and field stress state. In *Proceedings of the Asia-Pacific Conference on Unsaturated Soils*, Quilin.
- Fredlund, D.G. (2017). Role of the soil-water characteristic curve in unsaturated soil mechanics. In *Proceedings of the 19th International Conference on Soil Mechanics and Geotechnical Engineering* (The Blight Lecture, (Honours lecture), pp. 57-80), Seoul.
- Fredlund, D.G. (2019a). Determination of unsaturated soil property functions for engineering practice. In *Proceedings of the African Regional Conference on Soil Mechanics and Geotechnical Engineering* (The Jerry Jennings Memorial Lecture), Cape Town.
- Fredlund, D.G. (2019b). State of practice for use of the soil-water characteristic curve (SWCC) in geotechnical engineering. *Canadian Geotechnical Journal*, 56(8), 1059-1069. <http://dx.doi.org/10.1139/cgj-2018-0434>.
- Fredlund, D.G., & Morgenstern, N.R. (1977). Stress state variables for unsaturated soils. *Journal of the Geotechnical Engineering Division*, 103(GT5), 447-466.
- Fredlund, D.G., & Xing, A. (1994). Equations for the soil-water characteristic curve. *Canadian Geotechnical Journal*, 31(3), 521-532. <http://dx.doi.org/10.1139/t94-061>.
- Fredlund, D.G., Xing, A., & Huang, S.Y. (1994). Predicting the permeability function for unsaturated soils using the soil-water characteristic curve. *Canadian Geotechnical Journal*, 31(4), 533-546. <http://dx.doi.org/10.1139/t94-062>.
- Fredlund, D.G., & Zhang, F. (2013). Combination of shrinkage curve and soil-water characteristic curves for soils that undergo volume change as soil suction is increased. In *Proceedings of the 18th International Conference on Soil Mechanics and Geotechnical Engineering*, Paris, France.
- Houston, S.V. (2019). It is time to use unsaturated soil mechanics in routine geotechnical engineering practice. *Journal of Geotechnical and Geoenvironmental Engineering*, 145(5), 1-10. [http://dx.doi.org/10.1061/\(ASCE\)GT.1943-5606.0002044](http://dx.doi.org/10.1061/(ASCE)GT.1943-5606.0002044).
- Kasim, F., Fredlund, D.G., & Gan, J.M.-M. (1998). The effects of steady state rainfall on the matric suction conditions in a slope. In *Proceedings of the 2nd International Conference on Unsaturated Soils, UNSAT-98* (Vol. 1, pp. 78-83), Beijing, China.
- Klute, A. (1965). Laboratory measurement of hydraulic conductivity of unsaturated soil. In C.A. Black, D.D. Evans, J.L. White, L.E. Ensminger & F.E. Clark (Eds.), *Methods of soil analysis* (Monograph, No. 9, Part 1, pp. 253-261). Madison, WI: American Society of Agronomy.
- Klute, A. (1986). Water retention: laboratory methods. In A. Klute (Ed.), *Methods of soil analysis, part 1 – physical and mineralogical methods* (pp. 635-662). Madison, WI: American Society of Agronomy.
- Lu, N., & Griffiths, D.V. (2004). Profiles of steady state suction stress in unsaturated soils. *Journal of Geotechnical and Geoenvironmental Engineering*, 130(10), 1063-1076. [http://dx.doi.org/10.1061/\(ASCE\)1090-0241\(2004\)130:10\(1063\)](http://dx.doi.org/10.1061/(ASCE)1090-0241(2004)130:10(1063)).
- Morgenstern, N.R. (2012). Foreword. In D.G. Fredlund, H. Rahardjo & M.D. Fredlund (Eds.), *Unsaturated soil mechanics in engineering practice* (pp. xiii). New York: John Wiley & Sons.
- Pham, H.Q., Fredlund, D.G., & Barbour, S.L. (2003). A practical hysteresis model for the soil-water characteristic curve for soils with negligible volume change. *Geotechnique*, 53(2), 293-298. <http://dx.doi.org/10.1680/geot.2003.53.2.293>.
- Rahardjo, H., Kim, Y., & Satyanaga, A. (2019). Role of unsaturated soil mechanics in geotechnical engineering. *International Journal of Geo-Engineering*, 10(1), 8. <http://dx.doi.org/10.1186/s40703-019-0104-8>.
- Srivastava, R., & Yeh, T.-C.J. (1991). Analytical solutions for one-dimensional, transient infiltration toward the water table in homogeneous and layered soils. *Water Resources Research*, 27(5), 753-762. <http://dx.doi.org/10.1029/90WR02772>.
- Taylor, D.W. (1948). *Fundamentals of soil mechanics*. New York: John Wiley & Sons.
- Tarantino, A., & El Mountassir, G. (2013). Making unsaturated soil mechanics accessible for engineers: preliminary hydraulic-mechanical characterisation and stability assessment. *Engineering Geology*, 165, 89-104. <http://dx.doi.org/10.1016/j.enggeo.2013.05.025>.
- Terzaghi, K. (1943). *Theoretical soil mechanics*. New York: John Wiley & Sons.
- Terzaghi, K., & Peck, R.B. (1967). *Soil mechanics in engineering practice*. New York: John Wiley & Sons.
- Vanapalli, S. K., & Mohamed, F. M. O. (2006). Bearing capacity of model footings in unsaturated soils. In T. Schanz (Ed.), *Experimental unsaturated soil mechanics* (pp. 483-493). Berlin: Springer. [https://doi.org/10.1007/3-540-69873-6\\_48](https://doi.org/10.1007/3-540-69873-6_48).

- van Genuchten, M.T. (1980). A closed-form solution for predicting the hydraulic conductivity of unsaturated soils. *Journal of Soil Science of America*, 44(5), 892-898. <http://dx.doi.org/10.2136/sssaj1980.03615995004400050002x>.
- Zhang, L.L., Fredlund, D.G., Zhang, L.M., & Tang, W.H. (2004). Numerical study of soil conditions under which matric suction can be maintained. *Canadian Geotechnical Journal*, 41(4), 569-582. <http://dx.doi.org/10.1139/t04-006>.





## Application of in situ tests in unsaturated soils to analysis of spread footings

Gerald A. Miller<sup>1#</sup> , Rodney W. Collins<sup>2</sup> , Kanthasamy K. Muraleetharan<sup>1</sup> ,  
Tareq Z. Abuawad<sup>1</sup> 

Article

### Keywords

Standard penetration test  
Cone penetration test  
Pressuremeter test  
Unsaturated clay  
Spread footing  
Bearing capacity

### Abstract

Spread footings are often supported in the upper zone of the soil profile, which is frequently unsaturated. It is common in geotechnical practice to use in situ testing to assess soil properties throughout the zone of influence for footings. These tests regularly include the Standard Penetration Test (SPT), and sometimes the Cone Penetration Test (CPT), and Pre-bored Pressuremeter Test (PMT). Yet degree of saturation is often not considered in the analysis of the test results. To investigate the importance of partial saturation, SPTs, CPTs, and PMTs were conducted at two test sites over two years covering dry and wet periods. Water content and suction profiles were established for each test date to assess their impact on the in situ tests. Results from this study revealed that changes in moisture content and suction had an important influence on the results of in situ tests and the soil parameters derived from these tests. Specifically, undrained shear strengths estimated from SPT penetration resistance and CPT tip resistance using empirical and semi-empirical equations, respectively, were significantly lower during wet periods compared to dry periods. Consequently, estimated bearing capacities for a shallow foundation varied considerably from dry to wet periods. Similarly, PMT limit pressures were significantly impacted by increases in moisture content. Associated reductions in limit pressures resulted in large reductions in predicted allowable bearing capacity. While PMT modulus did appear to decrease with increasing moisture, its impact on settlement was offset by the decrease in allowable bearing pressure under wet conditions.

## 1. Introduction

In situ tests are commonly used as part of geotechnical investigations. Basic parameters obtained from these tests are used to predict soil properties and in turn to estimate bearing capacity and settlement of foundations. Researchers at the University of Oklahoma conducted in situ tests over a two-year period at two unsaturated soil test sites and collected water content and suction data in parallel. Results of this work revealed that basic test parameters and derived properties can vary significantly depending on seasonal variations in moisture conditions. Results from the Standard Penetration Test (SPT), Cone Penetration Test (CPT), and Pressuremeter Test (PMT), demonstrating these seasonal variations at the two clayey test sites are presented in this paper. In addition, variations in the predicted bearing capacity and settlement of a spread footing are presented and discussed in light of these seasonal variations in test parameters.

## 2. Background: predicting spread footing behavior using results of in-situ tests

### 2.1 Overview

Soil properties interpreted from in-situ tests are many, including drained and undrained shear strength parameters and elastic modulus for settlement analysis. Using the interpreted parameters, bearing capacity and elastic settlement of footings can be estimated using a drained or undrained analysis as appropriate. In the following sections two equations for estimating the undrained shear strength from SPT and CPT are presented, for use in a total stress analysis of spread footing bearing capacity at the clay test sites. In addition, for the PMT, equations for predicting bearing capacity and settlement based on the pressuremeter limit pressure and modulus, respectively, are also presented. Equations presented are provided as examples and their inclusion is not intended to

<sup>#</sup>Corresponding author. E-mail address: gamiller@ou.edu

<sup>1</sup>University of Oklahoma, School of Civil Engineering and Environmental Science, Norman, OK, USA.

<sup>2</sup>Building and Earth, Birmingham, AL, USA.

Submitted on April 7, 2021; Final Acceptance on May 12, 2021; Discussion open until November 30, 2021.

<https://doi.org/10.28927/SR.2021.065321>



This is an Open Access article distributed under the terms of the Creative Commons Attribution License, which permits unrestricted use, distribution, and reproduction in any medium, provided the original work is properly cited.

be an endorsement of their use over others that are available. The goal is to illustrate how the predicted soil properties from these equations can vary due to varying moisture conditions in an unsaturated profile; and consequently, how this impacts predicted bearing capacity and settlement of footings. The reader should keep in mind that the applicability of equations presented in this section may be questioned on the basis of actual drainage conditions during field testing, and because in the development of these equations, generally saturated drained or undrained conditions were assumed to prevail. In the case of unsaturated soils, the drainage conditions are vastly more complicated because of the presence of the air phase and the fact that excess pore pressures are governed by factors that extend beyond temporal volume change tendencies in the soil. Nevertheless, in practice the degree of saturation is not widely addressed in developing foundation recommendations, although it should be.

In the last decade researchers have been working on the problem of shallow foundations on unsaturated soils (Le et al., 2013; Oh & Vanapalli, 2013a, b, 2018; Vanapalli & Mohamed, 2013; Mohamed & Vanapalli, 2015; Tang et al., 2017a, b; Akbari Garakani et al., 2020) and various approaches for modeling and analysis have been presented. In this paper, the use of in situ testing to obtain parameters for estimating bearing capacity and settlement in unsaturated soils is explored. Of particular interest is how the in situ test results vary seasonally, and what impact this has on estimated bearing capacity and settlement if partially saturated conditions are not considered in the estimation of soil properties.

This paper demonstrates the possible consequences of not considering the moisture content at the time of in situ testing, relative to predicted soil properties, bearing capacity and settlement. The results highlight the necessity of developing methods for practitioners to address the influence of moisture content and suction on in situ test results for application to bearing capacity and settlement analysis. Preliminary recommendations for addressing these issues are provided.

## 2.2 Bearing capacity

For the purpose of this paper, the Terzaghi (1943) equation for ultimate bearing capacity of a square footing under general shear failure will be used. Ultimate bearing pressure,  $q_u$ , is given by Equation 1.

$$q_u = 1.3cN_c + \gamma_1 D_f N_q + 0.4\gamma_2 B N_\gamma \quad (1)$$

For a total stress analysis of clays, the total stress friction angle,  $\phi_p$ , is assumed equal to zero with  $c$  equal to the undrained shear strength,  $c_u$ ,  $N_c$  equal to 5.7,  $N_q$  equal to one,  $N_\gamma$  equal to zero, and  $\gamma_1$  equal to the total unit weight above the bearing level. For effective stress analysis of sand,  $c$  is equal to zero,  $N_c$  and  $N_\gamma$  depend on the effective stress friction angle  $\phi'$ , and,  $\gamma_1$  and  $\gamma_2$  are equal to the weighted average effective unit weights considering the position of the water table.

Fredlund et al. (2012) offer suggestions for predicting bearing capacity of unsaturated soils where the contribution of matric suction is captured via the cohesion,  $c$ , for a drained analysis. They also discuss a total stress approach based on strengths obtained from unconfined compression tests. For the purpose of this paper, Equation 1 was evaluated using a total stress approach for clays, with the governing strength parameters predicted from SPT and CPT results. In this way, the influence of seasonal variability in saturation and suction on the predictions will be revealed through the variation in interpreted soil parameters. This approach is indicative of the state of practice in areas where unsaturated soil mechanics has not been incorporated into the analysis of bearing capacity and settlement.

## 2.3 Standard Penetration Test (SPT)

The SPT is among the most widely used in situ test in geotechnical practice. It offers the advantage of providing a sample simultaneously while conducting the test. There are numerous correlations for estimating properties of sands and clays based on the SPT  $N$ -value. Equation 2 is but one example for estimating undrained shear strength,  $c_u$  (Hara et al., 1974), of clay.

$$c_u \text{ (kPa)} = 29N^{0.72} \quad (2)$$

Correlations between  $N$  and  $c_u$  are known to be unreliable; however, the authors have found that Equation 2 is reasonable compared to other methods of determining  $c_u$ . While not desirable, sometimes the SPT along with soil index properties provide the only means of estimating mechanical properties of soils for a given project.

## 2.4 Cone Penetration Test (CPT)

A CPT uses a friction cone and is a rapid profiling tool that provides near continuous records of tip resistance,  $q_c$ , and sleeve friction,  $f_s$ . The CPT can be used to estimate soil types and various soil properties. The cone can be equipped with a sensor to detect pore water pressure during penetration; however, since the research discussed in this paper involved unsaturated soils, reliable measurements of pore water pressures during penetration could not be obtained. As with the SPT, the undrained shear strength of clay can be estimated from the CPT using available correlations such as that represented by Equation 3 (Kulhawy & Mayne, 1990).

$$c_u = \frac{q_c - \sigma_o}{N_k} \quad (3)$$

Unlike Equation 2, Equation 3 is semi-empirical with its theoretical basis in bearing capacity theory; however, the determination of the bearing capacity factor  $N_k$  is based on empirical data. Factor  $N_k$  reported by Drnevich et al. (1988)

varies between about 5 and 25 for a wide range of clays; a value around 15 appears to be a reasonable first order approximation (Drnevich et al., 1988) for a wide range of clays. A value of  $N_k$  equal 20 was conservatively selected by the authors, in part because it seems to provide more reasonable values for the overconsolidated residual clays we have worked with.

## 2.5 Pressuremeter test (PMT)

The pressuremeter can be used to directly estimate the ultimate bearing pressure of a shallow foundation via Equation 4 (Briaud, 1992).

$$q_u = kp_{Le}^* + \gamma D_f \quad (4)$$

For  $D_f/B$  of 0.5, the recommended bearing capacity factor for clay is about 0.9 (Briaud, 1992). The pressuremeter is an in situ test that provides a stress-stress curve that can be used to directly determine the modulus of elasticity. The pressuremeter modulus can be used to predict settlement,  $S$ , using Equation 5 (Ménard & Rousseau, 1962; Briaud, 1992).

$$S = \frac{2}{9E_d} q_{net} B_o \left( \lambda_d \frac{B}{B_o} \right)^\alpha + \frac{\alpha}{E_c} q_{net} \lambda_c B \quad (5)$$

If the pressuremeter modulus,  $E_p$ , is constant with depth, Equation 5 reduces to Equation 6, where the constant  $C$  depends on the soil type and ratio  $B/B_o$ .

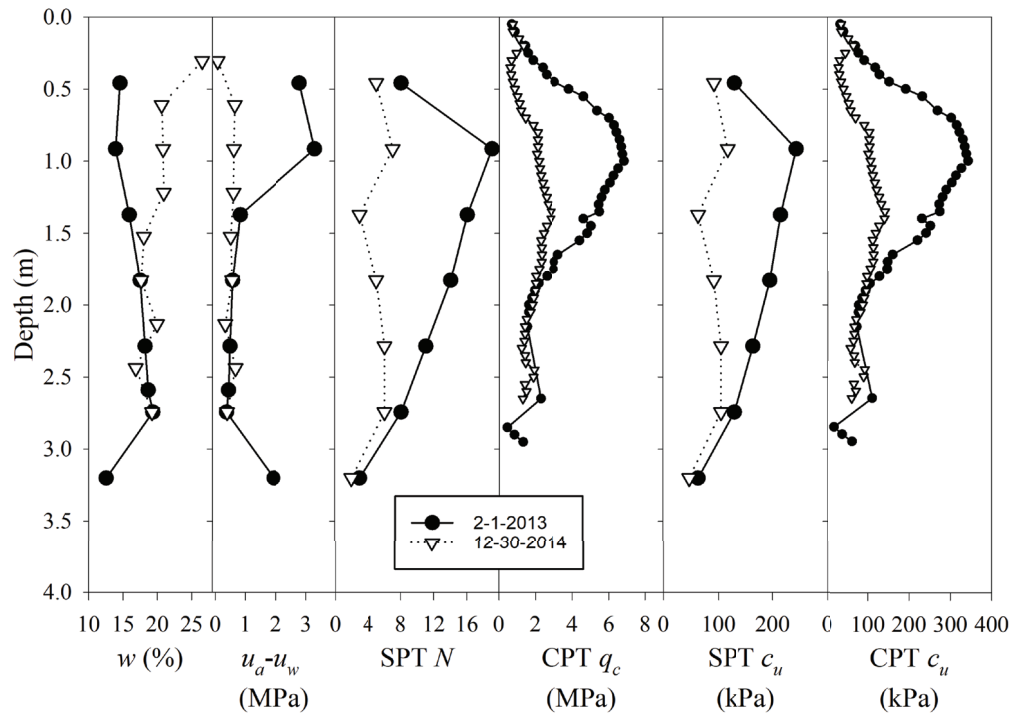
$$S = C \frac{q_{net} B}{E_p} \quad (6)$$

For a square footing, the shape factors are both about 1.1 and the rheological factor is 1 for overconsolidated clay. Thus, for a square footing on overconsolidated clay having a uniform  $E_p$  with depth, the constant  $C$  is about 1.3.

## 3. Results of in situ testing and foundation analysis in unsaturated soil

### 3.1 Standard penetration and cone penetration testing at two clay sites

Results of SPT and CPT testing at two different test sites on two different days are shown in Figures 1 and 2. On each testing date, one SPT and three CPT profiles were conducted and moisture content samples were collected. As discussed by Collins (2016) and Miller et al. (2018), the matric suction was estimated from gravimetric water content data using a soil-water characteristic curve (SWCC) developed for the test soils at each site using total suction measurements, pressure plate data and empirical curve fitting

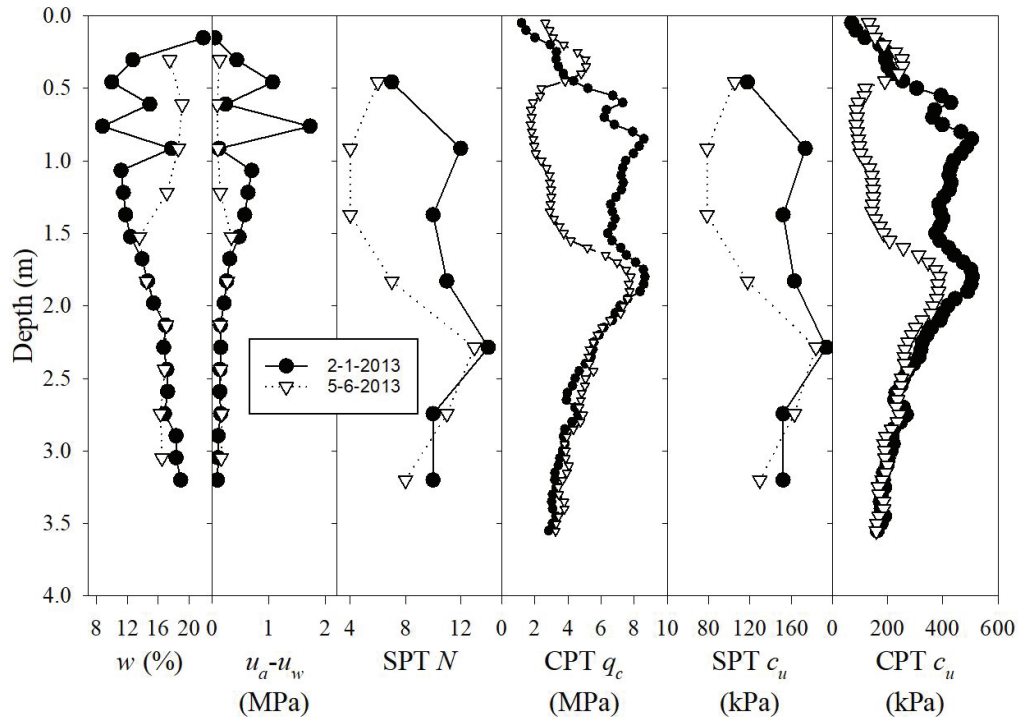
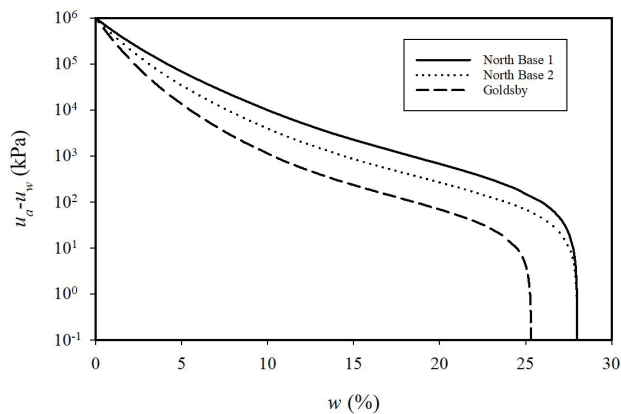


**Figure 1.** Results of SPT and CPT at North Base Test Site on two different test dates.

**Table 1.** Average soil properties for layers at North Base and Goldsby.

Depths (m)	Test Soil Site Name	UCSC Classification	LL	PI	%F*	%S <sup>#</sup>	n <sup>+</sup>	G <sub>s</sub> <sup>^</sup>
0.3-0.9	North Base-Layer 1	CL, Lean clay	47	29	91	9	0.414	2.72
0.9-3	North Base-Layer 2	CL, Lean clay	35	19	89	11	0.364	
0-1.5	Goldsby-Layer 1	CL, Lean clay	32	11	92	8	0.439	2.71
1.5-3	Goldsby-Layer 2	CL, Lean clay with sand	30	9	80	20	0.417	

\*% fines; <sup>#</sup>% sand; <sup>+</sup>porosity; <sup>^</sup>specific gravity of solids.

**Figure 2.** Results of SPT and CPT at Goldsby Test Site on two different test dates.**Figure 3.** Soil Water Characteristic Curves used to estimate matric suction from gravimetric water content.

using the method of Zapata et al. (2000). The soil layering and average properties at each site are listed in Table 1, while the SWCCs used to estimate matric suction from the gravimetric water content are provided in Figure 3. Measurements of total

suction revealed significant osmotic suction when the soil was near saturation; however, changes in matric suction are generally more meaningful relative to mechanical behavior (e.g. Fredlund et al., 2012) and therefore, matric suction was used in the analysis.

The impact of the change in water content and suction is clearly revealed in the trends of the SPT  $N$  values and CPT  $q_c$  values with depth in Figures 1 and 2. Interestingly, at both sites the SPT  $N$  values on the two dates below about 2.0 m continued to show some differences even though it appeared that water content and suction below 2.0 m was quite similar. On the other hand, the CPT  $q_c$  values on the two dates tended to converge at a lesser depth, closer to where the moisture content differences became minimal. Two possible contributors to this observation include, first, the fact that the SPT starts 0.3 m above the plotted test depth and so is influenced by soil above the actual point where the  $N$  value is plotted. Second, matric suction during wetting may be lower than predicted from a single SWCC that does not account for hysteresis. Because of hysteresis, for a given

water content during a period of wetting, the matric suction would be less than during drying, but using a single SWCC does not account for this. Thus, actual values of matric suction in Figures 1 and 2, would be lower for the inverted triangles, corresponding to the wetting event, relative to the solid circles at the same water content.

Predicted undrained shear strengths using Equation 2 with SPT  $N$  values and Equation 3 with CPT  $q_c$  values are shown side by side in Figures 1 and 2. The average undrained shear strengths from SPT and CPT in a layer extending from 0.5 to 2 m for each site and each date are summarized in Table 2 along with average water content, suction,  $N$  value and  $q_c$ . Also, shown in Table 2 are the predicted bearing capacities for each case, assuming a 1 m square footing is embedded 0.5 m, and using the average undrained strengths in a total stress analysis with Equation 1 and total unit weight,  $\gamma_t$ , of 18 kN/m<sup>3</sup>. In the last two columns of Table 2 are the factors of safety (FS) for the dry season date (assumed to be 3) and the wet season date calculated due to the change in  $q_u$  from dry to wet seasons. These FS values indicate that if the SPT or CPT are conducted in a dry season and used for footing design, the wet season FS could be about half of the original FS. This suggests great caution is needed in the interpretation of SPT and CPT results in unsaturated soils, particularly during drying seasons. What is needed is a practical method for interpreting SPT and CPT with consideration of moisture content changes from dry to wet seasons. The SPT and CPT values of undrained shear strength agree reasonably well for the higher  $PI$  North Base soil compared to the lower  $PI$  Goldsby soil. This highlights the uncertainty in empirical correlations and the importance of using more than one approach for estimating important soil mechanical properties. It is noted that  $c_u$  estimated based on SPT was lower in both cases, probably due to the significant conservatism built into SPT correlations. Also, these correlations are fundamentally more applicable to saturated than unsaturated clay soils.

The data in Table 2 indicate that on average the moisture content in the zone of interest for this footing increased about 4% at both sites and the average decrease in undrained

shear strength and ultimate bearing capacity was about 50% considering both the  $q_c$  and  $N$  values at both sites.

### 3.2 Pressuremeter testing at two clay sites

Results of pressuremeter tests at the North Base and Goldsby test sites on different dates over a nearly 2-year period are shown in Figures 4 and 5, respectively. These figures summarize the interpreted limit pressures,  $P_L$ , and pressuremeter moduli,  $E_p$ , for tests at three different depths, along with the natural moisture content and daily rainfall from a nearby weather station (Mesonet, 2021, Norman Station). The Mesonet weather station is less than 0.2 km from the North Base site and about 9.0 km north of the Goldsby site. The pressuremeter testing began in a relatively dry period in the beginning of 2013 when soil moisture contents were low. Then, rainfall events increased in frequency and magnitude until mid-November of 2013. There was an increase in soil moisture content at the test sites during this time and consequently, there is a noticeable decrease in the trend of pressuremeter limit pressures. The pressuremeter moduli also appear to generally decrease over this period, being more noticeable at the North Base site. During this period of wetting there was a total of 118 cm of rainfall. Following this period of wetting there was a dry spell between mid-November 2013 and mid-March 2014 during which only about 4 cm of rainfall occurred. Interestingly, the natural water contents did not decrease much during this period, which was over the colder winter months, but did show a steady decrease throughout the rest of 2014. 2014 was much drier with a total rainfall of 57 cm compared to 120 cm in 2013.

The influence of the changing water contents on the pressuremeter parameters at both North Base and Goldsby test sites is revealed in Figures 6 and 7, respectively. In these figures, the limit pressure and modulus, normalized by the vertical total stress, are plotted against the natural water content and corresponding matric suction estimated from the SWCC. The parameters were normalized by vertical overburden pressure to account for the differences in total stress state, which reflects the initial net normal stress state, at the three

**Table 2.** Average properties and bearing capacity.

Test Site	Avg. $w$	Avg. $u_a-u_w$	Avg. N	Avg. $q_c$	SPT	CPT	SPT	CPT	SPT	CPT
					Avg. $c_u$	Avg. $c_u$	$q_u$	$q_u$		
	(%)	(kPa)		(kPa)	(kPa)	(kPa)	(kPa)	(kPa)	(kPa)	$FS$
North Base										
2/1/2013	15.5	1883	14.3	4809	194	231	1447	1721	3	3
12/30/2014	19.6	579	5.0	2068	91	102	683	765	1.4	1.3
Goldsby										
2/1/2013	12.9	569	9.7	7301	148	428	1106	3180	3	3
5/6/2013	16.5	180	4.7	3893	88	194	661	1447	1.8	1.4



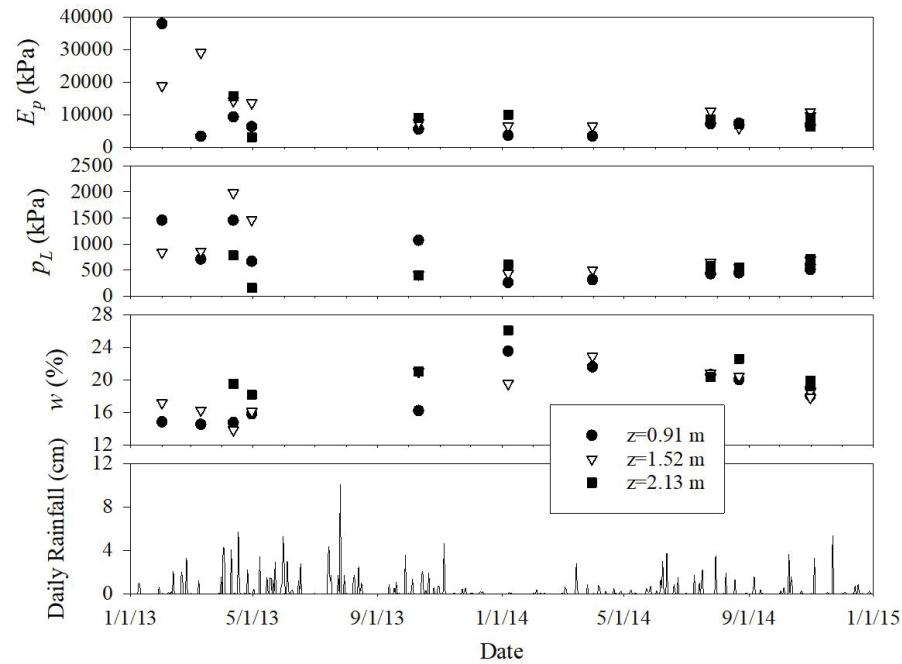


**Figure 4.** Pressuremeter limit pressure and modulus, and corresponding water content for the North Base test site for three test depths on different dates. Rainfall data obtained from a nearby weather station (Norman station, Mesonet 2021).

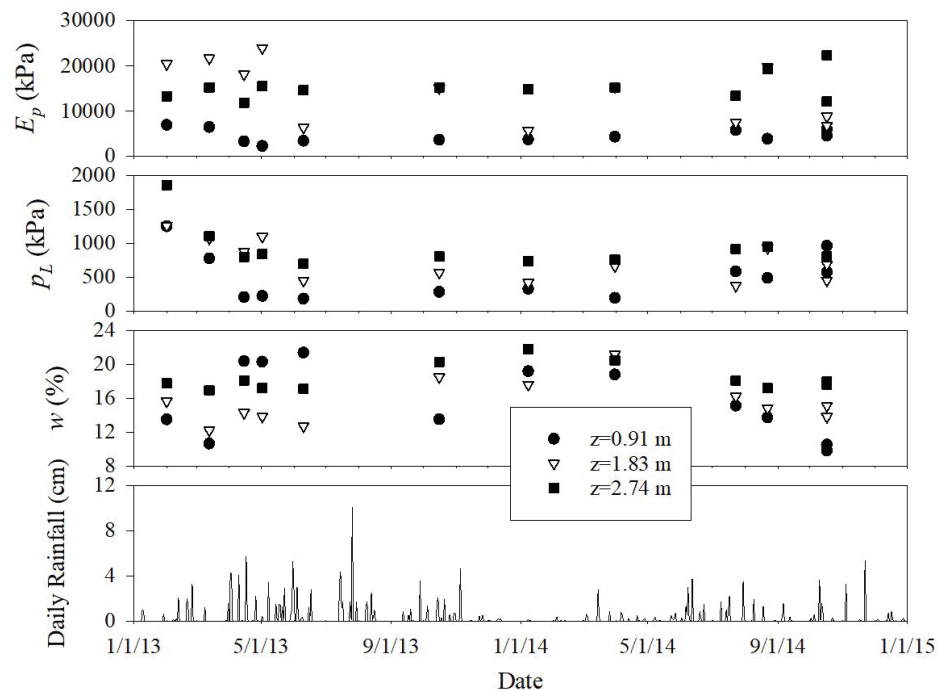


**Figure 5.** Pressuremeter limit pressure and modulus, and corresponding water content for the Goldsby test site for three test depths on different dates. Rainfall data obtained from a nearby weather station (Norman station, Mesonet 2021).

test depths. There is a fair amount of scatter in the data, which is largely attributed to the natural variations in soil properties at these sites. Nevertheless, there appears to be rather strong trends in the variation of normalized limit pressure with water content and suction. The trends in normalized modulus are

not as statistically robust as the limit pressures; however, they do show expected decreasing trends with increasing moisture content. The scatter in the pressuremeter modulus data is due in part to the subjectivity in selecting the near linear portion of the pressuremeter curve to interpret the modulus; a small

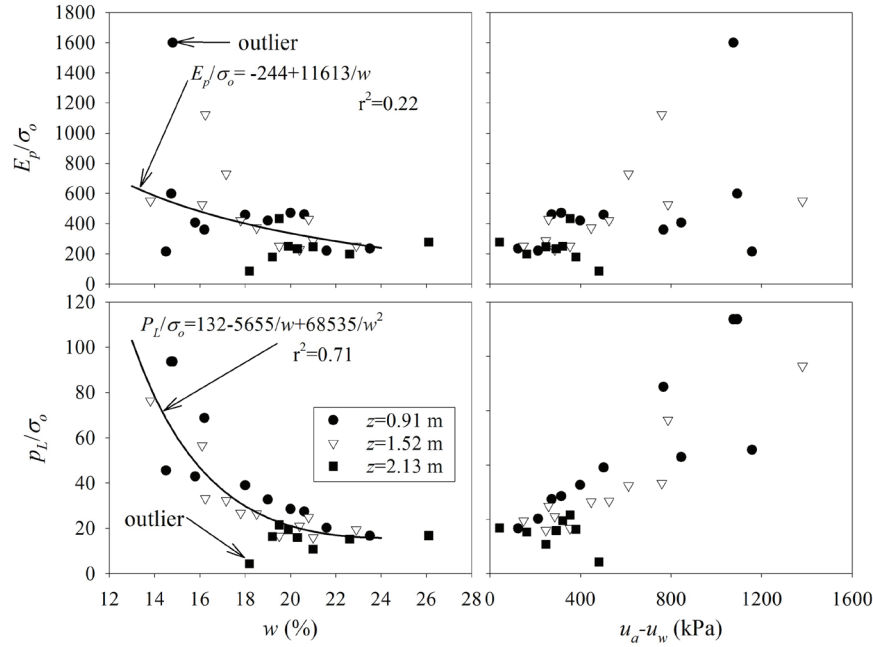


**Figure 6.** Normalized pressuremeter limit pressure and modulus versus water content and matric suction for North Base.

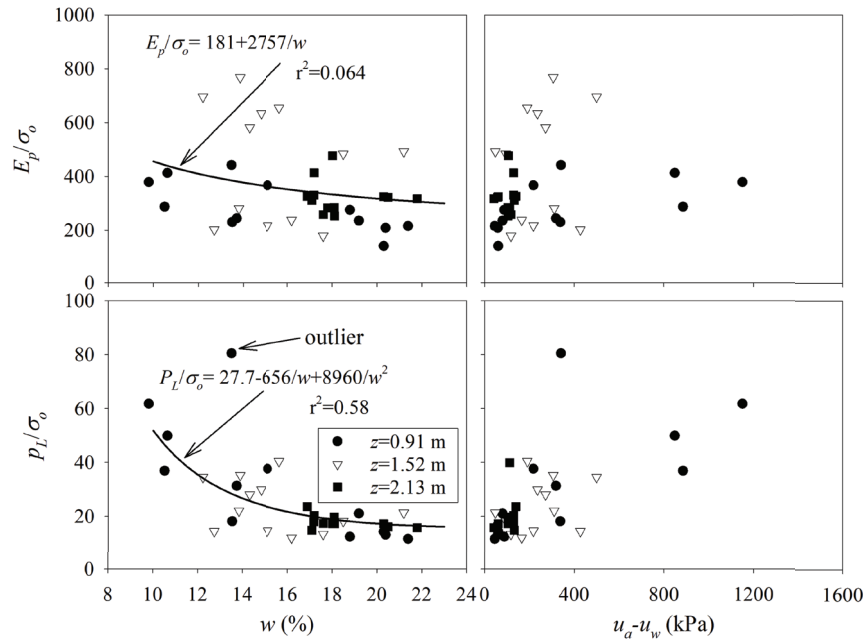


**Figure 7.** Normalized pressuremeter limit pressure and modulus versus water content and matric suction for Goldsby.

difference in the slope makes a large difference in the calculated modulus. Also, the pressuremeter modulus is more sensitive to disturbance around the borehole.

In Figures 8 and 9, the variation in predicted allowable bearing capacity and settlement using Equations 4 and 6 due to variations in water content during the testing period are presented. The water contents for the upper two test depths

were averaged to represent the moisture content in the zone of influence for bearing capacity (1-m wide square footing) while the moisture contents for all three test depths were averaged to represent the zone on influence for settlement. Pressuremeter limit pressures and moduli used in Equations 4 and 6 were calculated using the regression equations shown in Figures 6 and 7.



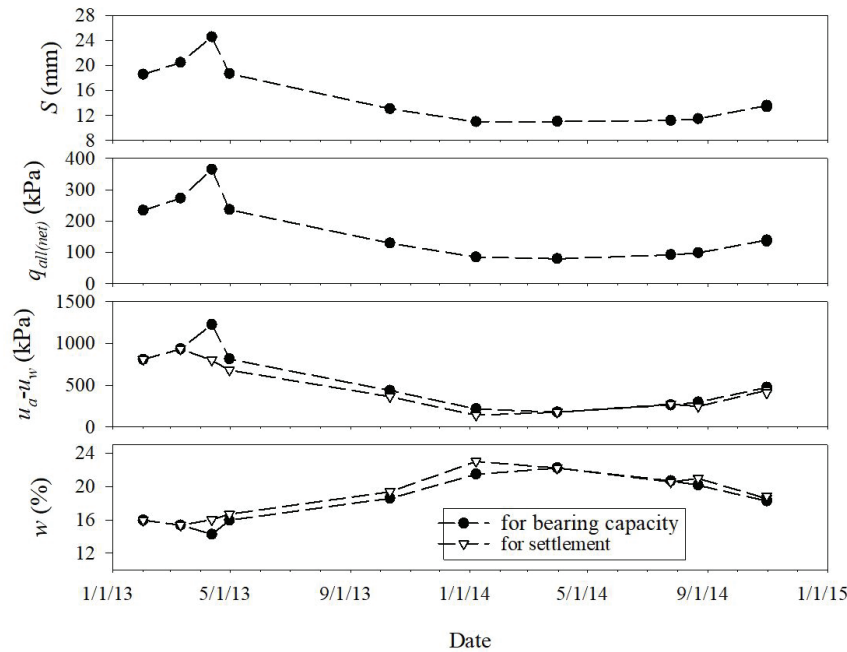


**Figure 8.** Predicted allowable bearing capacity and settlement in relation to variations in average moisture contents and matric suction within the zone of influence for bearing capacity and settlement during the testing period at North Base.

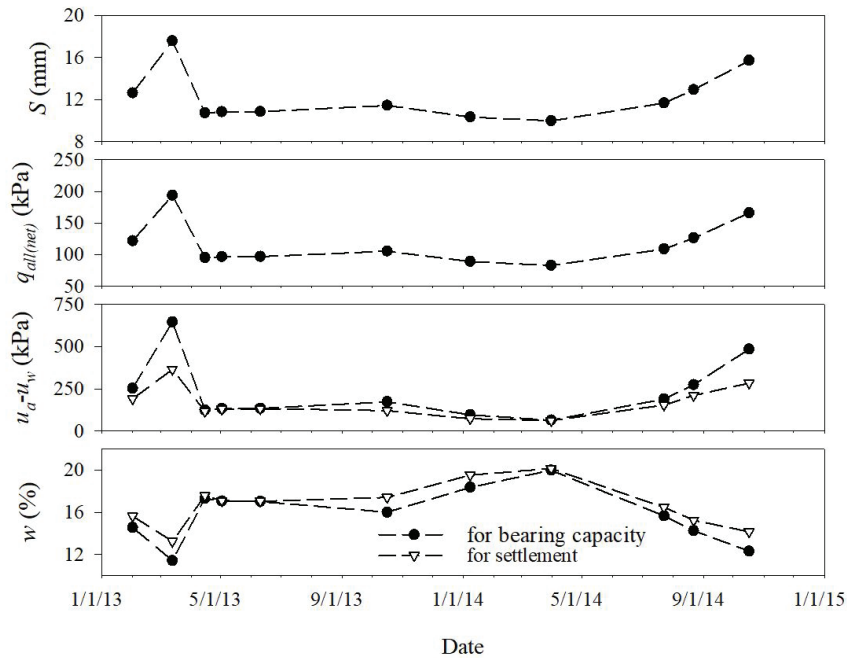


**Figure 9.** Predicted allowable bearing capacity and settlement in relation to variations in average moisture contents and matric suction within the zone of influence for bearing capacity and settlement during the testing period at Goldsby.

Figure 8 reveals that during the test period the predicted net allowable bearing pressure, assuming a factor of safety of three, varied between 80 and 366 kPa with corresponding settlement of 11 mm to 25 mm for the North Base site. For Goldsby in Figure 9, the predicted allowable bearing capacity and settlement ranged from 83 to 194 kPa and 10 to

18 mm, respectively. While the predicted range of settlements is not overly concerning, the change in allowable bearing capacity is alarming at both sites. Even though the modulus decreased with increasing moisture content, predicted settlements also decreased due to the decrease in allowable bearing pressures. The maximum predicted allowable bearing

pressure corresponding to dry conditions at North Base is 4.6 time greater than the minimum obtained during wet conditions. This implies that the allowable bearing pressure for dry conditions is greater than the ultimate bearing pressure for wet conditions. Or in other words, the factor of safety can drop below one if the footing is designed for dry conditions. The results of these pressuremeter tests emphasize the need for caution when interpreting PMT results in partially saturated clays, particularly during a dry period.

#### 4. Discussion

Results of in situ testing during dry and wet periods discussed in previous sections highlight the need to account for the influence of partial saturation on test parameters and resulting foundation analysis. To properly account for unsaturated soil mechanics in the analysis of foundation bearing capacity and settlement requires estimation of unsaturated soil parameters and soil water characteristic behavior. However, unsaturated soil mechanics in this regard has not yet been widely implemented in practice. Some advancements in the analysis of foundations on partially saturated soil have also been made as noted previously, but are not yet widely employed in practice. Furthermore, the state of knowledge regarding interpretation of in situ tests in unsaturated soils is still rather limited, in spite of some recent significant advancements in research (e.g. Mohamed & Vanapalli, 2015; Yang & Russell, 2015; Miller et al., 2018). Nevertheless, in situ tests are being conducted every day in unsaturated soil profiles and used in developing shallow foundation recommendations, especially the SPT. Practitioners need some interim, practical suggestions for addressing the impacts of partial saturation on their foundation recommendations, and other geotechnical problems where derived soil properties depend on in situ test results.

To assess the moisture conditions and potential impact on results of in situ tests in unsaturated soils, geotechnical engineers can employ a number of strategies. For example, the usual field and laboratory testing activities could be supplemented with the following:

- 1) Examining historical weather records for a site can help to determine whether the current conditions may be more dry or wet. Some states like Oklahoma also provide drought monitoring which contributes greatly to this assessment;
- 2) At a minimum, on the day of testing, collect frequent moisture content samples in the unsaturated zone, and if possible determine or estimate matric suction at the same depths. Matric suction can be estimated from the SWCC, which can also be estimated using the method of Zapata et al. (2000), for example;
- 3) If the soil is drier than the wettest condition expected for the site, which could be near saturation, the in situ test parameters corresponding to wet conditions could be estimated for use in geotechnical analysis. This

step has a great deal of uncertainty associated with it because of the lack of published data and procedures needed to make such predictions. However, not considering the consequences of wetter conditions is not an acceptable alternative. For soil profiles that are somewhat uniform in character with depth, it is possible that plotting the moisture content, even from a single day, versus the test parameters or normalized test parameters obtained at different depths may provide some insight. Otherwise, published data such as the normalized pressuremeter data in Figures 6 and 7 could be used to gain some insight into expected changes in the test results due to wetter conditions. Similar plots are shown in Figures 10, 11, 12 and 13, for SPT and CPT parameters from the North Base and Goldsby test sites. While there is significant scatter in these plots, there are reasonable trends exhibited and in some cases coefficients of determination are significant.

Figures 10 and 11 present SPT data obtained on different dates at the North Base and Goldsby sites, respectively, and representing lean clay layers with different plasticity and sand content as indicated in Table 1. The data are limited but do show some fairly substantial trends with moisture content and estimated matric suction, most notably for the North Base site. In Figures 10 and 11, the field SPT  $N$  values are presented along with  $N$  values corrected to standard energy and overburden pressure denoted as  $(N_1)_{60}$ . For calculating  $(N_1)_{60}$ , a hammer efficiency of 80% was assumed for the automatic hammer, borehole correction factor was 1.0, sampler correction factor was 1.0, rod length factor was 0.95, and the correction for overburden pressure ( $C_N$ ) was that of Liao & Whitman (1986), where  $C_N = (1/\sigma_v)^{0.5}$ . By correcting for overburden pressure the influence of net normal stress is to some extent accounted for, and use of  $(N_1)_{60}$  makes the use of the correlations more universal.

In Figures 12 and 13, CPT  $q_c$  data are presented with respect to moisture content and estimated suction. Plots are shown with  $q_c$  and  $q_c$  normalized by vertical total stress. Expressions for  $q_c$  and normalized  $q_c$  are presented as a function of water content and matric suction. Significant trends are evident and can be exploited for estimating changes in  $q_c$  due to wetting. Additional data from the literature and a method for interpreting CPT  $q_c$  data from unsaturated soils are presented in the paper by Miller et al. (2018).

For the purpose of estimating bearing capacity and settlement of foundations based on properties derived from in situ tests in unsaturated soils, it would seem most logical to predict the test parameters at moisture contents corresponding to the wettest states, near saturation. Then these parameters could be used to predict the soil properties, bearing capacity and settlement using the equations presented previously (e.g. Equations 1-5). The correlation equations for clay soil properties, such as those for undrained strength, are likely most applicable to clayey soils in the saturated state where

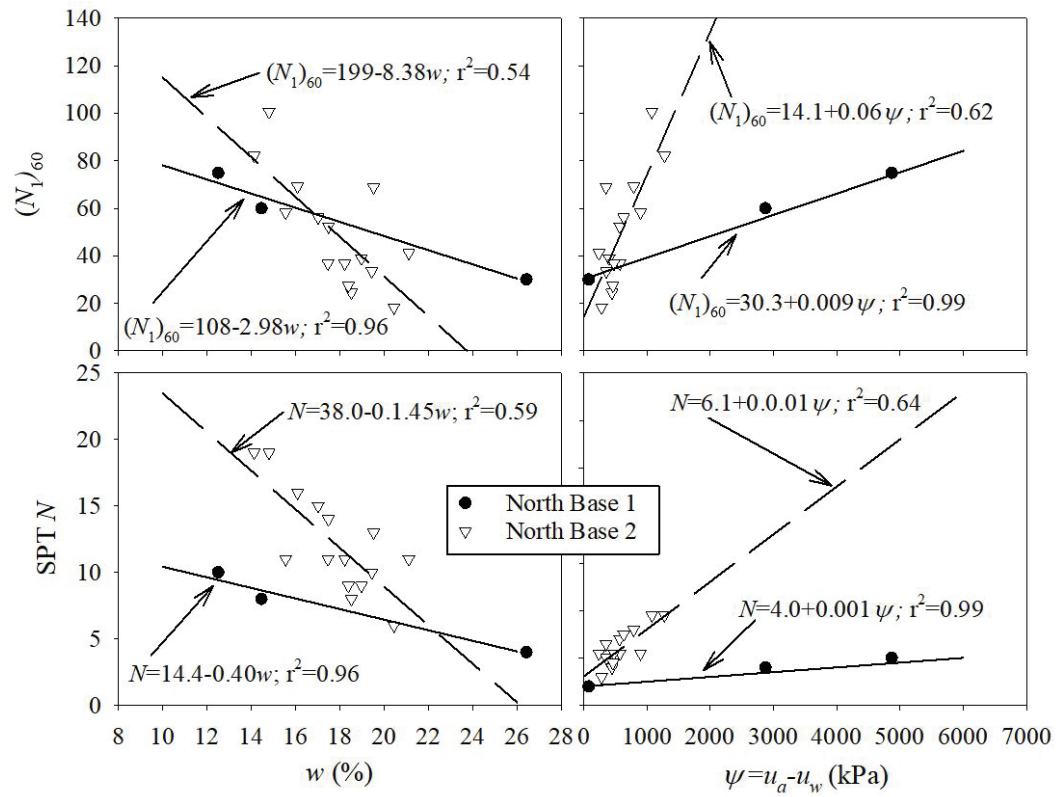


Figure 10. SPT  $N$  and  $(N_1)_{60}$  versus water content and matric suction for North Base site.

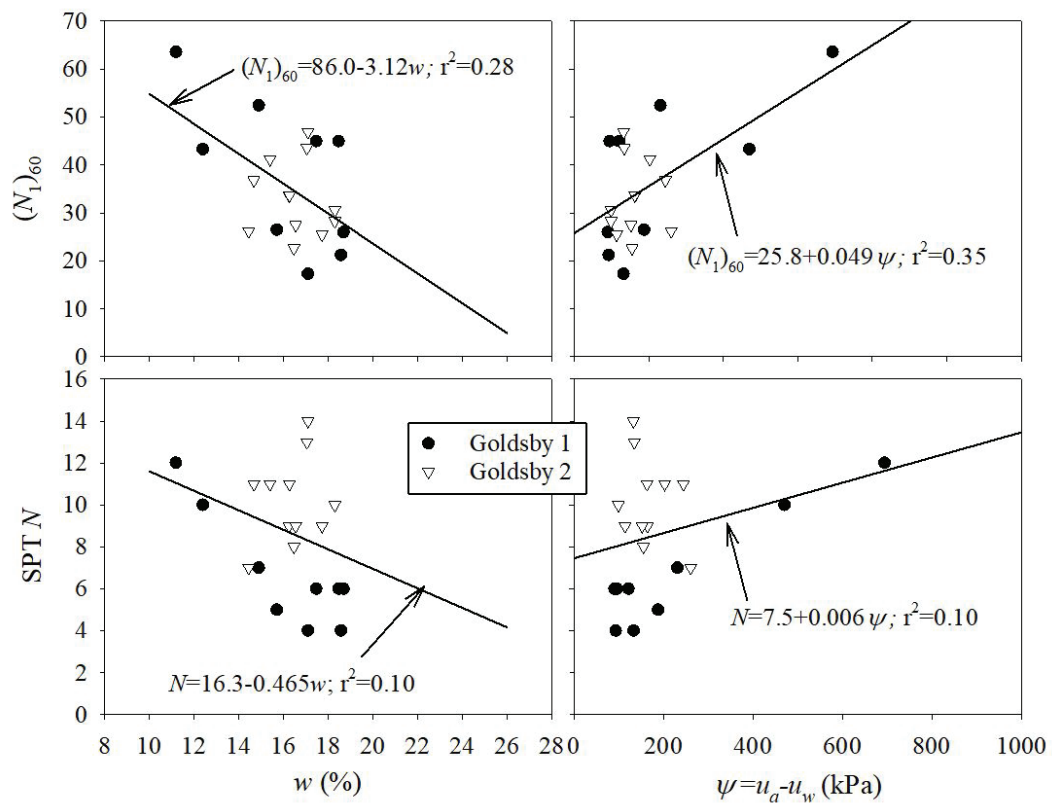
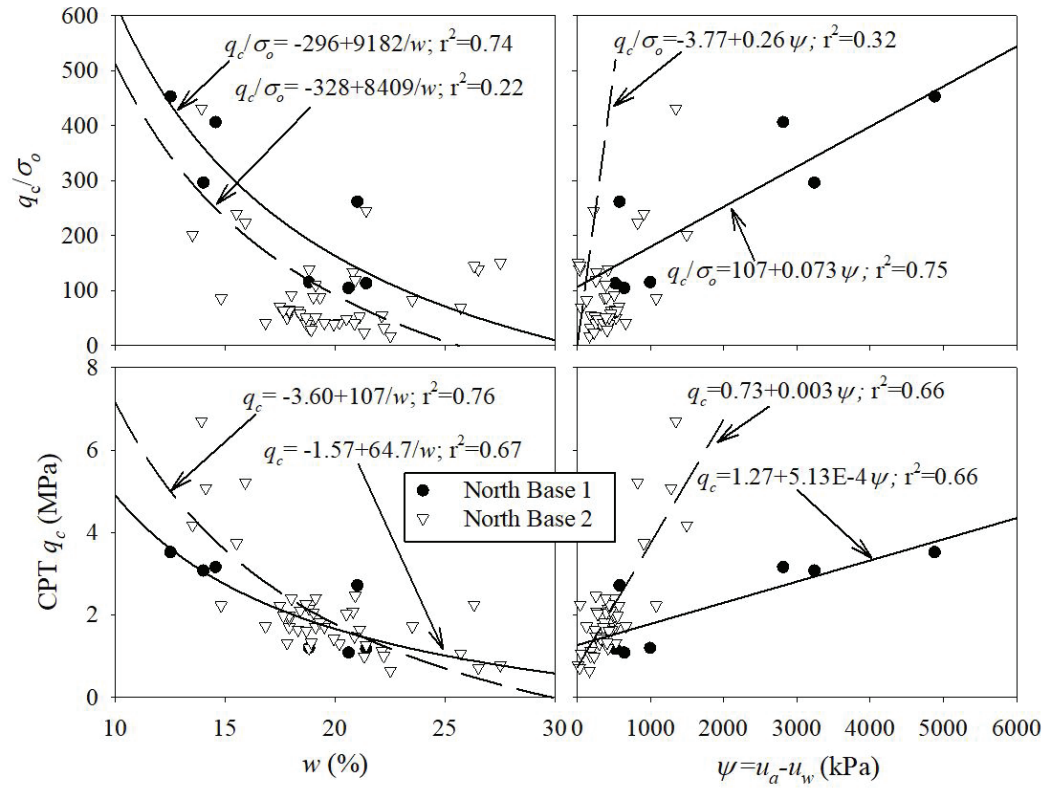
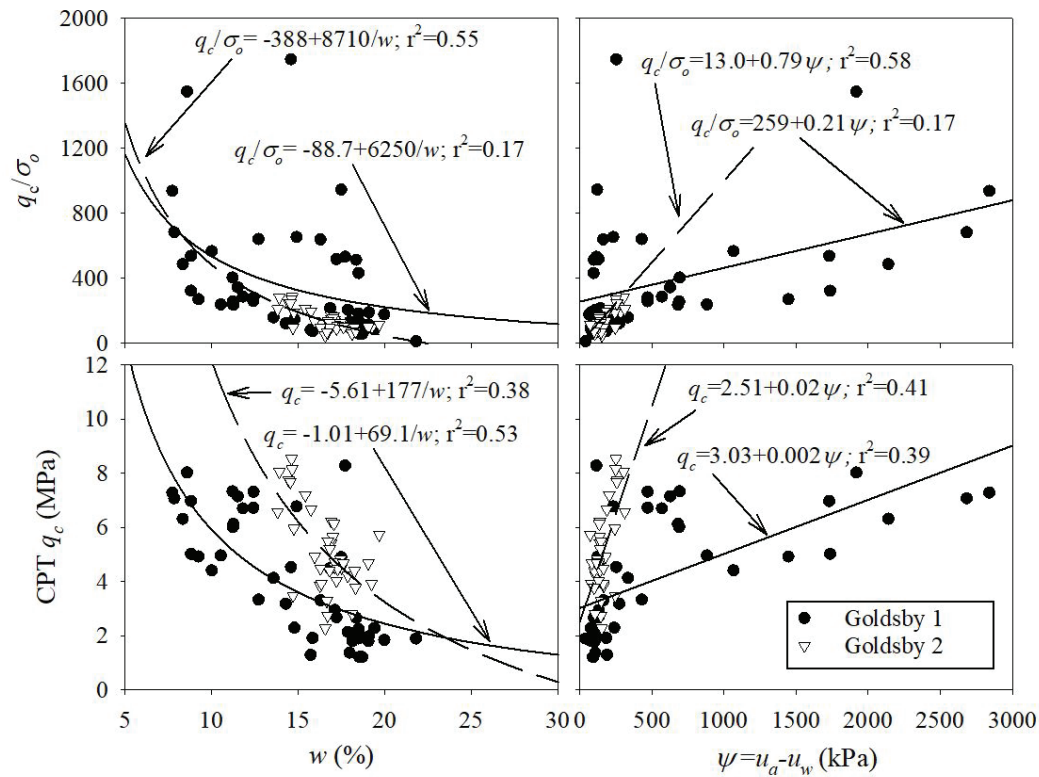


Figure 11. SPT  $N$  and  $(N_1)_{60}$  versus water content and matric suction for Goldsby site.



**Figure 12.** CPT  $q_c$  and  $q_c/\sigma_o$  versus water content and matric suction for North Base site.



**Figure 13.** CPT  $q_c$  and  $q_c/\sigma_o$  versus water content and matric suction for Goldsby site.

undrained conditions may prevail during testing. For unsaturated states, the use of such correlations is questionable because of the likelihood of partial drainage during the tests. This is a topic in need of a great deal of additional research.

## 5. Conclusions

In situ tests were conducted at two clay test sites over a period of two years, encompassing dry and wet soil conditions. Companion moisture contents were obtained throughout the depth of testing on test dates and matric suction was estimated based on soil water characteristic curves. SPT  $N$  values and CPT  $q_c$  values corresponding to different moisture conditions were used to estimate undrained shear strength using empirical equations and bearing capacity of a footing was estimated using a total stress analysis. Pressuremeter limit pressures and moduli were determined from tests under different moisture conditions and also used to predict bearing capacity and settlement of a footing. The following conclusions are based on this work.

- 1) Substantial reductions in SPT  $N$  values and CPT  $q_c$  values occurred due to increases in moisture content. Values of SPT  $N$  and corrected  $(N_1)_{60}$  plotted against moisture content and matric suction exhibit trends that can be exploited for predicting changes in these parameters. Similarly, values of  $q_c$  and normalized  $q_c$  plotted against moisture content and matric suction exhibited useful trends;
- 2) Undrained shear strengths calculated using empirical correlations for  $q_c$  and  $N$  values obtained on dry and wet days were substantially different. Corresponding allowable bearing capacities for wet days were substantially lower than for dry days;
- 3) Pressuremeter limit pressure was significantly affected by decreasing moisture contents. Significant trends were found between normalized limit pressure and moisture content and suction for the clayey soils tested. Pressuremeter moduli also exhibited decreasing trends with increasing moisture, but exhibited more scatter and appeared less sensitive to moisture changes compared to limit pressures. Predicted allowable bearing capacity based on the pressuremeter limit pressure for wet conditions was significantly lower compared to dry conditions. Predicted settlements were less concerning and more sensitive to the decrease in applied allowable bearing pressure than the change in modulus due to increased moisture content.

## Acknowledgements

The authors are grateful to the Oklahoma Department of Transportation (ODOT) and Oklahoma Transportation Center for their financial support of field research Grant

No. OTCREOS11.1-45. Additional thanks to ODOT for conducting, along with the second author, the cone penetration tests and test borings with standard penetration tests on field testing days.

## Declaration of interest

There were no competing interests or conflicts of interest associated with the conduct of this research or the development of this paper.

## Authors' contributions

Gerald A. Miller: conceptualization (equal), funding acquisition, formal analysis (equal), supervision (lead), writing-original draft. Rodney W. Collins: conceptualization (equal), formal analysis (equal), investigation, data curation, writing-review and editing (equal). Kanthasamy K. Muraleetharan: supervision (supporting), writing-review and editing (equal). Tareq Z. Abuawad: writing-review and editing (equal).

## List of symbols

$q_u$	ultimate bearing pressure of a square footing
$c$	cohesion term in ultimate bearing pressure equation
$N_c, N_q, N_\gamma$	bearing capacity factors dependent on the friction angle, $\phi$
$\phi$	friction angle of soil
$\gamma_1$ and $\gamma_2$	the soil unit weight above and below the bearing level, respectively
$D_f$	depth to bearing level
$B$	footing width
$c_u$	undrained shear strength
$\phi_t$	total stress friction angle
$\phi'$	effective stress friction angle
$N$	field value of penetration resistance from the Standard Penetration Test (SPT)
$q_c$	tip resistance from the Cone Penetration Test (CPT)
$f_s$	skin friction from the CPT
$\sigma_o$	in situ vertical total stress
$N_k$	empirical parameter for estimating $c_u$ from the Cone Penetration Test
$k$	a bearing capacity factor,
$p_{Le}^*$	geometric mean of net limit pressure from the Pressuremeter Test (PMT)
$p_L$	limit pressure from the PMT
$\gamma$	total unit weight above the bearing level
$S$	settlement predicted using elastic modulus obtained from the PMT
$E_p$	elastic modulus obtained from PMT results
$E_d$	PMT modulus within a zone of about $8B$ thick below the footing
$E_c$	PMT modulus within a zone of about $B/2$ thick below the footing



$q_{net}$	net bearing pressure below a footing
$B_o$	reference footing width equal to 60 cm
$\alpha$	rheological factor
$\lambda_d$	shape factor for the deviatoric term
$\lambda_c$	shape factor for the spherical term
$C$	constant for predicting settlement of a square footing from PMT results
LL	liquid limit
PI	plasticity index
%F	percent of fines by weight
%S	percent of sand by weight
$w$	soil gravimetric water content
$\psi$	$u_a - u_w$ = soil matric suction
$FS$	factor of safety for bearing capacity
$r^2$	coefficient of determination
$(N_1)_{60}$	SPT N corrected to standard energy and effective overburden pressure
$C_N$	correction factor accounting for overburden pressure

## References

- Akbari Garakani, A., Sadeghi, H., Saheb, S., & Lamei, A. (2020). Bearing capacity of shallow foundations on unsaturated soils: analytical approach with 3D numerical simulations and experimental validations. *International Journal of Geomechanics*, 20(3), 04019181. [http://dx.doi.org/10.1061/\(ASCE\)GM.1943-5622.0001589](http://dx.doi.org/10.1061/(ASCE)GM.1943-5622.0001589).
- Briaud, J.L. (1992). *The pressuremeter*. Rotterdam: Balkema.
- Collins, R.W. (2016). *In situ testing and its application to foundation analysis for fine-grained unsaturated soils* [PhD. Thesis]. University of Oklahoma. Retrieved in April 7, 2021, from <https://hdl.handle.net/11244/47092>
- Drnevich, V.P., Mayne, P.W., & Kemper, J.B. (1988). Profiling OCR in stiff clays by CPT and SPT. *Geotechnical Testing Journal*, 11(2), 139-147. <http://dx.doi.org/10.1520/GTJ10960J>.
- Fredlund, D.G., Rahardjo, H., & Fredlund, M.D. (2012). *Unsaturated soil mechanics in engineering practice*. Hoboken: John Wiley & Sons. <http://dx.doi.org/10.1002/9781118280492>.
- Hara, A., Ohta, T., Niwa, M., Tanaka, S., & Banno, T. (1974). Shear modulus and shear strength of cohesive soils. *Soil and Foundation*, 14(3), 1-12. [http://dx.doi.org/10.3208/sandf1972.14.3\\_1](http://dx.doi.org/10.3208/sandf1972.14.3_1).
- Kulhawy, F.H., & Mayne, P.W. (1990). *Manual on estimating soil properties for foundation design* (No. EPRI-EL-6800). Ithaca: Cornell University. Retrieved in April 7, 2021, from [https://www.geoengineer.org/storage/publication/20489/publication\\_file/2745/EL-6800.pdf](https://www.geoengineer.org/storage/publication/20489/publication_file/2745/EL-6800.pdf)
- Le, T.M.H., Gallipoli, D., Sanchez, M., & Wheeler, S. (2013). Rainfall-induced differential settlements of foundations on heterogeneous unsaturated soils. *Geotechnique*, 63(15), 1346-1355. <http://dx.doi.org/10.1680/geot.12.P.181>.
- Liao, S.S., & Whitman, R.V. (1986). Overburden correction factors for SPT in sand. *Journal of Geotechnical Engineering*, 112(3), 373-377. [http://dx.doi.org/10.1061/\(ASCE\)0733-9410\(1986\)112:3\(373\)](http://dx.doi.org/10.1061/(ASCE)0733-9410(1986)112:3(373)).
- Ménard, L., & Rousseau, J. (1962). L'évaluation des tassements, tendances nouvelles. *Sols Soils*, 1(1), 13-29 (in French).
- Mesonet. (2021). *Oklahoma Mesonet*. Retrieved in April 7, 2021, from <http://mesonet.org/>
- Miller, G.A., Tan, N.K., Collins, R.W., & Muraleetharan, K.K. (2018). Cone penetration testing in unsaturated soils. *Transportation Geotechnics*, 17, 85-99. <http://dx.doi.org/10.1016/j.trgeo.2018.09.008>.
- Mohamed, F.M., & Vanapalli, S.K. (2015). Bearing capacity of shallow foundations in saturated and unsaturated sands from SPT-CPT correlations. *International Journal of Geotechnical Engineering*, 9(1), 2-12. <http://dx.doi.org/10.1179/1939787914Y.0000000082>.
- Oh, W.T., & Vanapalli, S.K. (2013a). Interpretation of the bearing capacity of unsaturated fine-grained soil using the modified effective and the modified total stress approaches. *International Journal of Geomechanics*, 13(6), 769-778. [http://dx.doi.org/10.1061/\(ASCE\)GM.1943-5622.0000263](http://dx.doi.org/10.1061/(ASCE)GM.1943-5622.0000263).
- Oh, W.T., & Vanapalli, S.K. (2013b). Scale effect of plate load tests in unsaturated soils. *International Journal of GEOMATE*, 4(2), 585-594. <http://dx.doi.org/10.21660/2013.8.2h>.
- Oh, W.T., & Vanapalli, S.K. (2018). Modeling the stress versus settlement behavior of shallow foundations in unsaturated cohesive soils extending the modified total stress approach. *Soil and Foundation*, 58(2), 382-397. <http://dx.doi.org/10.1016/j.sandf.2018.02.008>.
- Tang, Y., Taiebat, H.A., & Russell, A.R. (2017a). Bearing capacity of shallow foundations in unsaturated soil considering hydraulic hysteresis and three drainage conditions. *International Journal of Geomechanics*, 17(6), 04016142. [http://dx.doi.org/10.1061/\(ASCE\)GM.1943-5622.0000845](http://dx.doi.org/10.1061/(ASCE)GM.1943-5622.0000845).
- Tang, Y., Taiebat, H.A., & Senetakis, K. (2017b). Effective stress based bearing capacity equations for shallow foundations on unsaturated soils. *AGH Journal of Mining and Geoengineering*, 12(2), 59-64. [http://dx.doi.org/10.6310/jog.2017.12\(2\).2](http://dx.doi.org/10.6310/jog.2017.12(2).2).
- Terzaghi, K. (1943). *Theoretical soil mechanics*. New York: John Wiley & Sons. <http://dx.doi.org/10.1002/9780470172766>.
- Vanapalli, S.K., & Mohamed, F.M. (2013). Bearing capacity and settlement of footings in unsaturated sands. *International Journal of GEOMATE*, 5(1), 595-604. <http://dx.doi.org/10.21660/2013.9.3k>.
- Yang, H., & Russell, A.R. (2015). Cone penetration tests in unsaturated silty sands. *Canadian Geotechnical Journal*, 53(3), 431-444. <http://dx.doi.org/10.1139/cgj-2015-0142>.
- Zapata, C.E., Houston, W.N., Houston, S.L., & Walsh, K.D. (2000). Soil-water characteristic curve variability. In C. D. Shackelford, S. L. Houston & N.-Y. Chang (Eds.), *Advances in unsaturated geotechnics* (pp. 84-124). Reston: ASCE. [http://dx.doi.org/10.1061/40510\(287\)7](http://dx.doi.org/10.1061/40510(287)7).



## Hydromechanical behavior of unsaturated soils: Interpretation of compression curves in terms of effective stress

John S. McCartney<sup>1#</sup> , Fatemah Behbehani<sup>1</sup> 

Article

### Keywords

Effective stress  
Suction stress  
Yielding  
Suction hardening  
Compacted soils

### Abstract

This state-of-the-art paper on the hydromechanical behavior of unsaturated soils focuses on the interpretation of the compression curves of unsaturated soils in terms of effective stress, with the goal of understanding the relative impacts of suction on the effective stress, net yield stress, effective yield stress and slope of the virgin compression line (VCL) during a monotonic increase in net stress. A database of compression curves was compiled for both high and low plasticity fine-grained soils under a wide range of suctions, isotropic or oedometric stress states, drainage conditions (constant suction or constant water content) and preparation techniques (impact compaction, static compaction, consolidation from slurry). Most of the compression curves plotted in terms of effective stress revealed a consistent hardening response with increasing suction and a slight suction dependency on the slope VCL. Interpretation of the compression curves in terms of effective stress led to load-collapse curves with a similar shape for a wide range of soils. Most soils evaluated had a greater rate of increase in effective yield stress with suction than the rate of increase in suction stress with suction, implying that these compacted soils may be susceptible to collapse upon wetting. Inconsistent trends were observed in some studies, which were attributed partially to natural variability but also experimental issues and limitations on the range of conditions investigated. Accordingly, recommendations are provided for future studies on the compression curves of unsaturated soils to ensure that results can be clearly interpreted in terms of effective stress.

### 1. Introduction

Several studies have demonstrated that the effective stress principle can be used to interpret the shear strength of unsaturated soils so that a unified shear strength model can be applied to both saturated, unsaturated, and dry soils (Khalili et al., 2004; Lu & Likos, 2006; Lu et al., 2010). While early studies like Escario & Saez (1986) and Gan et al. (1988) observed that application of suctions greater than the air entry suction led to nonlinear increases in apparent cohesion, the shear strength values of these unsaturated soils plotted in terms of effective stress fell onto the same effective stress failure envelope as saturated and dry soils with negligible drained cohesion values. These observations were also confirmed for soils under high suction magnitudes by Alsherif & McCartney (2015), who performed shear strength tests on unsaturated soils at low degrees of saturation using the vapor flow technique and found that the effective stress principle was valid over the full range of suction. More recently, studies have demonstrated that the effective stress principle can be used to interpret the small-strain shear

modulus of unsaturated soils (Khosravi & McCartney, 2012; Dong et al., 2016).

Despite the success in interpreting shear strength and shear modulus data in terms of effective stress, fewer studies have interpreted the volume change of unsaturated soils in terms of effective stress. This is perhaps due to the influence of early studies on the collapse of unsaturated soils during wetting. For example, Jennings & Burland (1962) performed collapse upon wetting tests on compacted soils and observed a decrease in volume during a reduction in effective stress (associated with a reduction in suction and increase in degree of saturation due to wetting). One of their conclusions was that the effective stress principle is not valid in unsaturated soils as soils should expand during a reduction in effective stress. Accordingly, many experimental studies on the compression response of unsaturated soils followed the double oedometer approach of Jennings & Knight (1957a), where the compression curves of saturated and as-compacted specimens were interpreted in terms of net

<sup>#</sup>Corresponding author. E-mail address: mccartney@ucsd.edu

<sup>1</sup>University of California, Department of Structural Engineering, San Diego, CA, USA.

Submitted on April 10, 2021; Final Acceptance on May 22, 2021; Discussion open until November 30, 2021.

<https://doi.org/10.28927/SR.2021.065721>



This is an Open Access article distributed under the terms of the Creative Commons Attribution License, which permits unrestricted use, distribution, and reproduction in any medium, provided the original work is properly cited.

stress (the difference in total stress and pore air pressure) to predict the amount of collapse or swelling during wetting. Further, early theories for the volume change of unsaturated soils like the Matyas & Radhakrishna (1968) considered the volume changes due to suction (wetting or drying) and net stress to be independent.

More recent studies have refuted the concerns on the application of the effective stress principle to the interpretation of volume change data. Khalili et al. (2004) explained that collapse occurs due a reduction in the effective yield stress with wetting, resulting in an unstable stress state causing a reduction in volume even when the effective stress decreases. Khalili et al. (2004) noted that elasto-plastic constitutive models that use the effective stress principle can capture the collapse phenomena observed by Jennings & Burland (1962). Khalili et al. (2004) evaluated data from the literature to show that elastic strains are directly related to the effective stress state in unsaturated soils to prove the validity of the effective stress principle in capturing volume change behavior and noted that soils susceptible to collapse would have a greater increase in effective yield stress with suction than the increase in effective stress with suction.

The goal of this state-of-the-art study is to reinterpret data from the literature to better understand the role of effective stress in the volume change of unsaturated soils, with a specific focus on the volume change encountered during a monotonic increase in net stress. As many studies have presented the compression curves of unsaturated soils in terms of net stress, a reinterpretation of the data may help to isolate the effects of suction on the shape the compression curve, most importantly the yield stress and the slope of the virgin compression line (VCL). Accordingly, the main objective of this study is to understand relationships between the suction, yield stress, and effective stress from a database of compression curves of unsaturated high and low plasticity fine-grained soils under a wide range of suctions, isotropic or oedometric stress states, drainage conditions (constant suction or constant water content) and preparation techniques (impact compaction, static compaction, consolidation from slurry). The intention of this study is not to use the information from the database to calibrate different constitutive models, but instead to compare the relative rates of increase in yield stress and effective stress with increasing suction. It is important to note that although interpretation of shear strength data in terms of effective stress leads to a clear unification of trends among unsaturated, saturated, and dry soils, the same unification is not expected for the volume change of unsaturated soils as the suction and degree of saturation influence the effective stress as well as the yield stress and the slope of the VCL. As the reinterpretation of the compression curves in terms of effective stress requires more information than the interpretation in terms of net stress, a secondary goal of this study is to provide lessons learned on what information should be collected as part of future testing programs.

## 2. Background

The effective stress is a key variable that permits application of continuum mechanics principles to fluid-filled, deformable porous media (Bishop & Blight, 1963; Khalili et al., 2004). The effective stress definition in unsaturated soils was first proposed by Bishop (1959):

$$\sigma'_{ij} = (\sigma_{ij} - u_a \delta_{ij}) + \chi(u_a - u_w) \delta_{ij} \quad (1)$$

where  $\sigma'_{ij}$  is the effective stress tensor,  $\sigma_{ij}$  is the total stress tensor,  $u_a$  and  $u_w$  are the pore air and water pressures, respectively,  $\chi$  is the effective stress parameter, and  $\delta_{ij}$  is the Kronecker delta. The difference between the total stress tensor and air pressure is referred to as the net stress tensor  $\sigma_{ij}^{net}$ , while the difference in pore air and water pressures is the matric suction  $\psi$ .

Many definitions for the effective stress parameter have been proposed, including  $\chi$  equal to the degree of saturation (Bishop, 1959, Nuth & Laloui, 2008),  $\chi$  equal to the effective saturation (Bolzon & Schrefler, 1995; Lu et al., 2010), or  $\chi$  as a function of the ratio of the air entry suction to suction (Khalili & Khabbaz, 1998). Khalili & Khabbaz (1998) noted that the relationship between the effective stress parameter and degree of saturation may not be unique due to hydraulic hysteresis, which was demonstrated by Khalili & Zargarbashi (2010) in experiments involving multistage shearing tests after drying and wetting. On the other hand, Lu et al. (2010) noted the practical advantage of using the effective saturation as the effective stress parameter as it permitted incorporation of a soil-water retention curve (SWRC) model such as that of van Genuchten (1980) directly into the effective stress definition. Further, Khosravi & McCartney (2012) demonstrated that using a hysteretic SWRC model in the effective stress equation following the approach of Lu et al. (2010) was useful in interpreting variations in shear modulus during wetting and drying. Lu et al. (2010) defined the concept of suction stress to incorporate the impacts of all particle-interaction mechanisms in the definition of the effective stress, as follows:

$$\sigma'_{ij} = (\sigma_{ij} - u_a \delta_{ij}) + \sigma_s \delta_{ij} \quad (2)$$

where  $\sigma_s$  is the suction stress. Mathematically the suction stress is equal to the product of the effective stress parameter and suction as noted in Equation 1, but physically it is meant to be a single variable that encompasses all interactions between particles due to capillarity, cementation, adsorptive forces, or van der Waals forces. The van Genuchten (1980) SWRC model is given as follows:

$$S_e = \left( \frac{S - S_{res}}{1 - S_{res}} \right) = \left[ \frac{1}{1 + (\alpha_{vG} \psi)^{N_{vG}}} \right]^{\frac{1}{1 - N_{vG}}} \quad (3)$$

where  $S_e$  is the effective saturation,  $S$  is the degree of saturation,  $S_{res}$  is the residual degree of saturation and  $\alpha_{vG}$  and  $N_{vG}$  are fitting parameters.

Early studies on the volume change of unsaturated soils focused on characterizing collapse during wetting at high net stresses (e.g., Jennings & Knight, 1957b; Jennings & Burland, 1962; Matyas & Radhakrishna, 1968) or swelling during wetting at low net stresses (e.g., Blight, 1965; Brackley, 1973), and only few characterized the changes in yield stress of soils with increasing suction (e.g., Dudley, 1970). In the extension of the modified Cam-clay model to unsaturated soils that led to the development of the Barcelona Basic Model (BBM), Alonso et al. (1990) identified the need to include a yield surface that governs the increase in net yield stress with increasing suction which was referred to as the Load-Collapse (LC) curve. The development of the BBM led to several studies focused on the characterization of the yielding of unsaturated soils during compression, many of which are revisited in this study. Following the pioneering concepts in the BBM, several hydro-mechanical, elasto-plastic frameworks were developed to simulate the impacts of changes in net stress, effective stress and matric suction on the volume change of unsaturated soils. The ability of these frameworks to predict the hydro-mechanical behavior of unsaturated soil is influenced by the stress state definition. While the BBM and other elasto-plastic models used independent state variables (Alonso et al., 1990; Wheeler & Sivakumar, 1995; Bolzon et al. 1996; Cui et al., 1995; Sheng et al., 2004), other studies used the generalized effective stress concept (Loret & Khalili, 2002; Gallipoli et al., 2003; Wheeler et al., 2003; Tamagnini, 2004; Romero & Jommi, 2008; Khalili et al., 2008; Zhou et al., 2012a, b; Della Vecchia et al., 2013). An advantage of using the generalized effective stress concept is that a smaller number of material properties may be needed to simulate the complex volume change behavior of unsaturated soils, and the yield surface is always concave (Khalili et al., 2008). Further, it may be easier to consider the effects of hydraulic hysteresis in an elasto-plastic framework by incorporating the soil-water retention curve (SWRC) (Wheeler et al., 2003; Gallipoli et al., 2003; Tamagnini, 2004) or the air entry suction (Khalili et al., 2008) in the definition of the generalized effective stress concept. Sheng et al. (2008) was able to incorporate the effects of hysteresis in the SWRC into an elasto-plastic model that used independent stress state variables.

Regardless, a common feature of these elasto-plastic models is that they incorporate an LC curve acting as the yield limit transition from an elastic to an elasto-plastic volumetric soil response during compression of unsaturated soils. In general, most LC curves indicate an increase in either the net yield stress or effective yield stress with increasing suction, an effect commonly referred to as “suction hardening”. Some studies like Uchaipichat & Khalili (2009) and Uchaipichat & Khalili (2009) observed suction hardening in the relationship between the effective yield stress and suction but a decrease (softening) in net yield stress with suction, although this observation may depend on the soils and compaction conditions being tested. Many analytical expressions have been proposed to

characterize the LC curve for unsaturated soils have been proposed in the literature, and several were summarized by Mun et al. (2017). LC curves have been defined in the net stress vs. suction space (Alonso et al., 1990), effective stress vs. suction space (Salager et al., 2008; Tourchi & Hamidi, 2015), effective stress vs. degree of saturation space (Gallipoli et al., 2003; Romero & Jommi, 2008), effective stress vs. modified suction space (i.e., suction multiplied by the porosity) (Wheeler et al., 2003), and effective stress vs. effective saturation space (Zhou et al., 2012b). In several constitutive models, the shape of the LC curves is linked with the shape of the VCL for the unsaturated soil, which has been assumed to be a function of suction (Alonso et al., 1990) or effective saturation (Zhou et al., 2012b). However, Wheeler et al. (2002) noted issues with fitting the VCL of the BBM to data, and Mun & McCartney (2017) noted that the links between the LC curve and VCL may not be valid when predicting pressurized saturation of soils at high stresses.

### 3. General compression response of unsaturated soils

Before investigating the experimental compression curves from the literature, it is important to review the general compression curves of an unsaturated soil under different suctions in terms of effective stress. The schematic shown in Figure 1a shows hypothetical compression curves for different compacted soil specimens during constant suction compression tests with drained air and water. Several features can be noted from this figure that are expected when interpreting compression curves in terms of effective stress. First, application of suction to the soil will increase the effective stress, which will lead to an elastic contraction. This will also lead to a shift in the starting point of the compression curves. Loading the soil to higher stresses will follow an elastic relationship until reaching the yield stress, which depends on the suction and the shape of the LC curve. After this point, greater deformations will be noted as the soil deforms along a VCL that may depend on the suction or degree of saturation (Alonso et al., 1990; Zhou et al., 2012b). Actual compression curves are expected to be more nonlinear than the idealized curves in Figure 1a so the slope of the VCL will change with increasing normal stress. At high stresses, the compression curves for unsaturated specimens will converge with that of a saturated specimen after all pore air has been expelled or dissolved into the pore water. Mun & McCartney (2017) noted that greater pressures are required to reach this point of pressurized saturation for specimens with lower initial degrees of saturation. During compression, the degree of saturation will increase as the volume of voids decreases, as shown in Figure 1b. During the increase in degree of saturation, the suction stress will change. Further, the shape of the SWRC of the soil will change, leading to an increase in the air entry suction of



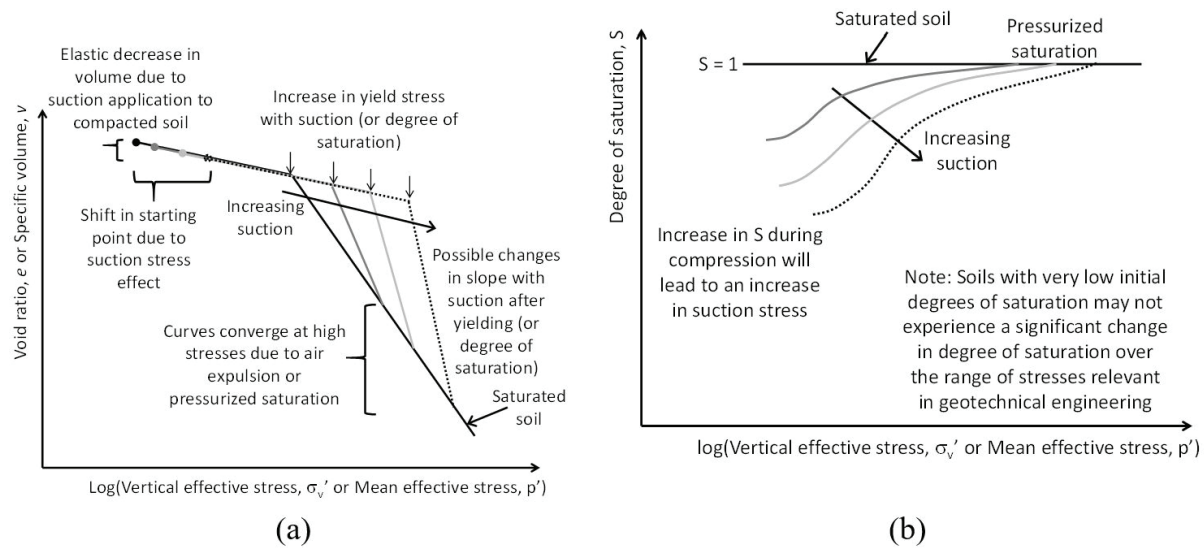


**Figure 1.** Hypothetical hydro-mechanical behavior of unsaturated soils during drained compression with constant suction: (a) Compression curves in terms of effective stress; (b) Increases in degree of saturation during drained compression.

the soil. This may lead to difficulties in using the effective stress definition of Khalili & Khabbaz (1998) to consider compression of unsaturated soils to high stresses. At the same time, it should be noted that during compression of relatively dry soils under high suctions, negligible changes in degree of saturation can be expected over the range of stresses representative of geotechnical problems.

Some additional observations can be drawn from the typical shapes of the compression curves of unsaturated soils interpreted in terms of net stress. Jennings & Knight (1957b) observed that the net stress compression curve for collapsible soils will typically plot above the curve for a saturated soil, while the net stress compression curve for an expansive soil will plot below the curve for a saturated soil. These observations may help interpret the range of compression curve shapes in the database.

Despite the observation of suction hardening observed by many studies, the fundamental cause behind the increase in yield stress with suction is not well understood, as it is independent from the interparticle connections that affect the effective stress state. Suction hardening could be due to a stiffening of the soil structure associated with the formation of the unsaturated soil and the distribution in water throughout the specimen associated with different degrees of saturation. Relatively few studies have studied the effects of soil structure, which could be achieved by comparing the LC curves for soils prepared using compaction with those consolidated from a slurry. While several studies have investigated the volume change behavior of soils consolidated from slurry (Fleureau et al., 1993; Dong et al., 2020), only the volume change due to changes in suction was monitored in these studies, and the net stress was not increased monotonically to evaluate the effects of suction on the yield stress. In addition, few studies have isolated the

impact of soil structure associated with compaction from the effects of suction on the yield stress. For example, Mun & McCartney (2017) performed drained compression tests on soils compacted to the same initial density but different compaction water contents. The observed yield stresses could be affected by both the soil structure from compaction at different water contents (dry and wet of optimum) or by the applied suction. It was not possible to investigate these issues in this study with the data available in the literature, but they are interesting topics for future research.

#### 4. Database and methodology

A database of compression curves from the literature for different fine-grained soils was collected to evaluate the impacts of suction on the yield stress and effective stress (or suction stress). Several studies have investigated the volume change behavior of unsaturated soils but focused on the impact of suction application on the shrinkage response of soils (Fleureau et al., 1993; Dong et al., 2020) or the transient process of wetting leading to collapse (Kato & Kawai, 2000; Pereira & Fredlund, 2000; Sun et al., 2000, 2007), so these studies were not included in the database. A total of 25 studies were identified who presented the results from compression curves on unsaturated soils. The details of these studies are summarized in Table 1, including the soil type according to the unified soil classification scheme (USCS), the suction control method, the suction range, the drainage conditions, stress state, the method to estimate the degree of saturation if available, and the stress state used to report the compression curves.

The approach followed in this study was to reinterpret the compression curves in terms of effective stress, then to investigate linkages between the suction and parameters

**Table 1.** Summary of compression studies on unsaturated soils in the literature.

Study	Soil Type	Preparation Technique	Suction Control/ Drainage	Suction Range (kPa)	Drainage	Compression	Degree of Saturation Estimate	Reported Stress State
Wheeler & Sivakumar (1995)	Kaolinite (CL)	Static compaction to 400 kPa	Axis translation	100-300	Drained	Oedometer	Outflow	Net
Sharma (1998)	Bentonite-Kaolin (CH)	Static compaction to 400 kPa	Axis translation	100-300	Drained	Oedometer	Outflow	Net
Maâtouk et al. (1995)	Silt (ML)	Tamped	Axis translation	0-600	Drained	Isotropic	None	Net
Rampino et al. (1999)	Decomposed granite (ML)	Compacted	Axis translation	0-400	Drained	Isotropic/Oedometer	Outflow	Net
Al-Mukhtar et al. (1999)	Na-Laponite (CH)	Compacted	Vapor equilibrium	0-298000	Drained	Oedometer	CWC assumed	Net
Cunningham et al. (2003)	Silty Clay (CL)	Static compaction to 200 kPa	Tensiometer/Vapor equilibrium	0-1000	Drained	Isotropic	CWC assumed	Net
Lloret et al. (2003)	Bentonite (CH)	Static compaction to 20 MPa	Vapor equilibrium	0-500000	Drained	Oedometer	CWC assumed	Net
Cuisinier & Masrouri (2005)	Silt-Bentonite (ML)	Compacted	Vapor equilibrium/Osmotic	0-39700	Drained	Oedometer	CWC assumed	Net
Villar (2005)	MX80 Bentonite (CH)	Static compaction	Vapor equilibrium	0-1400	Drained	Oedometer	CWC assumed	Net
Geiser et al. (2006)	Sion Silt (ML)	Slurry consolidated	Axis translation	0-280	Drained	Isotropic	Outflow	Net/ Effective
Jotisankasa et al. (2007)	Silt-Clay (CL)	Compacted	Tensiometer/Filter Paper	0-31800	CWC	Oedometer	CWC	Net
Thu et al. (2007)	Coarse Kaolinite (ML)	Compacted	Axis translation	0-300	Drained	Isotropic	SWRC	Net
Casini (2008)	Jossigny Silt (ML)	Compacted	Axis translation	0-200	Drained	Oedometer	SWRC	Net/ Effective
Salager et al. (2008)	Sion Silt (ML)	Slurry consolidated	Axis translation	0-300	Drained	Isotropic/Oedometer	SWRC	Net/ Effective
Uchaipichat & Khalili (2009)	Bourke Silt (ML)	Compacted	Axis translation	0-300	Drained	Isotropic	None	Net/ Effective
Sun et al. (2010)	Pearl Clay (CL)	Compacted	Axis translation	100-150	Drained	Isotropic	Outflow	Net
Tang & Cui (2010)	MX80 Bentonite (CH)	Static compaction to 40 MPa	Vapor equilibrium	0-110000	Drained	Isotropic	SWRC	Net
Uchaipichat (2010)	Kaolinite	Compacted	Axis translation	0-300	Drained	Isotropic	None	Effective
Ye et al. (2012)	GMZ01 Bentonite (CH)	Compacted	Vapor equilibrium	0-110000	Drained	Oedometer	None	Net
Coccia & McCartney (2016)	Bonny Silt (ML)	Compacted to $e=0.75$ to $0.82$	Axis translation	0-40	Drained	Isotropic	Outflow	Effective
Khosravi et al. (2016)	Bonny Silt (ML)	Compacted to $e=0.69$	Axis translation	0-55	Drained	Isotropic	Outflow	Net/ Effective
Mun & McCartney (2017)	Boulder Clay (CL)	Compacted to $e=0.51$	Axis translation at compacted	0-150	Drained	Isotropic	Outflow	Effective
Khosravi et al. (2018)	Bonny Silt (ML)	Compacted to $e=0.85$	Axis translation	0-100	Drained	Isotropic	Outflow	Net
Li et al. (2018)	Boughrara clay (CH)	Compacted	Vapor equilibrium	200-8000	Drained	Oedometer	Electrical Res.	Net
Haeri et al. (2019)	Loess (CL)	Compacted	Axis translation	0-400	Drained	Oedometer	SWRC	Net

representing the shapes of the compression curves. While some of these studies provided a comprehensive evaluation of the evolution in key variables during volume change (net stress, void ratio, suction, degree of saturation) along with measurement of a soil-water retention curve (SWRC), others provided less information and required careful interpretation. Most of the tests were performed in constant suction conditions (drained air and water), while one was performed in constant water content (CWC) conditions (drained air but undrained water). However, in some of the high suction tests, constant water content conditions could be assumed due to the small changes in water content during compression. The compression curves presented by Sivakumar (1993), which were also presented by Wheeler & Sivakumar (1995), Sharma (1998), Thu et al. (2007), Coccia & McCartney (2016), and Mun & McCartney (2017) were all obtained using constant rate of strain testing, while the other studies in Table 1 were obtained using incremental loading. The term yield stress is used to represent the mean apparent preconsolidation stress obtained from isotropic compression tests or the vertical apparent preconsolidation stress obtained from oedometer tests. In some studies, the variation in degree of saturation during compression was obtained and reported from outflow measurements or electrical resistivity sensors, but in other studies no information on the degree of saturation during compression was provided. In some of these cases, a constant degree of saturation was assumed based on the SWRC, while in other cases the degree of saturation was estimated from phase relationships using the initial gravimetric water content and the measured void ratio based on a constant water content assumption. Because the degree of saturation was estimated in some of the studies, the results presented in this study are only useful for assessment of general trends and should not be used to calibrate constitutive models. When defining the effective stress using Equation 1, the effective stress parameter was assumed to be the degree of saturation as this was the most consistently available piece of information from most of the studies considered in the database. An implication of this assumption is that the suction

stress in Equation 2 is equal to the product of the degree of saturation and suction. As most of the soils evaluated in this study have a small residual degree of saturation, the effective saturation and degree of saturation are similar. As the degree of saturation may evolve during compression, the suction stress at the point of yielding was used to define the trend with increasing suction. The air entry suction is provided for as many of the soils as possible which permits evaluation of the effective stress using the approach of Khalili & Khabbaz (1998), but this was not used in the analysis as the air entry suction may evolve during compression. If the actual yield stress was not identified in the relevant study, the yield stress was defined using Casagrande's method of finding the intersection between tangent lines fit to the initial and final parts of the compression curve.

## 5. Results

Selected compression curves from the database are presented in Figures 2 through 16 in terms of both net stress and effective stress, with results presented in the order of publication of the study. Wheeler & Sivakumar (1995) was one of the earliest studies to present the results of compression curves for compacted kaolinite clay with information on the degree of saturation evolution during compression. The compression curves shown in Figures 2a and 2b in terms of net stress and effective stress, respectively, reflect a clear rightward shift in the compression curves after reinterpretation using the effective stress principle. A clear evolution in the yield stress with increasing suction is observed, even though the specimens all had different initial void ratios and that yielding was observed shortly after the beginning of compression for the different specimens. Similar trends were observed for the results from compacted kaolinite-bentonite mixtures presented by Sharma (1998) in Figure 3. Although not shown, the results from Maâtouk et al. (1995) showed suction hardening in a compacted silt over a wider range of suction than evaluated in previous studies. The results from Rampino et al. (1999) for compacted decomposed granite

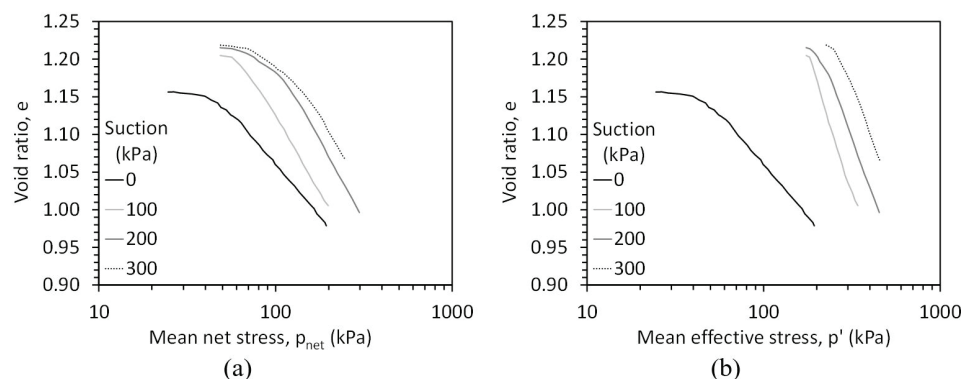


**Figure 2.** Compression curves from Sivakumar (1993) and Wheeler & Sivakumar (1995): (a) Reported curves in terms of net stress; (b) Reinterpreted curves in terms of effective stress.

in Figure 4 show how application of the effective stress differentiates the curves at elevated suctions. Comparison of the results in Figures 2 through 4 indicates that the effective stress VCLs for the unsaturated soils are approximately parallel for the range of effective stresses are applied. A comment from these figures is that if the volume changes during application of suction to the specimens had been tracked in these two studies, it may have been possible to define the initial elastic slope of the effective stress compression curves and better identify the yield stress.

The study by Lloret et al. (2003) was one of the first to investigate the compression curves of compacted high plasticity clay over a wide range of suction values. Although the study by Al-Mukhtar et al. (1999) also evaluated the compression response of high plasticity clays in the high suction range (greater than 1000 kPa), the range of net stresses applied were not sufficient to cause yielding of the soil. The results from Lloret et al. (2003) in Figures 5a and 5b show that the application of high suctions to the high plasticity clay led to a reduction in the initial void ratio, but that the shift of the curves led to VCLs that are clearly parallel.

Although yielding was not apparent in the highest suction tests, the data points are still approximately parallel to the lower suction tests. Cunningham et al. (2003) also applied a wide range of suctions to a compacted silty clay. Although the specimens evaluated had a range of initial void ratios, application of the effective stress principle showed interesting results in Figures 6a and 6b. All the compression curves for unsaturated soils in effective stress space were collocated with the compression curve for saturated soil, different from the hypothetical curves in Figure 1a. In this case, yielding seemed to occur as soon as the compression curves for the unsaturated soils approached the saturated compression curve. This interesting observation could have been due to the much higher initial void ratio of the saturated specimen, and to the limited range of net stresses used to compress the unsaturated soils. Cuisinier & Masrouri (2005) evaluated the compression curves of a high plasticity clay over a wide range of suctions as shown in Figures 7a and 7b. Similar to the curves of Lloret et al. (2003), the compression curves in effective stress space were approximately parallel to each other but were steeper than the curve for saturated soil, which

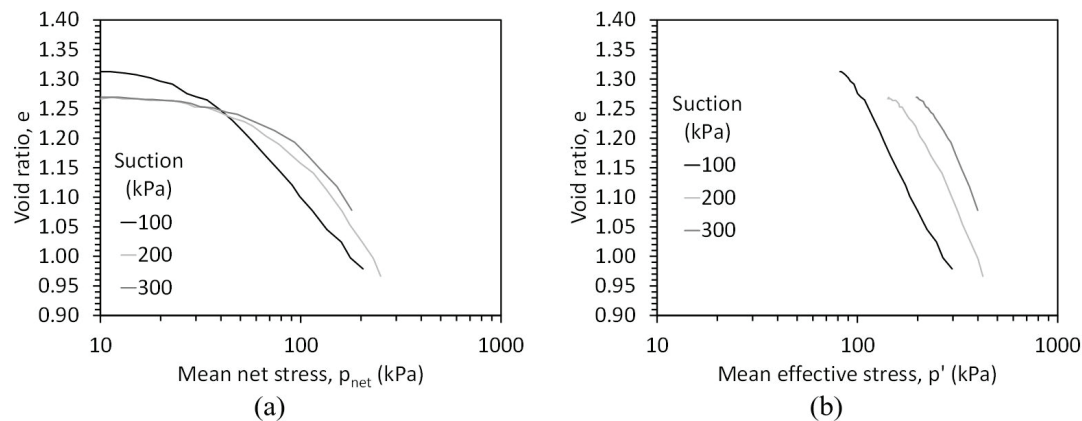


**Figure 3.** Compression curves from Sharma (1998): (a) Reported curves in terms of net stress; (b) Reinterpreted curves in terms of effective stress.

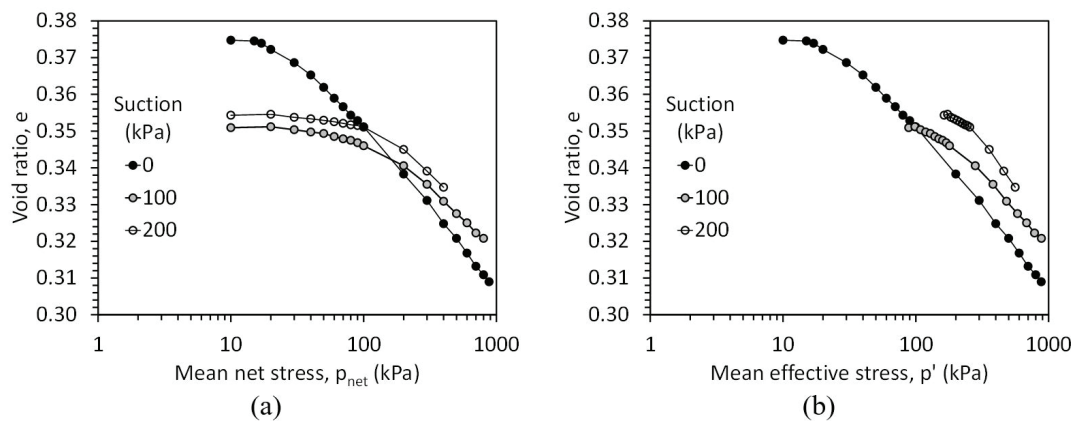


**Figure 4.** Compression curves from Rampino et al. (1999): (a) Reported curves in terms of net stress; (b) Reinterpreted curves in terms of effective stress.

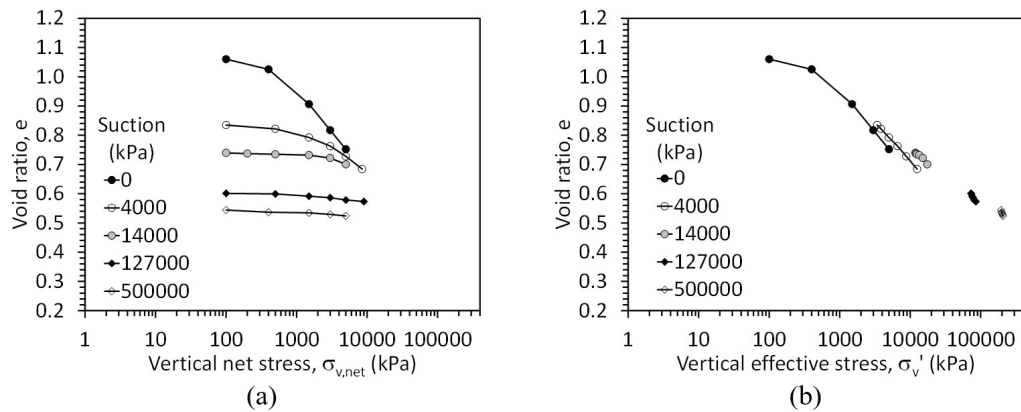


**Figure 5.** Compression curves from Lloret et al. (2003): (a) Reported curves in terms of net stress; (b) Reinterpreted curves in terms of effective stress.

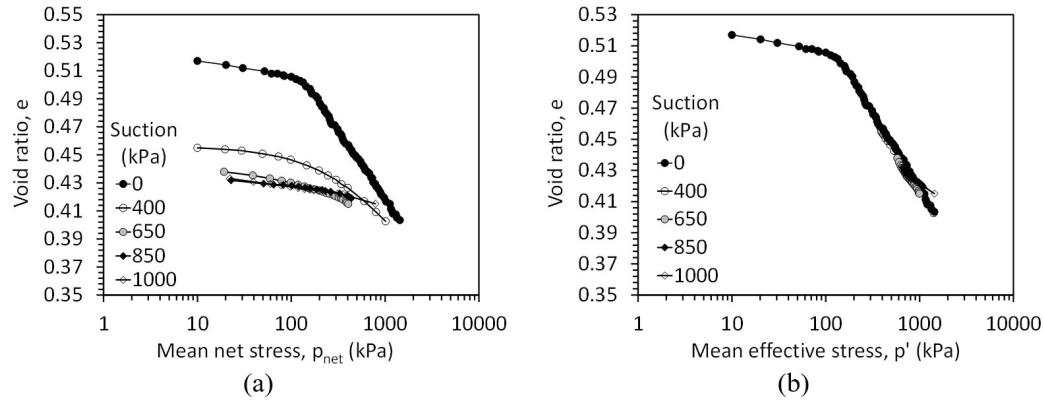


**Figure 6.** Compression curves from Cunningham et al. (2003): (a) Reported curves in terms of net stress; (b) Reinterpreted curves in terms of effective stress.

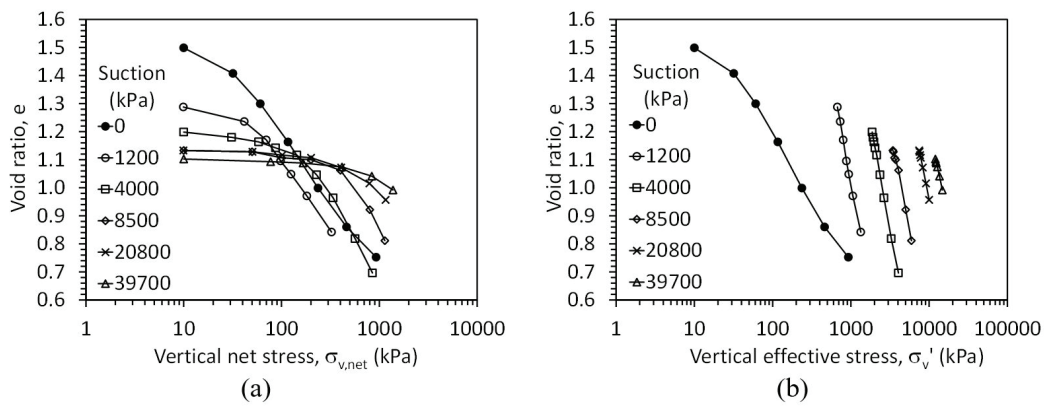


**Figure 7.** Compression curves from Cuisinier & Masroui (2005): (a) Reported curves in terms of net stress; (b) Reinterpreted curves in terms of effective stress.

had a much larger initial void ratio. Although the points of yielding are clear in the net stress space in Figure 7a, they are not as apparent in effective stress space in Figure 7b. Villar (2005) presented drained compression curves on compacted MX80 bentonite performed after swelling from high suctions. The results shown in Figures 8a and 8b are similar to those of Lloret et al. (2003) although the point of yielding was more apparent in the high suction test.

The study of Jotisankasa et al. (2007) perhaps has the most comprehensive evaluation of suction hardening of a soil over the widest range of conditions. Constant water content tests were performed, in which case the suction changes during compression. Accordingly, the initial degrees of saturation for the specimens are shown in Figures 9a and 9b. The suction was tracked using a high capacity tensiometer for the tests with initial degrees of saturation greater than 0.36, and the filter paper method was used



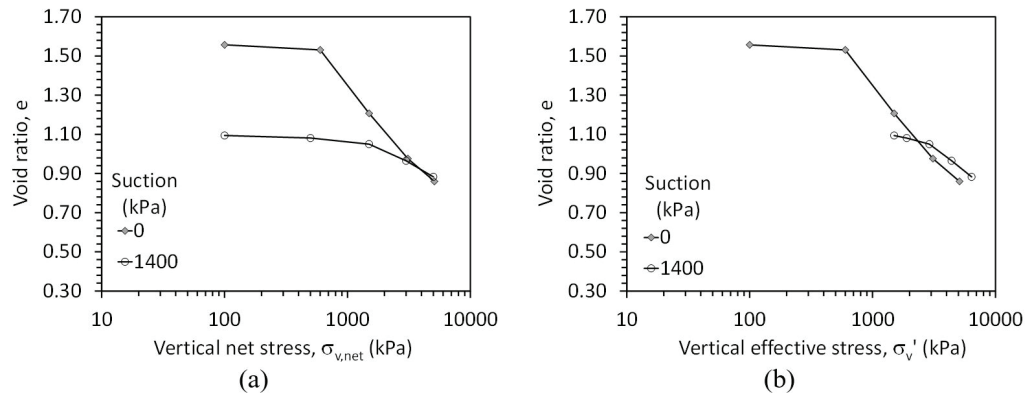


**Figure 8.** Compression curves from Villar (2005): (a) Reported curves in terms of net stress; (b) Reinterpreted curves in terms of effective stress

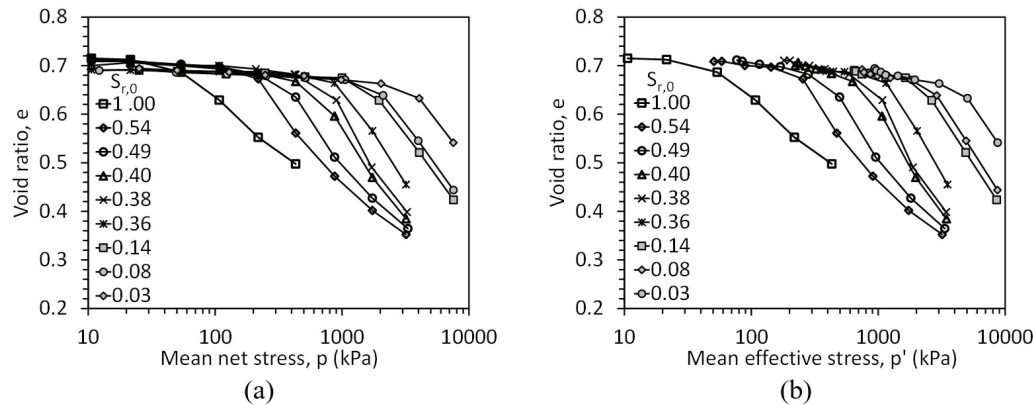


**Figure 9.** Compression curves from Jotisankasa et al. (2007): (a) Reported curves in terms of net stress; (b) Reinterpreted curves in terms of effective stress.

for the lower initial degrees of saturation. Although application of the effective stress principle leads to a shift to the right for the compression curves for unsaturated soils, the shapes of the curves remain the same, which is a different observation from the results presented in the previous figures. Casini (2008) was one of the first studies to report compression curves in terms of effective stress, and although similar trends were observed to those of Jotisankasa et al. (2007), the initial void ratio of each specimen were slightly different.

Although the results from Geiser et al. (2006) and Salager et al. (2008) on compacted Sion silt are not shown here, both studies presented compression curves in terms of effective stress only. Although the yield stress values in terms of net and effective stress were reported, neither study presented the evolution in degree of saturation during compression. These studies were the first to note that the yield stress in terms of effective stress should not change until the suction is greater than the air entry value. Uchaipichat & Khalili (2009) presented the compression curves for compacted Bourke silt in Figures 11a and 11b. An interesting observation from this study is that the net yield stress decreased with suction, while the effective yield stress increased with suction. The degree of saturation was not presented in this study, but the effective

stress was defined using the initial air entry suction. This study also found that the yield stress does not change until the suction is greater than the air entry suction, which was confirmed by the test at a suction of 10 kPa which was below the air entry suction of 50 kPa. Similar observations in the yield stress were made by Uchaipichat (2010), although the compression curves were only presented in terms of effective stress. The compression curves from Thu et al. (2007) in Figure 12 are similar to those of Rampino et al. (1999), while the compression curves of Tang & Cui (2010) in Figure 13 are similar to those of Lloret et al. (2003) and Cuisinier & Masroui (2005) except at the highest suction value. Ye et al. (2012) presented compression curves from GMZ bentonite, but only in terms of net stress without information on the degree of saturation.

Mun & McCartney (2017) presented compression curves for soils that were compacted to different initial water contents but at the same initial void ratio, as shown in Figure 14a and 14b. The initial suction in the specimen was measured using the tensiometer technique then applied using the axis translation technique. The shapes of the curves are similar to the hypothetical curves in Figure 1a, and high enough stresses were applied to reach pressurized

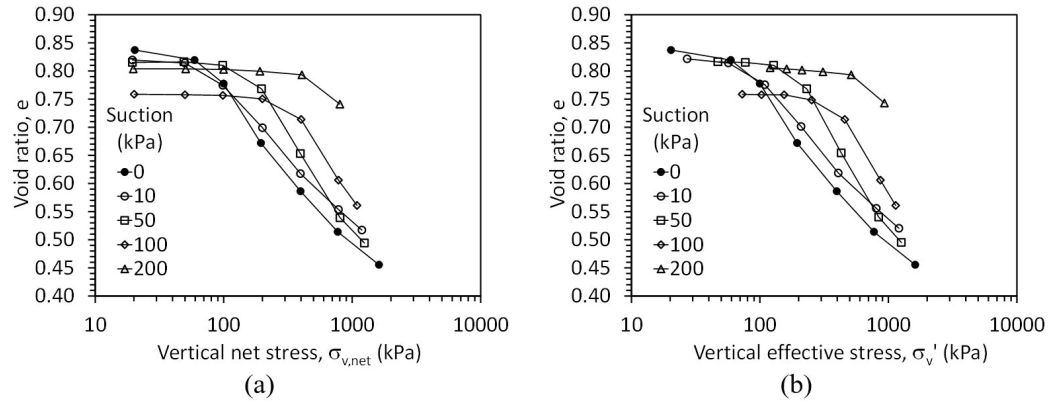


**Figure 10.** Compression curves from Casini (2008): (a) Reported curves in terms of net stress; (b) Reported curves in terms of effective stress.

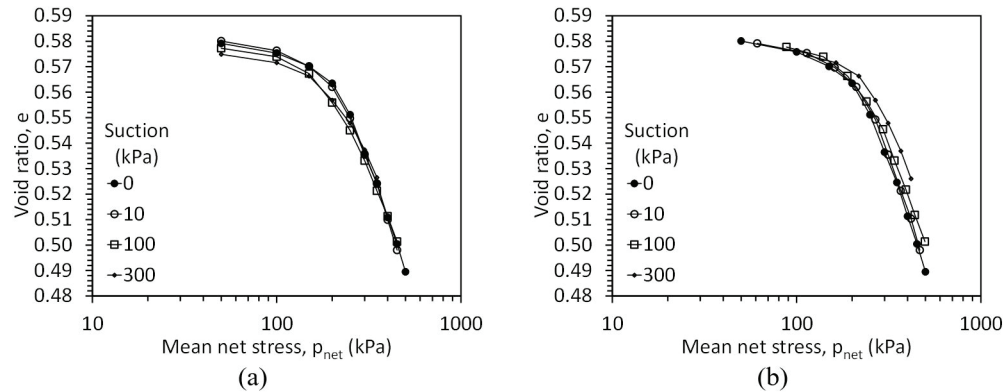


**Figure 11.** Compression curves from Uchaipichat & Khalili (2009): (a) Reported curves in terms of net stress; (b) Reinterpreted curves in terms of effective stress.

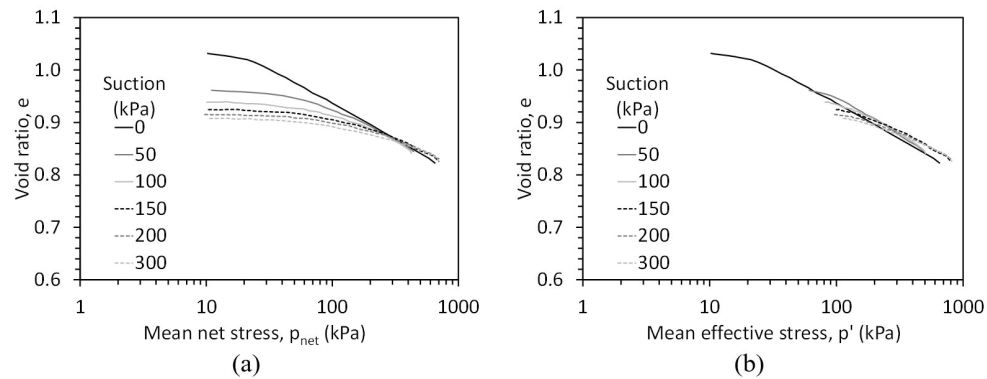


**Figure 12.** Compression curves from Thu et al. (2007): (a) Reported curves in terms of net stress; (b) Reinterpreted curves in terms of effective stress.

saturation. The shapes of the net and effective stress curves are similar, consistent with the observations of Jotisankasa et al. (2007). The compression curves of Khosravi et al. (2018) are shown in Figure 15a and 15b for Bonny silt. This soil was also characterized by Coccia & McCartney (2016) and Khosravi et al. (2016), albeit for different compaction conditions. The effective compression curves in Figure 15b mimic those of the hypothetical compression curves in Figure 1a to an

intermediate stress level. The compression curves from a compacted Loess reported by Haeri et al. (2019) are shown in Figure 16a and 16b. Similar to the results from Mun & McCartney (2017), they show a tendency to pressurized saturation at high stresses, especially for the lower suctions. Finally, Li et al. (2018) presented compression curves for a high plasticity clay over a range of suctions and used an innovative electrical resistivity technique to monitor the

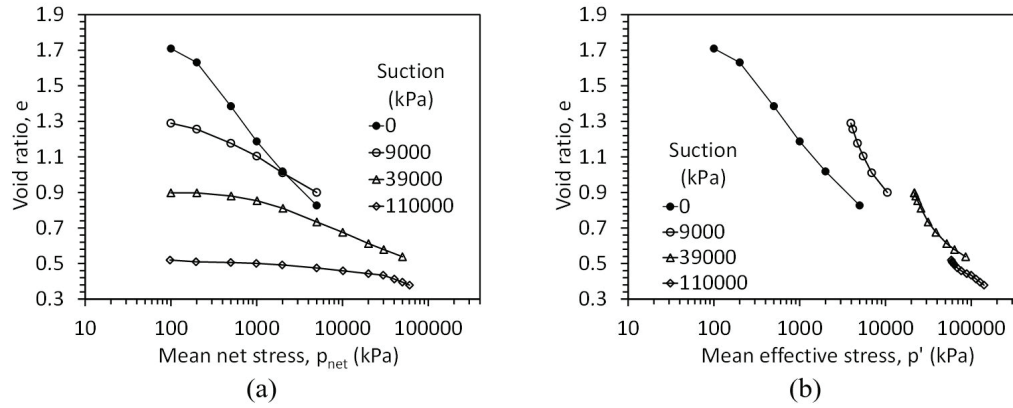


**Figure 13.** Compression curves from Tang & Cui (2010): (a) Reported curves in terms of net stress; (b) Reinterpreted curves in terms of effective stress.

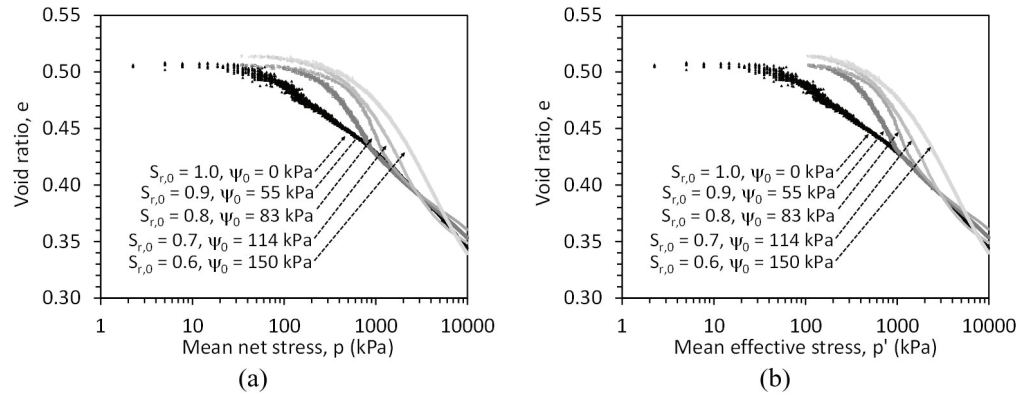


**Figure 14.** Compression curves from Mun & McCartney (2017): (a) Reinterpreted curves in terms of net stress; (b) Reported curves in terms of effective stress.

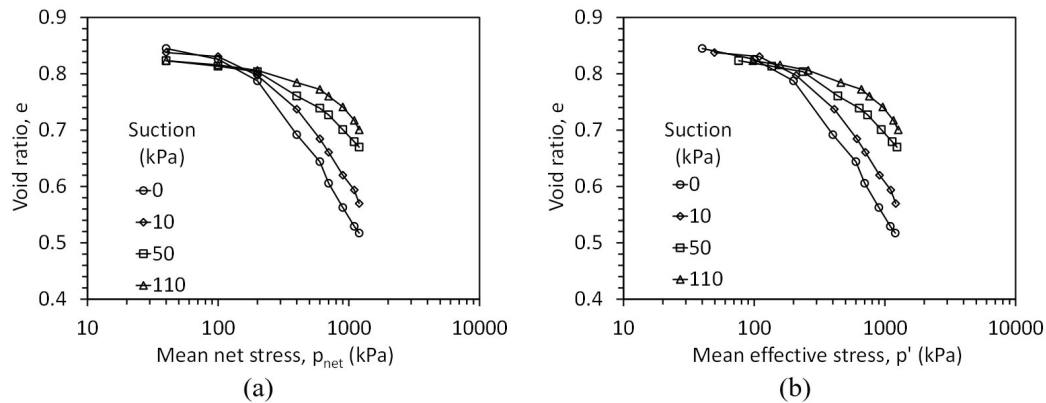


**Figure 15.** Compression curves from Khosravi et al. (2018): (a) Reported curves in terms of net stress; (b) Reinterpreted curves in terms of effective stress.

evolution in degree of saturation. They also tracked the change in void ratio during wetting or drying of compacted specimens to reach the target suction values.

## 6. Analysis

A plot of the suction versus the suction stress at yielding (i.e., the product of suction and the degree of saturation at

yielding) for low suction magnitudes (below 1000 kPa) is shown in Figure 17a. Although all the curves intersect at the origin, this point was not included to better show the trends in the data. In general, most of the soils show a linear trend between suction and suction stress at yielding. The different slopes for these soils are due to the different shapes of the soil-water retention curves of the soils. As the suction and suction stress at higher suction magnitudes vary over a wider

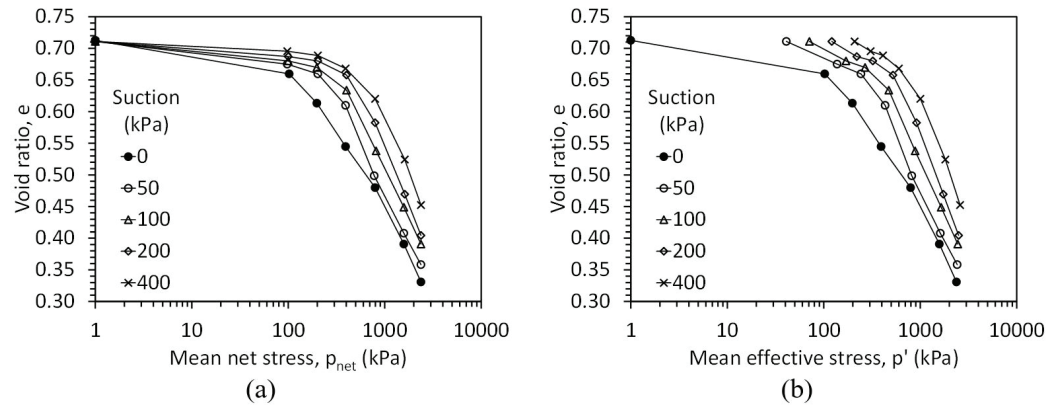


**Figure 16.** Compression curves from Haeri et al. (2019): (a) Reported curves in terms of net stress; (b) Reinterpreted curves in terms of effective stress.

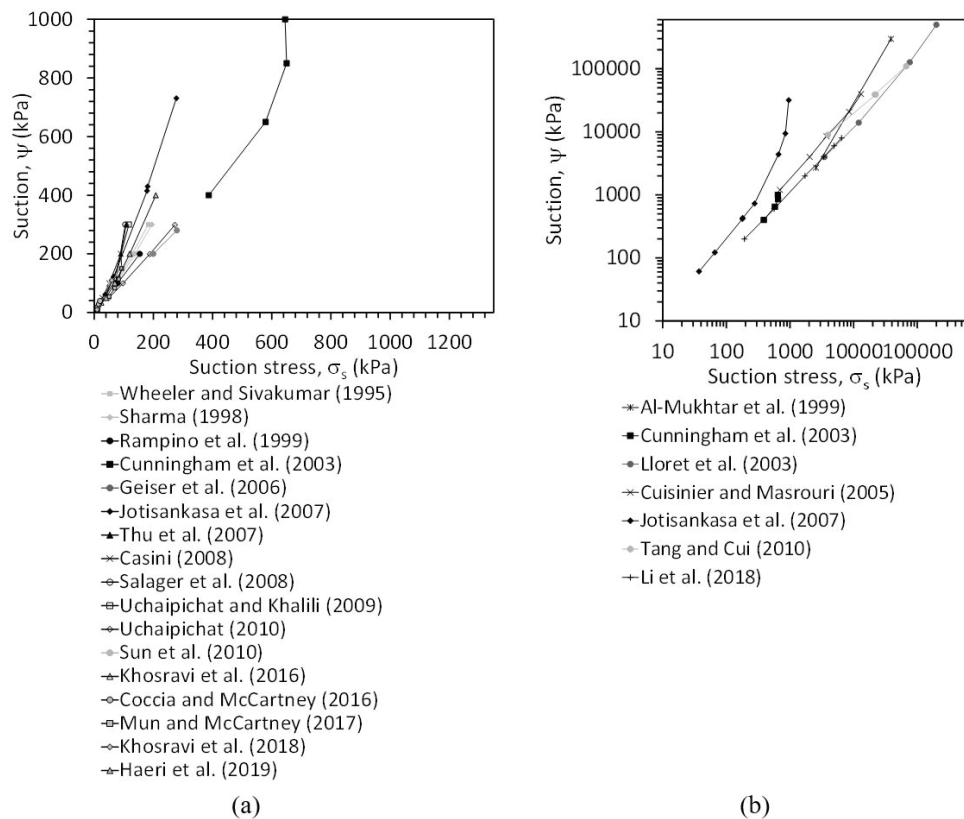


**Figure 17.** Suction vs. suction stress at the point of yielding: (a) Soils at low suctions (less than 1000 kPa); (b) Soils at high suctions.

range of values, the plot of suction versus the suction stress for high suctions is shown on a log-log scale in Figure 17b. The trends are more nonlinear in the high suction range, although the log-log slopes are very similar for many of the soils. For simplicity, the term suction is used interchangeably in Figures 18a and 18b even though the suction should be referred to as matric suction when capillarity is the dominant water retention mechanism, and the suction should be referred to as total suction when using Kelvin's law to calculate the suction from the relative humidity of the pore air.

A plot of the suction versus the net yield stress is shown in Figure 18a. Different from the plot in Figure 17a, a much wider range of trends is observed in this figure. This demonstrates the variability in the net yield stress for different soils, which could be due to incorrect identification of the point of yielding from a relative flat compression curve plotted in terms of net stress. Similar conclusions can be drawn from the plot of suction versus net yield stress for soils tested at high suctions in Figure 18b, where a range of trends with both positive and negative intercepts is observed. However,

when the results at low suctions are presented in terms of effective stress in Figure 19a, a more consistent behavior is noticed among the different soils, even though there is still greater variability than in the suction stress trends. The same can be said for the results at high suctions presented in terms

of effective stress in Figure 19b, where the effective yield stress relationships fall into a tighter band.

A synthesis of the hydro-mechanical properties governing the shape of the SWRC and the compression curves for the unsaturated soils evaluated in the database is summarized in

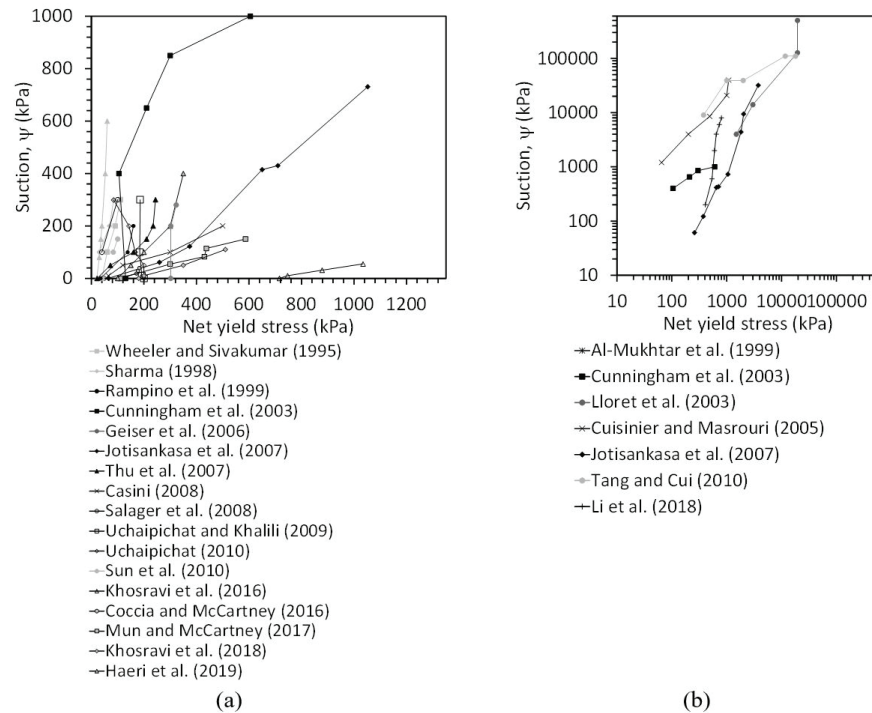


**Figure 18.** Suction vs. net yield stress: (a) Soils at low suctions (less than 1000 kPa); (b) Soils at high suctions.

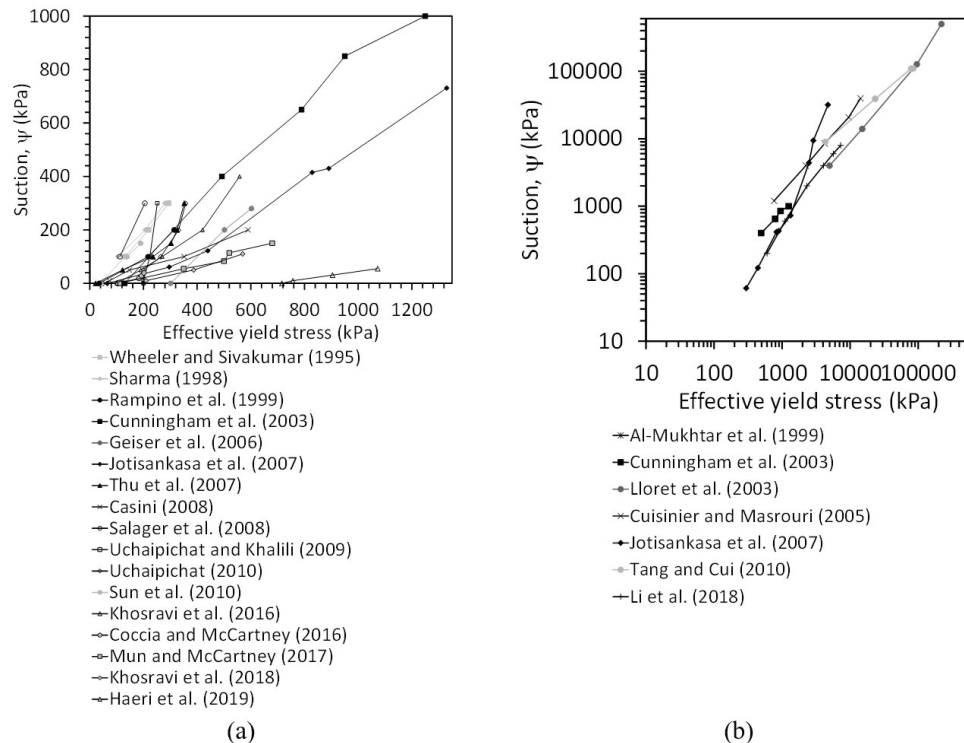


**Figure 19.** Suction vs. effective yield stress: (a) Soils at low suctions (less than 1000 kPa); (b) Soils at high suctions.



Table 2. This includes the parameters of the van Genuchten (1980) SWRC model fitted to the SWRC data presented in the studies, the estimated air entry suction, the slopes of the relationships between suction stress and suction, the slopes of the relationships between net and effective yield stresses and suction, and the slopes of the relationships between the VCL slope and suction. As the goal of this study is to understand the relative rates of increase in yield stress and effective stress with increasing suction, simple linear relationships were fitted to the yield stress and suction stress data. Although it is acknowledged that more advanced coupled relationships between suction, yield stress, and effective stress are available as summarized in the background sections, the simple linear relationships were found to provide a reasonable fit for most of the soils evaluated and the slopes summarized in

Table 2 can be used for qualitative comparison purposes. The slopes in Table 1 were defined such that the suction is on the ordinate axis and the yield stress, suction stress, and VCL slope are on the abscissa. This definition was selected to be consistent with the way that the LC curve is typically presented, with the suction on the ordinate axis and the net yield stress on the abscissa. Following this definition, a small slope value means that the variable (suction stress, yield stress, or slope of the VCL) has a larger change with a unit change in suction than a large slope value. The  $R^2$  values for the fitted relationships are typically greater than 0.95, with a minimum  $R^2$  of 0.75 for the most nonlinear relationship. Other important hydromechanical variables noted in Figure 1 include the slopes of the recompression lines and the point of pressurized saturation, but insufficient information

**Table 2.** Summary of hydro-mechanical parameters of unsaturated soils from the literature.

Study	van Genuchten (1980) Drying Path SWRC Parameters			$\psi_{acv}$ (kPa)	(Suction)/ (Suction Stress)	Net Yield Stress at $\psi=0$	(Suction)/ (Net Yield Stress)	(Suction)/ Effective Yield Stress)	(Suction)/ (Compression Curve Slope)
	$N_{VG}$	$\alpha_{VG}$ (kPa <sup>-1</sup> )	$S_{res}$						
Wheeler & Sivakumar (1995)	NR	NR	NR	NR	1.80	40	3.89	1.23	5E-04
Sharma (1998)	NR	NR	NR	NR	1.65	ND	3.41	1.12	9E-04
Maâtouk et al. (1995)	NR	NR	NR	NR	ID	20	16.9	ID	ID
Rampino et al. (1999)	NR	NR	NR	20	1.33	35	4.55	1.03	1E-05
Al-Mukhtar et al. (1999)	1.48	0.0002	0.00	ID	8.16	NY	NY	NY	-5E-07
Cunningham et al. (2003)	2.32	0.001	0.07	400	1.97	130	1.11	0.81	-2E-05
Lloret et al. (2003)	NR	NR	NR	3500	2.54	800	6.84	2.31	3E-07
Cuisinier & Masroui (2005)	NR	NR	NR	NR	3.06	50	31.51	2.81	5E-06
Villar (2005)	1.80	0.00003	0.00	6000	ID	600	ID	ID	-1E-05
Geiser et al. (2006)	2.15	0.014	0.11	50	1.00	NY	3.86	0.80	ID
Jotisankasa et al. (2007)	1.51	0.007	0.05	45	2.77	65	0.87	0.66	9E-07
Thu et al. (2007)	2.80	0.009	0.17	60	4.04	22	1.20	0.94	-5E-05
Casini (2008)	2.04	0.079	0.37	5	2.34	59	0.41	0.35	7E-05
Salager et al. (2008)	2.28	0.009	0.12	50	6.00	110	3.33	2.15	3E-05
Uchaipichat & Khalili (2009)	3.15	0.025	0.03	50	4.95	200	-21.3	5.68	-7E-05
Sun et al. (2010)	1.29	0.020	0.00	40	1.48	ND	2.94	0.99	9E-06
Tang & Cui (2010)	1.95	0.00002	0.00	10000	1.59	200	5.48	1.26	-8E-07
Uchaipichat (2010)	1.49	0.00158	0.00	18	1.12	200	-2.23	1.50	1E-05
Ye et al. (2012)	NR	NR	NR	NR	ID	582	16.4	ID	ID
Coccia & McCartney (2016)	1.38	0.158	0.03	10	2.66	103	1.90	1.11	-3E-04
Khosravi et al. (2016)	2.60	0.019	0.06	10	1.54	716	0.16	0.14	-1E-03
Mun & McCartney (2017)	1.81	0.010	0.00	40	2.19	110	0.34	0.29	3E-04
Khosravi et al. (2018)	1.91	0.016	0.00	20	1.99	180	0.32	0.28	-2E-04
Li et al. (2018)	1.10	0.003	0.00	400	1.24	ND	21.1	1.18	-5E-06
Haeri et al. (2019)	3.00	0.100	0.00	10	2.10	100	1.60	0.93	2E-04

Note: NR = Not Reported; NY = No Yielding; ID = Insufficient Data.

was available to characterize these for the majority of the soils in the database.

A plot of the gradient in suction with suction stress versus the gradient in suction with effective yield stress is shown in Figure 20. If the two gradients fall onto the line of unity, a similar increase in both variables would occur

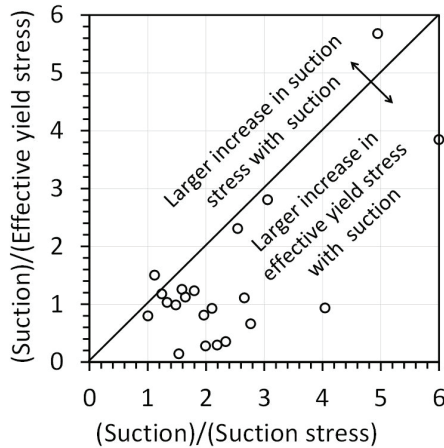


**Figure 20.** Slopes of suction vs. suction stress and suction vs. effective yield stress for different studies in the literature. Note: smaller slopes indicate greater increases in the variable with increasing suction.

with an increase in suction. Approximately half of the soils evaluated plot close to the line of unity. However, all but two of the soils plot below the line of unity, indicating that the soils exhibit a greater increase in effective yield stress with suction than the increase in suction stress with suction. The two points that plot above the line of unity were the two that had decreases in the net yield stress with increasing suction. According to Khalili et al. (2004), this indicates that the soils that plot below the line of unity will be susceptible to collapse upon wetting.

Plots of the relationships between suction and the slope of the VCL for the soils tested at low and high suction ranges are shown in Figures 21a and 21b. A low suction, the slopes of the VCLs range from 0.01 to 0.42, while at high suctions much larger slopes of VCLs are noted ranging from 0.018 to 0.83. The abnormally large slopes of the VCLs were observed for some soils at high suctions because the compression curves at the highest stress ranges in these tests were still showing a nonlinear decrease after yielding and may not have yet stabilized at the actual VCL. The trends in the slopes of the VCLs with increasing suction are generally flat, indicating that suction does not have a major effect on the slope of the VCL for these soils. In other words, the VCL for the unsaturated soils is parallel to the VCL for saturated soil for the range of effective stresses

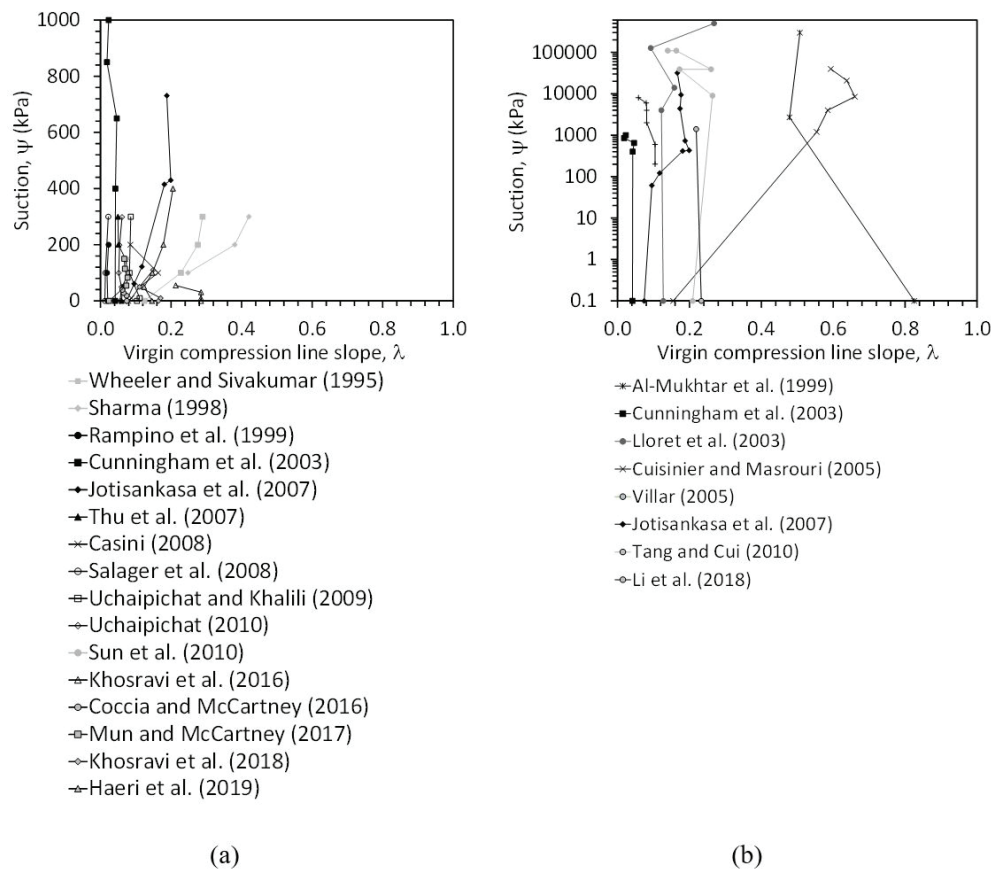


**Figure 21.** Suction vs. slope of the virgin compression line: (a) Soils at low suctions (less than 1000 kPa); (b) Soils at high suctions (values at saturation shown at a suction of 0.1 kPa).

investigated in these studies. As summarized in the last column of Table 2, most of the soils have a small positive rate of increase in the slope of the VCL with suction with a magnitude less than  $2 \times 10^{-4}$ . Three soils have larger positive rates of increase in the slope of the VCL with suction while two soils showed large negative rates of increase in the slope of the VCL with suction. A positive rate of increase reflects a trend like that shown in Figure 1a, where the VCLs for unsaturated soils converge with the VCL for saturated soil, while a negative rate of increase reflects a diverging trend. It is expected that if higher magnitudes of net stress had been applied that a positive rate of increase would eventually be observed for all the unsaturated soils, similar to the trends in the compression curves observed by Jotisankasa et al. (2007) and Mun & McCartney (2017) in Figures 9 and 14, respectively.

## 7. Conclusion and recommendations for future testing

This state-of-the-art paper presents the results from the analysis of a database of compression curves for unsaturated soils with the goal of understanding trends in the effective stress (or suction stress), yield stress, and slope of the VCL with increasing suction. Suction hardening was observed in nearly all the soils evaluated, and the effective yield stress curves were found to have more uniform shapes when compared with the net yield stress curves. The effective yield stresses generally showed a linearly increasing trend with increasing suction. Similar behavior was noted for soils tested at both high and low suctions, although the soils at high suctions often were not compressed to high enough net stresses to fully exhibit yielding. For all but two of the soils, the rate of increase in the effective yield stress with increasing suction was greater than the rate of increase in the suction stress with increasing suction. However, the rate of increase in the effective yield stress with increasing suction was only significantly greater for about half of the soils evaluated. The slopes of the VCLs for unsaturated soils were typically steeper than the slopes of the VCLs for saturated soils, with a few soils showing the opposite trend due to lower net stresses applied.

The observations from this study emphasize the importance of tracking the degree of saturation during compression of unsaturated soils, as this is a critical component to calculating the effective stress. A related recommendation is that all studies focused on the unsaturated behavior of soils should present the soil-water retention curve along with any scanning paths that may occur during testing. The observations also emphasize the importance of tracking changes in volume of unsaturated soils during initial suction application, as this may provide insight into the elastic behavior of the soil before yielding occurs during application of net stresses. Inconsistent comparisons between the compression curves for

saturated and unsaturated soils may have occurred because of large differences between the void ratios at the beginning of compression, which may have been caused by uncertainty in the volume changes occurring during suction application. The observations from this study indicate that it is critical to apply sufficiently high stresses to unsaturated soils to induce yielding, especially for heavily compacted soils or soils at high suction magnitudes. Future areas of research on this topic include characterizing the yielding behavior of unsaturated soils prepared using slurry consolidation to better understand the role of the soil structure induced by compaction and studying fundamental linkages between the yield stress and slope of the VCL.

## Acknowledgements

The authors appreciate the support from US Department of Energy Nuclear Energy University Program grant CFA-20-20093. The views in this paper are those of the authors alone.

## Declaration of interest

The authors have no conflicts of interest.

## Authors' contributions

John S. McCartney: conceptualization, methodology, writing – original draft preparation, data curation. Fatemah Behbehani: investigation, data curation, reviewing and editing.

## List of symbols

$e$	Void ratio.
$N_{vG}$	Parameter of the van Genuchten (1980) SWRC model.
$p'$	Mean effective stress.
$p_{net}$	Mean net stress.
$S$	Degree of saturation.
$S_e$	Effective saturation.
$S_{res}$	Residual degree of saturation.
$v$	Specific volume.
$\alpha_{vG}$	Parameter of the van Genuchten (1980) SWRC model.
$\sigma_s$	Suction stress.
$\sigma_v'$	Vertical effective stress.
$\sigma_{v,net}$	Vertical net stress.
$\lambda$	Effective stress parameter.
$\psi$	Suction.

## References

- Al-Mukhtar, M., Alcover, J.-F., & Bergaya, F. (1999). Oedometric and water-retention behavior of highly

- compacted unsaturated smectites. *Canadian Geotechnical Journal*, 36(4), 675-684. <http://dx.doi.org/10.1139/t99-035>.
- Alonso, E.E., Gens, A., & Josa, A. (1990). A constitutive model for partially saturated soils. *Geotechnique*, 40(3), 405-430. <http://dx.doi.org/10.1680/geot.1990.40.3.405>.
- Alsherif, N.A., & McCartney, J.S. (2015). Thermal behaviour of unsaturated silt at high suction magnitudes. *Geotechnique*, 65(9), 703-716. <http://dx.doi.org/10.1680/geot.14.P.049>.
- Bishop, A.W. (1959). The principle of effective stress. *Teknisk Ukeblad*, 106(39), 859-863.
- Bishop, A.W., & Blight, G.E. (1963). Some aspects of effective stress in saturated and unsaturated soils. *Geotechnique*, 13(3), 177-197. <http://dx.doi.org/10.1680/geot.1963.13.3.177>.
- Blight, G.E. (1965). A study of effective stress for volume change. In *Proceedings of the Symposium on Moisture Equilibria and Moisture Changes in the Soils Beneath Covered Areas* (pp. 259-269). Guildford: Butterworths.
- Bolzon, G., & Schrefler, B.A. (1995). State surfaces of partially saturated soils: an effective pressure approach. *Applied Mechanics Reviews*, 48(10), 643-649. <http://dx.doi.org/10.1115/1.3005044>.
- Bolzon, G., Schrefler, B.A., & Zienkiewicz, O.C. (1996). Elastoplastic soil constitutive laws generalised to partially saturated states. *Geotechnique*, 46(2), 270-289. <http://dx.doi.org/10.1680/geot.1996.46.2.279>.
- Brackley, I.J.A. (1973). Swell pressure and free swell in a compacted clay. In *Proceedings of the 3rd International Conference on Expansive Soils* (Vol. 1, pp. 169-176), Haifa. Jerusalem: Academic Press.
- Casini, F. (2008). *Effetti del grado di saturazione sul comportamento meccanico di un limo* [Ph.D. thesis]. "Sapienza" Università degli Studi di Roma.
- Coccia, C.J.R., & McCartney, J.S. (2016). Thermal volume change of poorly draining soils I: critical assessment of volume change mechanisms. *Computers and Geotechnics*, 80, 26-40. <http://dx.doi.org/10.1016/j.compgeo.2016.06.009>.
- Cui, Y.J., Delage, P., & Sultan, N. (1995). An elastoplastic model for compacted soils. In E. E. Alonzo & P. Delage (Eds.), *Proceedings of the 1st International Conference on Unsaturated Soils* (Vol. 2, pp. 703-709), Paris. Rotterdam: Balkema.
- Cuisinier, O., & Masrouri, F. (2005). Hydromechanical behaviour of a compacted swelling soil over a wide suction range. *Engineering Geology*, 81(3), 204-212. <http://dx.doi.org/10.1016/j.enggeo.2005.06.008>.
- Cunningham, M.R., Ridley, A.M., Dineen, K., & Burland, J.J. (2003). The mechanical behaviour of a reconstituted unsaturated silty clay. *Geotechnique*, 53(2), 183-194. <http://dx.doi.org/10.1680/geot.2003.53.2.183>.
- Della Vecchia, G., Jommi, C., & Romero, E. (2013). A fully coupled elastic-plastic hydro-mechanical model for compacted soils accounting for clay activity. *International Journal for Numerical and Analytical Methods in Geomechanics*, 37(5), 503-535. <http://dx.doi.org/10.1002/nag.1116>.
- Dong, Y., Lu, N., & Fox, P.J. (2020). Drying induced consolidation of soils. *Journal of Geotechnical and Geoenvironmental Engineering*, 146(9), 04020092. [http://dx.doi.org/10.1061/\(ASCE\)GT.1943-5606.0002327](http://dx.doi.org/10.1061/(ASCE)GT.1943-5606.0002327).
- Dong, Y., Lu, N., & McCartney, J.S. (2016). A unified model for small-strain shear modulus of variably saturated soil. *Journal of Geotechnical and Geoenvironmental Engineering*, 142(9), 04016039. [http://dx.doi.org/10.1061/\(ASCE\)GT.1943-5606.0001506](http://dx.doi.org/10.1061/(ASCE)GT.1943-5606.0001506).
- Dudley, J.H. (1970). Review of collapsing soils. *Journal of Soil Mechanics and Foundation Engineering*, 96(3), 925-947. <http://dx.doi.org/10.1061/JSFEAQ.0001426>.
- Escario, V., & Saez, J. (1986). The shear strength of partly saturated soils. *Geotechnique*, 36(3), 453-456. <http://dx.doi.org/10.1680/geot.1986.36.3.453>.
- Fleureau, J.M., Kheirbek-Saoud, S., Soemitro, R., & Taibi, S. (1993). Behaviour of clayey soils on drying-wetting paths. *Canadian Geotechnical Journal*, 30(2), 287-296. <http://dx.doi.org/10.1139/t93-024>.
- Gallipoli, D., Wheeler, S.J., & Karstunen, M. (2003). Modelling the variation of degree of saturation in a deformable unsaturated soil. *Geotechnique*, 53(1), 105-112. <http://dx.doi.org/10.1680/geot.2003.53.1.105>.
- Gan, J.K.M., Fredlund, D.G., & Rahardjo, H. (1988). Determination of the shear strength parameters of an unsaturated soil using the direct shear test. *Canadian Geotechnical Journal*, 25(3), 500-510. <http://dx.doi.org/10.1139/t88-055>.
- Geiser, F., Laloui, L., & Vulliet, L. (2006). Elasto-plasticity of unsaturated soils: laboratory test results on a remoulded silt. *Soil and Foundation*, 46(5), 545-556. <http://dx.doi.org/10.3208/sandf.46.545>.
- Haeri, S.M., Garakani, A.A., Roohparvar, H.R., Desai, C.S., Ghafouri, S.M.H.S., & Kouchesfahani, K.S. (2019). Testing and constitutive modeling of lime-stabilized collapsible loess. I: experimental investigations. *International Journal of Geomechanics*, 19(4), 04019006. [http://dx.doi.org/10.1061/\(ASCE\)GM.1943-5622.0001364](http://dx.doi.org/10.1061/(ASCE)GM.1943-5622.0001364).
- Jennings, J.E.B., & Burland, J.B. (1962). Limitations to the use of effective stresses in partly saturated soils. *Geotechnique*, 12(2), 125-144. <http://dx.doi.org/10.1680/geot.1962.12.2.125>.
- Jennings, J.E.B., & Knight, K. (1957a). The prediction of total heave from the double oedometer test. *Transactions of the South African Institution of Civil Engineers*, 7, 285-291.
- Jennings, J.E.B., & Knight, K. (1957b). The additional settlement of foundations due to a collapse of structure of sandy subsoils on wetting. In *Proceedings of the 4th International Conference on Soil Mechanics* (Vol. 1, pp. 316-319), London.
- Jotisankasa, A., Ridley, A., & Coop, M. (2007). Collapse behavior of a compacted silty clay in the suction-monitored oedometer apparatus. *Journal of Geotechnical and Geoenvironmental Engineering*, 133(7), 867-877. [http://dx.doi.org/10.1061/\(ASCE\)1090-0241\(2007\)133:7\(867\)](http://dx.doi.org/10.1061/(ASCE)1090-0241(2007)133:7(867)).

- Kato, S., & Kawai, K. (2000). Deformation characteristics of a compacted clay in collapse under isotropic and triaxial stress state. *Soil and Foundation*, 40(5), 75-90. [http://dx.doi.org/10.3208/sandf.40.5\\_75](http://dx.doi.org/10.3208/sandf.40.5_75).
- Khalili, N., & Khabbaz, M.H. (1998). A unique relationship for  $\chi$  for the determination of shear strength of unsaturated soils. *Geotechnique*, 48(5), 681-688. <http://dx.doi.org/10.1680/geot.1998.48.5.681>.
- Khalili, N., & Zargarbashi, S. (2010). Influence of hydraulic hysteresis on effective stress in unsaturated soils. *Geotechnique*, 60(9), 729-734. <http://dx.doi.org/10.1680/geot.09.T.009>.
- Khalili, N., Geiser, F., & Blight, G.E. (2004). Effective stress in unsaturated soils, a review with new evidence. *International Journal of Geomechanics*, 4(2), 115-126. [http://dx.doi.org/10.1061/\(ASCE\)1532-3641\(2004\)4:2\(115\)](http://dx.doi.org/10.1061/(ASCE)1532-3641(2004)4:2(115)).
- Khalili, N., Habte, M.A., & Zargarbashi, S. (2008). A fully coupled flow deformation model for cyclic analysis of unsaturated soils including hydraulic and mechanical hysteresis. *Computers and Geotechnics*, 35(6), 872-889. <http://dx.doi.org/10.1016/j.compgeo.2008.08.003>.
- Khosravi, A., & McCartney, J.S. (2012). Impact of hydraulic hysteresis on the small-strain shear modulus of unsaturated soils. *Journal of Geotechnical and Geoenvironmental Engineering*, 138(11), 1326-1333. [http://dx.doi.org/10.1061/\(ASCE\)GT.1943-5606.0000713](http://dx.doi.org/10.1061/(ASCE)GT.1943-5606.0000713).
- Khosravi, A., Rahimi, M., Gheibi, A., & Mahdi Shahrabi, M. (2018). Impact of plastic compression on the small strain shear modulus of unsaturated silts. *International Journal of Geomechanics*, 18(2), 04017138. [http://dx.doi.org/10.1061/\(ASCE\)GM.1943-5622.0001031](http://dx.doi.org/10.1061/(ASCE)GM.1943-5622.0001031).
- Khosravi, A., Sajjad, S., Dadashi, A., & McCartney, J.S. (2016). Evaluation of the impact of drainage-induced hardening on the small strain shear modulus of unsaturated soils. *International Journal of Geomechanics*, 16(6), 1-10. [http://dx.doi.org/10.1061/\(ASCE\)GM.1943-5622.0000614](http://dx.doi.org/10.1061/(ASCE)GM.1943-5622.0000614).
- Li, Z.-S., Derfouf, F.-E.M., Benchouk, A., Abou-Bekr, N., Taibi, S., & Fleureau, J.-M. (2018). Volume change behavior of two compacted clayey soils under hydraulic and mechanical loadings. *Journal of Geotechnical and Geoenvironmental Engineering*, 144(4), 04018013. [http://dx.doi.org/10.1061/\(ASCE\)GT.1943-5606.0001851](http://dx.doi.org/10.1061/(ASCE)GT.1943-5606.0001851).
- Lloret, A., Villar, M.V., Sanchez, M., Gens, A., Pintado, X., & Alonso, E.E. (2003). Mechanical behaviour of heavily compacted bentonite under high suction changes. *Geotechnique*, 53(1), 27-40. <http://dx.doi.org/10.1680/geot.2003.53.1.27>.
- Loret, B., & Khalili, N. (2002). An effective stress elastic-plastic model for unsaturated porous media. *Mechanics of Materials*, 34(2), 97-116. [http://dx.doi.org/10.1016/S0167-6636\(01\)00092-8](http://dx.doi.org/10.1016/S0167-6636(01)00092-8).
- Lu, N., & Likos, W.J. (2006). Suction stress characteristic curve for unsaturated soil. *Journal of Geotechnical and Geoenvironmental Engineering*, 132(2), 131-142. [http://dx.doi.org/10.1061/\(ASCE\)1090-0241\(2006\)132:2\(131\)](http://dx.doi.org/10.1061/(ASCE)1090-0241(2006)132:2(131)).
- Lu, N., Godt, J., & Wu, D. (2010). A closed-form equation for effective stress in unsaturated soil. *Water Resources Research*, 46(5), 1-14. <http://dx.doi.org/10.1029/2009WR008646>.
- Maâtouk, A., Leroueil, S., & La Rochelle, P. (1995). Yielding and critical state of collapsible unsaturated silty soil. *Geotechnique*, 45(3), 465-477. <http://dx.doi.org/10.1680/geot.1995.45.3.465>.
- Matyas, E.L., & Radhakrishna, H.S. (1968). Volume change characteristics of partially saturated soils. *Geotechnique*, 18(4), 432-448. <http://dx.doi.org/10.1680/geot.1968.18.4.432>.
- Mun, W., & McCartney, J.S. (2017). Constitutive model for the drained compression of unsaturated clay to high stresses. *Journal of Geotechnical and Geoenvironmental Engineering*, 143(6), 04017014. [http://dx.doi.org/10.1061/\(ASCE\)GT.1943-5606.0001662](http://dx.doi.org/10.1061/(ASCE)GT.1943-5606.0001662).
- Mun, W., Coccia, C.J.R., & McCartney, J.S. (2017). Application of hysteretic trends in the preconsolidation stress of unsaturated soils. *Geotechnical and Geological Engineering*, 36(1), 193-207. <http://dx.doi.org/10.1007/s10706-017-0316-7>.
- Nuth, M., & Laloui, L. (2008). Effective stress concept in unsaturated soils: clarification and validation of a unified framework. *International Journal for Numerical and Analytical Methods in Geomechanics*, 38(7), 771-801. <http://dx.doi.org/10.1002/nag.645>.
- Pereira, J.H.F., & Fredlund, D.G. (2000). Volume change behavior of collapsible compacted gneiss soil. *Journal of Geotechnical and Geoenvironmental Engineering*, 126(10), 907-916. [http://dx.doi.org/10.1061/\(ASCE\)1090-0241\(2000\)126:10\(907\)](http://dx.doi.org/10.1061/(ASCE)1090-0241(2000)126:10(907)).
- Rampino, C., Mancuso, C., & Vinale, F. (1999). Laboratory testing on an unsaturated soil: equipment, procedures, and first experimental results. *Canadian Geotechnical Journal*, 36(1), 1-12. <http://dx.doi.org/10.1139/t98-093>.
- Romero, E., & Jommi, C. (2008). An insight into the role of hydraulic history on the volume changes of anisotropic clayey soils. *Water Resources Research*, 44(5), 1-16. <http://dx.doi.org/10.1029/2007WR006558>.
- Salager, S., François, B., El Youssoufi, M.S., Laloui, L., & Saix, C. (2008). Experimental investigations of temperature and suction effects on compressibility and pre-consolidation pressure of a sandy silt. *Soil and Foundation*, 48(4), 453-466. <http://dx.doi.org/10.3208/sandf.48.453>.
- Sharma, R. (1998). *Mechanical behaviour of unsaturated highly expansive soil* [PhD thesis]. University of Oxford.
- Sheng, D., Fredlund, D.G., & Gens, A. (2008). A new modelling approach for unsaturated soils using independent stress variables. *Canadian Geotechnical Journal*, 45(4), 511-534. <http://dx.doi.org/10.1139/T07-112>.
- Sheng, D., Sloan, S., & Gens, A. (2004). A constitutive model for unsaturated soils: thermomechanical and computational aspects. *Computational Mechanics*, 33(6), 453-465. <http://dx.doi.org/10.1007/s00466-003-0545-x>.
- Sivakumar, V. (1993). *A critical state framework for unsaturated soils* [PhD thesis]. University of Sheffield.



- Sun, D., Matsuoka, H., Yao, Y.-P., & Ichihara, W. (2000). An elasto-plastic model for unsaturated soil in three-dimensional stresses. *Soil and Foundation*, 40(3), 17-28. [http://dx.doi.org/10.3208/sandf.40.3\\_17](http://dx.doi.org/10.3208/sandf.40.3_17).
- Sun, D., Sheng, D., & Xu, Y. (2007). Collapse behavior of unsaturated compacted soil with different initial densities. *Canadian Geotechnical Journal*, 44(6), 673-686. <http://dx.doi.org/10.1139/t07-023>.
- Sun, D., Sun, W., & Xiang, L. (2010). Effect of degree of saturation on mechanical behavior of unsaturated soils and its elastoplastic simulation. *Computers and Geotechnics*, 37(5), 678-688. <http://dx.doi.org/10.1016/j.compgeo.2010.04.006>.
- Tamagnini, R. (2004). An extended Cam-clay model for unsaturated soils with hydraulic hysteresis. *Geotechnique*, 54(3), 223-228. <http://dx.doi.org/10.1680/geot.2004.54.3.223>.
- Tang, A.M., & Cui, Y.J. (2010). Experimental study on hydro-mechanical coupling behaviours of highly compacted expansive clay. *Journal of Rock Mechanics and Geotechnical Engineering*, 2(1), 39-43. <http://dx.doi.org/10.3724/SP.J.1235.2010.00039>.
- Thu, T.M., Rahardjo, H., & Leong, E.-C. (2007). Soil-water characteristic curve and consolidation behavior for a compacted silt. *Canadian Geotechnical Journal*, 44(3), 266-275. <http://dx.doi.org/10.1139/t06-114>.
- Tourchi, S., & Hamidi, A. (2015). Thermo-mechanical constitutive modeling of unsaturated clays based on the critical state concepts. *Journal of Rock Mechanics and Geotechnical Engineering*, 7(2), 193-198. <http://dx.doi.org/10.1016/j.jrmge.2015.02.004>.
- Uchaipichat, A. (2010). Hydraulic hysteresis effect on compressibility of unsaturated soils. *ARP Journal of Engineering and Applied Science*, 5(10), 92-97.
- Uchaipichat, A., & Khalili, N. (2009). Experimental investigation of thermo-hydro-mechanical behaviour of an unsaturated silt. *Geotechnique*, 59(4), 339-353. <http://dx.doi.org/10.1680/geot.2009.59.4.339>.
- van Genuchten, M.T. (1980). A closed form equation for predicting the hydraulic conductivity of unsaturated soils. *Soil Science Society of America Journal*, 44(5), 892-898. <http://dx.doi.org/10.2136/sssaj1980.03615995004400050002x>.
- Villar, M.V. (2005). *MX-80 bentonite: thermo-hydro-mechanical characterisation performed at CIEMAT in the context of the prototype project* (Technical Report, No. 1053). Departamento de Impacto Ambiental de la Energía.
- Wheeler, S.J., & Sivakumar, V. (1995). An elasto-plastic critical state framework for unsaturated soils. *Geotechnique*, 45(1), 35-53. <http://dx.doi.org/10.1680/geot.1995.45.1.35>.
- Wheeler, S.J., Gallipoli, D., & Karstunen, M. (2002). Comments on the use of Barcelona Basic Model for unsaturated soils. *International Journal for Numerical and Analytical Methods in Geomechanics*, 26(15), 1561-1571. <http://dx.doi.org/10.1002/nag.259>.
- Wheeler, S.J., Sharma, R.J., & Buisson, M.S.R. (2003). Coupling of hydraulic hysteresis and stress-strain behaviour in unsaturated soils. *Geotechnique*, 53(1), 41-54. <http://dx.doi.org/10.1680/geot.2003.53.1.41>.
- Ye, W.M., Zhang, Y.W., Chen, B., Zheng, Z.J., Chen, Y.G., & Cui, Y.J. (2012). Investigation on compression behaviour of highly compacted GMZ01 bentonite with suction and temperature control. *Nuclear Engineering and Design*, 252, 11-18. <http://dx.doi.org/10.1016/j.nucengdes.2012.06.037>.
- Zhou, A.-N., Sheng, D., Sloan, S.W., & Gens, A. (2012a). Interpretation of unsaturated soil behaviour in the stress – saturation space, I: volume change and water retention behavior. *Computers and Geotechnics*, 43, 178-187. <http://dx.doi.org/10.1016/j.compgeo.2012.04.010>.
- Zhou, A.-N., Sheng, D., Sloan, S.W., & Gens, A. (2012b). Interpretation of unsaturated soil behaviour in the stress – saturation space, II: constitutive relationships and validations. *Computers and Geotechnics*, 43, 111-123. <http://dx.doi.org/10.1016/j.compgeo.2012.02.009>.



## An improved framework for volume change of shrink/swell soils subjected to time-varying climatic effects

Austin H. Olaiz<sup>1#</sup> , Mohammad Mosawi<sup>1</sup> , Claudia E. Zapata<sup>1</sup> 

Article

### Keywords

Shrink/swell volume change  
Time-varying climatic effects  
Soil-climate interaction  
Mitchell's closed-form solution  
Soil suction envelopes  
Unsaturated soil moisture flow

### Abstract

The ability to estimate soil volume change as a function of time is a valuable tool in the design or forensic analysis of shallow foundations and pavement structures. This paper presents an improved framework for estimating the volume change of shrink/swell soils due to time-varying climatic effects using the Lytton et al. (2005) approach with the suction envelope models created by Vann & Houston (2021) and updated considerations of short-term varying climate. The procedure can be easily implemented in any country due to its mechanistic-empirical nature. The authors present an example calculation of the proposed framework using the data from an American Association of State Highway and Transportation Officials (AASHTO) Long-Term Pavement Performance (LTPP) Seasonal Monitoring Program (SMP) section, located approximately 80 miles northeast of Dallas, Texas. The volume change estimated from the proposed framework was compared to 70 measured data points from sections from the SMP study and the results look promising. The models are universal and can be used in any part of the world provided measured data is available to calibrate for local conditions. Ongoing calibration effort with the remaining LTPP SMP sections will allow obtaining calibration factors for the proposed framework that will improve the estimation of the volume change predictions under pavements and facilitate the implementation into current design procedures.

## 1. Introduction

The ability to estimate soil volume change as a function of time is a valuable tool in the design of shallow foundations of pavement structures. Specifically pertaining to pavement design, estimating soil volume change as a function of time allows for the prediction of the potential cumulative International Roughness Index (IRI). The time-varying volume change can also be a valuable tool in the forensic analysis of existing foundation movement of a lightly loaded structure on shallow footings.

This paper presents an improved framework for estimating the volume change of shrink/swell soils due to time-varying climatic effects using the Lytton et al. (2005) approach with the suction envelope models created by Vann & Houston (2021). The proposed framework for estimating soil volume change of shrink/swell soils as a function of time is presented as an example calculation with data from an AASHTO Long-Term Pavement Performance (LTPP) Seasonal Monitoring Program (SMP) section TX 48-1068 (FHWA, 1995), which is located approximately 80 miles northeast of Dallas, Texas.

The SMP study includes measured data from 1/1994 to 9/1997 for the TX 48-1068 section. The construction date of the TX48-1068 section is 3/1987. As such, the example calculation will use the time frame of 3/1987 to 9/1997 so that a comparison of predicted and measured volume change can be performed.

## 2. Volume change of shrink/swell soils

The determination of the magnitude of potential soil volume change is a key focus of geotechnical engineering as it causes significant infrastructure damage each year. Studies have been published, which empirically relate soil index properties (Atterberg limits, gradation, mineralogy, etc.), along with soil engineering properties (density, moisture content, swell pressure, etc.), to volume change.

Direct laboratory measurements of the volume change potential of a soil helps improve the estimation of potential volume change in the field. The 1-D oedometer "Response to Wetting Test" as described in ASTM D4546 (ASTM, 2021) is the common type of laboratory test for volume

<sup>#</sup>Corresponding author. E-mail address: Austin.Olaiz@asu.edu

<sup>1</sup>Arizona State University, School of Sustainable Engineering and The Built Environment, Tempe, AZ, USA.

Submitted on April 10, 2021; Final Acceptance on July 14, 2021; Discussion open until November 30, 2021.

<https://doi.org/10.28927/SR.2021.065621>



This is an Open Access article distributed under the terms of the Creative Commons Attribution License, which permits unrestricted use, distribution, and reproduction in any medium, provided the original work is properly cited.

change determination. One key difference from the laboratory oedometer test compared to the field conditions the soil will experience is the final degree of saturation. The response to wetting test inundates the sample, driving to almost full saturation. However, it is the probability that the soil will reach this moisture level over the period of the structure/pavements design life is very low (Houston & Houston, 2017).

A common method for volume change estimation is the Potential Vertical Rise published by the Texas Department of Transportation (TxDOT, 1978), which includes both empirical-based relationships and result from an oedometer test. In 2005, the Texas DOT updated the approach to determining the volume change of expansive soils using the work by Lytton et al. (2005), which encompassed a suction-based approach. The study concluded that the previous empirical-based approach significantly over-estimated the soil heave and did not account for the shrinkage of the soil during dry climatic periods.

A thorough literature review of volume change estimates of unsaturated soil (oedometer-based, or suction-based) was performed by Vann (2019). The authors of this paper have carefully reviewed this relative literature summary as part of the research leading up to this paper.

The suction-based approach by Lytton et al. (2005) for estimating the volume change of shrink/swell soils which was adopted by the Texas DOT and the Post-Tensioning Institute for the design of slabs on ground (PTI, 2004, 2008), was the compilation of efforts of several related studies including: Lytton (1977), McKeen & Hamberg (1981), Holtz & Gibbs (1956), Covar & Lytton (2001), Lytton et al. (2004). The approach encompasses the volumetric strain caused by changes in both stress states of the soil (matric suction and net normal stress) and uses the closed-form solution of the Richard's unsaturated moisture flow equation (Bear, 1972) developed by Mitchell (1979) to estimate the soil volume-change as a function of time when no groundwater table is present. The relationship between the change in each stress state and the volumetric strain, referred to as the compression indices, must be directly measured or empirically determined.

One limitation of the Mitchell equation (1979) used in the Lytton et al. (2005) framework is that the climate boundary condition is assumed and modelled to be a sinusoidal pattern. Aubeny & Long (2007) proposed an improvement to this limitation by fitting a Fourier equation to the climate data. The Fourier fit to the climate data allows for the irregularities of climate data to be captured and allows for the development of asymmetrical suction profiles. Aubeny & Long (2007) also studied the uncertainty of the key variables required in the Mitchell's equation (1979) for the change in soil suction with time. The study concluded that the diffusion coefficient ( $\alpha$ ) had significant ranges for a given soil, low reproducibility, and discrepancies between lab and field measurements, and was dependent upon the number of climatic cycles per year ( $n$ ) when performing a back-calculation from the depth of equilibrium suction.

Vann & Houston (2021) developed correlations between the 30-year Thornthwaite Moisture Index (Thornthwaite, 1948; Witczak et al., 2006) and soil suction envelopes using measured data from over 40 geotechnical studies (Vann, 2019). The suction envelope correlations to the *TMI* allow for key aspects of the Aubeny & Long (2007) approach to estimating volume change of shrink/swell soils as function of time to be determined without the need to measure or estimate the diffusion coefficient or number of climatic cycles per year.

This paper presents an improved framework for estimating the volume change of shrink/swell soils due to time-varying climatic effects. This framework builds upon the work presented by Lytton et al. (2005) and incorporates the latest suction envelope models proposed by Vann & Houston (2021). The framework presented is applicable to uncovered sites where the groundwater table effects are negligible, but it has been calibrated to account for covered areas and for the spatial variation between the pavement center and edges.

### 3. Framework outline

The following outline summarizes the steps of the improved framework for estimating the volume change of shrink/swell soils due to time-varying (monthly) climatic effects:

1. Weather station identification and data extraction
2. 30-year and monthly Thornthwaite Moisture Index per Witczak et al. (2006)
3. Determination of suction envelope parameters per Vann & Houston (2021)
  - a. Depth to stable suction
  - b. Magnitude of stable suction
  - c. Limits of suction variation at the surface
  - d. Climatic parameter ( $r$ )
4. Back-calculation of variables for Mitchell (1979) equation
5. Development of long-term wet and dry suction profiles
6. Initial estimation of monthly changes in suction at the surface per Perera (2003)
7. Adjustment to estimation of monthly changes in suction using limits of suction variation at the surface from Vann & Houston (2021)
8. Fourier equation fit to the monthly suction change at the surface per Aubeny & Long (2007)
9. Generation of monthly suction profile per Aubeny & Long (2007)
10. Suction profile adjustments for varying surface boundary conditions
11. Determination of net normal stress profile
12. Estimation of suction compression index (assuming value is not directly measured)
13. Calculation of strain monthly
14. Calculation of volume change monthly

### 3.1 Step 1: climate data

A Season Monitoring Program (SMP) pavement section approximately 80 miles northwest of Dallas, Texas (TX 48-1068) is used to provide an example for the proposed framework (FHWA, 2021). For the purposes of this example calculation, the climate data was gathered from the weather station nearest to the site and identified using the open-access Thornthwaite Moisture Index (*TMI*) GIS map developed by Olaiz (2017), which uses the National Oceanic and Atmospheric Administration's (NOAA) 30-year climate normal database for the United States. Figure 1 presents an excerpt for the GIS map, which has the Paris, TX weather station selected.

The "Station ID" shown in the pop-up window in Figure 1 (USC00416794) is the only data needed for the purposes of this study. However, the remaining data shown may be helpful to get an understanding of the general climatic conditions at the site.

The NOAA climate data associated with each station in the country can be extracted from the online NOAA FTP site. It is recommended that the extracted weather data be filtered to contain the necessary variables for computation of the Thornthwaite Moisture Index (Witczak et al., 2006):

- Year
- Month
- Monthly Precipitation (cm)
- Monthly Average Temperature (Celsius)

Note that the Vann & Houston (2021) models used in the proposed analysis correlate the suction envelope parameters

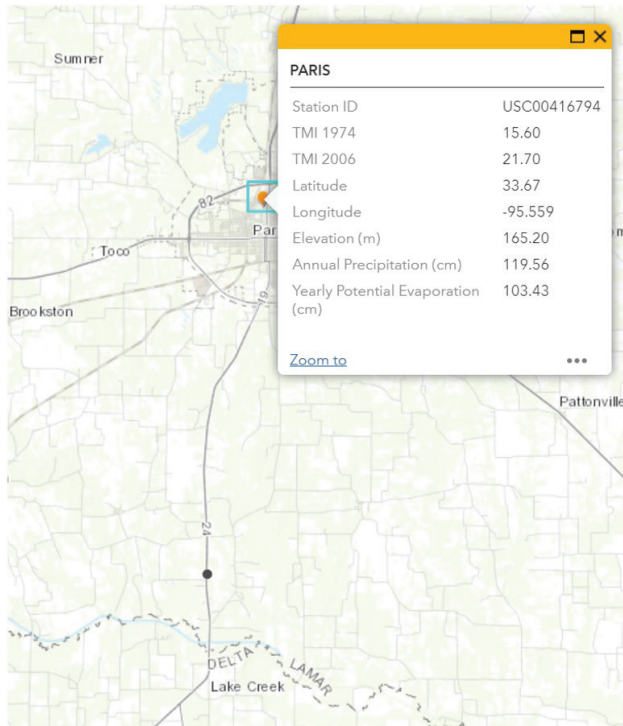


**Figure 1.** Paris (Texas) weather station (NOAA ID USC00416794) data from online *TMI* GIS map (Olaiz, 2017).

to a 30-year *TMI* value. As such, the climate data from the NOAA database for station USC00416794 was extracted for the date range of 9/1967 to 9/1997 (the last date of measured data from the SMP study for the TX 48-1068 section).

### 3.2 Step 2: monthly and 30-year Thornthwaite Moisture Index (*TMI*) (Witczak et al., 2006)

To determine yearly *TMI* for each month, first the potential evapotranspiration (*PET*) for each month must be calculated:

$$PET(cm) = f_1 f_2 1.6 \left( \frac{10t}{I} \right)^a \quad (1)$$

where,  $f_1$  is the fraction of the number of days in month divided by the average number of days in month, 30;  $f_2$  is the fraction of the number of hours in a day divided by the base of 12 h in a day;  $t$  is the mean monthly temperature in degrees Celsius;  $I$  is the annual heat index; and  $a$  is a coefficient.

$$I = \sum_{i=1}^{12} \left( \frac{t_i}{5} \right)^{1.514} \quad (2)$$

where,  $t_i$  is the mean temperature for the  $i^{\text{th}}$  month, and

$$a = 6.75I^3 \times 10^{-7} - 7.71I^3 \times 10^{-5} + 1.792I \times 10^{-2} + 0.49239 \quad (3)$$

The *TMI* (Witczak et al., 2006) can now be determined by:

$$TMI = 75 \left( \frac{P}{PET} - 1 \right) + 10 \quad (4)$$

where,  $P$  is the precipitation for the given month.

To visualize the climate data over time, the monthly average temperature, monthly rainfall, and the calculated *TMI* can be plotted (Figure 2). For the example calculation at the TX 48-1068 SMP section, the 30-year weather data was analyzed (9/1967 to 9/1997). For the comparison of measured *versus* predicted data, measured elevation change data was also extracted from the LTPP-SMP database between 3/1987 and 9/1997.

The 30-year *TMI* value (Witczak et al., 2006) calculated from the NOAA data set for the USC00416794 station is +29.6. This value does differ slightly from the +21.7 value previously shown on the *TMI* GIS map (Figure 1) due to the difference in date ranges used in the Olaiz (2017) study.

### 3.3 Step 3: suction envelope parameters (Vann & Houston, 2021)

The suction envelope defines the maximum and minimum suction values at the surface and within the subsurface to a depth of stable suction. The suction envelopes are established using the following parameters: (1) equilibrium suction,  $\psi_e$ ,



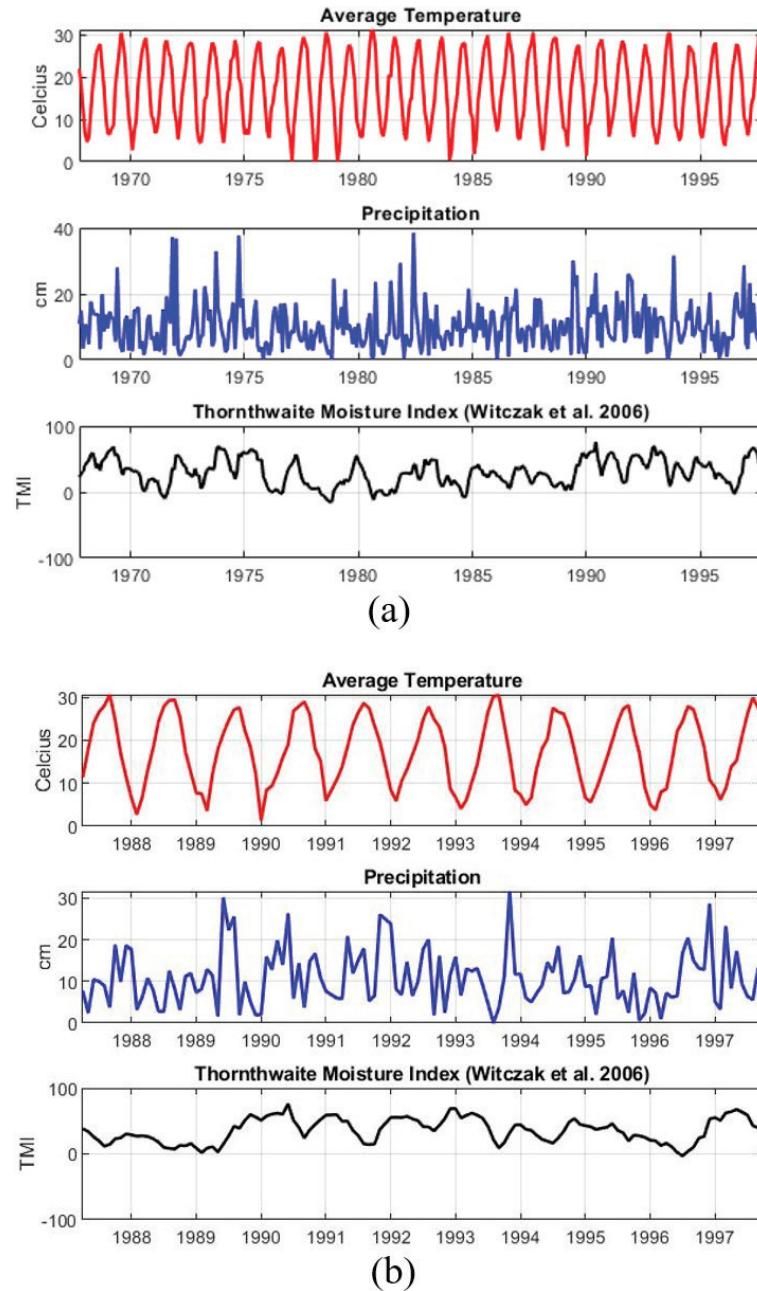


**Figure 2.** Monthly average temperature and rainfall data for NOAA weather station USC00416794 with the calculated yearly *TMI* (Witczak et al., 2006) between (a) 9/1967 and 9/1997 and (b) 3/1987 and 9/1997.

(2) depth to equilibrium suction,  $D_{\psi_e}$ , (3) change in suction at the ground surface,  $\Delta\psi$ , and (4) climate parameter,  $r$ .

The depth at which the climate-driven fluctuations in soil suction begins to stabilize, or equilibrate is determined using the Vann & Houston (2021) model (Figure 3) relatively flat uncovered sites subjected to natural climate surface flux conditions:

The equation for the Depth to Equilibrium Suction ( $D_{\psi_e}$ ) versus *TMI* regression shown above is:

$$D_{\psi_e} = 1.617 + \frac{2.617}{1 + e^{(2.36 + 0.1612TMI)}} \quad (5)$$

With an  $R^2 = 0.9045$  and standard error = 0.3147 m.

The stable, or equilibrium, suction value is determined using the Vann & Houston (2021) model (Figure 4). The soil suction unit of pF (log to the base 10 of soil suction in centimeters of water) was used in the Vann & Houston (2021) study due to its extensive

use in the geotechnical practice, with regards to unsaturated soils. Note that log of suction in kPa units is approximately equal to suction in pF units, minus 1 (i.e.,  $4.0 \text{ pF} = 3.0 \log(\text{suction (kPa)})$ ).

The equation for the Equilibrium Suction ( $\psi_e$ ) as a function of  $TMI$  is:

$$\psi_e (\text{pF}) = 0.0002TMI^2 - 0.0053TMI + 3.9771 \quad (6)$$

With an  $R^2 = 0.6539$  and a standard error = 0.1959 pF.

The limits of the potential surface flux, or potential change in suction at the surface, is determined using the Vann & Houston (2021) model (Figure 5).

The equation for the potential change in suction at the surface ( $\Delta\psi$ ) as a function of  $TMI$ , as shown above is:

$$\Delta\psi (\text{pF}) = 1.2109e^{(-0.005TMI)} \quad (7)$$

With an  $R^2 = 0.9184$  and a standard error = 0.1835 pF.

Aubeny & Long (2007) presented illustrative suction envelopes, developed from unsaturated flow analyses (Mitchell, 1980), to demonstrate that asymmetrical soil suction envelopes are expected, depending on the climate

( $TMI$ ). Aubeny & Long introduced a climate parameter,  $r$ , that is the percentage of the total anticipated change in soil suction at the surface, ( $\Delta\psi$ ), comprising the wet side of the suction envelope. The climatic parameter can be expressed in terms of the equilibrium suction ( $\Psi_e$ ) and the minimum ( $\Psi_{wet}$ ) and maximum ( $\Psi_{dry}$ ) suction at the surface ( $z = 0$ ):

$$r = \frac{(\psi_e - \psi_{wet,z=0})}{(\psi_{dry,z=0} - \psi_{wet,z=0})} = \frac{(\psi_e - \psi_{wet,z=0})}{\Delta\psi} \quad (8)$$

Houston & Vann created a relationship between the climatic parameter and  $TMI$  (Figure 6).

The equation for the climatic parameter ( $r$ ) as a function of  $TMI$  as shown above is:

$$r = 0.3725e^{(-0.009TMI)} \quad (9)$$

With an  $R^2 = 0.7998$  and a standard error = 0.1132.

Table 1 presents the suction envelope parameters for the SMP TX 48-1068 section which had 30-year  $TMI$  of 29.6.

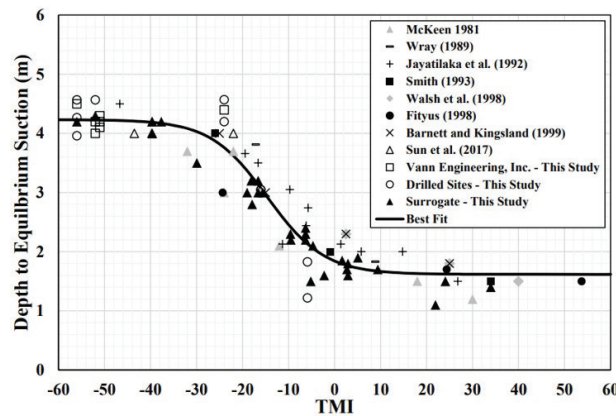


**Figure 3.** Relationship between  $TMI$  and the depth to constant soil suction for uncovered and non-irrigated sites (Vann & Houston, 2021).

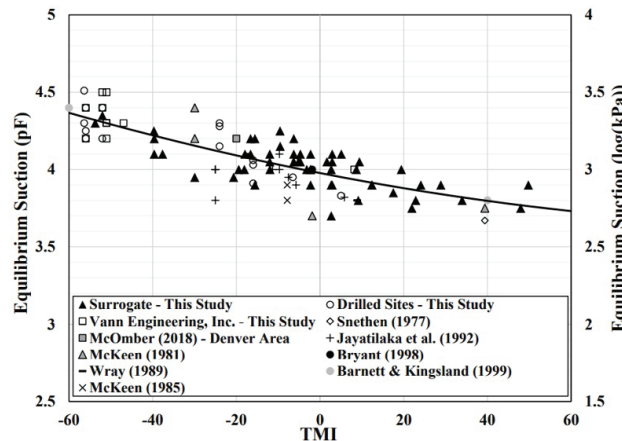


**Figure 4.** Equilibrium Suction vs.  $TMI$  with Literature Values (Vann & Houston, 2021).

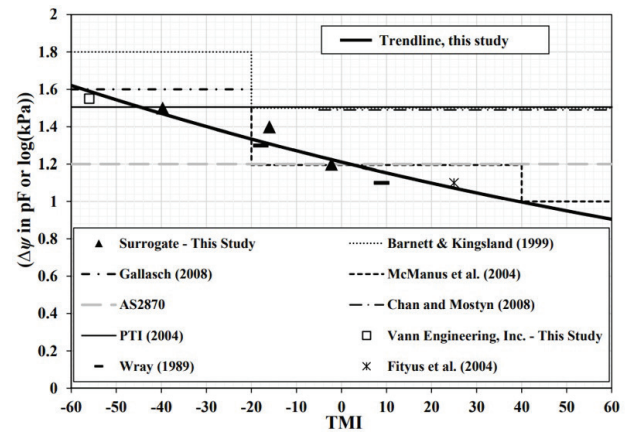


**Figure 5.** Limits of the potential change in suction at the surface vs.  $TMI$  with literature values (Vann & Houston, 2021).

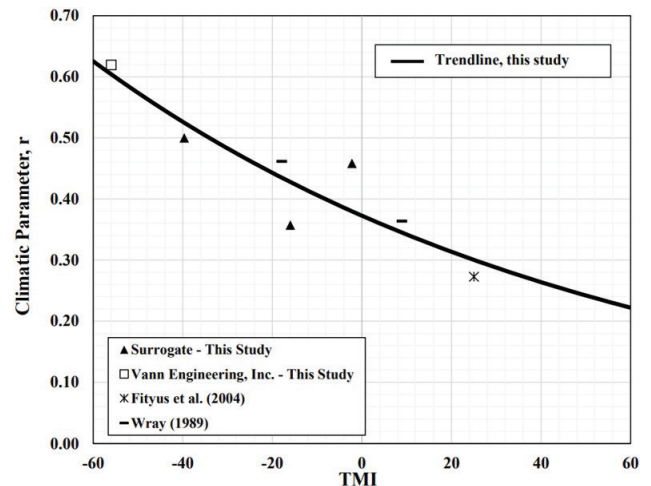


**Figure 6.** Relationship between the Climate Parameter,  $r$ , and  $TMI$  (Vann & Houston, 2021).

**Table 1.** Suction envelope parameters for the SMP TX 48-1068 per Vann & Houston (2021) with a  $TMI = 29.6$ .

Suction Envelope Parameter	Value
Depth to Equilibrium Suction ( $D_{\psi_e}$ )	1.62 m
Equilibrium Suction ( $\psi_e$ )	3.84 pF
Change in suction at the surface ( $\Delta\psi$ )	1.044 pF
Climatic parameter ( $r$ )	0.2854

### 3.4 Step 4: back calculation of variables for Mitchell's equation (1980)

The suction envelope can now be generated using the simplified unsaturated flow equation derived by Mitchell in 1980. The adjustment to the equation by Aubeny & Long (2007) for asymmetrical suction envelopes has also been incorporated into this study.

The Mitchell (1979) equation for change in suction with depth and time, simplified by (Naiser, 1997) to consider only the extreme suction cases (wet and dry), by taking the time variable to infinity, is used to obtain the shape of the envelopes.

$$\psi(z) = \psi_e + \Delta\psi e^{\left(-z\sqrt{\frac{n\pi}{\alpha}}\right)} \quad (10)$$

where,  $\psi$  is units of pF and  $z$ ,  $n$  and  $\alpha$  are in consistent units,  $\psi(z)$  is the suction value at any depth  $z$ ,  $n$  is the frequency of suction cycles, and  $\alpha$  is the diffusion coefficient.

The suction change with depth is a function of change in suction at the surface ( $\Delta\psi$  in pF units) and the equilibrium suction ( $\psi_e$ ).

Once the key parameters of the profiles are established for any given  $TMI$ , all information required for the Mitchell (1980) flow computations (such as the ratio of the diffusion coefficient to the number of seasonal cycles per year) can be back-calculated (Vann, 2019). The  $n$ ,  $\alpha$ ,  $\pi$  terms in the Mitchell (1980) equation, are back-calculated using the known equilibrium depth,  $D_{\psi_e}$ , change in suction at surface,  $\Delta\psi$ , and the 0.2 pF difference (Lytton et al., 2005; Vann, 2019), wet to dry, at the depth of equilibrium.

$$\frac{n\pi}{\alpha} = \left( \frac{\ln\left(\frac{0.2 \text{ pF}}{\Delta\psi}\right)}{-D_{\psi_e}} \right)^2 \quad (11)$$

The suction profile can now be generated using Equations 10 and 11 and the previously computed components of the surrogate suction, where suction is in pF units and depth is in meters.

### 3.5 Step 5: development of the wet and dry suction envelope

The suction envelope defines the boundary conditions for the suction value at any depth within the soil profile. At the

ground surface, the minimum (wet) and maximum (dry) suction values can be determined using the following expressions:

$$\psi_{wet_{z=0}} = \psi_e - r\Delta\psi \quad (12)$$

$$\psi_{dry_{z=0}} = \psi_{wet_{z=0}} + \Delta\psi \quad (13)$$

The minimum (wet) and maximum (dry) suctions for the TX 48-1068 section are 3.54 and 4.58, respectively.

The step size, or thickness of depth intervals ( $dz$ ) must be determined. A sensitivity analysis should be performed to determine the number of steps ( $n_s$ ) needed for the analysis; however, a value of 20 steps has been found to be sufficient for the volume change calculation performed in this study. The step size is computed by:

$$dz = \frac{D_{\psi_e}}{(n_s - 1)} \quad (14)$$

The step size for the SMP TX 48-1068 section is 8.526 cm using 20 steps with a depth of equilibrium suction of 1.62 m.

The wet and dry limit suction curves are iteratively calculated as the depth ( $z$ ) is increased from 0 (ground surface) to the depth of equilibrium suction.

$$\psi(z_i)_{wet} = \psi_e - r\Delta\psi e^{\left(-z_i\sqrt{\frac{n\pi}{\alpha}}\right)} \quad (15)$$

$$\psi(z_i)_{dry} = \psi_e + (1-r)\Delta\psi e^{\left(-z_i\sqrt{\frac{n\pi}{\alpha}}\right)} \quad (16)$$

The suction for the SMP TX 48-1068 section is shown in Figure 7.

### 3.6 Step 6: initial estimate of monthly changes in suction at the surface (Perera, 2003)

It is important to note that the following steps for determining the suction at the surface over time are specific to a deterministic approach for estimating historic ground movements. Such approach can be used for a case study, forensic analysis, or calibration efforts based on measured data. The suction at the surface over time can also be modeled using a stochastic analysis with randomly generated monthly  $TMI$  values based on the historic averages and standard deviations. The second type of analysis can be used for designs of future structures; however, an example of such analysis is not presented in this paper.

In 2003, Perera studied the relationship between in-situ moisture content, suction,  $TMI$ , and index soil properties. He developed correlations for two models: the  $TMI-P_{200}$  model, which is valid for granular base materials; and the  $TMI-P_{200}/wPI$  model, used to estimate the equilibrium suction of subbase and subgrade materials (Rosenbalm, 2011). The two models are briefly explained in the following paragraphs.

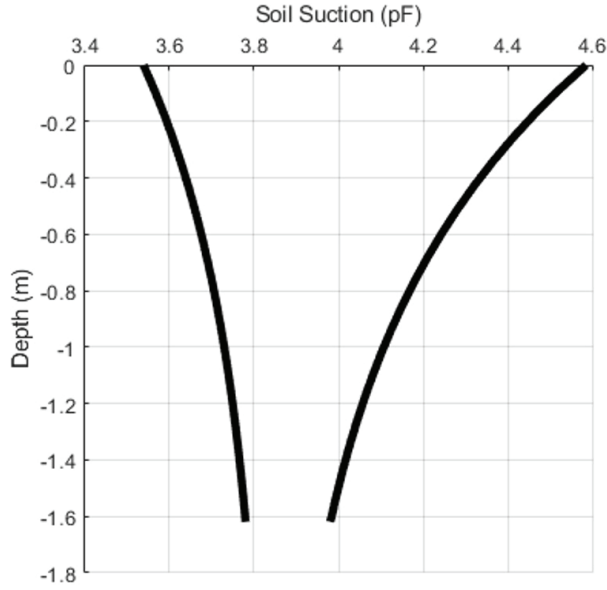


**Figure 7.** Suction envelope for the SMP TX 48-1068 section using the Vann & Houston (2021) models.

The  $TMI-P_{200}/wPI$  model is of interest to this study. This model was developed for fine-grained material, which makes it suitable for expansive soils. For such materials, in addition to  $P_{200}$ , the weighted plasticity index,  $wPI$ , property was added, where:

$$wPI = \left( \frac{P_{200}}{100} \right) PI \quad (17)$$

The  $wPI$  for the example in Paris, TX site is 18.4 based on the percent passing the #200 sieve of 74% and a  $PI$  of 20.

The following equation is used to calculate suction based  $TMI$ ,  $P_{200}$ , and  $wPI$  (Perera 2003).

$$\Psi = 0.3 \left[ e^{\left[ \frac{\beta}{TMI + \gamma} \right]} + \delta \right] \quad (18)$$

where,  $\Psi$  is the matric suction of the soil; and  $\beta, \gamma$ , and  $\delta$  are regression constants.

Rosenbalm developed equations for each regression constant. These equations are used when  $wPI$  is less than 0.5 (Rosenbalm, 2011):

$$\beta = 2.56075(P_{200}) + 393.4625 \quad (19)$$

$$\gamma = 0.09625(P_{200}) + 132.4875 \quad (20)$$

$$\delta = 0.025(P_{200}) + 14.75 \quad (21)$$

The following equations are used when  $wPI \geq 0.5$ :

$$\beta = 0.006236(wPI)^3 - 0.7798334(wPI)^2 + 36.786486(wPI) + 501.9512 \quad (22)$$

$$\gamma = 0.00395(wPI)^3 - 0.04042(wPI)^2 + 1.454066(wPI) + 136.4775 \quad (23)$$

$$\delta = -0.01988(wPI)^2 + 1.27358(wPI) + 13.91244 \quad (24)$$

### 3.7 Step 7: adjustment to the estimation of monthly changes in suction at the surface (Vann & Houston, 2021)

It has been observed by the authors that the suction at the surface calculated using the Perera (2003) model typically will not reach the long-term minimum and maximum suction values observed by Vann & Houston (2021). This may not cause a significant issue if the analysis period is relatively short (e.g., less than ten years), however; for the purpose of pavement design, which typically incorporates a design life of 20+ years, it is recommended that the surface suction values determined from the Perera model be adjusted so that they will reach the limits observed by Vann & Houston (2021). This can be conducted by normalizing the maximum and minimum suction values from the Perera model to the previously computed potential change in suction at the surface ( $\Delta \Psi$ ).

$$\begin{aligned} (\Psi_i)_{norm} &= (\Psi_{wet})_{z=0} + \\ \Delta \Psi &\left( \frac{(\Psi_i)_{z=0} - (\Psi_{Perera})_{min}}{(\Psi_{Perera})_{max} - (\Psi_{Perera})_{min}} \right) \end{aligned} \quad (25)$$

After iterating the process for each month, the adjusted surface suction values can be plotted to help visualize adjustment (Figure 8).

### 3.8 Step 8: fourier equation fit to the monthly surface suction (Aubeny & Long, 2007)

In order to model the suction changes as a function of time and depth, an equation must be developed to represent the variation of suction at the surface. Typically, a simple sinusoidal fit has been used to represent the surface suction variation with time. However, Aubeny & Long (2007), proposed that a Fourier transform can be used to improve the goodness of fit. As such, an 8<sup>th</sup> degree Fourier series is used in this analysis to fit an equation to the highly variable surface suction data.

In general, the Fourier series is a sum of sine and cosine functions that describes a periodic signal. It is represented in either the trigonometric form or the exponential form.

$$y = a_0 + \sum_{i=1}^n a_i \cos(iwx) + b_i \sin(iwx) \quad (26)$$



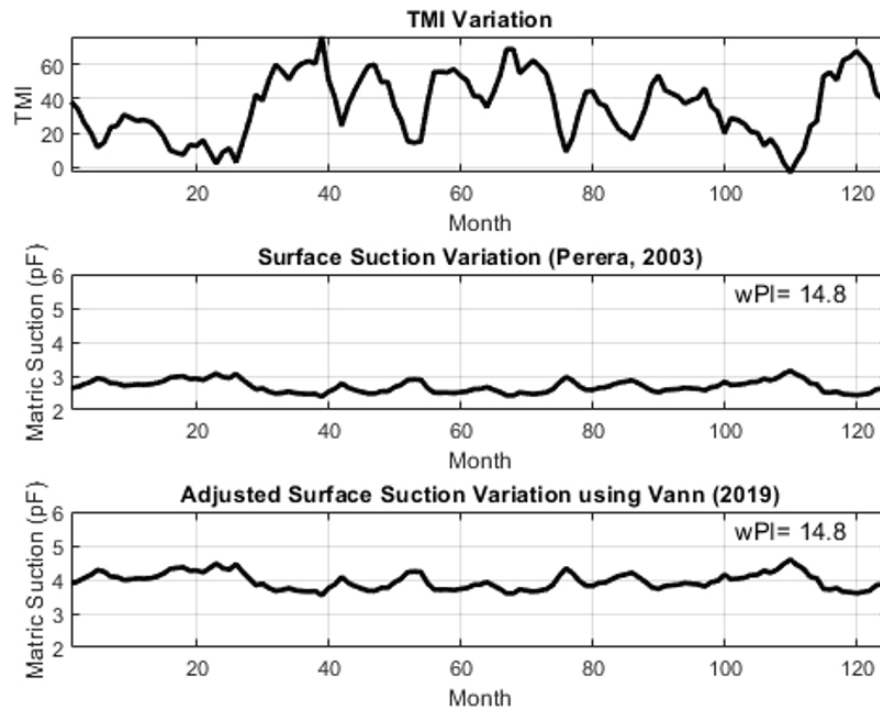


**Figure 8.** Monthly *TMI*, Perera (2003) surface suction, and the Vann (2019) adjusted surface suction for the TX 48-1068 section for the date range 3/1987 to 9/1997.

where,  $x$  represents time (for this analysis),  $a_0$  models a constant (intercept) term in the data and is associated with the  $i = 0$  cosine term,  $w$  is the fundamental frequency of the signal,  $n$  is the number of terms (harmonics) in the series, and  $1 \leq n \leq 8$ , and  $a_i$  and  $b_i$  are the fitting parameters. Additional background information on the Fourier series can be found on MathWorks help center (MathWorks, 2021).

Figure 9 presents the 1<sup>st</sup> and 8<sup>th</sup> order Fourier fit to the Vann & Houston (2021) adjusted surface suction for the TX 48-1068. The 1<sup>st</sup> order fit closely represents the original approach to modeling the surface suction flux by Lytton et al. (2005) using Mitchell (1979) equation. The adjusted  $R^2$  for the 1<sup>st</sup> order Fourier fit to the suction data is 0.2903, while the 8<sup>th</sup> order Fourier fit increases the adjusted  $R^2$  to 0.7056.

One limitation of requiring an equation to represent the surface suction, is that generally the equation fit will not be able to encompass the maximum and minimum values of the individual monthly data. For purposes of the shrink/swell volume change analysis, the inclusion of the peaks of the surface suction can provide more accurate and conservative representation of extreme events. As such, the Fourier surface suction equation can be normalized between the maximum and minimum values of the surface suction; however, this additional step was not performed as part of the example analysis presented in this paper.

Note that the initial suction is a function of the *TMI* value for that month. The initial suction (time = 0) can be adjusted using a phase shift of the Fourier equation. Lytton et al. (2005),

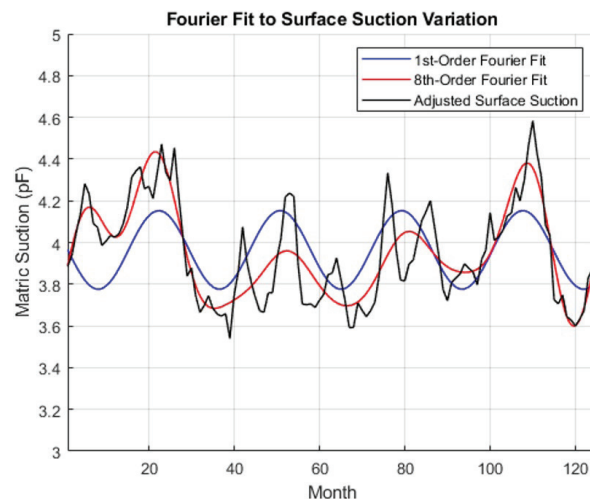


**Figure 9.** 1<sup>st</sup> and 8<sup>th</sup> order Fourier fit to the surface suction data for the TX 48-1068 section for the date range 3/1987 to 9/1997.

provided values of phase shifts for different initial conditions of the soil (wet, dry, and equilibrium). The example calculation in this report does not include the phase shift for the initial conditions.

### 3.9 Step 9: monthly suction profile (Aubeny & Long, 2007)

The next step is to model the suction profile change with time using Aubeny & Long's (2007) adjusted 1979 Mitchell equation.



$$u(y,t) = U_e - (U_{dry} - U_{wet}) \sum_{k=1}^{\infty} \alpha_k \exp(-\sqrt{\lambda k}) \cos(\tau k - \sqrt{\lambda k}) \quad (27)$$

where,  $y$  is the depth,  $\lambda = \pi y^2 n_\lambda / \alpha_k$ ,  $\tau = 2\pi t n_\lambda$ ,  $n_\lambda$  = lowest frequency of cyclic suction variation, and  $\alpha_k = (2/k\pi) \sin(k\pi r)$  with  $k = 1, 2, 3, \dots$

For a given point in time, the suction profile can be estimated using the Aubeny & Long approach. Figure 10 presents the estimated suction at time = 1 month for the TX 48-1068 SMP site. Note that the long-term or extreme boundaries of the suction profile are known from the Vann (2019) correlations with the 30-year *TMI* value previously presented herein.

The monthly change in suction at each depth can be determined by calculating the following months suction profile and taking the difference of the two values at each depth. It is this ongoing change in soil suction with time that drives the volume change of shrink/swell soils. Figure 11 shows the suction profiles for  $t = 1$  month, and  $t = 2$  months, for the TX 48-1068 SMP site. Figure 12 shows the suction profiles for month 1 through month 12.

Figure 13 presents the monthly suction profiles over the date range 3/1987 to 9/1997 life for TX 48-1068 SMP section. From the figure, the significant swings of the suction profile from wet to dry, over the date range 3/1987 to 9/1997, can be observed. The monthly change in suction

at each depth in the soil profile can be determined from this model.

To account for hysteresis effects associated with the wetting and drying of soil, it is important to record if the

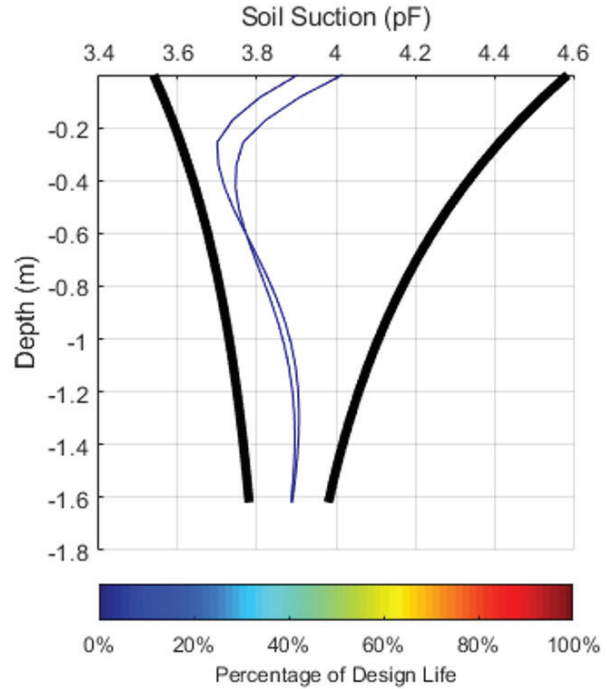


**Figure 11.** The estimated initial suction profiles (time = 2 months) for TX 48-1068 section.

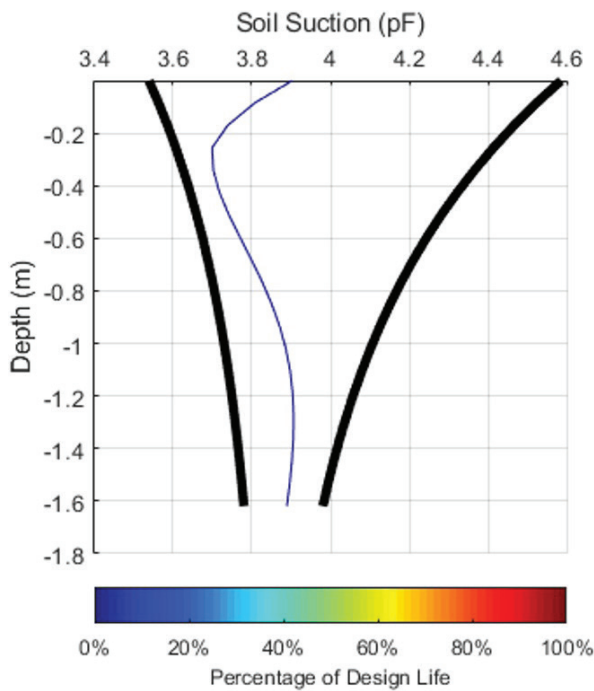


**Figure 10.** The estimated initial suction profile (time = 1 month) for TX 48-1068 section.

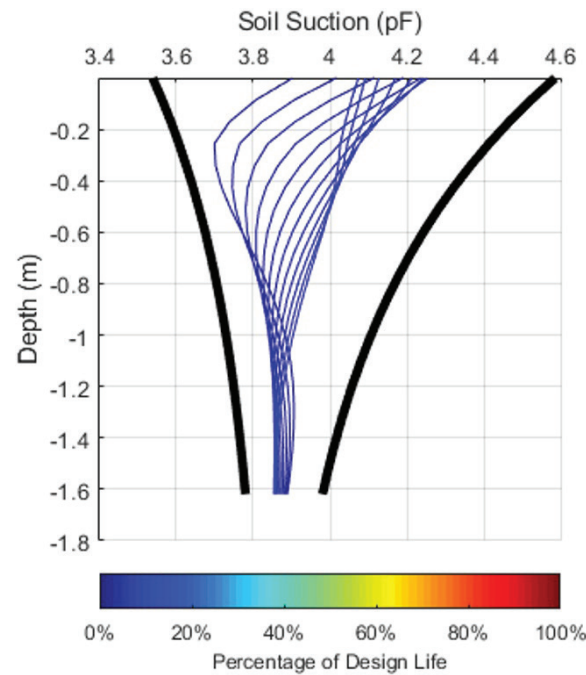


**Figure 12.** The estimated initial suction profiles (time = 12 months) for TX 48-1068 SMP section.

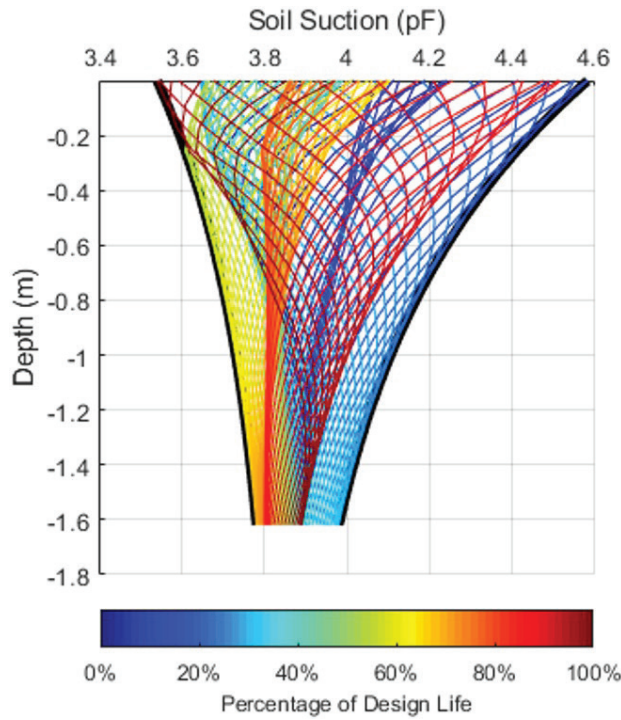


**Figure 13.** Monthly suction profiles over the date range 3/1987 to 9/1997.

soil is wetting or drying at each depth and time during the iterative analysis. This information will be used during the strain calculation discussed later in this report.

### 3.10 Step 10: suction profile adjustments due to varying boundary conditions

It is possible that the project site has a variable groundwater table, nearby vegetation, or is constructed using a moisture barrier. If any of these boundary conditions are present, the suction envelope and profile must be adjusted. (e.g. the suction profile will reach osmotic suction at the groundwater table depth). No variable boundary conditions were included in this example calculation.

### 3.11 Step 11: net normal stress profile

The net normal, or overburden stress, is a key component of shrink/swell volume change determination as it will help reduce potential soil swelling and can increase soil shrinkage. The overburden stress profile is determined using the conventional total stress approach.

$$\sigma_z = \sum (\gamma_{soil} z) \quad (28)$$

Note that the water content is subject to change over time as the soil suction changes, which will affect the magnitude of the net normal stress. However, for purposes of this example calculation, the effect of the changing water

content on the net normal stress is negligible and is not included in the analysis.

If there are foundation loads or increases overburden stresses due to pavement layers above the subject soil profile, an increase of stress will be applied throughout the net normal stress profile.

### 3.12 Step 12: suction compression index (Covar & Lytton, 2001)

The most widely accepted method for estimating volumetric strain is the one developed for the Texas DOT and the Federal Highway Administration, FHWA, by Lytton et al. (2005), which is as follows:

$$\frac{\Delta V}{V} = -\gamma_h \log \left( \frac{h_f}{h_i} \right) - \gamma_\sigma \log \left( \frac{\sigma_f}{\sigma_i} \right) - \gamma_\pi \log \left( \frac{\pi_f}{\pi_i} \right) \quad (29)$$

where,  $\frac{\Delta V}{V}$  is the volumetric strain (volume change with respect to initial volume);  $\gamma_h$  is the the matric suction compression index;  $\gamma_\sigma$  is the mean principal stress compression index;  $\gamma_\pi$  is the osmotic suction compression index;  $h_i$  is the initial matric suction;  $h_f$  is the final matric suction;  $\sigma_i$  is the initial mean principal stress;  $\sigma_f$  is the final mean principal stress;  $\pi_i$  is the initial osmotic suction; and  $\pi_f$  is the final osmotic suction.

Although, total suction is the sum of matric suction and osmotic suction, Fredlund wrote “Matric suction in a soil mass change is a result of moisture infiltration and evaporation at the ground surface. Osmotic suction in the soil does not appear to be highly sensitive to modest changes in the water content of the soil. As a result, a change in the total suction is quite representative of a change in the matric suction.” (Fredlund et al., 2012). Also, Lytton wrote: “It is the change of matric suction that generates the heave and shrinkage, while osmotic suction rarely changes appreciably.” (Lytton et al., 2005). Thus, the change in matric suction is responsible to shrinkage and heave and osmotic suction does not affect enough to be concerned (Lytton et al., 2005; Fredlund et al., 2012). Thus, the equation can be rewritten as:

$$\frac{\Delta V}{V} = -\gamma_h \log \left( \frac{h_f}{h_i} \right) - \gamma_\sigma \log \left( \frac{\sigma_f}{\sigma_i} \right) \quad (30)$$

Note that the net normal stress portion of the equation is added if the soil is wetting (swelling) and subtracted if the soil is drying (shrinking).

The Suction compression index,  $\gamma_h$ , is a parameter used to relate total suction to volume change to predict heave or shrinkage in expansive soils. This value can either be measured or estimated using soil index properties (Atterberg limits and gradation) as described in Covar & Lytton (2001).

First, the mineralogical zone is determined using Figure 14 with soils plasticity index ( $PI$ ) and liquid limit ( $LL$ ).

The zone for the TX 48-1068 SMP section site is Zone 2, using a  $LL = 60\%$  and a  $PI = 40\%$ .

The percent fine clay ( $\%fc$ ) is then calculated using the percent passing #200 sieve ( $P_{200}$ ) and the percent clay ( $\%clay$ ) obtained via hydrometer testing.

$$\%fc = \left( \frac{\%clay}{P_{200}} \right) \quad (31)$$

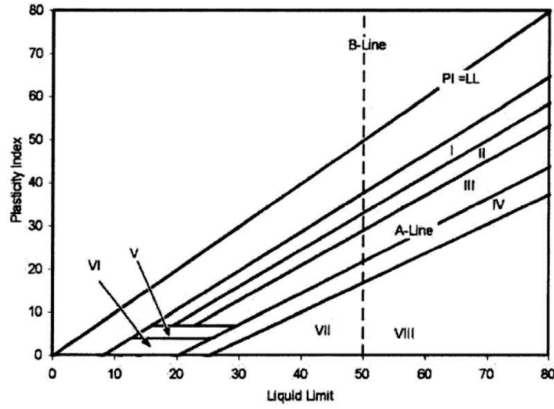


**Figure 14.** Mineralogical zones for soil (Covar & Lytton, 2001), units in %.

The  $\%fc$  for the example site is 21.05%, using a  $\%clay = 20\%$  and  $P_{200} = 95\%$ .

The average suction compression index ( $\gamma_0$ ) can now be determined using the charts developed by Covar & Lytton (2001), which are separated by mineralogical zones (Figure 15).

The average suction compression index for the TX 48-1098 SMP section is 0.051 using Zone 1,  $\%fc = 43.78\%$ ,  $LL = 38\%$ , and  $PI = 20\%$ .

The adjusted suction compression index ( $\gamma_h$ ) is now determined by:

$$\gamma_h = \gamma_0 (\%fc) \quad (32)$$

The adjusted suction compression index for TX 48-1098 SMP section site is 0.0223.

The hysteresis effects of the soil are now accounted for using the equations from the PTI (2008) Manual. The wetting and drying suction compression indices must be calculated for each depth and time of the analysis using the recorded wetting/drying information from Step 9.

$$\gamma_{swell} = \gamma_h e^{(\gamma_h)} \quad (33)$$

$$\gamma_{shrink} = \gamma_h e^{(-\gamma_h)} \quad (34)$$

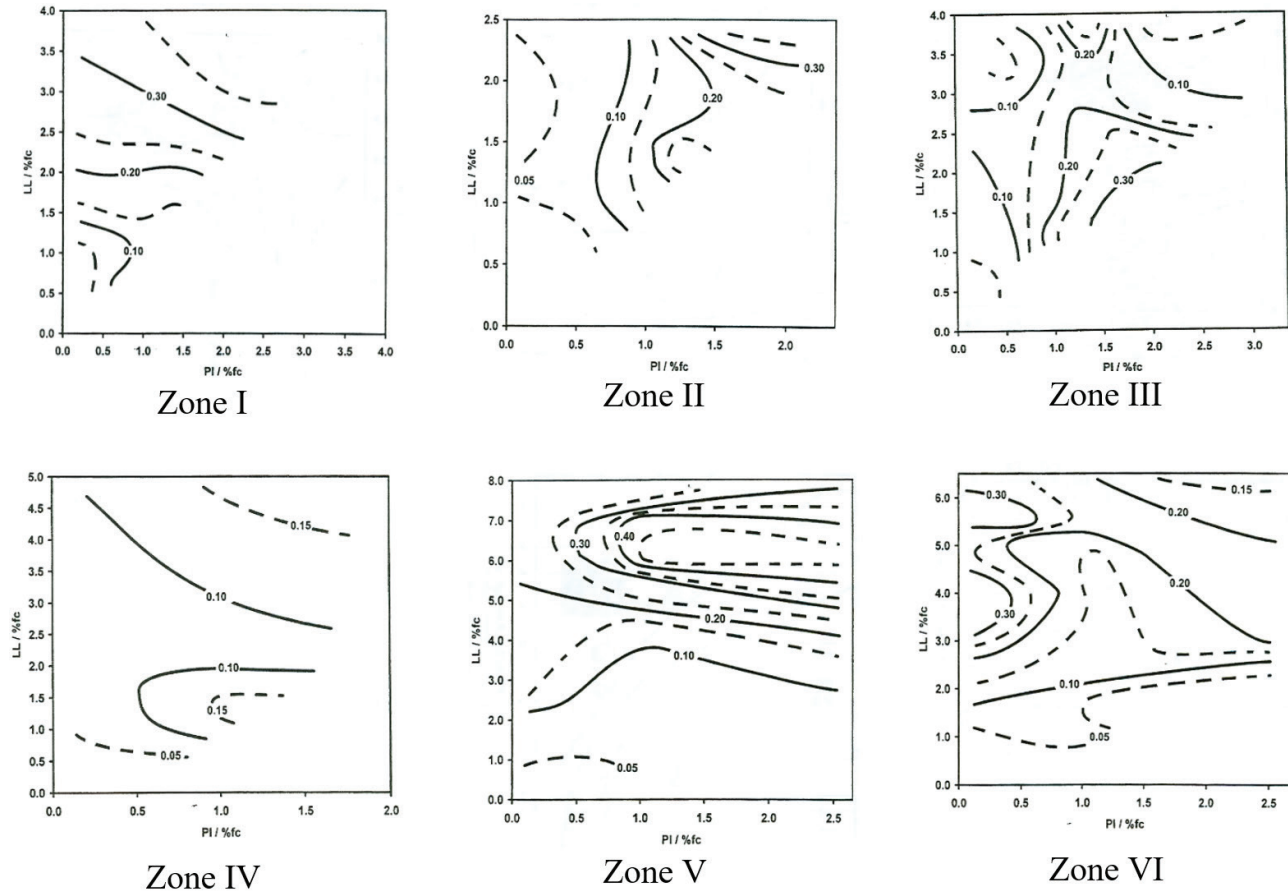


**Figure 15.** Suction Compression Index based on Mineralogical Classification and Soil Index Properties (Covar & Lytton, 2001).

### 3.13 Step 13: monthly strain calculation

The mean principal stress compression index,  $\gamma_\sigma$ , can be calculated using its relation to the compression index,  $C_c$ , and void ratio,  $e$ , as follows (Lytton et al., 2005):

$$\gamma_\sigma = \frac{C_c}{1 + e_0} \quad (35)$$

where,  $C_c$  is the compression index; and  $e_0$  is the void ratio. For purposes of this example calculation, the mean principal stress compression index was assumed to be 10% of the suction compression index as recommended by Lytton et al. (2005).

The mean principal stress must be iteratively determined at each depth and time step, as it is a function of the net normal stress and the wetting/drying condition.

$$\sigma = \frac{1 + 2K_0}{3} \sigma_z \quad (36)$$

where,  $\sigma_z$  is the previously calculated vertical stress at a point below the surface in the soil mass; and  $K_0$  is the 1-D at-rest lateral earth pressure coefficient.

$$K_0 = e \left( \frac{1 - \sin(\phi')}{1 + \sin(\phi')} \right) \left( \frac{1 + d \sin(\phi')}{1 - k \sin(\phi')} \right)^n \quad (37)$$

Values of coefficients  $e$ ,  $d$ ,  $k$ , and  $n$  for different soil conditions are given in Table 2.

The angle of internal friction,  $\phi'$ , can be estimated from its empirical correlation with plasticity index,  $PI$ , based on triaxial compression tests.

$$\phi' = 0.0016PI^2 - 0.3021PI + 36.208 \quad (38)$$

The internal angle of friction for the TX 48-1068 SMP site is  $30.8^\circ$  using a  $PI = 20$ .

Using the data developed from the iterative steps discussed above, and the suction-overburden-strain relationships, the volume change over time can be estimated. Figure 16 presents the volume change estimation for the Paris, TX site.

### 4. Estimated volume change comparison to measured data

The estimated volume change from the proposed framework for the TX 48-1068 site was compared to the measured data gathered from the LTPP SMP database. The estimated data was normalized to the value of the first measurement. Figure 17 presents the measured and estimated volume change for the TX 48-1068 SMP section.

**Table 2.** Lateral earth pressure parameter coefficients.

Conditions	$K_0$	$e$	$d$	$k$	$n$
Cracked	0	0	0	0	1
Drying (Active)	1/3	1	0	0	1
Equilibrium (at rest)	1/2	1	1	0	1
Wetting (within movement active zone)	2/3	1	1	0.5	1
Wetting (below movement active zone)	1	1	1	1	1
Swelling near surface (passive earth pressure)	3	1	1	1	2

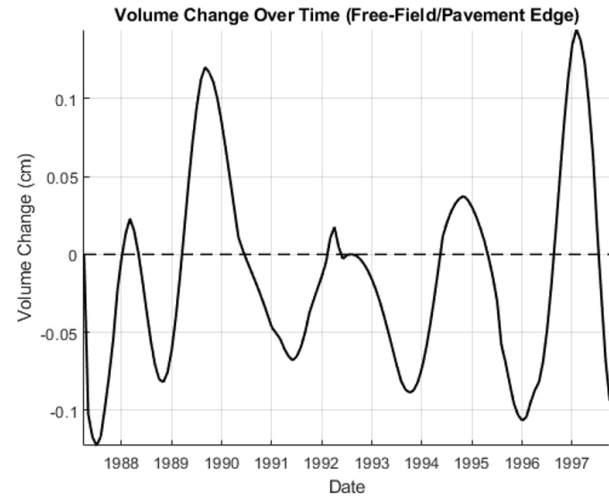


**Figure 16.** Volume change over time for the TX 48-1068 site.

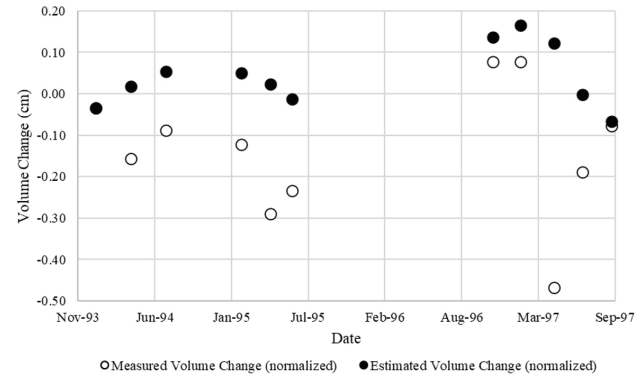


**Figure 17.** Measured vs. estimated volume change normalized to the initial measurement for the TX 48-1068 SMP Section.

A preliminary analysis of the proposed framework presented in this paper was performed on eight more sections from Alabama, Colorado, Montana, Nebraska, South Dakota and Texas from the LTPP SMP program. The resulting comparison, presented in Figure 18, of the estimated volume change and the measured field data for 70 data points yielded a coefficient of correlation of 0.45. This result is promising, and the data allows for a calibration of the model to the field conditions once all the parameters have been defined.



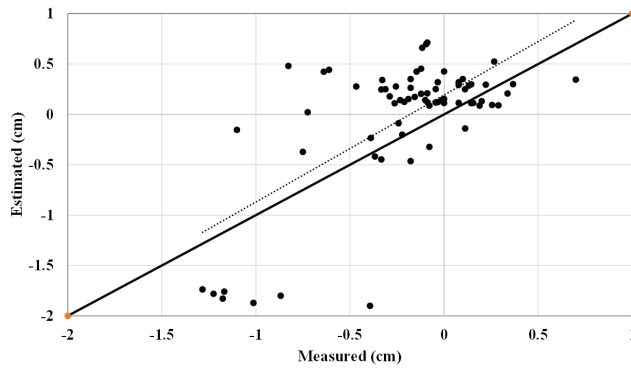


**Figure 18.** Measured vs. estimated volume change normalized to the initial measurement for the eight SMP sections.

## 5. Conclusions

This paper presented a preliminary mechanistic-empirical framework for the estimation of volume change. The models are universal and can be used in any part of the world provided measured data is available to calibrate for local conditions. Ongoing calibration effort with the remaining LTPP SMP sections will allow obtaining calibration factors for the proposed framework that will improve the estimation of the volume change predictions under pavements and facilitate the implementation into current design procedures.

## Acknowledgements

This work is based on part of research funded by the National Academies of Science, Engineering, and Medicine Transportation Research Board's (TRB) National Cooperative Highway Research Program (NCHRP) 01-59. The opinions, conclusions, and interpretations are those of the authors and not necessarily of NCHRP.

## Declaration of interest

The authors have no conflict of interests pertaining to the material included in this paper.

## Authors' contributions

Austin Olaiz: conceptualization, formal analysis, methodology, writing – original draft. Mohammad Mosawi: data curation, formal analysis, writing – original draft. Claudia Zapata: conceptualization, funding acquisition, project administration, supervision, writing – review & editing.

## List of symbols

$a$	a coefficient
$a_0$	constant (intercept) term, associated with the $i=0$ cosine term

$a_i$	fitting parameter
$b_i$	fitting parameter
$C_c$	compression index
$D_{\psi_e}$	depth to equilibrium suction
$dz$	thickness of depth intervals
$e$	void ratio
$f_1$	fraction of the number of days in month divided by the average number of days in month, 30
$f_2$	fraction of the number of hours in a day divided by the base of 12 h in a day
$h_i$	initial matric suction
$h_f$	final matric suction
$I$	annual heat index
$K_0$	lateral earth pressure coefficient
$n$	frequency of suction cycles
$n_\lambda$	lowest frequency of cyclic suction variation
$n_z$	number of steps needed for the analysis
$P$	precipitation for the given month
$P_{200}$	percent passing #200 sieve
$PI$	plasticity index
$t$	mean monthly temperature in degrees Celsius
$t_i$	mean temperature for the $i^{\text{th}}$ month
$r$	climate parameter
$w$	fundamental frequency of the signal
$wPI$	weighted plasticity index
$x$	time of the analysis
$z$	depth
$\alpha$	diffusion coefficient
$\beta, \gamma, \delta$	regression constants
$\Delta V / V$	volumetric strain
$\gamma_h$	matric suction compression index
$\gamma_{soil}$	unit weight of the soil
$\gamma_\sigma$	mean principal stress compression index
$\gamma_\pi$	osmotic suction compression index
$\varnothing'$	angle of internal friction
$\pi_i$	initial osmotic suction
$\pi_f$	final osmotic suction
$\sigma_f$	final mean principal stress
$\sigma_i$	initial mean principal stress
$\sigma_z$	net normal, or overburden, stress
$\Delta\psi$	change in suction at the ground surface
$\psi$	matric suction
$\psi_e$	equilibrium suction
$\psi_{wet,z=0}$	minimum (wet) suction at the surface ( $z = 0$ )
$\psi_{dry,z=0}$	maximum (dry) suction at the surface ( $z = 0$ )
$\psi(z)$	suction value at any depth $z$
$\%fc$	percent of fine clay



## References

- ASTM D4546. (2021). *Standard Test Methods for One-Dimensional Swell or Collapse of Soils*. ASTM International, West Conshohocken, PA. <https://doi.org/10.1520/D4546-21>
- Aubeny, C., & Long, X. (2007). Moisture diffusion in shallow clay masses. *Journal of Geotechnical and Geoenvironmental Engineering*, 133(10), 1241-1248.
- Bear, J. (1972). *Dynamics of fluids in porous media*. American Elsevier.
- Covar, A.P., & Lytton, R.L. (2001). *Estimating soil swelling behavior using soil classification properties*. ASCE.
- Federal Highway Administration – FHWA (1995) *LTPP seasonal monitoring program site installation and initial data collection section 481068*. FHWA, Paris, TX.
- Federal Highway Administration – FHWA (2021). *LTPP InfoPave*. Retrieved in July 21, 2021, from <https://infopave.fhwa.dot.gov/>
- Fredlund, D.G., Rahardjo, H., & Fredlund, M.D. (2012). *Unsaturated soil mechanics in engineering practice*. Wiley.
- Holtz, R.D., & Gibbs, H. (1956). Engineering properties of expansive clays. *Transactions of the American Society of Civil Engineers*, 121(1), 641-677.
- Houston, S., & Houston, W. (2017). A suction-oedometer method for computation of heave and remaining heave. In *Proceedings of the 2nd PanAm Conference on Unsaturated Soils*, Dallas. <https://doi.org/10.1061/9780784481677.005>
- Lytton, R., Aubeny, C., & Bulut, R. (2004). *Design procedure for pavements on expansive soils: volume 1 - Report 0-4518-1/0-4518*. Texas Department of Transportation, Austin, TX.
- Lytton, R., Aubeny, C., & Bulut, R. (2005). *Design procedures for soils on expansive soils: volume 1 - Report FHWA/TX-05/0-4518*. Texas Department of Transportation, Austin, TX.
- Lytton, R.L. (1977). Foundations in expansive soils. In C.S. Desai & J.T. Christian (Eds.), *Numerical methods in Geotechnical Engineering* (pp. 427-458). McGraw-Hill.
- MathWorks (2021). *Help center - Fourier series*. Retrieved in July 21, 2021, from <https://www.mathworks.com/help/curvefit/fourier.html>
- McKeen, R.G., & Hamberg, D.J. (1981). Characterization of expansive soils. *Transportation Research Record: Journal of the Transportation Research Board*, (790), 73-78.
- Mitchell, P.W. (1979). *The structural analysis of footings on expansive soil*. Kenneth W.G. Smith & Associates.
- Mitchell, P.W. (1980). The concepts defining the rate of swell of expansive soils. In *Proceedings of the 4th International Conference on Expansive Soils*, Denver.
- Naiser, D. (1997). *Procedures to predict vertical differential soil movement for expansive soil* [Master's thesis]. Texas A&M University, College Station, TX.
- Olaiz, A. H., Singhar, S. H., Vann, J. D., & Houston, S. L. (2017). Comparison and applications of the Thornthwaite moisture index using GIS. In L. R. Hoyos, J. S. McCartney, S. L. Houston, & W. J. Likos (Eds.), *PanAm Unsaturated Soils 2017: Applications, Geotechnical Special Publication 302* (pp. 280–289). Reston, VA: ASCE
- Perera, Y.Y. (2003). *Moisture equilibria beneath paved areas* [Unpublished doctoral dissertation]. Arizona State University.
- Post-Tensioning Institute – PTI (2004). *Design of post-tensioned slabs-on-ground* (3rd ed.). PTI.
- Post-Tensioning Institute – PTI (2008). *Design & construction of post-tensioned slabs-on-ground* (3rd ed.). PTI.
- Rosenbalm, D. (2011). *Reliability associated with the estimation of soil resilient modulus at different hierarchical levels of pavement design* [Master's thesis]. Arizona State University. Retrieved in July 21, 2021, from <http://hdl.handle.net/2286/R.I.14453>
- Texas Department of Transportation – TxDOT (1978). *Method for determining the potential vertical rise, PVR - TxDOT-124-E*. TxDOT, Austin, TX.
- Thornthwaite, C. (1948). An approach toward a rational classification of climate. *Geographical Review*, 38(1), 55-94.
- Vann, J.D. (2019). *A soil suction-oedometer method and design soil suction profile recommendations for estimation of volume change of expansive soils* [Doctoral dissertation]. Arizona State University. Retrieved in July 21, 2021, from <http://hdl.handle.net/2286/R.A.216886>
- Vann, J.D., & Houston, S. (2021). Field Suction Profiles for Expansive Soil. *Journal of Geotechnical and Geoenvironmental Engineering*, 147(9), 04021080. [https://doi.org/10.1061/\(ASCE\)GT.1943-5606.0002570](https://doi.org/10.1061/(ASCE)GT.1943-5606.0002570).
- Witczak, M.W., Zapata, C.E., & Houston, W.N. (2006). *Models incorporated into the current enhanced integrated climatic model: NCHRP 9-23 Project findings and additional changes after version 0.7 - Final report, Project NCHRP 1-40D*. AASTHO & FHWA, Washington, DC.

## The role of unsaturated soil mechanics in unconventional tailings deposition

Paul Simms<sup>1#</sup> 

Article

### Keywords

Unsaturated soils  
Elasto-plastic  
Large strain consolidation  
Desiccation  
Shear strength  
Tailings

### Abstract

Desiccation (water loss by drying or freeze-thaw sufficient to generate matric suction), can influence the performance of a tailings deposit both positively and negatively. The significance of desiccation is largest in tailings that have been dewatered prior to deposition, by thickening or filtration. Such tailings can be “stacked” or deposited with a significant slope, which usually implies that a substantial volume of tailings remain above water. Under such conditions the tailings, by accident or by design, may undergo desiccation before burial by fresh tailings. Desiccation can contribute substantially to strength, above and beyond the contribution arising from increase in density, through stress history effects. For some deposits, it is required practice that at least some tailings undergo desiccation to improve, particularly when those tailings form a structural part of a deposit. If, however, tailings remain exposed to the atmosphere in an unsaturated state for some period of time, this may have potential negative consequences through oxidation of sulphide minerals and the formation of acid drainage. This paper describes previous research on the strength gained through desiccation in tailings, and on modelling work that incorporates unsaturated soil phenomena into consolidation analysis. Both types of research are applied to a real field site, providing an example of how novel improvements to tailings management can arise out of application of principles of unsaturated soil mechanics.

## 1. Introduction

Mining involves the excavation of significantly large volume of rock or soil for purposes of extracting a specific commodity: most often the commodity itself (e.g. gold, copper, bauxite, rare earth metals, etc) is a small fraction of the total volume of geologic material that is processed. Most of this geologic material is combined with large amounts of water to facilitate grinding and/or mineral separation. Due to this reason, mining inevitably results in the generation of large volumes of high water content slurry, with particles size generally ranging from a sandy silt for mining of rock, to finer particles containing clay minerals when the parent material is a soil (such as for bauxite or oil sands operations). In all cases, the tailings are transported as a high water content slurry between different operations in the mill (Willis, 2006). At the majority of mines, the tailings are deposited directly into a dammed impoundment, where the water content is usually at least twice their liquid limit (Vick, 1990). New mines show a trend of increasing production rates, and mines that process over 200,000 m<sup>3</sup> of rock a day, with mine lives in the order of

decades, are becoming more common. Such rates of mining results in large tailings deposits, often covering several square kilometres, with dam heights in certain scenarios reach up to 400 m. The dams of impoundments themselves are some of largest earth structures in the world.

Unfortunately, tailings dams fail with some regularity, at a rate of 4 or 5 a year. Some of these failures have resulted in loss of life and up to billions of dollars in damage to property and / or associated environmental cleanup costs (Rico et al., 2008). This includes the well-known failure at Brumadinho in Brazil, which killed about 300 people in 2019. Other failures of significance that have been analyzed in the geotechnical literature include the Mount Polley failure in Canada in 2014 (Zabolotnii et al., 2021), the los Frailes dam failure in 1998 in Southern Spain, and the Merriespruit failure (Fourie et al., 2001). Tailings dams fail for a variety of reasons, including poor foundation conditions, poor water level control, and damage due to seismic events. Industry response to these failures has been twofold: either to improve the level of care afforded to tailings dam design and maintenance through changes in regulation or management culture, or to implement

<sup>#</sup>Corresponding author. E-mail address: Paul.simms@carleton.ca

<sup>1</sup>Carleton University, Department of Civil and Environmental Engineering, Ottawa, Canada.

Submitted on April 23, 2021; Final Acceptance on July 27, 2021; Discussion open until November 30, 2021.

<https://doi.org/10.28927/SR.2021.066721>



This is an Open Access article distributed under the terms of the Creative Commons Attribution License, which permits unrestricted use, distribution, and reproduction in any medium, provided the original work is properly cited.

technologies that improve the geotechnical performance of the tailings themselves.

The most common alternatives technologies involve dewatering the tailings to some degree before deposition, either by thickening in large ( $> 20$  m high) thickeners, or through filtration, which facilitates quicker consolidation. Often, such thickened or filtered tailings are transported by pipeline, conveyer, or truck, to various points in a tailings impoundment. As the dewatered tailings possess a small undrained shear strength ( $< 1$  kPa and often measured using rheometry and referred to as a yield stress) at their initial state out of the pipe, they will naturally stack (Mizani et al., 2013; Henriquez & Simms, 2009) and form discrete layers. This allows for evaporation to assist in further dewatering and densification of the tailings, before deposition cycles around again and those tailings are buried (Simms, 2017). An example of such a deposit is shown in Figure 1, where the deposition point is changed every 2 weeks, such that one circuit of the embankment is completed each year. Figure 2, from a different site, shows the difference between older more desiccated tailings, and a younger layer deposited on top.

How such deposition schemes are conducted are typically based on the operator's experience. This paper will show that hydro-mechanical analysis, which includes consideration of unsaturated soil mechanics, may provide helpful guidance to these types of operations.

Figure 3 indicates conceptually the progress of dewatering of a given layer of thickened or filtered tailings. Initially, the tailings dewater through sedimentation and consolidation. Depending on the commodity and the extent of initial dewatering, deformations at this stage are large: void ratios reduce from values above 2 (sometimes as high as 5) to close to 1. Simultaneously, the upper part of the layer may begin to desaturate. With the addition of a new layer, several behaviours will manifest, including the effect of additional weight on the previously desiccated tailings, the acceleration of consolidation of the new layer due to rewetting occurring in the bottom layer, and the potential for wetting-induced collapse in the previously desiccated lower layers.

The hydro-mechanical evolution of a tailings deposit is therefore somewhat complex. The reader may wonder if indeed it is worthwhile to consider this complexity. It may well be worthwhile, for two main reasons. The extent of desiccation or desaturation is important to the tailings impoundment: desiccation leads to an increase in strength through multiple mechanisms, however, if a layer of tailings becomes desaturated and remains so for an extensive period of time there may be a potential risk of acid generation. The paper proceeds by i) briefly reviewing the positive and negative effects associated with the unsaturated behaviour, then; ii) providing some data from large laboratory experiments and the field on multilayer deposition of tailings; and finally; iii) showing examples of numerical simulation of a field site.

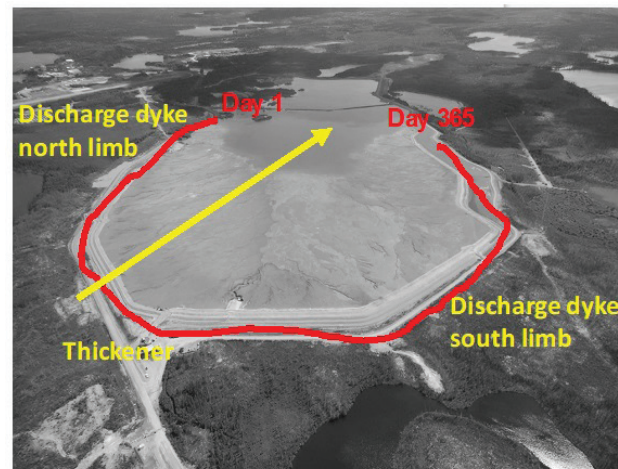


**Figure 1.** Example of a thickened tailings deposit, where deposition is cycled from different points on a perimeter embankment – here the circuit is complete in 1 year.



**Figure 2.** A thickened tailings site, where a relatively fresh layer can be distinguished from the underlying desiccated layer (Courtesy Jason Crowder).

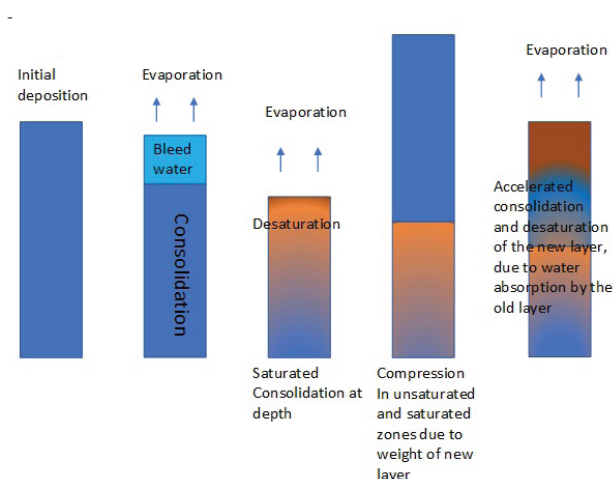


**Figure 3.** Phenomena contributing to post-deposition dewatering in layered tailings deposits (modified from Qi & Simms, 2018).



## 2. Desiccation and its consequences for strength and acid generation

### 2.1 Strength

Desiccation imparts additional strength to tailings by i) contributing to higher density; ii) an increase in effective stress through matric suction, that would be dissipated if the tailings are re-wetted; and iii) stress history effects. The last effect is most relevant to the contribution to strength by desiccation to tailings that are subsequently buried and rewetted. In the scientific literature, the stress path experienced by the tailings has been explored for relatively thin layers (100 mm to 300 mm), where samples are allowed to desiccate, are rewetted to eliminate matric suctions (by application of water until ponding is observed and/or measured suctions are dissipated), and then samples are either trimmed or extracted using thin-wall tubes, and subsequently tested in simple shear or tri-axial devices (Al-Tarhouni et al., 2011; Daliri et al., 2014, 2016). Trimmed samples are usually obtained from short columns (~ 100 mm); samples extracted using thin-walled tubes are extracted from large (1m by 1m in plan) physical simulations of multilayer deposition (drybox tests). An example of sampling from one of the larger multilayer drybox tests is shown in Figure 4.

The samples obtained from the columns or drybox tests are trimmed and placed in element testing apparatus, where they are subsequently consolidated before shearing. This generates a stress path that comprises initial sedimentation, consolidation, desiccation, rewetting, and then consolidation, the last simulating burial of a layer of tailings by a substantial thickness of newer tailings. Subsequent results are shown for a gold tailings with the following properties: Specific gravity, liquid limit, plastic limit, and shrinkage limit were determined as 2.89, 22.5%, 20%, and 18% respectively; while the  $D_{90}$ ,  $D_{50}$ ,  $D_{30}$ , and  $D_{10}$  values are 120, 30, 12, 1.5  $\mu\text{m}$ , respectively. Figures 5 through 7 show the Water-retention curve / soil-water



**Figure 4.** Drying box test (1m × 1m in plan) showing extraction of samples with thin-walled tubes (from Daliri et al., 2016).

characteristic curve (WRC), examples of stress paths before shearing, and the results of constant volume simple shear tests in terms of shear stress and strain. In terms of stress path

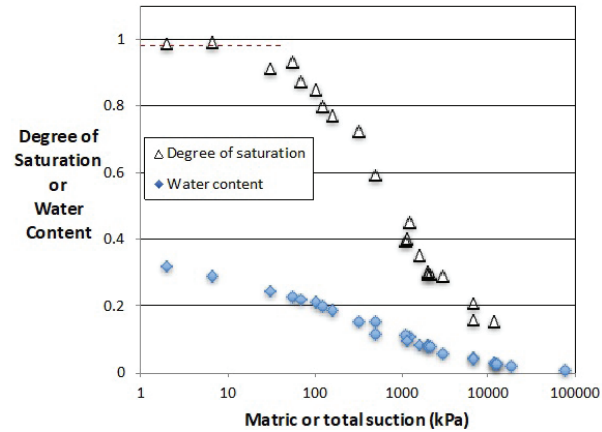


**Figure 5.** WRC of the gold tailings samples shown in subsequent figures, obtained by conventional axis-translation for suction below 500 kPa, and paired measurements of total suction (Dewpoint Hygrometer) and water content for higher measurements.

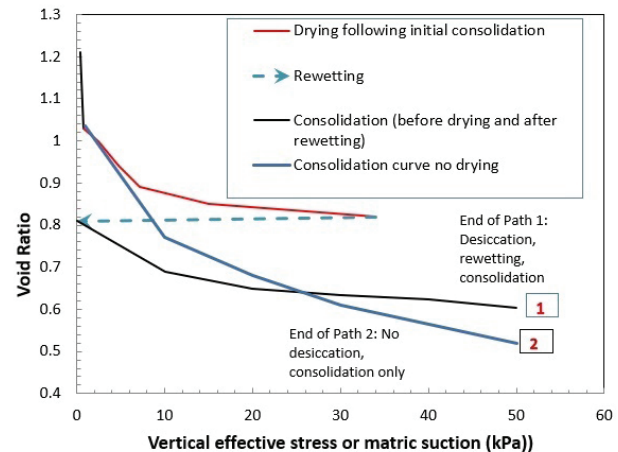


**Figure 6.** Example of stress paths imposed on laboratory samples before element testing.

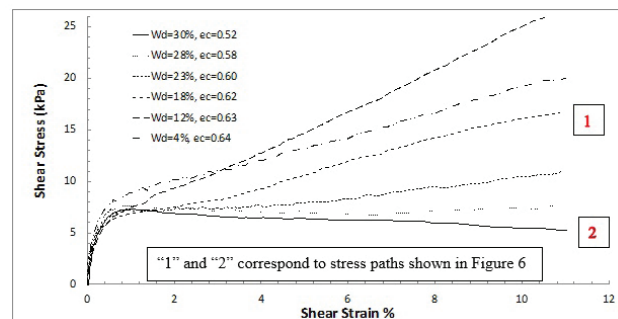


**Figure 7.** Shear strength in constant volume simple shear of gold tailings desiccated, re-wet, and then consolidated to 50 kPa. “Wd” is water content after initial desiccation but before rewetting, “ec” is the void ratio after rewetting and consolidation to 50 kPa.

(Figure 6), the most interesting finding is that the previously desiccated samples are less compressible than samples that have never been desiccated (virgin material). Similarly, Figure 7 shows that as the initial degree of desiccation increases, the tailings exhibit greater degrees of strain hardening, built only up to a point - the amount of strain hardening in the sample desiccated to 4% water content, is less than the strain hardening for the sample desiccated to 12%. Figure 7 also shows that the desiccated tailings are stronger despite having higher void ratios than the virgin tailings.

These results conform qualitatively to expected elasto-plastic behaviour in unsaturated soils, in that suction will contribute to strength through expansion of the yield surface. However, the more common elasto-plastic formulations of unsaturated soils are not concerned with the manner of strength increase shown in Figure 7, that is an increase in dilation. Most elasto-plastic unsaturated soils models aim to emulate behavior observed in clayey soils: on a strength basis, this is expansion or contraction of yield surface that produces a peak strength declining to a residual value at large strains. Therefore, quantitative explanation of the behaviour shown in Figure 7 is a potential avenue for future research.

In terms of practice, the changes in shear strength behaviour are quite significant. The behavior of the virgin sample (no desiccation) shows strain softening behavior, that is, the strength decreased with strain. It is thought that this behavior is associated with long runouts and their associated catastrophic effects (e.g. Fourie et al., 2001).

Another way to represent the influence of desiccation on strength is through field vane measurements. Figure 8 shows vane shear strength data for thickened gold tailings from both drybox tests shown previously as well field data from near surface measurements at two gold mines. The data from Musselwhite is collected and presented by Kam et al. (2011). The vane measurements show similar trends to the element shear strength, in that the desiccated–rewet samples show a maximum value as degree of desiccation increases. For comparison, the peak strength from the simple shear test in Figure 7 for the un-desiccated sample is shown, using the water content of the consolidated sample, which gives a sense of the magnitude of the suction-related effects on strength. Figure 8 also shows how the field measurements are potentially influenced by both current matric suction values, and also by stress history. The range in the Musselwhite data suggests that some of these measurements are influenced by matric suctions that are present during the vane measurements, while the values on the low end likely represent stress history effects only, presumably taken during wetter conditions after the dissipation of matric suctions. Figure 8 clearly shows the relevance of unsaturated soil mechanics in interpreting conventional measurements, as for some sites, such field vane measurements are used to judge the timing of embankment raises, when these are partially constructed on top of the

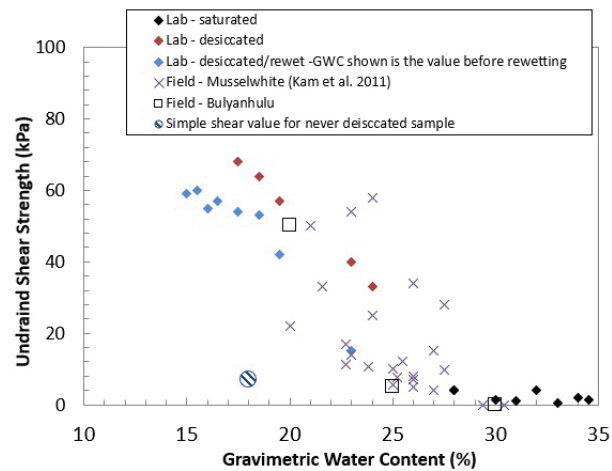


**Figure 8.** Influence of desiccation and subsequent rewetting in laboratory and field shear strengths for gold tailings from two mines (Bulyanhulu and Musselwhite) as measured by a shear vane.

tailings., and the strength of the tailings themselves are critically important. Clearly the stress history effect is the most reliable and the key contributor to shear strength out of all the possible contributing effects of matric suction (which include lower density, present suction values, stress history).

## 2.2 Desaturation and potential for acid generation

The major negative potential impact of desiccation on tailings performance is the increased risk of acid generation, which occurs via oxygen transport into the tailings, the oxygen serving as the principal oxidant to dissolve certain minerals that are unstable under oxidizing conditions. The dissolution of some of these minerals, the most common being pyrite ( $\text{FeS}_2$ ), results in the generation of very low pH water, which in turn leads to the dissolution of other minerals, eventually generating water with low pH and very high concentration of dissolved mass. This water is termed acid drainage, and its generation and its effects have been studied for many decades, the following reference list far from being exhaustive: Aubertin et al. (2016), Simms et al. (2000), Blowes & Jambor (1990), Singer & Stumm (1970).

In terms of unsaturated soil behaviour, the key parameter is the degree of saturation, which governs the effective diffusion coefficient of oxygen into the tailings. There are a set of different equations to predict the variation in oxygen diffusion with saturation (Aachib et al., 2004), but they all plot quite close to the relationship shown in Figure 9. In thickened or filtered tailings deposits, acid generation seems to occur only if i) there is a sufficient quantity of acid generating minerals, ii) significant desaturation occurs (degree of saturation  $< 0.8$ ), and iii) the tailings remain at this low saturation for at least a month. References to specific sites is given in Simms (2017).



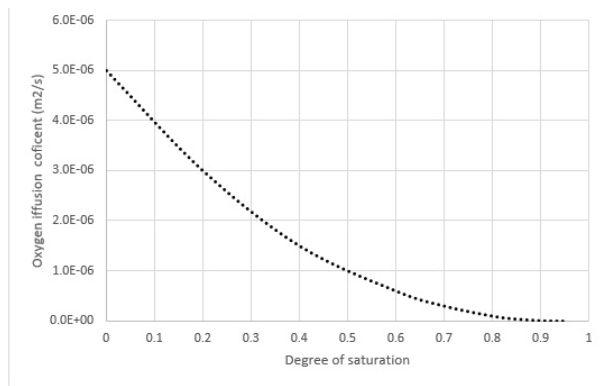


**Figure 9.** Variation of oxygen diffusivity with saturation using Millington-Quirk model.

### 3. Predicting the variation in void ratio, stress, state and degree of saturation in a given tailings deposition plan

#### 3.1 Theoretical concepts

The preceding text has shown that the effect of desiccation can be positive in terms of strength, but there is some risk to increased poor geo-environmental performance due to sulphide mineral oxidation. Therefore, hydro-mechanical analysis of potential tailings deposition plans, or analysis of existing operations or pilots with the view to optimization, would be valuable to assist mines to maximize performance of their tailings deposition operations.

As shown in Figure 3, several simultaneous and coupled processes influence volume change and desaturation in a multi-layer deposition scheme. The most rigorous analysis therefore requires consideration of large strain consolidation, unsaturated flow with dependency of constitutive relationships on both density and degree of saturation, and considerations of yield surface effects by both mechanical and hydraulic loading. Fortunately, there exists a significant literature on the elasto-plastic behavior of unsaturated soils, with associated soil models such as the Basic Barcelona Model (BBM), the modified state surface model (MSSM), the Glasgow coupled model (GCM), and several others (a recent summary is presented by Qi et al., 2020). These models, however, have been applied in the context of buffer design for nuclear waste repository. The application to tailings requires is for generally lower range of total stress, and additionally, the deformations of tailings can be large, which requires a large strain consolidation analysis.

This author and his colleagues have developed the UNSATCON model, which is designed to analyze this kind of tailings deposition scheme. The model combines large strain consolidation with the aforementioned elasto-plastic soil models, using the piecewise-linear approach to large strain consolidation developed by Fox & Berles (1997). This model and its applicability to field cases and laboratory studies for monotonic dewatering is presented in Qi et al. (2017a, b), while the addition of elasto-plastic unsaturated

soil models in described in Qi et al. (2020). The authors have subsequently implemented several of the aforementioned elasto-plastic constitutive models for unsaturated soils in the UNSATCON platform, including:

- i) the modified State Surface Method (SSM) proposed by Zhang & Lytton (2009) coupled to a simple void ratio dependent water retention curve;
- ii) the well-known Barcelona Basic Model (BBM) (Alonso et al., 1990), coupled to the same simple water retention model;
- iii) the SSM and BBM models coupled to bounding plasticity water-retention model of Gallipoli & Bruno (2017); and
- iv) the Glasgow Coupled Model (GCM), first proposed by Wheeler et al. (2003)

The UNSATCON framework incorporating these various elasto-plastic unsaturated soil models has been tested on the multilayer drybox type tests described in the first section for different types of tailings (Qi, 2017; Qi et al., 2020). When calibrated to the same basic material parameters, these models give similar global results when analyzing multilayer tailings deposition, though there are some differences that may have important implications considering large deposits. For example, GCM type models consider the influence of cumulative plastic strain due to repeated wetting-drying cycles, which cannot be considered by some other models. The difference between models is explored in detail in Qi et al. (2020), and will not be repeated here. Rather, this paper will focus on the general behaviours of such models and the associated practical implications for tailings deposit simulation.

The material parameters required for this type of analysis are the saturated large strain consolidation properties (hydraulic conductivity as a function of void ratio, and void ratio as a function of vertical effective stress), and the water retention curve/soil-water characteristic curve. If the latter is measured with a standard axis translation test where volume change is measured, that information is sufficient to calibrate the unsaturated parameters of the models.

The key components of the analysis are a generalized set of functions to describe volume change, and a volume change dependent water retention curve. The generalization of the volume change relationships is shown Figures 10a and 10b, the former being simply the standard formulation for saturated soils. In 10b, stress history effects can be both from suction or stress, causing the elastic surface to move low values of void ratio and so progressively change the yield surface. Put another way, 10b combines the shrinkage curve with the compressibility function to define the 3D volume change surface.

The physical relevance of this to tailings deposits, is that if a layer of tailings experiences substantial desiccation, due the high suctions, that layer of tailings will likely remain in the elastic region with respect to volume change for a considerable thickness of overlying tailings. For example, if the void ratio corresponding to virgin compression under 100 kPa matric suction is in the neighborhood of the same

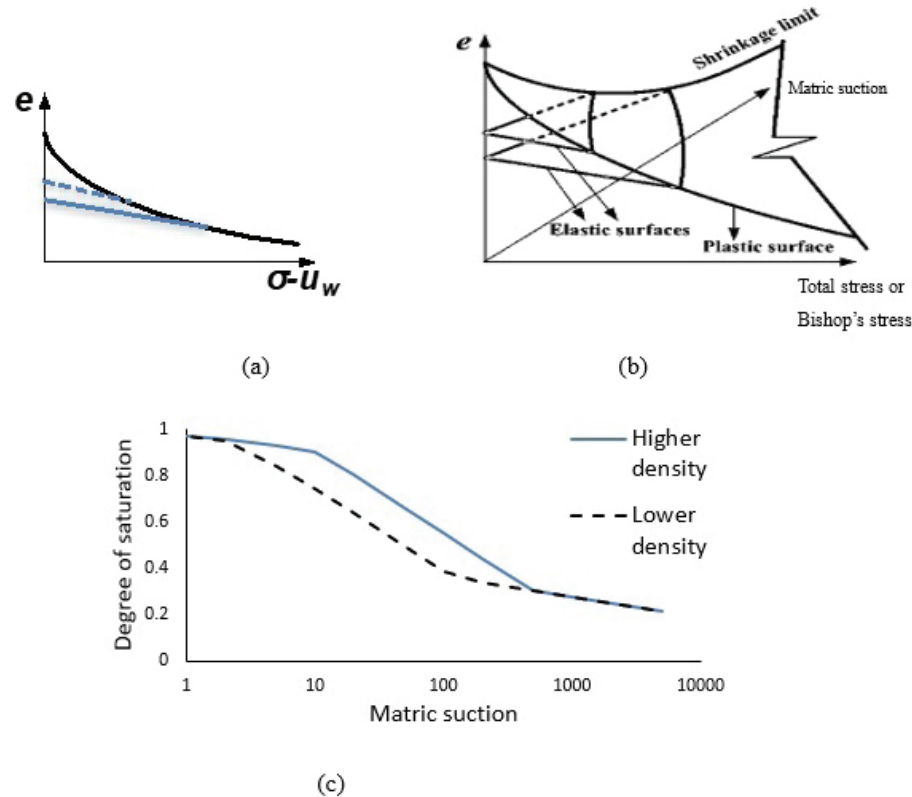


**Figure 10.** Representation of the key concepts for hydro-mechanical coupling (a) unload-reload behavior in a saturated soil; (b) generalization of this behaviour to unsaturated conditions, where the elastic and plastic constitutive functions are now dependent on two variables; (c) void ratio dependency of a water retention curve.

value of total stress for 70 kPa, this will mean that it could require burial by 5 m for volume change to reach again to the plastic surface. Put another way, essentially desiccation can lead to substantial pre-consolidation pressures in the first layer, that will not be succeeded by either future drying, and not be loading until substantial thickness of tailings are deposited. This situation is most relevant for hard rock tailings, for their comparatively lower hydraulic conductivity generates a more uniform distribution of matric suction.

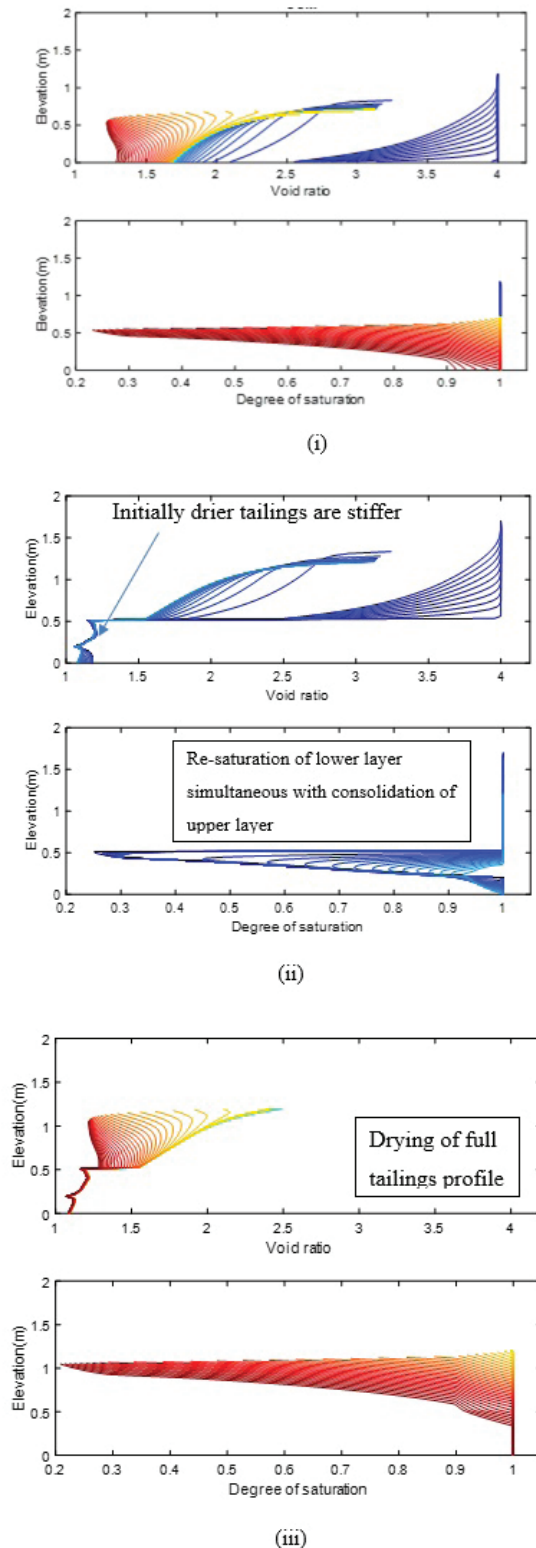
Figure 10c illustrates the dependency of the WRC on void ratio. The dependency of the air entry value on void ratio is particularly important to water exchange between fresh and old tailings. Having a softer tailings will allow for greater contribution of evaporation to volume change as opposed to desaturation, which will allow for greater strength and less risk of acid generation.

Figure 11 shows detailed outputs from analysis of relatively soft and clayey tailings. The tailings initially undergo self-weight consolidation, reaching a typical profile of void ratio vs depth by the yellow line. Thereafter, after the rate of bleed water generation drops below the evaporation rate, the tailings begin to desiccate and subsequently desaturate, the lowest void ratio being reached at the surface (here nearer the shrinkage limit), the tailings at the bottom reaching lower matric suctions corresponding to higher

degrees of saturation. With the placement of the new layer there is a visible compression in the underlying tailings, as the bottom tailings are still largely saturated, and have not experienced the same degree of desiccation, are softer, and therefore compress more under the weight of the new tailings. Eventually, after the second layer consolidates (accelerated by adsorption of water by the bottom layer), the whole profile undergoes evaporation. The final void ratio profile is not only a function of variation in load, but it also influenced variation in stress history, as the yield surface (Figure 10b) is at different locations for different depths.

### 3.2 Example application to a field site

To highlight the significance of the elasto-plastic unsaturated behaviour to practical applications, the following describes in brief the analysis of real thickened tailings site in Northern Ontario, Canada. Tailings are deposited at gravimetric water contents of approximately 50%. The deposition rate (volume of the tailings as they come out the end of the pipe / divided by the impoundment footprint) is about 2.5 m per year. The tailings are deposited from various spigots, using the same deposition scheme shown in Figure 1, Deposition covers the whole area in roughly 1 year.



**Figure 11.** Example of UNSATCON outputs simulating deposition of two layers (i) Initial self-weight consolidation to yellow line, thereafter drying once evaporation rate exceeds bleed water generation; (ii) initial compression and short term interactions after placement of new layer; (iii) eventual second drying phase.

The climate in northern Ontario, Canada is relatively cold and wet. Figure 12 shows gravimetric water contents measured in the field near the surface of a thickened tailings. The figure is annotated to show the water content at deposition. It is clear that there are two trends, one for late Fall or Spring, where the evaporation rate is very low, the other for Summer where the evaporation rate is substantial. From May to September, the average potential evaporation rate is  $\sim 1.5$  mm/day.

The UNSATCON model was employed to analyze this data (Qi & Simms, 2018). A column test was used to back calculate the large strain consolidation properties, and a water-retention curve was measured, which was sufficient to calibrate all the properties. A modified state surface model was employed to simulate the elasto-plastic behaviour. Of significance, the hydraulic conductivity function for this site is relatively high ( $5 \times 10^{-6} \text{ m/s}$ ). The model was run over a range of plausible rates of rise (the one-dimensional rate of filling, assuming no water release after deposition), to examine whether the model could reproduce the field data, and then to examine sensitivity of performance to deposition rate.

The modelling results are shown in Figures 13 and 14 for three different deposition rates (2, 2.5 and 3 m per year),

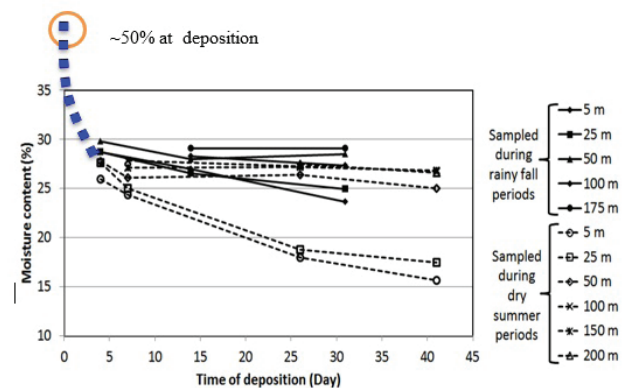


**Figure 12.** Gravimetric water contents samples at a thickened tailings site. Data from Kam et al. (2011). Distance in legend refers to distance from deposition point.

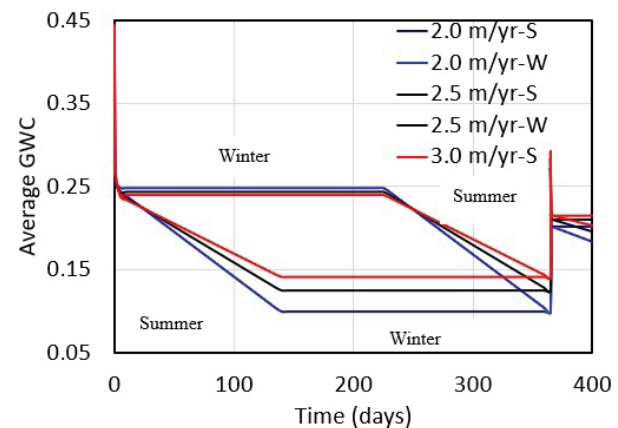


**Figure 13.** Simulated average GWC in the first layer.

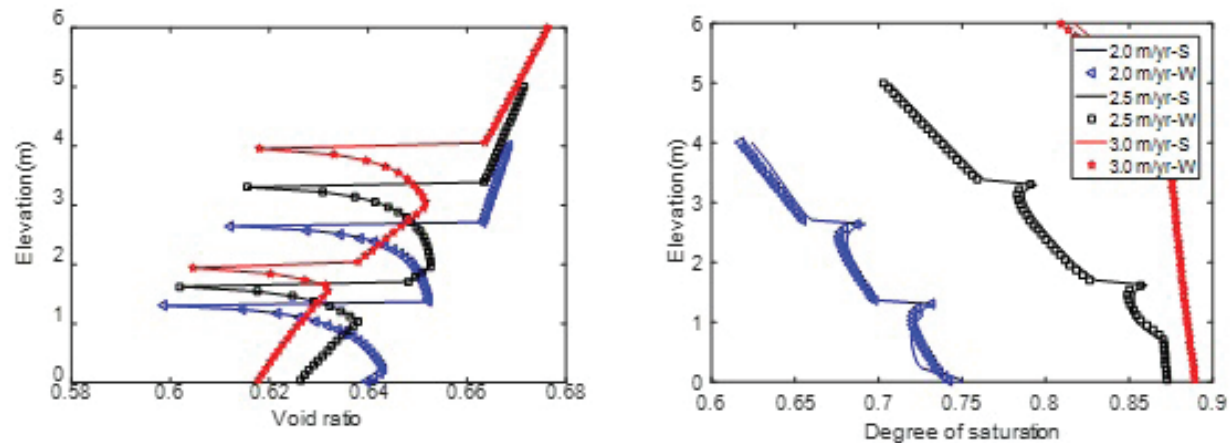


**Figure 14.** Simulated profiles of degree of saturation and void ratio for different deposition schemes (Rate of deposition, deposition at beginning of summer or winter) (modified from Qi, 2017).

and different deposition times, either beginning of summer or beginning of winter. Regardless of timing of deposition, as in the measured water contents, consolidation dominates the early behaviour, the same water content being achieved in the fresh layer regardless of the season. In the tailings are deposited at the beginning of summer, then the contribution to dewatering by evaporation begins to reduce the water content and void ratio of tailings, while for winter deposition this effect is delayed until to the start of summer. Both methods of deposition, however, end up at the same state at the end of a year.

Figure 14 shows the profiles of degree of saturation and void ratio at the end of three years for all deposition schemes. The range of void ratios is relatively small (0.60 to 0.66) for all deposition scenarios, and all have a significant stress history with respect to desiccation. This is largely due to the favourable consolidation properties of the tailings, which means that they consolidate quickly. Due to this reason, a relatively small amount of time is required for evaporation to induce a desiccation effect. Indeed, shear vane strengths at this site measured in the top layer have values in the range of 30 kPa to 60 kPa.

The degree of saturation, however, is much more variable, the highest deposition rate keeps degree of saturations above 0.85, while for the slowest rate the degree of saturation drops below 0.65. Therefore, if a site is susceptible to acid drainage, it is clear that this kind of analysis can suggest optimal deposition rates. In this case, a deposition rate of 3 m per year would be preferred, as the void ratios are still low, and the tailings still experience substantial desiccation and associated strength gain, while keeping the degree of saturation higher. Practically, this could be achieved by limiting the footprint, or depositing cell by cell using internal dykes.

The void ratios are slightly lower at the top of each old layer. This occurs because the i) contributive effects of total stress (increases with depth) and suction (increases with elevation), and ii) for the points at high elevation, high suctions develop with comparatively low total stresses, which is followed by a substantial increase in total stress following deposition of the next layer, followed by a high degree of

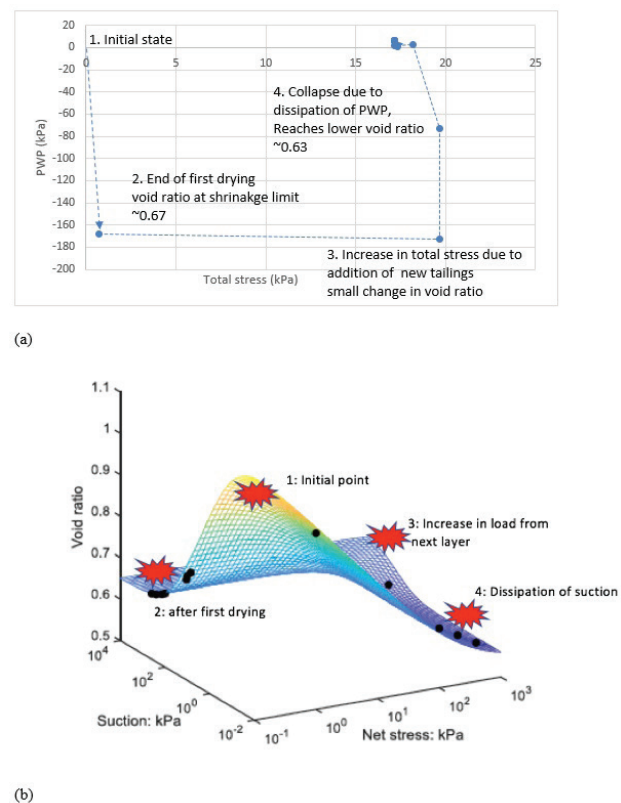


**Figure 15.** Stress path for a point near the surface of layer 1, as layer 2 is deposited: (a) suction and total stress space; (b) overlaid on plastic surface.

suction dissipation – these conditions favour collapse. The substantial increase in total stress, followed by a large decrease in suction, allow the tailings to move to the low suction and high stress part of the plastic constitutive surface (that is, close to the 0 suction plane, or saturated behaviour), which is more compressible. An example stress path is shown in Figure 15, for a point near the surface of layer 1 as it is buried by layer 2.



#### 4. Summary and opportunities for future research

The goal of this paper was to illustrate the applicability of unsaturated soil mechanics to design or optimization of thickened or filtered tailings impoundments. To summarize, desiccation is the key parameter that affects the strength of the tailings through stress history effects. These effects manifest in some tailings in terms of increased dilatancy in element testing. The most common negative impact is desaturation and the associated increased risk of acid generation in susceptible tailings. It was shown that consolidation analysis incorporating elasto-plastic unsaturated behaviour can replicate the essential phenomena in multi-layer deposition. Finally, one such analysis was applied to a real field site, showing that useful information of help to operations can come out of such numerical analyses.

The paper has focused on the implications elasto-plastic behaviour in unsaturated soils for multi-layer tailings behaviour, but other aspects are important, for example, the magnitude of the evaporative boundary conditions, the role of cracks, or cold regions applications where freeze-thaw not drying is the driver of desiccation. For evaporation it is generally found from back-analysis of several sites (both thickened, and traditional tailings impoundments in arid climates) (Qi et al., 2017b; Newson & Fahey, 2003; Fujiyasu et al., 2000) and in the large multilayer laboratory tests (Simms et al., 2019), that the effective evaporation can be taken reasonably to be  $0.7 \times PE$  (the potential evaporation). This will generally be a larger net flux the predicted by 1-D unsaturated flow models with coupled soil-atmosphere boundary conditions commonly available in many geotechnical software suites, probably because of the influence of cracks (Simms et al., 2019).

Cracking during desiccation in tailings is studied in the above references, but also with respect to modelling the desiccation process (Rodríguez et al., 2007; Yao et al., 2002). In exploring the modelling of tailings in the large drying box types tests, the authors' own experience is that most important influence of cracking, aside from prolonging high rates of evaporation, is the increasing uniform distribution of water content afforded by the effective shortening of the drainage path of water from within the tailing to some exposed surface. This can usually be accounted for, and the distribution of water content within a layer of tailings can be reasonably reproduced, through an upward adjustment of hydraulic conductivity, approximately half an order of magnitude (Qi, 2017). This effect is more dominant in the clayey tailings than hard rock tailings. Cracks are typically filled in or closed under the deposition of successive layers, though there may be some residual effect on the overall strength of a deposit, which is unknown.

Also unknown is the fundamental reason for the particular change in strength behaviour of hard rock tailings when desiccated, that is, an increase in dilatancy. Daliri et al.

(2014), looking at SEM pictures obtained on freeze-dried samples of gold tailings, speculated that suction rearranges the internal structure of the tailings matrix, possibly increasing attraction and coating of coarser particles with finer smaller particles, resulting in increased effective particle size, but this is unproven. As stated previously, this effect is quite different than that predicted by elasto-plastic unsaturated models, in term of strength behaviour.

Potentially, similar analysis can be done with respect to desiccation by freeze-thaw effects: similarities between the water-retention curve and soil-freezing characteristic curves are much studied in the literature, including for tailings (Schafer & Beier, 2020). Strengthening tailings and immobilized tailings pore-waters by turning the tailings into "permafrost" is practiced at several mines in Northern Canada: deposition management is based largely on accumulated operation experience. With expected variation in climate expected to increase, application of similar unsaturated soil concepts to deposition in cold regions probably could also assist deposition optimization at these mines.

#### Acknowledgements

The author gratefully acknowledges the invitation from the Technical Committee of the Pan-Am Conference on Unsaturated Soils to write a paper on this topic. The author expresses thanks to his colleagues and students who have contributed to the work referenced in this paper, in particular, Professor Siva Sivathayalan at Carleton University and Professor Sai Vanapalli at the University of Ottawa; and former students Farzad Daliri, Senior Geotechnical Engineer at Hatch, BC, Canada, and Shunchao Qi, Associate Professor, Sichuan University, China.

#### Declaration of interest

The author has no conflicts of interest to declare and there is no financial interest to report.

#### References

- Aachib, M., Mbonimpa, M., & Aubertin, M. (2004). Measurement and prediction of the oxygen diffusion coefficient in unsaturated media, with applications to soil covers. *Water, Air, and Soil Pollution*, 156(1-4), 163-193. <http://dx.doi.org/10.1023/B:WATE.0000036803.84061.e5>.
- Alonso, E.E., Gens, A., & Josa, A. (1990). A constitutive model for partially saturated soils. *Geotechnique*, 40(3), 405-430. <http://dx.doi.org/10.1680/geot.1990.40.3.405>.
- Al-Tarhouni, M., Simms, P., & Sivathayalan, S. (2011). Cyclic behaviour of reconstituted and desiccated-rewet thickened gold tailings in simple shear. *Canadian Geotechnical Journal*, 48(7), 1044-1060. <http://dx.doi.org/10.1139/t11-022>.









- Aubertin, M., Bussière, B., Pabst, T., James, M., & Mbonimpa, M. (2016). Review of the reclamation techniques for acid-generating mine wastes upon closure of disposal sites. In A. Farid, A. De, K. R. Reddy, N. Yesiller & D. Zekkos (Eds.), *Geo-Chicago 2016: geotechnics for sustainable energy* (GSP 270, pp. 343-358). Reston: American Society of Civil Engineers.
- Blowes, D.W., & Jambor, J.L. (1990). The pore-water geochemistry and the mineralogy of the vadose zone of sulphide tailings, Waite Amulet, Quebec, Canada. *Applied Geochemistry*, 5(3), 327-346. [http://dx.doi.org/10.1016/0883-2927\(90\)90008-S](http://dx.doi.org/10.1016/0883-2927(90)90008-S).
- Daliri, F., Kim, H., Simms, P., & Sivathayalan, S. (2014). Impact of desiccation on monotonic and cyclic shear strength of thickened gold tailings. *Journal of Geotechnical and Geoenvironmental Engineering*, 140(9), 04014048. [http://dx.doi.org/10.1061/\(ASCE\)GT.1943-5606.0001147](http://dx.doi.org/10.1061/(ASCE)GT.1943-5606.0001147).
- Daliri, F., Simms, P., & Sivathayalan, S. (2016). Shear and dewatering behaviour of densified gold tailings in a laboratory simulation of multi-layer deposition. *Canadian Geotechnical Journal*, 53(8), 1246-1257. <http://dx.doi.org/10.1139/cgj-2014-0411>.
- Fourie, A.B., Blight, G.E., & Papageorgiou, G. (2001). Static liquefaction as a possible explanation for the Merriespruit tailings dam failure. *Canadian Geotechnical Journal*, 38(4), 707-719. <http://dx.doi.org/10.1139/t00-112>.
- Fox, P.J., & Berles, J.D. (1997). CS2: a piecewise-linear model for large strain consolidation. *International Journal for Numerical and Analytical Methods in Geomechanics*, 21(7), 453-475. [http://dx.doi.org/10.1002/\(SICI\)1096-9853\(199707\)21:7<453::AID-NAG887>3.0.CO;2-B](http://dx.doi.org/10.1002/(SICI)1096-9853(199707)21:7<453::AID-NAG887>3.0.CO;2-B).
- Fujiyasu, Y., Fahey, M., & Newson, T. (2000). Field Investigation of evaporation from freshwater tailings. *Journal of Geotechnical and Geoenvironmental Engineering*, 126(6), 556-567. [http://dx.doi.org/10.1061/\(ASCE\)1090-0241\(2000\)126:6\(556\)](http://dx.doi.org/10.1061/(ASCE)1090-0241(2000)126:6(556)).
- Gallipoli, D., & Bruno, A.W. (2017). A bounding surface compression model with a unified virgin line for saturated and unsaturated soils. *Geotechnique*, 67(8), 703-712. <http://dx.doi.org/10.1680/jgeot.16.P.145>.
- Henriquez, J., & Simms, P. (2009). Dynamic imaging and modelling of multi-layer deposition of gold paste tailings. *Minerals Engineering*, 22(2), 128-139. <http://dx.doi.org/10.1016/j.mineng.2008.05.010>.
- Kam, S., Girard, J., Hmidi, N., Mao, Y., & Longo, S. (2011). Thickened tailings disposal at Musselwhite Mine. In R. J. Jewell & A. B. Fourie (Eds.), *Proceedings of the 14<sup>th</sup> International Conference on Paste and Thickened Tailings*, Perth, Australia. [http://dx.doi.org/10.36487/ACG\\_rep/1104\\_21\\_Kam](http://dx.doi.org/10.36487/ACG_rep/1104_21_Kam).
- Mizani, S., He, X., & Simms, P. (2013). Application of lubrication theory to modeling stack geometry of high density mine tailings. *Journal of Non-Newtonian Fluid Mechanics*, 198, 59-70. <http://dx.doi.org/10.1016/j.jnnfm.2013.03.002>.
- Newson, T.A., & Fahey, M. (2003). Measurement of evaporation from saline tailings storages. *Engineering Geology*, 70(3-4), 217-233. [http://dx.doi.org/10.1016/S0013-7952\(03\)00091-7](http://dx.doi.org/10.1016/S0013-7952(03)00091-7).
- Qi, S. (2017). *Numerical investigation for slope stability of expansive soils and large strain consolidation of soft soils* [Doctoral dissertation, Université d'Ottawa]. University of Ottawa. Retrieved in April 23, 2021, from <https://ruor.uottawa.ca/handle/10393/37019>.
- Qi, S., & Simms, P. (2018). Analysis of dewatering and desaturation of generic field deposition scenarios for thickened tailings. In R. J. Jewell & A. B. Fourie (Eds.), *Proceedings of the 21<sup>st</sup> International Seminar on Paste and Thickened Tailings* (pp. 401-412). Crawley, Australia: Australian Centre for Geomechanics, University of Western Australia. [http://dx.doi.org/10.36487/ACG\\_rep/1805\\_33\\_Simms](http://dx.doi.org/10.36487/ACG_rep/1805_33_Simms).
- Qi, S., Simms, P., & Vanapalli, S. (2017a). Piecewise-linear formulation of coupled large-strain consolidation and unsaturated flow. I: model development and implementation. *Journal of Geotechnical and Geoenvironmental Engineering*, 143(7), 04017018. [http://dx.doi.org/10.1061/\(ASCE\)GT.1943-5606.0001657](http://dx.doi.org/10.1061/(ASCE)GT.1943-5606.0001657).
- Qi, S., Simms, P., Vanapalli, S., & Soleimani, S. (2017b). Piecewise-linear formulation of coupled large-strain consolidation and unsaturated flow. II: testing and performance. *Journal of Geotechnical and Geoenvironmental Engineering*, 143(7), 04017019. [http://dx.doi.org/10.1061/\(ASCE\)GT.1943-5606.0001658](http://dx.doi.org/10.1061/(ASCE)GT.1943-5606.0001658).
- Qi, S., Simms, P., Daliri, F., & Vanapalli, S. (2020). Coupling elasto-plastic behaviour of unsaturated soils with piecewise linear large-strain consolidation. *Geotechnique*, 70(6), 518-537. <http://dx.doi.org/10.1680/jgeot.18.P.261>.
- Rico, M., Benito, G., Salgueiro, A.R., Diez-Herrero, A., & Pereira, H.G. (2008). Reported tailings dam failures: a review of the European incidents in the worldwide context. *Journal of Hazardous Materials*, 152(2), 846-852. PMID:17854989. <http://dx.doi.org/10.1016/j.jhazmat.2007.07.050>.
- Rodríguez, R., Sánchez, M., Ledesma, A., & Lloret, A. (2007). Experimental and numerical analysis of desiccation of a mining waste. *Canadian Geotechnical Journal*, 44(6), 644-658. <http://dx.doi.org/10.1139/t07-016>.
- Schafer, H., & Beier, N. (2020). Estimating soil-water characteristic curve from soil-freezing characteristic curve for mine waste tailings using time domain reflectometry. *Canadian Geotechnical Journal*, 57(1), 73-84. <http://dx.doi.org/10.1139/cgj-2018-0145>.
- Simms, P. (2017). 2013 Colloquium of the Canadian Geotechnical Society: geotechnical and Geoenvironmental behaviour of high-density tailings. *Canadian Geotechnical Journal*, 54(4), 455-468. <http://dx.doi.org/10.1139/cgj-2015-0533>.
- Simms, P., Soleimani, S., Mizani, S., Daliri, F., Dunmola, A., Rozina, E., & Innocent-Bernard, T. (2019). Cracking, salinity and evaporation in mesoscale experiments on

- three types of tailings. *Environmental Geotechnics*, 6(1), 3-17. <http://dx.doi.org/10.1680/jenge.16.00026>.
- Simms, P.H., Yanful, E.K., St. Arnaud, L., & Aubé, B. (2000). A laboratory evaluation of metal release and transport in flooded pre-oxidized mine tailings. *Applied Geochemistry*, 15(9), 1245-1263. [http://dx.doi.org/10.1016/S0883-2927\(00\)00003-2](http://dx.doi.org/10.1016/S0883-2927(00)00003-2).
- Singer, P.C., & Stumm, W. (1970). Acidic mine drainage: the rate-limiting step. *Science*, 167(3921), 12-34. <http://dx.doi.org/10.1126/science.167.3921.1121>.
- Vick, S.G. (1990). *Planning, design and analysis of tailings dams*. Vancouver: BiTech Publishers Ltd.
- Wheeler, S.J., Sharma, R.S., & Buisson, M.S.R. (2003). Coupling of hydraulic hysteresis and stress-strain behaviour in unsaturated soils. *Geotechnique*, 53(1), 41-54. <http://dx.doi.org/10.1680/geot.2003.53.1.41>.
- Willis, B. (2006). *Mineral processing technology*. Oxford: Elsevier.
- Yao, D.T., de Oliveira-Filho, W.L., Cai, X.C., & Znidarcic, D. (2002). Numerical solution for consolidation and desiccation of soft soils. *International Journal for Numerical and Analytical Methods in Geomechanics*, 26(2), 139-161. <http://dx.doi.org/10.1002/nag.196>.
- Zabolotnii, E., Morgenstern, N., & Wilson, G.W. (2021). Mesh sensitivity in numerical models of strain-weakening systems. *Computers and Geotechnics*, 136, 104253. <http://dx.doi.org/10.1016/j.compgeo.2021.104253>.
- Zhang, X., & Lytton, R.L. (2009). Modified state-surface approach to the study of unsaturated soil behavior. Part I: basic concept. *Canadian Geotechnical Journal*, 46(5), 536-552. <http://dx.doi.org/10.1139/T08-136>.



## Behavior of unsaturated cohesive-frictional soils over a whole range of suction/thermo-controlled stress paths and modes of deformation

Laureano R. Hoyos<sup>1#</sup> , Roya Davoodi-Bilesavar<sup>1</sup> , Ujwalkumar D. Patil<sup>2</sup> ,  
Jairo E. Yepes-Heredia<sup>3</sup> , Diego D. Pérez-Ruiz<sup>4</sup> , José A. Cruz<sup>5</sup> 

Article

### Keywords

Suction-controlled testing  
Triaxial testing  
True triaxial testing  
Plane strain testing  
Ring shear testing  
Resonant column testing

### Abstract

The present work documents some of the most recent experimental evidence of the thermo-hydro-mechanical behavior of compacted soils over a whole range of suction- and/or thermo-controlled stress paths and modes of deformation, including data from a series of triaxial, true triaxial, plane strain, ring shear, and resonant column tests conducted on different types of cohesive-frictional soils in the low-to-medium matric suction range under either room temperature or thermally controlled conditions. The work has been accomplished at the Advanced Geomechanics Laboratory of the University of Texas at Arlington, focusing primarily on the following essential features of unsaturated soil behavior: (1) Loading-collapse and apparent tensile strength loci assessed from suction-controlled triaxial and true triaxial testing on clayey sand, (2) Critical state lines from suction-controlled plane strain testing on silty soil, (3) Peak and residual failure envelopes from suction-controlled ring shear testing on clayey soil, (4) Frequency response curves and cyclic stress-strain hysteretic loops from thermo-controlled, constant-water content resonant column testing on clayey soil, and (5) Residual failure envelopes from suction/thermo-controlled ring shear testing on clayey soil. The work is intended to serve as a succinct yet reasonably thorough state-of-the-art paper contribution to PanAm-UNSAT 2021: Third Pan-American Conference on Unsaturated Soils, Rio de Janeiro, Brazil, July 21-25, 2021.

## 1. Introduction

Over the last five decades, intensive research efforts undertaken worldwide have defined the threshold of the state-of-the-knowledge of unsaturated soil behavior. The adoption of matric suction and the excess of total stress over air pressure, i.e., net normal stress, as the relevant stress state variables, has facilitated the investigation of essential features of unsaturated soil response, via either the axis-translation or the vapor transfer technique, for a wide range of matric and total suction states. It is the relative success of these techniques that has prompted researchers in the discipline to devote countless hours to fine-tuning myriad details of standardized soil testing devices, and thus keep the focus of their efforts on expanding and upgrading the capabilities of such devices for testing unsaturated soil materials.

The present work documents some of the most recent experimental evidence of the thermo-hydro-mechanical behavior of compacted soils over a whole range of suction- and/or thermo-controlled stress paths and modes of deformation, including data from a series of triaxial, true triaxial, plane strain, ring shear, and resonant column tests conducted on different types of compacted cohesive-frictional soils in the low-to-medium matric suction range under either room temperature or thermally controlled conditions.

The work focuses primarily on the following essential features of unsaturated soil behavior: (1) Comparative analysis of loading-collapse and apparent tensile strength loci assessed from both suction-controlled triaxial and true triaxial testing on clayey sand, (2) Critical state lines from suction-controlled plane strain testing on silty soil, (3) Peak and residual failure envelopes from suction-controlled ring

<sup>#</sup>Corresponding author. E-mail address: hoyos@uta.edu

<sup>1</sup>University of Texas, Department of Civil Engineering, Arlington, USA.

<sup>2</sup>University of Guam, School of Engineering, Mangilao, Guam, USA.

<sup>3</sup>Texas A&M University, Department of Civil and Environmental Engineering, Texas, USA.

<sup>4</sup>Pontificia Universidad Javeriana, Departamento de Ciencias de la Ingeniería, Cali, Colombia.

<sup>5</sup>Universidad Militar Nueva Granada, Facultad de Ingeniería, Bogotá, Colombia.

Submitted on April 23, 2021; Final Acceptance on June 10, 2021; Discussion open until November 30, 2021.

<https://doi.org/10.28927/SR.2021.066621>



This is an Open Access article distributed under the terms of the Creative Commons Attribution License, which permits unrestricted use, distribution, and reproduction in any medium, provided the original work is properly cited.

shear testing on clayey soil, (4) Frequency response curves and cyclic stress-strain hysteresis loops from thermo-controlled, constant-water content resonant column testing on clayey soil, and (5) Residual failure envelopes from suction/thermo-controlled ring shear testing on clayey soil.

The first section of the work is devoted to the hydro-mechanical response of compacted cohesive-frictional soils under isothermal and suction-controlled conditions via the axis-translation technique. Key modifications made to standardized triaxial, true triaxial, plane strain, and ring shear devices, in order to make them suitable for suction-controlled testing via axis-translation, are summarily described and illustrated.

The second section of the work is devoted to the thermo-hydro-mechanical response of compacted cohesive-frictional soils under non-isothermal and either constant-water content or suction-controlled conditions. Key modifications made to standardized resonant column and ring shear devices, in order to make them suitable for suction/thermo-controlled testing of soils over a whole range of shear strain amplitudes, are also summarily described.

The present work does not make any pretenses to absolute originality or even a thoroughly comprehensive literature review, given the extent and importance of the work accomplished by other researchers and scholars on the subject to this date. It is rather intended to serve as a succinct yet reasonably thorough state-of-the-art paper contribution to PanAm-UNSAT 2021: The Third Pan-American Conference on Unsaturated Soils, with particular emphasis on essential features of unsaturated soil behavior that have not been thoroughly addressed in the existing literature, largely due to a lack of suitable testing devices.

## 2. Hydro-mechanical behavior: recent evidence

### 2.1 Experimental program and scope

Over the last three decades, several critical-state based constitutive models, incorporating suction as an independent stress state variable, have been postulated for unsaturated soils with varying degrees of success in capturing the true nature of soil response (e.g., Alonso et al., 1990; Toll, 1990; Sivakumar, 1993; Maatouk et al., 1995; Wheeler, 1996; Cui & Delage, 1996; Bolzon et al., 1996; Adams & Wulfsohn, 1997; Rampino et al., 2000; Sivakumar & Wheeler, 2000; Tang & Graham, 2002; Wang et al., 2002; Chiu & Ng, 2003; Thu et al., 2007; Hoyos et al., 2012). Additional experimental evidence for a wider variety of soils, however, particularly for materials that are cohesive-frictional in nature, is still sorely needed to conclusively substantiate their validation.

In this regard, triaxial testing continues to be the most universally used method to characterize unsaturated soil behavior, owing primarily to its versatility in accommodating the required modifications for suction-controlled testing via

the axis-translation technique (e.g., Estabragh et al., 2004; Zhang & Li, 2011; Liu & Muraleetharan, 2012; Usmani et al., 2012; Estabragh & Javadi, 2014). In nature, however, soil deposits well above the ground-water table are intrinsically heterogeneous, and hence may be subject to a state of three-dimensional anisotropic tensions and stress gradients. Therefore, accurate predictions of unsaturated soil response require that the constitutive relations be valid for all principal stress paths that are likely to be experienced in the field. It is in this context that a suction-controlled true triaxial (cubical) apparatus becomes of paramount importance (e.g., Hoyos & Macari, 2001; Matsuoka et al., 2002; Reis et al., 2011).

Despite recent advances in suction-controlled triaxial (TX) and true triaxial (TTX) testing of unsaturated soils, there is a glaring lack of experimental substantiation of test results obtained from one technique based on results from the other, which constitutes a first chief motivation under this section of the present work (Hydro-mechanical Behavior). As previously mentioned, a comparative analysis of loading-collapse and apparent tensile strength loci, assessed from both suction-controlled TX and suction-controlled TTX testing on clayey sand, was accomplished. (Results are summarized in the following subsection.)

Suction-controlled TX testing was carried out in a fully automated, double-walled triaxial system, as shown in Figure 1a, featuring the following key items: (1) Base pedestal with 15-bar ceramics, (2) Top cap with coarse porous stones, (3) Inner cell water inlet, (4) Pore water pressure inlet, (5) Differential pressure transducer, (6) Pore air pressure inlet, (7) Flushing inlet, (8) Flushing outlet, (9) Outer cell water outlet, and (10) Soil volume change outlet. A typical cylindrical specimen has a 71.1 mm (2.8 in) diameter and a 142.2 mm (5.6 in) height. A detailed description of the main components and earlier performance verification tests is presented by Patil (2014).

Likewise, suction-controlled TTX testing was accomplished in a servo-controlled cubical cell with similar features, except with the cubical soil sample resting on a bottom wall assembly, as shown in Figure 1b, featuring the following key items: (1) Stainless steel bottom wall, (2) Cubical base pedestal, (3) Full set of symmetrically spaced coarse porous stones, and (4) Full set of symmetrically spaced 5-bar ceramics. Silicon rubber membranes form a pressure seal between each wall assembly and the core reaction frame of the cubical test cell, thus acting as the fluid barrier for distilled water pressurizing the top and four lateral faces of the specimen. A typical cubical specimen measures 76.2 mm (3 in) per side. A detailed description of the main components and earlier performance verification testing is presented by Pérez-Ruiz (2009).

A second chief motivation under this section of the work was the assessment of critical state lines from suction-controlled plane strain (PS) testing on silty soil. (Results are summarized in a subsequent subsection.) It is well known that plane strain analyses may render far more accurate predictions



for a vast majority of geotechnical infrastructure, including slopes, embankments, tunnels and pavements, given the particular geometries, loading paths and boundary conditions that such geosystems normally undergo. The majority of plane strain (biaxial) devices reported to date, however, only allow for soil testing under fully dry or saturated conditions (e.g., Wood, 1958; Vardoulakis & Graf, 1985; Drescher et al., 1990; Alshibli et al., 2004). In this work, suction-controlled PS testing was carried out in a fully automated, Vardoulakis type of biaxial apparatus, as shown in Figure 1c, featuring the following key items: (1) Bottom base plate; (2) U-shaped base frame, coupled with a Schneeberger type sliding table; (3) Bottom pedestal housing a 5-bar ceramic; and (4) Cuboid specimen. Two 8-mm thick rigid walls, made of Type 304 stainless steel, prevent the specimen from deforming along the intermediate principal axis. A typical cuboid specimen has a 90 mm (3.5 in) height, a 60 mm (2.4 in) width, and a 30 mm (1.2 in) depth. A detailed description of the main components and earlier performance verification is presented by Cruz et al. (2011).

The last chief motivation under this first section of the work was the assessment of peak and residual failure envelopes from suction-controlled ring shear (RS) testing

on clayey soil. (Results are also summarized in a subsequent subsection.) Despite the crucial importance of peak and residual shear strength properties of compacted clayey soils, there is very limited experimental evidence of unsaturated soil behavior under large deformations as the soil is being subjected to controlled suction states. In recent years, a few researchers have expanded the capabilities of Bromhead-type RS devices for soil testing under suction-controlled conditions (e.g., Infante-Sedano et al., 2007; Merchán et al., 2011). More comprehensive efforts, however, have yet to be undertaken to generate a thorough set of suction-dependent peak/residual failure envelopes for compacted clayey soil. In this work, suction-controlled RS testing was carried out in a fully automated RS apparatus, as shown in Figure 1d, featuring the following key items: (1) Outer wall of bottom annular platen housing a full set of 5-bar ceramics, (2) Inner wall of bottom annular platen, and (3) Spare set of 5-bar ceramics. A typical ring-shaped specimen has a 152.4 mm (6 in) outer diameter, a 96.5 mm (3.8 in) inner diameter, and an average thickness of 15.0 mm (0.6 in). A detailed description of the main components and performance verification is presented by Velosa (2011) and Yepes (2015).

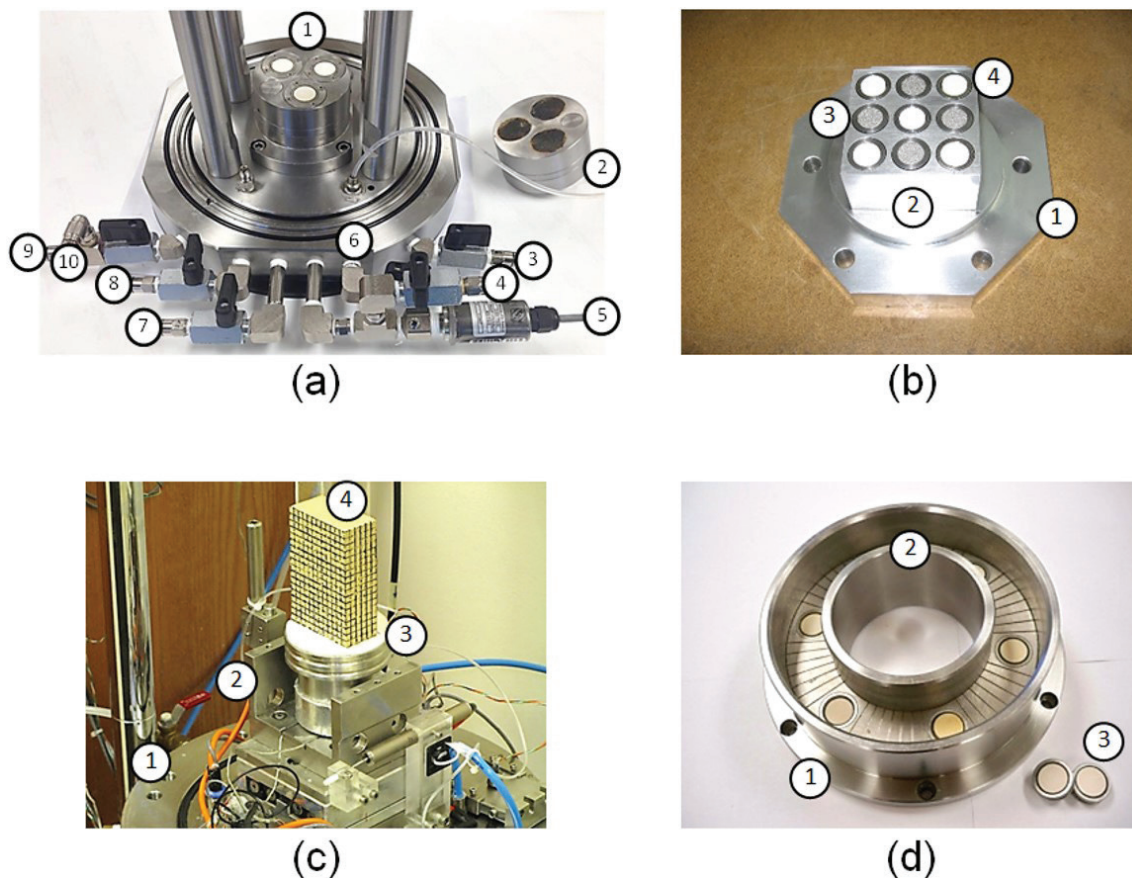


**Figure 1.** Key modifications to advanced soil testing devices for implementing axis-translation technique: (a) Triaxial, (b) True triaxial, (c) Plane strain, (d) Ring shear.

## 2.2 Suction-controlled triaxial (TX) vs. true triaxial (TTX) testing

The Barcelona Basic Model (BBM), introduced by Alonso et al. (1990), and the Oxford Model (OM), by Wheeler & Sivakumar (1995), have become two of the most popular critical state based constitutive frameworks postulated to date for unsaturated soils. The OM formulation is similar to that of the original BBM; however, it postulates that all the essential model parameters are suction-dependent and ought to be experimentally predetermined for a particular matric suction state.

A first distinctive feature of the original BBM is the assumption of a monotonic decrease of the volumetric stiffness parameter  $\lambda(s)$  with increasing matric suction, which in turn defines a Loading-Collapse (LC) yield locus in the  $p:s$  plane as a full set of preconsolidation pressures for each associated value of suction. Another distinctive feature of the original BBM is the postulation of an Apparent Tensile Strength (ATS) locus as a full set of apparent tensile strength values for each associated value of suction. Both conceptual loci are illustrated in Figure 2, which shows the experimental LC and ATS curves assessed from a series of suction-controlled triaxial TX and TTX testing on compacted SP-SC soil: poorly graded clayey sand.

The LC locus on the positive  $p:s$  quadrant was obtained from a series of hydrostatic compression tests conducted on statically compacted samples (cylindrical or cubical) of SP-SC soil under sustained matric suction states of 50, 100, 200, or 350 kPa. In each case, pore-fluid equalization was followed by a ramped consolidation from an initial net mean stress of 50 kPa to a final net mean stress of 600 kPa. The experimental data points in Figure 2 represent values of preconsolidation pressures obtained for each corresponding matric suction using either testing device. Likewise, the ATS locus on the negative  $p:s$  quadrant was obtained from a short series of conventional triaxial compression tests, and

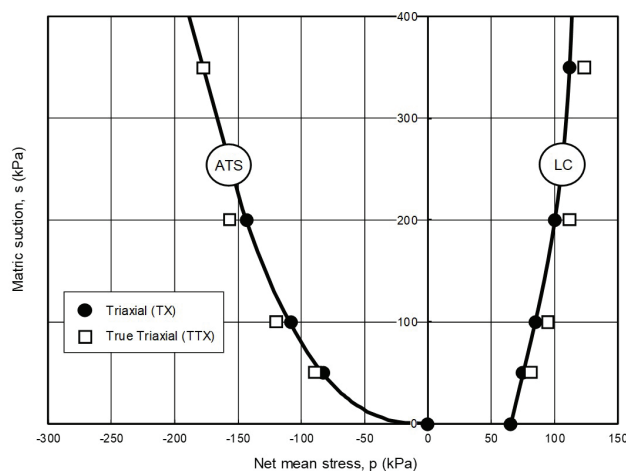


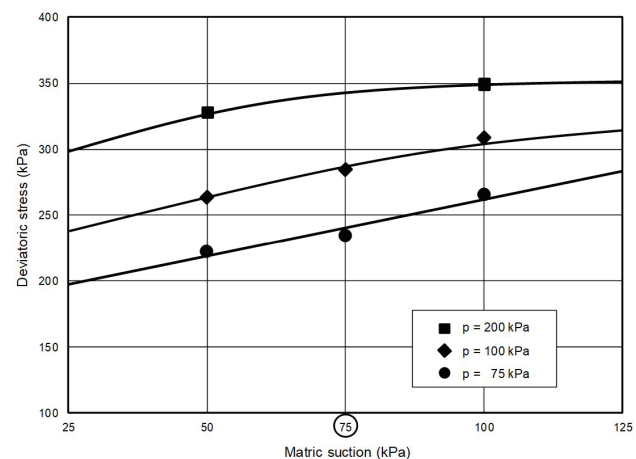
**Figure 2.** Loading-collapse (LC) and apparent tensile strength (ATS) curves from suction-controlled triaxial (TX) and true triaxial (TTX) testing on compacted SP-SC soil.

the corresponding critical state lines, conducted on statically compacted samples (cylindrical or cubical) of the same SP-SC soil and for the same range of sustained matric suction states (50 - 350 kPa).

Results strongly suggest the existence of a non-linear ATS locus, independent of the testing method: triaxial or true triaxial. The apparent tensile strength is indeed expected to reach a constant value (plateau) at significantly higher suction states ( $s \rightarrow \infty$ ), in a similar fashion as the original BBM formulation for preconsolidation pressures on the LC locus (Sheng et al. 2008), as shown in Figure 2. Even more suggestive, however, is the virtually identical response of SP-SC soil from suction-controlled TX and TTX testing, regardless of the level of induced matric suction and despite potential inconsistencies in the boundary conditions imposed on the test samples. It is worth mentioning that the Silastic Type J-RTV cubical membranes proved to yield best possible performance, especially in terms of minimal stress concentration at their corners (e.g., Sture & Desai, 1979; Janoo, 1986). These results serve as a contribution to what it might become a preliminary basis for the substantiation of test results obtained from one method, when implementing the axis-translation technique, based on results from the other.

## 2.3 Suction-controlled plane strain (PS) testing

A full set of critical state lines (CSLs) obtained from suction-controlled PS testing on compacted ML soil (low compressibility silt) is shown in Figure 3. The material is an artificially mixed soil, made of predominantly silty sand and kaolin clay. A typical specimen, as shown in Figure 1c, was prepared by uniaxial consolidation of a slurry mixture made of 75% fine sand and 25% kaolin. The CSLs were obtained from a series of conventional triaxial compression tests carried out on identically prepared cuboid specimens of ML soil under sustained matric suction states of 50, 75, or 100 kPa, and initial values of net mean stress of 75, 100, and 200 kPa.



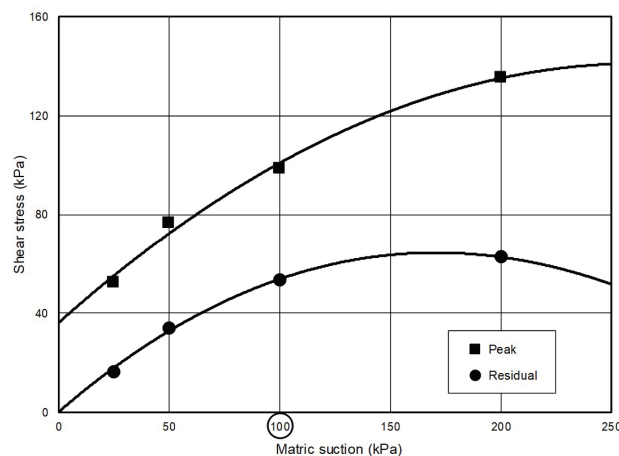
**Figure 3.** Critical state lines (CSLs) from suction-controlled plane strain (PS) testing on compacted ML soil.

Figure 3 shows the effect of increasing net normal stress on the position and slope of the CSLs of ML soil as projected onto the deviatoric stress vs. matric suction plane. Although not definitively conclusive, given the limited set of experimental datapoints, results clearly suggest an increasingly nonlinear CSL with increasing net normal stress, even under suction-controlled PS conditions. This can be directly attributed to the already (and thoroughly) demonstrated correspondence between the nonlinear nature of shear strength envelopes for most unsaturated soils, with increasing matric suction, and their respective soil-water characteristic curve (e.g., Vanapalli et al, 1996; Lu & Likos, 2004).

Within the regime of relatively low suction, and prior to the air-entry pressure, the soil pores remain essentially saturated, and the shear strength envelope is reasonably linear. As the soil becomes unsaturated, the reduction in the pore-water volume within this regime effectively reduces the contribution of matric suction toward shear strength. This effect becomes more readily apparent as the net normal stress increases, as effectively shown in Figure 3. It is worth noting that the air-entry value of the ML soil used in this work is approximately 75 kPa, beyond which the nonlinearity of the CSLs becomes increasingly manifest.

## 2.4 Suction-controlled ring shear (RS) testing

Peak and residual failure envelopes obtained from suction-controlled RS testing on compacted CL soil (low plasticity clay) are shown in Figure 4. The soil consists of 18% sand, 50% silt, and 32% clay. A typical RS specimen was prepared by statically compacting the loose soil-water mixture directly into the bottom annular platen of the RS apparatus, as featured in Figure 1d, via an upper annular platen. The upper annular platen itself features a full set of coarse porous stones for simultaneous pore-air pressure control in the RS specimen, thus allowing for implementation of the axis-translation technique.



**Figure 4.** Peak and residual failure envelopes from suction-controlled ring shear (RS) testing on compacted CL soil.

The assessment of peak and residual shear strength of compacted CL soil was accomplished under constant matric suction states ranging from 25 to 200 kPa, for a net normal stress of 100 kPa, which was attained via the upper annular platen during the in-place static compaction process. Once the soil attained at least 90% consolidation, a suction-controlled shearing was carried out at an average rotational speed of 0.023°/min, corresponding to an equivalent horizontal displacement rate of 0.025 mm/min. Shearing was terminated when it was readily apparent that a residual stress had been reached. This shearing rate is slightly lower than that reported in previous works where higher total suction values (up to 100 MPa) were induced via relative-humidity based techniques (e.g., Infante-Sedano et al., 2007).

Figure 4 shows the effect of matric suction on both peak and residual failure envelopes of CL soil as projected onto the shear stress vs. matric suction plane. The patterns are strikingly similar to those observed in the experimental CSLs obtained for compacted ML soil from suction-controlled PS testing (Figure 3), namely: (1) Both envelopes remain essentially linear within a range of relatively low values of suction, and (2) The nonlinearity of either envelope becoming more manifest with increasing suction beyond a threshold value. It is also worth noting that the air-entry value of the CL soil used in this work is approximately 100 kPa.

As has been demonstrated from extensive suction-controlled direct shear and triaxial testing on a wide variety of unsaturated soils, within the regime of relatively low suction, and prior to the air-entry pressure, the soil pores remain essentially saturated, the shear strength envelope is reasonably linear, and the beta angle ( $\phi^b$ ) with respect to suction remains effectively equal to the friction angle ( $\phi'$ ), as it is readily observed in Figure 4. Results also suggest a more pronounced (and detrimental) effect of increasing matric suction on the residual shear strength of compacted clay soil, as compared to that on its peak shear strength.

## 3. Thermo-hydro-mechanical behavior: recent evidence

### 3.1 Experimental program and scope

A considerable portion of the increasingly ubiquitous geothermal infrastructure across the world is located in traditionally earthquake prone areas while being supported by soil deposits well above the phreatic surface. To date, however, there is hardly any comprehensive study at the laboratory scale that had focused on a thorough characterization of strength-stiffness properties of unsaturated cohesive-frictional soils over a relatively large range of shear strain amplitudes (0.001% to 0.1%) and under simultaneous thermal conditioning of the pore fluids, which constitutes a first chief motivation under this second section of the work (Thermo-hydro-mechanical Behavior).



Cyclic triaxial testing has proved to be a potentially suitable approach to studying the effect of elevated temperatures on unsaturated soil response under repeated loading, particularly the resilient modulus  $M_R$  (e.g., Ng & Zhou, 2014). The non-destructive resonant column (RC) technique, however, has proved to be sufficiently reliable for similar purposes, particularly the assessment of shear-wave velocity, shear modulus, and material damping, and is relatively inexpensive compared to most cyclic triaxial or cyclic simple shear apparatuses. Furthermore, most conventional devices are not suitable to capture small-strain behavior adequately and hence vastly underestimate soil stiffness.

In this work, an existing RC apparatus has been upgraded in order to investigate the dynamic response of compacted clayey soil via thermo-controlled, constant-water content RC testing, with particular emphasis on confinement/moisture/thermal effects on frequency response curves and cyclic shear stress vs. shear strain hysteresis loops. (Results are summarized in the following subsection.) The upgraded RC apparatus, as shown in Figure 5a, features the following key items: (1) Bottom base plate, (2) Base pedestal with optional 5-bar ceramics, (3) Omega Type K thermocouple, and (4) Cyclic torque actuator with Model SR-DF-FO-250 fiber-optics proximitor probe. A Type HTC-250 digital convection heater, featuring an internal fan, was also adapted to the main cell of the RC device for thermal conditioning of the soil sample, ranging from 20 to 60 degrees Celsius. A typical cylindrical specimen has a 70 mm (2.75 in) diameter and a

150 mm (5.9 in) height. A detailed description of the main components and performance verification and calibration testing is presented by Davoodi-Bilesavar (2020).

One last chief motivation under this section of the work was the assessment of residual failure envelopes from suction/thermo-controlled ring shear (RS) testing on clayey soil (results are summarized in a subsequent subsection). Drilled shaft foundations above ground water table which are also used as part of ground-source heat pump systems, hence referred to as energy foundations, have proved to be a promising technology for increasing the energy efficiency of heating-cooling systems. Thermally induced changes in shear strength of surrounding soils may have a significant impact on some of their key design parameters, including side shear resistance, and therefore the overall performance of these foundations (e.g., Cekerevac & Laloui, 2004; Uchaipichat & Khalili, 2009; Alsherif & McCartney, 2016; Cheng et al., 2017). To date, however, there is hardly any comprehensive study at the laboratory scale that has focused on a thorough characterization of shear strength behavior of soils, from peak to residual, over a wider range of shear deformations and simultaneous thermal conditioning of the pore-fluids.

In this work, suction/thermo-controlled RS testing was carried out in an upgraded version of the suction-controlled RS apparatus illustrated in Figure 1d, thus featuring all of the essential items for implementing the axis-translation technique. The upgraded version, however, as shown in Figure 5b, features the additional key items: (1) Thermal band, wrapping

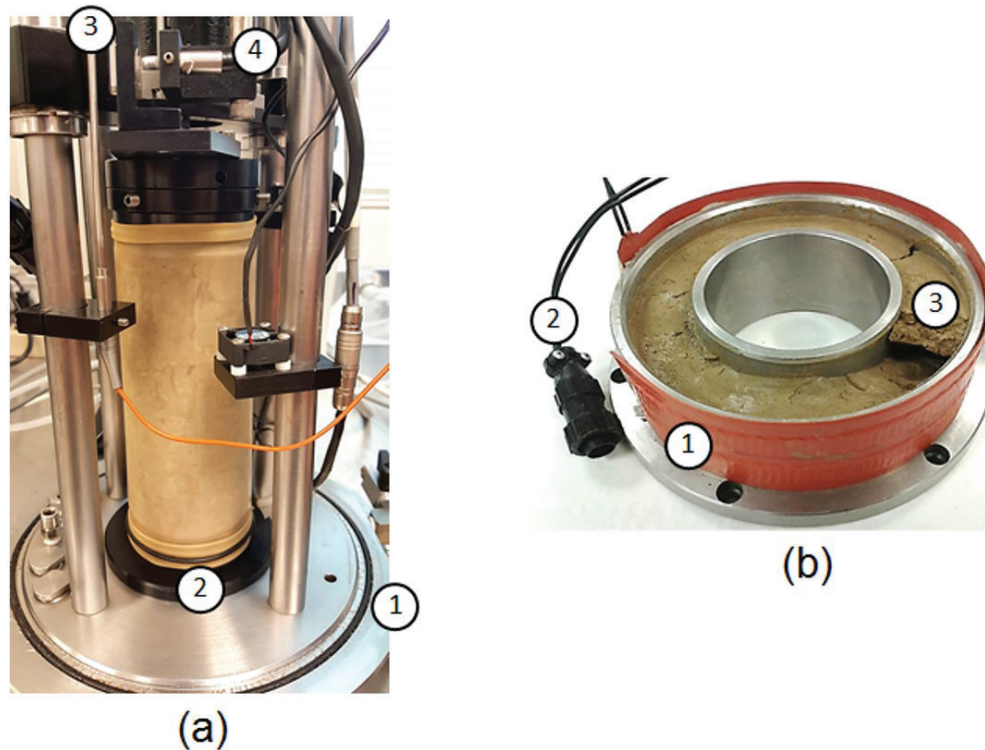


**Figure 5.** Key modifications for thermo-hydro-mechanical testing of soil over a whole range of shear strain amplitudes: (a) Resonant column, (b) Ring shear.

bottom annular platen; (2) Heating lead wire, connecting to a convection heater; and (3) Clayey soil specimen failed under elevated temperature. A Type HTC-250 digital convection heater, featuring an internal fan, was also adapted to the main cell of the RS device for thermal conditioning of the soil, ranging from 20 to 60° C. The upper annular platen, which seats right on top of the specimen, features an Omega Type K thermocouple for direct measurements of soil temperature induced by the featured thermal band around the bottom annular platen. The typical ring-shaped specimen featured the same dimensions as those illustrated in Figure 1d, namely, a 152.4 mm (6 in) outer diameter, a 96.5 mm (3.8 in) inner diameter, and an average thickness of 15.0 mm (0.6 in). A detailed description of its main components and performance verification is presented by Yepes (2015).

### 3.2 Thermo-controlled resonant column (RC) testing

Typical frequency response curves (FRCs) obtained from thermo-controlled RC testing on a sample of CL soil compacted at optimum moisture content ( $w = 13.6\%$ ) are shown in Figure 6. The soil consists of 20% sand, 28% silt, and 52% clay, thus classifying as low plasticity clay as per the USCS. Likewise, typical FRCs obtained from a CL soil sample compacted on wet side of optimum ( $w = 17\%$ ) are shown in Figure 7. In both cases, the test sample was subjected to an identical multistage stress/thermal history prior to RC testing, summarized as follows.

The sample was first allowed to consolidate for at least 24 hrs under a 5 psi (34.5 kPa) confinement, after which the convection heater was set to room temperature (25° C) and thermal conditioning of the soil allowed for at least 3 hours. A first FRC was generated by sweeping the input-torque frequency range, typically between 100-280 Hz, with a 0.1 kN-m magnitude cyclic torque. The temperature was then gradually increase to 60° C, under constant 5 psi (34.5 kPa) confinement, and thermal conditioning allowed for another 3 hours, after which a new FRC was generated. The convection heater was then shut off and the soil allowed to cool down back to room temperature (25° C).

After soil cooling, and given the non-destructive nature of the RC technique for cyclic torques of 0.1 kN-m magnitude or less, the confinement was raised to 20 psi (138 kPa) and the sample subjected to the same thermal history prior to further RC testing. After the sample was taken apart, the moisture content was measured at its middle, top, and bottom to assess the amount of water loss during cyclic thermal loading. No significant water loss was observed in any of the test samples (less than 1% loss on average), thus rendering all trials as constant-water content RC tests.

The RC test essentially involves a soil column with fixed-free end conditions that is excited to vibrate in one of its natural modes. The FRCs shown in Figure 6a were generated upon thermal conditioning of the test soil to a temperature of 25° C. Results corroborate the critical influence that the

level of confinement has been observed to have over a soil column under resonance, with a significant rightward shift of the FRC under higher confinement of 20 psi (138 kPa), which can be directly attributed to the ensuing increase in rigidity (stiffness) of the soil skeleton, and hence the resonant frequency. Conversely (and consequently), the maximum shear strain amplitude induced at resonance by the 0.1 kN-m torque is observed to decrease with increasing confining pressure.

Likewise, the FRCs shown in Figure 6b were generated upon thermal conditioning of the test soil to a temperature of 60° C. Results corroborate the general behavioral trends noted for 25° C, namely, a significant rightward shift of the FRC under higher confinement, and thus lower shear strain amplitude at resonance. However, RC testing under 60° C is observed to yield lower values of resonant frequencies (Hz) and concomitantly higher values of shear strain amplitudes (%) at resonance, as compared to those generated from RC testing under 25° C. This is strongly indicative of an increasingly detrimental effect of rising temperatures on soil stiffness, a behavioral trend that appears to substantiate findings from previous work related to thermal effects on shear strength properties of compacted clayey soils (e.g., Cekerevac & Laloui, 2004; Alsherif & McCartney, 2016).

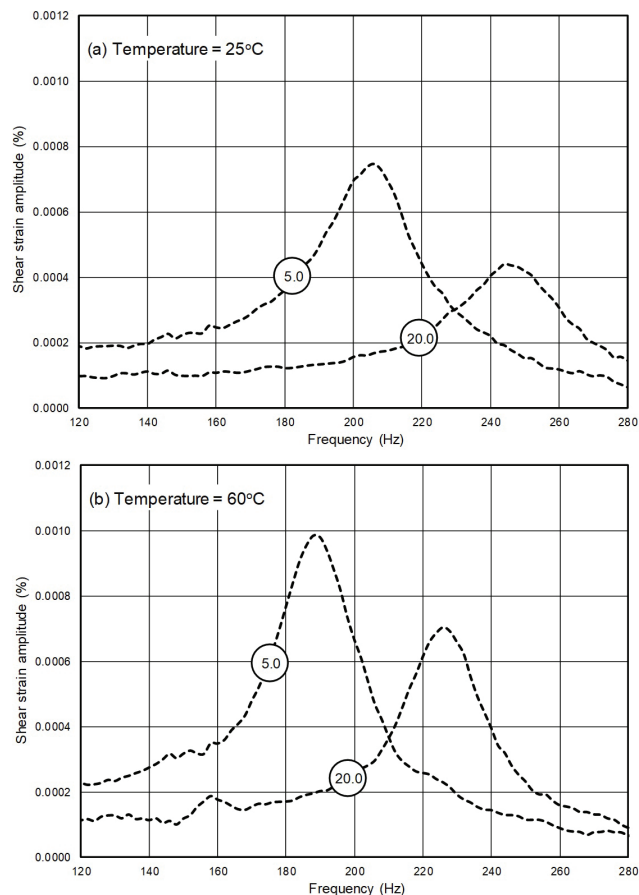


**Figure 6.** Frequency response curves (FRCs) from thermo-controlled RC testing on CL soil compacted at optimum moisture ( $w = 13.6\%$ ): (a) Temperature = 25° C, (b) Temperature = 60° C.



It is worth restating that all the FRCs shown in Figure 6 correspond to CL soil compacted at optimum gravimetric moisture content ( $w = 13.6\%$ ), which corresponds to a matric suction of 400 kPa, as per the soil-water characteristic curve (Davoodi-Bilesavar, 2020). The intent was to induce an initial suction state beyond the air-entry value of the soil (60 kPa) and well into the drying loop of the SWCC. On the other hand, all the FRCs shown in Figure 7 correspond to CL soil compacted on wet side of optimum ( $w = 17\%$ ), which now corresponds to a lower matric suction of 40 kPa. In this latter case, the intent was to induce an initial matric suction just below the air-entry value of the soil, and the resulting FRCs virtually replicate the same trends observed in Figure 6 for CL soil compacted at optimum moisture.

The set of FRCs shown in Figure 7, however, appears to suggest a far less detrimental effect of rising temperatures on soil stiffness, that is, for clayey soils compacted at relatively high moisture contents, and hence initial matric suctions below their air-entry value. This is substantiated by the minimal decrease observed in resonant frequencies, and thus minimal increase in shear strain amplitudes, from

25 to 60° C, which is also in conformity with findings from previous work related to thermal effects on shear strength behavior.

The influence of the initial (compaction induced) matric suction can be readily assessed by comparing the main RC test outputs in Figures 6 and 7, respectively. For instance, for 5 psi (34.5 kPa) confinement and 25° C temperature, the output resonant frequency experiences a rather drastic decrease, from 208 to 128 Hz, as the compaction induced suction decreases almost tenfold from 400 kPa ( $w = 13.6\%$ ) to 40 kPa ( $w = 17\%$ ). Likewise, for 60° C temperature, the output resonant frequency decreases from 190 to 126 Hz for the same difference in compaction induced matric suctions. The same trends can be observed for higher confinements (20 psi) and also in terms of both resonant frequencies and shear strain amplitudes.

The main focus of this subsection of the work has been on small-strain stiffness of compacted CL soil. It is well known, however, that the cyclic behavior of soils is nonlinear and hysteretic; consequently, the shear modulus and damping are heavily shear strain dependent. It is hence worth mentioning that the applied 0.1 kN-m torque proved to yield shear strain amplitudes far below a threshold limit (0.01%), thus rendering the CL soil response from all RC testing as low-amplitude or purely linear (a more thorough assessment of shear moduli, damping ratios, and threshold strain amplitudes is far beyond the intended scope of the present work).

Figures 8a and 8b show the cyclic hysteretic stress-strain loops obtained from two additional, identically prepared specimens of CL soil under temperatures of 25 and 60° C, respectively. The loops were both generated under a 5 psi (34.5 kPa) confinement, with the specimens compacted on wet side of optimum ( $w = 17\%$ ), yielding initial suctions of 40 kPa and 42 kPa (verified via filter paper), respectively. In both cases, the frequency of the applied torque was set to the same value corresponding to resonance in Figures 7a and 7b, respectively.

It can be readily observed that the range of maximum shear strain amplitudes generated in the loops (0.002% - 0.003%) is reasonably close to that observed in the corresponding FRCs (Figure 7). Moreover, a slightly degraded secant modulus (slope of hysteretic loop) is observed with increasing temperature, which is consistent with the general trends emerging from Figures 6 and 7. On the other hand, equivalent viscous damping can be evaluated from the area enclosed by the hysteretic loops (e.g., Hardin & Drnevich, 1972; Prakash, 1981; Kramer, 1996). The results hence confirm the inverse proportionality that exist between shear modulus and damping, even under thermally controlled conditions, that is, larger areas enclosed by the loops, and larger shear strain amplitudes induced by the same cyclic shear stress, with increasing temperature.

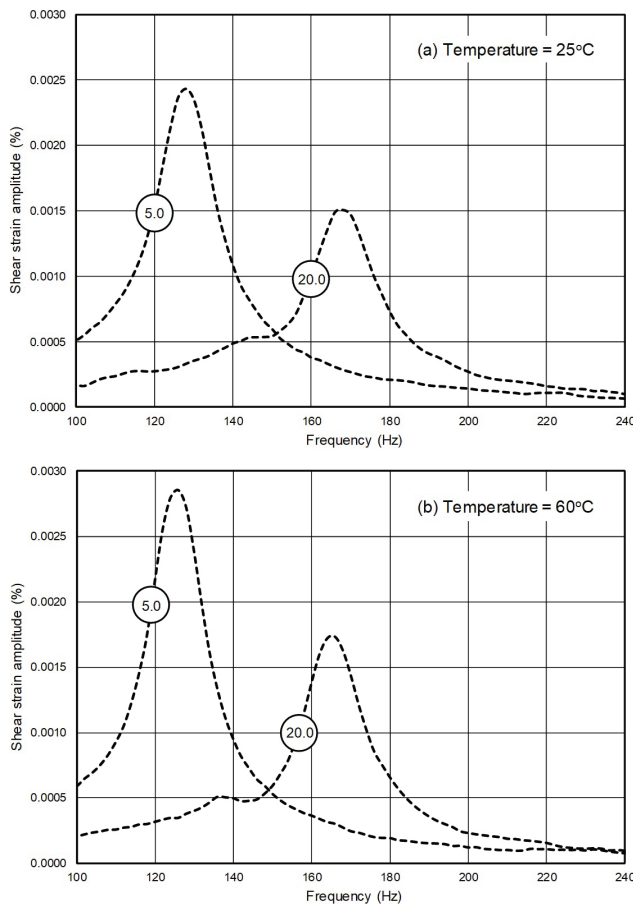


**Figure 7.** Frequency response curves (FRCs) from thermo-controlled RC testing on CL soil compacted on wet side of optimum ( $w = 17\%$ ): (a) Temperature = 25° C, (b) Temperature = 60° C.

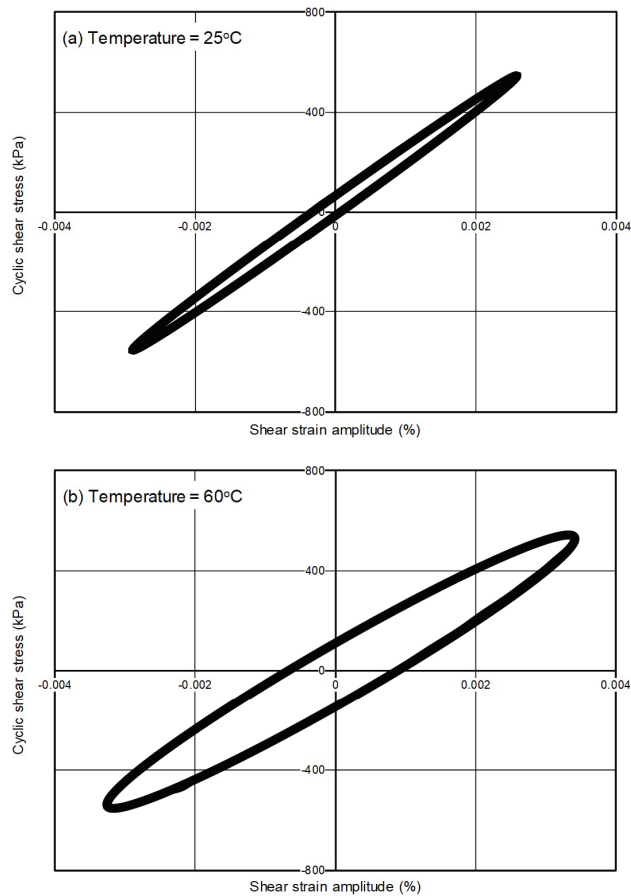


**Figure 8.** Stress-strain hysteresis loops from thermo-controlled RC testing on compacted CL soil: (a) Temperature = 25° C, (b) Temperature = 60° C.

### 3.3 Suction/thermo-controlled ring shear (RS) testing

The residual failure envelope obtained from suction/thermo-controlled RS testing on three identically prepared samples of compacted CL soil (low plasticity clay) is shown in Figure 9. The soil is virtually identical to the test material used for generating the peak and residual failure envelopes shown in Figure 4 via suction-controlled RS testing under isothermal conditions. In this case, however, each RS sample was subjected to a multistage stress/suction/thermal history prior to shearing, summarized as follows.

The RS specimen was prepared by statically compacting the loose soil-water mixture directly into the bottom annular platen of the RS apparatus via the upper annular platen. The sample was first allowed to consolidate under a vertical stress of 100 kPa. Once the soil attained at least 90% consolidation, the pore-air pressure was gradually increased to a target value and the pore-fluids allowed to come under equilibrium (equalization stage) under a matric suction state of 50 kPa via the axis-translation technique. The convection heater was then set to a constant temperature of either 20, 30, or 40° C, and thermal conditioning of the soil allowed for

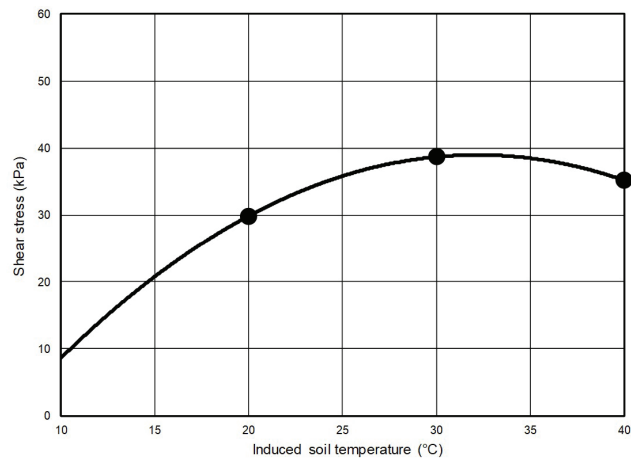


**Figure 9.** Residual failure envelope from suction/thermo-controlled ring shear (RS) testing on compacted CL soil.

at least 3 hours via the thermal band wrapped around the bottom annular platen, as illustrated in Figure 5b. The soil temperature was thoroughly verified by the Omega Type K thermocouple adapted to the upper annular platen.

Upon complete stress/suction/thermal conditioning of the soil, and for procedural consistency purposes, each suction/thermo-controlled RS testing was conducted at the same average rotational speed of 0.023°/min, with the shearing phase terminated when it was readily apparent that a residual stress had been reached. The convection heater was finally shut off and the soil allowed to cool down back to room temperature (approximately 25° C).

For one particular set of experimental variables, namely, net normal stress of 100 kPa, matric suction of 50 kPa, and soil temperature of 25° C, the resulting residual failure envelope, as shown in Figure 9, yields a value of residual shear strength of approximately 35 kPa, which is reasonably close to that generated from suction-controlled RS testing on same CL soil, as shown in Figure 4. This serves as further evidence of the potential suitability of the upgraded RS device for thermo-controlled testing. More importantly, however, the resulting envelope appears to support the notion of a “threshold” temperature beyond which the residual shear strength of compacted clayey soil experiences an increasingly detrimental effect with increasing temperature, very much like the effect of increasing matric suction on a would-be “residual” beta angle ( $\phi^B$ ), as shown in Figure 4.

## 4. Concluding remarks

As mentioned earlier as the present work was being introduced in its intent and scope, the main objective was to synthesize some of the most recent experimental evidence of thermo-hydro-mechanical behavior of cohesive-frictional soils over a whole range of suction- and/or thermo-controlled stress paths and modes of deformation, with particular

emphasis on essential features of unsaturated soil behavior that are yet to be thoroughly investigated in the literature.

The virtually identical response of SP-SC soil from suction-controlled TX and TTX testing, in terms of both LC and ATS loci; the nonlinearity of CSLs of ML soil with increasing matric suction, even under suction-controlled PS conditions; the similar patterns observed in peak and residual failure envelopes of CL soil from suction-controlled RS testing; the increasingly detrimental effect of rising temperatures on CL soil stiffness via thermo-controlled RC testing; the inverse proportionality observed between shear modulus and damping under thermally controlled conditions, as evidenced by cyclic hysteretic loops; and finally, the evidence of a “threshold” temperature beyond which the residual shear strength of CL soil decreases progressively with increasing temperature stand as the most enlightening features of unsaturated soil behavior that the present work has gained further insights on.

In a far more general sense, however, the results from the relatively short series of triaxial, true triaxial, plane strain, ring shear, and resonant column tests accomplished in this work underscore the crucial importance of keeping a research focus on expanding and upgrading the capabilities of standardized testing techniques for a thorough and proper characterization of the engineering response of unsaturated soil materials, as well as the significant amount of room still available for further investigative efforts.

The present experimental effort would have been ideally accomplished on the same type of soil in order to facilitate the analysis and comparison of behavioral trends assessed from the different testing methods. However, each individual soil type, and the corresponding experimental program, was investigated under the auspices of different sponsors and programs based on proposals pursuing a wide range of research ideas in the fascinating subject of unsaturated soil mechanics.

## Acknowledgements

The core systems of the upgraded TX, TTX and RS devices were developed under the auspices of the U.S. National Science Foundation (NSF): Awards MRI-1039956, MRI-0216545 and CMS-0626090, respectively. This support is gratefully acknowledged. Any findings, conclusions or recommendations expressed in this material are those of the authors and do not necessarily reflect the views of the NSF. The authors would also like to acknowledge the invaluable suggestions made by Drs. Anand J. Puppala, Aritra Banerjee and Arcesio Lizcano throughout this effort, as well as the technical advice from Mr. Peter Goguen of Geotechnical Consulting and Testing Systems (GCTS). Last but not least, the authors appreciate the opportunity offered by Drs. Tacio M.P. de Campos, Fernando A.M. Marinho, and Gilson Gitirana Jr. to submit a state-of-the-art paper contribution to PanAm-UNSAT 2021.

## Declaration of interest

The authors acknowledge the absence of any conflicting interests throughout the course and conduct of the present experimental research effort.

## Authors' contributions

Laureano R. Hoyos: conceptualization and original draft preparation. Roya Davoodi-Bilesavar: resonant column testing. Ujwalkumar D. Patil: triaxial testing. Jairo E. Yepes: ring shear testing. Diego D. Pérez-Ruiz: true triaxial testing. José A. Cruz: plane strain testing.

## References

- Adams, B.A., & Wulfsohn, D. (1997). Variation of the critical-state boundaries of an agricultural soil. *European Journal of Soil Science*, 48(4), 739-748. <http://dx.doi.org/10.1111/j.1365-2389.1997.tb00573.x>.
- Alonso, E.E., Gens, A., & Josa, A. (1990). A constitutive model for partially saturated soils. *Geotechnique*, 40(3), 405-430. <http://dx.doi.org/10.1680/geot.1990.40.3.405>.
- Alsherif, N.A., & McCartney, J.S. (2016). Yielding of silt at high temperature and suction magnitudes. *Geotechnical and Geological Engineering*, 34(2), 501-514. <http://dx.doi.org/10.1007/s10706-015-9961-x>.
- Alshibli, K.A., Godbold, D.L., & Hoffman, K. (2004). The Louisiana plane strain apparatus for soil testing. *Geotechnical Testing Journal*, 27(4), 337-346. <http://dx.doi.org/10.1520/GTJ19103>.
- Bolzon, G., Schrefler, B.A., & Zienkiewicz, O.C. (1996). Elasto-plastic soil constitutive laws generalized to partially saturated states. *Geotechnique*, 46(2), 279-289. <http://dx.doi.org/10.1680/geot.1996.46.2.279>.
- Cekerevac, C., & Laloui, L. (2004). Experimental study of thermal effects on the mechanical behavior of a clay. *International Journal for Numerical and Analytical Methods in Geomechanics*, 28(3), 209-228. <http://dx.doi.org/10.1002/nag.332>.
- Cheng, Q., Kaewsong, R., Zhou, C., & Ng, C.W.W. (2017). A double cell triaxial apparatus for testing unsaturated soil under heating and cooling. In: A. Ferrari & L. Laloui (eds), *Advances in Laboratory Testing and Modelling of Soils and Shales (ATMSS)* (Springer Series in Geomechanics and Geoengineering). Cham: Springer.. [https://doi.org/10.1007/978-3-319-52773-4\\_21](https://doi.org/10.1007/978-3-319-52773-4_21).
- Chiu, C.F., & Ng, C.W.W. (2003). A state-dependent elasto-plastic model for saturated and unsaturated soils. *Geotechnique*, 53(9), 809-829. <http://dx.doi.org/10.1680/geot.2003.53.9.809>.
- Cruz, J.A., Hoyos, L.R., & Lizcano, A. (2011). A novel suction-controlled biaxial apparatus for unsaturated soils. In: N. Khalili, A. Russell & A. Khoshghalb (Eds.), *Unsaturated*

- Soils: Research and Applications* (vol. 1, pp. 233-237). Taylor & Francis. <https://doi.org/10.1201/B17034-14>.
- Cui, Y.J., & Delage, P. (1996). Yielding and plastic behaviour of an unsaturated compacted silt. *Geotechnique*, 46(2), 291-311. <http://dx.doi.org/10.1680/geot.1996.46.2.291>.
- Davoodi-Bilesavar, R. (2020). *Dynamic properties of cohesive-frictional soils via thermo-controlled resonant column testing* [Unpublished doctoral dissertation]. University of Texas.
- Drescher, A., Vardoulakis, I., & Han, C. (1990). A biaxial apparatus for testing soils. *Geotechnical Testing Journal*, 13(3), 226-234. <http://dx.doi.org/10.1520/GTJ10161J>.
- Estabragh, A., & Javadi, A. (2014). Effect of soil density and suction on the elastic and plastic parameters of unsaturated silty soil. *International Journal of Geomechanics*, 15(5), 04014079. [http://dx.doi.org/10.1061/\(ASCE\)GM.1943-5622.0000422](http://dx.doi.org/10.1061/(ASCE)GM.1943-5622.0000422).
- Estabragh, A.R., Javadi, A.A., & Boot, J.C. (2004). Effect of compaction pressure on consolidation behavior of unsaturated silty soil. *Canadian Geotechnical Journal*, 41(3), 540-550. <http://dx.doi.org/10.1139/t04-007>.
- Hardin, B.O., & Drnevich, V.P. (1972). Shear modulus and damping in soils: measurement and parameter effects. *Journal of the Soil Mechanics and Foundations Division*, 98(6), 603-624. <http://dx.doi.org/10.1061/JSFEAQ.0001756>.
- Hoyos, L., Perez-Ruiz, D., & Puppala, A. (2012). Modeling unsaturated soil response under suction-controlled true triaxial stress paths. *International Journal of Geomechanics*, 12(3), 292-308. [http://dx.doi.org/10.1061/\(ASCE\)GM.1943-5622.0000159](http://dx.doi.org/10.1061/(ASCE)GM.1943-5622.0000159).
- Hoyos, L.R., & Macari, E.J. (2001). Development of a stress/suction-controlled true triaxial testing device for unsaturated soils. *Geotechnical Testing Journal*, 24(1), 5-13. <http://dx.doi.org/10.1520/GTJ11277J>.
- Infante-Sedano, J.A., Vanapalli, S.K., & Garga, V.K. (2007). Modified ring shear apparatus for unsaturated soils testing. *Geotechnical Testing Journal*, 30(1), 39-47. <http://dx.doi.org/10.1520/GTJ100002>.
- Janoo, V.C. (1986). *Drained and undrained behavior of sand under high pressures* [Unpublished doctoral dissertation]. University of Colorado at Boulder.
- Kramer, S.L. (1996). *Geotechnical Earthquake Engineering*. Prentice-Hall.
- Liu, C., & Muraleetharan, K. (2012). Coupled hydro-mechanical elastoplastic constitutive model for unsaturated sands and silts. II: Integration, calibration, and validation. *International Journal of Geomechanics*, 12(3), 248-259. [http://dx.doi.org/10.1061/\(ASCE\)GM.1943-5622.0000147](http://dx.doi.org/10.1061/(ASCE)GM.1943-5622.0000147).
- Lu, N., & Likos, W.J. (2004). *Unsaturated Soil Mechanics*. John Wiley & Sons.
- Maatouk, A., Leroueil, S., & La Rochelle, P. (1995). Yielding and critical state of a collapsible unsaturated silty soil. *Geotechnique*, 45(3), 465-477. <http://dx.doi.org/10.1680/geot.1995.45.3.465>.
- Matsuoka, H., Sun, D.A., Kogane, A., Fukuzawa, N., & Ichihara, W. (2002). Stress-strain behaviour of unsaturated soil in true triaxial tests. *Canadian Geotechnical Journal*, 39(3), 608-619. <http://dx.doi.org/10.1139/t02-031>.
- Merchán, V., Romero, E., & Vaunat, J. (2011). An adapted ring shear apparatus for testing partly saturated soils in the high suction range. *Geotechnical Testing Journal*, 34(5), 433-444. <http://dx.doi.org/10.1520/GTJ103638>.
- Ng, C.W.W., & Zhou, C. (2014). Cyclic behaviour of an unsaturated silt at various suctions and temperatures. *Geotechnique*, 64(9), 709-720. <http://dx.doi.org/10.1680/geot.14.P.015>.
- Patil, U.D. (2014). *Response of unsaturated intermediate geomaterials over a wider range of suction states using a double-walled triaxial testing device* [Doctoral dissertation]. University of Texas. <http://hdl.handle.net/10106/24761>.
- Pérez-Ruiz, D.D. (2009). *A refined true triaxial apparatus for testing unsaturated soils under suction-controlled stress paths* [Doctoral dissertation]. University of Texas. <http://hdl.handle.net/10106/1764>.
- Prakash, S. (1981). *Soil Dynamics*. McGraw-Hill.
- Rampino, C., Mancuso, C., & Vinale, F. (2000). Experimental behavior and modelling of an unsaturated compacted soil. *Canadian Geotechnical Journal*, 37(4), 748-763. <http://dx.doi.org/10.1139/t00-004>.
- Reis, R.M., de Azevedo, R.F., Botelho, B.S., & Vilar, O.M. (2011). Performance of a cubical triaxial apparatus for testing saturated and unsaturated soils. *Geotechnical Testing Journal*, 34(3), 177-185. <http://dx.doi.org/10.1520/GTJ103256>.
- Sheng, D., Fredlund, D.G., & Gens, A. (2008). A new modeling approach for unsaturated soils using independent stress variables. *Canadian Geotechnical Journal*, 45(4), 511-534. <http://dx.doi.org/10.1139/T07-112>.
- Sivakumar, V. (1993). *A critical state framework for unsaturated soil* [Doctoral dissertation]. University of Sheffield. <https://theses.whiterose.ac.uk/21744>.
- Sivakumar, V., & Wheeler, S.J. (2000). Influence of compaction procedure on the mechanical behaviour of an unsaturated compacted clay. Part 1: wetting and isotropic compression. *Geotechnique*, 50(4), 359-368. <http://dx.doi.org/10.1680/geot.2000.50.4.359>.
- Sture, S., & Desai, C.S. (1979). Fluid cushion truly triaxial or multiaxial testing device. *Geotechnical Testing Journal*, 2(1), 20-33. <http://dx.doi.org/10.1520/GTJ10585J>.
- Tang, G.X., & Graham, J. (2002). A possible elasto-plastic framework for unsaturated soils with high-plasticity. *Canadian Geotechnical Journal*, 39(4), 894-907. <http://dx.doi.org/10.1139/t02-024>.
- Thu, T.M., Rahardjo, H., & Leong, E.C. (2007). Critical state behavior of a compacted silt specimen. *Soil and Foundation*, 47(4), 749-755. <http://dx.doi.org/10.3208/sandf.47.749>.

- Toll, D.G. (1990). A framework for unsaturated soil behaviour. *Geotechnique*, 40(1), 31-44. <http://dx.doi.org/10.1680/geot.1990.40.1.31>.
- Uchaipichat, A., & Khalili, N. (2009). Experimental investigation of thermo-hydro-mechanical behaviour of an unsaturated silt. *Geotechnique*, 59(4), 339-353. <http://dx.doi.org/10.1680/geot.2009.59.4.339>.
- Usmani, A., Ramana, G., & Sharma, K. (2012). Stress-strain-volume change modeling of Delhi silt in triaxial compression and extension. *International Journal of Geomechanics*, 12(3), 323-326. [http://dx.doi.org/10.1061/\(ASCE\)GM.1943-5622.0000144](http://dx.doi.org/10.1061/(ASCE)GM.1943-5622.0000144).
- Vanapalli, S.K., Fredlund, D.G., Pufahl, D.E., & Clifton, A.W. (1996). Model for the prediction of shear strength with respect to soil suction. *Canadian Geotechnical Journal*, 33(3), 379-392. <http://dx.doi.org/10.1139/t96-060>.
- Vardoulakis, I., & Graf, B. (1985). Calibration of constitutive models for granular materials using data from biaxial experiments. *Geotechnique*, 35(3), 299-317. <http://dx.doi.org/10.1680/geot.1985.35.3.299>.
- Velosa, C.L. (2011). *Unsaturated soil behavior under large deformations using a fully servo/suction-controlled ring shear apparatus* [Doctoral dissertation]. University of Texas. <http://hdl.handle.net/10106/5875>.
- Wang, Q., Pufahl, D.E., & Fredlund, D.G. (2002). A study of critical state on an unsaturated silty soil. *Canadian Geotechnical Journal*, 39(1), 213-218. <http://dx.doi.org/10.1139/t01-086>.
- Wheeler, S.J. (1996). Inclusion of specific water volume within an elastoplastic model for unsaturated soil. *Canadian Geotechnical Journal*, 33(1), 42-57. <http://dx.doi.org/10.1139/t96-023>.
- Wheeler, S.J., & Sivakumar, V. (1995). An elasto-plastic critical state framework for unsaturated soils. *Geotechnique*, 45(1), 35-53. <http://dx.doi.org/10.1680/geot.1995.45.1.35>.
- Wood, C.C. (1958). *Shear strength and volume change characteristics of compacted soil under conditions of plane strain* [Unpublished doctoral dissertation]. University of London.
- Yepes, J.E. (2015). *Thermo-hydro-mechanical behavior of unsaturated clayey soils via thermo/suction-controlled ring shear testing* [Doctoral dissertation]. University of Texas. <http://hdl.handle.net/10106/25512>.
- Zhang, X., & Li, L. (2011). Limitations in the constitutive modeling of unsaturated soils and solutions. *International Journal of Geomechanics*, 11(3), 174-185. [http://dx.doi.org/10.1061/\(ASCE\)GM.1943-5622.0000076](http://dx.doi.org/10.1061/(ASCE)GM.1943-5622.0000076).



## The new expertise required for designing safe tailings storage facilities

Gordon Ward Wilson<sup>1#</sup> 

Article

### Keywords

Filtered tailings  
Dry stack tailings  
Design  
Mine waste management

### Abstract

The global mining community has seen a dangerous sequence of failures in tailings dams, beginning with Mount Polley mine, followed by the Samarco, Cadia Valley and Córrego do Feijão mines. This sequence of failures began on August 4, 2014, at the Mount Polley tailings storage facility in British Columbia, Canada. The initial failure in the embankment at the Mount Polley tailings storage facility had substantial impact on the global mining industry. The Independent Expert Engineering Investigation and Review Panel (IEEIRP) tasked with the investigation of the breach in the tailings dam at Mount Polley made major contributions for new guidelines. The incident has given rise to comprehensive recommendations for best available tailings technologies (BAT) based on principles such as the elimination of surface water from impoundments with the promotion of unsaturated conditions in the tailings through drainage provisions. The application of these BAT principles for the surface storage of tailings leads to the use of filtered tailings technology. Filtered tailings technology or “dry stack tailings” can satisfy each of the BAT components when the impoundment is properly designed and constructed. The implementation of the best available technologies for the physical stability (BAT-PS) of tailings impoundments competes directly with the best available technologies for the chemical stability (BAT-CS) of reactive tailings that may produce acid and metalliferous drainage. The new expertise in mine waste management required to achieve both BAT-PS and BAT-CS are discussed in the present paper.

## 1. Introduction

The global mining community has recently witnessed a series of serious failures in the tailings dams at the Mount Polley, Samarco, Cadia Valley and Córrego do Feijão mines. This sequence of failures began on August 4, 2014, at the Mount Polley tailings storage facility in British Columbia, Canada.

In the case of the Mount Polley failure, approximately 25 million m<sup>3</sup> of water and tailings were released into Polley Lake, Hazeltine Creek and Quesnel Lake. The breach occurred suddenly at about 1:00 am and without warning in the perimeter embankment. Fortunately, there was no loss of life. The British Columbia Ministry of Energy and Mines created an Independent Expert Engineering Investigation and Review Panel (IEEIRP) to investigate the breach, and the panel released its report on January 30, 2015. The report can be found at Mount Polley Independent Expert Engineering Investigation and Review Panel (2015).

The Samarco dam disaster in Minas Gerais, Brazil, occurred at about 4:30 pm on November 5, 2015, when the Fundão tailings underwent a catastrophic and fatal liquefaction flow slide, and approximately 44 million m<sup>3</sup> of mine tailings flowed into the Doce River. The cause of the liquefaction flow slide was attributed to lateral extrusion of slimes that had intruded into the sand dam. The full report from the Fundão Tailings Dam Review Panel released August 25, 2016, may be found at Fundão Tailings Dam Review Panel (2016).

The failure at the Cadia Valley Operations in New South Wales, Australia, was not catastrophic but was certainly most significant in attracting the attention of the global mining community. The failure occurred with the wall of the Northern Tailings Storage Facility (NTSF) slumping laterally into the Southern TSF. Prominent cracks within the South face of the NTSF were seen in the morning of March 9, 2018. Significant ground heave was observed at the toe of the NTSF at about 4:00 pm, which prompted the evacuation of the worksite and a small number of downstream residents. A section of the wall

<sup>#</sup>Corresponding author. E-mail address: ward.wilson@ualberta.ca

<sup>1</sup>University of Alberta, Department of Civil & Environmental Engineering, Edmonton, Alberta, Canada.

Submitted on June 25, 2021; Final Acceptance on August 25, 2021; Discussion open until November 30, 2021.

<https://doi.org/10.28927/SR.2021.067521>



This is an Open Access article distributed under the terms of the Creative Commons Attribution License, which permits unrestricted use, distribution, and reproduction in any medium, provided the original work is properly cited.

with a width of about 300 m displaced southward by about 170 m. The failure is best described as a mobile slump, and by March 14, 2018, the volume of slump material displaced was calculated to be about 1.3 million m<sup>3</sup>. The failure at Cadia Valley Operations had no fatalities. The Independent Technical Review Board released its final report on April 17, 2019, and it can be found at Newcrest (2019).

The failure of Feijão Dam I occurred on January 25, 2019, at approximately 12:28 pm. The fatal failure was a sudden, catastrophic liquefaction flow slide. The failure was recorded on high quality video, and the failure was seen to extend across most of the face of the dam. Collapse of the downstream face of the dam was complete in less than 10 seconds. Approximately 9.7 million m<sup>3</sup> of material that represented about 75% of the tailings contained in the dam was released in less than five minutes. The report of the expert panel on the technical causes of the failure of Feijão Dam I was published on December 12, 2019, and can be found at Feijão Dam I Expert Panel (2019).

All four of these major and prominent failures occurred within a period of less than five years. Moreover, these failures occurred in contemporary tailings dams constructed under good conditions and with no environmental extremes or usual stresses. These failures have generated an unprecedented response in the global mining community. The old paradigm of business as usual has completely evaporated. For example, in Canada, leading entities such as the Canadian Dam Association and Mining Association of Canada, as well as the International Council on Mining and Metals, have published new and comprehensive guidelines. The author believes that the Mount Polley IEEIRP provided a major contribution for many of these new guidelines in that a component of the mandate given to the IEEIRP was to recommend best available tailings technologies to improve dam safety. These will be discussed in the following section of this paper.

## 2. Recommendations arising from the Mount Polley failure

According to the Mount Polley IEEIRP report, the failure on August 4, 2014, occurred as a slump in a short section of approximately 250 m within the 40 m to 50 m high perimeter embankment at the Mount Polley tailings storage facility. The slump was caused by a sudden foundation failure in the embankment. The crest of the embankment dropped approximately 2 m, which allowed the high water level in the pond to overtop the crest of the dam and cause a large breach to form and down cut by rapid erosion. There were no eye witnesses who observed the failure at 1:00 am. The foundation failure formed in the glaciolacustrine unit at the base of the slide, which failed in undrained loading. A comprehensive three-dimensional numerical modelling program showed that the collapse occurred with the strain-weakening of a thin shear band in the glaciolacustrine unit at the base of the

slide (Zabolotnii, 2020). The failure mechanism articulated by Zabolotnii (2020) was not recognized during the original design of the embankment.

As noted in Wilson et al. (2017), as a result of the comprehensive enquiry completed at Mount Polley, the IEEIRP recommended the implementation of best available tailings technologies (BAT). In terms of risk-based dam safety practice, “the panel does not accept the concept of a tolerable failure rate for tailings dams” and advocated the implementation of the best available tailings technology based on the BAT principles outlined as follows:

1. eliminate surface water from the impoundment,
2. promote unsaturated conditions in the tailings with drainage provisions, and
3. achieve dilatant conditions throughout the tailings deposit by compaction.

The application of these BAT principles for the surface storage of tailings leads to the use of filtered tailings technology. Filtered tailings technology or “dry stack tailings” can satisfy each of the BAT components when the impoundment is properly designed and constructed. The panel refers to the Greens Creek mine in Alaska, USA, shown in Figure 1, as an example of where “dry stack tailings” has been successfully implemented. It is important to note that the regional climate regime is paramount in the design of any tailings impoundment, but in this case, the Greens Creek mine was selected by the panel due to its proximity to the province of British Columbia.

The application of the best available technologies for the physical stability (BAT-PS) of tailings impoundments requires new knowledge and new expertise. This new knowledge and expertise must overcome the inherent or embedded ignorance (Morgenstern 2020) that exists in tailings management. The term ignorance carries a negative connotation and that is not the intent of its use here. The definition of ignorance by the Merriam-Webster is simply lack of knowledge, education, awareness, and it is within this context that the term is used herein. Two examples of problems associated with embedded ignorance are illustrated here to help articulate the challenges for the design, operation and closure of many



**Figure 1.** Filtered dry stack tailings at Greens Creek mine, Alaska (Wilson & Robertson 2015).

tailings storage facilities generally found in the base and precious metal industries.

### 3. Challenges with physical and chemical stability

Implementation of BAT principles creates serious challenges with current best practice. The principle of physical stability (BAT-PS) strongly competes with the best available technologies for the chemical stability (BAT-CS) of reactive tailings. The application of BAT-PS principles is to drain and dry the tailings profile, which results in increased oxidation potential for acid rock drainage and metal leaching (ARD/ML) in reactive tailings. In contrast, the maintenance of fully saturated conditions in a tailings profile along with the use of water covers for the closure of potentially acid generating waste has been considered best practice to prevent or limit acid generation in several jurisdictions. Figure 2 illustrates the preferred solution of using water covers for the prevention and control of ARD. Water covers are routinely employed as a preferred strategy for the long-term closure of reactive tailings worldwide as outlined by the global acid rock drainage (GARD) guide (INAP, 2014). However, the containment of a permanent water pond on a tailings dam for closure creates an everlasting geo-hazard that requires perpetual monitoring and maintenance.

The examples shown on the left side of Figure 2 are ideal closure configurations for sub-aqueous disposal, since the tailings and water cover do not require above ground containment structures and both chemical and physical stability (i.e. BAT-CS and BAT-PS) are completely satisfied. On the contrary, with the examples shown on the right side of Figure 2, while satisfying chemical stability (BAT-CS), the condition for long-term physical stability (BAT-PS) is most certainly not guaranteed. The required confinement of a water cover above the surrounding topography is a permanent geo-hazard that must be maintained into perpetuity. Tailings

dams that require regular inspections and maintenance eliminate the possibility of walk away at closure, impose complexities with monitoring and increase long-term risk. In fact, strict application of a risk-based approach dictates the probability of failure over longer time scales is arguably approaching 100%.

### 4. Challenges associated with unsaturated soil mechanics

The use of filtered tailings at Green Creek eliminates the surface water pond from the waste facility, promotes unsaturated conditions in the tailings with drainage provisions and achieves dilatant conditions throughout the tailings deposit by the use of mechanical compaction. While these characteristics promote BAT-PS, the de-watering of tailings to produce an acceptable filtered product can be expensive, especially in the case of pressure filtration. In addition, the implementation of filtering tailings at sites with high tonnages is also very challenging.

The primary issue with dry stack tailings impoundments is that they form positive topographic structures that rise above the surrounding terrain and water tables. Consequently, they form unsaturated mined earth structures, as a result of drainage to the foundation and water losses to the atmosphere due to evaporative drying. Figure 3 shows the surface of a dewatered tailings deposit with a layer of unoxidized tailings overlying oxidized tailings. The tailings profile is unsaturated, and the lower layer of reactive tailings has oxidized with the ingress of atmospheric oxygen. The upper unoxidized layer of fresh thickened tailings, deposited after the underlying tailings were already oxidized, can be expected to oxidize with time in the same way as the previous lower lift of acid-forming tailings. In summary, the BAT-PS principles for the elimination of surface water from the impoundment and the promotion of unsaturated conditions in the tailings can be seen to directly contradict the general principles laid

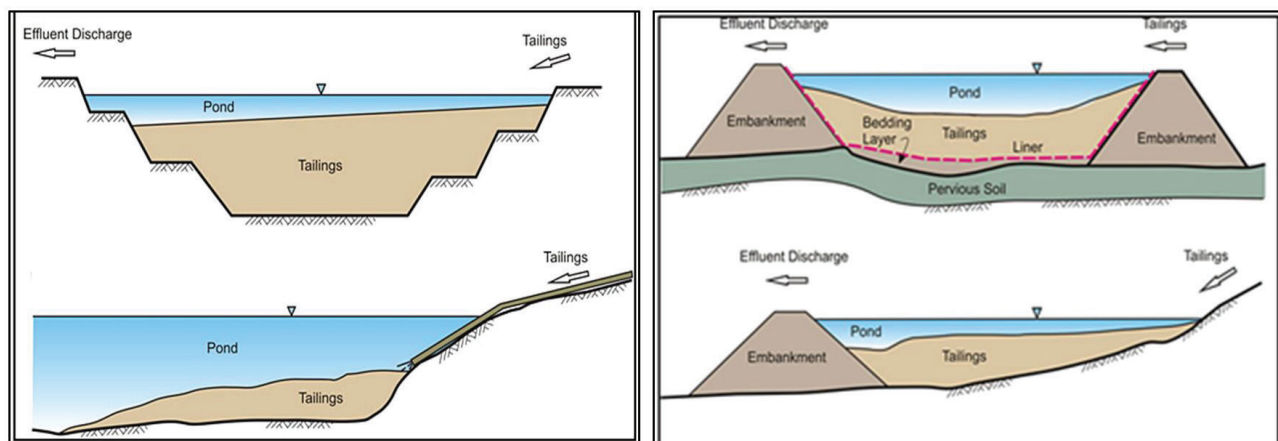


**Figure 2.** Sub-aqueous disposal for chemical stability (modified from INAP, 2014).





**Figure 3.** Thickened tailings with unoxidized layer overlying oxidized tailings.

out in the GARD guide (INAP, 2014) for the prevention of ARD and metalliferous drainage or BAT-CS. Mine waste professionals are left with a serious and competing conflict in their design criteria.

A key component for the design of de-watered tailings deposits is the degree of water saturation within the tailings profile. Tailings profiles with water saturation levels greater than 85% are considered resistant to oxygen diffusion and subsequent ARD. Figure 4 shows the effective diffusion coefficient of oxygen ( $D_e$ ) as a function of the degree of saturation ( $S$ ). The figure shows that  $D_e$  decreases by several orders of magnitude as the degree of saturation increases from zero to 100%. Furthermore, the decrease in  $D_e$  becomes most significant in the range of 85% saturation; thus, maintaining  $S$  at 85% or greater has become a target or criteria in the design of mitigative measures to control or prevent ARD in potentially acid forming (PAF) mine waste materials.

Satisfying the condition for physical stability (BAT-PS) in tailings is controlled in part by the degree of saturation. Saturated contractive tailings are the most susceptible to liquefaction, while dry tailings are generally non-liquefiable. While saturated tailings are most resistant to the diffusion of oxygen that drives ARD (BAT-CS), saturated tailings are the least desirable in terms of physical stability (BAT-PS). However, it is generally accepted that tailings profiles with water saturation levels less than 85% are considered resistant to liquefaction. A degree of water saturation equal to 85% marks a key design target or metric for both BAT-CS and BAT-PS, albeit in an inverted or overturned fashion. In summary, successful implementation of the BAT principles

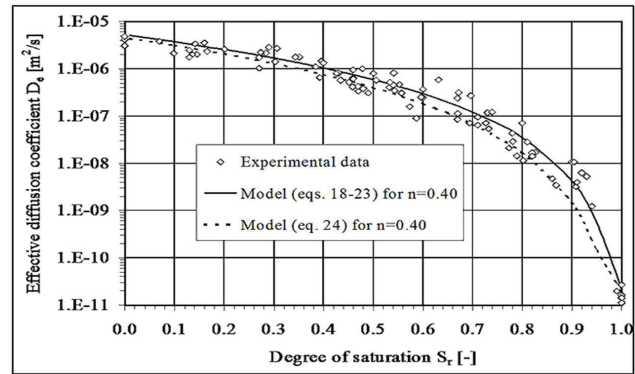


**Figure 4.** Oxygen diffusion coefficient versus degree of saturation (Aubertin, 2005).

for both PS and CS demands insight and knowledge of the field of unsaturated soil mechanics.

A degree of water saturation equal to 85% appears to be a key target for achieving both chemical and physical stability in reactive tailings (Aubertin, 2005). Figure 5 shows a typical soil–water characteristic curve (SWCC) for tailings. The SWCC controls water saturation as a function of matric suction. Generally, a value of  $S = 85\%$  (based on the tangent technique) corresponds to a very important point on the SWCC known as the air entry value (AEV). The AEV corresponds to the value of matric suction at which the largest pores drain and air enters the matrix of the tailings (i.e. bubbles). It is important to note that while air bubbles exist in the matrix, the air phase is not continuous. This explains why the diffusion coefficient for oxygen  $D_e$  decreases dramatically at  $S = 85\%$ , corresponding to the AEV. In a similar way, the development of air bubbles at the AEV reduces the potential for liquefaction since excess porewater pressures can be dissipated with the flow of water to the air-filled voids in the largest pores of the tailings matrix. In summary, the AEV corresponds to an optimum point on the SWCC for the simultaneous minimization of both oxygen diffusion in reactive tailings and porewater pressure generation in liquefiable tailings.

Controlling the saturation profile demands the coupling of the net infiltration rate with hydraulic properties of the tailings that in turn are controlled by the SWCC, AEV and unsaturated permeability ( $k_{sat}$ ) function of the tailings (Bussi re & Guittonny-Larchev que, 2021). In general, under downward drainage with a hydraulic gradient of unity, the long-term steady state net percolation rate (shown in Figure 6) entering the surface of the tailings profile must be equal to the unsaturated hydraulic conductivity (as defined by the SWCC and AEV) of the tailings. Furthermore, the infiltration rate is determined on the basis of coupling hydraulic properties of the surface of the tailings or cover system with the microclimatic conditions. In summary, the final cover

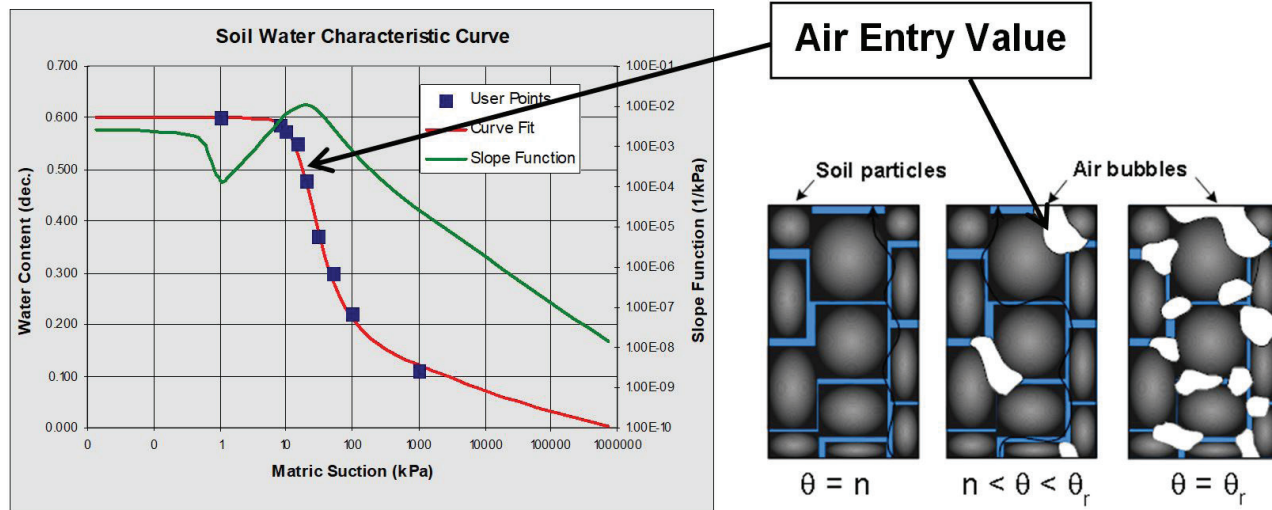


Figure 5. Typical soil-water characteristic curve for tailings.

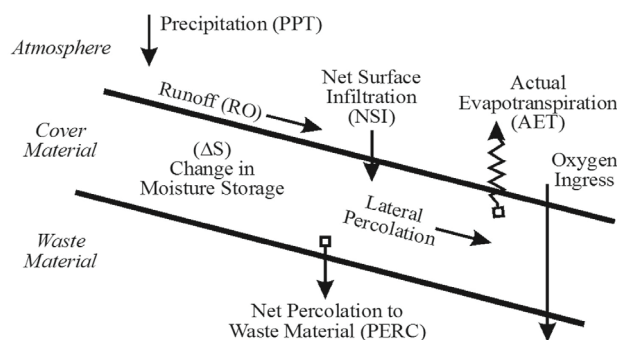


Figure 6. Components of the surface water budget and net percolation for tailings. Source: Mine Environment Neutral Drainage (MEND) Program (2017).

system design for closure must provide infiltrative fluxes that optimize unsaturated flow conditions in the tailings.

## 5. Challenges for designing new tailings management facilities

As stated above in Section 2, the IEEIRP advocated the implementation of the best available tailings technologies based on BAT principles. Furthermore, the IEEIRP declared that the application of these BAT principles for the surface storage of tailings leads to the use of filtered tailings technology. Filtered tailings technology or “dry stack tailings” can satisfy each of the BAT components when the impoundment is properly designed and constructed. Designing dry stack tailings systems that satisfy both BAT-CS and BAT-PS will

require rigorous application of the principles and theory for unsaturated soil mechanics outlined above.

The IEEIRP referred to the Greens Creek mine shown in Figure 1 as an example of where “dry stack tailings” has been successfully implemented. Numerous other dry stack facilities have been constructed or are under construction, or are being planned, as mentioned in the MEND (Mine Environment Neutral Drainage (MEND) Program, 2017) report. Some of the new dry stack facilities currently being considered are at mine sites with productions in excess of 100,000 tonnes per day. Figure 7 below shows an example of the large dry stack system proposed at Rosemont mine in Arizona, USA. The design, analysis, instrumentation, monitoring and assessment of dry stack tailings systems is radically different when compared to conventional tailings dams.

Dry stack tailings systems, by definition are positive topographic tailings deposits that are intended to remain permanently unsaturated, and therefore, special or nonconventional theory (i.e. unsaturated soil theory), methods of analysis, laboratory test procedures and field instrumentation are required. To illustrate the difference, the seepage analysis required for a conventional slurry impoundment with a water pond compared with that for a dry stack tailings system can be considered. The principal upper boundary condition for the surface of the conventional tailings impoundment is a head boundary condition that is established by the elevation of the pond. However, no such boundary condition exists for a dry stack tailings deposit. The surface boundary condition for seepage in a dry stack tailings deposit is a flux boundary condition established on the basis of coupled soil–atmosphere modelling determined by the hydraulic properties of the surface of the tailings cover together with microclimatic and atmospheric forcing conditions.



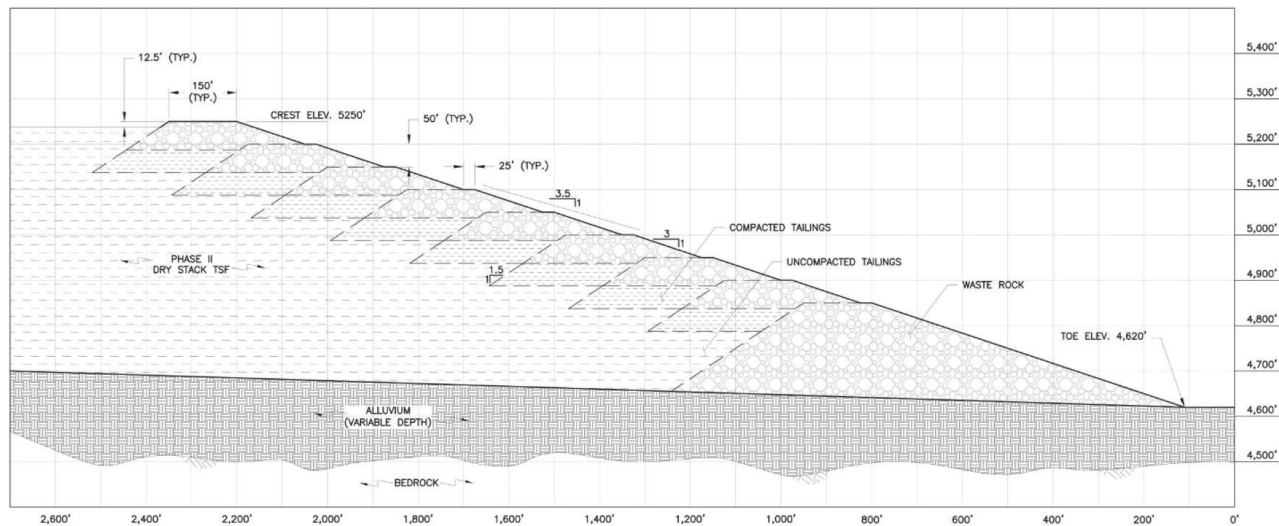


**Figure 7.** Rosemont dry stack tailings (AMEC Earth and Environmental, 2009).

The prediction and measurement of actual evaporation is perhaps the most difficult variable to quantify and requires highly advanced instrumentation such as the eddy covariance (ECV) apparatus shown in Figure 8. Inverse (or back) analyses are also often used and require the installation of water content probes in the tailings profile. Nevertheless, evaporation is routinely determined on the basis of pan evaporation measurements or methods of analysis based on micro-meteorological measurements for solar or net radiation, temperature, relative humidity and wind speed. However, these methods provide estimates solely for potential evaporation, which can be a source of great error since actual rates of evaporation are much less than potential values; thus, the simple water balance equation becomes highly indeterminate.

In addition to the difficulty in defining appropriate boundary conditions for modelling unsaturated flow in dry stack tailings, equally difficult challenges arise for the in-situ measurement of porewater pressures and associated hydraulic heads. In the case of conventional saturated slurry tailings deposits, porewater pressures and hydraulic heads are measured with conventional piezometers such as the Casagrande piezometer and/or vibrating wire piezometers. However, such instruments are virtually useless in dry stack tailings unless saturated conditions are forming, such as at the base of a stack. Conventional piezometers will still be required in dry stack systems but only to check if saturation is developing that might be causing dangerous conditions for instability.

Proper instrumentation for the monitoring of porewater conditions in unsaturated dry stack tailings will require the installation of instruments to measure matric suction. Figure 9 illustrates an example of an instrument for the measurement of matric suction as low as 1 kpa known as the Fredlund thermal conductivity sensor. Such instruments will need to be installed within the profiles of dry stack

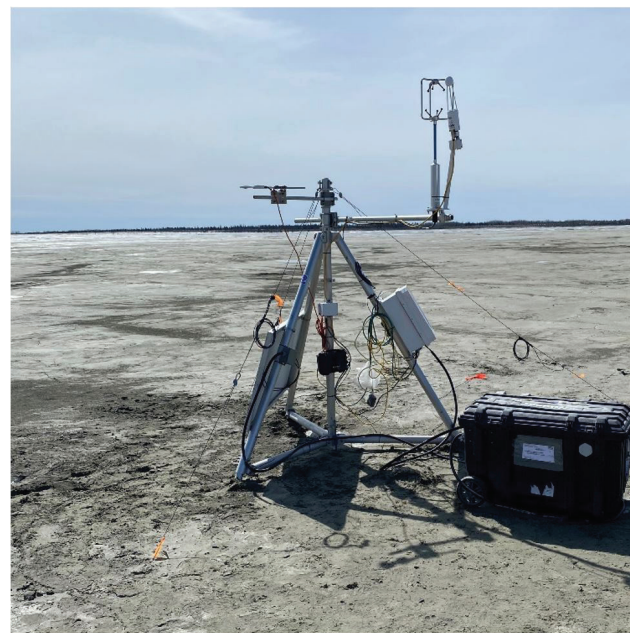


**Figure 8.** Eddy covariance instrumentation (ECV) on a tailings surface.

tailings, similar to the nested profiles commonly used for conventional piezometers.

The determination of soil property functions for saturated/unsaturated flow in dry stack tailings is perhaps the most important component of seepage modelling for dry stack systems. Seepage modelling in an unsaturated system is controlled by the SWCC and the associated permeability function for the tailings as shown in Figure 5. However, the SWCC, which is a function of the particle size distribution, is also strongly influenced by total stress and density as can be seen in Figure 10. The key components in the design of a dry

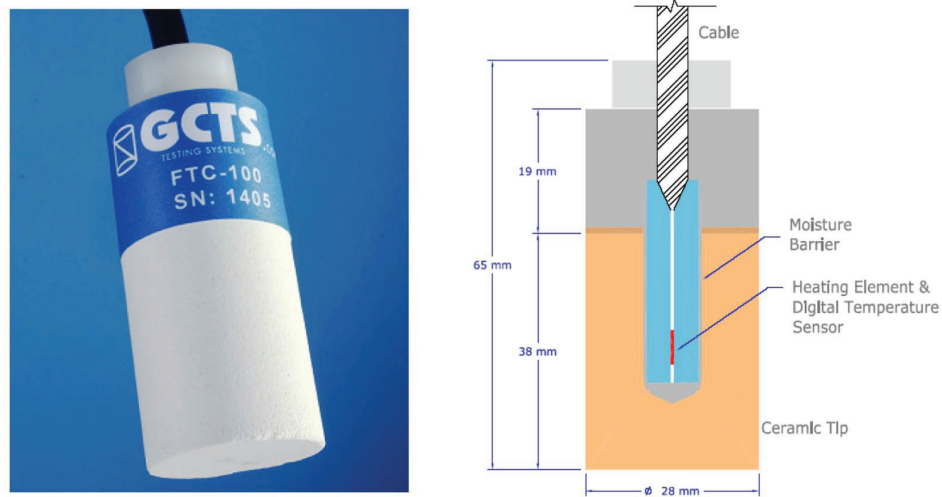


**Figure 9.** Fredlund thermal conductivity sensor (FTC-100). Source: GCTS (2021).

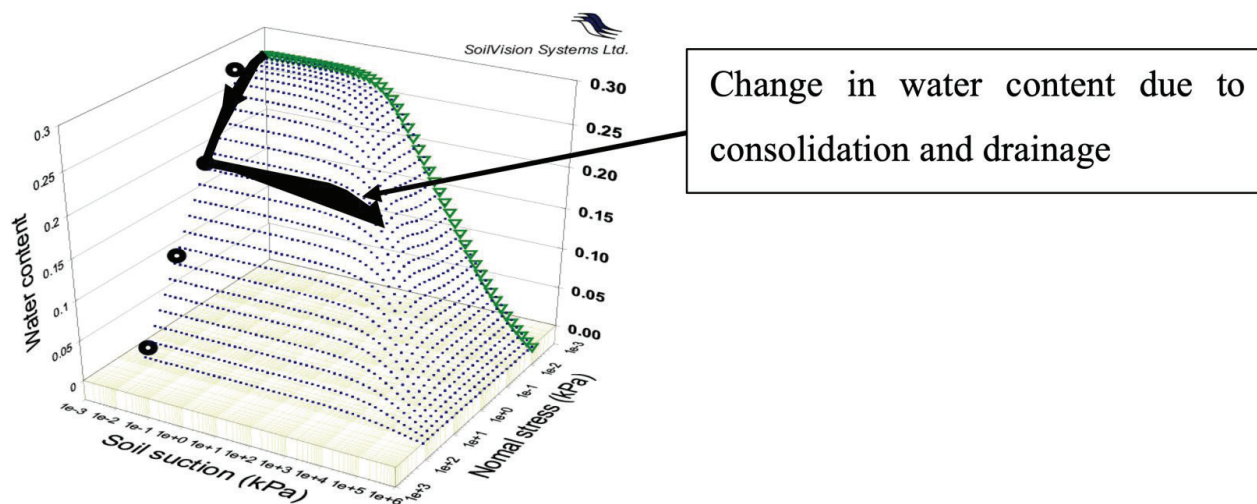


**Figure 10.** An example constitutive surface for a saturated/unsaturated tailings profile, showing a potential stress path for loading (after Fredlund, 2000).

stack system are to achieve physical stability (BAT-PS) and dilatant conditions throughout the tailings deposit by compaction and/or in-situ stress. The determination and application of the constitutive surfaces for dry stack tailings, such as the example presented in Figure 10, will be paramount in terms of coupling the seepage analysis with the stress analysis.

## 6. Summary and conclusions

The failure in the embankment at the Mount Polley tailings storage facility in British Columbia, Canada has had substantial impact on the global mining industry. The Independent Expert Engineering Investigation and Review Panel (IEEIRP) for

the breach in the tailings dam at Mount Polley made major contributions to new guidelines. The incident has given rise to comprehensive recommendations for the best available tailings technologies (BAT) based on principles such as the elimination of surface water from impoundments with the promotion of unsaturated conditions in the tailings through drainage provisions. The application of these BAT principles for the surface storage of tailings leads to the use of filtered tailings technology. Filtered tailings technology or “dry stack tailings” can satisfy each of the BAT components when the impoundments are properly designed and constructed.

The implementation of the best available technologies for the physical stability (BAT-PS) of tailings impoundments

competes directly with the best available technologies for the chemical stability (BAT-CS) of reactive tailings that may produce acid and metalliferous drainage. Mine waste management methods directed at achieving both BAT-CS and BAT-PS were discussed in the present paper. The application of unsaturated soil theory and special methods of analysis, laboratory testing and field instrumentation will be required for designing new tailings management facilities.

## Declaration of interest

The author has no conflict of interest to declare, and there is no financial interest to report.

## References

- AMEC Earth and Environmental. (2009). *Rosemont Copper Company dry stack tailings storage facility final design report*. Retrieved in June 25, 2021, from <https://www.rosemonteis.us/sites/default/files/technical-reports/011978.pdf>
- Aubertin, M. (2005). *Coefficient of diffusion versus degree of saturation for saturated porous media*. [Figure is from an unpublished presentation, which has since been reproduced in Chapter 6 of the Global Acid Rock Drainage Guide published by the International Network for Acid Prevention (INAP) in 2014]. Retrieved in June 25, 2021, from [http://www.gardguide.com/index.php?title=Chapter\\_6](http://www.gardguide.com/index.php?title=Chapter_6)
- Bussière, B., & Guittonny-Larchevêque, M. (2021). *Hard rock mine reclamation: from prediction to management of acid mine drainage*. Boca Raton: CRC Press.
- Feijão Dam I Expert Panel. (2019). *Report of the Expert Panel on the Technical Causes of the Failure of Feijão Dam I*. Retrieved in December 12, 2019, from <http://www.b1technicalinvestigation.com>
- Fredlund, M.D. (2000). *The role of unsaturated soil property functions in the practice of unsaturated soil mechanics* [Doctoral thesis, University of Saskatchewan]. University of Saskatchewan's repository. Retrieved in June 25, 2021, from <http://hdl.handle.net/10388/etd-10212004-002824>
- Fundão Tailings Dam Review Panel. (2016). *Report on the immediate causes of the failure of the Fundão dam*. Retrieved in August 25, 2016, from <http://fundaoinvestigation.com/wp-content/uploads/general/PR/en/FinalReport.pdf>
- GCTS. (2021). Retrieved in June 25, 2021, from <https://www.gcts.com/product/soil-water-characteristic-curve>
- International Network for Acid Prevention. (2014). *Global acid rock drainage guide (rev 1)*. Retrieved in June 25, 2021, from [www.gardguide.com](http://www.gardguide.com)
- Mine Environment Neutral Drainage (MEND) Program. (2017). *Study of tailings management technologies (MEND Report 2.50.1)*. Retrieved in June 25, 2021, from [http://mend-nedem.org/wp-content/uploads/2.50.1Tailings\\_Management\\_TechnologiesL.pdf](http://mend-nedem.org/wp-content/uploads/2.50.1Tailings_Management_TechnologiesL.pdf)
- Morgenstern, N.R. (2020) Tailings dam safety: have we resolved the crisis? In *Tailings and Mine Waste 2020 Conference* (Keynote Lecture).
- Mount Polley Independent Expert Engineering Investigation and Review Panel. (2015). *Report on Mount Polley Tailings Storage Facility Breach*. Retrieved in January 30, 2015, from <https://www.mountpolleyreviewpanel.ca/final-report>
- Newcrest. (2019). *Report on NTSF embankment failure*. Retrieved in June 25, 2021, from [https://www.newcrest.com/sites/default/files/2019-10/190417\\_Report%20on%20NTSF%20Embankment%20Failure%20at%20Cadia%20for%20Ashurst.pdf](https://www.newcrest.com/sites/default/files/2019-10/190417_Report%20on%20NTSF%20Embankment%20Failure%20at%20Cadia%20for%20Ashurst.pdf)
- Wilson, G.W., & Robertson, A. (June, 2015). The value of failure. *Geotechnical News* (pp. 24-28).
- Wilson, G.W., Wickland, B., & Weeks, B. (2017). Designing tailings and waste rock systems for chemical and physical stability. In *Proceedings of the 9th Australian Acid and Metalliferous Drainage (AMD) Workshop*, Burnie, Tasmania.
- Zabolotnii, E. (2020). *Three-dimensional slope stability effects in the failure at the Mount Polley Tailings Storage Facility* [Doctoral thesis, University of Alberta]. University of Alberta's repository. <https://doi.org/10.7939/r3-78me-0x79>.

## Unsaturated soils in the context of tropical soils

José Camapum de Carvalho<sup>1#</sup> , Gilson de F. N. Gitirana Jr.<sup>2</sup> 

Article

### Keywords

Tropical soils  
Unsaturated soils  
Aggregation  
Weathering  
Soil-water characteristic curve  
Particle-size distribution

### Abstract

The practice of geotechnical engineering in tropical climate regions must consider the use of unsaturated soil concepts. However, these concepts must also take into account the specific behavior traits of tropical soils, particularly those related to soil aggregation, pore structure, and mineralogy. This paper will initially present considerations on the typical properties of unsaturated tropical soils as well as fundamental concepts. Throughout the article, several engineering problems will be presented alongside reflections on the complex interaction between the numerous variables involved in the modeling and engineering practice of tropical unsaturated soil behavior. The paper addresses issues related to soil formation, chemical and mineral composition, physical properties, tropical soil classification, and structural characteristics of soils. Issues related to compaction and the influence of weathering, geomorphology and bioengineering are also addressed.

## 1. Introduction

The engineering practice is generally based on the experience built over time, with new scientific and technological advances being introduced gradually. Critical thinking, the central pillar of engineering, is often set aside to prioritize the application of standards and regulations that, in most cases, are not mandatory. The lack of critical thinking may have greater consequences when dealing with soils that present complex soil behavior, such as unsaturated tropical soils. Unfortunately, standards do not consider the particular behavior of unsaturated and tropical soils, even when developed in countries where these types of soils are predominant. For instance, drying of specimens in preparation for soil characterization tests is recommended by most standards, but it may greatly affect testing results because of the potential degradation of the aggregates present in deeply weathered soils.

The books *Laterite Soil Engineering: Pedogenesis and Engineering Principles* (Gidigas, 2012) and *Tropical Residual Soils* (edited by Fookes, 1997) present a broad perspective on tropical soils, ranging from their formation and characterization to their behavior and uses. However, tropical soils have characteristics that remain poorly studied and that depend on the degree of transformation suffered during their genesis. It is important to note that the properties and

behavior of tropical soils bear a faint link with their origin, as illustrated the studies of Mortari (1994) and Cardoso (1995) on the behavior of tropical soils from the Federal District, Brazil. These authors showed that the particle-size distribution, the Atterberg limits, and the Skempton activity index of these soils depends on and the Claystone, Slate, and Metarhythmite formations from which these residual soils developed.

The experimental determination and the use of soil properties require the consideration of what they represent and the contextualization in time, space, and general environmental conditions. This is particularly true for unsaturated tropical soils. Static and non-contextualized interpretations of soil behavior generally lead to the adoption of simplifications and poor engineering decisions and planning.

Regarding the relevance of time effects, geotechnical engineering practice is frequently focused on the present and on the past geological periods. Little consideration is given to what will happen to construction materials in the future. In the case of unsaturated soils, temporal contextualization has a great relevance since soil moisture and consequently its behavior often varies over time and follows a cyclical pattern. These fluctuations impose changes in the physicochemical properties of the soil. For example, cyclical variations of water content can be of great relevance to the fatigue of

<sup>#</sup>Corresponding author. E-mail address: camapumdecarvalho@unb.br

<sup>1</sup>Universidade de Brasília, Department of Civil and Environmental Engineering, Brasília, DF, Brasil.

<sup>2</sup>Universidade Federal de Goiás, School of Civil and Environmental Engineering, Goiânia, GO, Brasil.

Submitted on July 18, 2021; Final Acceptance on September 16, 2021; Discussion open until November 30, 2021.

<https://doi.org/10.28927/SR.2021.068121>



This is an Open Access article distributed under the terms of the Creative Commons Attribution License, which permits unrestricted use, distribution, and reproduction in any medium, provided the original work is properly cited.



pavement structures and to the development of erosive processes (Lima, 2003).

Regarding the spatial context, materials are generally studied under laboratory conditions that do not reproduce the dynamic balance with the environment, nor most of the geomorphological, biological, and geological factors, including structural geology and hydrogeology (Diniz et al., 2012; Jesus et al., 2012; Jesus et al., 2017; Oliveira & Ribeiro, 2017; Romão & Souza, 2017). For instance, the imposition of new drainage conditions on unsaturated soil due to the development of erosion processes or due to the construction of a road cut, imposes new hydraulic gradients that influence soil behavior (Lima, 2003).

Unsaturated and tropical soils can also be affected by intentional or unintended chemical changes in the soil itself or the environment in which they are found. An example of unintentional chemical changes occurs when executing concrete piles in situ in an unsaturated soil profile. The initial suction in the concrete, a porous material put in direct contact with the soil, is generally close to zero. The surrounding soil suction, being greater than zero, will result in the migration of chemical elements and compounds from the concrete into the soil. This may result, in the case of deeply weathered tropical soil profiles, in textural degradation over time (Wanderley Neto, 2020). As an example of intentional chemical alterations, soil stabilization depends on the mineralogical characteristics significantly associated with the weathering profile and moisture fluctuations resulting from the soil-atmosphere interaction (Ayala, 2020).

Structural characteristics of soils from weathering profiles can also play an essential role in soil behavior. Chemicals introduced for soil stabilization, such as lime, cement, or ash, do not immediately penetrate the aggregates and microaggregates present in deeply weathered tropical soils or the clay packages present in slightly weathered tropical soils. In deeply weathered soils, ionic exchanges are combined with the solubilization of minerals, such as gibbsite, hematite, and goethite, affecting the soil textural stability. In slightly weathered soils, ionic exchanges are predominant, interfering with the interactions between particles. The effects on highly weathered soils were shown by Ayala (2020), who studied soils stabilized with hydrated lime. Pérez (2018) showed that agricultural fertilizers also provoke changes in soil aggregates and microaggregates. It is also important to note that studies on the influence of suction on the hydromechanical behavior of soils are almost always based on analyzes of matric suction; however, when introducing chemical effects, osmotic suction becomes relevant (Pérez, 2018, Ramírez et al., 2017).

The several issues described herein highlight the importance of understanding the properties and behavior of tropical unsaturated soils and their impacts on the performance of geotechnical structures. A broader view is required, considering the role of soil suction, structural stability, and macro and microaggregate interactions. In this context,

this paper presents the analysis of physical, chemical, and mineralogical properties in the context of the behavior of unsaturated soils, with particular emphasis on tropical soil behavior. The particular behavior of natural and compacted soils will be considered. Finally, the temporal and spatial impact on the weathering process and behavior of unsaturated tropical soils will be discussed.

## 2. Properties of tropical soils

### 2.1 Mineralogy of weathering profiles of tropical regions

Weathering profiles formed in tropical regions depend on factors such as climate, microclimate, geology, structural geology, hydrogeology, geomorphology, and drainage conditions. Therefore, an assessment in the broad sense is necessary (Gusmão Filho, 2002). This particularity limits the validity for tropical soils, especially for deeply weathered ones, of existing correlations between physical properties and behavior developed for soils with different characteristics.

Figure 1 exemplifies a tropical weathering profile typical of the Federal District, Brazil, presenting the mineralogical composition based on data obtained by Rodrigues (2017). The gibbsite content, which is higher near the ground surface, remains constant between 2 m and 4 m in depth and then decreases with depth. The opposite behavior is observed for kaolinite. This pattern occurs because gibbsite comes from the weathering of kaolinite (Cardoso, 2002). Kaolinite, in this case, is probably originated from the weathering of muscovite. It should be noted that in recently deposited sedimentary soils formed from erosive processes acting on weathered tropical soils that formed over centuries and millennia, the mineralogical profile shown in Figure 1 is generally inverted (Santos, 1997).

Figure 1 shows also that there is great similarity between the quartz and the gibbsite contents, along the entire profile. That similarity can be attributed to the fact that the quartz

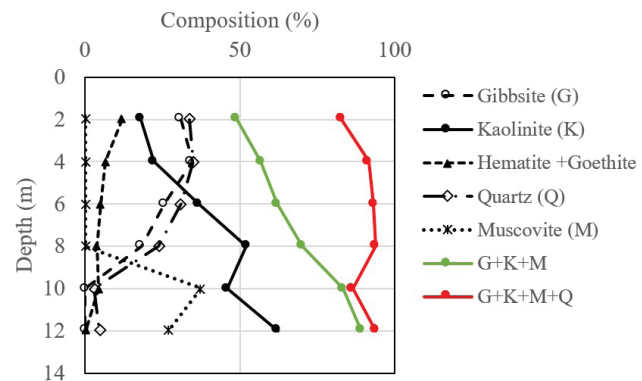


Figure 1. Mineralogy of a soil profile from the Federal District, Brazil.



is neoformed, as explained by Senaha (2019). In this case, quartz would be formed from silicon released when kaolinite is weathered, producing gibbsite. Such neoformation also occurs during the formation of kaolinite from clay minerals 2:1, as indicated by the parallel profiles of kaolinite and quartz content obtained for Manaus, Brazil (Lima, 1999).

In the neoformed condition, quartz is present in significant quantities inside the aggregations, as observed in laterites of the Federal District (Figure 2a). Phyllosilicates preserved inside these laterites were also observed (Figure 2b). The minerals present in the soil under these conditions do not influence the hydromechanical behavior of the soil, which relativizes the importance of mineralogical composition in the study of the behavior of unsaturated tropical soils and the definition of the soil-water characteristic curve itself.

Leaching processes result in changes in the soil properties and in the mineralogical composition along the profiles of tropical soils. Figure 1 shows that the sum of the fractions of gibbsite, kaolinite, muscovite, and quartz results in quantities that are smaller at 2 m and 10 m in depth. The near ground surface region is affected by the infiltration of rainwater, generating the migration of the gibbsite formed at a depth of 2 m. The soil in the region near 10 m in depth is less porous and less permeable, resulting in the accumulation of water during the rainy season, which is subsequently exfiltrated during the dry season, thus causing the gradual migration of kaolinite to lower depths.

The mineralogy of tropical soils has significant impacts on the selection of adequate chemical stabilization techniques. Its consideration must be integrated into the structural analysis, as the presence of compounds such as iron and aluminum oxyhydroxides directly impact the aggregation status of these soils. The increase in soil pH produced by

stabilizers such as lime and Portland cement enables the solubilization of gibbsite, making the aggregates present in deeply weathered soils fragile, as shown by Rezende (2003) and Ayala (2020). Delgado (2007) showed, when studying tropical soils subjected to chemical stabilization, that lime affects the shape of the soil-water characteristic curve and the soil's mechanical behavior. The influence of chemical stabilization depends on the level of weathering suffered by the soil, on the conditions in which that weathering process took place, on the soil mineralogy, and on the level of aggregation (Rezende, 2003; Pessoa, 2004; Aguiar, 2014). Such findings imply the need for a detailed analysis when dealing with chemically stabilized tropical soils.

Testing methodologies used to investigate the mechanical behavior of tropical soils subjected to chemical treatments or contamination must be carefully designed. In general, contaminated mixtures or soils are not subjected in the laboratory to the same water flow conditions imposed by the unsaturated conditions and variations that occur in the field. For example, oxide-hydroxides of aluminum and solubilized iron can be carried by unsaturated seepage, affecting the mechanical behavior and the soil-water characteristic curve of the soil. These effects were observed by Ayala (2020) when comparing results obtained for laboratory curing conditions and those found in situ.

When studying the properties and behavior of tropical soils, whether saturated or not, it is necessary to understand the particularities of behavior. For example, scattering in testing results may have specific causes and not simply imply in testing errors. Freitas (2018) shows that mineralogy can cause unexpected results. In his dissertation, he shows that the simple compressive strength of a tropical soil stabilized with the addition of rice husk ash and Portland cement, when

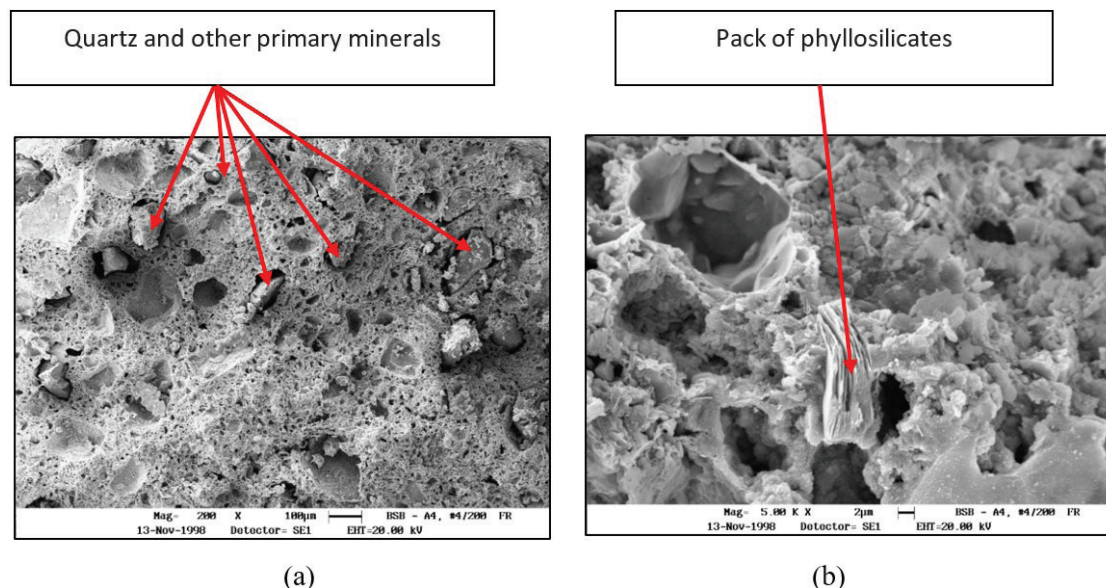


**Figure 2.** Microstructure of the interior of a laterite from the Federal District, Brazil.

plotted as a function of the degree of saturation, showed a highly scattered result. However, when plotted as a function of the saturation degree divided by the sum of the hematite and goethite contents, these same results led to a good correlation.

## 2.2 Structural properties of weathering profiles in tropical regions

Figure 3 shows typical microstructures of soil profiles submitted to the process of tropical weathering. Microstructures of a deeply weathered soil (Figures 3a, 3b, 3c), of a soil with an intermediate degree of weathering (Figure 3d), and of a slightly weathered soil (Figures 3e, 3f) are illustrated. It is noteworthy that the profile of tropical soil corresponding to Figure 3 did not present a water table in subsurface exploration drilling up to 13 m in depth.

Figure 3a shows that the soil collected at 2 m in depth is predominantly composed of aggregates, with macropores between them. These aggregates have micropores, as shown in Figures 3b and 3c. At 5 m in depth (Figure 3c) aggregates are still present but the macropores between them are relatively smaller. In the transitional soil present at 8 m in depth (Figure 3d) the aggregates decrease in size and independent particles and primary minerals are found. At 10 m in depth, the slightly weathered soil horizon is reached (Figure 3e), presenting clay packs that appear to replace the aggregates found in the deeply weathered soil. In deeper layers corresponding to the saprolite the chemical-mineralogical weathering is relatively small, with significant fractions of primary minerals being found (Figure 3f). The laterites may (Figure 4a) or may not (Figure 4b) have internal pores, and these may vary from micro to macropores. This microstructural analysis combined with the mineralogical analysis exemplified in the previous section shows that in tropical weathering profiles, mineralogical and structural transformations go hand in hand.

The structural characteristics that are present in most tropical weathering profiles result in unconventional behavior. For this reason, caution is necessary when analyzing the behavior of these soils and the correspondence between testing results and field monitoring data. For example, the results presented by Guimarães (2002) show measured N-values in standard penetration tests for depths from 1 m to 6 m that range from 2 to 4. These low N-values are due to the fact that the drilling and penetration procedures lead to alterations in the soil structure. Although the highest N-values were obtained for the dry period, when the suction is higher, the results are not consistent with the actual behavior of the soil, leading to estimations of load capacity based on the N-values that are lower than the results from load tests, as shown by Guimarães (2002).

Figure 5 shows load test results versus estimated load capacity values calculated using three methods, two of which use the N-values from SPT tests (Décourt & Quaresma Filho, 1978; Aoki & Velloso, 1975) and a third method that uses the maximum torque in standard penetration tests

(Décourt, 1996). Load tests and SPT tests were carried out at different times of the year (Guimarães, 2002). The results obtained for concrete piles immediately after concreting and 15 days after concreting are also shown in Figure 5. Despite the differences between the values estimated by the different methods, the results show that the load test results were higher when the values calculated from the N-SPT values were lower. The load test result obtained for the concrete pile immediately after concreting was superior to that obtained 15 days after concreting. In addition to the influence of the soil structure change generated during the SPT sampler penetration, these two sets of results indicate that the higher the suction acting on the soil, the greater the uptake of concrete chemical elements by the soil, resulting in strength loss. Ayala (2020) observed similar behavior when treating the same soil with lime.

Figure 6a shows the N-SPT values versus the sum of the logarithm value of suction in pF and of the vertical stress, also in pF, divided by the void ratio. Figure 6b shows the results of the maximum torque measured after the SPT sampler penetration versus the same variable used in Figure 6a, with exception of the use of horizontal stresses. The normalizations using the void ratio are based on the principles proposed by Camapum de Carvalho & Pereira (2002). Considering that the maximum torque was measured after driving the SPT sampler, its similarity with the N-SPT results show that in this test the soil structure is also affected. The larger scatter in Figure 6a is attributed to a lower level of soil structural change compared to the conditions imposed in the torque test (Figure 6b). The points excluded from the trend are located in the transition zone, between the slightly weathered soil and the highly weathered soil. It should be noted that the heterogeneity indicated in this figure is usual, as the N-SPT and maximum torque results were obtained at different times of the year. Thus, the temperature (Lima, 2018) and water content (Guimarães, 2002; Mascarenha, 2003) throughout the soil profile do not remain constant for the same depth. The corresponding changes in soil suction affect not only the soil shear strength but also its susceptibility of structural change during sampler driving.

Load tests carried out on Straus piles, precast, and excavated with mechanized and manual augers with approximately the same diameter (30 cm) and the same length (8 m) present different results (Figure 7), with the worst results being those obtained for precast and excavated by hand auger. The lower results for the precast piles are due to the destruction of the soil structure by the blows required to drive the pile. The lower results for the hand drilled pile may be attributed to the fact that water is used during the excavation process. An intermediate result was obtained for the Straus pile. The pile excavated with a mechanized auger showed the highest bearing capacity. In summary, it is observed that breaking the soil structure and increasing the water content of tropical soils decrease their mechanical strength.



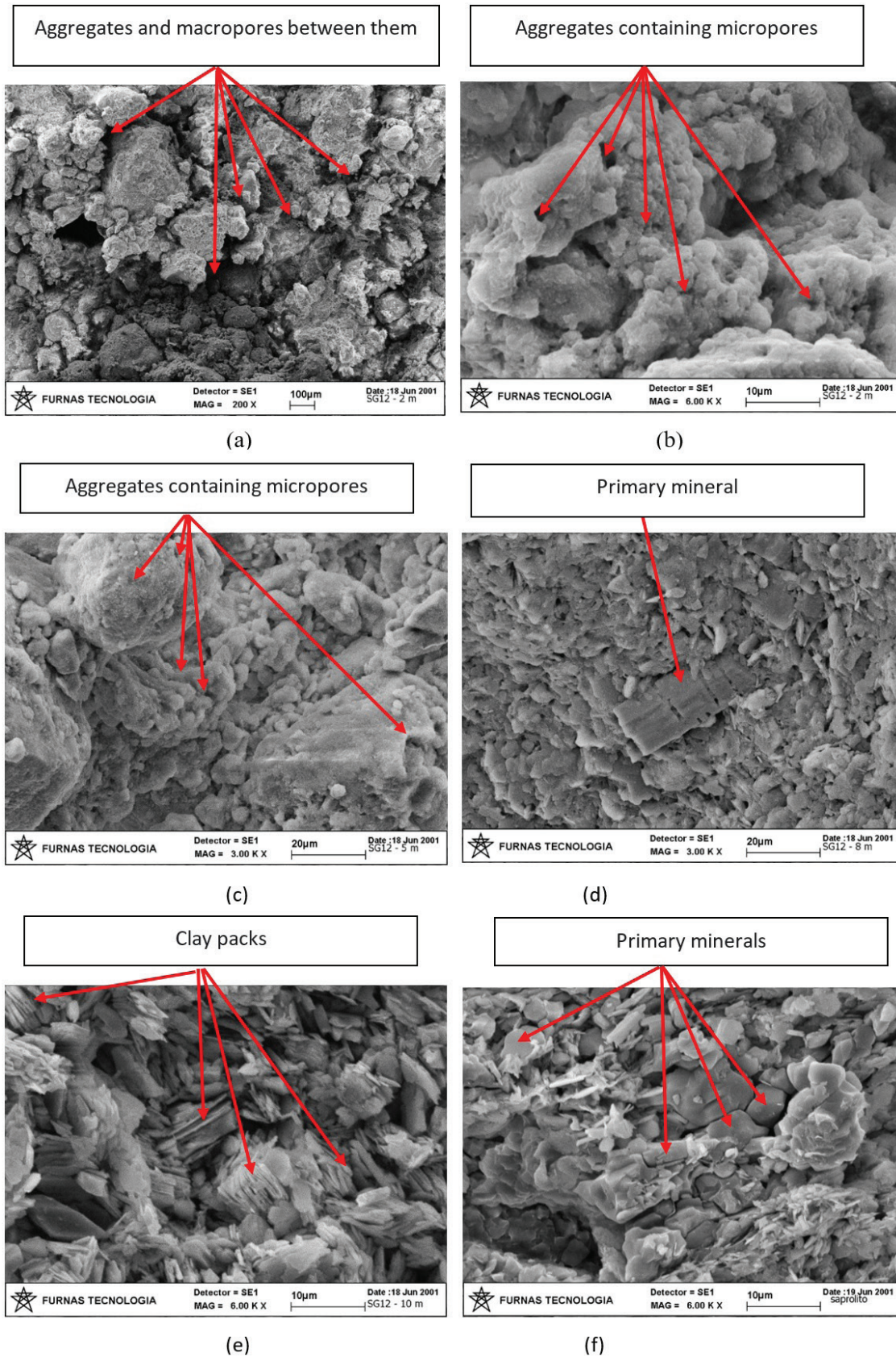


**Figure 3.** Microstructure of soils along a weathering profile: deeply weathered soil (a, b, and c); moderately weathered soil (d); slightly weathered soil (e and f).

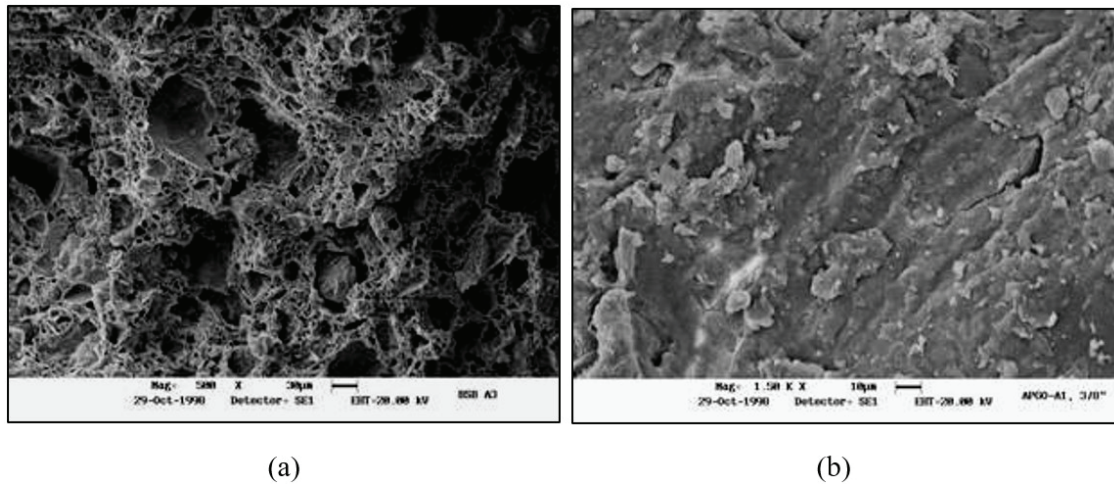


**Figure 4.** Lateritic aggregates from the Federal District and Goiânia, Brazil: (a) laterites with pores; (b) laterites without pores.

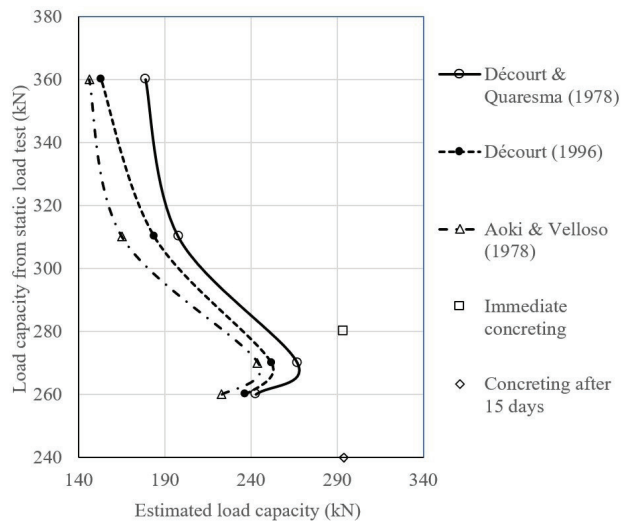


**Figure 5.** Estimated load capacity versus load test results on collapsible tropical soils in the Federal District, Brazil.

The shear strength envelopes of tropical soils under unsaturated conditions may, in some cases, present particular behavior that can be interpreted based on the structural behavior of the soil. Camapum de Carvalho (1981) showed typical results, such as strength increased due to prior drying of the soil and ascending envelopes, with increasing friction angles. In cases where the strength of the cementing bridges between the aggregates is constant, it is common to obtain a shift of the envelope at higher stresses while maintaining its slope approximately constant (Figure 8, CS1). That shift occurs due to the breakage of the cement links, implying a loss of cohesion. However, when the resistance of cementing links in the soil changes with the level of confining stress, a curved envelope is observed (Cardoso, 2002). In direct shear tests, when the contact surface between particles is augmented as a result of the structural collapse of the soil

with the increase of the confining stress, the shear strength also increases, which when divided by a constant area reflects in a pseudo-increase in the shear strength since the effective contact area is not corrected (Figure 8, CS2). This behavior can be better understood through the model presented by Camapum de Carvalho & Gitirana Junior (2005). Lateritic soils with a low degree of cementation in and between aggregates (Figure 8, LS) and saprolitic soils (Figure 8, SS) tend to present linear shear strength envelopes.

Cardoso (2002) showed that in moderately weathered soils significant dispersion in shear strength results could occur as a function of confining stress. This is due to the greater heterogeneity of these soils (Figure 8, TS). It is important to note that the shear strength envelopes shown in Figure 8 can be shifted as a result of changes in the degree of saturation and in the matric suction. Eventual changes in the friction angle can occur as a result of the loss of strength of the aggregates due to the reduction of matric suction or by chemical actions.

### 2.3 The soil-water characteristic curves of tropical soils

Before discussing unsaturated tropical soils' physical properties and behavior, it is relevant to present typical shapes of soil-water characteristic curves (SWCC) generally found when studying these soils. Figure 9 shows the types of SWCC behavior most commonly observed for fine-grained lateritic soils (TLS), saprolitic soils free of expansive clay minerals (SS), saprolitic soils containing expansive clay minerals (SSE), well-graded laterite gravel (WGG), uniform laterite gravel (UG) and gap-graded laterite gravel (GOG). It is noteworthy that the curves shown in Figure 9 are only general models of behavior and may vary from soil to soil.

The general shape of the SWCCs, their air-entry values (AEVs), and the slopes of the SWCCs depend on the particle-size distribution, on soil mineralogy, and on soil porosity. However, soil structure and microstructure



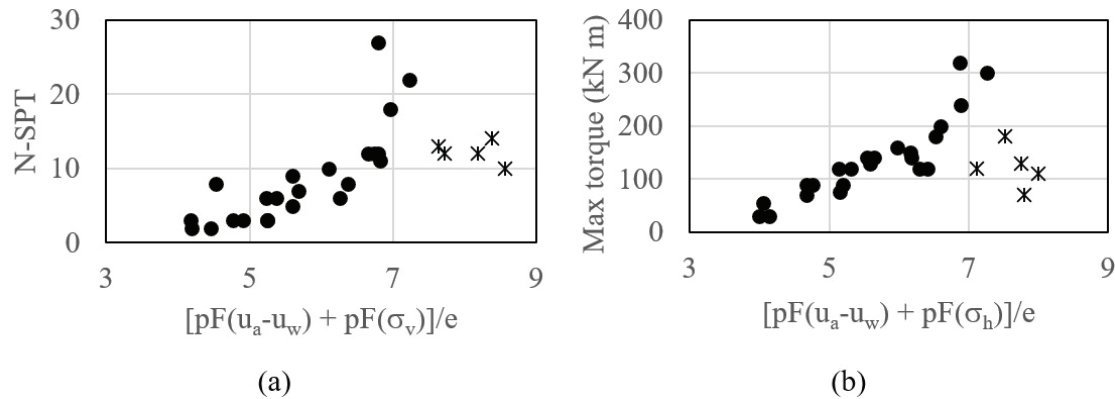


**Figure 6.** Effect of normalized stress state variables on: (a) NSPT; (b) maximum torque.

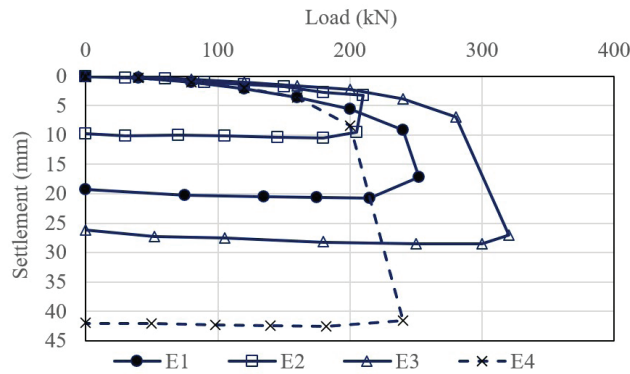


**Figure 7.** Results of static load tests on piles (modified from Rodrigues et al., 1998).

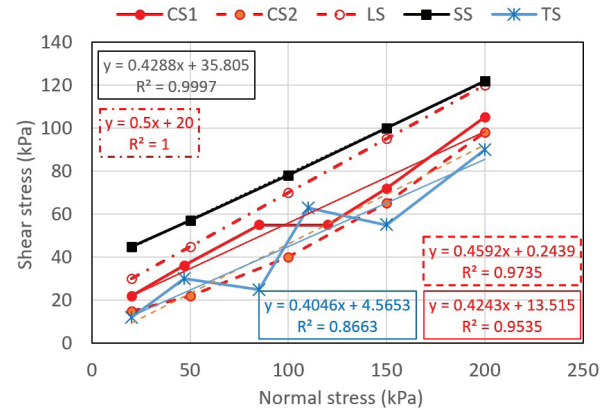


**Figure 8.** Shear strength envelopes of tropical soils.

also play a significant role. In the case of the three gravelly materials (i.e., WGG, UG, and GOG), the AEVs of the macropores indicated in Figure 9 are followed by a plateau. The existence of this plateau will depend on the occurrence of these macropores in significant amounts, which is linked to the level of particle aggregation and soil porosity. The AEVs for the micropores of the three gravelly soils are also shown, followed by the residual water content region. This behavior is observed for microstructures of aggregates similar to the one in Figure 4a. However, it is not observed when the microstructure assumes the characteristics of Figure 4b. For the gap-graded lateritic gravel (GOG), the SWCC often presents an AEV at an intermediate level, corresponding to mesopores arising from the loss of continuity in the grain size distribution and, consequently, in the pore-size distribution.

The typical SWCC for lateritic soils shown in Figure 9 has a bimodal shape, with the first drainage section corresponding to the macropores and the second to the micropores (Camapum de Carvalho & Leroueil, 2004). This behavior is generally attributed to aggregated materials. Multimodal curves are sometimes observed and can be modeled by extending existing fitting equations, such as that proposed by Gitirana Junior & Fredlund (2004).

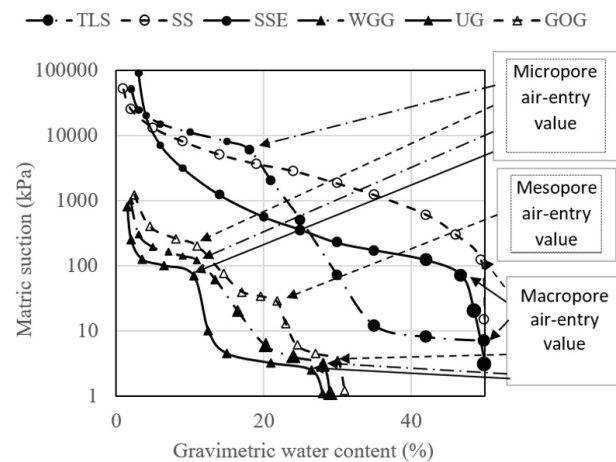


**Figure 9.** Typical soil-water characteristic curves of soils from tropical weathering profiles.

It is interesting to note that in the macroporosity zone, where matric suction is relatively low, the aggregates' volume tends to be relatively constant. However, when entering the residual zone of the macropores, the amount of aggregate volume change will depend on the level of



internal cementation. The solubilization of these cementing agents due to the chemical action of the medium may also provoke volume change of aggregates. The slope of the SWCC in the macropore's residual zone will depend on the variation in pore-size between aggregates and between non-aggregated particles.

Aggregates lose saturation when their AEV is reached. From a practical point of view, this observation has great relevance. It is current practice in geotechnical engineering to air dry the soil in preparation of soil characterization and even hydro-mechanical testing of remolded/compacted soils. When the water content of the air-dried sample becomes lower than that corresponding to the AEV of the micropores, the aggregates tend to remain unsaturated when the soil is subsequently wetted. The forced drying of soil aggregates results in differences between laboratory testing and field conditions. The excessive drying of samples may also produce micro-cracks in the aggregates, compromising their textural stability. In summary, great attention is required in terms of the representativeness of sample preparation methods of soils with aggregations.

Suction values that produce drainage in the microporosity zone, although generally very high, have a decreased effectiveness in contributing to the improvement of the mechanical behavior of the soil. In this stage, suction starts to act predominantly inside the aggregates, thus reducing its contribution to the state of stress between the aggregates, and, consequently, to the mechanical behavior of the soil as a whole. Figure 10 illustrates this behavior and indicates that the maximum values of the simple compressive strength (SCS) and of the tensile strength (TSDC) correspond to the AEV of the micropores (Valencia et al., 2007; Valencia et al., 2019).

The typical SWCC for saprolitic soils free of expansive clay minerals follows a pattern commonly found in sedimentary soils, because in this case the particles are dispersed or flocculated, but not aggregated (Camapum de Carvalho, 1985; Camapum de Carvalho et al., 2002a). The AEV and the slope of these curves will depend on the soil porosity, particle-size distribution, pore-size distribution, and soil

mineralogy. Typically, these soils do not show significant compressibility with increased suction after AEV.

Finally, considering the typical SWCC of saprolitic soils containing expansive clay minerals, attention is drawn to its loss of linearity after air entry. This loss of linearity may be attributed to the change in hydration of the expansive clay minerals, causing the volume of the particles to vary and, consequently, generating changes in soil porosity. This behavior is not observed in soils with low content of expansive clay minerals and when such minerals do not have a relevant structural function.

Studies analyzing SWCCs of expansive soils have generally focused on bentonite materials. However, these studies should be extended to tropical saprolitic soils containing expansive clay minerals. Barreto (2019) proposed a method for considering the effect of soil porosity of expansive non-tropical soils. Tripathy et al. (2014) present a study of SWCCs of three clays, designated as MX80 bentonite, Yellow bentonite, and Speswhite kaolin. In defining the SWCCs as a function of the void ratio, the authors considered the values of specific gravity obtained for the dehydrated minerals, respectively, 2.80, 2.84, and 2.61. Such consideration leads, in the case of expansive clay minerals, to high void ratio values. However, in these cases, it is critical to define the interparticle water content. Interparticle pores and the corresponding water content control the hydromechanical behavior and even other properties, such as the Atterberg limits. This interpretation of the relevant water content was also presented by Chen et al. (2019), when analyzing the hydraulic conductivity of a unsaturated compacted bentonite. The literature has treated the pore space corresponding to the basal interplanar distance as "microporosity" (Sedighi & Thomas, 2014; Navarro et al., 2015; Chen et al., 2019). However, when analyzing the properties and behavior of tropical soils, it is suggested to reserve the term microporosity only for the intra-aggregate pore space. In special cases, depending on the pore size, pores existing outside the aggregates and between independent particles may also be referred to as micropores.

## 2.4 Physical characteristics of tropical soils

The physical characteristics generally considered in studies of tropical soils are the specific weight of the particles, particle-size distribution, pore structure, Atterberg limits, porosity, and gravimetric water content. From these characteristics, others can be calculated, such as the degree of saturation and the dry unit weight. However, when interpreting these characteristics, little attention is paid to the pore structure and effects of hydration or dehydration. Emphasis will be placed here on the study of the specific weight of particles and particle-size distribution and their impacts on the analysis of soil porosity. The interference of these studies on the properties and behavior of unsaturated soils will also be considered. A great focus will be placed

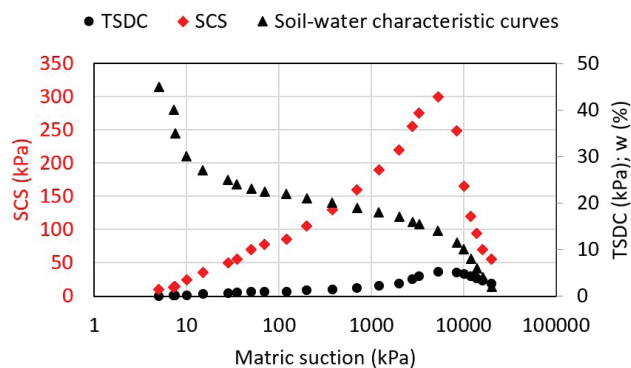


**Figure 10.** Suction influence on the behavior of aggregated tropical soils (modified, Valencia et al., 2007, 2019)

on the peculiarities of tropical soils that distinguish them from sedimentary soils.

#### 2.4.1 The specific weight of particles

The specific weight of particles corresponds to the chemical-mineralogical composition of the soil. This association is particularly relevant in deeply weathered tropical soils (i.e., lateritic soils) and must consider their texture. The specific weight of the particles also changes with the hydration level of expansive clay minerals, which are often present in slightly weathered tropical soils (i.e., saprolitic soils). It should also be taken into account that aggregates and micro aggregates present in deeply weathered tropical soils have internal pores that are not connected to the external environment, thus generating a decrease in the value of the specific weight of the particles (Palocci et al., 1998).

The concept of an “apparent” specific weight of the particles is useful in the interpretation of the behavior of deeply weathered soils containing voids inside the aggregates, including their SWCCs and their general hydromechanical behavior (Camapum de Carvalho & Pereira, 2002; Camapum de Carvalho et al., 2002a, b; Camapum de Carvalho, 2017). This concept and the corresponding modeling approach are presented in Camapum de Carvalho et al. (2015a) and are based on the concepts shown in Figure 11. The model for the

interpretation of soil behavior was based on tests carried out on soils from Goiânia, Brazil (Figure 11a) and the Federal District, Brazil (Figure 11b). In this conceptual model, iron spheres were used to symbolize iron concretions, and glass spheres were used to represent aluminum concretions. The iron spheres were hypothetically assigned a relative density of 5. In the case of glass, a relative density equal to 2.5 was considered. This model will also be used, due to its simplicity, when dealing with other physical indices.

Figure 11a shows a compact laterite without pores in its interior, except for those corresponding to cracks, which are represented by spheres. In this case, both the mechanical behavior and the SWCC will be influenced by the pores existing between the aggregates and/or between the microaggregates. In Figure 11b, the aggregates have internal voids. According to Figure 11b, these voids may or may not be connected to the external environment, between the aggregates. The communication between the pores in deeply weathered tropical soils influences the material's behavior and its SWCC (Figure 9). The connected internal voids impact soil water content, global void ratio, and degree of saturation but do not interfere with the soil properties and behavior, as shown by Camapum de Carvalho et al. (2002b) when analyzing the collapse of a soil profile from the Federal District, Brazil. Camapum de Carvalho et al. (2002a), when analyzing the transformation model of the SWCC proposed

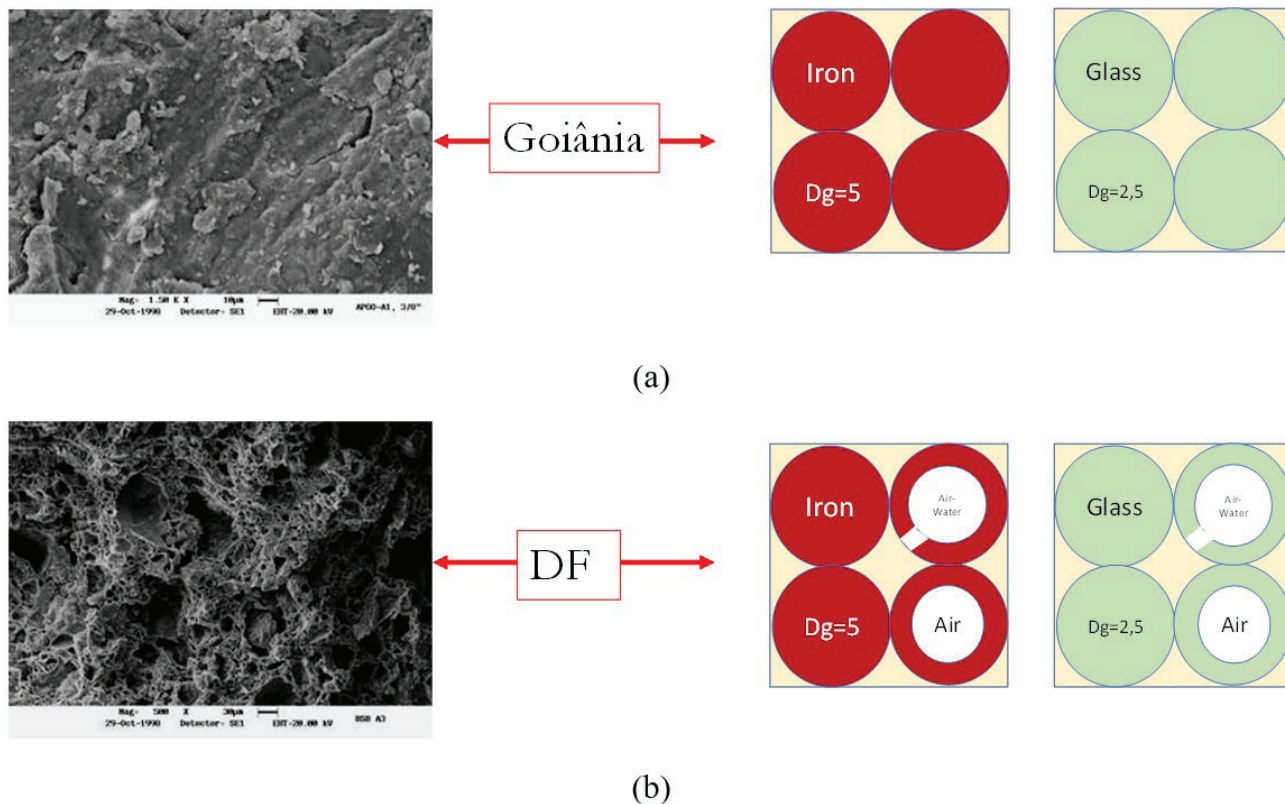


**Figure 11.** Model of pore-volume distribution in laterites and lateritic soils: (a) concretion from Goiânia, Brazil; (b) concretion from the Federal District (DF), Brazil.

by Camapum de Carvalho & Leroueil (2004), demonstrated the need to consider the pore structure in this analysis.

Slightly weathered tropical soils without expansive clay minerals may present expansion only of structural nature (i.e., increase in the distance between particles). In this case, the analysis of soil properties and behavior under unsaturated conditions may follow standard procedures. However, for slightly weathered tropical soils with expansive minerals, the swelling of these soils can be both structural and mineralogical (i.e., swelling of the particles themselves). Figure 12 shows that with the expansion of clay minerals, the volume of solids expands according to the increase in the interplanar basal distance (Camapum de Carvalho et al., 2019). In this case, it is necessary to consider the volume change of the expansive clay minerals and their impacts in the relative density of the particles. It is also important to realize that structural volume changes directly affect the void ratio, while mineralogical volume changes do not. Therefore, since the hydromechanical behavior is a function of the void ratio, it will not directly correspond with the global volume variation in the case of soils containing expansive clay minerals. Due to the difficulties in separating the two types of volume change, studies generally do not make such a distinction (Consoli et al., 2020). In studies applied to the analysis of bentonites, mineral expansion due to increased basal interplanar distance has generally been considered as a variation of soil microporosity (Sedighi & Thomas, 2014; Navarro et al., 2015; Chen et al., 2019) that does not necessarily interfere with the hydromechanical behavior.

To summarize, the analysis of the specific weight of the particles and its influence on the mechanical behavior of soils requires several considerations:

- It is necessary to consider the weathering profile and the variation of its chemical-mineralogical composition;
- Any analysis of deeply weathered tropical soils considering the void ratio requires attention towards the effect of the pore structure;
- Any analysis of slightly weathered tropical soils with expansive clay minerals requires attention towards the hydration or dehydration of clay minerals, with important impact on physical indexes;
- The definitions and analyses of the SWCCs obtained of deeply weathered tropical soils require considering the pore structure;
- The definitions and analyses of the SWCCs of slightly weathered tropical soils require considering, when present, the hydration or dehydration of the expansive clay minerals.

Adequate interpretation of the specific weight of the particles is essential in dealing with practical engineering problems and in the interpretation of laboratory testing data. For example, Camapum de Carvalho et al. (2019) showed, when analyzing the particle-size distribution curve of a bentonite obtained in hydrometer tests, that it is essential to consider the specific weight of the particles in a hydrated state. The same authors, when analyzing the relationship

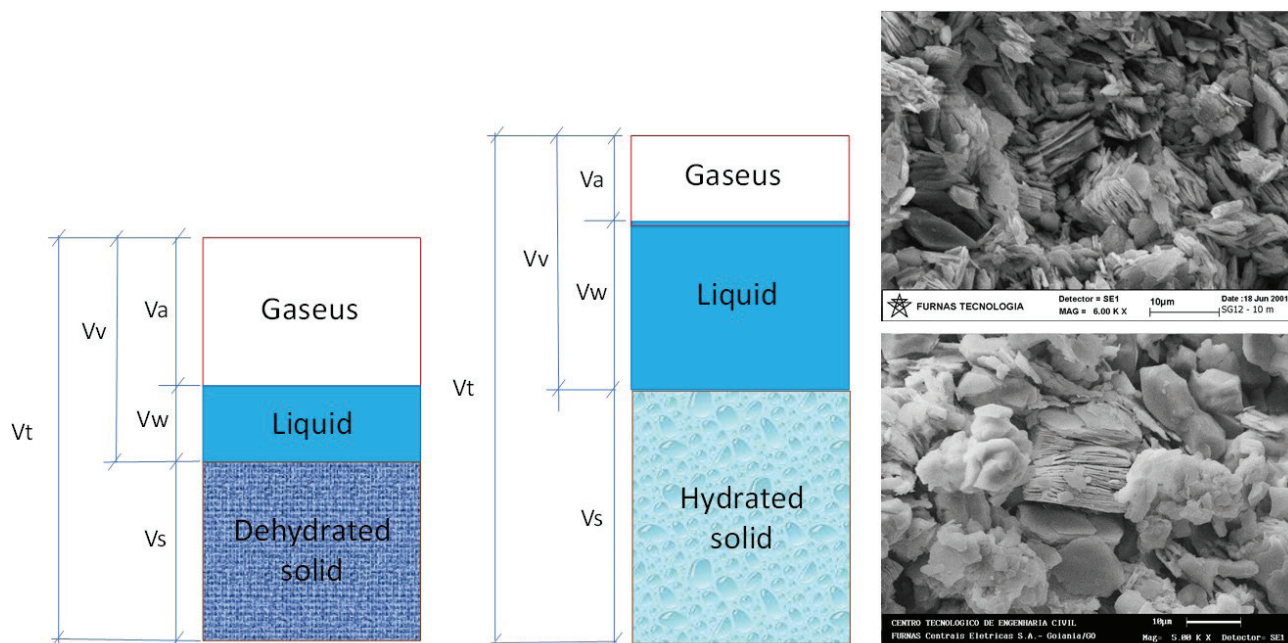


**Figure 12.** Impact of mineral expansion on the volume of solids.



between the void ratio corresponding to the liquid limit with the Skempton activity coefficient, found that meaningful results are only obtained if the particle-size distribution used is computed considering the specific weight of the particles in the hydrated state.

#### 2.4.2 Particle-size distribution

Important information regarding the structural characteristics of tropical soils that affect their behavior may be obtained from the particle-size distribution (PSD). Particle-size analysis methodologies and the interpretation of results must consider the use of the soil, active suctions, and temporal dynamics. Figure 13, obtained for a deeply weathered and aggregated soil (lateritic soil) shows that the PSD can be highly dependent on the sample preparation method (Roseno & Camapum de Carvalho, 2007). For this reason, PSD analyses of tropical soils must always include tests with and without the use of ultrasound and/or deflocculants. The PSDs obtained without dispersion offer information regarding the in-situ state of the soil. In situations where the soil is subjected to chemical stabilization (e.g., pavement structures) or the flow of contaminants (e.g., landfill covers and liners), the impact of these elements on the texture and aggregation must be investigated. In the event of disaggregation effects from soil treatment, it becomes relevant to include the use of deflocculant in the analyses. Obviously, changes in osmotic suction may take place and need to be accounted for.

Ayala (2020), when studying a lateritic soil stabilized with hydrated lime, determined PSDs using hydrometer tests considering: a) the pure soil (SP); b) the soil stabilized with 4% hydrated lime one day after mixing (4% 1D); c) soil obtained from crumbling a compacted cylindrical specimen prepared without the addition of lime (SP 1A); and d) soil from another crumbled specimen mixed with 4% of lime (4% 1A) and kept buried in situ for a year. Figure 14a shows that

the presence of lime affected the textural stability of both treated and untreated soils. Figure 14b, obtained for a soil studied by Delgado (2007), shows that depending on the lime content added to the soil, it can promote its disaggregation or aggregation. The addition of 2% lime disaggregated the soil. In the case of 6% lime content, it practically did not affect the stability of the aggregates or, more likely, it increased disaggregation and aggregation. Finally, with 8% lime, the soil suffered aggregation. These results show the importance of understanding the properties and behavior of tropical soils subjected to chemical stabilization or placed in contact with chemical products, common situations in geotechnical works such as the construction of pavement structures, embankments, dams, foundations, and retaining walls.

Rezende (2003) showed for a lateritic soil treated with 2% of lime that the chemical affected the textural stability and altered the SWCC (Figure 15). The influence of lime on the SWCC obtained by Rezende (2003) was, however, different from that verified in the study carried out by Botelho (2000), thus indicating that the chemical agent can act to

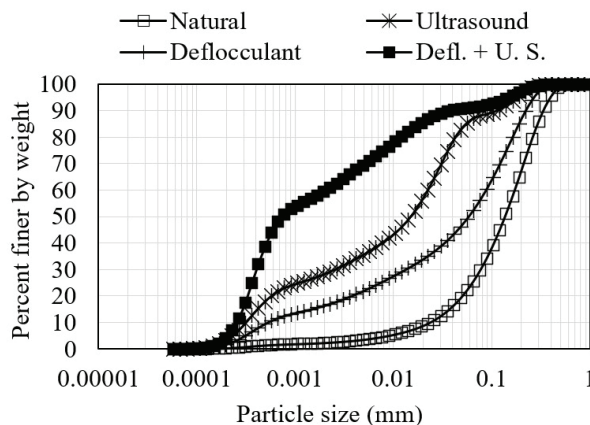
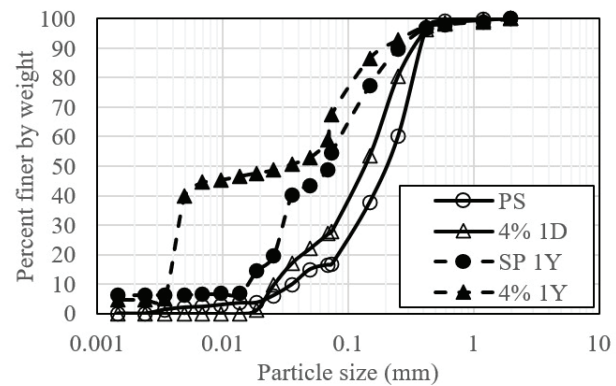
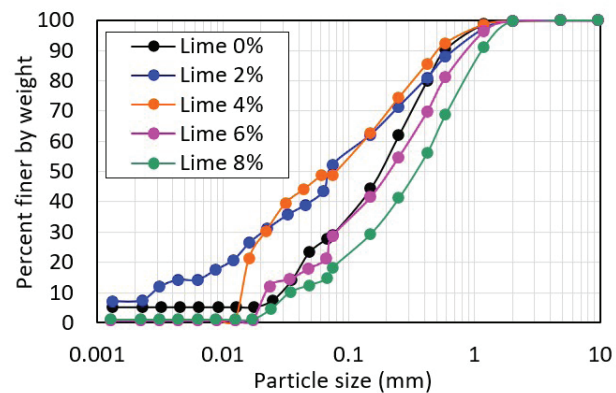


**Figure 13.** Particle-size distribution curves of a highly weathered soil collected at 4 m in depth, Federal District, Brazil (Modified from Roseno & Camapum de Carvalho, 2007).



(a)



(b)

**Figure 14.** Particle-size distribution curves of lateritic soils treated with lime: (a) modified from Ayala (2020); (b) modified from Delgado (2007).

aggregate or disaggregate the soil, depending on soil and the chemical agent itself.

Concrete placed in contact with the unsaturated soils can also be considered a contamination source, as shown by Wanderley Neto (2020), based on direct shear tests were performed on concrete-soil interfaces. The specimens were molded using concrete and a semi-statically compacted lateritic soil. Water content and void ratios corresponded to that of the soil found in the field. Matric suction was measured using the filter paper technique. Direct shear tests were carried out after 10, 14, 28, 60, and 90 days of curing. For the curing time equal to zero, the matric suction in the soil was equal to 4.1 kPa and in the concrete equal to zero. Figure 16 shows the results obtained by Wanderley Neto (2020) for the lateritic-concrete soil interfaces and the suctions measured using the filter paper technique on the soil surface and on the concrete surface. The results show that both cohesion and friction angle increase up to 60 days of curing, decreasing thereafter. The suction in the soil and the concrete increases until 60 days of curing, tending to equalize and stabilize after that time. As deteriorations occurred in the soil-concrete interface between 60 and 90 days, it is useful to analyze the destabilizing effect of the aggregates. Figure 17 presents shear stress results as a function of cure time for different vertical stresses. For the lowest confining stress (50 kPa), there is already a decrease in strength when passing from 28 to 60 days of cure, which demonstrates the loss of stability of the aggregates.

The instability of aggregates verified by Ayala (2020) and Wanderley Neto (2020) may be explained by the penetration of chemical compounds in the aggregate. Under favorable pH conditions, iron and aluminum oxide hydroxides are solubilized. Another example of the instability of aggregates was observed by Silva et al. (2008) when analyzing, 32 years after its construction, a tieback wall built on lateritic soil. Soil volumetric collapse resulted in excessive residual deformations (Figure 18) and the low residual stresses of the ground anchors. It was observed that the collapse was

due to the loss of stability of the aggregations, as a result of chemical migration from the concrete into the aggregates.

#### 2.4.3 Atterberg limits

The atterberg limits of tropical soils are strongly affected by the state of soil aggregation, chemical composition, and mineralogy. Figure 19 shows the plasticity chart containing data of the tropical weathering soil profile shown in Figure 3. These liquid limits and plasticity indices were originally

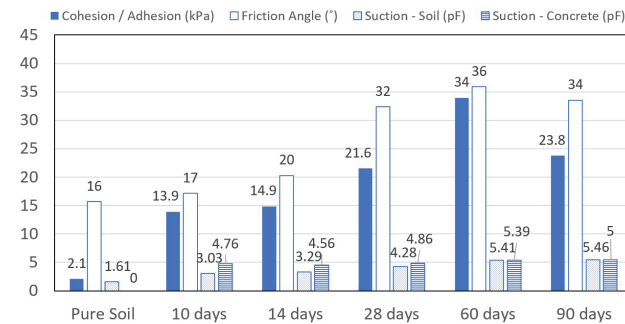


Figure 16. Soil-concrete interaction (Wanderley Neto, 2020).

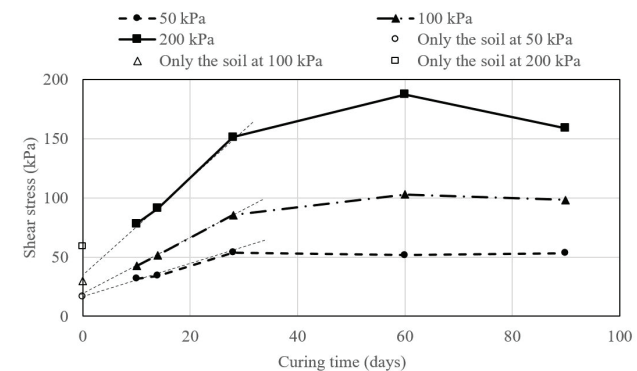


Figure 17. Shear strength in the soil - concrete interface as a function of curing time (Wanderley Neto, 2020).

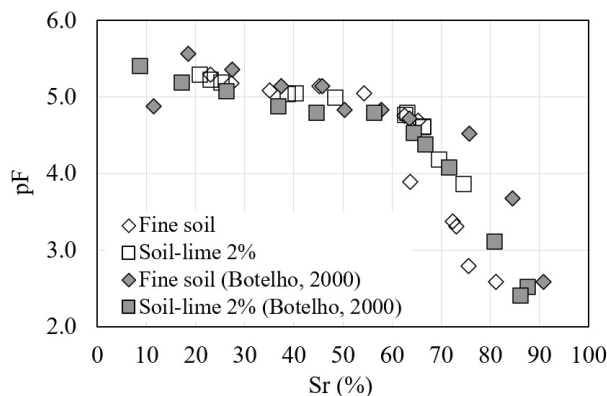


Figure 15. Soil-water characteristic curves of pure lateritic soils and stabilized soils with lime (modified from Rezende, 2003).

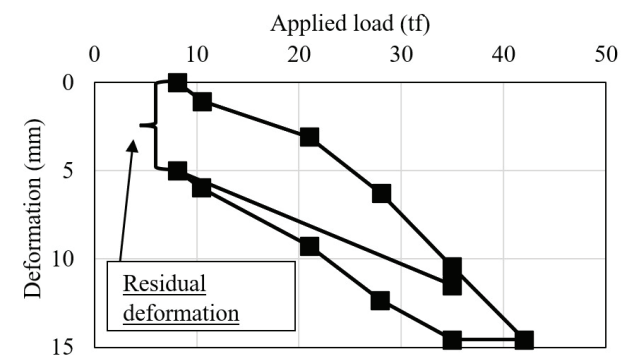


Figure 18. Load test on a ground anchor (modified from Silva et al., 2008).



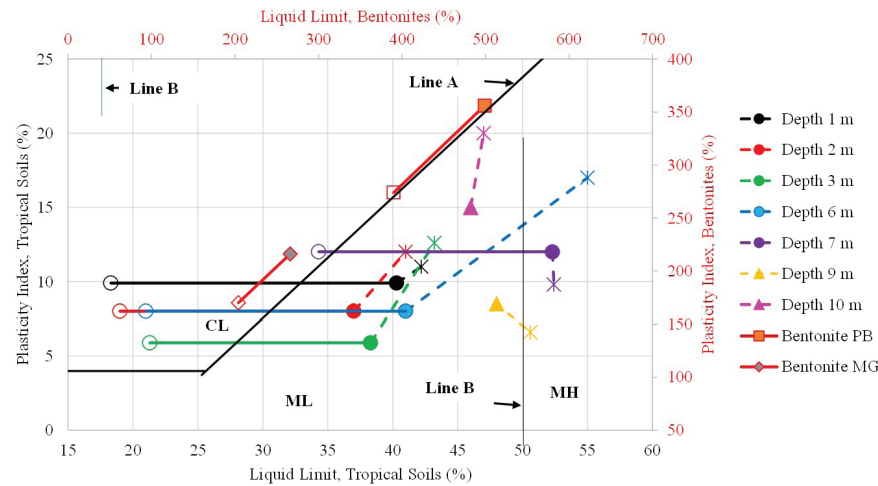


Figure 19. Plasticity chart and tropical soil's data under several conditions.

obtained by Carvajal et al. (2005). The data is presented for: a) the natural soil (filled markers); b) the soil disaggregated using ultrasound ("x" markers); and c) values adjusted by subtracting the intra-aggregate saturation water contents (empty markers). In the latter case, the intra-aggregate water content was estimated considering the content of aggregates and the water content corresponding to the micropore AEV, according to the bimodal SWCC model presented by Camapum de Carvalho & Leroueil (2004). The volume of micropores of aggregates was considered constant when going from the liquid limit to the plastic limit. However, depending on the stability of the aggregates, some volume change may occur. The results from Figure 19, combined with the plasticity chart by Vargas (1977), show that the weathered tropical soils (1 m to 7 m deep) move from the silt-clay classification to soils containing sand, which is more consistent with the soil texture in a natural state (Guimarães, 2002).

Figure 19 shows that disaggregation leads to higher liquid limits and plasticity index values. It is noteworthy that the samples collected at 9 m and 10 m in depth correspond to slightly weathered soils that do not present aggregations. These soils contain clay packages that are easily destroyed by ultrasound. Figure 19 also demonstrated that soil disaggregation releases active particles that can interact with water. These results indicate that the intra-aggregate water content does not contribute to the soil properties measured by the liquid limit and plastic index. Balduzzi & Mayor (1981) reached similar conclusion, based on studies carried out at the Federal University of Paraíba, towards better classification of tropical soils. According to these authors, tropical soils present superior mechanical properties when compared to soils from temperate climate regions with similar plasticity. As explained herein, the water content that effectively defines soil behavior is lower than the global water content (Camapum de Carvalho, 2017; Camapum de Carvalho et al., 2002b). As a result, Balduzzi & Mayor (1981) point out that the plastic limits of tropical soil

can vary significantly depending on the method of sample preparation. This finding may be extended to a greater or lesser degree, depending on the soil, to other tests aimed at evaluating the hydromechanical behavior of tropical soils.

The data presented by Campos et al. (2008) for a bentonite from the state of Paraíba, Brazil ( $w_L = 499\%$ ,  $PI = 356\%$ ), and for a bentonite from the state of Minas Gerais, Brazil ( $w_L = 266\%$ ,  $PI = 216\%$ ) are also shown in Figure 19. To estimate the amount of water occupying the basal interplanar distances, the model presented by Camapum de Carvalho et al. (2019) was used. The results presented in Figure 19, subtracting from the global moisture the water occupying the basal interplanar distances (empty markers), show significant variations in the liquid limits and the plasticity index value. Global void ratios were calculated assuming a saturated state and considering the total water content or only the free water (i.e., subtracting basal interplanar water). For the bentonite from Paraíba, the void ratios corresponding to the liquid and plastic limits went from 13.37 and 3.83 to 5.68 and 1.74, respectively. For the bentonite from Minas Gerais, the same values went from 6.83 and 1.285 to 3.20 and 0.60, respectively. These results underscore the importance of disregarding interplanar basal water content in the interpretation of properties and behavior of expansive clay minerals.

Additional factors must be considered in the case of deeply weathered tropical soils and slightly weathered tropical soils containing expansive clay minerals. Considering the results presented by Carvajal et al. (2005), Fleureau et al. (1993), Guimarães (2002) and Khalili et al. (2004), Figure 20 presents correlations between the liquid and plastic limits and the product of the void ratio and the macropore AEV in pF. The soil data from Guimarães (2002) indicate that superior correlations are obtained when subtracting from  $w_L$  and  $w_p$  the water content present inside the aggregates and taking only the void ratio corresponding to the inter-aggregate pores, as proposed by Camapum de Carvalho et al. (2015a). Figure 20 show also

that when considering only interparticle moisture and porosity in the analysis of expansive soils, the data points preset a superior fit to the trends originally proposed by Camapum de Carvalho et al. (2017) and Bigdeli (2018). This fact highlights the need for such consideration when slightly weathered tropical soils have expansive clay minerals.

In order to highlight the importance of the chemical-mineralogical composition of tropical soils, Figure 21 shows correlations between the aggregate contents determined in the studies carried out by Lima (2003) and the activity coefficients determined according to Skempton (1953) and according to the EMBRAPA (2006) methodology, with the latter being based on the cation exchange capacity (CTC). Superior correlations are obtained using the EMBRAPA (2006) methodology, indicating the need to review how the Atterberg limits of deeply weathered tropical soils (aggregate

soils) are determined and highlighting the importance of chemistry composition for the state of soil aggregation. The data presented in this section corroborates the analyzes shown in Figure 19 and demonstrates the need for further studies on the impact of aggregations and the corresponding structure of pores in the case of deeply weathered soils and of the effect of the presence of expansive clay minerals in slightly weathered soils.

## 2.5 Soil classification

Soil classification is an important element in Geotechnical Engineering. Its purpose is not to precisely define the hydromechanical behavior of the soil but to indicate the expected general behavior. Design based on parameters estimated from classification indexes should be completely avoided in the case of tropical soils, due to their particular characteristics, properties, behavior, and temporal dynamics. The adoption of theoretical models for estimating SWCCs also requires attention, since it depends on the pore-size distribution, pore structure, and on the chemical-mineralogical characteristics. In this context, there is a need to establish a link with the specific behavior and properties of tropical unsaturated soils.

Deeply weathered soils, fine-grained lateritic soils, and lateritic gravels require the consideration of aggregate porosity and stability against the environment and construction-related loads. The slope of the dry branch of the compaction curve (defined by Nogami & Villibor, 1995) and its relevance for soil classification deserves further analysis, including the behavior of coarse-grained soils. The slope of the dry branch may be linked to variations in suction and/or breaking of aggregates, which depends on the compaction water content. The mass loss immersion test, used to evaluate soil erodibility, may also serve to identify the presence of soil expansion when the soil detaches from the mold. The detachment occurs by shear in the contact plane between the part of the specimen extracted from the mold.

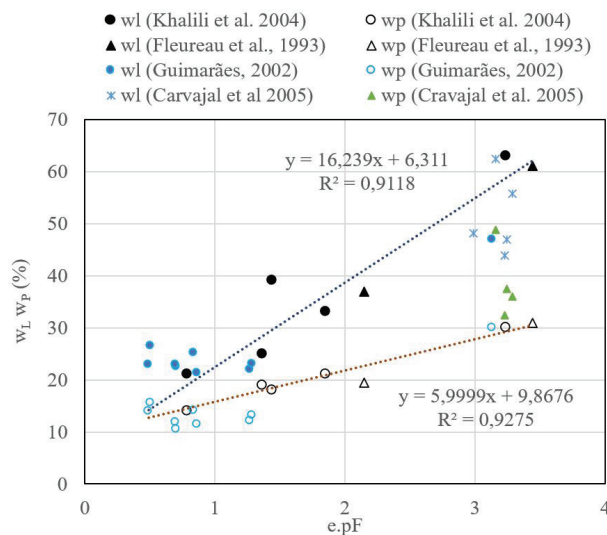


**Figure 20.** Relationship between the air-entry value transformed by the void ratio and the corrected plastic and liquid limits (modified from Camapum de Carvalho et al., 2017)

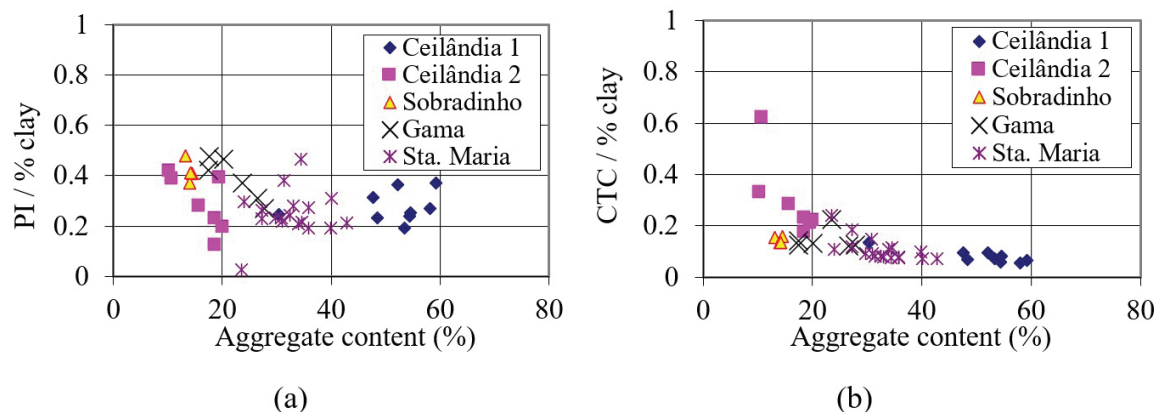


**Figure 21.** Aggregate content as a function of: (a) plasticity index; (b) cation exchange capacity (modified from Camapum de Carvalho et al., 2015b).

In traditional classification models, the use of texture as a classification element must be combined with analyzes related to aggregate stability and the distribution of pores in the soil. In this sense, considering the shape of the SWCC (e.g., Figure 9) is relevant for understanding the properties and behavior of tropical soils and for adopting classifications that are more integrated to engineering practice. Another aspect to be analyzed, in the specific case of coarse-grained tropical soils, is the potential PSD discontinuity that may lead to piping erosion (Camapum de Carvalho et al., 1999).

The use of the Atterberg limits in traditional classification systems applied to tropical soils requires two important factors to be considered: a) if the soil is in an aggregated state (i.e., lateritic soil), it is necessary to subtract from  $w_L$  and  $w_p$  the water present in the interior of micro-aggregates; b) if the soil is slightly weathered and has expansive clay minerals (i.e., saprolitic soils), the water integrating the hydration of these clay minerals must be subtracted from  $w_L$  and  $w_p$ . It is important to note that these two factors still need further study. The approach presented here aims to encourage researchers to further these studies.

### 3. Compaction of tropical soils

The compaction of tropical soils requires the understanding of unsaturated and saturated behavior. As the water content is increased, the dry unit weight in the dry-of-optimum branch increases due to: a) the lubricating effect of water, an effect not always preponderant; b) the reduction of suction and the corresponding decrease in the resistance to the compaction process, with effects that depend on the presence of inter-aggregate water (Camapum de Carvalho et al., 2012); c) particle breakage, which is common in aggregate materials such as laterite gravels. Further increase in the water content will lead to the occlusion of the air phase, generating positive pore-water pressures during compaction, and reducing the effective compaction energy. These are the mechanisms that result in the wet-of-optimum compaction conditions.

Given the particularities of tropical soils, some points deserve to be highlighted:

- due to the presence of different levels of aggregation and aggregate stability, deeply weathered soils may present compaction curves with two dry unit weight peaks;
- the crushing of aggregates during the compaction process affects the distribution and structure of pores, the resulting SWCC and suctions acting on the soil, and the dry unit weight;
- in deeply weathered soils (i.e., lateritic soils), where the compaction water content partially fills the macropores, suction is relatively small. As a result, little effect of suction is observed in the compaction

and mechanical behavior of the soil (Camapum de Carvalho, 2004; Parreira et al., 2004);

- in slightly weathered soils (i.e., saprolitic soils), the SWCCs are generally unimodal. The influence of suction on the compaction process and on the soil behavior will depend on the size and distribution of the pores;
- Lambe's theory regarding the influence of water content and compaction energy on the soil structure is only applicable to saprolitic soils. Particle orientation does not occur in highly weathered tropical aggregated soils;
- when a tropical soil is stabilized with asphalt emulsion, the compaction curve must be represented as a function of the fluid content and not the moisture content. The emulsion interferes with the effect of suction, interparticle lubrication, air phase occlusion, and pore-water pressure;
- when the soil has a significant amount of expansive clay minerals, the hydration water content of these clay minerals must be subtracted from the global water content. The weight of these hydrated particles must be taken into account in the calculation of the dry unit weight.

The characteristics of tropical lateritic and saprolitic soils define the shape of the compaction curve and the mechanical behavior of the soil, as illustrated by Nogami & Villibor (1995) in Figures 3.8 and 3.9 of the book "*Pavimentação de baixo custo com solos lateríticos*".

Guimarães et al. (1997) showed that the disintegration of the soil using a chemical agent promotes the increase in maximum dry unit weight (Figure 22, black markers). Nevertheless, the mechanical behavior is worsened (Figure 22, red markers). The penetration resistance curves obtained for the natural and disaggregated soil are affected by the different

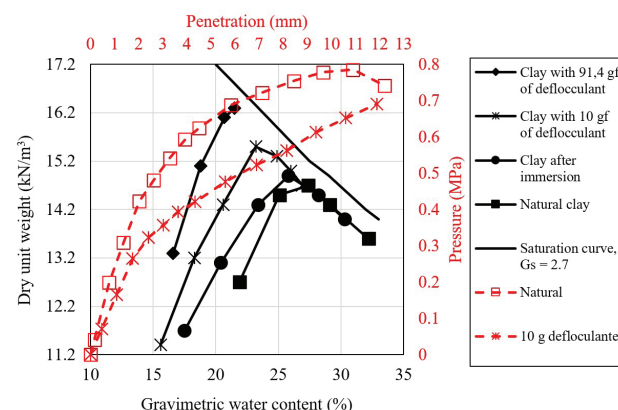


**Figure 22.** Influence of dispersion on the compaction and resistance of a lateritic soil (modified from Guimarães et al., 1997).

structures and aggregations present in the natural soil and by the dispersed particles in the disaggregated soil. In addition, the reuse of tropical soil and its prior drying can affect the compaction results (Aquino et al., 2008).

The aggregates in deeply weathered tropical soils are affected by the chemical actions of the environment. Therefore, it is necessary to consider the quality of the water used in compaction. The composition of the water used in laboratory studies is often different from that of the water in the field. The solubilization and, in some instances, the leaching of chemical compounds such as iron and aluminum oxides and hydroxides can promote textural and structural instability in deeply weathered soils (Farias et al., 2002).

Figure 23 shows the impact of water quality on the compaction curves of a deeply weathered soil collected at 5 m in depth and of a slightly weathered soil, collected at 9 m in depth (Coelho et al., 2016). The stream water used for compaction was contaminated by domestic sewage. These results show that, in slightly weathered soil, the water quality affects the optimum water content, but has little effect in the maximum dry unit weight. This finding indicated the potential influence of the osmotic suction. For the deeply weathered soil, there is an increase in the dry unit weight when using polluted stream water, indicating the occurrence of instability of the aggregates. These results show the importance of using, in the laboratory investigations, the same water that will be used in the field.

The method of sample preparation can also affect the compaction curve of tropical soils. Figure 24 presents Proctor compaction results obtained for four soils from Urucu, AM, Brazil (Pessoa, 2004). Filled markers correspond to the air-dried soil and the empty markers correspond to testing results using samples that were not air-dried. For the studied soils, air drying resulted in higher optimum water contents and lower dry unit weights. Different results can be obtained for other soils, depending on the sensitivity of its structure to drying.

It is suggested that when studying the compactability of a tropical soil, one should pay attention to variations in the specific weight of particles in situ, the aggregate stability, and the structural and/or mineralogical expansion of the soil. Finally, incorporating iso-suction curves into the compaction curve constitutes important complementary information that allows evaluating how the suction is varying depending on the compaction condition (Camapum de Carvalho & Leroueil, 2004; Camapum de Carvalho et al., 2012).

#### 4. Effective water content and porosity

The study and analysis of the properties and behavior of tropical soils require consideration of the “effective porosity” and “effective water content”, as these are the effective parameters that define the hydromechanical behavior of the soil. The void ratio ( $e$ ) and global water content ( $w$ ) are based on the weight and volume of solids dried at 105 °C. The effective void ratio ( $e'$ ) and the effective water content

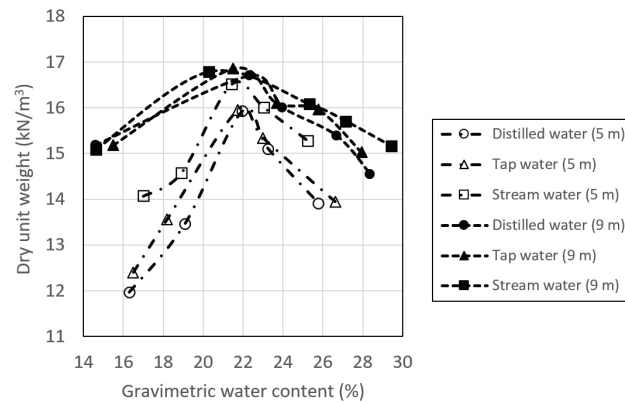


**Figure 23.** Influence of water quality on the compaction curve of tropical soils (modified from Coelho et al., 2016).

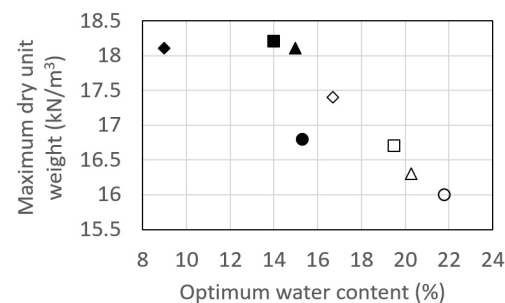


**Figure 24.** Influence of sample drying on the optimal compaction condition (modified from Pessoa, 2004).

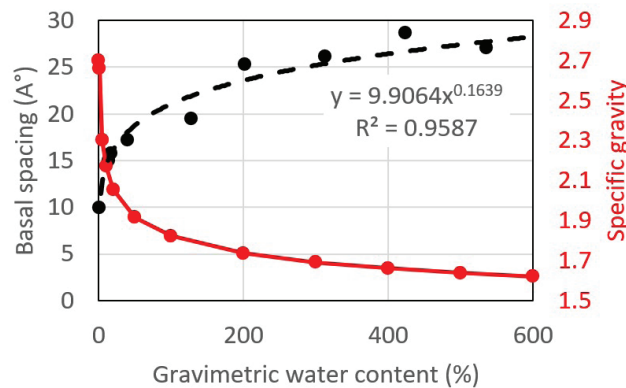
( $w'$ ) may be computed based on the following methodology: a) for soils with aggregations, only the inter-aggregate voids and water content must be considered. Depending on the water contents and suction, aggregates may be assumed to be saturated and the water contained in them may be incorporated in the weight and volume of solids; b) for active clay minerals, the volume of voids and the water content corresponding to the hydration water must be excluded, thus reducing their densities. Additional assumptions are required. The basal interplanar distance equation shown in Figure 25 (Camapum de Carvalho et al., 2019) was adopted for the calculations of smectite hydration and corresponding specific density presented herein. The data shown in Figure 25 corresponds to a material from the same region where the bentonite studied by Consoli et al. (2020) was collected. Smectites may be assumed to have an average number of layers of 10 and an average diameter of 1 mm.

Figure 26 presents the analysis of compaction curves where the dry unit weight was replaced by the void ratio (regular and effective). The data corresponding to a lateritic soil compacted in normal Proctor conditions (LSPN-e) and intermediate Proctor energies (LSPI-e) was originally presented by Delgado (2002). The dataset for the mixtures of bentonite (B) with kaolin (K) in the proportions 10%B



/ 90%B and 50%B / 50%B was originally presented by Consoli et al. (2020). That bentonite is composed of 70% of smectite, approximately. The slightly weathered tropical soil studied by Delgado (2002) and the bentonite-kaolin mixtures studied by Consoli et al. (2020) present some common minerals. Slightly weathered tropical soils often present 5% to 10% of expansive clay minerals and kaolinite is also often created during weathering. Quartz is also frequently present in tropical weathering profiles, either as a residual mineral or as a newly formed mineral (Senaha, 2019). These common mineral occurrences have motivated the comparisons presented herein. Figure 26 shows the significant difference between the values of global and effective void ratio and moisture contents.

This analysis approach can also be applied to other materials, with varying degrees of aggregation, such as construction waste (Camapum de Carvalho 2017) and sandy-quartzose soils (Machado and Vilar, 1998; Camapum de Carvalho & Pereira, 2002). The effective parameters  $e'$  and  $w'$  have also been used in the analysis of the SWCC and of the volumetric collapse of tropical soils (Camapum



**Figure 25.** Effect of gravimetric water content on basal interplanar distance and on density of a bentonite (modified from Camapum de Carvalho et al., 2019).

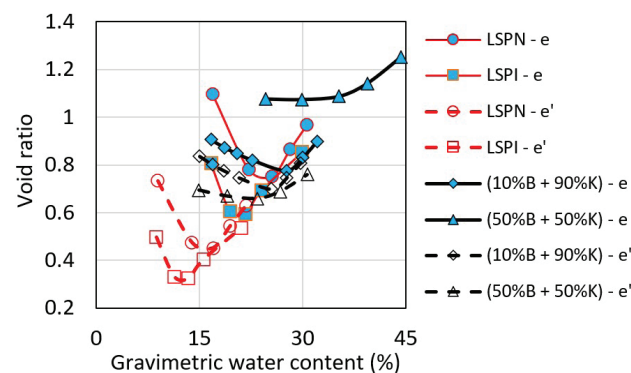


**Figure 26.** Compaction curves (modified from Delgado, 2002; Consoli et al., 2020)

de Carvalho et al., 2002a; Camapum de Carvalho et al., 2002b). Finally, when studying chemical stabilization, the cation exchange capacity and exchangeable ions should be considered.

The swelling results presented by Consoli et al. (2020) for mixtures of kaolin, bentonite, and Portland cement were analyzed using the effective parameters  $e'$  and  $w'$ . Figure 27 was obtained considering that swelling is directly proportional to the smectite content and inversely proportional to the Portland cement content, water content, and void ratio. Smectite content was used in the normalization attempt, to isolate the effect of mineralogical expansion and to disregard kaolinite structural expansion (Mielenz & King, 1955 apud Grim, 1962). Figure 27 shows that no clear trend is found when considering global parameter  $e$  and  $w$ . Swelling is better defined in terms of the effective parameters  $e'$  and  $w'$ . The need to include the Portland cement fraction should also be recognized. Figure 27 shows also that the transition zone, before the relatively constant swelling behavior, corresponds to a global water content that matches a minimum basal spacing shown in Figure 25. In summary, the use of effective void ratio and effective water contents allows the establishment of meaningful relationships between the state variables.

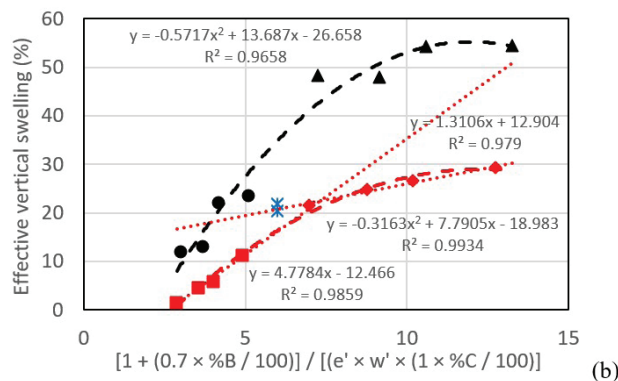
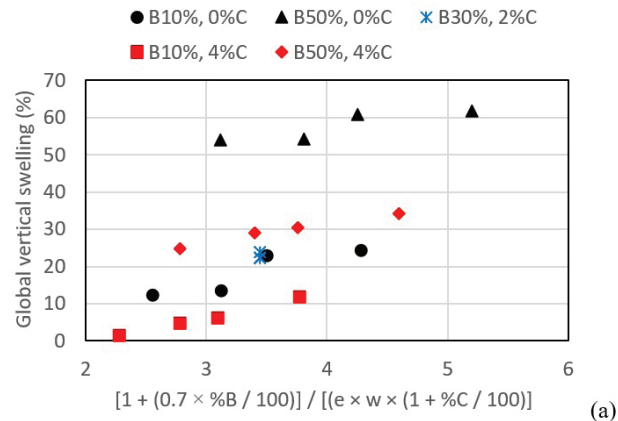


**Figure 27.** Analysis of swelling considering: (a) global parameters; (b) effective parameters.

## 5. Temporal and spatial aspects

The impact of time and terrain morphology on tropical soil behavior is related to the level of weathering, mineralogical and chemical composition, structure and physical state, climate, geomorphology, and anthropogenic effects. Therefore, treating engineering problems that involve tropical soils as being static in time is an inadequate approach. Results from Lima (2003), obtained during studies of erosion gullies in the Federal District, Brazil, illustrate the effects of geomorphology and time. Figure 28a shows that the clay content increases when approaching the face of the erosion slope. These findings reveal the degradation of clay aggregates over time, as the gully gradually exposes the soil to the weather conditions. In connection with the change in texture, the sum of the iron and aluminum oxide/hydroxides increases when approaching the erosion edge. Figure 28b shows SWCCs determined by Lima (2003) for undisturbed specimens taken from the same gully erosion location. Well 1 was located 3 m from the edge of the erosion slope and well 2 was located 20 m from the edge. The accelerated weathering observed in the specimens from well 1 modifies the retention properties of the soil, increasing the AEV.

Table 1 shows the data obtained from direct shear indicating a slight increase in the effective friction angle and a significant reduction in effective cohesion when approaching

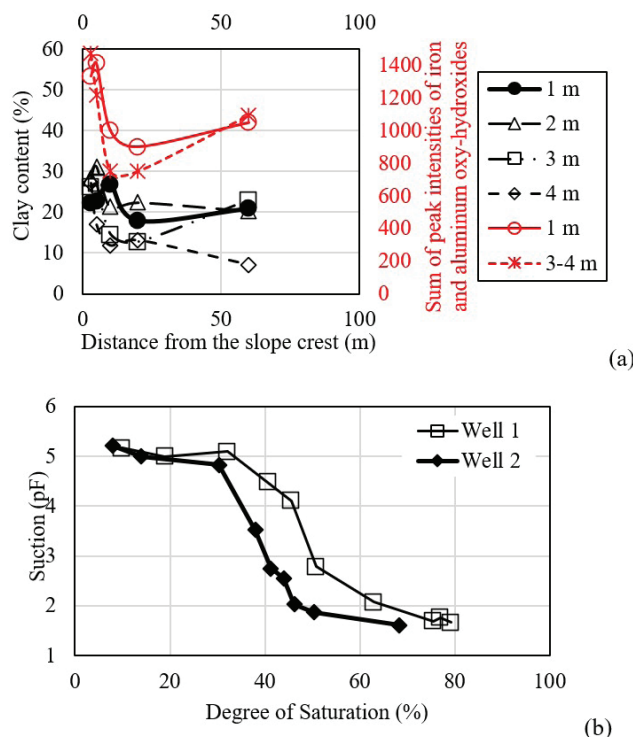


**Figure 28.** Temporal effects of weathering near an erosion gully: (a) soil composition; (b) soil-water characteristic curves (modified from Lima, 2003).

the erosion edge, despite the increase in clay content and the presence of iron and aluminum hydroxides. This means that the fine particles produced due to weathering have negligible interaction with the soil matrix. The decrease in cohesion is related to the leaching process that occurred in the original structure due to the flow towards the slope. Lima (2003) shows that the factors of safety for the gully slope (height of 15 m and slope angle of 70°) were higher when considering the shear strength parameters from specimens taken from well 2, when compared to the results based on well 1. These factors of safety show the significance of the accelerated soil weathering and degradation. To summarize, the study of erosion gullies in tropical soils clearly demonstrates temporal impacts on the behavior of the soil that should not be neglected.

Another example of temporal effects arise from the analysis of geological data related to slope failures. During a recent conference organized in remembrance to the tragic slope failure events that occurred in 2011 in the state of Rio de Janeiro, Ana Carolina F. Campello (Universidade Federal do Rio de Janeiro) presented the dating of hillside failures that occurred over several past centuries. Figure 29 shows information presented on sediment accumulations over time and information from Marcott et al. (2013) on the temperature variations over the last 11,000 years. The plot shows that during the warming and cooling phases of the

**Table 1.** Shear strength parameters from direct shear tests for wells 1 and 2 (Lima, 2003).

Depth (m)	Well 1, 3 m to the slope edge		Well 2, 20 m to the slope edge	
	c' (kPa)	$\phi'$ (°)	c' (kPa)	$\phi'$ (°)
1	2.2	23.9	4.2	20.8
3	8.7	27.7	23.5	26.1

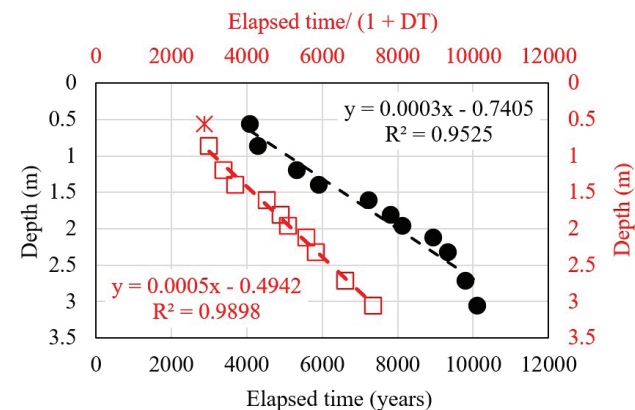


**Figure 29.** Accumulation of sediments as a function of the elapsed time and as a function of elapsed time normalized by the thermal variation.

planet there was an expansion of the soil profile in relation to time. Thermal variations in the time scale were introduced in Figure 29 by dividing the year of occurrence of the sediment accumulation by  $(1 + DT)$ , where  $DT$  is the thermal variations in the respective sediment accumulation periods. The data normalization led to the linearization of the results, except for the most recent years of accumulation of sediment. This shows the impact of extreme events, anthropic interventions, changes in the microclimate and in the quality of rainwater. This simple and brief analysis highlights the importance of the temperature in altering the soil, which indicates that factors such as insolation and wind must be considered, as they alter the hydrological conditions in the unsaturated media.

The unsaturated soils predominate in most geotechnical works in tropical climate regions and are influenced by weather and drainage conditions. In this context, subsurface and surface morphology plays a significant role. Camapum de Carvalho et al. (2007) present the analysis of a slope of a 12 m excavation that failed in 2005 (Figure 30a). The slide occurred on the concave side of a curved section. Other failures have been observed in the region, under similar conditions, such as the slide shown in Figure 30b. Numerical analyzes and physical modeling (Camapum de Carvalho et al., 2007; Jesus, 2013) demonstrated that the slope morphology influences not only the stress state, but also the saturated/unsaturated seepage conditions near the slope surface. Concave slopes present converging flow near the toe and higher water tables. The opposite effect is observed in convex slopes. The increase in the water table in concave slopes goes against the favorable effects of stress arching.

Some conclusions can be drawn from the analysis of these slopes failures. Terrain morphology must be considered, including its influence on saturated/unsaturated seepage.

The two-dimensional analysis of slope stability does not represent adequately concave and convex slopes. The region right next to the corner where two vertical slopes meet should be carefully analyzed, as it may be negatively influenced by a higher water table. It is expected that these effects of geomorphology will be accumulated over time.

## 6. Life in the soil and unsaturated behavior

Vegetation, insects, and microscopic organisms can affect the properties and behavior of tropical soils, by changing the characteristics of the environment (Bernardes & Gomes, 2012) and the physical state of the soil itself (Valencia, 2009; Gómez Muñetón, 2013; Guimarães et al., 2017). For example, plants promote the movement of chemical compounds in soils and generate organic matter that influences the aggregation and distribution of pores (Momoli et al., 2017). Termites affect the hydraulic properties of the soil and often incorporate substances that aggregate the particles (Conciani et al., 2009). Bacteria present in tropical soils can affect the cementation and distribution of pores (Valencia, 2009; Gómez Muñetón, 2013). Therefore, temporal, climatic, and geomorphological aspects must also be combined with the influence of living organisms. Figure 31 shows growing bacteria naturally occurring in a tropical soil from erosive processes in the Federal District, Brazil. Studies have been carried out on the use of bacteria to stabilize these erosive processes, by promoting soil cementation through crystallization of chemical compounds. This cementation provides a change in the matric suction acting on the soil and on its mechanical behavior (Figure 32).



**Figure 30.** Slope failures in excavations (Camapum de Carvalho et al., 2007).



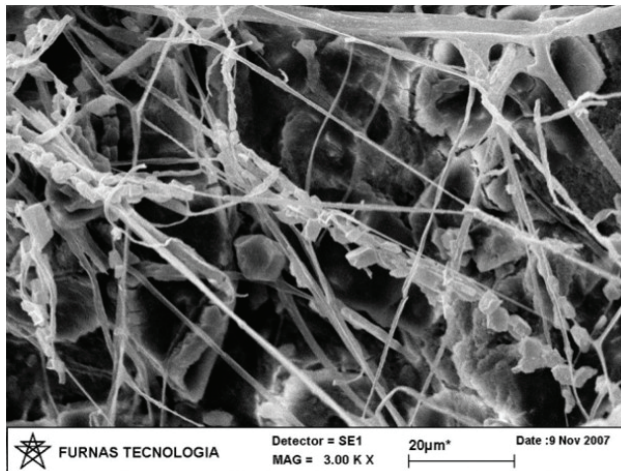


**Figure 31.** Formation of crystals by bacteria present in the soil (Valencia, 2009).

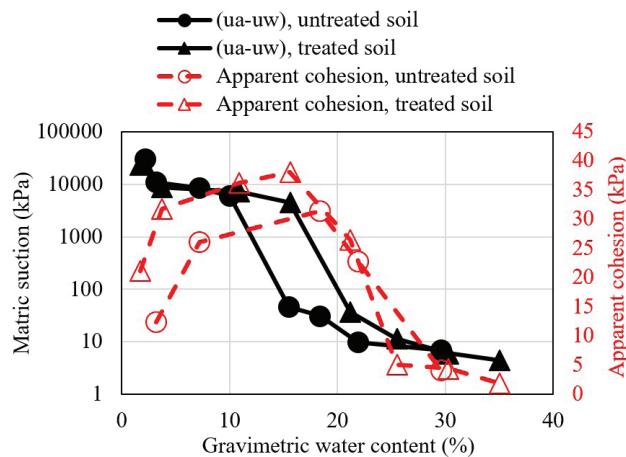


**Figure 32.** SWCC and apparent cohesion of a soil in a natural state and modified by the action of bacteria (modified from Valencia, 2009).

## 7. Final remarks

The practice of geotechnical engineering and the use of theories and concepts for unsaturated soils in tropical regions requires the consideration of the particularities of the weathering profiles and their temporal and spatial dynamics. Microstructure, chemical-mineralogical composition, pore structure and distribution, the chemistry of the environment, the geomorphology, and the climatic conditions need to be accounted for.

Classification systems and hydromechanical behavior models developed for sedimentary soils and temperate and cold climate soils are generally also applicable to slightly weathered tropical soils and saprolitic soils. However, its applications to deeply weathered tropical soils and lateritic soils require adaptations that were discussed in this article.

The comparison of the PSD obtained from test with and without the use of deflocculants and ultrasound provide important quantitative information on the soil pore structure, volume of aggregates, and aggregate stability. The representative particle size analysis will depend on the problem at hand. For example, problems where the soil is in contact with domestic sewage requires PSD analyses with and without deflocculants. The evaluation of pavement structures requires PSD tests with and without the use ultrasound. However, if this soil is subjected to chemical action, deflocculants and ultrasound are recommended. In problems involving the chemical stabilization of soils or the presence of fertilizers, it is recommended to evaluate the effect of these compounds on the PSD.

Studies and analyzes of the properties and behavior of natural and compacted unsaturated tropical soils require consideration of their sensitivity to the chemistry of the environment and their alterability as a function of climatic and spatial conditions. In many cases, the temperature has an immediate effect on tropical soils' behavior and on the SWCC. The paper also highlighted the importance of living organisms to the soil's behavior.

Given the complex temporal and spatial dynamics acting on the properties and behavior of tropical soils, it is often necessary to have simplified analysis approaches. The transformed SWCC model proposed by Camapum de Carvalho & Leroueil (2004) offers a useful alternative. However, in the case of aggregated soils, it is also necessary to consider the pore structure, as exemplified by Camapum de Carvalho et al. (2002a). When it comes to the analysis of the mechanical behavior, the use of transformation or normalization models of suction in relation to the void ratio is suggested, taking into account conditions where the parameter is directly proportional to porosity, such as in volumetric collapse (Camapum de Carvalho et al., 2002b), or inversely proportional, such as in shear strength (Camapum de Carvalho & Pereira, 2002). It should be noted that these models do not replace detailed laboratory studies and field monitoring.

Most of the topics discussed herein require further studies and a continuing advance in the understanding of the complex phenomena involving tropical unsaturated soils. The scientific research and engineering practice require consideration of the current State-of-the-Art and State-of-the-Practice, technical standards, the exercise of observation, and, especially, the reflection which is the philosophical basis of engineering. To put this perception into practice, it is necessary to exercise thinking that is free of ties to the norms, dogmas, and previously set knowledge. Past experience should not be neglected, but should be followed without losing sight that it is always evolving, especially in the complex field of geotechnical engineering.



## Acknowledgements

The authors are grateful to academic advisors throughout their education and to colleagues and students who contributed to the consolidation of the understandings shown in this paper. They thank the University of Brasília, the Federal University of Goiás, and the scientific research funding bodies CNPq, CAPES, FAP-DF, and FAPEG for the support they received throughout their academic lives. The authors thank Fernando Carolino da Silva, Juliana Alarcón Posse, and Luiz Felipe R. Varrone, for their support in formatting this article.

## Declaration of interest

The authors declare that they do not have conflicts of interest that could have interfered with the contents of the paper.

## Author's contributions

José Camapum de Carvalho: conceptualization, formal analysis, funding acquisition, writing – original draft; Gilson de F. N. Gitirana Jr.: formal analysis, writing – review & editing.

## List of symbols

AEV	Air-entry value
CTC	Cation exchange capacity
$c'$	Effective cohesion
$e$	Void ratio
$e'$	Effective void ratio
PI	Plasticity index
$G_s$	Specific gravity
N-SPT	Number of blows
PSD	Particle-size distribution
SPT	Standard penetration test
SWCC	Soil-water characteristic curve
$w$	Gravimetric water content
$w'$	Effective gravimetric water content
$w_L$	Liquid limit
$w_p$	Plastic limit
$\phi'$	Effective friction angle

## References

- Aguiar, L.A. (2014). *Análise do comportamento mecânico de solos compactados e estabilizados quimicamente para uso em barragens* [Doctoral thesis, University of Brasília]. University of Brasília's repository. <https://www.geotecnia.unb.br/index.php/pt/producao-academica/teses-e-dissertacoes>
- Aoki, N., & Velloso, D.A. (1975). An approximate method to estimate the bearing capacity of piles. In *Proceedings of the 5th Panamerican Conference on Soil Mechanics and Foundation Engineering* (Vol. 1, pp. 367-376). Buenos Aires: Sociedad Argentina de Mecánica de Suelos e Ingeniería de Fundaciones.
- Aquino, F.R., Guimarães, R.C., Aguiar, L.A., Miranda, C.O.P., Cabral, M.P., & Camapum de Carvalho, J. (2008). Influência dos métodos de compactação e preparação de amostras no comportamento da curva de compactação de solos tropicais. In *Anais do 19º Congresso Brasileiro de Mecânica dos Solos e Engenharia Geotécnica* (pp. 1755-1762). São Paulo: ABMS.
- Ayala, R.J.L. (2020). *Melhoria de solos com fibras provenientes da indústria avícola* [Doctoral thesis, University of Brasília]. University of Brasília's repository. <https://www.geotecnia.unb.br/index.php/pt/producao-academica/teses-e-dissertacoes>
- Balduzzi, F., & Mayor, P.A. (1981). *La classification des sols rouges tropicaux à l'aide de l'essai Moisture Condition. Rapport interne J 341/2*. Institut d Technique de Foundations et de Mécanique des Sols (in French).
- Barreto, P.N.M. (2019). *A new method to correct the void ratio for expansive soil* [Master of Applied Science in Civil Engineering, The College of Graduate Studies]. The University of British Columbia's repository. <https://open.library.ubc.ca/cIRcle/collections/ubctheses/24/items/1.0378422>
- Bernardes, R.S., & Gomes, L.N.L. (2012). Qualidade da água e suas relações com a infiltração no solo. In J.C. Carvalho, G.F.N. Gitirana Junior, E.T.L. Carvalho (Eds.), *Tópicos sobre infiltração: teoria e prática aplicadas a solos tropicais* (pp. 143-156). Faculdade de Tecnologia, Universidade de Brasília. Retrieved in July 18, 2021, from <https://www.geotecnia.unb.br/index.php/pt/producao-academica/livros>
- Bigdeli, A. (2018). *Evaluation and control of collapsible soils in okanagan-thompson region* [Doctoral thesis. The University of British Columbia]. The University of British Columbia's repository. <https://open.library.ubc.ca/cIRcle/collections/ubctheses/24/items/1.0372367>
- Botelho, F.V.C. (2000). Influência da compactação e estabilização na curva característica dos solos lateríticos. [Unpublished research report]. University of Brasília (in Portuguese).
- Camapum de Carvalho, J. (1981). *Influência das energias térmica e mecânica em propriedades de engenharia selecionadas de alguns solos lateríticos do Norte e Nordeste do Brasil* [Master's dissertation, Federal University of Paraíba]. Federal University of Paraíba's repository. [https://repositorio.ufpb.br/?locale=pt\\_BR](https://repositorio.ufpb.br/?locale=pt_BR)
- Camapum de Carvalho, J. (1985). *Etude du comportement mécanique d'une marne compactée* [Unpublished doctoral thesis]. I.N.S.A. – Toulouse (in French).
- Camapum de Carvalho, J. (2004). Propriedades e comportamento de solos tropicais não-saturados. In *Anais do 5º Simpósio*

- Brasileiro de Solos Não Saturados* (Vol. 2, pp. 597-616). São Paulo, Brasil: ABMS.
- Camapum de Carvalho, J. (2017). Solo como material de Construção. In G. C. Isaia (Ed.), *Materiais de Construção Civil e Princípios de Ciência e Engenharia de Materiais* (pp. 538-574). IBRACON (in Portuguese).
- Camapum de Carvalho, J., & Gitirana Junior, G.F.N. (2005). Considerações sobre parâmetros de resistência de solos tropicais. In *Anais do 2o Simpósio sobre Solos Tropicais e Processos Erosivos no Centro-Oeste, Goiânia* (pp. 183-191). Goiânia: UFG.
- Camapum de Carvalho, J., & Leroueil, S. (2004). Curva característica de sucção transformada. *Solos e Rochas*, 27(3), 231-242.
- Camapum de Carvalho, J., & Pereira, J.H.F. (2002). Une approche pour la description des propriétés des sols non saturés. In *Proceedings of the 3rd International Conference on Unsaturated Soils, UNSAT 2002* (Vol. 2, pp. 501-506). Recife, Brazil (in French).
- Camapum de Carvalho, J., Guimarães, R.C., & Pereira, J.H.F. (2002a). Courbes de retention d'eau d'un profil d'alteration. In *Proceedings of the 3rd International Conference on Unsaturated Soils, UNSAT 2002* (Vol. 1, pp. 289-294). Recife, Brazil. (in French).
- Camapum de Carvalho, J., Pereira, J.H.F., & Guimarães, R.C. (2002b). Effondrement de sols tropicaux. In *Proceedings of the 3rd International Conference on Unsaturated Soils, UNSAT 2002* (Vol. 2, pp. 851-856). Recife, Brazil (in French).
- Camapum de Carvalho, J., Guimarães, R.C., Siddiqua, S., Bigdeli, A., & Barreto, P.N.M. (2017). Relação entre a plasticidade do solo e o ponto de entrada de ar na curva característica de retenção de água. In *GEOCENTRO 2017* (pp. 734-739). São Paulo, Brasil: ABMS.
- Camapum de Carvalho, J., Marinho, F.A.M., Oliveira, O.M., & Gitirana Junior, G.F.N. (2012). Contribuição ao entendimento do comportamento dos solos não saturados. In *Anais do XVI Congresso Brasileiro de Mecânica dos Solos e Engenharia Geotécnica* (pp. 1-9). São Paulo, Brasil: ABMS.
- Camapum de Carvalho, J., Pastore, E.L., Pereira, J.H.F., Franco, H.A., & Brostel, R.C. (1999). Estudo e solução para os problemas de erosão interna nas lagoas de estabilização de Recanto da Emas - DF. In *Anais do 4º Congresso Brasileiro de Geotecnica Ambiental* (pp. 1-9). São Paulo, Brasil: ABMS.
- Camapum de Carvalho, J., Rezende, L.R., Cardoso, F.B.F., Lucena, L.C.F.L., Guimarães, R.C., & Valencia, Y.G. (2015a). Tropical Soils for Highway Construction: peculiarities and Considerations. *Transportation Geotechnics*, 5, 3-19. <http://dx.doi.org/10.1016/j.trgeo.2015.10.004>.
- Camapum de Carvalho, J., Barbosa, M.C., Mendonça, R.M.G., Farias, W.M., & Cardoso, F.B.F. (2015b). Propriedades químicas, mineralógicas e estruturais de solos naturais e compactados. In J. Camapum de Carvalho, G.F.N. Gitirana Junior, S.L. Machado, M.M.A. Mascarenha, & F.C. Silva Filho (Orgs.), *Solos não saturados no contexto geotécnico* (pp. 39-78). ABMS. Retrieved in July 18, 2021, from <https://www.abms.com.br/biblioteca/>
- Camapum de Carvalho, J., Silva, F.C., Barreto, P.N.M., Pérez, A.C., Guimarães, R.C., & Oliveira, R.B. (2019). Aspectos químico-mineralógicos e as propriedades e comportamento dos solos expansivos. In *Anais do II GeoBASE - II Seminário Geotécnico Bahia/Sergipe* (pp. 277-286). São Paulo, Brasil: ABMS.
- Camapum de Carvalho, J., Valencia, Y.G., Santos, M.A.A., & Gitirana Junior, G.F.N. (2007). Estabilidad de un talud cóncavo considerando condiciones en 3D. In *XIII Conferencia Panamericana de Mecánica de Suelos e Ingeniería Geotécnica* (pp. 988-993). SVDG e ISSMGE (in Spanish).
- Campos, I.C.O., Guimarães, E.M., & Camapum de Carvalho, J. (2008). Busca de entendimento da curva característica de materiais expansivos. In *Anais do XIV COBRAMSEG* (pp. 1535-1542). São Paulo, Brasil: ABMS.
- Cardoso, F.B.F. (1995). *Análise química e mineralógica e micromorfológica de solos tropicais colapsíveis e o estudo da dinâmica do colapso* [Master's dissertation, University of Brasília]. University of Brasília's repository. <https://www.geotecnia.unb.br/index.php/pt/producao-academica/teses-e-dissertacoes>
- Cardoso, F.B.F. (2002). *Caracterização físico-química e estrutural de solos tropicais do Distrito Federal* [Doctoral thesis, University of Brasília]. University of Brasília's repository. <https://www.geotecnia.unb.br/index.php/pt/producao-academica/teses-e-dissertacoes>
- Carvajal, H.E.M., Camapum de Carvalho, J., & Fernandes, G. (2005). Influência da desagregação nos limites de Atterberg. In *Anais do II Simpósio Sobre Solos Tropicais e Processos Erosivos no Centro-Oeste, Goiânia, Brazil* (pp. 217-225). Goiânia: UFG. Retrieved in July 18, 2021, from <https://gecon.eec.ufg.br/p/18785-publicacoes>
- Chen, T., Sedighi, M., Jivkov, A., Suresh, C., & Seetharam, S.C. (2019). Unsaturated hydraulic conductivity of compacted bentonite: revisit of microstructure effects. In L. Zhan, Y. Chen & A. Bouazza (Eds.), *Proceedings of the 8th International Congress on Environmental Geotechnics* (pp. 544-550). [https://doi.org/10.1007/978-981-13-2224-2\\_67](https://doi.org/10.1007/978-981-13-2224-2_67).
- Coelho, J. A., Aquino, S. C. N., & Camapum de Carvalho, J. (2016). Análise da influência da qualidade da água na compactação de solos tropicais. In *Anais do 45ª RAPV, 19º ENACOR* (pp. 1-13). Brasília.
- Conciani, R., Matos, T.H.C., & Camapum de Carvalho, J. (2009). O cupim como modificador das propriedades e comportamento de um solo tropical. In *Anais do IV Simpósio Sobre Solos Tropicais e Processos Erosivos no Centro-Oeste e de Minas Gerais* (pp. 1-12). Uberlândia, MG.

- Consoli, N.C., Araújo, M.T., Ferrazzo, S.T., Rodrigues, V.L., & Rocha, C.G. (2020). Increasing density and cement content in expansive soils stabilization: conflicting or complementary procedures for reducing swelling? *Canadian Geotechnical Journal*, 58, 866-878. <http://dx.doi.org/10.1139/cgj-2019-0855>.
- Décourt, L. (1996). Análise e projetos d fundações profundas – Estacas. In F. Falconi, C.N. Corrêa, C. Orlando, C. Schimdt, W.R. Antunes, P.J. Albuquerque, W. Hachich & S. Niyama (Orgs.), *Fundações teoria e prática* (pp. 263-297). ABMS/ABEF.
- Décourt, L., & Quaresma Filho, A.R. (1978). Capacidade de carga de estacas a partir de valores de SPT. In *Anais do VI Congresso Brasileiro de Mecânica dos Solos e Engenharia de Fundações* (pp. 45-53). São Paulo, Brasil: ABMS.
- Delgado, A.K.C. (2002). *Influência da sucção no comportamento de um perfil de solo tropical compactado* [Master's dissertation, University of Brasília]. University of Brasília's repository. <https://www.geotecnia.unb.br/index.php/pt/producao-academica/teses-e-dissertacoes>
- Delgado, A.K.C. (2007). *Estudo do comportamento mecânico de solos tropicais característicos do Distrito Federal para uso na pavimentação rodoviária* [Doctoral thesis, University of Brasília]. University of Brasília's repository. <https://www.geotecnia.unb.br/index.php/pt/producao-academica/teses-e-dissertacoes>
- Diniz, N.C., Romão, P.A., & Carvajal, H.E.M. (2012). Aspectos geológicos e infiltração. In J.C. Carvalho, G.F.N. Gitirana Junior, E.T.L. Carvalho (Eds.), *Tópicos sobre infiltração: teoria e prática aplicadas a solos tropicais* (pp. 89-99). Faculdade de Tecnologia, Universidade de Brasília. Retrieved in July 18, 2021, from <https://www.geotecnia.unb.br/index.php/pt/producao-academica/livros>
- EMBRAPA. (2006). *Sistema brasileiro de classificação de solos*. Brasília, DF: EMBRAPA – Empresa Brasileira de Pesquisa Agropecuária. Retrieved in July 18, 2021, from <https://ainfo.cnptia.embrapa.br/digital/bitstream/item/93143/1/sistema-brasileiro-de-classificacao-dos-solos2006.pdf>
- Farias, W.M., Cardoso, F.B.F., Martins, E.S., & Camapum de Carvalho, J. (2002). A Influência do oxi-hidróxido de Fe matricial no comportamento mecânico de solos tropicais. In *Anais do XII COBRAMSEG* (Vol. 1, pp. 547-554). São Paulo, Brasil.
- Fleureau, J.M., Kheirbek-Saoud, S., Soemitro, R., & Taibi, S. (1993). Behaviour of clayey soils on drying-wetting paths. *Canadian Geotechnical Journal*, 30, 287-296. <http://dx.doi.org/10.1139/t93-024>.
- Fookes, P.G. (1997). *Tropical residual soils*. Geological Society Pub House.
- Freitas, J.E. (2018). *Uso de cinza da casca de arroz na estabilização de solos para uso em pavimento rodoviário* [Master's dissertation, University of Brasília]. University of Brasília's repository. <https://www.geotecnia.unb.br/index.php/pt/producao-academica/teses-e-dissertacoes>
- Gidigas, M.D. (2012). *Laterite soil engineering: pedogenesis and engineering principles*. Elsevier Scientific Publishing Company.
- Gitirana Junior, G.F.N., & Fredlund, D.G. (2004). Soil-water characteristic curve equation with independent parameters. *Journal of Geotechnical and Geoenvironmental Engineering*, 130(2), 209-212. [http://dx.doi.org/10.1061/\(ASCE\)1090-0241\(2004\)130:2\(209\)](http://dx.doi.org/10.1061/(ASCE)1090-0241(2004)130:2(209)).
- Gómez Muñetón, C.M. (2013). *Avaliação geotécnica de um perfil de solo tratado biotecnologicamente para fins de pavimentação* [Doctoral thesis, University of Brasília]. University of Brasília's repository. <https://www.geotecnia.unb.br/index.php/pt/producao-academica/teses-e-dissertacoes>
- Grim, R.E. (1962). *Applied clay mineralogy*. McGraw-Hill.
- Guimarães, R.C. (2002). *Propriedades, comportamento e desempenho de estacas escavadas em um perfil de intemperismo* [Master's dissertation, University of Brasília]. University of Brasília's repository. <https://www.geotecnia.unb.br/index.php/pt/producao-academica/teses-e-dissertacoes>
- Guimarães, R.C., Camapum de Carvalho, J., & Farias, M.M. (1997). Contribuição ao estudo da utilização de solos finos em pavimentação. In *Anais do I Simpósio Internacional de Pavimentação de Rodovias de Baixo Volume de Tráfego - I SIMBRATA* (Vol. 1, pp. 469-478). Rio de Janeiro, Brasil.
- Guimarães, R.C., Silva, H.H.A.B., Oliveira, R.B., Valencia, Y.G., Farias, W.M., & Camapum de Carvalho, J. (2017). A micromorfologia no contexto das erosões de borda de reservatório. In M.M. Sales, J. Camapum de Carvalho, M.M.A. Mascarenha, M.P. da Luz, N.M. de Souza, & R.R. Angelim (Orgs.), *Erosão em borda de reservatório* (pp. 209-227). Universidade Federal de Goiás. Retrieved in July 18, 2021, from <https://gecon.ecc.ufg.br/p/18785-publicacoes>
- Gusmão Filho, J.A. (2002). *Solos: da formação geológica ao uso na engenharia*. EDUFPE.
- Jesus, A.S. (2013). *Investigação multidisciplinar de processos erosivos lineares: estudo de caso da cidade de Anápolis - GO* [Doctoral thesis, University of Brasília]. University of Brasília's repository. <https://www.geotecnia.unb.br/index.php/pt/producao-academica/teses-e-dissertacoes>
- Jesus, A.S., Lima, C.V., & Camapum de Carvalho, J. (2012). A interação entre a geomorfologia e os processos de infiltração. In J.C. Carvalho, G.F.N. Gitirana Junior, E.T.L. Carvalho (Eds.), *Tópicos sobre infiltração: teoria e prática aplicadas a solos tropicais* (pp. 75-88). Faculdade de Tecnologia, Universidade de Brasília. Retrieved in July 18, 2021, from <https://www.geotecnia.unb.br/index.php/pt/producao-academica/livros>
- Jesus, A.S., Sousa, M.S., Nascimento, D.T.F., Romão, P.A., & Camapum de Carvalho, J. (2017). A influência de aspectos geomorfológicos, de cobertura do solo e climáticos no surgimento e evolução de processos erosivos

- no entorno de reservatório. In M.M. Sales, J. Camapum de Carvalho, M.M.A. Mascarenha, M.P. da Luz, N.M. de Souza, & R.R. Angelim (Orgs.), *Erosão em borda de reservatório* (pp. 171-194). Universidade Federal de Goiás. Retrieved in July 18, 2021, from <https://gecon.eec.ufg.br/p/18785-publicacoes>
- Khalili, N., Geiser, F., & Blight, G. (2004). Effective stress in unsaturated soils: review with new evidence. *International Journal of Geomechanics*, 4(2), 115-126. [http://dx.doi.org/10.1061/\(ASCE\)1532-3641\(2004\)4:2\(115\)](http://dx.doi.org/10.1061/(ASCE)1532-3641(2004)4:2(115)).
- Lima, M.C. (1999). *Contribuição ao estudo do processo evolutivo de boçorocas da área urbana de Manaus* [Master's dissertation, University of Brasília]. University of Brasília's repository. <https://www.geotecnia.unb.br/index.php/pt/producao-academica/teses-e-dissertacoes>
- Lima, M.C. (2003). *Degradação físico-química e mineralógica de maciços junto às voçorocas* [Doctoral thesis, University of Brasília]. University of Brasília's repository. <https://www.geotecnia.unb.br/index.php/pt/producao-academica/teses-e-dissertacoes>
- Lima, M.R.C. (2018). *Estudo de técnicas alternativas para monitoramento ótico de tensões, deformações e temperatura em obras de engenharia* [Doctoral thesis, University of Brasília]. University of Brasília's repository. <https://www.geotecnia.unb.br/index.php/pt/producao-academica/teses-e-dissertacoes>
- Machado, S.L., & Vilar, O.M. (1998). Estudo da compressibilidade e resistência de solos não saturados ao longo de um perfil típico da cidade de São Carlos-SP. In *Anais do XI COBRAMSEG* (Vol. 2, pp. 991-999). Brasília. (in Portuguese).
- Marcott, S.A., Shakun, J.D., Clark, P.U., & Mix, A.C. (2013). A reconstruction of regional and global temperature for the past 11,300 years. *Science*, 339, 1198-1201. <http://dx.doi.org/10.1126/science.1228026>.
- Mascarenha, M.M.A. (2003). *Influência do recarregamento e da sucção na capacidade de carga de estacas escavadas em solos porosos colapsíveis* [Master's dissertation, University of Brasília]. University of Brasília's repository. <https://www.geotecnia.unb.br/index.php/pt/producao-academica/teses-e-dissertacoes>
- Mielenz, R.C., & King, M.E. (1955). Physical-chemical properties and engineering performance of clays. In J.A. Pask, M.D. Turner (Eds.), *Proceedings of the First National Conference on Clays and Clay Technology: California Division of Mines Bulletin: 169* (pp. 196-254).
- Momoli, R.S., Camapum de Carvalho, J., & Cooper, M. (2017). Erosão hídrica em solos cultivados. In M.M. Sales, J. Camapum de Carvalho, M.M.A. Mascarenha, M.P. da Luz, N.M. de Souza, & R.R. Angelim (Orgs.), *Erosão em borda de reservatório* (pp. 369-397). Universidade Federal de Goiás. Retrieved in July 18, 2021, from <https://gecon.eec.ufg.br/p/18785-publicacoes>
- Mortari, D. (1994). *Caracterização geotécnica e análise do processo evolutivo das erosões no Distrito Federal* [Master's dissertation, University of Brasília]. University of Brasília's repository. <https://www.geotecnia.unb.br/index.php/pt/producao-academica/teses-e-dissertacoes>
- Navarro, V., Asensio, L., Morena, G., Pintado, X., & Yustres, Á. (2015). Differentiated intra- and inter-aggregate water content models of mx-80 bentonite. *Applied Clay Science*, 118, 325-336. <http://dx.doi.org/10.1016/j.clay.2015.10.015>.
- Nogami, J.S., & Villibor, D.F. (1995). *Pavimentação de baixo custo com solos lateríticos*. Villibor.
- Oliveira, M.C., & Ribeiro, J.F. (2017). Impactos na vegetação em área de implantação de reservatório no bioma cerrado. In M.M. Sales, J. Camapum de Carvalho, M.M.A. Mascarenha, M.P. da Luz, N.M. de Souza, & R.R. Angelim (Orgs.), *Erosão em borda de reservatório* (pp. 195-208). Universidade Federal de Goiás. Retrieved in July 18, 2021, from <https://gecon.eec.ufg.br/p/18785-publicacoes>
- Palocci, A., Camapum de Carvalho, J., Pereira, J.H.F., & Silva, P.R. (1998). Considerações sobre a granulometria de alguns solos do Centro-Oeste. In *Anais do XI COBRAMSEG* (Vol. 2, pp. 1001-1005). Brasília.
- Parreira, A.B., Takeda, M.C., & Luz, M.P. (2004). Avaliação da influência do período de imersão nos resultados do ensaio CBR de solos tropicais. In *Anais do 5º Simpósio Brasileiro de Solos Não Saturados* (Vol. 1, pp. 383-388). São Paulo, Brasil: ABMS/EESC-USP. Retrieved in July 18, 2021, from <https://www.abms.com.br/biblioteca/>
- Pérez, A.C. (2018). *Influência de insumos agrícolas em propriedades físicas de solos tropicais* [Master's dissertation, University of Brasília]. University of Brasília's repository. <https://www.geotecnia.unb.br/index.php/pt/producao-academica/teses-e-dissertacoes>
- Pessoa, F.H.C. (2004). *Análise dos solos de Urucu para fins de uso rodoviário* [Master's dissertation, University of Brasília]. University of Brasília's repository. <https://www.geotecnia.unb.br/index.php/pt/producao-academica/teses-e-dissertacoes>
- Ramírez, A.Q., Valencia, Y.G., & Valencia, L.A.L. (2017). Efecto de los lixiviados de residuos sólidos en un suelo tropical. *Revista DYNA*, 84(203), 283-290 (in Spanish). <http://dx.doi.org/10.15446/dyna.v84n203.63875>.
- Rezende, L.R. (2003). *Estudo do comportamento de materiais alternativos utilizados em estruturas de pavimentos flexíveis* [Doctoral thesis, University of Brasília]. University of Brasília's repository. <https://www.geotecnia.unb.br/index.php/pt/producao-academica/teses-e-dissertacoes>
- Rodrigues, A.A., Camapum de Carvalho, J., Cortopassi, R.S., & Silva, C.M. (1998). Avaliação da adaptabilidade de métodos de previsão de capacidade de carga a diferentes tipos de estacas. In *Anais do XI COBRAMSEG* (Vol. 3, pp. 1591-1598). Brasília.
- Rodrigues, S.M. (2017). *Caracterização mineralógica e microestrutural de um perfil intemperizado de Brasília*. [Unpublished research report]. Anápolis, GO: State University of Goiás. (in Portuguese).



- Romão, P.A., & Souza, N.M. (2017). Aspectos geológicos e hidrogeológicos na deflagração e evolução da erosão hídrica em margens de reservatórios. In M.M. Sales, J. Camapum de Carvalho, M.M.A. Mascarenha, M.P. da Luz, N.M. de Souza, & R.R. Angelim (Orgs.), *Erosão em borda de reservatório* (pp. 153-170). Universidade Federal de Goiás. Retrieved in July 18, 2021, from <https://gecon.eec.ufg.br/p/18785-publicacoes>
- Roseno, J.L., & Camapum de Carvalho, J. (2007). Avaliação granulométrica de um perfil de solo tropical usando o granulômetro a laser. In *Anais do III Simpósio sobre Solos Tropicais e Processos Erosivos no Centro-Oeste* (pp. 136-147). Cuiabá, MT.
- Santos, R.M.M. (1997). *Caracterização geotécnica e análise do processo evolutivo das erosões no município de Goiânia* [Master's dissertation, University of Brasília]. University of Brasília's repository. <https://www.geotecnia.unb.br/index.php/pt/producao-academica/teses-e-dissertacoes>
- Sedighi, M., & Thomas, H.R. (2014). Micro porosity evolution in compacted swelling clays. *Applied Clay Science*, 101, 608-618. <http://dx.doi.org/10.1016/j.clay.2014.09.027>.
- Senaha, S.C.F. (2019). *A quartzilização em perfis de intemperismo tropical* [Master's dissertation, University of Brasília]. University of Brasília's repository. <https://www.geotecnia.unb.br/index.php/pt/producao-academica/teses-e-dissertacoes>
- Silva, C.M., Cordão Neto, M.P., Ribeiro, L.F.M., & Soares, E. (2008). Perda da capacidade de carga de tirantes executados na argila porosa de Brasília. In *Anais do XIV Congresso Brasileiro de Mecânica dos Solos e Engenharia Geotécnica* (pp. 367-372). São Paulo, Brasil: ABMS.
- Skempton, A.W. (1953). The colloidal "activity" of clay. In *Proceedings of the 3rd International Conference on Soil Mechanics* (Vol. 1, pp. 57-61). Zurich.
- Tripathy, S., Tadza, M.Y.M., & Thomas, H.R. (2014). Soil-water characteristic curves of clays. *Canadian Geotechnical Journal*, 51(8), 869-883. <http://dx.doi.org/10.1139/cgj-2013-0089>.
- Valencia, Y.G. (2009). *Influência da biomineralização nas propriedades físico - mecânicas de um perfil de solo tropical afetado por processos erosivos* [Doctoral thesis, University of Brasília]. University of Brasília's repository. <https://www.geotecnia.unb.br/index.php/pt/producao-academica/teses-e-dissertacoes>
- Valencia, Y.G., Camapum de Carvalho, J., & Gitirana, G. (2019). Metodologias simples para determinar em solos parcialmente saturados a envoltória de resistência ao cisalhamento. *Revista EIA*, 16(32), 43-53. <https://doi.org/10.24050/reia.v16i32.1218>.
- Valencia, Y.G., Santos, M.A.A., Camapum de Carvalho, J., Farias, M.M., & Gitirana Júnior, G.F.N. (2007). Una metodología simple para determinar la envoltente de resistencia al corte de suelos no saturados: resultados experimentales y validación. In *Conferencia Panamericana de Mecánica de Suelos e Ingeniería Geotécnica, Isla de Margarita* (pp. 710-715). Venezuela: SVDG & ISSMGE (in Spanish).
- Vargas, M. (1977). *Introdução à mecânica dos solos*. McGraw-Hill.
- Wanderley Neto, R.V. (2020). *Estudo experimental de interfaces solo-concreto no contexto de solos não saturados* [Master's dissertation, University of Brasília]. University of Brasília's repository. <https://www.geotecnia.unb.br/index.php/pt/producao-academica/teses-e-dissertacoes>



## ***CASE STUDY***

***Soils and Rocks***  
**v. 44, n. 3**





## Unsaturated mine tailings disposal

Luciano A. Oldecop<sup>1#</sup> , Germán J. Rodari<sup>1</sup> 

Case Study

### Keywords

Tailings dewatering  
Filtered tailings  
Flocculant  
Tailings air-drying  
Tailings compressibility  
Dry stacking

### Abstract

Filtered tailings is the disposal technology that is most likely to yield an unsaturated state of the tailings. Such state has important benefits. A dam to contain the mine wastes is no longer needed, the risk of polluting seepage is minimized, and liquefaction of tailings is prevented. Filtering also allows most of the water mixed with the tailings to be recovered and reused in the process. The resulting material can be handled with traditional soil moving equipment to form a stack, for instance. While the idea is simple, the multiple phenomena involved in the tailings unsaturated disposal make up a complex process. The present work is based on a case study, the Casposo Mine filtered tailings disposal facility, located in the central Andes of Argentina. Throughout ten years of operation, a series of field and laboratory studies have been carried out to characterize the phenomena that intervene in the disposal of filtered tailings. Two stages were studied in detail: air drying upon tailings discharge and tailings compression under the weight of the subsequent lifts of the stack. Flocculant agents were found to have an outstanding influence in the tailings behaviour. Because of the multiple influencing factors, the process outcome (namely, the tailings water content and their void ratio) is highly variable. To deal with such variability, projects must include enough redundancy. In this regard, the case study's incorporation of waste rock layers interspersed between tailings layers was a successful experience.

## 1. Introduction

Filtered tailings is a currently well-established technology for mine tailings disposal. Among the disposal methods, it is the one which allows achieving an unsaturated state of the disposed tailings in the most consistent manner. This is indeed a very desirable goal in a tailings deposit because of the multiple benefits of the unsaturated state. First and foremost, the need of a dam is eliminated. Moreover, a large fraction of the process water can be recovered, which otherwise is permanently trapped within the tailings voids, lost by evaporation or underground seepage. Recovered water can be reused in the extraction process allowing to save a high fraction of the process water. In the case of metal lixiviation, it also yields higher recovery ratios and spare of chemical additives. Moreover, unsaturated tailings are less prone to static or dynamic liquefaction failures. According to Franks et al. (2021), filtered tailings facilities show less than the half to one fifth the incidence of stability issues of the other tailings disposal methods (in % of the total number of facilities of each type). Contaminating leakages are also

less likely since there is no permanent hydraulic head acting over water-proof linings or barriers installed at the bottom of the disposal facility. Lastly, tailings dewatering reduces the volume and footprint of the disposal facility. The usual arrangement of a filtered tailings disposal facility is simply a stack (Figure 1a). Construction methods involve typical earthmoving equipment, front-loaders, trucks, dozers, graders and eventually compaction rollers. Conveyor belts are also used as an alternative means of placing the tailings in the stack (Lara et al., 2013).

In view of the above considerations, the use of filtered-tailings technology appears quite straightforward. However, the ultimate goal of storing the tailings in a permanent unsaturated condition has many implications, not only for the design of the facility but also for its operation, mainly due to the variable nature of the tailings water content. In the first place, the selection of the tailings water content at filter output is a trade-off between a desirable amount of dewatering and the technical constraints of the filtering method. Standard practice involves thickening of the slurry before filtration. Moreover, the filter output moisture of tailings is intrinsically variable,

#Corresponding author. E-mail address: oldecop@unsj.edu.ar

<sup>1</sup>Instituto de Investigaciones Antisísmicas "Ing. Aldo Bruschi", Facultad de Ingeniería, Universidad Nacional de San Juan, San Juan, Argentina.

Submitted on June 1, 2021; Final Acceptance on July 15, 2021; Discussion open until November 30, 2021.

<https://doi.org/10.28927/SR.2021.067421>



This is an Open Access article distributed under the terms of the Creative Commons Attribution License, which permits unrestricted use, distribution, and reproduction in any medium, provided the original work is properly cited.

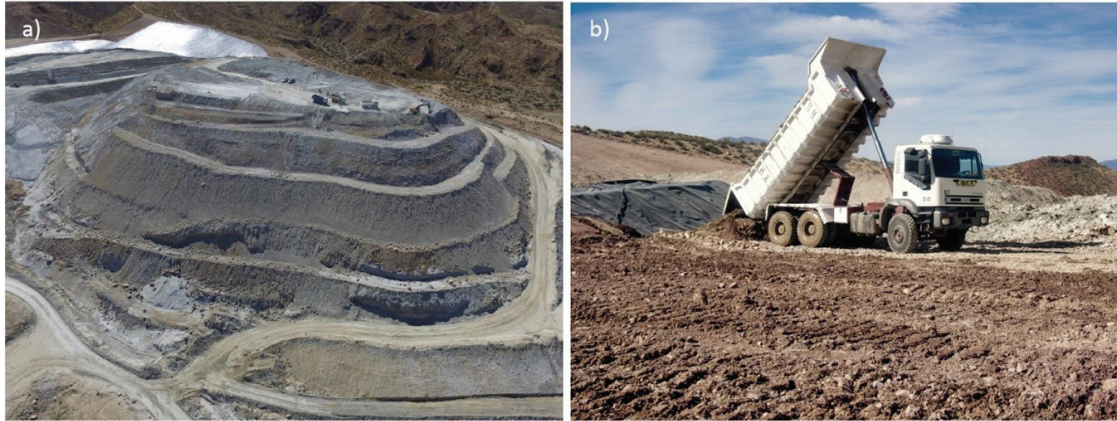


**Figure 1.** (a) Stack of filtered tailings under construction. Casposo Mine, San Juan, Argentina (Photo: courtesy of Casposo Argentina, published with permission); (b) Tailings transport and distribution with conventional earthmoving equipment requires achieving trafficability.

because of the variability of the ore grain size distribution and changes in its mineralogical composition affecting the filter performance (Crystal et al., 2018).

In any case, the achieved moistures are relatively high from a geotechnical standpoint. The commonly specified moistures of tailings at filter output (termed “filter cake”) typically range between 15 and 25% in weight (Wang et al., 2014; Hogg, 2010; Ulrich, 2019). Nonetheless, some mining operations specify higher moistures up to 30 or even 40% (Crystal et al., 2018, Copeland et al. 2006). It is worth noting that in the metallurgist usage water content is defined as water weight divided by the mixture weight (solids plus water), which differs from the geotechnical definition of the gravimetric water content (GWC), i.e., water weight divided by solids weight. Hence the above-referred moisture range translates into a GWC range of 18 to 67%. From a geotechnical perspective, it would be desirable for the moisture achieved by filtration to be close to the Proctor optimum. Nonetheless, such a condition is hardly achievable for many tailings (Ulrich, 2019). In fact, filtered tailings are delivered from the plant in a rather high saturation state.

Later, during the transport, discharge and spreading operations, water content can further change by segregation and water bleeding, drainage, evaporation, rainfall, or snowmelt. Additional factors affect the evolution of water content. For instance, the tailings production rates affect the timing of lifts placing and, hence, the period during which the recently discharged tailings remain exposed to atmosphere. Also, the placing procedure used, the spreading method, the lift height and the discharge area have influence on the evolution of water content. Finally, the site climate and meteorology factors are obviously relevant. Hence, the final water content of tailings in the deposit is far from being constant and rather difficult to control.

A key parameter in the disposal process is the moisture of tailings at the time of covering them with the following lift, also termed the target water content. In the first place,

moisture determines trafficability (Ulrich, 2019), which is vital when tailings transport and distribution rely on trucks and earthmoving machinery (Figure 1b). If compaction is specified in the standard placing procedure, a water content close to the Proctor optimum value should be approached. In any case, upon covering a tailings layer with the following lift of the stack, air-drying is mostly interrupted. In addition, from that moment on, overburden stresses will grow steadily due to the deposit rise. As a result, the saturation degree tends to increase due to volume reduction. Thus, if the intended goal is to keep tailings unsaturated, the target water content should be low enough to counteract the expected volume reduction during consolidation. So, it turns out that the whole disposal process is not as simple as it appears at first sight since the result depends on many mechanisms and factors.

Several surveys have been carried out at Casposo Mine (Argentina) filtered tailings deposits along the decade elapsed since the mining operations started. The facility was specifically designed based on unsaturated soils mechanics concepts. The overall performance of the deposit was quite satisfactory, with no significant issues and having passed some moderate intensity earthquakes without visible effects. The goal of the survey program was to gather basic information for characterising the processes and factors previously mentioned. The present paper summarizes the lessons learned during this process as well as some general conclusions and recommendations.

## 2. Case description

Casposo is a moderate size gold and silver mine located in the east foothills of the Andes, in San Juan Province, Argentina. Metal extraction is done by milling followed by tank lixiviation with cyanide solution. To date, the exploitation has already been run for a decade, being the reserves close to exhaustion.

A distinct feature of this case is that filters are used for dewatering the mine tailings ahead of their disposition. It is

the first and, so far, the only experience in Argentina with filtered tailings. While processed, the ore pulp has a solids content of 53% in weight (computed as the weight of solids divided by the mixture weight). The whole dewatering process, involving the addition of a flocculating agent, thickening, and vacuum belt filters (Figure 2) allows recovering about 60% of the process water. Fresh water is sprinkled over the tailings travelling on the belt filter to rinse the pregnant solution. All the recovered water is reused in the process after going through a treatment for the separation of the dissolved metals. The tailings delivered by the filter have a mean solids content of 70% in weight. The plant was projected for an ore processing rate of 1000 tons/day.

The host rock of the mineral deposit includes rhyolite and andesite, while the mineralized veins are composed mostly by quartz. The solids specific gravity of tailings particles is 2.72 (ASTM, 2014). Grain size distribution of tailings is shown in Figure 3.  $D_{50}$  is 0.05 mm and  $C_u = 6$ . The content of

clay-sized particles is about 1% in weight and, consistently, Atterberg limits are  $LL = 20.2$ ,  $PL = 17.6$ ,  $PI = 2.6$ . Hence, the material would be considered a non-plastic silt in the Unified Soil Classification System. Two additional grain size distributions are displayed in Figure 3. One corresponds to mine ore milled in the lab to nearly the same grain size distribution as tailings and no further treatment. This was used as reference material for studying the influence of the metallurgical process on tailings properties. The third curve corresponds to waste rock which is also a component of the tailings disposal facility, as later explained.

Retention curve data were obtained with filter paper method (ASTM, 2016a; Kim et al., 2017), vapour equilibrium with saline solutions (Delage et al., 1998), and chilled mirror device (ASTM, 2016b). Figure 4a depicts the results of the two series of tests conducted on specimens of milled ore and actual tailings, respectively. All specimens were prepared from a known weight of oven-dried tailings, adding



**Figure 2.** Vacuum belt filter at Casposo Mine. (a) Tailings being fed to the filter band; (b) Tailings at filter output.

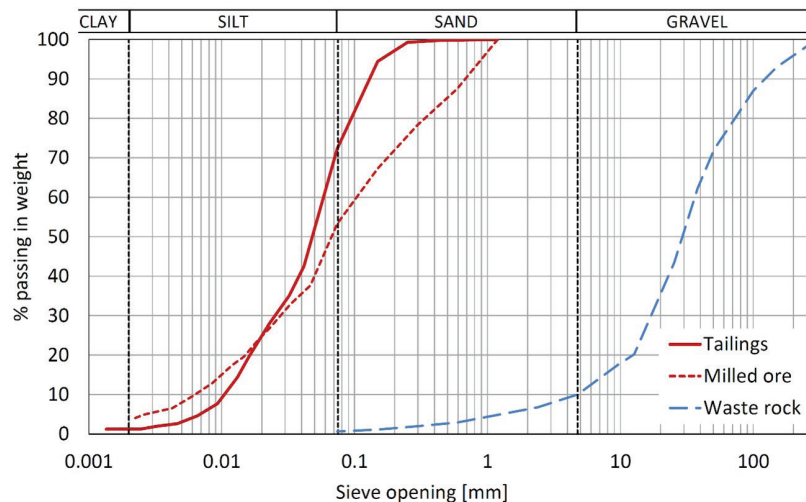


**Figure 3.** Grain size distribution of tailings milled ore and waste rock.



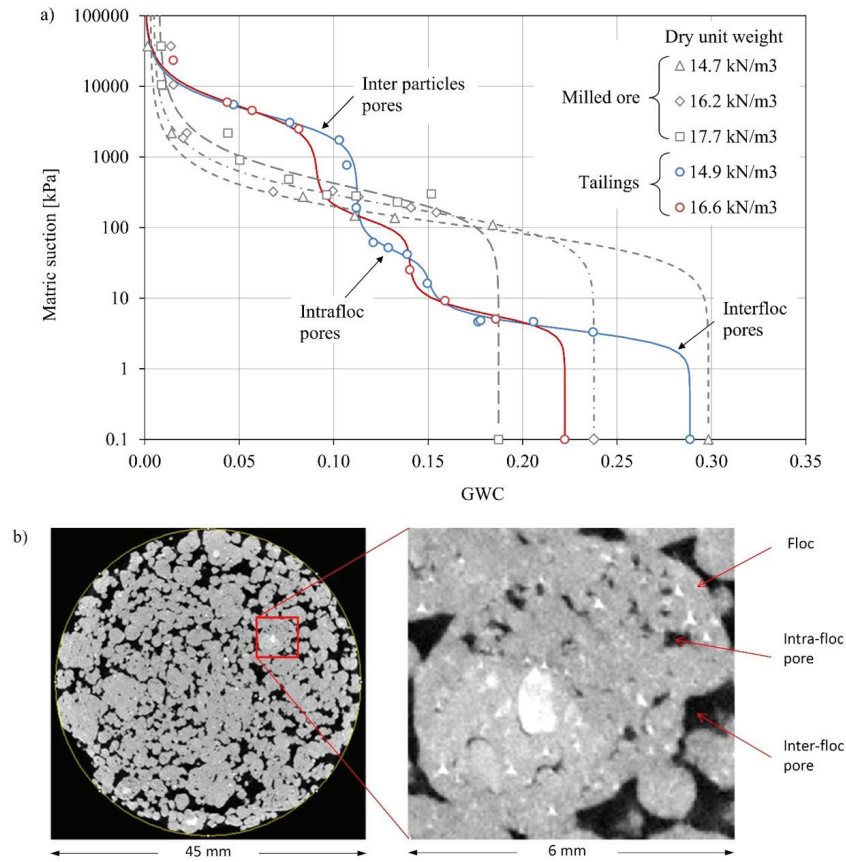


**Figure 4.** (a) Retention curves of Casposo Mine milled ore and tailings at different unit weights; (b) X-ray Tomography results on Casposo Mine tailings sample prepared at 10.5 kN/m<sup>3</sup> dry unit weight.

the amount of distilled water needed to achieve the desired water content, and measuring the suction with the appropriate method. The points obtained with the latter methods are those with suctions above 1000 kPa. Strictly speaking, they are total suction values. However, measurements made with the chilled mirror device on samples of tailings leachate yielded zero reading for the osmotic suction component. Hence, total suction measurements can be considered equivalent to matric suction with reasonable approximation. In the filter paper technique, the paper was put in contact with the specimen and, therefore, measurements correspond to matric suctions.

From the beginning of mine operation, chemical additives incorporated while in the metallurgical process were suspected of having strong effects on the tailings behaviour. Certainly, some striking differences can be observed in the two sets of data displayed in Figure 4a. Milled ore retention curves have the shape of a typical silty soil. These data were fitted with a van Genuchten (1980) (VG) expression.

On the other hand, the retention curve points obtained for the tailings suggest, at least, bimodal or even trimodal distribution of pore sizes. An example of natural soil showing similar features is peat (Rezanezhad et al., 2012). Such drastic difference between milled ore and tailings is attributable to the effects of the flocculant agent (a long-chain polymer)

added in the extraction process. Figure 4b shows the result of an x-ray tomography performed on a tailings sample, where flocs, inter-floc and intra-floc pores are clearly visible. A third inter-particle pore system can be inferred, though not visible in the tomography due to image resolution limitations. Tailings retention curve data points were fitted with a weighted sum of three VG expressions as proposed by Ross & Smettem (1993):

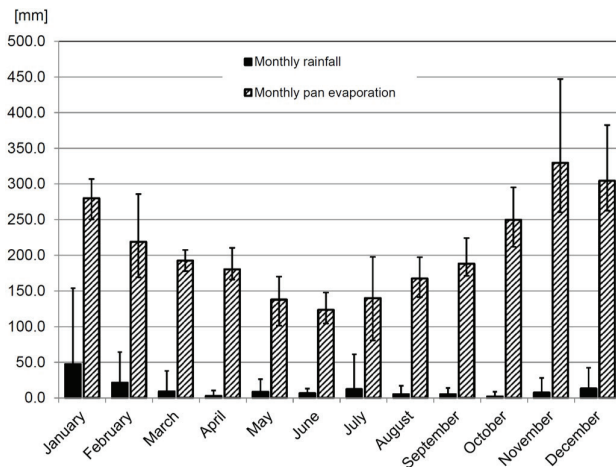
$$S(\psi) = S_r + (1 - S_r) \sum_{i=1}^3 \frac{e_i}{e} \left[ 1 + (\psi / P_{0i})^{1/(1-\lambda_i)} \right]^{-\lambda_i}, \text{ with } \sum_{i=1}^3 e_i = e \quad (1)$$

where  $S$  is the degree of saturation,  $\psi$  is suction,  $S_r$  is the residual degree of saturation,  $e_i$  are the partial void ratios of each pore system,  $e$  is the material void ratio,  $P_{0i}$  and  $\lambda_i$  the VG expression parameters. Curve fitting parameters are indicated in Table 1.  $S$ -values were then converted to GWC according to the specimen's dry unit weight.

While preparing the retention curve specimens, it also became evident that the unit weight range achievable with each material was quite different. For tailings, dry unit weights higher than 17 kN/m<sup>3</sup> are only achievable with heavy compaction or confining stress levels beyond the range of interest for this work. Moreover, tailings can attain very loose states, with unit weights as low as 11 kN/m<sup>3</sup>.

**Table 1.** Retention curve parameters.

Material	Dry unit w. [kN/m <sup>3</sup> ]	$S_r$	Inter-particle pores			Intra-floc pores			Inter-floc pores		
			$e_1/e$	$P_{01}$ [kPa]	$\lambda_1$	$e_2/e$	$P_{02}$ [kPa]	$\lambda_2$	$e_3/e$	$P_{03}$ [kPa]	$\lambda_3$
Milled ore	14.7	0.01	1.00	75.8	0.52	---	---	---	---	---	---
	16.2	0.02	1.00	139.5	0.51	---	---	---	---	---	---
	17.7	0.05	1.00	259.5	0.50	---	---	---	---	---	---
Tailings	14.9	0.00	0.39	3300.0	0.60	0.13	43.3	0.75	0.48	3.4	0.75
	16.6	0.00	0.41	4200.5	0.60	0.22	123.7	0.75	0.37	5.4	0.75


**Figure 5.** Casposo site precipitation and evaporation. (reprinted from Oldecop et al. (2017) by permission from Springer Nature ©2017).

However, lab specimens with such low unit weights are impossible to handle for performing measurements with the filter paper method. This aspect is addressed again in the paper when analysing the oedometer tests. Otherwise, specimens of milled ore for filter paper method hold only for relatively low moisture states (for instance, under 18% for the 14.7 kN/m<sup>3</sup> specimen as it follows from the lack of higher GWC points in Figure 4a). Datasets with zones of lacking points were fitted with curves that follow a similar pattern as the complete series.

Finally, it is worth mentioning that the site climate is arid, with a year-round water deficit (Figure 5). Mean annual precipitation is 150 mm and mean annual evapotranspiration is 1250 mm. Most rainfall occurs in summer when evaporation is higher, causing their effects to cancel out to some extent.

### 3. The tailings disposal process

At the filter outlet, tailings were loaded in trucks, transported to the disposal facility, dumped, and spread with a bulldozer, forming layers roughly 1 m in thickness. The stack is placed over a water-proof barrier covering all the valley floor. Such a barrier is underlain by a subdrain layer which allows bypassing uncontacted surface and subsurface waters (very scarce at the site) and covered by a

top drainage layer for collecting contacted waters eventually draining from tailings.

Newly deposited tailings need to undergo some air-drying to become trafficable. The arid site climate grants significant drying in a relatively short time. No compaction was applied. Instead, once drying has progressed far enough, a layer of waste rock (also roughly 1 m thick) was spread over the air-dried tailings to create a new work-platform, where trucks could travel and dump the following tailings layer. Besides the improved trafficability, the design alternating tailings and waste rock layers provides some additional strengths to the deposit:

- Free drainage of tailings with eventual excess water;
- Capillary barrier effect at the bottom of each tailings layer;
- Structural reinforcement.

Eventual excesses of water may occur for a variety of reasons: variability of filter performance, rainfall events, temporary rise of the ore processing rate or temporary shortage of the deposition area due to constructive issues, etc. In any event, the draining capability provided by the waste rock layers adds flexibility and redundancy to the operation, since eventual excess waters can drain with no harmful consequences. Some trench drains, also filled with waste rock, were built-in to collect the drained water, leading it to the bottom draining layer. Thereafter, water is collected in a reservoir at the downstream toe of the stack. All contacted waters are recycled in the mineral extraction process. Furthermore, the capillary barrier effect prevents deep percolation. Thereby, rainfall water is always kept in the topmost layer from where it is readily eliminated by capillary rise and evaporation. Finally, as for most fine-grained materials, the shear strength of tailings depends on the water content (or matric suction). Hence, introducing reinforcement layers of the coarse-grained waste rock adds redundancy to the stability of the deposit, reducing its sensibility to eventual water excess.

Figure 6 illustrates the stages of the tailings disposal process explained in the previous section, and the corresponding phase diagrams for each stage. Key parameters regarding water management are  $w_f$  = gravimetric water content at filter output;  $w_0$  = target gravimetric water content by the time of covering a layer with the following lift and  $w_c$  = final gravimetric water



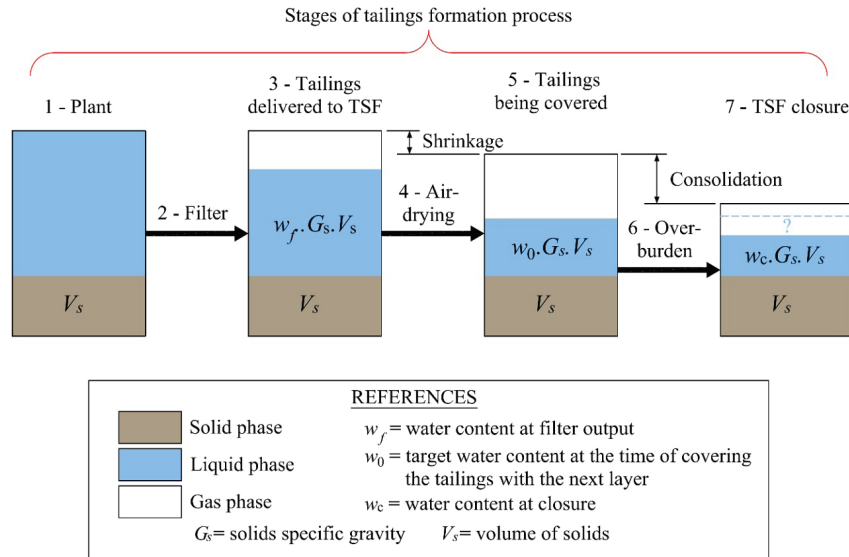


**Figure 6.** Phase diagrams of tailings along the stages of their disposal process.

content of tailings, i.e., by the closure of the facility. Moreover, the final void ratio  $e_c$  is also a relevant parameter since, together with  $w_c$ , determine the degree of saturation at closure.

A primary design hypothesis assumed in the design phase was that little to no moisture change would occur after tailings cover by the following layer. Hence,  $w_c$  should result nearly equal to  $w_0$ , allowing to estimate the final saturation water content by estimating the final void ratio  $e_c$ , assuming that the tailings compressibility properties are known. As shown in the following sections, tailings layers do not seem to behave that way, essentially, because drainage of tailings starts ahead of saturation. Otherwise, recharge could occur in already covered layers with waters draining from upper layers. So, in the end, the closure water content,  $w_c$ , could be lower or higher than  $w_0$ . In any case, volume reduction under the increasing overburden loads will increase the degree of saturation during Stage 6. Therefore, the final degree of saturation is certainly difficult to evaluate.

Regarding the conceptual model presented above (Figure 6) two basic phenomena are worth to study:

- Tailings air-drying which determines the required duration of the air-drying period (Stage 4) needed to achieve  $w_0$ .
- Tailings volume reduction due to consolidation (Stage 7) which shall determine the selection of the target water content,  $w_0$ .

Considerable effort was devoted to study these two aspects. The methods and results are described in the following sections.

#### 4. Tailings air-drying

Tailings air-drying is an essential component of the disposal scheme used in the case study. The process, namely the tailings-atmosphere interaction, was studied both ahead and

during the mine exploitation phases. The available timespan for air-drying (Stage 4) is controlled by the lift placing cycle, which, in turn, is determined by the available working area and the tailings production rate. Hence, for a given set of external constraints (climate, tailings properties, filter performance and production rate), an appropriate stack geometry is required to ensure that the length of the air-drying period always spans the time for achieving the target water content,  $w_0$ .

The evolution of the water content of tailings during the air-drying stage was monitored by means of random sampling of the tailings as layers were placed, simultaneously recording the time-since-placing at each sampling point. Samples were taken from the mid-height of the layers and GWC was determined by oven-drying (ASTM, 2019). The data set gathered along a four-year sampling period, is shown in Figure 7. A first attempt was made analysing the data grouped by season, in the supposition that meteorological factors would considerably differ from one season to another and this would influence the tailings desiccation rate. No definitive trends were observed and hence, it was decided to carry on with the analysis of the data set as a whole. The following expression was fitted by minimum squares (Rodari & Oldecop, 2021):

$$w_0 = (a - b)e^{-ct} + b + \epsilon_w(0, s) \quad (2)$$

where  $w_0$  is a random variable,  $t$  is air-drying time elapsed since placing of tailings,  $a$ ,  $b$ , and  $c$  are fitting parameters and  $\epsilon_w$  is the residue assumed as normally distributed with zero-mean and standard deviation  $s$ .

Some conclusions can be drawn from Figure 7:

- The water content from samples gathered in the deposit bears a significant variability, attributable not only to

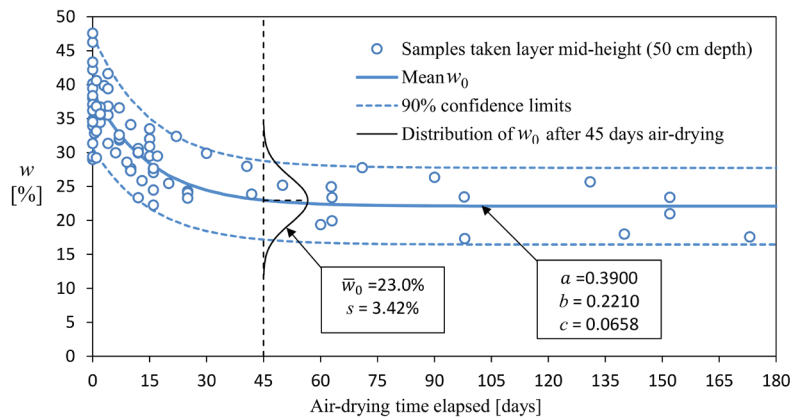


**Figure 7.** Evolution of GWC in the upper tailings layer while exposed to the atmosphere, determined by random sampling at the layer mid-height (modified from Rodari & Oldecop (2021) in print, reproduced with permission).



**Figure 8.** Exploration trenches dug in the upper tailings layer while exposed to the atmosphere.

the initial variability caused by filter performance, but also to the action of meteorological factors.

- The desiccation process gradually slows down during the initial period (lasting 45 to 60 days in the case studied) and becomes almost nil thereafter. This can be attributed to the formation of a very dry superficial zone in the tailings layer (see Figure 8), in which capillary rise is impeded by loss of liquid phase continuity.
- At the time of covering a certain tailings layer with the following waste lift, the water content,  $w_0$ , within the tailings being buried, can be described as a normally distributed random variable, with a mean value given by ec. (1) and a standard deviation obtained by variance analysis of the residuals. In Figure 7 such distribution is depicted for an air-drying period of 45 days, for instance.

A second method was used to study the tailings drying process. Water content profiles were obtained in trenches dug in the top layer during the air-drying stage (Figure 8), for various times elapsed since tailings placing. In-situ unit weight was also determined in the same sites at two or three different heights within the layer (ASTM, 2007). A summary of the results of those surveys is presented in Figure 9. Desiccation proceeds from an initial (estimated) uniform profile ( $w_f$  with a mean value of 41%). The profiles from days 7 and 10 suggest loss of water from both the layer top boundary (surface evaporation) and bottom boundary (drainage). In the following weeks, drying continues mainly by capillary rise and evaporation from the layer upper surface. Between days 45 and 50 the profile seems to approach a limit, suggesting that, beyond that period, drying reaches a standstill. The average GWC in the 50-days profile is 23.6% (indicated

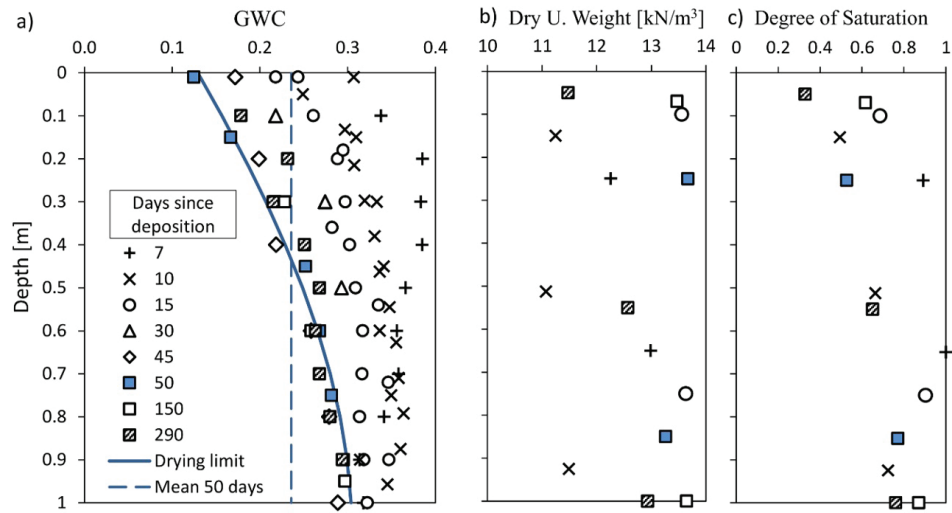


**Figure 9.** GWC and unit weight profiles surveyed in the upper tailings layer while exposed to the atmosphere (adapted from Rodari & Oldecop (2021) in print, reproduced with permission). (a) GWC profiles for different periods elapsed since deposition; (b) In-situ dry unit weight determinations; (c) Computed degree of saturation profiles.

**Table 2.** Testing conditions of tailings and milled ore specimens.

MATERIAL	ID	MOUNTING	TEST INITIATION		TEST END		
		GWC $w_f$	GWC $w_0$	Void ratio $e_0$	Max. applied stress [kPa]	GWC $w_c$	Void ratio $e_c$
Tailings	T1	0.409	0.409	1.497	1540	0.205	0.561
	T2	0.406	0.336	1.504	1582	0.201	0.554
	T3	0.394	0.206	1.400	1542	0.196	0.573
	T4	0.386	0.212	1.425	1582	0.200	0.569
Milled ore	O1	0.250	0.250	0.840	1570	0.148	0.402
	O2	0.150	0.150	0.901	1570	0.150	0.472
	O3	0.100	0.100	1.510	1570	0.100	0.618

ID: Specimen identification, GWC: gravimetric water content.

with dash line in Figure 9). This is roughly consistent with the GWC data gathered with random sampling (Figure 7).

The dry unit weight data (Figure 9b) do not reveal a clear relationship with the time elapsed since placing of the tailings layer nor with the depth. The measured values are noticeably low. Simultaneous determinations of dry unit weight and GWC allowed to compute the in-situ degree of saturation which is depicted in Figure 9c. These values are consistent with the interpretation made in the previous paragraph.

## 5. Tailings compressibility

Compressibility of tailings was primarily studied by means of oedometer tests. Specimens were prepared and tested attempting to mimic the tailings disposal process depicted in Figure 6 (for a more straightforward interpretation, moisture and void ratios characterising the test specimens were named with the same notation defined in Figure 6). The testing procedure comprised the following stages: 1) Oven-dry

tailings were mixed with water to reach the mounting water content  $w_f$ ; 2) Tailings were poured in the oedometer ring with no compaction. The resulting void ratio was computed from the poured tailings mass and the ring volume 3) The specimen was allowed to air-dry until reaching a specific target water content  $w_0$ ; 3) During a 24hs-period the specimen was kept isolated from the environment, to allow moisture uniformization within the specimen.; 4) Load was applied in steps, recording the vertical strain and mass of water expelled by the specimen. In some specimens the air-drying stage was omitted and, hence,  $w_0$  is equal to  $w_f$  in those tests. The testing device is a piston-cylinder assembly, allowing drainage from both upper and lower specimen ends. The water expelled was measured at each stage of the test by collecting and weighting the drained water. Table 2 summarizes the conditions of all specimens tested. Figure 10 displays the oedometer results in the compression plane (void ratio vs. vertical stress).

Some interesting observations can be made regarding the results depicted in Figure 10. The first feature that

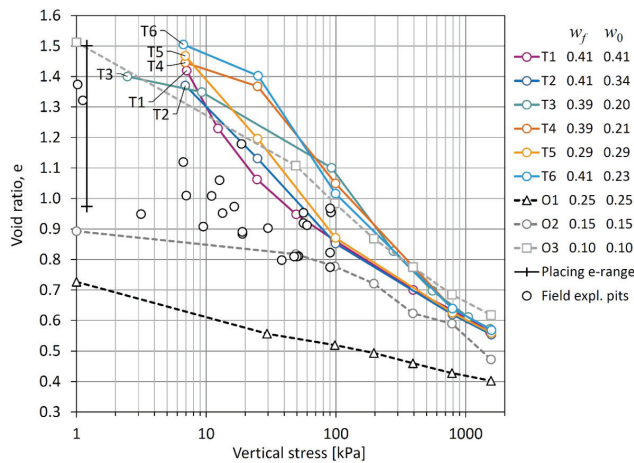


**Figure 10.** Oedometer tests performed on specimens of tailings and milled ore specimens, prepared at different initial water contents. Results shown in the compression plane. Additionally, points of void ratio vs. vertical stress obtained from in situ measurements in field exploration pits are included.

stands out is the relationship between the void ratios and the mounting water content of each specimen. In the milled ore, higher pore indexes are attained for lower preparation water contents. The loosest state is achieved with  $w_f = 10\%$ , while the densest state corresponds to  $w_f = 25\%$ , for which the material is almost saturated. This appears to be attributable to the bulking effect caused by the action of the capillary water menisci. The effect diminishes for higher water contents and completely vanishes at saturation. In contrast, tailings attain void ratios similar to the loosest state of the milled ore, but for much higher water contents (30-40%). The difference could be ascribed to the action of the flocculant agent.

To get a field reference to check how representative are the laboratory compressibility data of the real behaviour of tailings, information gathered in exploration pits dug at different stages of the deposit construction are used, i.e., in-situ dry unit weight (ASTM, 2007) and water content of tailings (ASTM, 2019). The vertical stress at each measurement point was calculated from the known depth and the estimated unit weight of the overburden layers. The in-situ void ratios were calculated from the unit weight determinations. Thereby, void ratio vs. stress points representing the encountered field states were included in Figure 10. Although the field datapoints cover only a limited range of stresses (since the limited depth of the exploration pits), the data cloud is fairly consistent with the compression lines obtained from oedometer tests. A second notable feature of this field dataset is the notably wide variability range of void ratios, though with a trend to narrow as the vertical stress increases.

The compression lines obtained for the tailings show a dependence on the testing water content,  $w_0$ . The specimens with lower  $w_0$  (near 20%) are initially less deformable than the specimens with higher  $w_0$  (30-40%). In fact, a similar trend is observed to a lesser extent also between the

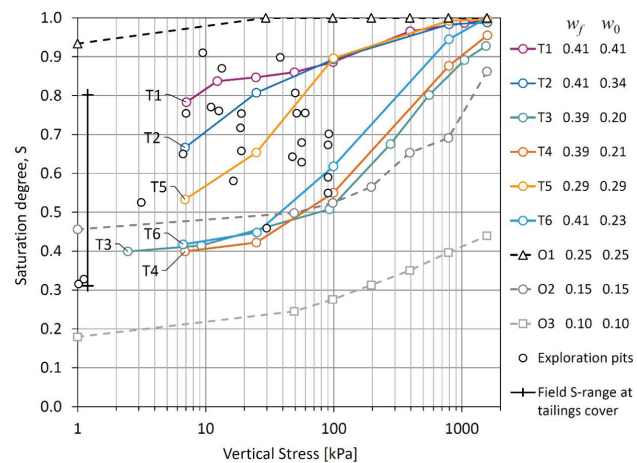


**Figure 11.** Oedometer tests performed on specimens of tailings and milled ore specimens, prepared at different initial water contents. Results shown in saturation vs. vertical stress plot. Additionally, points of degree of saturation vs. vertical stress obtained from in situ measurements in field exploration pits are included.

specimens with  $w_0$  of 30 and 40%. This can be explained by the effect of suction on increasing the material stiffness. However, compression lines tend to converge into one for high stresses (above 1000 kPa). This is a second difference in the behaviour with the milled ore specimens, which compression lines do not merge in the range of stresses of interest for this study.

Since the expelled water was measured for each loading step, the evolution of the degree of saturation could also be computed. It is interesting to note that no tested specimen was observed to drain by its upper end, suggesting that drainage mostly occurs by gravity-driven water flow and, likely, with no pore pressure build-up. Figure 11 shows the plot of degree of saturation vs. vertical stress. Milled ore specimens show a typical behaviour for a non-plastic silt. The specimen with 25% GWC, being close to saturation at the beginning of the test, reaches saturation in the first load step. The other two milled ore specimens, prepared and tested at 15% and 10% GWC, did not expel any water during the test and did not reach saturation under the applied stresses.

By contrast, the behaviour of the tailings is notably different. All the tailings specimens expelled water at some loading step. The degree of saturation increased gradually but the 100% saturation condition is approached at considerably high-stress levels. A striking contrast is given by the milled ore specimen with  $w_0 = 25\%$  which reaches saturation under 30 kPa vertical stress while all tailings specimens reach saturation above 900 kPa, even with extreme values of  $w_0 = 40\%$ . Figure 11 also includes field data points computed from in situ dry unit weight and water content measurements and the vertical stress estimated as explained before for Figure 10. Field data are fairly consistent with the experiments and, again, display a notable variability.



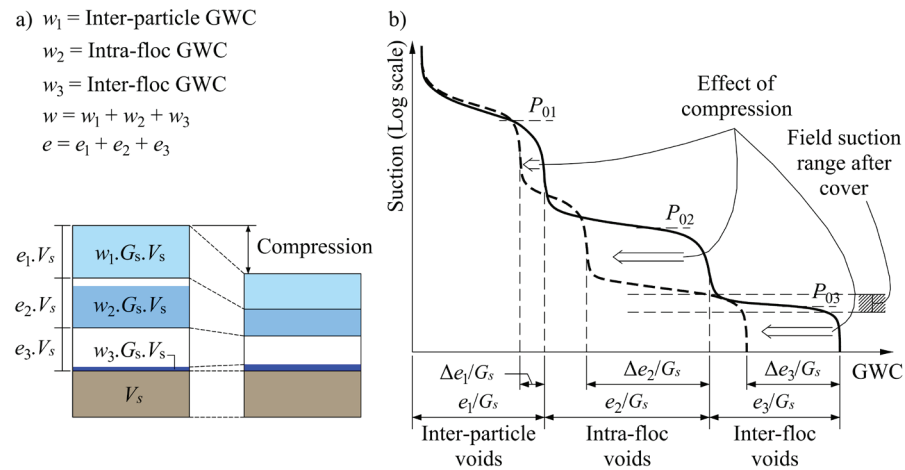


**Figure 12.** Conceptual model proposed for explaining the tailings behaviour observed in the field and in laboratory tests during the compression stage (referred as stage 6 in Figure 6). (a) Phase diagrams; (b) Retention curves.

## 6. Discussion

The observed behaviour of the tailings evidently departs from that of a typical silty soil. A possible explanation is proposed based on the observed multimodal pore structure, by means of the conceptual model depicted in Figure 12. According to such model, the inter-floc pore system is large enough to form a free-draining network. This is supported by the pore size that can be observed in the X-ray tomography (Figure 4b) and the notably low air entry value that results from the fitting of the retention curve for that pore system ( $P_{03} = 3.4 - 5.4$  kPa). Under increasing confining stresses, it can be assumed that flocs are squeezed, causing the intra-floc pores to collapse. The water expelled from the flocs drains through the inter-floc pore system. Hence, the intra-floc pores are the ones that act as the main capillary water storage. The air entry value of the intra-floc pores is  $P_{02} = 43 - 124$  kPa, which means that this pore system can support without desaturating the capillary height equivalent to the thickness of a 1-meter-thick layer of tailings. Finally, the high air entry value of the inter-particle pore system leads to think that the water stored there would drain neither by gravity nor by squeezing. The only way to extract this water would be evaporation.

The proposed model explains the mechanism by which the tailings can drain water well before reaching saturation. It also explains why saturation is only reached under unexpectedly high stress levels for relatively elevated water contents, when compared to the milled ore tests.

The behaviour of tailings described here means an obstacle to the estimation of the final state of tailings by the time of deposit closure. As referred in section 3, the hypothesis of constant GWC during the compression stage does not hold, at least for the tailings studied here. More laboratory research is needed to formulate a constitutive model enabling to make a precise estimation of the final

degree of saturation. In any case, given the behaviour depicted in Figure 12 and considering the variability of  $w_0$ , it can be concluded that the saturation condition would have been reached only marginally in the deepest layer, at the point of greatest height in the central zone of the Casposo deposit (the worst-case location within the deposit).

## 7. Conclusions

The basic phenomena involved in filtered tailings disposal were studied for a particular study case, during follow-up surveys carried out throughout almost a decade of operation of Casposo Mine tailings disposal facility. The facility performed notably well, under the normal operation actions, meteorological events, and moderate seismic shaking.

Although metallurgical tailings can be assimilated to some types of soil, such as silt, based on similarities in grain size distribution and plasticity properties, the case study suggests that their hydromechanical behavior can differ dramatically from soils due to the treatment applied during the metal extraction process.

Disposal of filtered tailings turn out to be a complex process mainly because of the large number of factors determining the outcome of the process, namely the final water content of tailings and their void ratio. The interactions between the mine, the processing plant and the tailings disposal facility must be carefully considered during the design stage since many design constraints arise from those interactions. For example, the area of deposition platforms at different building heights, the cadence of lifts, the need for contingency areas for placing tailings with excess water, the need for rainfall water management, etc.

A conceptual model for the whole tailings disposal process was proposed. Then, this work focused on two particular stages of the process: 1) tailings air-drying after discharge into the deposit and before covering with the following lift

of the stack; and 2) tailings compression under the increasing overburden due to the growth of the stack in height.

In arid climates, it seems viable to rely on air-drying to achieve a significant additional water loss in the recently placed tailings. Two features of the drying process are worthy of note: 1) unless the tailings are reworked by ploughing or some similar technique, the drying process will reach a halt sometime after discharge (two months in the study case) and, 2) the outcome of the drying stage, namely the so-called target water content, bears a significant variability. Hence, specifying single-value target moisture seems completely unsuitable for the deposit design and operation. Using a probabilistic criterion would be much more appropriate and useful.

Multiple factors seem to influence tailings compression. The initial void ratio, resulting from the tailings being dumped from trucks plus some spreading work with bulldozers, appears to be strongly influenced by the water content of the tailings at discharge, which, in turn, depends on the filter performance. This, plus other possible unknown factors, result in a significant variability observed in the void ratio and degree of saturation obtained from field measurements in exploration pits. The laboratory work done so far indicates that compression of the studied tailings involves uncommon mechanisms, such as flocs mechanical behaviour and multimodal porosity water retention and flow. These aspects deserve additional research.

The capability to cope with the variability of the whole tailings disposal process is a key aspect to ensure its viability. Variability needs to be accommodated through redundancy and increased safety margins. An interesting feature of the studied deposit is the inclusion of waste rock layers interspersed between tailings layers. Besides ensuring trafficability with no compaction, the deposit benefited from an ample flexibility to accommodate the variability of the tailings water content, allowing drainage, and preventing stability issues.

## Acknowledgements

This work was developed as part of the cooperation agreement between Casposo Argentina and Fundación UNSJ. The authors gratefully acknowledge the funding and support received.

## Declaration of interest

The authors have no conflicts of interest to declare. All co-authors have observed and affirmed the paper's contents and there is no financial interest to report.

## Authors' contributions

**Luciano A. Oldecop:** Conceptualization, Data curation, Methodology, Supervision, Validation, Writing – original draft. **Germán J. Rodari:** Conceptualization, Data curation, Visualization, Writing – original draft.

## List of symbols

$D_{50}$	Sieve opening allowing to pass 50% of the sample weight
$C_u$	Grain size distribution uniformity coefficient
$LL$	Liquid limit
$PI$	Plasticity index
$S$	Degree of saturation
$\psi$	Suction
$\gamma_w$	Water specific weight
$G_s$	Solids specific gravity
$S_r$	Residual degree of saturation
$e$	Void ratio
$e_i$	Partial void ratio of the $i$ -pore system. $i = 1$ Inter-particle, 2 Intra-floc, 3 Inter-floc.
$P_{0i}$	Air entry value of the $i$ -pore system. $i = 1$ Inter-particle, 2 Intra-floc, 3 Inter-floc.
$\lambda_i$	VG parameter $i$ -pore system. $i = 1$ Inter-particle, 2 Intra-floc, 3 Inter-floc.
$w_f$	Water content at filter output. Mounting water content of oedometer specimens.
$w_0$	Target water content by the time of covering tailings with the following lift of the stack. Testing initial water content of oedometer specimens
$w_c$	Water content at facility closure. Test-end water content of oedometer specimens
$V_s$	Volume of solids
$e_0$	Void ratio by the time of covering tailings with the following lift of the stack. Initial void ratio of oedometer specimens
$e_c$	Void ratio at facility closure. Test-end void ratio of oedometer specimens.
$t$	Air-drying time elapsed (equal to the time elapsed since placing of tailings)
$a, b, c$	Fitting parameters of Equation 2
$\epsilon_w$	Residue of Equation 2, normally distributed with zero-mean
$s$	Standard deviation of $\epsilon_w$
$w_i$	Water content of the $i$ -pore system. $i = 1$ Inter-particle, 2 Intra-floc, 3 Inter-floc.

## References

- ASTM D1556–07. (2007). *Standard Test Method for Density and Unit Weight of Soil in Place by the Sand-Cone Method*. ASTM International, West Conshohocken, PA.
- ASTM D854-14. (2014). *Standard Test Methods for Specific Gravity of Soil Solids by Water Pycnometer*. ASTM International, West Conshohocken, PA.
- ASTM D5298-16. (2016a). *Standard Test Method for Measurement of Soil Potential (Suction) Using Filter Paper*. ASTM International, West Conshohocken, PA.

- ASTM D6836-16. (2016b). *Standard Test Methods for Determination of the Soil Water Characteristic Curve for Desorption Using Hanging Column, Pressure Extractor, Chilled Mirror Hygrometer, or Centrifuge*. ASTM International, West Conshohocken, PA.
- ASTM D2216-19. (2019). *Standard Test Methods for Laboratory Determination of Water (Moisture) Content of Soil and Rock by Mass*. ASTM International, West Conshohocken, PA.
- Copeland, A.M., Lyell, K.A., & van Greunen, P. (2006). Disposal of belt filtered tailings – skorpion zinc case study: feasibility, design and early operation. In: R. Jewell, S. Lawson and P. Newman (Eds.), *Proceedings of the Ninth International Seminar on Paste and Thickened Tailings*. Perth: Australian Centre for Geomechanics.
- Crystal, C., Hore, C., & Ezama, I. (2018). Filter-pressed dry stacking: design considerations based on practical experience. In: *Tailings and Mine Waste 2018 – Proceedings of the 24th International Conference on Tailings and Mine Waste* (pp. 209-219). Colorado: Colorado State University/University of British Columbia.
- Delage, P., Howat, M., & Cui, Y.J. (1998). The relationship between suction and swelling properties in a heavily compacted unsaturated clay. *Engineering Geology*, 50, 31-48.
- Franks, D.M., Stringer, M., Torres-Cruz, L.A., Baker, E., Valenta, R., Thygesen, K., Matthews, A., Howchin, J., & Barrie, S. (2021). Tailings facility disclosures reveal stability risks. *Scientific Reports*, 11, 5353. <http://dx.doi.org/10.1038/s41598-021-84897-0>.
- Hogg, C.S. (2010). Filtered tailings in Western Australian iron ore projects. Comparison of filtered tailings with other tailings disposal methods. In: R. Jewell & A.B. Fourie (Eds.), *Proceedings of the First International Seminar on the Reduction of Risk in the Management of Tailings and Mine Waste* (pp. 463-472). Perth: Australian Centre for Geomechanics. [https://doi.org/10.36487/ACG\\_rep/1008\\_38\\_Hogg](https://doi.org/10.36487/ACG_rep/1008_38_Hogg).
- Kim, H., Prezzi, M., & Salgado, R. (2017). Calibration of Whatman Grade 42 filter paper for soil suction measurement. *Canadian Journal of Soil Science*, 97(2), 93-98. <http://dx.doi.org/10.1139/cjss-2016-0064>.
- Lara, J.L., Pornillos, E.U., & Muñoz, H.E. (2013). Geotechnical-geochemical and operational considerations for the application of dry stacking tailings deposits – state-of-the-art. In: R.J. Jewell, A.B. Fourie, J. Cadwell, & J. Pimenta (Eds.), *Paste 2013*. Perth: Australian Centre for Geomechanics.
- Oldecop, L.A., Rodari, G.J., & Muñoz, J.J. (2017). Atmosphere interaction and capillary barrier in filtered tailings. *Geotechnical and Geological Engineering*, 35, 1803-1817. <https://doi.org/10.1007/s10706-017-0210-3>.
- Rezanezhad, F., Price, J.S., & Craig, J.R. (2012). The effects of dual porosity on transport and retardation in peat: a laboratory experiment. *Canadian Journal of Soil Science*, 92, 1-10. <https://doi.org/10.4141/cjss2011-050>.
- Rodari, G. & Oldecop, L.A. (2021), Secado de colas filtradas en contacto con la atmósfera. *Boletín Geológico y Minero*, 132(3), in print. <https://doi.org/10.21701/bolgeomin>.
- Ross, P.J., & Smettem, R.J. (1993). Describing soil hydraulic properties with sums of Simple functions. *Soil Science Society of America Journal*, 57, 26-29.
- Ulrich, B. (2019) Practical thoughts regarding filtered tailings. In: A.J.C. Paterson, A.B. Fourie & D. Reid (Eds.), *Proceedings of the 22nd International Conference on Paste, Thickened and Filtered Tailings* (pp. 71-79). Perth: Australian Centre for Geomechanics. [https://doi.org/10.36487/ACG\\_rep/1910\\_01\\_Ulrich](https://doi.org/10.36487/ACG_rep/1910_01_Ulrich).
- van Genuchten, M.T. (1980). A closed-form equation for predicting the hydraulic conductivity of unsaturated soils. *Soil Science Society of America Journal*, 44(5), 892-898. <http://dx.doi.org/10.2136/sssaj1980.03615995004400050002x>.
- Wang, C., Harbottle, D., Liu, Q., & Xu, Z. (2014). Current state of fine mineral tailings treatment: a critical review on theory and practice. *Minerals Engineering*, 58, 113-131.

## Brasília municipal solid waste landfill: a case study on flow and slope stability

José Fernando Thomé Jucá<sup>1#</sup> , Alison de Souza Norberto<sup>1</sup> ,

José Ivan do Santos Júnior<sup>1</sup> , Fernando A. M. Marinho<sup>2</sup> 

CASE STUDY

### Keywords

MSW Landfill  
Slope stability  
Hydraulic and mechanical parameters  
Leachate; Pore liquid pressures

### Abstract

For geotechnical and environmental reasons, landfills are positioned above the regional water table and thus are formed in unsaturated conditions. This condition can be different if the drainage system and the rain regime of the site are such that they create a level of internal liquid in the landfill. During January and February 2019, excessive movements occurred in the slopes of the Brasília sanitary landfill. A geotechnical investigation indicated that the raised leachate level caused by the clogging of the drainage system contributed to the landfilled waste movements. The limit equilibrium analysis was used to predict the relationship between leachate level and slope stability. In order to understand the process that led to the rupture, flow and stability analysis by limit equilibrium were performed. The parameters associated with flow, water retention capacity, and shear strength were obtained based on literature evaluations. In addition, data from tests were used, which allowed to define more accurately the distribution of pore pressures of liquid that led to the failure. This study allowed to define the cause of failure and also to establish the role of the drainage system in maintaining the stability of the landfill. The studies indicated that although the gain of shear strength of landfill due to the unsaturated condition is negligible, the process of flow in unsaturated medium, associated with climatic aspects, are fundamental for a medium- and long-term analysis.

## 1. Introduction

Slope stability analysis for Municipal Solid Waste landfill has been the focus of many technical publications; however, few papers have addressed the influence of leachate on the landfill stability, considering the climatic aspect and hence, the unsaturated conditions of the waste mass, which occur up to the leachate level in the landfill and from there the conditions of the waste mass become saturated. This paper presents a case study of a landfill failure that involved a small movement of waste induced by an excessive pore liquid pressure, caused by the obstruction of the drainage system.

Excessive infiltration of rainwater, without adequate control, increases the waste saturation and raises the level of internal leachate in the landfill, inducing a reduction in gas permeability. If the generated gas finds it difficult to escape through the roof or be captured by the gas capture system, this pressure can add to the liquid pressure. It is exactly this combination of reduced gas permeability, as result of saturation, that makes it difficult to assess the role

of gas pressure in instability processes. Merry et al. (2006) present a theoretical study to define the effect of gas pressure generation along the landfill. This effect is significant when the saturated hydraulic conductivity of the landfill is less than approximately  $10^{-6}$  m/s. If there is complete saturation of the landfill, the excess gas pressure would be approximately 0.6 kPa per meter of landfill height. The authors suggest that to take this effect into account in the stability analyses, the simplest way is to use a specific weight for the liquid higher. According to Merry et al. (2006) and based on the data shown later in the text, the saturated hydraulic conductivities of landfills can range from  $10^{-8}$  m/s to  $10^{-4}$  m/s. Under these conditions, saturated waste, Merry et al. (2006) indicates that the equivalent specific weight of the liquid, to take into account the gas pressure in the stability analysis, can reach up to 110 kN/m<sup>3</sup>. The heterogeneity characteristics of the landfill can generate an inhomogeneous pressure distribution of liquid and gas. Not even a well-distributed monitoring system can guarantee the correct determination of liquid and gas pressures in the landfill. The use of resistivity to detect

#Corresponding author. E-mail address: jucah@ufpe.br

<sup>1</sup>Universidade Federal de Pernambuco, Technology Center, Department of Civil and Environmental Engineering, Recife, PE, Brasil.

<sup>2</sup>Universidade de São Paulo, São Paulo, SP, Brasil.

Submitted on May 18, 2021; Final Acceptance on July 15, 2021; Discussion open until November 30, 2021.

<https://doi.org/10.28927/SR.2021.067321>



This is an Open Access article distributed under the terms of the Creative Commons Attribution License, which permits unrestricted use, distribution, and reproduction in any medium, provided the original work is properly cited.



regions with the greatest presence of water has been very efficient (e.g. Rosqvist et al., 2007; Dumont et al., 2016).

During January and February of 2019 excessive movements occurred in the slopes of the Brasília sanitary landfill. A geotechnical investigation indicated that the raised leachate level caused by the clogging of the drainage system contributed to the landfilled waste movements. In this work, the slope stability analysis was carried out analyzing the influence of rain and the consequent generation of leachate considering the flow in unsaturated medium. The back analysis of the study of the Brasília MSW landfill slope stability aimed to identify the reasons for the excessive movements of the landfilled mass.

A back-analysis was performed considering information from site observations and data from an electro-resistivity survey. This case led to a general assessment of the design procedures for the landfill that included the flow analysis associated with the equilibrium stability analysis. The flow analysis took into account the precipitation and local evaporation, and the analysis was carried out for a period of two years after the completion of the landfill. The analyses made it possible to evaluate the change in the stability scenarios, through the variation of the factor of safety (FoS), associated with the pore pressure profiles developed according to the climatic conditions. The case shows that the amount of leachate present in a landfill is critical and should always be kept low, based on an efficient drainage system. The organic matter present in the Brasília landfill is around 47% in volume. In the biodegradation process, part of this organic matter is transformed into liquids and gases at different times that vary according to the amount of waste and its degradation capacity. In other words, the contribution of organic waste to the total volume of leachate leaving the landfill is difficult to accurately estimate. However, if the landfill is isolated from incoming rain, the volume of liquids generated could be only 10% of the volume of biodegradable organics, depending on its moisture and density. Thus, it is precipitation and its infiltration into the landfill that control the generation of leachate.

## 2. General aspects of the landfill

The municipal solid waste landfill of Brasília is located at the Administrative Region of Samambaia, in the Federal District, between the Melchior stream and the DF-180 highway, close to the sewage treatment stations Melchior and Samambaia, at 30 km from the center of Brasília. Brasília is 1087 m above sea level and has a tropical climate, with hot and humid springs (September to December) and summers (December to March) and cold, dry autumns (March to June) and winters (June to September). The average annual rainfall is 1443 mm and presents an annual average relative humidity of 68%, ranging from 49% in August to 79% in December. Temperature ranges between 22°C and 40°C. Annual rainfall varies widely, from months without rain

to periods of intense rain of 400 to 500 mm per month, as shown in Figure 1.

The Brasília Landfill project was conceived and adapted to the planialtimetric conditions of the land surface, considering aspects such as vegetation, available areas, access, and distance to rivers, streams, and springs. The implantation of the Brasília Landfill began in 2015 and is taking place in 4 sequential phases. Phase 1 contemplates the implementation of an initial area of approximately 110,000 m<sup>2</sup>, located on the east side of the waste disposal area itself. Phase 2 is located in the central portion, Phase 3 in the southwest region, which should also be used as a soil storage area during the implementation and operation of the Phases that precede it, and finally, Phase 4 should be performed over the previous Phases. At the end of the construction, the landfill will occupy a total area of 320V and will have accumulated an amount of 8.2 million tons. The general arrangement of the landfill with the identification of the phases can be seen in Figure 2. The characteristics and properties of the subsoil were studied through in situ geotechnical investigation. For Phase 1, it was carried out based on 23 Standard Penetration Tests (SPT). The subsoil consists of a top layer of sandy clay 3m thick and SPT of 5, followed by a layer of sandy silt 6m thick and average SPT of 12. The water level varied between 3.50 m and 6.70 m, from the foundation level.

The MSW of Brasília receives around 2200 t of waste daily. The predominant composition of the waste is food and garden waste (47%), followed by plastics (15%), paper and cardboard (11%), and clothes and wood (7%), the rest being sand, gravel, and stones. The geotechnical and environmental monitoring of the Brasília MSW landfill was carried out after the excessive movements in January 2019 through the installation and maintenance of monitoring instruments, such as: vector piezometers and superficial landmarks, which are intended to monitor parameters linked to the stability and safety of the landfill. Groundwater monitoring wells as well as surface water monitoring are used to assess the region's water quality. Routine visual inspection is also carried out

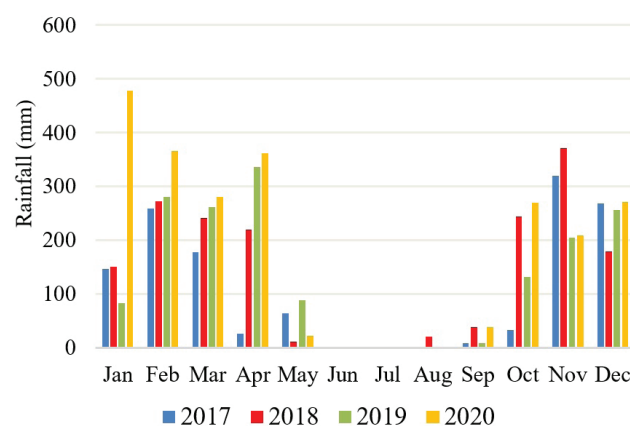
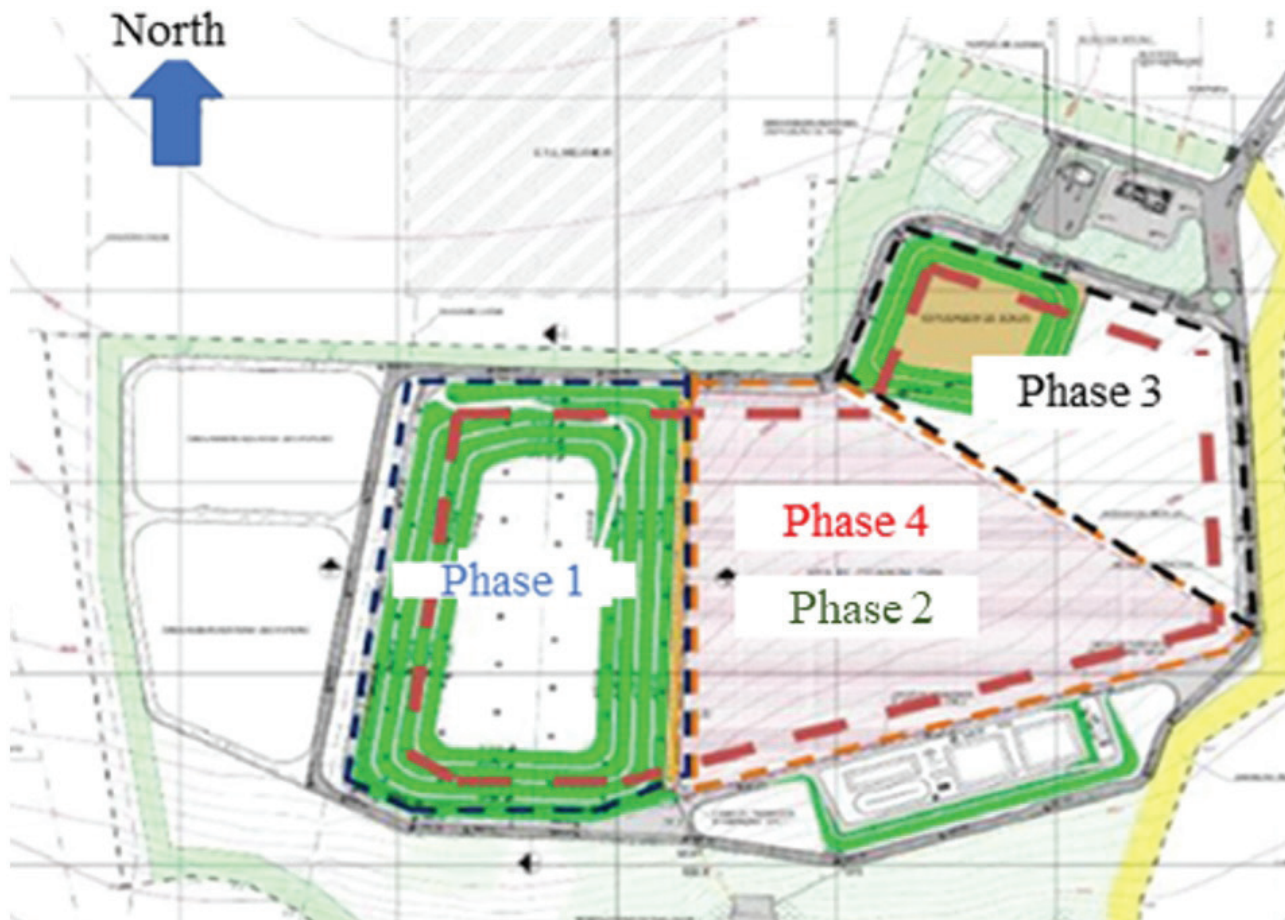


Figure 1. Rainfall at the Brasília Landfill between 2017 and 2020.



**Figure 2.** Locations of the construction phases of the Brasília MSW landfill.

to check features that may indicate stability and security problems.

### 3. Characteristics of the base liner and drainage system

In Phase 1, the landfill base liner was built with a thickness of 1.5 m of compacted clay soil, aiming a hydraulic conductivity equal to or less than  $10^{-9}$  m/s. Overlying the base liner, a 2 mm HDPE geomembrane was installed, textured on both sides, with seams made by thermal fusion. The mechanical protection of the HDPE geomembrane, both at the base and on the slopes, was carried out by means of a soil layer with a thickness of 0.5 m.

The leachate drainage system at the base of the Phase 1 of Brasília MSW (BMSW) landfill was implanted above the mechanical protection layer, where a HDPE geomembrane was used, and following the declivities defined in project, with 3.5% in the South-North direction and 0.7% in the East-West direction. The drainage system implanted is herringbone type with a main drain working with secondary drains that collect the leachate to the accumulation ponds. Vertical

draining wells is also installed, starting over the main drains. The latter should also work as a gas drainage system. These drains were filled with limestone, which had no restrictions for its use in Brazilian technical standards. During the landfill operation, some problems occurred with the drainage system causing clogging or reduction in hydraulic conductivity to flow the leachate. Some studies have explained this problem by the use of limestones (about 50% of calcium carbonate) with significant concentration of fines (unwashed stone), although reports of similar problems have not been found in Brazilian landfills (Carvalho & Pfeiffer, 2019). Limestone was the main cause the problems, other minor causes may have been caused by movements in the drainage system. On the other hand, limestone was present in horizontal drains as well as vertical leachate drains and gas drains. There were excavations in specific places to investigate the clogging of liquid drains that confirmed as hypotheses raised about the effects of using limestone in drainage systems. On the other hand, in the south area of Phase 1, the drainage system also indicated problems of low gradients, because the low slope of the drainage system induces lower flow velocities, accentuating the observed clogging problems. This area corresponds to the places where leachate overflow problems,

excess of pore liquid pressures, and excessive movements in the landfill slope were observed.

#### 4. Characteristics of the landfill soil cover

The cover system plays a key role in the water balance of landfills. This system controls the surface water and also the water that infiltrates and/or evaporates, thus having a direct influence on the volume of liquid (leachate) that is captured by the drainage system. This entire system is responsible for the variation of water content and pore pressures of liquids within the landfill and consequently, the landfill stability. The interaction between the roofing system and the atmosphere goes beyond the entry and exit of water. The atmospheric air ( $N_2$  and  $O_2$ ) penetrates the landfill due to variations in atmospheric pressure, leading to a series of biochemical reactions that generate gases ( $CH_4$ ,  $CO_2$ ,  $H_2S$ , among others) that tend to escape from the landfill. Thus, in the same soil element of the roof, there is simultaneously a flow of liquid and gases associated with climatic variations, water content, soil suction, air permeability, and hydraulic conductivity (e.g., Jucá & Maciel, 1999; Marinho et al., 2001; Maciel & Jucá, 2011). In this way, the system also has the function of minimizing gas emissions to the atmosphere. Its execution must be done with extreme care, adapting the conditions of compaction and thickness to the characteristics of the landfill and the local climate. In the specific case of BMSW landfill, the material used in the execution of the cover system is a sandy silt. The estimated infiltration is about 50% of the rain, which allows an excessive intake of water to the landfill, increasing the volume of leachate, Melchior et al. (2010) reports in his article that there was an infiltration of 42% of rain in the compacted soil layer. In field tests with double rings, the water infiltration range varies from 15 to 20 mm/h. The layer thickness was initially designed to be

0.6 m, but it showed variations during execution and there was no compaction control.

#### 5. The occurrence of slope instability

From February to April 2019, the south area of Brasília landfill presented excessive movements associated with the excess of leachate that overflowed in different points of the slopes and through the existing gas drains. These excessive movements were also identified in the drainpipes and an intense erosive process of the covering soils.

Figure 3a presents an overview of phase 1 of the landfill construction with an indication of the region that suffered the failure, and positions where the leaks were observed. Figure 3b illustrates the tipping of one of the gas drains after the failure.

In Figure 4a, one of the gas drainage systems completely taken by the leachate is shown. In Figure 4b, the leachate leak is identified on the road.

#### 6. Post failure investigation

##### 6.1 Back-analysis

##### 6.1.1 Mechanical and hydraulic parameters of the landfill

The observational method associated with flow and stability analysis (limit equilibrium) provides a very efficient and simple tool for identifying the causes of failure or malfunctions in geotechnical structures. The geotechnical problems related to landfills of municipal solid waste (MSW) present intrinsic difficulties due to the characteristics of the material with which it is dealing. Back-analysis of failures requires knowledge of the parameters involved in the behaviour

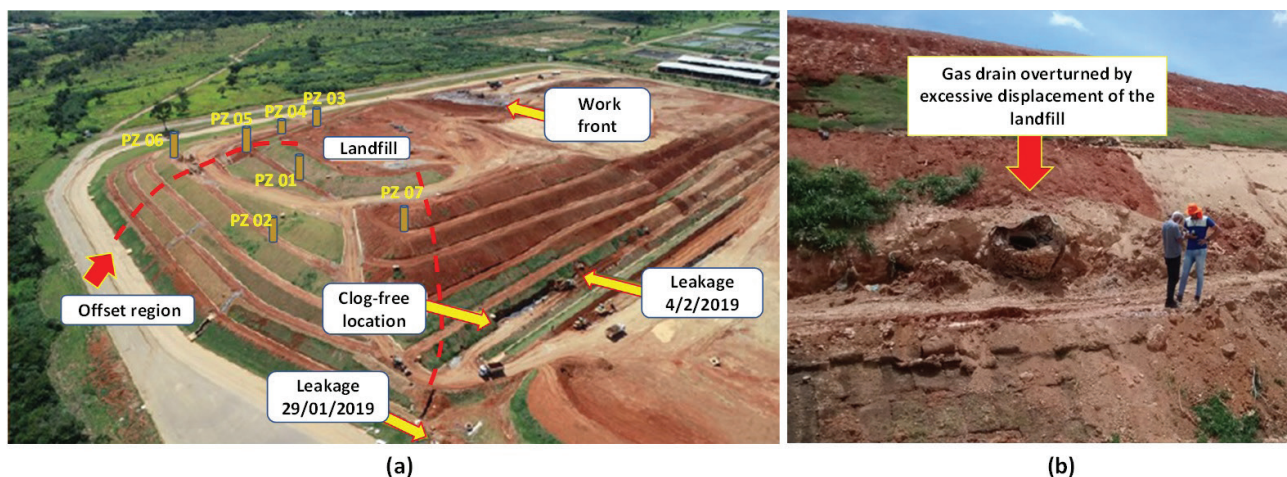


**Figure 3.** Region where the rupture movement occurred: (a) aerial view of the landfill with the location of leachate leaks and failure zone; (b) tilt of the vertical gas drain.





**Figure 4.** Leachate leaks: (a) gas drainage with leachate; (b) flow of leachate along the road.

of the materials. These parameters, which are predominantly mechanical and hydraulic in nature, govern the behaviour of the landfill. Associated with this are the biochemical aspects that affect the material and the drainage system. The failure mechanism must also be defined, establishing whether the failure occurred in a drained or undrained condition, or if there is a combination of the two mechanisms. Geometric characteristics of both the landfill section and the failure surface may also generate uncertainties in the analyses.

Thus, in order to carry out a back-analysis, it is necessary to define, with maximum accuracy, the parameters less susceptible to variations or the ones we are more confident about. In the case of MSW landfills, this is a task that is always subject to criticism. In the present study, which is based on a case of excessive movement of a MSW landfill, an attempt was made to establish a procedure that would allow not only to identify the predominant cause for the excessive movements but also to create a procedure that allows a conceptually more consistent definition of the project. It should be noted that the adopted procedure aims to be relatively easy to be adopted in engineering practice.

MSW landfills are located in positions that tend to leave the waste in an unsaturated condition. In other words, they are above the ground water level. This condition can change if there is any deficiency in the drainage system associated with an intense rainfall regime that creates an internal level of liquid. Based on data from the literature, the variation of the saturated hydraulic conductivity of the landfill in depth

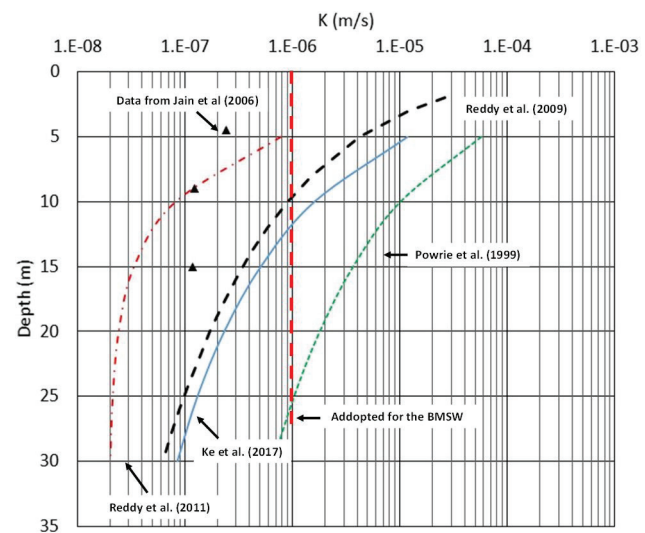


**Figure 5.** Variation of saturated hydraulic conductivity of MSW with depth according to literature and the value used for the present analyses (data from Jain et al., 2006; Ke et al., 2017; Powrie et al., 1999; Reddy et al., 2009, 2011).

was defined and the shear strength parameters were also based on literature as a start point for the back analysis.

### 6.1.2 Hydraulic parameters

Any embankment, whether carried out with solid urban waste, from mining tailings or even soil from a controlled borrow pit, is subject to climatic conditions. The infiltration of water plays a fundamental role in the stability of these structures and the project must take into account the climatic aspects of the site. Infiltrations are linked to seasonal climatic variations and can affect the stability of the structure in the medium and long term. These landfills are generally designed to remain unsaturated. This unsaturated condition, in the case of landfills of solid urban waste, does not contribute significantly to the strength of the material, which indicates that the gain of strength due to the unsaturated state is in general negligible. However, the unsaturated condition of municipal solid waste creates a different flow pattern than it would be if the material were saturated.

In this case, an unsaturated flow analysis is essential, taking into account appropriate parameters. The determination of the variation in hydraulic conductivity with saturation or suction (called permeability function) is not usually obtained through laboratory tests. Its determination is made through models that make use of the saturated hydraulic conductivity and the water retention curve (van Genuchten, 1980). In the specific case of BMSW, no data were available on saturated hydraulic conductivity and water retention curve, and an evaluation based on the literature was necessary. Figure 5 presents data on hydraulic conductivity as a function of the depth of the solid waste landfill, for several studies found in the literature (e.g., Powrie et al., 1999; Jain et al., 2006;



Reddy et al., 2009; Reddy et al., 2011; Ke et al., 2017). Based on these studies, a single value of  $10^{-6}$  m/s was adopted as the hydraulic conductivity value.

Similarly, data from the literature were taken to assess which water retention curve (SWRC) would be adopted for studies at BMSW. Figure 6 shows SWRCs obtained from the literature. It is observed that the volumetric water content is the condition closest to saturation, although it does not reflect porosity, varies between 60% and 70%. In addition, the various authors obtained curves with bi-modal behaviour. The interpretation of the suction water content relationships in unsaturated soils has always deserved much discussion and little convergence of opinions. In urban solid waste this issue is even more complex, few studies show repeatability and easy interpretations. The question of linearity or not of this relationship can be strongly influenced by the composition of the residues and the moisture retention capacity of each one of these fractions. Higher percentages of organic matter and materials such as paper and cardboard have a higher retention capacity than materials such as glass, plastics and metals. Organic fractions degrade and can change this composition over time. Furthermore, this same composition can change other properties of the waste, such as its permeability and compressibility, modifying the suction – water content ratio

of the waste. The adoption of the nonlinear model is more associated with samples obtained at greater depths (higher stress level and older or more decomposed) and better expresses the long-term behaviour. Based on the analysis of the curves from the literature, a bimodal curve was adopted for the present work as shown in Figure 6 and its parameters are shown in Table 1.

### 6.1.3 Shear strength parameters

Similarly, data from the literature were obtained for the shear strength parameters of urban solid waste to be adopted

**Table 1.** SWRC parameters adopted for the BMSW.

Parameters	BMSW
$\alpha_1$	1.327 1/kPa
$n_1$	7.948
$m_1$	0.87418
$\theta_1$	61.55%
$\alpha_2$	0.1514 1/kPa
$n_2$	3.121
$m_2$	0.67959
$\theta_2$	38.45%
$\theta_s$	71.5%

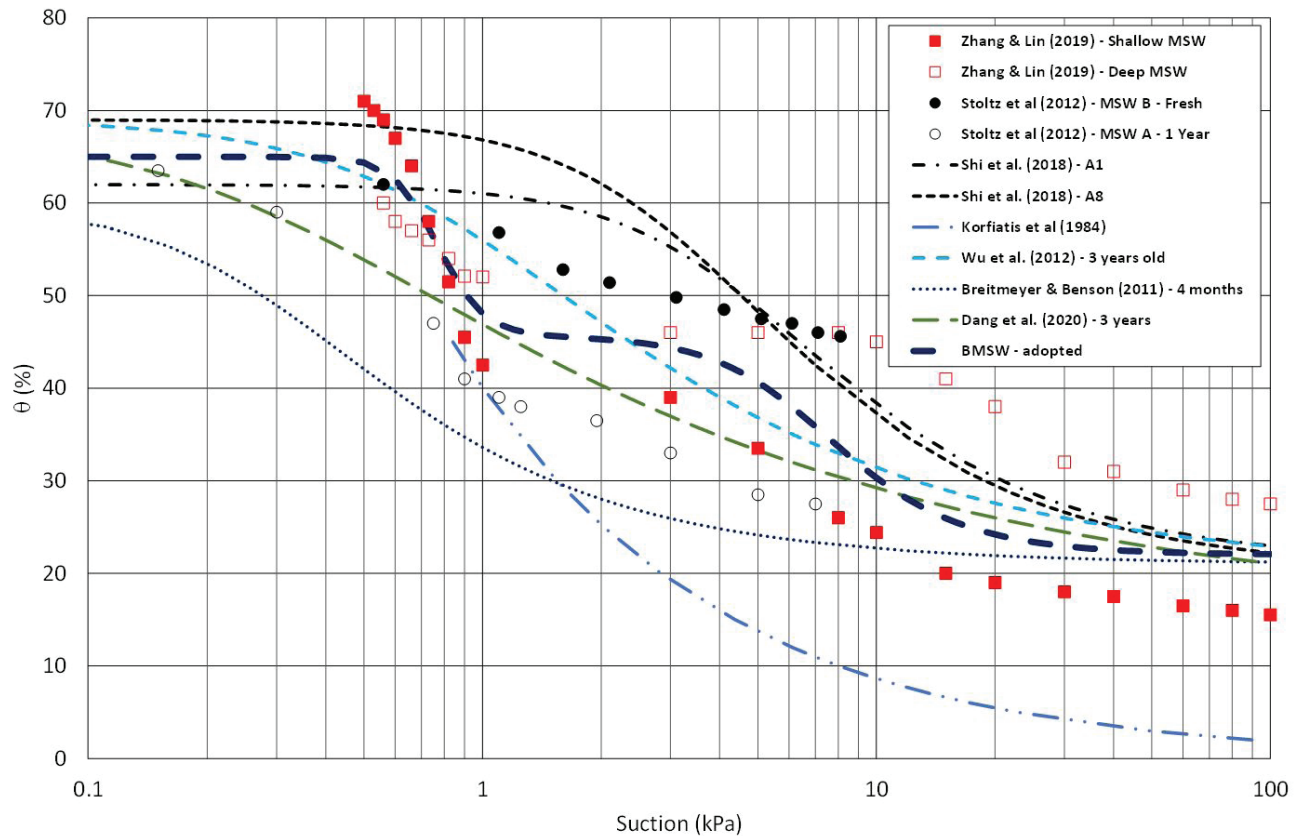


**Figure 6.** Soil water retention curve for MSW according to literature and the curve used for the present study (data from Breitmeyer & Benson, 2011; Dang et al., 2020; Korfiatis et al., 1984; Shi et al., 2018; Stoltz et al., 2012; Wu et al., 2012; Zhang & Lin, 2019).

for studies. In Figure 7, several shear strength envelopes found in the literature are presented, alongside the envelope used in this research.

#### 6.1.4 Pore liquid pressure

In order to be able to carry out the back analysis, it is necessary to know or estimate the pore liquid pressure in the landfill. As in Phase 1 of the construction of the landfill, piezometers or water level meters had not yet been installed, it was decided to obtain an instantaneous picture of the moisture condition of the waste by performing an electrical resistance survey.

After the initiation of the failure process of the landfill in Phase 1, an investigation was carried out by means of electrical tomography, performed in the longitudinal and transversal directions of the landfill. These results, together with the data of the instrumentation, installed after the failure, were used to infer the pore liquid pressure distribution in the landfill at the time of failure. After a careful interpretation it was possible to have an approximate view of the level of leachate inside the landfill, which at the time of the test (January 2020) indicated a liquid level at about 10 m from the base layer of the first cell, as can be seen in Figure 8.

## 7. Back analysis of the failure

With the interpretation of the pore liquid pressure distribution and the shear strength parameters adopted it was possible to evaluate the failure using limit equilibrium analysis. The analyses were performed using the software Slope/w. The original slope presents a geometry of 1V:2H, with berms of 2 m wide, each 5 m. Figure 9a illustrates the final geometry adopted for the back analysis. The interpretation of the humidity zones identified in the electrical survey (shown in Figure 8) and converted to pore liquid pressure is indicated in Figure 9b. The conversion was based on the moisture distribution associated with the back analysis. That is, maintaining the moisture distribution and imposing pore-pressures that induce a safety factor equal to one.

In the analysis, software from the GeoStudio package was used, the Seep/W was used for the flow and climatic aspects modelling and the Slope/W for the stability analyses. The observed failure zone from the field is replicated in the analysis with a factor of safety of one, as shown in Figure 10, suggesting that the combination of parameters is in agreement with the failure mode. The rupture surface was delimited from the displacement observed in the field. Therefore, the BMSW landfill failure mode was due to excess of pore pressure.

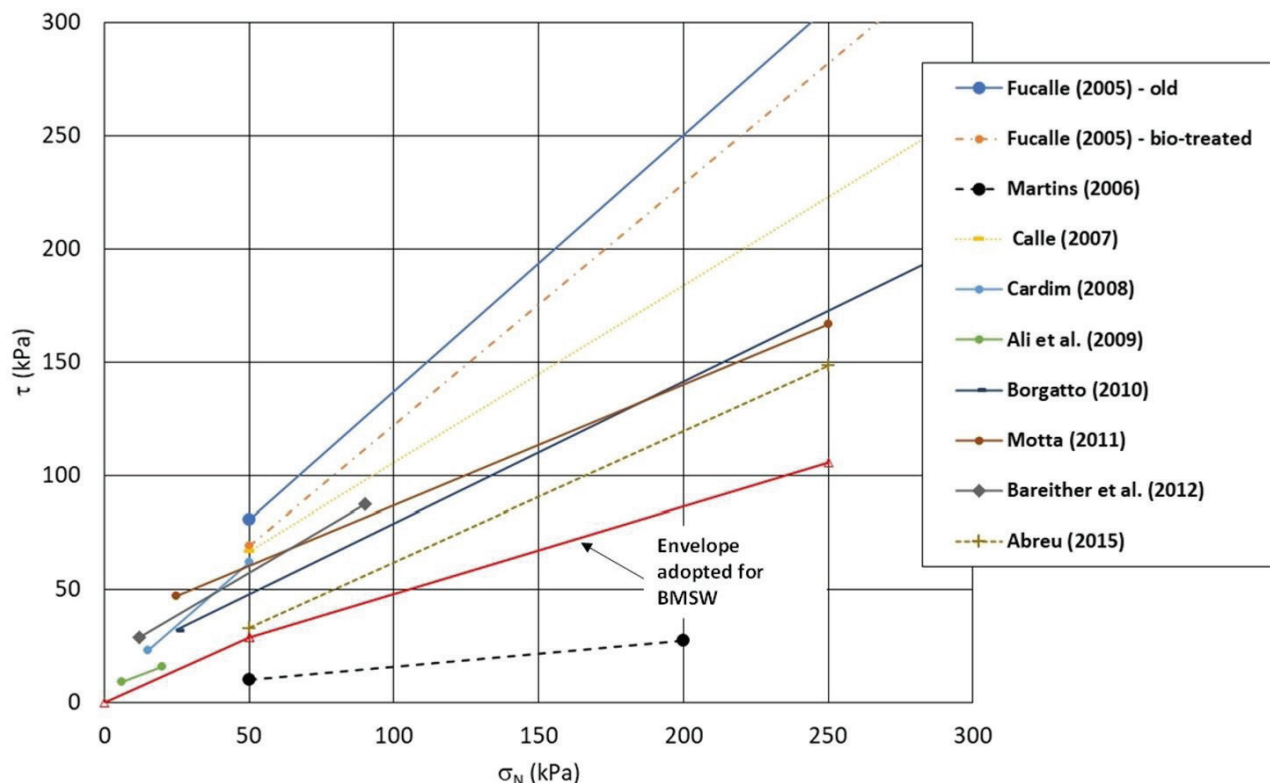


**Figure 7.** Shear strength envelopes for MSW and the bi-linear envelope used for the present study (data from Abreu, 2015; Ali et al., 2009; Bareither et al., 2012; Borgatto, 2010; Calle, 2007; Cardim, 2008; Fucalle, 2005; Martins, 2006; Motta, 2011).

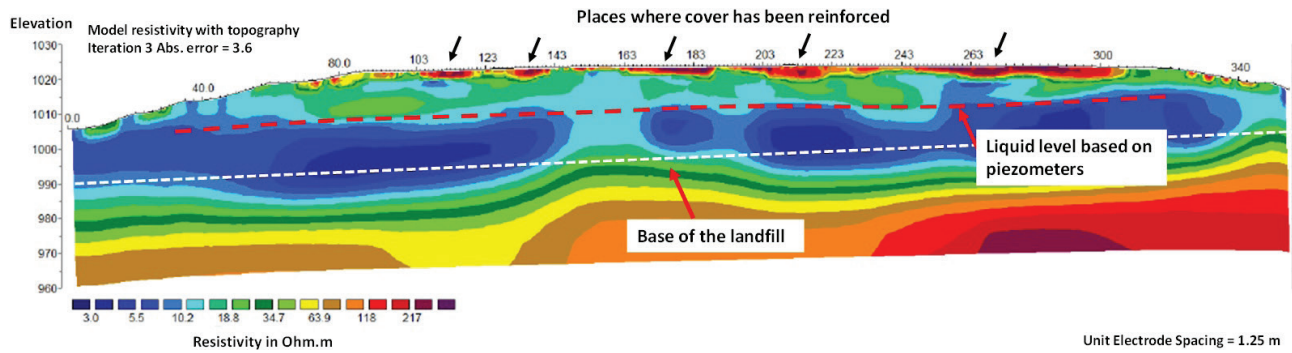


**Figure 8.** Geoelectric profile of Phase 1 after failure (Cunha & Borges, 2020).

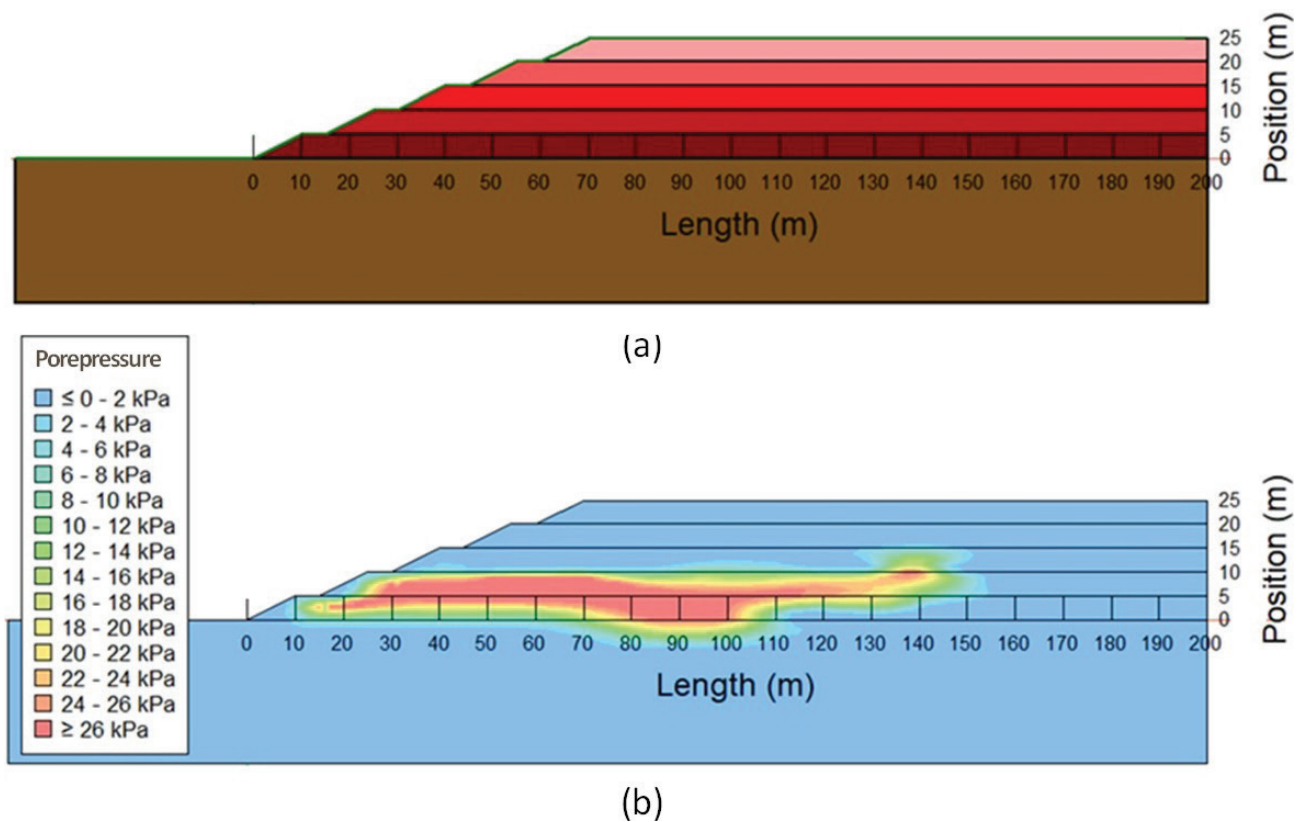


**Figure 9.** (a) section of the BMSW Landfill; (b) pore water pressure adopted to the back analysis.

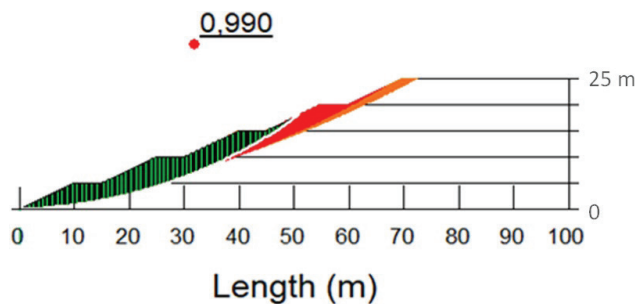


**Figure 10.** Surface equivalent to the field situation.

### 7.1 The local climate and the variation of the safety factor

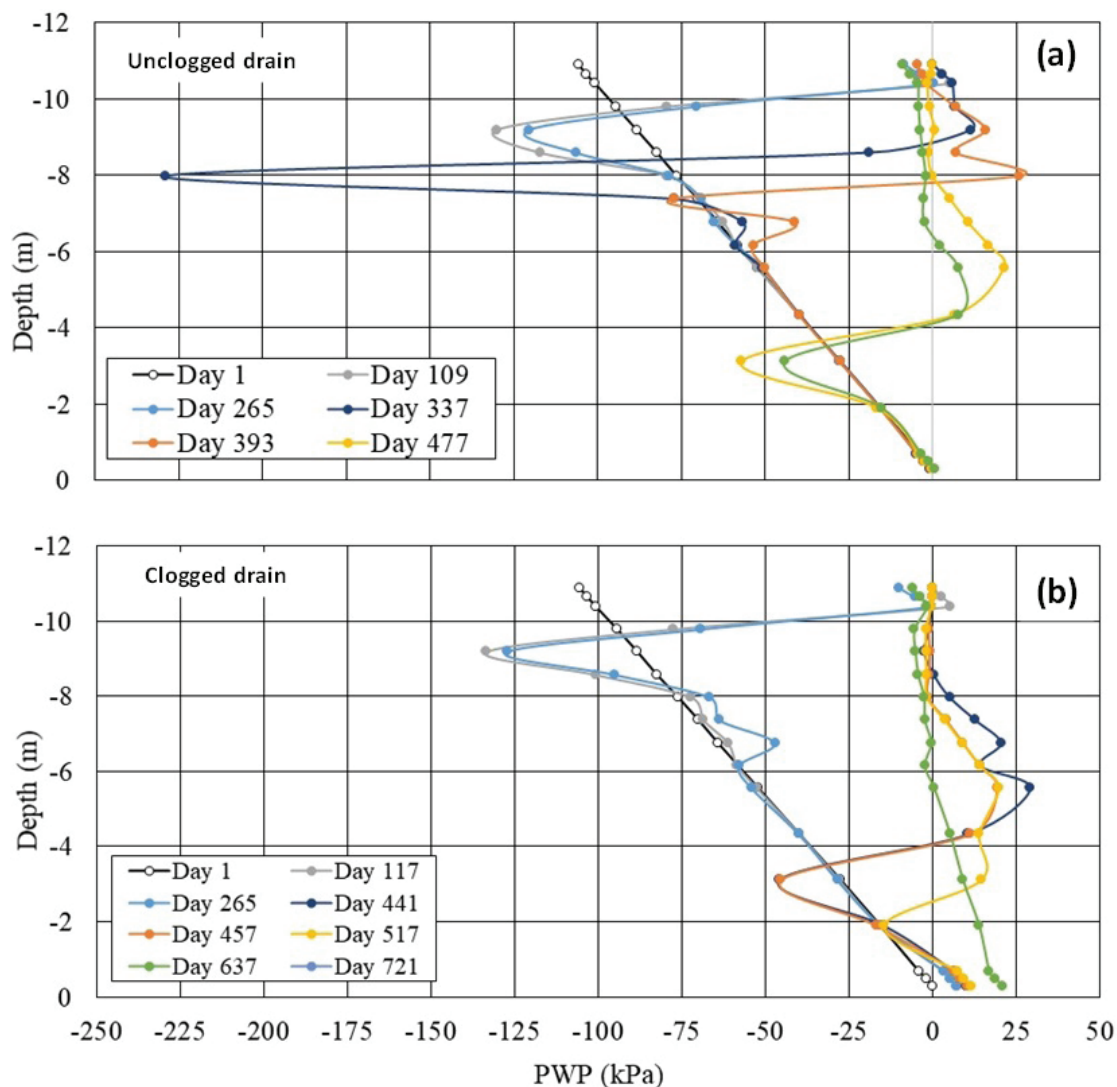
In order to better identify the reasons for the increase in the pore pressure causing the failure, an analysis was carried out combining the effects of the climate and the analysis of stability by limit equilibrium. The climatic conditions of the place where the landfill is located were established, adopting precipitation data. Considering the location of the landfill, Penman-Monteith model was used to take evaporation into account. The study replicated the climatic condition for

two years, with the initial condition of pore pressure being the equilibrium situation from the base of the landfill. In transient analyses the landfill is unsaturated, and therefore with a high gas permeability. Thus, gas pressure was not considered in the analyses.

The original design of the landfill adopted a herringbone drain at the base of the landfill. This system, when it is compromised due to some type of clogging, generates a rapid increase in the pore pressure. As landfills, in general, are very subject to chemical processes that can speed up clogging, the use of horizontal blankets is recommended. The analysis carried out in the present study is in two dimensions, and therefore, it is only possible to consider obstructions in one section. Thus, only two analyses were performed: one with the drain blocked (case 1) and the other without obstruction (case 2). The analyses were made considering the horizontal blanket with 0.40 m height and adopting a saturated permeability of  $10^{-3}$  m/s.

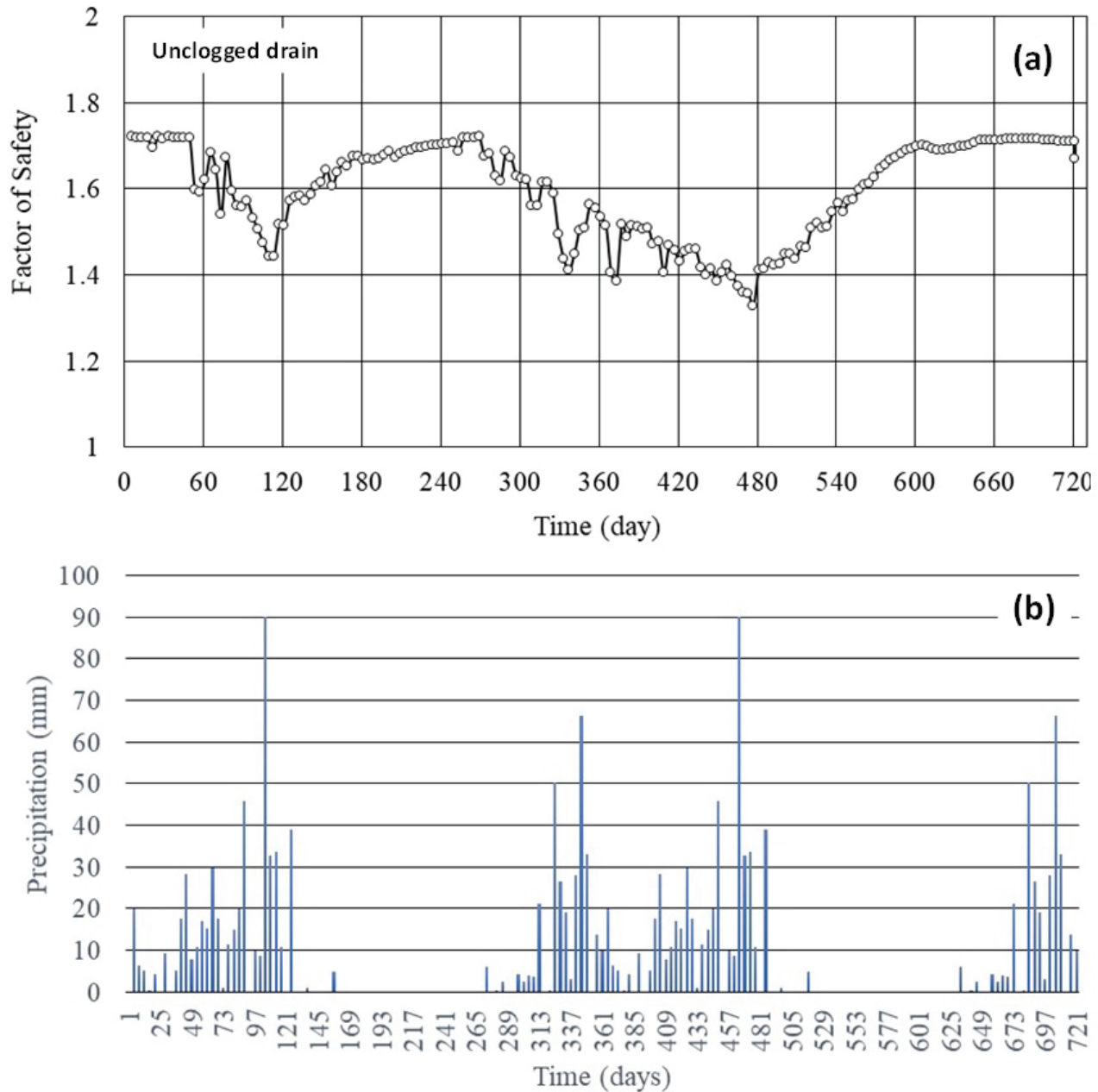
In case 1, the boundary condition adopted induced a full efficiency of drainage system, during the 2 years analysis. For case 2, a condition of variable obstruction was considered along the drainage system, simulating the clogging process that occurred in the field. The obstruction was induced over 30 m from the drain outlet. The hydraulic conductivity along the section considered obstructed varied from  $10^{-8}$  m/s to  $10^{-10}$  m/s, the obstruction being considered in a regressive way, being the largest obstruction at the exit point of the landfill drainage ( $10^{-10}$  m/s) and reducing to ( $10^{-8}$  m/s) at 30 m from the leachate exit. Using the software Seep/w (unsaturated flow considering local climate for two years) and Slope/w (limit equilibrium analysis), the analyses were performed for case 1 and 2.

Figure 11 shows the suction profiles over the two years of the analysis, for the case of the unobstructed drain (Figure 11a) and the case of the obstructed drain (Figure 11b). It should be noted that for the lower 4 m of the profile, the



**Figure 11.** Pore liquid pressure profiles for: (a) unclogged drain; (b) clogged drain.





**Figure 12.** Evaluation of the Factor of Safety for an unclogged drain with time with the precipitation applied to the model.

section closest to the drainage system, there is an increase in the pore liquid pressure when the drain has its drainage limited by the obstruction. Although this phenomenon (increase of pore-water pressure) does not occur in the first year, the increase in the liquid pressure at the base of the landfill is clear in the second year. It should be noted that this was the time taken between the completion of the landfill and its failure.

By incorporating pore liquid pressure profiles over time in the stability analysis, there is an expected variation in the safety factor. This variation is linked to precipitation

and evaporation, that is, to the local water balance, and the efficiency of the drainage system. Figures 12 and 13 show the variation of FoS over time, together with the rainfall adopted. In both cases, the response of the FoS to rainfall is clear. In the situation of the system without obstruction, the FoS reaches a value below 1.4, but at the end of the second year, it still maintains a FoS above 1.7.

In the case where the system undergoes a clogging process, the FoS already reaches a value below 1.4 in the first year, and this value suffers a degradation from the second rainy season, reaching values below 1.2.

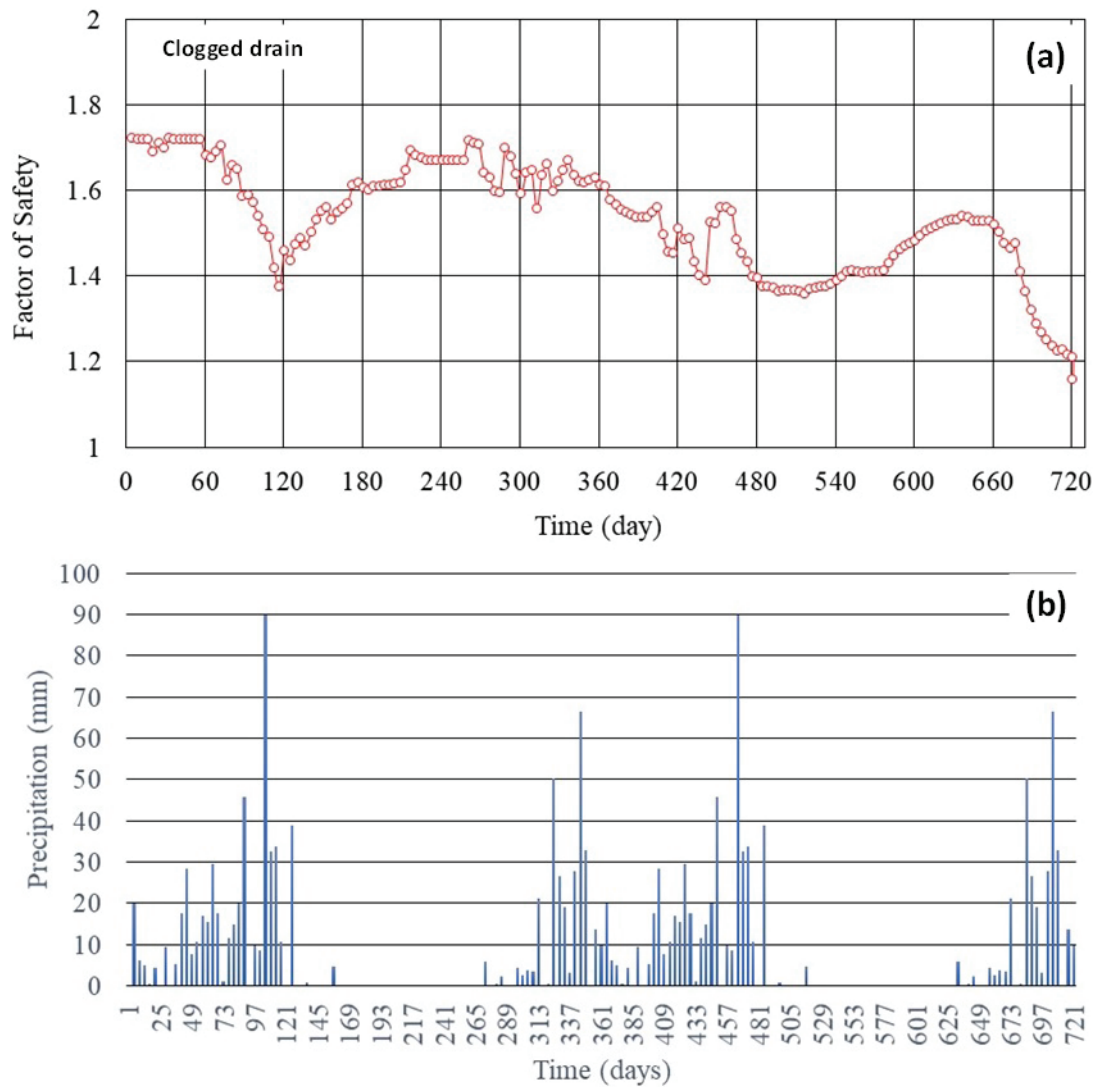


**Figure 13.** Evaluation of the Factor of Safety for a clogged drain with time with the precipitation applied to the model.

## 8. Conclusion

The present case once again brings to light important design aspects to be considered in municipal solid waste landfill projects. These aspects range from considerations about the internal drainage system to the cover system and its drainage project. In addition, analysis procedures—such as, climate association, flow in unsaturated media, and stability analysis must be incorporated.

Some specific observations and conclusions are:

- In many Brazilian landfills, control and testing data to obtain mechanical and hydraulic parameters are quite difficult. This paper presents alternatives for obtaining these parameters and makes an analysis that allows an assessment of the slope stability. However, it is emphasized that it is necessary to obtain specific parameters for the projects, taking into account the

characteristics of the local waste and the soils, both those of the foundation and those that will be used from borrow pits;

- Drainage systems in the form of herringbone has severe limitations in its efficiency. This effect is accentuated due to climatic conditions, the cover system, and the operation of the landfill. In most cases, a draining blanket system is more effective. In a system with a horizontal blanket, the occasional obstruction still allows drainage by another section, so it is considered safer to adopt this type of drainage system;
- Although the present analysis was limited to two years, it was possible to evaluate the behaviour of FoS over this period. It is suggested that the behaviour for longer periods be evaluated, using local rainfall data and parameters obtained for the landfill itself;

- Some aspects are important to control the stability of the landfill in the long term, such as: a well-dimensioned and permanently maintained cover system; and a monitoring system that allows the assessment of any clogging of the drainage system or the formation of leachate pockets.

## Acknowledgements

The authors are very grateful to the Regulatory Agency for Water, Energy and Sanitation of the Federal District (ADASA) and the Federal District Urban Cleaning Service (SLU – DF).

## Declaration of interest

The authors have no conflict of interests regarding the matter included in this paper.

## Authors' contributions

José Fernando Thomé Jucá: Writing, reviewing, editing, investigation. Alison de Souza Norberto: Writing, reviewing, editing, investigation. José Ivan do Santos Júnior: Writing, reviewing, editing, investigation. Fernando Antônio Medeiros Marinho: Writing, reviewing, editing, investigation.

## References

- Abreu, A.E.S. (2015). *Geophysical investigation and shear strength of municipal solid wastes with different landfilling ages waste* [Doctoral thesis, University of São Paulo]. University São Paulo's repository (in Portuguese). <https://doi.org/10.11606/T.18.2015.tde-03082015-115017>.
- Ali, L., Ali, S., & Maqbool, A. (August 2009). Large direct shear test apparatus for in situ testing of municipal solid waste landfill sites. In *Proceedings of the GeoHunan International Conference*, Changsha, Hunan. [https://doi.org/10.1061/41041\(348\)13](https://doi.org/10.1061/41041(348)13).
- Bareither, C.A., Benson, C.H., & Edil, T.B. (2012). Effects of waste composition and decomposition on the shear strength of municipal solid waste. *Journal of Geotechnical and Geoenvironmental Engineering*, 138(10), 1161-1174. [https://doi.org/10.1061/\(asce\)gt.1943-5606.0000702](https://doi.org/10.1061/(asce)gt.1943-5606.0000702).
- Borgatto, A.V.A. (2010). *Study of the geomechanical properties of pre-treated municipal solid waste* [Doctoral thesis, Federal University of Rio de Janeiro]. Federal University of Rio de Janeiro's repository (in Portuguese). <http://www.coc.ufrj.br/en/doctoral-thesis/349-2010/3891-andre-vinicius-azevedo borgatto>.
- Breitmeyer, R.J., & Benson, C.H. (2011). Measurement of unsaturated hydraulic properties of municipal solid waste. In *Proceedings of the Geo-Frontiers 2011: Advances in Geotechnical Engineering* (pp. 1433-1442). Dallas, TX. [https://doi.org/10.1061/41165\(397\)147](https://doi.org/10.1061/41165(397)147).
- Calle, J.A.C. (2007). *Geomechanical behavior of urban solid waste* [Doctoral thesis, Federal University of Rio de Janeiro]. Federal University of Rio de Janeiro's repository (in Portuguese). <http://www.coc.ufrj.br/pt/teses-de-doutorado/151-2007/1091-jose-antonio-cancino-calle>.
- Cardim, R.D. (2008). *Estudo da resistência de resíduos sólidos urbanos por meio de ensaios de cisalhamento direto de grandes dimensões* [Master's dissertation, University of Brasília]. University of Brasília's repository (in Portuguese). <https://repositorio.unb.br/handle/10482/3290>.
- Carvalho, E.H., & Pfeiffer, S.C. (2019). *Studies of the causes of clogging on leachate drainage system in Brasília landfill* (Technical report). Consortium Samambaia.
- Cunha, S.L., & Borges, W. R.B. (2020). *Report ASB 01/2020 - Profile of electrical tomography acquired at the top of cell 01 of the landfill in Brasília on 01/21/2020*. Institute of Geology, University of Brasília.
- Dang, M., Chai, J., Xu, Z., Qin, Y., Cao, J., & Liu, F. (2020). Soil water characteristic curve test and saturated-unsaturated seepage analysis in Jiangcungou municipal solid waste landfill, China. *Engineering Geology*, 264, <https://doi.org/10.1016/j.enggeo.2019.105374>.
- Dumont, G., Pilawski, T., Dzaomuhlo-Lenieregue, P., Hilgsmann, S., Delvigne, F., Thonart, P., et al (2016). Gravimetric water distribution assessment from geoelectrical methods (ERT and EMI) in municipal solid waste landfill. *Waste Management (New York, N.Y.)*, 55, 129-140. <https://doi.org/10.1016/j.wasman.2016.02.013>.
- Fucale, S.P. (2005). *Influence of reinforcement components in the resistance of municipal waste* [Unpublished doctoral thesis]. Federal University of Pernambuco (in Portuguese).
- Jain, P., Powell, J., Townsend, T.G., & Reinhart, D.R. (2006). Estimating the hydraulic conductivity of landfilled municipal solid waste using the borehole permeameter test. *Journal of Environmental Engineering*, 132(6), 645-652. [https://doi.org/10.1061/\(asce\)0733-9372\(2006\)132:6\(645\)](https://doi.org/10.1061/(asce)0733-9372(2006)132:6(645)).
- Jucá, J.F.T., & Maciel, F.J. (1999). Permeabilidade ao gás de um solo compactado não saturado. In *4º Congresso Brasileiro de Geotecnia Ambiental - REGEO 99: Vol. 1* (pp. 384-391). São José dos Campos, SP. (in Portuguese).
- Ke, H., Hu, J., Xu, X.B., Wang, W.F., Chen, Y.M., & Zhan, L.T. (2017). Evolution of saturated hydraulic conductivity with compression and degradation for municipal solid waste. *Waste Management (New York, N.Y.)*, 65, 63-74. <https://doi.org/10.1016/j.wasman.2017.04.015>.
- Korfiatis, G.P., Demetracopoulos, A.C., Bourdinos, E.L., & Nawy, E.G. (1984). Moisture transport in a solid waste column. *Journal of Environmental Engineering*, 110(4), 780-796. [https://doi.org/10.1061/\(ASCE\)0733-9372\(1984\)110:4\(780\)](https://doi.org/10.1061/(ASCE)0733-9372(1984)110:4(780)).
- Maciel, F.J., & Jucá, J.F.T. (2011). Evaluation of landfill gas production and emissions in a MSW large-scale experimental cell in Brazil. *Waste Management (New*

- York, N.Y.), 31, 966-977. <https://doi.org/10.1016/j.wasman.2011.01.030>.
- Marinho, F.A.M., Andrade, M.C.J., & Jucá, J.F.T. (2001). Air and water permeability of a compacted soil used in a solid waste landfill in Recife, Brazil. In R.N. Yong and H.R. Thomas (Eds.), *Proceedings of the 3rd BGA Geoenvironmental Engineering Conference* (pp. 437-442). Edinburgh.
- Martins, H.L. (2006). *Avaliação da resistência de resíduos sólidos urbanos por meio de ensaios de cisalhamento direto em equipamento de grandes dimensões* [Doctoral thesis, Federal University of Minas Gerais]. Federal University of Minas Gerais's repository (in Portuguese). <http://hdl.handle.net/1843/FRPC-6ZNJ2D>.
- Melchior, S., Sokollek, V., Berger, K., Vielhaber, B., & Steinert, B. (2010). Results from 18 years of in situ performance testing of landfill cover systems in Germany. *Journal of Environmental Engineering*, 136(8), 815-823. [https://doi.org/10.1061/\(asce\)ee.1943-7870.0000200](https://doi.org/10.1061/(asce)ee.1943-7870.0000200).
- Merry, S.M., Fritz, W.U., Budhu, M., & Jesionek, K. (2006). Effect of gas on pore pressures in wet landfills. *Journal of Geotechnical and Geoenvironmental Engineering*, 132(5), 553-561. [https://doi.org/10.1061/\(asce\)1090-0241\(2006\)132:5\(553\)](https://doi.org/10.1061/(asce)1090-0241(2006)132:5(553)).
- Motta, E.Q. (2011). *Shear strength evaluation of municipal solid waste with co-disposal of sewage sludge through large-scale direct shear testing* [Doctoral thesis, Federal University of Pernambuco]. Federal University of Pernambuco's repository (in Portuguese). <https://repositorio.ufpe.br/handle/123456789/5382>.
- Powrie, W., Ceng, F., & Beaven, R.P. (1999). Hydraulic properties of household waste and implications for landfills. *Proceedings of the Institution of Civil Engineers: Geotechnical Engineering*, 137(4), 235-247. <https://doi.org/10.1680/geng.1997.137.4.235>.
- Reddy, K.R., Gangathulasi, J., Parakalla, N.S., Hettiarachchi, H., Bogner, J.E., & Lagier, T. (2009). Compressibility and shear strength of municipal solid waste under short-term leachate recirculation operations. *Waste Management & Research*, 27(6), 578-587. <https://doi.org/10.1177/0734242X09103825>.
- Reddy, K.R., Hettiarachchi, H., Gangathulasi, J., & Bogner, J.E. (2011). Geotechnical properties of municipal solid waste at different phases of biodegradation. *Waste Management (New York, N.Y.)*, 31(11), 2275-2286. <https://doi.org/10.1016/j.wasman.2011.06.002>.
- Rosqvist, H., Dahlin, T., Linders, F., & Meijer, J.E. (2007). Detection of water and gas migration in a bioreactor landfill using geoelectrical imaging and a tracer test. In *Proceedings of the 11th International Waste Management and Landfill Symposium - Sardinia 2007* (pp. 267-274). Italy: CISA.
- Shi, J., Wu, X., Ai, Y., & Zhang, Z. (2018). Laboratory test investigations on soil water characteristic curve and air permeability of municipal solid waste. *Waste Management & Research*, 36(5), 463-470. <https://doi.org/10.1177/0734242X18766223>.
- Stoltz, G., Tinet, A.-J., Staub, M.J., Oxarango, L., & Gourc, J.-P. (2012). Moisture retention properties of municipal solid waste in relation to compression. *Journal of Geotechnical and Geoenvironmental Engineering*, 138(4), 535-543. [https://doi.org/10.1061/\(asce\)gt.1943-5606.0000616](https://doi.org/10.1061/(asce)gt.1943-5606.0000616).
- van Genuchten, M. (1980). A closed-form equation for predicting the hydraulic conductivity of unsaturated soils. *Soil Science Society of America Journal*, 44, 892-898. <https://doi.org/10.2136/sssaj1980.03615995004400050002x>.
- Wu, H., Wang, H., Zhao, Y., Chen, T., & Lu, W. (2012). Evolution of unsaturated hydraulic properties of municipal solid waste with landfill depth and age. *Waste Management (New York, N.Y.)*, 32(3), 463-470. <https://doi.org/10.1016/j.wasman.2011.10.029>.
- Zhang, W., & Lin, M. (2019). Evaluating the dual porosity of landfilled municipal solid waste. *Environmental Science and Pollution Research International*, 26(12), 12080-12088. <https://doi.org/10.1007/s11356-019-04607-2>.





## ***REVIEW ARTICLES***

***Soils and Rocks***  
**v. 44, n. 3**



## Review of expansive and collapsible soil volume change models within a unified elastoplastic framework

Sandra L. Houston<sup>1#</sup> , Xiong Zhang<sup>2</sup> 

Review Article

### Keywords

Volume change of unsaturated soils  
Expansive soils  
Collapsible soils  
Elastoplastic models  
Oedometer methods

### Abstract

Numerous laboratory tests on unsaturated soils revealed complex volume-change response to reduction of soil suction, resulting in early development of state surface approaches that incorporate soil expansion or collapse due to wetting under load. Nonetheless, expansive and collapsible soils are often viewed separately in research and practice, resulting in development of numerous constitutive models specific to the direction of volume change resulting from suction decrease. In addition, several elastoplastic models, developed primarily for collapse or expansion, are modified by add-on, such as multiple yield curves/surfaces, to accommodate a broader range of soil response. Current tendency to think of unsaturated soils as either expansive or collapsible (or, sometimes, stable), has likely contributed to lack of development of a unified approach to unsaturated soil volume change. In this paper, common research and practice approaches to volume change of unsaturated soils are reviewed within a simple macro-level elastoplastic framework, the Modified State Surface Approach (MSSA). The MSSA emerges as a unifying approach that accommodates complex volume change response of unsaturated soil, whether the soil exhibits collapse, expansion, or both. Suggestions are made for minor adjustments to existing constitutive models from this review, typically resulting in simplification and/or benefit to some of the most-used constitutive models for unsaturated soil volume change. In the review of practice-based approaches, the surrogate path method (SPM), an oedometer/suction-based approach, is demonstrated to be consistent with the MSSA framework, broadly applicable for use with expansive and collapsible soils, and yielding results consistent with measured field stress-path soil response.

### 1. Introduction

An unsaturated soil exhibits volume change in response to changes in one or both stress state variables (net total stress and matric suction). For unsaturated soil volume change, changes in volume of the soil matrix and the water phase (commonly represented by the void ratio and gravimetric water content, respectively) occur, giving rise to well-known state surfaces in unsaturated soil mechanics (Matyas & Radhakrishna, 1968; Fredlund & Morgenstern, 1976, 1977; Lloret & Alonso, 1980, 1985). Figure 1 shows a representative schematic plot of the void ratio surface of Matyas & Radhakrishna (1968). As discussed in Wheeler & Karube (1996), volume change response of unsaturated soils is complex, particularly for changes in soil suction. An increase in net total stress always results in volume reduction of an unsaturated soil (AB or A'B' in Figure 1). However, essentially any soil with some clay content may compress or

expand in response to reduction of soil suction, depending on the magnitude of the net total stress and the initial soil suction, as well as soil structure (Jennings & Burland, 1962; Fredlund & Rahardjo, 1993; Delage & Graham, 1996; White, 2007). At low net total stress, a clay typically exhibits expansion upon wetting (AA' as shown in Figure 1a), but at high net total stress, it may exhibit compression upon wetting (BB' as shown in Figure 1). Computation of volume change requires the consideration of the initial soil state, including stress history, along with simultaneous consideration of both stress state variables of net total stress and matric suction. Thus, it can be difficult to intuit even the direction (compression or expansion) of suction-induced volume change.

Historically, geotechnical engineers have classified a soil that exhibits substantial increases in volume in response to wetting as expansive and soil that exhibits substantial

<sup>#</sup>Corresponding author. E-mail address: sandra.houston@asu.edu

<sup>1</sup>Arizona State University, Tempe, AZ, USA.

<sup>2</sup>Missouri University of Science and Technology, Rolla, MO, USA.

Submitted on March 11, 2021; Final Acceptance on June 16, 2021; Discussion open until November 30, 2021.

<https://doi.org/10.28927/SR.2021.064321>



This is an Open Access article distributed under the terms of the Creative Commons Attribution License, which permits unrestricted use, distribution, and reproduction in any medium, provided the original work is properly cited.



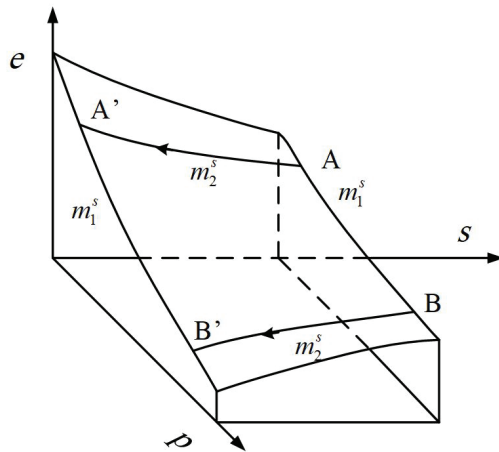


**Figure 1.** Warped state surfaces for void ratio of Matyas & Radhakrishna (1968), showing instantaneous state surface slopes with respect to matric suction and net total stress of Fredlund & Rahardjo (1993).

decreases in volume in response to wetting as collapsible. Such classifications are convenient short hands, as are other common generalizations – unsaturated fat clays increase in volume when wetted whereas unsaturated low-density silts decrease in volume when wetted; smectite clays of sedimentary origin expand upon wetting, and loessial soils collapse upon wetting. Further, expansive clays and collapsible soils, separately rather than together, are classified as natural hazards due to the potential for severe damage to infrastructure that can occur when soils exhibit large volume change upon wetting under load. Expansive soils result in an estimated \$15 billion annual cost of damage to infrastructure in the USA, more than £400 million a year in cost to British insurance companies, and are recognized as one of the most common causes of damage to roadways (Driscoll & Crilly, 2000; Jones, 2018; Jones & Jefferson, 2012; Nelson & Miller, 1992; Dessouky et al., 2012). Collapsible soils can cause severe damage to critical infrastructure, including canals, dams, pipelines, roads, and buildings (Knodel, 1992; Li et al., 2016; Fonte et al., 2017).

The long history of separation of expansive soil and collapsible soils in research and practice has resulted in the creation of many volume change constitutive models that are specific to the direction of volume change upon soil wetting (suction reduction). Some elastoplastic models are primarily for collapsible or expansive conditions, but empirically, and often inconsistently, incorporate multiple yield surfaces to accommodate both volume change responses. A constitutive model for evaluation of volume change of an expansive clay may not be best for predominantly collapsible soils and vice versa. This reality of emphasis on either expansive or collapsible response has not necessarily hampered progress in dealing with real-world unsaturated soil volume-change problems. But separation of expansive and collapsible soils has contributed, most likely, to lack of progress in the

development of a unified approach to calculation of volume change of unsaturated soils, which can lead to significant differences in volume change prediction, even for a specific field prototype.

More general volume change models are appropriate for heterogeneous soil profiles containing soil types with mixed (expansion or collapse) suction-changed induced volume change response, and to more homogenous soil profiles that exhibit both expansion and collapse upon wetting, depending on the net total stress conditions. It is the intent of this paper to briefly review available approaches to modeling expansive and collapsible soils and to present in more detail the modified state surface approach (MSSA), as a broadly applicable macro-level elastoplastic framework for modeling unsaturated soil volume change.

The MSSA, first introduced by Zhang & Lytton (2009a, b), allows for a soil response of expansion, collapse, or both and accommodates the full range of volume change response through the use of unique elastoplastic state surfaces for void ratio and water content. The MSSA is based on two independent stress state variables of matric suction and mean net stress and builds upon the traditional state surface approach (Matyas & Radhakrishna, 1968; Lloret & Alonso, 1980, 1985; Fredlund & Rahardjo, 1993). The MSSA was later extended to handle triaxial stress state conditions (Zhang, 2010), and coupled hydro-mechanical unsaturated soil behavior (Zhang & Lytton, 2012), with considerations of both mechanical and hydraulic hysteresis (Riad & Zhang, 2020, 2021). However, in this paper, only soil structure (void ratio) volume change constitutive models are considered, and companion volume change models for the water phase are not addressed. It will be demonstrated how existing approaches to modeling unsaturated soil volume change can be accommodated within the MSSA framework. Where minor adjustments to existing constitutive models are shown to be appropriate, according to the MSSA, such modifications will be shown to lead to overall simplification and some benefits, in general, in the constitutive modelling of unsaturated soils.

## 2. Overview of available constitutive models

Decades of research on expansive and collapsible soils has resulted in the development of numerous constitutive models for the estimation of volume change of unsaturated soils. Foundation engineering work resulted in practice-based models for the computation of vertical strains (deformations), under  $K_0$  conditions: (a) for expansive soils (Washington, 1983; Picornell & Lytton, 1984; Lytton, 1977; Fredlund et al., 1980; Nelson & Miller, 1992; Noorany & Houston, 1995; Overton et al., 2006; Adem & Vanapalli, 2013; Houston & Houston, 2018), and (b) for collapsible soils (Jennings & Knight, 1957; Houston et al., 1988; Washington, 1983; Barden et al., 1973; Houston & Houston, 1997). Many 1-D models are for problems of either expansion or collapse volume change due to monotonic suction change (typically

wetting) under constant confining stress (load), due to the importance of this boundary condition for many practical problems. A suction-oedometer method, termed the surrogate path method (SPM), is applicable to expansive and collapsible soils, and is a practice-based approach for estimation of 1-D volume change of unsaturated soil for monotonic change in soil suction under constant net total stress conditions (Houston & Houston, 2018; Singhal, 2010).

Fredlund & Rahardjo (1993) and Fredlund & Morgenstern (1976) set forth a general 3-D volume change model for unsaturated soils based on incremental elasticity, which was expanded upon by Vu & Fredlund (2004, 2006) in the analysis of wetting-induced expansive soil movements. Zhang (2005), Wray et al. (2005), and Zhang & Briaud (2015) also developed generalized 3-D volume change models for expansive soils based on incremental elasticity. Theoretically, both expansive and collapsible soil response can be modeled using incremental elasticity due to the ability to adjust soil parameters for various ranges in a stress state. However, unsaturated collapsible soils exhibit clear irrecoverable volume change, and the process is therefore truly elastoplastic (Alonso, 1987; Alonso et al., 1990). The emphasis to date has been on the use of incremental 3-D elastic models for problems of soil expansion, with few exceptions such as Lloret & Alonso (1980) and Pereira & Fredlund (1997) who used incremental elasticity for collapsible soils.

Several elastoplastic models using the two stress state variable approach for the estimation of volume change of unsaturated soils are available (Alonso et al., 1990, 1994, 1999; Gens & Alonso, 1992; Cui & Delage, 1996; Bolzon et al., 1996; Delage & Graham, 1996; Gens et al., 1996; Wheeler & Sivakumar, 1995; Wheeler, 1996; Wheeler et al., 2003; Dangla et al., 1997; Vaunat et al., 2000; Geiser et al., 2000; Khalili & Loret, 2001; Gallipoli et al., 2003a, b; Sheng et al., 2003a, b, 2004, 2008a, b; Tamagnini, 2004; Vassallo, et al., 2007; Costa & Alonso, 2009). The focus of early elastoplastic models was on unsaturated collapsible soil behavior due to the vast attention placed on the Barcelona Basic Model, BBM (Alonso et al., 1990). Within the BBM, soil expansion is typically accomplished through the introduction of an additional Suction Increase (SI) yield surface. While the use of multiple yield surfaces accomplishes the goal of well-matching laboratory test results, this approach often results in sharp transitions in soil response at the intersections of the yield surfaces, and some inconsistencies between the constitutive model and established virgin loading response of soils (Delage & Graham, 1996; Zhang & Lytton, 2009a, b). Zhang & Lytton (2009a, b) present a macro-level elastoplastic method, the modified state surface approach (MSSA), which makes use of a unique virgin loading state surface. The MSSA is theoretically applicable to both collapsible and expansive soils.

Alonso et al. (1999) proposed an elastoplastic constitutive model (BExM), incorporating soil responses at both the micro- and macro-levels to simulate wetting-induced swell of expansive soils, again making use of multiple

yield surfaces. Several other dual structure (micro-macro) constitutive models have been developed for expansive soils (e.g., Sánchez et al., 2005; Vilarrasa et al., 2016). Micro-macro constitutive models for collapsible soils, however, have not received a great deal of attention to date. Highly complex thermo-hydro-mechanical models have been developed, particularly for expansive soils, and mainly due to consideration of using clay-bentonite soil mixtures as part of a barrier system in the containment of radioactive wastes (Gens & Olivella, 2001; Lloret et al., 2003; Sánchez et al., 2005). At the research level, micro-macro constitutive models appear to play an important role, most notably in applications to nuclear waste isolation. On the other hand, dual-structure/micro-macro constitutive models require the determination of many parameters, too many of which can be obtained only by estimation from back-analysis, rather than by direct determination. Complex micro-macro models can also represent a deterrent to the application of unsaturated soil mechanics to routine geotechnical engineering problems.

Unsaturated soil volume change constitutive models may be macro-level or micro-macro level in nature. The micro-level structure of common expansive clay minerals allows firm absorption of water internal to particles, increasing the spacing between particles, and inducing swell macroscopically (Lin & Cerato, 2014; Sánchez et al., 2005). In collapsible soils, the water leads to the softening of clay particles that bind the open-void macro-structure of the soil together, contributing to the triggering of collapse (Liu et al., 2016). An understanding of the role of micro-level response to changes in the state of stress of unsaturated soil is important and can be particularly useful in the search and for selection of mitigation alternatives, and micro-level investigations lead to enhanced understanding of the role of water as a volume-change trigger (Bellil et al., 2018; Liu et al., 2016; Lin et al., 2013). However, it can be debated whether modeling of micro-level phenomena is required, or desirable, in the computation volume change of unsaturated soils (Vilarrasa et al., 2016; Alonso et al., 1999; Fredlund & Morgenstern, 1976; Fredlund, 1979; Houston, 2019).

Relatively simple macro-level approaches, requiring experimentally obtainable soil parameters, are available for the computation of volume change of unsaturated soils, whether the response is expansion or collapse, or both, as cited above. Such models may be based on coupled or uncoupled hydro-mechanical approaches, and may be 3-D incremental elastic or elastoplastic, or simply limited to 1-D monotonic loading conditions. An argument can be made for the use of the simplest appropriate model for the particular volume change case at hand. The MSSA, as first proposed by Zhang & Lytton (2009a, b, 2012) for isotropic conditions and then extended to triaxial stress states (Zhang, 2010; Zhang et al., 2016a) with consideration of coupled hydro-mechanical hysteresis (Riad & Zhang, 2020, 2021), is a generalized elastoplastic framework that is theoretically sound and generally appropriate across all known unsaturated

soil volume change responses. The MSSA is not a specific constitutive model itself but can be viewed as a unifying framework to study existing models and develop new models for unsaturated soils.

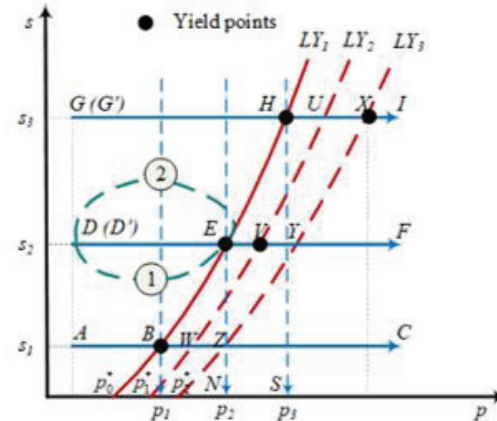
### 3. Modified state surface approach

Conventional elasto-plastic models for soils are developed in an incremental form according to classical elastoplasticity, which was first applied to solid materials such as metals. The use of simple stress-strain relationships, while convenient and straightforward where laboratory data is uncomplicated, is not particularly helpful for unsaturated soils where behavior is highly nonlinear and laboratory results have to be compared from multiple specimens with differing stress histories, and where multiple stress state variables influence the soil responses. In the development of commonly used unsaturated soil elastoplastic models, some of the inherent relationships between different components of the model have not been clearly explained in the past. In addition, unsaturated soil elastoplastic models have not taken full advantage of some features of material behavior, such as the uniqueness of the state boundary surface for virgin loading conditions. Due to unsaturated soil response being highly nonlinear and influenced by multiple factors, when the incremental form for elastoplastic behavior is used, huge challenges are created for the testing, constitutive model development and model calibration (D'Onza et al., 2015). By contrast, the MSSA takes full advantage of the uniqueness of the state boundary surface (elastoplastic virgin loading surface), simplifying the process of constitutive modeling. The MSSA can be used to deal with large amounts of potentially confusing data and synthesize the data into a usable form. The MSSA can be used to explain the elastoplastic behavior of unsaturated soils in a relatively simple way without undue complication.

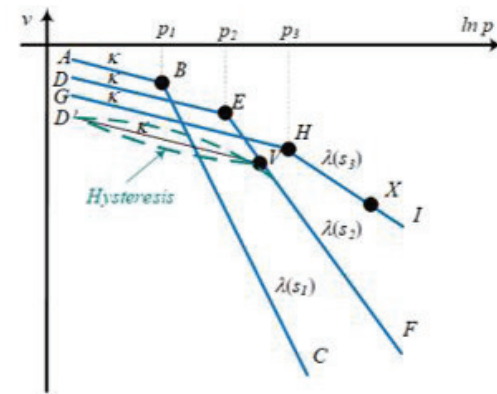
#### 3.1 Principle of the MSSA

The principle of the MSSA can be illustrated by Figure 2. Figure 2 shows the stress paths for three isotropic loading-unloading-reloading tests. Under an arbitrary constant suction  $s = s_2$ , the soil specimen has an initial condition of point D. The initial yield curve of the soil is  $LY_1$  with a preconsolidation stress of  $p_0^*$  at  $s = 0$  kPa and the yield stress at  $s = s_2$  is  $p_2$  at point E (Figure 2b). The soil is loaded from D to E to V, unloaded from V to D', and then reloaded from D' to V to F in Figure 2b which illustrates a typical soil response in the  $v$ - $\ln p$  plane when the hysteresis is neglected. The following observations can be made from the process:

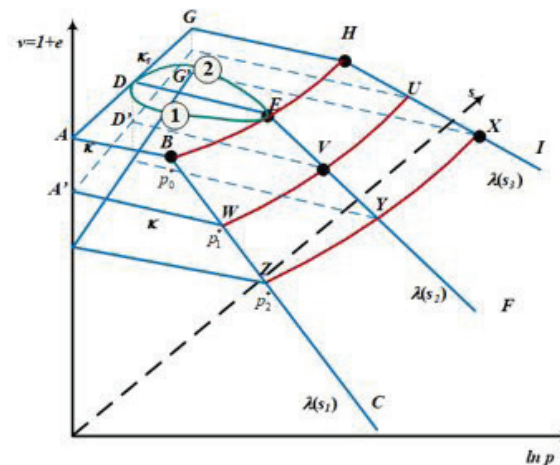
1. Regardless of stress path and stress history, the shape and position of the virgin loading curve EVF are always the same for the soil in the  $v$ - $\ln p$  plane. Plastic loading only changes the range of the virgin



(a)



(b)



(c)

**Figure 2.** Principle of the MSSA. (a) conventional interpretation of tests to determine parameters for the BBM (Alonso et al., 1990); (b) volume change upon loading at different suctions from suction controlled compression tests; (c) three-dimensional representation of volume change of the soil.



loading curve. For example, the initial virgin loading curve for the soil is EVF. After loading from D to E to V, the virgin curve for the soil is VF;

2. During an elastic loading or unloading process, for example, from D to E, from V to D', or from D' to V, the shape and position of the unloading-reloading curve remain unchanged in the  $v$ - $\ln p$  plane. During a plastic loading process, the shape and slope of the unloading-reloading curve remains unchanged in the  $v$ - $\ln p$  plane, but its position will change. Specifically, the unloading-reloading curve will move downward in parallel with the original unloading-reloading curve. The range of the elastic zone also expands due to the increase in the preconsolidation stress from  $p_0^*$  to  $p_1^*$ ;
3. The yield point V is the intersection of the unloading-reloading curve and the virgin loading curve for  $s = s_2$ .

It is worth noting that in nearly all existing constitutive models  $\kappa$  is assumed a constant. To keep the explanation simple,  $\kappa$  is assumed a constant in the following discussion. This assumption can be easily taken out in the use of the MSSA to handle more general cases of varying  $\kappa$ .

Consider two other stress paths from D to E, i.e. paths 1 and 2 as shown in Figure 2a, and in the elastic zone. Since stress paths 1 and 2 are in the elastic zone, the specific volume changes are stress path independent. The results obtained for the two stress paths should be the same and the volume in the elastic zone can be expressed as a surface ABEHGDA in the  $v$ - $p$ - $s$  space as shown in Figure 2c (Zhang & Lytton, 2009a, b).

Figure 2c shows the specific volume change for the stress paths in Figure 2a in the  $v$ - $p$ - $s$  space. All the elastic volume changes, such as stress paths 1 and 2 and DE are on the same surface of ABEHGDA. When there is a plastic loading, similar to the previous discussion, the shape and position of the virgin loading curve EVF are always the same in the  $v$ - $p$ - $s$  space regardless of the previous stress path and stress history in the elastic zone. It can also be proven that when there is unloading, any unloading stress path must fall on a lower elastic surface.

Compression tests can be performed at any arbitrary suction level, such as  $s_1$  and  $s_3$  as shown in Figures 2a and 2b. Consequently, the virgin curves at different suction levels as shown in Figure 2b will form a "plastic (virgin) loading surface" in the  $v$ - $p$ - $s$  space such as BEHUXYZWB in Figure 2c. The location and shape of the plastic surface will always remain the same in the  $v$ - $p$ - $s$  space and the plastic surface is unique. The uniqueness of the virgin state boundary surface is a fundamental assumption made in the constitutive modeling of elastoplastic soil behavior. The uniqueness of the state boundary surface for unsaturated soils has been experimentally verified by Wheeler & Sivakumar (1995). The plastic surface BEHUXYZWB in Figure 2c is the shape of the state boundary surface for isotropic conditions. In the

$v$ - $p$ - $s$  space, the following assertions can be made for the elastic and plastic surfaces:

1. The shape and position of the plastic surface are always the same for the soil in the  $v$ - $p$ - $s$  space. Virgin loading only changes the range of the plastic surface;
2. During an elastic loading or unloading process, the shape and position of the unloading-reloading elastic surface and the plastic surface remain unchanged in the  $v$ - $p$ - $s$  space. The specific volume of any isotropic elastic loading or unloading stress path must fall on the elastic surface in the  $v$ - $p$ - $s$  space. During a plastic loading process, the shape of the unloading-reloading elastic surface remains unchanged ( $\kappa$  and  $\kappa_s$  are constants for an assumed planar elastic surface), but its position will shift. Specifically, the unloading-reloading elastic surface will move downward in parallel with the original unloading-reloading elastic surface. For example, the unloading stress path V to D' will fall on the new elastic surface A'WVUG'D'. The volume change of any isotropic plastic loading stress path must fall on the plastic surface in the  $v$ - $p$ - $s$  space;
3. The yield curve is the intersection of the unloading-reloading elastic surface and the plastic surface.

The MSSA can be easily extended to the triaxial stress states in the  $v$ - $p$ - $q$ - $s$  space (which also considers deviator stress,  $q$ ) as follows (Zhang, 2010; Zhang et al., 2016a, b):

1. There is a unique state boundary surface in the elastoplastic region which is always unchanged in the  $v$ - $p$ - $q$ - $s$  space;
2. The elastic surface is movable, but only moves when there is plastic loading. The elastic surface is fixed when there is elastic loading or unloading;
3. All the soil responses will fall on either the elastic or plastic surface;
4. The intersection between the elastic and plastic hypersurface is the yield surface; and
5. The plastic hypersurface ends when the soil fails, which is at the critical state.

Zhang & Lytton (2012) extended the MSSA for the coupled hydro-mechanical behavior of unsaturated soils. Riad & Zhang (2020, 2021) further extended the MSSA to include the coupled hydro-mechanical hysteresis for unsaturated soils. However, here only the soil structure constitutive relationships are discussed.

### 3.2 Surfaces used in the BBM

The MSSA can be used to explain existing constitutive models in a simple way. As an example, Zhang & Lytton (2009a) derived the close-form expressions of the elastic and elastoplastic surfaces for the BBM (Equations 1, 2, and 3, below) and successfully used the MSSA to represent many unsaturated soil behaviors, including the stress path independency under isotropic conditions. Figure 3 shows the



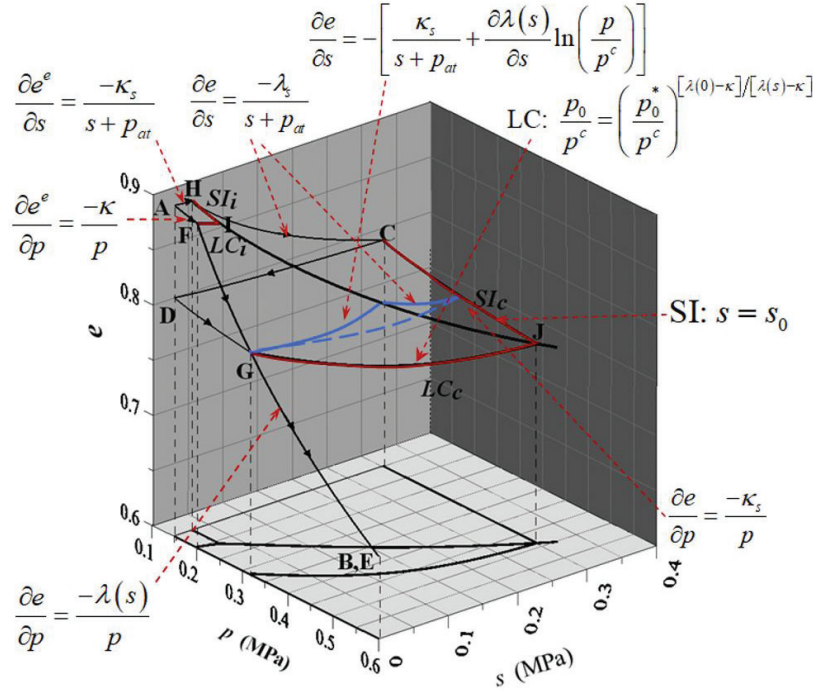


**Figure 3.** State Boundary Surface for the BBM (modified from Zhang & Lytton, 2009a).

elastic and plastic surfaces used in the BBM. They include an elastic surface AFIH and the plastic surface which is made up of two parts: a plastic collapsible surface FIJG (corresponding to the LC yield curve) and a plastic expansive surface HIJC (corresponding to the SI curve). The mathematical expressions for the three surfaces are as follows:

$$e^e = C_1 - \kappa \ln p - \kappa_s \ln(s + p_{at}) \quad (1)$$

(elastic surface AFIH)

$$e = C_2 - \kappa_s \ln\left(\frac{s + p_{at}}{p_{at}}\right) - \lambda(s) \ln\left(\frac{p}{p^c}\right) \quad (2)$$

(plastic collapsible surface FIJG)

$$e = C_3 - \kappa \ln p - \lambda_s \ln(s + p_{at}) \quad (3)$$

(plastic expansive surface HIJC)

where  $\lambda(s) = \lambda(0)[(1-r)\exp(-\beta s) + r]$ ,  $r$  = parameter controlling the slope of the virgin compression line,  $\beta$  = parameter controlling the slope of the virgin compression line for  $s \neq 0$ ,  $\lambda(0)$  = slope of the virgin compression line associated with the mean net stress at saturation ( $s=0$ );  $p^c$  = reference stress,  $C_2 = N(0)$  in the BBM = a constant,  $\lambda_s$  = slope of the virgin compression line associated with soil suction,  $p_{at}$  = atmospheric pressure,  $\kappa$  = slope of the unloading-reloading line associated to the mean net stress,  $\kappa_s$  = slope of the unloading-reloading line associated with soil suction, and  $C_1$  and  $C_3$  = are constants. The superscripts “e” represents the elastic change in the specific volume.

The LC yield curve is the intersection of the elastic surface and collapsible soil surface. In other words, the points on the LC curve must simultaneously satisfy Equations 1 and 2, which gives:

$$\ln\left(\frac{p}{p^c}\right) = \frac{C_4}{\lambda(s) - \kappa} \quad (4)$$

where  $C_4 = N(0) - C_1 + \kappa \ln(p^c) + \kappa_s \ln(p_{at})$  = constant. The yield stress when the soil is saturated is the preconsolidation stress, that is,  $p = p_0^*$  when  $s = 0$ , which gives:

$$C_4 = [\lambda(0) - \kappa] \ln\left(\frac{p_0^*}{p^c}\right) \quad (5)$$

Substituting Equation 4 into Equation 3, the yield curve equation in the BBM is obtained as follows:

$$p = p^c \left[ \frac{p_0^*}{p^c} \right]^{\frac{\lambda(0) - \kappa}{\lambda(s) - \kappa}} \quad (6)$$

Similarly, the SI yield curve is the intersection of the elastic surface and the plastic expansive soil surface. The points on the SI curve must simultaneously satisfy Equations 1 and 3 as expressed as follows.

$$s = e^{\frac{C_3 - C_1}{(\lambda_s - \kappa_s)}} - p_{at} = \text{constant} \quad (7)$$

Zhang (2010) also derived the plastic hardening equation for the BBM under a triaxial stress states as follows:

$$e = C_2 - \kappa \ln \frac{p}{p^c} - \kappa_s \ln \left( \frac{s + p_{at}}{p_{at}} \right) - (\lambda(s) - \kappa) \left[ \ln \left( p + \frac{q^2}{M^2(p + ks)} \right) - \ln p^c \right] \quad (8)$$

where  $q = \sigma_1 - \sigma_3$  = deviatoric stress,  $k$  = parameter that relates cohesion and suction, and  $M$  = slope of theoretical critical state line.

The above equations, and Figure 3, show the BBM model within the framework of the MSSA. The BBM was selected as an example to demonstrate how the MSSA principles can be used in describing existing elastoplastic models. Similarly, other elastoplastic models for unsaturated soils can be described within the MSSA framework, provided that the model maintains consistency with all of the requirements of traditional elastoplastic theory.

### 3.3 Relationship between MSSA and existing approaches

The MSSA is consistent with the existing theories of elastoplasticity for unsaturated soils. At present, most researchers first propose some constitutive relationships for specific soil behavior in the elastic and elastoplastic zones in incremental forms and then the constitutive relationships are assembled together into a constitutive model to predict soil behavior under arbitrary stress paths. For example, in the BBM, in the elastic zone, incremental formulations were developed to calculate the specific volume changes for an unsaturated soil due to net total stress and suction as follows:

$$\frac{\partial e^e}{\partial p} = \frac{-\kappa}{p} \quad (9)$$

$$\frac{\partial e^e}{\partial s} = \frac{-\kappa_s}{s + p_{at}} \quad (10)$$

Figure 3 also shows the partial derivatives of the BBM surfaces with respect to the net total stress and matric suction. When there are simultaneous changes in the net total stress and suction in the elastic region, the above two equations are assembled together to calculate the total void ratio change:

$$de^e = -\kappa \frac{dp}{p} - \kappa_s \frac{ds}{s + p_{at}} \quad (11)$$

The specific volume change from a known initial point to any stress state in the elastic region is the line integral of Equation 11, resulting in Equation 1. Equation 1 is the closed form expression for void ratio for the elastic surface of the BBM, which was obtained using the MSSA. When the constitutive relations are simple linear equations, the level of difficulty in using the MSSA and the conventional incremental formulation is about the same. Equations 9 and

10 can be obtained by taking partial derivatives of Equation 1 with respect to the net total stress and suction respectively, demonstrating that the incremental plasticity and MSSA methods are interchangeable.

Unsaturated soil behavior, however, is very complicated and notoriously highly nonlinear. It is hence very difficult to use the incremental approach to develop constitutive models for unsaturated soils. For example, use of the incremental formulation to develop the BBM under isotropic conditions requires the following two constitutive relations to describe the plastic collapsible surface (FIJG as shown in Figure 3, corresponding to the LC yield curve) in the original BBM:

$$\frac{\partial e}{\partial p} = \frac{-\lambda(s)}{p} \quad (12)$$

$$\frac{\partial e}{\partial s} = - \left[ \frac{\kappa_s}{s + p_{at}} + \frac{\partial \lambda(s)}{\partial s} \ln \left( \frac{p}{p^s} \right) \right] \quad (13)$$

While Equation 12 is simple and frequently adopted by most researchers, Equation 13 is very complicated and difficult to visualize, or even imagine. In addition, Equations 12 and 13 are interdependent (Zhang & Lytton, 2008). In the original BBM, such a complicated formulation was successfully avoided by properly selecting  $\lambda(s)$  and  $N(s)$  in integrated forms. However, such clever approaches to simplification are not commonly used for constitutive modelling of unsaturated soils.

Similarly, the following two constitutive relations to describe the plastic expansive soil surface (corresponding to the SI yield curve) in the original BBM:

$$\frac{\partial e}{\partial p} = \frac{-\kappa}{p} \quad (14)$$

$$\frac{\partial e}{\partial s} = - \frac{\lambda_s}{s + p_{at}} \quad (15)$$

Equation 14 is the same as Equation 9, which is caused by the assumed horizontal SI yield curve. Equations 13 and 15 are significantly different and are used to simulate the collapse and swelling upon wetting for unsaturated soils, respectively. More detailed comparison and explanation regarding Equations 12 to 15 will be made in the later sections.

Another simple example of challenges faced in use of incremental formulations can be made by introducing some dependency on suction in Equation 9 in elastic region, such as in Equation 16:

$$\frac{\partial e^e}{\partial p} = \frac{-\kappa}{p + s} \quad (16)$$

Equation 16 violates stress path independency in the elastic region, simply from the addition of suction in Equation 9. In the plot of Figure 2, Equations 9 and 10 are

used to describe the elastic surface, and taking two different paths, 1 and 2, in the elastic region results in arrival at the same void ratio, point E (Figure 2). However, if Equation 16 is adopted to replace Equation 9, the two different elastic region stress paths of 1 and 2 of Figure 2 will no longer give the same void ratio at point E within the  $p$ - $s$ - $v$  space of Figure 2c. This directly conflicts with the elasticity assumption in the elastic region, as mentioned by Wheeler & Karube (1996), but received little attention. The conflict with required stress path independency in the elastic zone is due to failure to adhere to Green's theorem, as discussed in detail by Zhang & Lytton (2008).

As can be seen, use of the incremental formulation approach makes it very difficult for constitutive modeling of highly nonlinear unsaturated soil behavior. Similar discussions have been provided by Zhang & Lytton (2008) regarding the SFG model (Sheng et al., 2008a). Instead, if the MSSA is used, one just needs to obtain the best-fit smooth functions for the elastic and plastic surfaces, matching the results from available isotropic compression tests. In this way, the constitutive model for isotropic conditions is obtained as well as the yield curve and its evolution with plastic hardening (Zhang et al., 2010; Zhang, 2016). After that, by simply taking partial derivatives of the elastic and elastoplastic surfaces, the incremental formulation of the elastoplastic model is obtained in a consistent way. Using the MSSA, there is no need to check consistency with laboratory/observed soil response since Green's theorem is automatically satisfied. When incremental formulations are used, consistency with observed soil response is not automatically assured, which can lead to violation of fundamentals of elastoplastic theory as discussed in the previous sections.

The MSSA can be used to describe some existing models within a unified framework, and also to develop new models. Zhang & Lytton (2009a) indicated that for the same experimental results of Karube (1986), the MSSA can be used to develop a simpler model compared to the BBM (6 model parameters in the MSSA model vs. 11 in the BBM). Also, for the specific Karube (1986) data, the MSSA predictions represent an improvement over those obtained using the BBM (Alonso et al. 1990).

### 3.4 Determination of yield curve and model development

An alternative way to develop a constitutive model using an incremental formulation is to define the elastic relationship and the yield curve and its evolution. As pointed out by Wheeler & Karube (1996, p. 1338), "[...] *in developing an elastoplastic model, it is therefore only necessary to define either the changing shape of the yield curve as it expands or the form of the normal compression lines for different values of suction.*" This approach is relatively straightforward and well-established for both saturated and unsaturated soils.

However, it is very difficult to accurately determine the yield curve and its evolution, as demonstrated below.

It was extensively accepted that the shape of the BBM LC yield curve can be independently determined from isotropic loading tests at varying constant suction using soil specimens with identical stress histories (Alonso et al., 1990, 1994, 1999; Gens & Alonso, 1992; Delage & Graham, 1996; Gens et al., 1996; Wheeler & Karube, 1996; Cui & Delage, 1996; Wheeler & Sivakumar, 1995; Vaunat et al., 2000; Robles & Elorza, 2002; Gallipoli et al., 2003a; Sheng et al., 2004; Wheeler, 1996; Wheeler et al., 2003; Thu et al., 2007). Figure 2a schematically illustrates the stress paths for three isotropic loading tests. Figure 2b shows the specific volume  $v$  versus  $\ln p$  curves for three isotropic loading tests under constant suction. The three yield points, determined by Casagrande's method (Casagrande, 1936) for each test, are B, E, and H, respectively, as shown in Figure 2b. These points are connected into a curve in Figure 2a to represent the initial shape of the BBM LC yield curve for the soil.

Although the above method is straightforward and well-established, it is difficult to implement correctly in the laboratory since it requires that all tested soil specimens have exactly identical stress histories. However, identical specimen history is only theoretically possible because loading, drying, and wetting can cause the soil to yield and the positions of the SI yield curves to change. In addition, even if identical specimens can be obtained, the soil may have different stress histories due to improper experimental design resulting from the initial positions of the LC and SI yield curves being unknown before the soil specimens are tested (Zhang et al., 2010). Numerous researchers reported that carefully prepared "identical specimens" were found to have different yield points when the soil specimens were tested following exact stress paths (Wheeler & Sivakumar, 1995; Rampino et al., 2000; Blatz & Graham, 2003). For soil specimens with different stress histories, their positions of LC and SI yield curves will be different. Furthermore, the Casagrande's method is an empirical method and cannot produce highly accurate results for the yield stress. Consequently, use of the above conventional method for obtaining the LC yield curve can lead to incorrect results.

Consider the MSSA principles represented in Figure 2, when the soil specimens have different stress histories, or the stress histories are changed during the soil preparation process, the actual test results could be D'V YF and G'XI in Figure 2c for the stress paths D'V YF and G'XI in Figure 2a. Since the patterns of the results for stress paths with different stress histories are very similar, such as DEVF and D'VF in Figure 2b, one can easily mistake yield point V as E and consider BVX as the shape of the yield curve, when in fact the point V belongs to another yield curve (UVW) different from the actual yield curve of BEH. It is noted that there are many other possibilities for the relative positions of the yield points, and therefore use of conventional methods for determination of the LC curve can result in yield curves with

shapes significantly different from either BVX or BEH. In addition, the above approach can only be used to estimate the initial shape of the yield curve. Typically only one yield curve is experimentally determined from three or more suction-controlled laboratory compression tests for each LC determination, and data on how the yield curve evolves during the plastic hardening process is often unavailable.

One important application of the MSSA is to determine the shape of yield curves and their evolution, as discussed in Zhang et al. (2010). The MSSA clearly defines the relationship between the form of the normal compression lines in the  $v: p$  plane and the shape of the yield curve as it expands in the  $s: p$  plane. According to MSSA, the yield curves are the intersection of the elastic and plastic surfaces. The evolution of the yield curves forms the plastic surface or, one can say that the plastic surface is a “trace” of the yield curves. Consider the case where three suction-controlled compression test specimens do not have the same stress history. In this case, results from the three isotropic compression tests could, for example, be ABC, D’VF, and G’XI as shown in Figure 2c, resulting in determination of three yield points B, V, and X, belonging to three different yield curves,  $LY_1$ ,  $LY_2$ , and  $LY_3$  (Figure 2a) respectively. As can be seen in Figure 2c, in the three-dimensional  $p-s-v$  plot the virgin normal compression curves BC, VF, and XI will fall on a unique plastic hardening surface while the elastic compression curves AB, D’V, and G’X belong to different elastic surfaces. According to the MSSA, the shape and position of the elastoplastic surface does not change during yielding (but the range of the plastic hardening surface will change). Consequently, the plastic hardening surface obtained from the three soil specimens with different stress histories, BCFIXV, is a subset of the plastic hardening surface that formed from the three theoretical soil specimens with the exactly the same stress history (BCFIHE). Using the principles of the MSSA, the virgin compression curves BC, VF, and XI establish the shape of the plastic surface, in spite of the use of non-identical soil specimens in the laboratory testing. The elastic surface (under an assumption of planar shape) is established by the constants  $\kappa$  and  $\kappa_s$  obtained from the laboratory compression tests. As long as the shape of the elastic and elastoplastic surfaces is well-fit by smooth functions, the shape of the yield curve is determined, and its evolution is established by a parallel shift of the elastic surface downward.

Use of the MSSA to obtain shapes of the yield surface and elastic surface does not require precise determination of the yield stress. If one is not certain whether the determined yield stress is accurate, an arbitrarily larger yield stress can be assumed, and the shape of the plastic surface will not be influenced. For example, Figure 4 compares the LC and SI yield curves obtained by Thu et al. (2007) and those obtained by Zhang et al. (2010) using the MSSA for the same experimental data. It was found that none of the soil specimens have the same stress histories and the shapes of the yield curves obtained from the conventional approach are misleading.

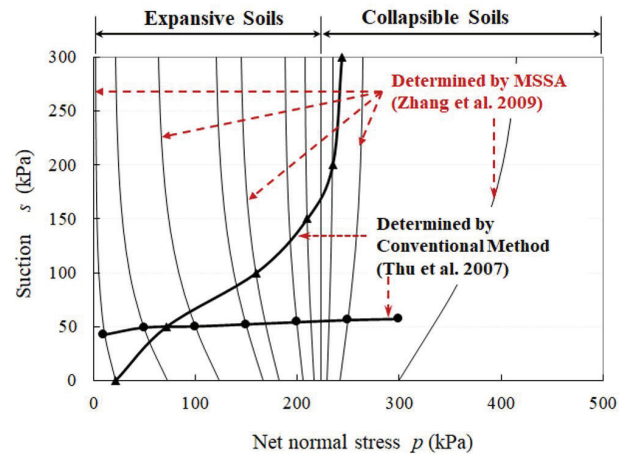
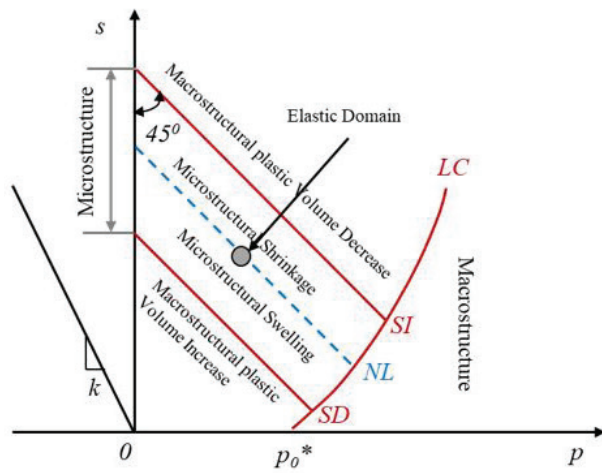


**Figure 4.** Comparison between yield curves obtained from different methods (modified from Zhang et al., 2010).

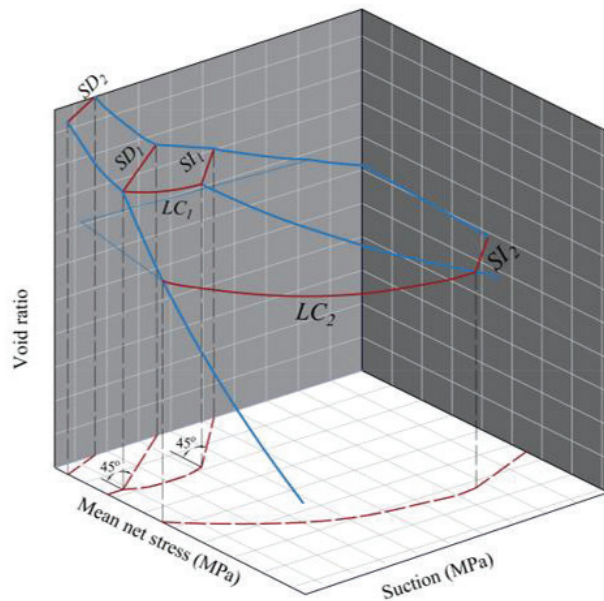
At present, multiple yield curves are increasingly used to model complicated unsaturated soil behavior, especially when mechanical and hydraulic hysteresis are involved. According to the above discussions, this approach is equivalent to assuming multiple plastic hardening surfaces, or different shapes of the virgin compression lines at different suction levels. The shapes of the virgin compression lines represent soil behavior under isotropic compression, and are best obtained by measurement using laboratory tests. For example, in the BBM, expansion of the LC and SI yield curves form two plastic hardening surfaces of FIJG and HIJC, as shown in Figure 3. Surfaces FIJG and HIJC as shown in Figure 3 are the “traces” of the LC and SI yield curves during their expansions. The evolution of the intersection of the LC and SI yield curves is an intersection curve IJ for the two plastic surfaces. It can be seen that the intersection points of the LC and SI yield curves represent a sharp discontinuity in unsaturated soil behavior, which was considered unlikely by Delage & Graham (1996). No available experimental results support the existence of such a sharp discontinuity.

Another example is the model for highly expansive clays proposed by Alonso et al. (1999) where two yield curves SI and SD, are introduced in addition to the LC yield curve, as well as a microstructural NL yield curve, as shown in Figure 5a. Alonso et al. (1999) use this multi-yield curve model to simulate strain accumulation due to plastic volume change resulting from wetting-drying cycles, taking into account the interaction between the macro and micro-structures, as shown in Figure 5a. A schematic plot of the corresponding elastic and elastoplastic surface of the Alonso et al. (1999) model is shown in Figure 5b. More experimental results are needed to prove or disapprove the assumed shapes of these added yield curves. The SI and SD yield curves are frequently used to simulate the hydraulic hysteresis of the degree of saturation during wetting-drying cycles as well as to obtain a good match between the measured and predicted volume change. Little effort, however, has been placed on





(a)



(b)

**Figure 5.** (a) yield curves for highly expansive soils in the BExM (Alonso et al., 1999); (b) schematic plot of possible corresponding State Boundary Surfaces.

examination of the consistency between the multiple yield curve models and the measured plastic (virgin) state surface for unsaturated soils. More research is needed in this direction.

### 3.5 Use of the MSSA to interpret unsaturated expansive soils and collapsible behavior in a unified system

As discussed previously, many researchers reported that unsaturated soils, when subjected to wetting, exhibit

expansive soil behavior under low confining stresses while experiencing collapse under high confining stresses (Jennings & Burland, 1962; Matyas & Radhakrishna, 1968; Fredlund & Rahardjo, 1993). In particular, nearly all early researchers found that the void ratio state surface is a warped surface, which represents the wetting-induced increase in soil volume (swelling) at a low value of net stress and the wetting-induced decrease in soil volume (collapse) at a high net stress shown schematically in Figure 1. For example, Lloret & Alonso (1985) suggested the expressions for the warped void ratio state surface as follows:

$$e = a + b \log p + c \log s + d \log p \log s \quad (17)$$

where  $a$ ,  $b$ ,  $c$ , and  $d$  are soil constants.

The warped state surface provides for wetting-induced swelling at low confining stress and the wetting-induced collapse at a high confining stress, explicitly including both volume change responses. These studies provided useful experimental data and insight to simulate unsaturated soil behavior. As pointed out by Delage & Graham (1996), the elastic and elastoplastic models are two different ways of modeling the same soil behavior.

Elastoplastic models were introduced as one method to address some limitations of nonlinear elastic SSA models, as summarized in Gens et al. (1996), Delage & Graham (1996) and Wheeler & Karube (1996). Alonso et al. (1990) developed the first elastoplastic model for unsaturated soil. It was considered that the BBM was developed for collapsible soils and slightly expansive soils (Alonso et al., 1990). Gens & Alonso (1992) and Alonso et al. (1999) discussed that the BBM has limitations in modeling the behavior of highly expansive soils, particularly the dependency of swelling strains and swelling pressures on the initial state (Brackley, 1973) and on the stress path (Justo et al. 1984), as well as strain accumulation during suction cycles (Pousada Presa, 1984; Dif & Bluemel, 1991). A revised version of the BBM, called the Barcelona Expansive Model (BExM), was introduced to address unique features of volume change response of highly plastic clay. Recently, Sánchez et al. (2005) developed a formulation for expansive soil modeling based on generalized plasticity concepts, while keeping the same basic features and assumptions in the BExM.

Both the BBM and BExM, in fact, have the ability to simulate the wetting-induced swelling at low confining stress and the wetting-induced collapse at high confining stress for unsaturated soils, through the introduction of the SI and SD yield curves at the low stress levels and retention of the original BBM LC yield curve at high stress level. Although predicted results for the BBM and BExM models have been demonstrated to match many experimental data, there has been little exploration of the implications of the fact that the plastic hardening process (the evolution of the SI and SD yield curves) should represent the virgin state surface. In other words, during constitutive modelling, producing good matches between the experimental results and model

predictions is necessary but not sufficient. Instead, the proposed constitutive model must simultaneously predict many constitutive behaviors of the same soil, in a consistent way. For example, as shown in Figure 3 and Figure 5b, the shapes of the various plastic yield surfaces of the BBM and BExM are significantly different from that of the experimental data by the researchers (e.g., Figure 1). The major reason that the plastic yield surfaces of these models deviate from the experimentally-determined virgin loading surface is caused by assumptions made in the introduction of the SI and SD yield curves. The discrepancy in the shape of the virgin loading surface between multi-yield surface models and experimental data can give the impression that elastoplastic models are dealing with unsaturated soil behavior that is significantly different from that observed by early researchers using SSA methods. Of course, this is not the case.

Since unsaturated soil behavior is closely related to the shape of yield curve, better representation of yield curve is needed to simulate the wetting –induced welling at a low confining stress and the wetting-induced collapse at a high confining stress for unsaturated soils in a unified system. Zhang & Lytton (2009b) analyzed the possible shape of yield curve for unsaturated expansive soils. According to the definition, the yield curve is the boundary separating the elastic and elastoplastic zones. Moving along the yield curve is a neutral loading process and will not generate plastic deformation. In an incremental formulation, the yield curves can be expressed as follows,

$$d\varepsilon_v^p = (m_1^s - m_1^{se})dp + (m_2^s - m_2^{se})ds = 0 \quad (18)$$

(On the yield curves)

where  $m_1^s$  = coefficient of total volume change with respect to mechanical stress in the elastoplastic zone,  $m_1^s = [1/(1+e_0)]\partial e/\partial p$ ,  $e_0$  is the initial void ratio,  $m_1^{se}$  = coefficient of volume change with respect to mechanical stress in the elastic zone, or bulk modulus of the soil in the elastic zone,  $m_1^{se} = [1/(1+e_0)]\partial e^e/\partial p$ ,  $m_2^s$  = coefficient of total volume change with respect to changes in the matric suction in the elastoplastic zone,  $m_2^s = [1/(1+e_0)]\partial e/\partial s$ , and  $m_2^{se}$  = coefficient of volume change with respect to changes in matric suction or coefficient of expansion due to matric suction change in the elastic zone  $m_2^{se} = [1/(1+e_0)]\partial e^e/\partial s$ .

Using Equation 18, Zhang & Lytton (2009b) analyzed the signs of the partial derivatives of the state boundary surfaces for the shapes of the BBM LC curve, and the represented unsaturated soil behavior. It was found that in the BBM, both  $m_1^s$  and  $m_1^{se}$  have negative signs on the LC yield curve and  $|m_1^s| > |m_1^{se}|$  as shown in Equations 9 and 12 respectively, representing that soil is compressed by the applied mechanical stress, and can yield due to p-loading

under constant matric suction if the soil stress state is on the yield curve. As represented by Equations 10 and 13, respectively,  $m_2^s$  is positive while  $m_2^{se}$  is negative. For the BBM LC conditions on soil parameters, Equation 16 results in that, on the yield curve, the yield stress will increase with an increase in the matric suction, as suggested by Alonso et al. (1990). A positive  $m_2^s$  is the key for successfully predicting collapsible soil behavior in the BBM because it leads to a reduction in the soil volume (collapse) upon wetting under constant net-normal stress. An LC yield curve with a shape that increases the net-normal stress for increasing suction predicts plastic (irrecoverable) volumetric strain when there is a decrease in matric suction and therefore a positive  $m_2^s$  leads to a reduction in the soil volume upon wetting. This was the reason why surface FIJC in Figure 3 was called “Plastic Collapsible Surface” by Zhang & Lytton (2009a, b).

In contrast, on surface HIJC (Figure 3), as well as the SI yield curve in Figure 3,  $m_2^s$  is negative, and  $m_2^{se}$  is also negative. Such a combination can be used to simulate an irrecoverable decrease in the soil volume with an increase in the matric suction beyond the yield suction and recoverable volume increase upon wetting. This increase in soil volume upon wetting is directly opposite to responses of collapsible soils upon wetting. Swell upon wetting is a typical response for unsaturated expansive soils. Commonly, only highly active clays with significant swelling upon wetting are considered to be expansive soils (Wray, 1995). All unsaturated soils with any plasticity (clay content) can exhibit swell upon wetting under low confinement (and compression upon wetting under high confinement). From the viewpoint of constitutive modeling, the common description of expansive soil as being highly active clays is too limited. All soils that swell upon wetting should be considered to be expansive for modeling purposes. This is why the surface HIJC (Figure 3) is named “plastic expansive surface” in Zhang & Lytton (2009a, b). It was also found that on the BBM plastic expansive surface HIJC, the following relationship exists:

$$m_1^s = m_1^{se} \quad (19)$$

Equation 19 is obtained by comparing Equation 9 and 14, and the condition is a result of the BBM assumption of a horizontal SI yield curve.

On the other hand, in the BExM, Gens & Alonso (1992) and Alonso et al. (1999) introduce two inclined 45° yield lines, SI and SD, to replace the original BBM SI proposal by Alonso et al. (1990), as shown in the  $p$ - $s$  plane of Figure 5a. On the 45° yield lines, both  $m_2^s$  and  $m_2^{se}$  are negative. Through incorporation of the SI and SD curves, the BExM can accommodate suction-change induced plastic expansive soil behavior, required to capture the accumulation of strains under cyclic wetting and drying. However, a 45° yield line means the soil is saturated such that an equal magnitude change in  $p$  or  $s$  yield the same magnitude of

change in volume, and the following equations always hold true on 45° yield lines:

$$m_1^s = m_2^s \text{ and } m_1^{se} = m_2^{se} \quad (20)$$

In the BExM (Alonso et al. 1999), a 45° yield line, NL, is related to the microstructural swelling effect, and two additional functions are proposed to link the micro-structural response to the macro-structural response. It is unlikely that all expansive soils are saturated or have the same shapes of yield curves, in general. In addition, it is challenging to calibrate the additional model parameters in the coupling micro-macro function.

Zhang & Lytton (2009b) argued that it is more reasonable to consider that the BBM and BExM restrictions in Equations 19 and 20 do not exist for unsaturated expansive soils in the general case. Instead, for all soils, saturated or unsaturated, the net total stress increase always results in soil compression and plastic deformation beyond yield stress, which means  $|m_1^s| > |m_1^{se}|$  and both have negative signs. It is not reasonable to assume that Equation 19 is satisfied for saturated or unsaturated soils because the virgin compression line is steeper than the unload line. In addition, Equation 20 does not result in reasonable conclusions for unsaturated soils, in general, because the 45° line of the SI and SD curves can only exist for saturated soil conditions. Further, when the restrictions of Equations 19 and 20 are removed, application of Equation 18 to stress states associated with volume increase upon wetting (expansion), gives yield curves on which suction decreases are associated with an increase in the net total stress as shown in Figures 6a and 6b. For stress states corresponding to volume decrease upon wetting (collapse), Equation 18 will result in yield curves on which suction increases are associated with an increase in net total stress, as shown in Figure 3a. Equation 18, without restrictions of Equations 19 and 20, as shown in Zhang & Lytton (2009b), is sufficiently general to accommodate volume change of expansion (Figure 6a), collapse (Figure 3), or both (Figure 4 and 7a).

Advantages of the above flexibility in use of Equation 18 was verified by reanalyzing the experimental results reported by Thu et al. (2007) as was shown in Figure 4. A yield curve on which yield stress decreases with an increase in the suction is very important for the constitutive modeling of unsaturated expansive soil behavior. Many soil behaviors, which were considered very complex previously such as those reported by Brackley (1975) and Justo et al. (1984) (Alonso, 1998), can now be easily modeled. For example, in the original BBM, this is considered illogical and the preconsolidation pressure  $p_0^*$  is restricted to be greater than  $p^c$  (Alonso et al., 1990; Wheeler et al., 2002) because a  $p_0^*$  less than  $p^c$  will lead to a decrease in the preconsolidation stress with an increase in the matric suction on the yield curve. By removing this

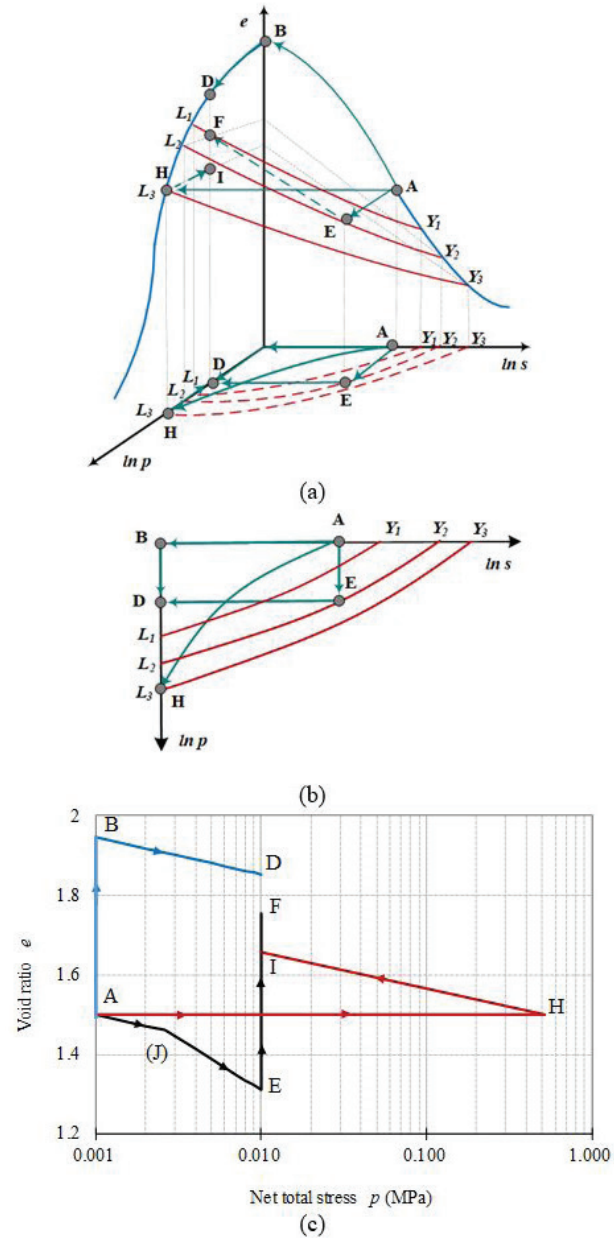


**Figure 6.** Simulation of experimental work by Brackley (1975) for Unsaturated Expansive Soils: (a) schematic plot in the  $e$ - $p$ - $s$  space; (b) stress paths in the  $p$ - $s$  plane; (c) predicted test results.

restriction ( $p_0^* > p^c$ ) the SI yield curve in the BBM can be discarded while expansive soil behavior can still be simulated.

Figure 6 shows the model predictions of the experimental results by Brackley (1975) using the MSSA, which includes three different tests on compacted high-plasticity clay with complex stress paths as follows: (i) first wetting from A to B and then loading the saturated specimen to a designated stress D ( $A \rightarrow B \rightarrow D$  as shown in Figure 6a), (ii) loading first to the target confining stress and then wetting ( $A \rightarrow E \rightarrow F$  as shown in Figure 6a), and (iii) confining the sample to the swelling pressure and unloading it to the target confining



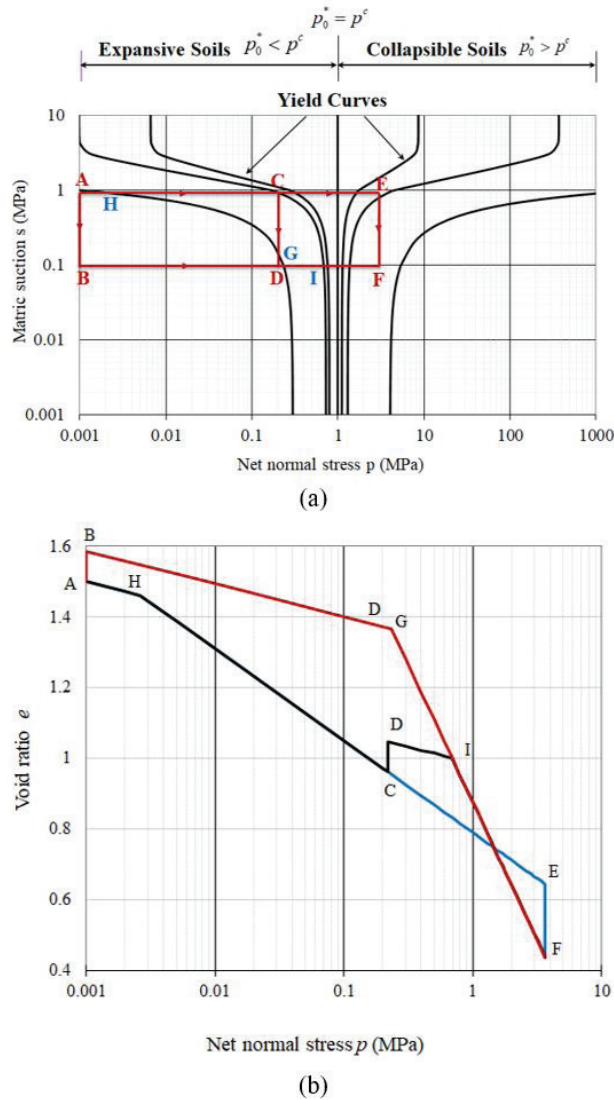


**Figure 7.** Prediction of Both Expansive and Collapsible Behavior in a Unified System: (a) MSSA Simulated Shapes of Yield Curves and Example Stress Paths; (b) predicted unsaturated soil response for stress paths in (a) (modified from Zhang & Lytton, 2009b).

stress (A→E→H→I as shown in Figure 6a). Similar tests were performed by Justo et al. (1984) and are considered as typical unsaturated expansive soil behavior (Alonso, 1998). Figure 6b shows the projection of the yield curves and stress paths in the  $p$ - $s$  plane. The yield curves have shapes of yield stress decreases with an increase in the suction, which is invoked to model unsaturated expansive soils. Figure 6c shows the predicted results, which are qualitatively consistent with the results from Brackley (1975) and Justo et al. (1984).

Zhang & Lytton (2009b) demonstrated that the MSSA can be used to model the behavior of both unsaturated expansive and collapsible soils in a unified system (Figure 7). Figure 7a shows the shapes of the yield curves used by Zhang & Lytton (2009b) to simulate the Brackley (1975) data. When

$p_0^* < p^c$ , unsaturated expansive soil behavior is simulated. When  $p_0^* = p^c$ , the LC curve is a vertical straight line, which is a transition from expansive soil behavior to collapsible soil behavior. When  $p_0^* > p^c$ , unsaturated collapsible soil behavior is simulated. The transition from the expansive soil behavior to collapsible soil behavior is smooth and the corresponding void-ratio constitutive surface has continuous first derivatives with respect to both the net total stress and the matric suction. Figure 7b shows the predicted results for different stress paths. As can be seen in Figure 7b, wetting the soil at a low net total stress of 0.2 MPa results in volume increase (swelling) from point C to D, while wetting the soil at a high net total stress of 3 MPa results volume decrease (collapse) from point E to F. The obtained plastic hardening surface is a warped surface similar to that as shown in Figure 1 on which soil behavior can smoothly change from expansive soil behavior at a low confining stress to collapsible soil behavior at high confining stress level.

In a summary, Figures 4, 6, and 7 show the applications of the MSSA to simulate either collapsible or expansive, or both collapsible and expansive soil behavior in a unified way. In fact, for any warped void ratio surface, such as Equation 17 (Lloret & Alonso, 1985), the MSSA framework can be used to simulate wetting-induced swelling at a low confining stress and wetting-induced collapse at a high confining stress for unsaturated soils, provided a smooth function can be well-fitted to laboratory test results. Under isotropic conditions, it is only required to separate the conventional void ratio surface into an elastic surface (most researchers used Equation 1) and an elastoplastic state boundary surface based upon the MSSA, and to obtain a smooth function for these surfaces. The MSSA, therefore, also represents a smooth bridge across the gap between the traditional state surface approach and elastoplastic constitutive models for unsaturated soils.

One limitation of the original MSSA is that the mechanical and hydraulic hysteresis due to cyclic drying-wetting cycles was not considered. Simulation of such behavior requires incorporating the concept of bounding surface and kinematical hardening, as proposed by Dafalias & Herrmann (1982) and Pastor et al. (1990). This can however be handled with relative simplicity by using the MSSA with an additional new reloading surface which shares the same shapes of yield curve as for the unloading surface. This has been demonstrated in Riad & Zhang (2020, 2021) and is beyond the scope of this paper.

## 4. Oedometer-based models for practice as viewed within an elastoplastic framework

### 4.1 Background

For most practice-based foundation engineering problems it is not necessary to consider the entire state surface for the



soil, or to implement all elements of an elastoplastic model. However, it is always necessary that soil volume change constitutive models, regardless of level of simplification, remain consistent with known unsaturated soil response. It is required, for example, that any volume-change method remains true to the two stress-state unsaturated soil principles. The MSSA was also used to provide a rigorous elastoplastic interpretation of  $K_0$  loading conditions for both saturated and unsaturated soils (Riad & Zhang, 2019; Zhang et al., 2016a, b). Herein, the MSSA is used as an effective framework from which to evaluate simplified  $K_0$  approaches for expansive and collapsible soil volume change analyses used in routine foundation design.

For foundation design, it is often adequate to assume 1-D,  $K_0$  conditions. For this reason, the oedometer device is used extensively in practice for the laboratory testing of expansive and collapsible soils. The ASTM D4546 (ASTM, 2014) response-to-wetting testing is routinely used in the characterization of collapsible and expansive soil sites (Noorany, 2017; Noorany & Houston, 1995; Houston, 2014; Nelson et al., 2006, 2015; Fredlund et al., 2012; Adem & Vanapalli, 2015; Houston, et al., 1988; Washington, 1971). Although several options exist within the ASTM D4546 procedure, Method B is often used in the USA to determine the response of an undisturbed (or representative compacted) specimen of soil to full submergence (full wetting to  $s = 0$ ), starting from field moisture (suction) and field net total stress (vertical stress) conditions (Houston, 2014; Nelson, et al., 2015). Traditional consolidometer testing equipment is used for the ASTM D4546 test, the net total stress (vertical stress) is held constant at the field value of overburden stress, the soil matric suction is reduced to zero by submergence, and no soil suction measurements are made. In performance of the ASTM D4546, Method B, response to wetting test, a field-appropriate soil-wetting path, along a small subset of the entire unsaturated soil state surface, is followed. This type of approach to soil testing and property determination is analogous to the stress path method proposed by Lambe (1967). By testing two or more companion specimens under a range of total stress values, the ASTM D4546, Method B, test can also be used to determine the applied stress level at which the void ratio of the specimen would just remain at its initial value when wetted to  $s = 0$  conditions (i.e., the swell pressure for an expansive soil).

Another commonly used oedometer test for expansive soils is the constant volume test, wherein an undisturbed specimen is placed within the oedometer rings, and vertical load is added to the specimen so as to keep the specimen volume constant during submergence. When, prior to wetting, the specimen is first loaded at in-situ moisture to field overburden, the stress that has to be applied to the specimen to avoid volume change upon submergence is termed the swell pressure, or the constant volume swell pressure,  $\sigma_{OCR}$ . In the USA, the swell pressure is often empirically estimated using a load-back test, wherein the load on the D4546 test

specimen (ASTM, 2014), after full wetting, is increased so as to return the swelled specimen back to its original height (ASTM D4546, Method C, loading-after-wetting test).

Here, some of the available oedometer-based methods for estimation of soil heave and soil collapse under 1-D,  $K_0$ , monotonic wetting conditions are reviewed in the context of elastoplastic volume change models and the unsaturated soil state surface. Currently, most 1-D,  $K_0$ , methods for estimation of volume change of unsaturated soils have been focused on expansive soils, and much less on collapsible soils. Adem & Vanapalli (2015) and Vanapalli & Lu (2012) provide comprehensive reviews of several methods used in the estimation of 1-D volume change of expansive soils, including methods by Briaud et al. (2003), Wray et al. (2005), Lytton (1997), Adem & Vanapalli (2013), Overton et al. (2006), and Vu & Fredlund (2004). Li et al. (2016) provide a general discussion of methods used for estimation of volume change for collapsible soils, although the methods reviewed are not focused on 1-D,  $K_0$ , monotonic wetting conditions. The review here is more limited, and primarily directed at the evaluation of simplified 1-D approaches in the context of more general SSA and elastoplastic methods, via the MSSA. Methods that do not directly, or at least indirectly, consider both soil suction and net total stress as controlling stress state variables are not consistent with known unsaturated soil response and are not considered here. Particular attention will be given to the surrogate path method (SPM), an oedometer-based method that can be used to estimate volume change of expansive or collapsible soils in response to suction change under field net total stress conditions (Singhal, 2010; Houston & Houston, 2018).

## 4.2 Fredlund method: oedometer based heave analyses

Fredlund & Morgenstern (1976) present the following incremental model for volume change of unsaturated soils in response to isotropically induced changes in suction and net mean total stress:

$$d\varepsilon_v = \frac{de}{1+e_0} = m_1^s dp + m_2^s ds \quad (21)$$

where  $m_1^s$  is the slope of the void ratio-net mean stress plane of the state surface and  $m_2^s$  is the slope of the matric suction plane of the state surface, and  $\varepsilon_v$  = volumetric strain.

Equation 21 was extended to 3-D by Fredlund & Rahardjo (1993), but is not shown here. In principle, Equation 21 is for either expansive or collapsible soils, depending on the sign of  $m_2^s$ , as discussed by Fredlund & Rahardjo (1993). However, considerably more attention was given to use of Equation 21 for soils exhibiting expansion in response to monotonic decrease in suction (wetting). For isotropic loading of an expansive soil, the unsaturated soil volume-change coefficients,  $m_1^s$  and  $m_2^s$ , can be related to the 1-D  $K_0$  loading coefficients,  $C_s$  and  $C_m$  (Figure 8). For 1-D,  $K_0$

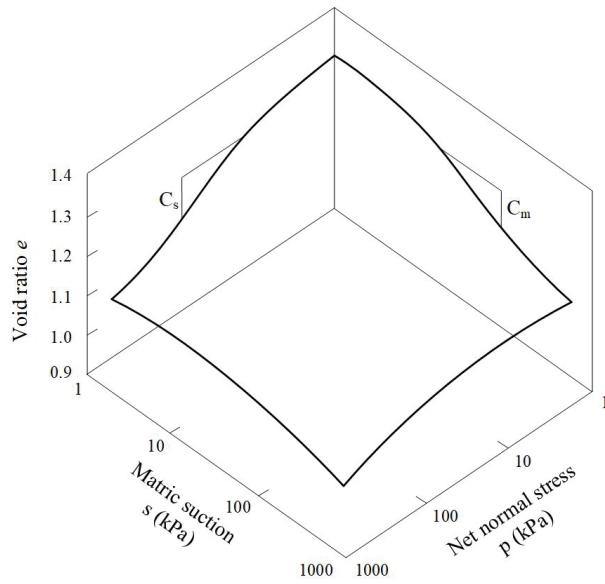


**Figure 8.** State Surface for Expansive Soils (modified from Fredlund & Rahardjo, 1993).

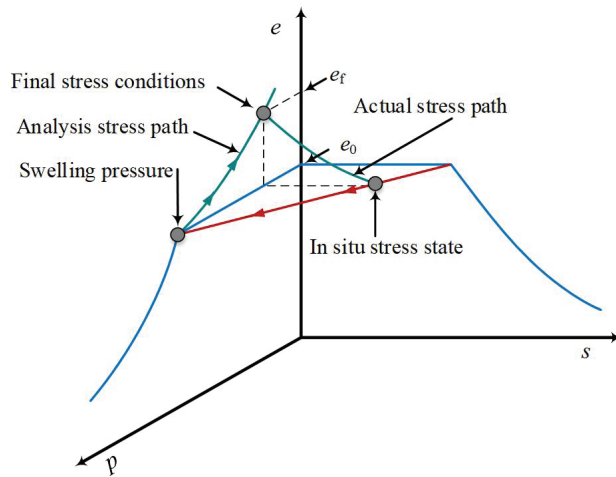


**Figure 9.** Schematic of the Fredlund Method for expansive soil showing an equivalent stress path approach for computation of heave from oedometer tests.

conditions, under an assumption of  $K_0 = 1$ , the volume change coefficients shown in Figure 8 and Equation 21 are related as follows:

$$m_{1-1D}^s = \frac{0.434}{1 + e_0} \frac{C_s}{(\sigma_v - u_a)} \quad (22)$$

$$m_{2-1D}^s = \frac{0.434}{1 + e_0} \frac{C_m}{s} \quad (23)$$

where  $m_{1-1D}^s$  = coefficient of total volume change with respect to mechanical stress under 1-D constrained loading,  $m_{2-1D}^s$  = coefficient of total volume change with respect to

changes in the matric suction under 1D constrained loading,  $C_s = K_0$  loading coefficient corresponding suction,  $C_m = K_0$  loading coefficient corresponding net total stress,  $u_a$  = pore air pressure, and  $\sigma_v$  = net vertical stress.

In the Fredlund oedometer-based 1-D method for estimation of soil heave (Fredlund & Rahardjo, 1993; Fredlund et al., 2012), the concept of an “equivalent matric suction” is used to translate the actual stress path (wetting of the soil in the field under constant net total stress conditions) onto the net total stress plane. The translated (or analysis, or surrogate) stress path in the total stress plane ( $s = 0$  plane), is shown in Figure 9. When suction is plotted on a logarithmic scale and  $s = 0$  is cited herein, it means that  $s$  is so small that there is no significant difference in the void ratio plotted on the lowest depicted suction plane and the void ratio for truly  $s = 0$  conditions. The constant volume oedometer tests is used in the translation (mapping) of the in-situ soil stress state (in terms of net total stress and suction) onto the net total stress plane ( $s = 0$ ). The swell pressure becomes the point on the  $C_s$  sloped curve (in the net total stress plane) where swell strain is zero upon full wetting of the specimen. The constant volume swell pressure, which Fredlund et al. (2012) recommend be corrected for sampling disturbance, is interpreted as the in-situ stress state of the specimen (overburden pressure plus matric suction equivalent). Fredlund & Rahardjo (1993) and Fredlund et al. (2012), place emphasis on measurement of the swell pressure, because the swell pressure is taken to be representative of the initial stress state of the soil. Fredlund et al. (2012) use the swell pressure, together with the matric suction equivalent concept, in lieu of measurement of the initial soil suction.

Once the swell pressure of the expansive soil is determined, Fredlund & Rahardjo (1993) provide numerous methods for obtaining the slope of the translated (analysis) state surface in the total stress plane,  $C_s$  (the swell index), as follows. Upon completion of the constant volume swell test, the specimen (remaining in the consolidometer device) is loaded to a stress well above the swell pressure, and then unloaded (i.e., a saturated soil consolidation test is performed on the constant volume swell test specimen). The slope of the unloading curve, from the post-constant volume swell pressure consolidation test, is defined as  $C_s$  under an assumption of saturated soil conditions and elastic soil state (unload conditions). Fredlund & Rahardjo (1993) also allow use of the unloading curve from a loading-after wetting free swell test as  $C_s$ , as well as determination of  $C_s$  from the unload curve of a traditional consolidation test on saturated soil. Estimation of  $C_s$  from a shrinkage curve (ASTM, 2018) or through correlations with Atterberg limits (Washington, 1971; Lytton, 1994), is also allowed. Fredlund & Rahardjo (1993) assert that problematic heave is commonly attributable to wetting at shallow depth, where net total stress values are relatively low, hence, their allowance for use of the token-load free swell test and token load constant swell pressure, in estimation of the volume-change soil parameters.

Fredlund et al. (2012) provide for the same methods of determination of  $C_s$  as Fredlund & Rahardjo (1993), but also include use of ASTM D4546 (ASTM, 2014) Method A or C (swell tests on “companion” specimens at various surcharge pressures) to obtain  $C_s$ . The use of multiple swell test specimens to define  $C_s$  addresses observed stress path/net total stress level dependencies of response-to-wetting of unsaturated soils (Justo et al., 1984; Noorany & Stanley, 1994; Noorany & Houston, 1995; Houston & Nelson, 2012; Houston et al., 1988).

In the Fredlund Method, the swell pressure and the slope,  $C_s$ , are used to establish the translated (analysis) stress path (Figure 9). Void ratio change in response to reduction of soil suction is estimated as follows:

$$\Delta e = C_s \log \left( \frac{P_f}{P_o} \right) \quad (24)$$

where  $\Delta e$  = change in void ratio between initial and final stress states (i.e.,  $e_f - e_o$ ),  $e_o$  = initial void ratio,  $e_f$  = final void ratio,  $C_s$  = swelling index,  $P_o$  = initial stress state is assumed to be equal to the sample disturbance-corrected swelling pressure, and  $P_f$  = final stress state.

The final stress state,  $P_f$ , includes net total stress changes and suction changes. The final suction conditions must be determined to compute the final stress state,  $P_f$ .

$$P_f = \sigma_v \pm \Delta \sigma_v - u_{wf} \quad (25)$$

where  $\Delta \sigma_v$  = change in total vertical stress due to the excavation, (i.e.,  $-\Delta \sigma_v$ ), or placement of fill (i.e.,  $+\Delta \sigma_v$ ), and  $u_{wf}$  = final pore-water pressure (final matric suction).

Using an incremental-elastic formulation of Equation 21, Vu & Fredlund (2006) provide for highly nonlinear stress state surface curves.  $C_s$  (in Equation 24) can be made to be very small in the low suction or low “translated” net total stress range, avoiding unrealistically large swell strain estimates due to the logarithm relationship assumed between void ratio and suction (and void ratio and net total stress).

In using the final pore-water pressure (suction) directly to define  $P_f$  (Equation 25), there is an underlying assumption that the expansive soil volume change occurs under saturated soil conditions (effective stress principles apply). Fityus & Buzzi (2009) also suggest the treatment of expansive soils as saturated. Vu & Fredlund (2004) introduce the degree of saturation as an empirical operator on the suction to establish the equivalent matric suction value to account for the fact that an equal magnitude change in soil suction and net total stress do not have the same effect on volume change. Fredlund et al. (2012) assert that, for expansive clays, any difference between the actual in-situ matric suction and the “equivalent matric suction” is primarily attributed to the difference in degree of saturation.

Fredlund et al. (2012) interpret the translated stress path line, having slope  $C_s$  in the net total stress plane, as a rebound curve, and therefore an elastic unload-reload surface. This conclusion is reached through the reasoning that field desiccated clay soils possess a very high pre-consolidation stress, such that the swell pressure is always lower than the pre-consolidation stress.

#### 4.3 Use of the MSSA to study test methods used in determination of $C_s$

Elastic (loading/unloading) response-to-wetting response seems to be a reasonable assumption for natural soils subjected seasonally to very wet (near  $s = 0$ ) cyclic conditions. However, for deeper field specimens and compacted specimens not previously subjected to full wetting to  $s = 0$ , the response-to-wetting would seem to be elastoplastic, in general. Therefore, within the framework of the MSSA, the volume change constitutive model of Fredlund & Rahardjo (1993) and Fredlund & Morgenstern (1976) could be considered as a state surface comprised of an elastic (reload/unload) segment and an elastoplastic (virgin loading) segment, depending on the soil stress history. For monotonic loading it is not necessary to separate the elastic and plastic components of volume change. However, it is necessary to consider the elastic and/or plastic nature of specimen response in the interpretation and use of laboratory oedometer tests, because there are implications with regard to the manner in which  $C_s$  is best determined for use with the Fredlund Method. The following discussion uses the MSSA to visualize stress paths commonly used in oedometer-based heave computations.

Figure 10 shows the unsaturated soil state surface corresponding to Figure 9 in  $\ln s$ - $\ln p$  space. In Figure 10, the

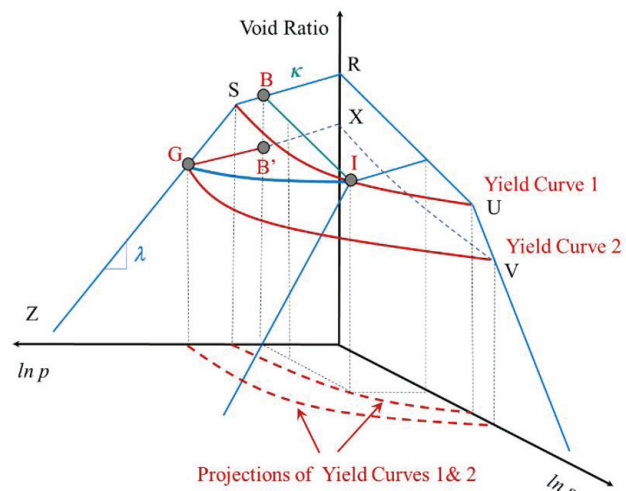


**Figure 10.** Use of the MSSA for interpretation of methods for obtaining  $C_s$ .

state surface is assumed to be elastoplastic (and therefore unique for isotropic loading). For 1-D,  $K_0$  conditions, under an assumption of  $K_0 = 1$ , the volume change coefficients are shown in Figures 8 and 10 are related as follows:

$$m_{1-1D}^s = \frac{0.434}{1+e_0} \frac{C_s}{(\sigma_v - u_a)} = \frac{1}{1+e_0} \frac{\lambda(0)}{(\sigma_v - u_a)} \quad (26)$$

$$m_{2-1D}^s = \frac{0.434}{1+e_0} \frac{C_m}{s} = \frac{1}{1+e_0} \frac{\lambda_s}{s} \quad (27)$$

Figure 10 shows an example field stress path IB followed under constant in-situ overburden stress and wetting of the soil to  $s = 0$ ; IB is the same as the actual stress path depicted in Figure 9. The path IB is also the path that is followed in the performance of the ASTM D4546 (ASTM, 2014), Method B, oedometer method, assuming that the specimen is essentially “undisturbed” (i.e., returned more or less to its field state upon reloading at in-situ moisture to field overburden stress). At point I, the state of the stress of the soil corresponds to the field suction (in-situ moisture condition) and field total stress (overburden stress). In the sample case depicted in Figure 10, the initial state of stress is assumed to be on a yield curve (i.e., the soil is in a virgin state of stress), and the actual path IB is then an elastic unload process. Figure 10 also shows the stress path of a constant volume wetting test of IG. Because expansive soils exhibit elastoplastic volume-change response, in general, the constant volume swell test can cause the soil to yield, as occurs in the example depicted in Figure 10. The analysis path of Figure 9 corresponds to GB' in Figure 10 for unloading of the soil to field overburden stress at approximately zero suction. Under elastic soil assumptions, in determining the position of B', the slope of GB' is  $\kappa$  (corresponding to  $C_s$ ), determined from an unload consolidation test on a saturated specimen (for example, one performed at the end of a constant volume swell test). Because the constant volume wetting (IG) is a plastic loading process, while the unloading process is elastic, point B' is located on a new elastic surface of GXV, which is below the original elastic surface of RSU. As can be seen, the stress path GB' results in a lower void ratio at field overburden stress compared to the void ratio obtained from the actual field stress path (IB). This result, lower void ratio for path GB' compared to path IB, is confirmed by the laboratory data of Brackley (1975) and qualitative analysis of Zhang & Lytton (2009b) as shown by the stress path A→H→I in Figure 6. Thus, the use of the unloading curve from a saturated specimen consolidation test in the determination of  $C_s$  can result in some degree of underestimate of the field swell strain. Only when paths IB and IG are both elastic are B and B' the same. If, instead,  $C_s$  is determined as the slope GB, where point B is obtained from a D4546, Method B, test, an improved estimate of the

field swell strains is expected because the analysis path would then become GB in the example of Figure 10.

Both the Fredlund Method and the Lytton Method (discussed subsequently) allow for use of the unload curve from a saturated consolidation test for determining  $C_s$ , along with other options. Although Fredlund et al. (2012) provide for the use of the overburden-stress swell test (ASTM D4546, 2014, Method B) to estimate  $C_s$ , Fredlund et al. (2012) does not require a particular oedometer test method of determination of  $C_s$  – rather, Fredlund requires a particular method of determination of swell pressure. Fredlund et al. (2012) argue that the difference between the  $C_s$  value obtained using the overburden swell test (ASTM D4546, Method B) and that obtained from the unloading of a saturated soil specimen (consolidation test) is small. Others, however, point to the importance of path-dependence in the determination of volume change response of unsaturated clays (Noorany & Stanley, 1994; Justo et al., 1984). If the expansive soil is always saturated and the soil volume change is elastic, then the difference between the use of the unload curve from a consolidation test and use of the ASTM D4546, Method B test in establishment of  $C_s$  may be small. If, on the other hand, the soil exhibits an elastic response for field loading conditions, but a plastic response is induced during the constant volume swell test, there may be significant differences in the  $C_s$  values determined by the ASTM D4546 method B test and the  $C_s$  determined from the unloading curve of a consolidation test.

#### 4.4 Nelson method: oedometer based heave analysis

Nelson & Miller (1992) use an approach to estimating 1-D soil expansion that is similar in concept to Fredlund & Rahardjo (1993). The primary difference between the Nelson et al. and the Fredlund & Rahardjo methods relates to the method used to determine the slope of the analysis (translated) state surface in the net total stress plane. Nelson et al. (2015) use the ASTM D4546 (ASTM, 2014), Method B test, performed on an undisturbed (or compacted, representative) specimen of soil under an applied constant stress equal to field overburden, in the determination of full-wetting (to  $s = 0$ ) swell strains. Use of a response-to-wetting oedometer test, performed at in-situ moisture and field overburden stress, in the establishment of fully-wetted field strains is an approach long advocated by Nelson and colleagues for expansive soils (Nelson et al., 1998), as well as by other researchers of both expansive and collapsible soils (Noorany & Stanley, 1994; Noorany & Houston, 1995; Houston et al., 1988; Houston & Nelson, 2012). In the Nelson Method, the ASTM D4546 test, method B, is used together with the swell pressure to obtain  $C_s$ . The advantage of the use of the ASTM D4546, Method B, test for determination of  $C_s$  was previously demonstrated in the example of Figure 10. The slope of the state surface for  $s = 0$  ( $C_s$ , Figure 8) is referred to as the swell index,  $C_H$ , by



Nelson et al. (2006, 2015) when the volume change surface is plotted in terms of vertical strain, rather than void ratio.

The Nelson et al. (2006) approach provides an estimate of the soil volume change (heave) when the soil becomes fully wetted to  $s = 0$  in the field. Based on the research of Chao (2007), Nelson et al. (2015) introduce an empirical approach, based on the degree of saturation, to correct computed swell strains for field wetting conditions resulting in the final degree of saturation less than 100%. In using a degree of saturation-based correction to full-wetting swell strains, the Nelson Method cannot properly account for reduced swell resulting from wetting to final field suction values greater than zero. Except for the special case where field suction is reduced to zero, the Nelson et al. approach to heave computation does not properly consider the effect of both stress state variables, total stress and matric suction. When the final degree of saturation of the field soil is 100%, Nelson et al. (2015) assume that the full-wetting swell strain is achieved, without consideration being given to the actual final field suction value that may exist under full saturation conditions. For expansive clays, the field degree of saturation can be quite high (even 100%) in the presence of rather large suction values due to the relatively high air-entry values of high plasticity clays. Indeed, it is common for an expansive clay heave analysis to proceed under the assumption of saturated soil conditions (Fredlund & Rahardjo, 1993; Fityus & Buzzi, 2009). Provided some significant matric suction remains in the soil after field wetting, the full wetting strain ( $s = 0$  strain, observed in the ASTM, 2014, laboratory test) will not be realized in the field. Thus, the Nelson method, in using degree of saturation, rather than soil suction, to account for partial wetting effects, results in an over-estimate of soil heave in the general case. It is primarily the failure to explicitly consider the role of soil suction, as required when using the MSSA or any other suction-based method, that results in overestimated heave when using Nelson's method.

#### 4.5 The Surrogate Path Method (SPM): oedometer based heave and collapse analyses

##### 4.5.1 Theoretical framework of the SPM

As with the Fredlund and Nelson Methods, the surrogate path method (SPM) considers only a relatively small segment of the 1-D void ratio constitutive surface, obtained under very specific loading conditions: (1)  $K_0$  boundary conditions and 1-D deformation, (2) constant net total stress during wetting, and (3) monotonic decrease of suction (soil wetting) (Singhal, 2010; Houston & Houston, 2018). Although the SPM was originally developed for expansive soils and conditions of soil wetting, the model can also be used to estimate soil collapse and suction increase (drying) shrinkage of expansive soils (Houston & Houston, 2018). For expansive soils, like the Nelson Method, the SPM is anchored to the ASTM D4546 (ASTM, 2014) over-burden swell test results for full

wetting conditions. This ASTM D4546, Method B, test result provides an actual measurement of a point on the  $s = 0$ , net total stress plane of the unsaturated soil state surface. Thus, the SPM is a suction-based method, requiring initial and final soil suction values. As with the Fredlund et al. (2012) method for estimation of soil heave, the SPM requires the estimation of final soil suction values. However, rather than using the constant volume swell pressure and "equivalent matric suction concept" to estimate the initial in-situ soil state, the SPM requires the measurement or estimation of the initial soil suction value. The initial soil suction value can be obtained by different means, including use of relative humidity devices (e.g. WP4C, Meter, Inc.), filter paper, correlations with soil-water characteristic curves, and high capacity tensiometers (Marinho & Teixeira, 2009; Houston & Houston, 2018; Fredlund et al., 2012).

The SPM is based on a two stress-state variable approach to unsaturated soil mechanics, and ensures that the correct (laboratory-observed) soil response is obtained at the endpoints of soil wetting (i.e., at full wetting to final  $s = 0$  and at zero wetting (final  $s =$  initial soil suction value). By using the ASTM D4546 test (ASTM, 2014), performed at overburden stress, the laboratory test specimen is made to follow the same stress path as that of the field prototype, resulting in a direct measurement of soil response for loading to  $s = 0$ . The SPM is a total stress-equivalent or "surrogate" path method, coupled with initial and final soil suction values and oedometer response-to-wetting (submerged specimen) tests (ASTM D4546, 2014).

Figure 11 is a graphical representation of the SPM for an expansive soil. In the SPM, an alternate net total stress path serves as a surrogate path (GQB, Figure 11) to the actual suction-change stress path (IFB, Figure 11a) in reaching the final swell strain,  $\epsilon_B$ , exhibited by an element of soil subjected to full wetting in the field. As with the Fredlund approach, the SPM can be used to estimate an actual segment of the void ratio state surface, such as IFB on Figure 11, for monotonic reduction in soil suction under constant confining stress. However, in practice, preference is for use of the translated (surrogate) stress path along the  $s = 0$  net total stress plane (BQG, Figure 11b). The actual stress path (IFB), corresponding to suction change along a fixed net total stress plane, is not determined directly in the laboratory for the SPM (due to requirements for suction control/measurement devices), but rather full wetting strain AB is estimated using commonly available oedometer tests and testing equipment, without suction control or measurement.

As with the Fredlund Method, the SPM is based on a traditional state surface approach, and it is not absolutely necessary to separate the elastic and plastic strains due to the restriction of the method to monotonic loading (wetting or drying). However, it is of interest to view the SPM within the context of the MSSA to confirm consistency of approach to known elastoplastic unsaturated soil volume-change response, in the general case.

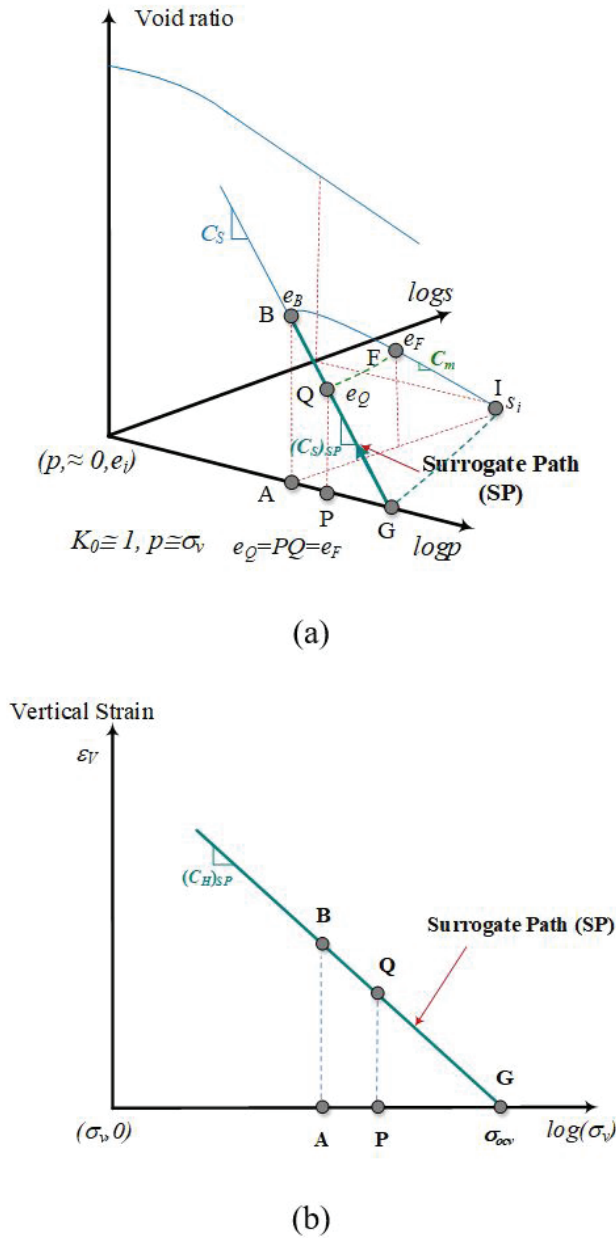


**Figure 11.** Graphical representation of SPM for expansive soils: (a) mapping of actual stress path to net total stress surrogate path; (b) surrogate path used for analysis.

In the SPM, a proportionality factor,  $R_w$  (the ratio of the final suction to the initial matric suction), is used to interpolate ASTM D4546 swell strains (ASTM, 2014) for final suction values intermediate between the initial suction and full wetting (matric suction of zero). As described by Houston & Houston (2018), the actual stress path, with slope  $C_m$ , is the path of line IFB (Figure 11a), where point I is at the original in-situ suction and point F represents the final suction after partial wetting. The void ratio (strain) at point F,  $\epsilon_F$ , is the desired quantity. The strain for partial wetting,

$\epsilon_F$ , is obtained by using the proportion of suction dissipated by wetting from I to F as a proportionality factor,  $R_w$ , in estimating the “final” net total stress,  $\sigma_p$ , at point P, Figure 11b.

For the SPM, the ASTM D4546 test specimen (ASTM, 2014) is first loaded at in-situ moisture to field (or prototype) net total stress conditions, and then submerged (fully wetted) under load. For soils that exhibit expansion, the swell index,  $C_H$ , is the slope of the swell strain versus log of “equivalent” total stress, along the “surrogate path” BG, Figure 11b. It is assumed that no swell occurs under constant volume swell pressure,  $\sigma_{ocv}$ , such that the full wetting swell strain,  $\epsilon_{ob}$ , at overburden stress,  $\sigma_{ob}$  (or overburden plus structural load, as appropriate) is:

$$\epsilon_{ob} = C_H \log \left( \frac{\sigma_{ocv}}{\sigma_{ob}} \right) \quad (28)$$

where  $C_H$  is the swelling index.

The constant volume swell pressure,  $\sigma_{ocv}$ , can be determined from a constant volume swell test. However, a sufficiently accurate estimate of  $\sigma_{ocv}$  can be obtained by simply performing two swell tests, one at  $\sigma_{ob}$  and one at a substantially higher net total stress and extrapolating to get  $\sigma_{ocv}$  (Houston & Nelson, 2012). Alternatively, the load-back procedure, with correction, can be used to approximate the constant volume swell pressure,  $\sigma_{ocv}$  (Nelson et al., 2006; Olaiz, 2017). The surrogate path BG, is established from the ASTM D4546 test result ( $\epsilon_{ob}$  at  $\sigma_{ob}$ ) and the constant volume swell pressure, requiring no suction measurements.

The partial wetting strain ( $\epsilon_{pw}$ ), realized in going from the initial suction value to the final suction value, is:

$$\epsilon_{pw} = C_H \log \left( \frac{\sigma_{ocv}}{\sigma_p} \right) \quad (29)$$

where

$$\sigma_p = \sigma_{ob} + R_w (\sigma_{ocv} - \sigma_{ob}) \quad (30)$$

$$\text{and } R_w = \frac{s_f}{s_i} \quad (31)$$

where  $s_i$  = initial matric suction and  $s_f$  = final matric suction. The suction proportionality factor  $R_w = 1$  for no wetting and  $R_w = 0$  for full wetting. The strain PQ at point P, along the surrogate path, was compared by Singhal (2010) to the actual strain  $\epsilon_F$  for numerous cases, and an excellent agreement was found.

Another way to view the SPM is as an interpolation method for going from known (measured) point I to measured point B along the IFB path in Figure 11a. The results of any volume change estimate are constrained to fall between known points I (zero strain) and B (strain at  $s = 0$ ). In establishment of the interpolation method, the ratio of the final to initial soil suction is used, together with an estimate of the constant volume swell pressure. The swell pressure is typically obtained from a load-back swell test (ASTM

D4546, 2014, Method C, loading-after-wetting), or from the log-scale slope of the net total stress path, at  $s = 0$ ,  $C_H$ , established by the full wetting strains of a series of at least two companion specimens at varying applied stress level (ASTM D4546, Method C and Method A). Although direct measurement of the swell pressure might seem ideal, the constant volume swell test is not easy to perform without computer control, and the results are sensitive to any minor swell that occurs during the test, as well as to other system compliances, such as compressibility of the measurement device components (Fredlund et al., 2012). In fact, the constant volume swell test is no longer available as an ASTM Standard. The results for strain obtained by the SPM are not particularly sensitive to the method of estimating the swell pressure (Singhal, 2010; Houston & Houston, 2018). The reason for this is that the SPM requires anchoring of the solution at initial suction ( $R_w = 0$  results in zero volume change) and zero suction (swell strain is that measured by the ASTM D4546 test at  $s = 0$ ). It could be argued that the estimation or measurement of initial suction, using currently available methods, is easier than the measurement of swell pressure. Regardless of one's position on this point, the focus of the SPM on initial and final suction estimation and/or measurement is quite consistent with the two stress-state variable unsaturated soil mechanics principles.

If the ASTM D4546 test specimen (ASTM, 2014) exhibits collapse, the SPM can be used, analogously, for estimation of partial wetting collapse strains (Houston & Houston, 2018). The SPM is used to estimate partial wetting strains,  $\epsilon_{pw}$ , from the D4546 fully wetted collapse strain,  $\epsilon_{ob}$ , by mapping the actual stress path along the void ratio state surface (with slope  $C_m$ ) onto the net total stress plane where  $s = 0$ , and establishing a surrogate path (SP) for collapse (Figure 12).

To establish the slope of the surrogate path, it is necessary to estimate a net total stress,  $\sigma_{G'}$ , for which fully wetted collapse strains are zero. The value of  $\sigma_{G'}$  can be estimated by testing an additional specimen, as identical as possible, using a smaller confining stress equal to 0.2 to  $0.3\sigma_{ob}$ . A straight line on the net total stress plane can be established between the two response-to-wetting test results to establish the surrogate path slope,  $(C_{col})_{sp}$ , analogous to  $(C_H)_{sp}$  for expansive soil. Although it may not be possible to obtain a perfectly identical companion specimen for natural soils, Houston & Houston (2018) report that  $\epsilon_{pw}$  is relatively insensitive to variations in the value of  $\sigma_{G'}$ , which can be introduced by sample variability. However, for profiles of high variability in soil cementation, a series of test specimens may be appropriate for establishment of  $C_{col}$  based on an average value of  $\sigma_{G'}$ .

The slope of the surrogate path for collapsible soil,  $(C_{col})$  is:

$$C_{col} = \frac{\epsilon_{ob}}{\log\left(\frac{\sigma_{p'}}{\sigma_{G'}}\right)} \quad (32)$$

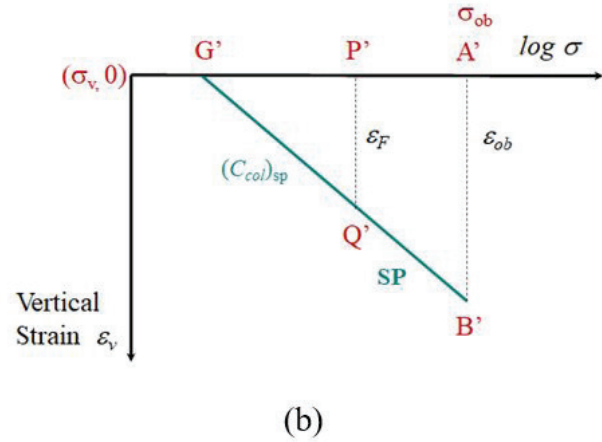
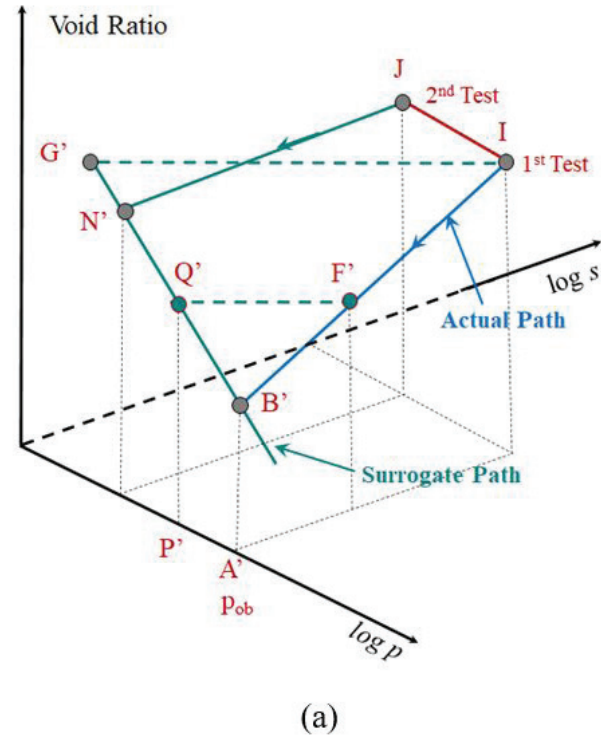


**Figure 12.** Graphical representation of SPM for collapsible soils: (a) mapping of actual stress path to net total stress surrogate path; (b) surrogate path used for analysis.

The partial wetting strain,  $\epsilon_{pw}$ , corresponding to the final suction value for field conditions, is calculated as follows:

$$\epsilon_{pw} = C_{col} \log\left(\frac{\sigma_{p'}}{\sigma_{G'}}\right) \quad (33)$$

$$\text{where } \sigma_{p'} = \sigma_{G'} + (1 - R_w)(\sigma_{ob} - \sigma_{G'}) \quad (34)$$

where  $\sigma_{G'}$  = stress level corresponding to zero volume change upon specimen submergence, and  $\sigma_{p'}$  = surrogate total stress for partial wetting conditions for collapsible soil.

The  $C_{col}$  value for collapsible soil should be given a negative sign to assure that subsequently computed partial wetting collapse strains are compressive. The expression for estimation of partial wetting collapse strains is analogous to that of  $\sigma_p$  for swelling, except that  $(I-R_w)$  is used instead of  $R_w$  because  $\sigma_{ob}$  is greater than  $\sigma_G$ . Due to observed threshold values of suction (degree of saturation) required to induce soil collapse (Houston & Houston, 1997), use of the SPM for collapse is slightly conservative for small degree of wetting of natural cemented soil.

The SPM makes use of oedometer tests performed on relatively undisturbed soil specimens. For natural cemented collapsible soils (not compacted soils), the dry strains observed in loading to appropriate net total stress, prior to wetting, should be added into the fully wetted strain for relatively undisturbed field samples exhibiting collapse, to account for sample disturbance effects (Houston & Houston, 1997). For soils exhibiting expansion upon full wetting, the fully wetted strain should be that associated with re-zeroing the LVDT after first loading “dry” to in-situ stress level, as a means of compensating to some extent for sampling distance. The above corrections for collapsible and expansive soils, respectively, go in the right direction for correcting for sampling disturbance.

#### 4.5.2 Use of the MSSA to evaluate the SPM

The SPM is consistent with the existing elastoplastic framework of unsaturated soils, as can be demonstrated using the MSSA. Figures 13 through 15 demonstrate the application of the SPM, within the context of the MSSA elastoplastic framework, for three example cases (A, B, and C) representing different initial conditions and different volume change responses (expansion or collapse) for unsaturated soil.

For the SPM, the ASTM D4546 test specimen (ASTM, 2014) is first loaded at in-situ moisture to field (or prototype) net total stress conditions, and then submerged (fully wetted) under load. If the net total stress is at a relatively low level, both the wetting path and the surrogate path are expected to fall in the elastic zone as shown for Case A in Figure 13. Point I represents the soil condition at the original in-situ suction and net total stress. The soil is fully wetted along the stress path of IFB, which has the same constant net total stress as that in the field, and point B represents the void ratio at zero suction after full wetting. The surrogate path is GQB, at the zero suction. The instantaneous slope of the surrogate path,  $m_r^s$  ( $C_H$  in log p-log s space), can be obtained by performing an ASTM D4546 test, Method B, to establish point B, and a second ASTM D4546 test, at a different net total stress level, obtaining slope  $C_H$  due to the assumed linear relationship between void ratio and log net mean stress along GQB. Alternatively, where companion specimens are not practical, Point G can be estimated by a load-back test, as described previously – or a constant volume swell test could be performed. For case A, the initial state

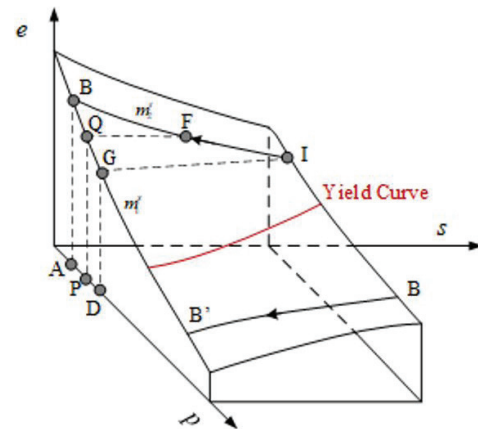


**Figure 13.** MSSA representation of the SPM under elastic conditions, example Case A.

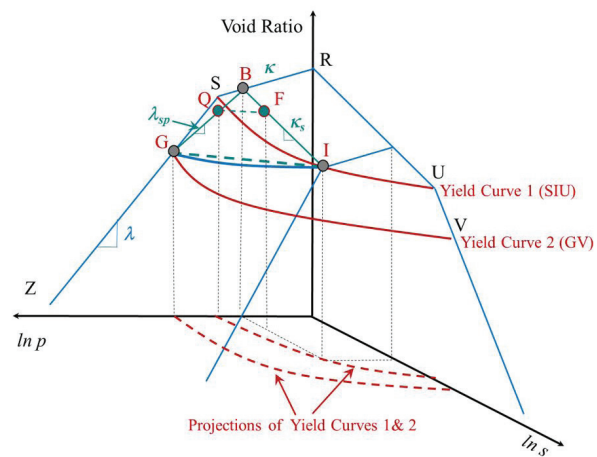


**Figure 14.** MSSA representation of the SPM for unsaturated expansive soils: example Case B.

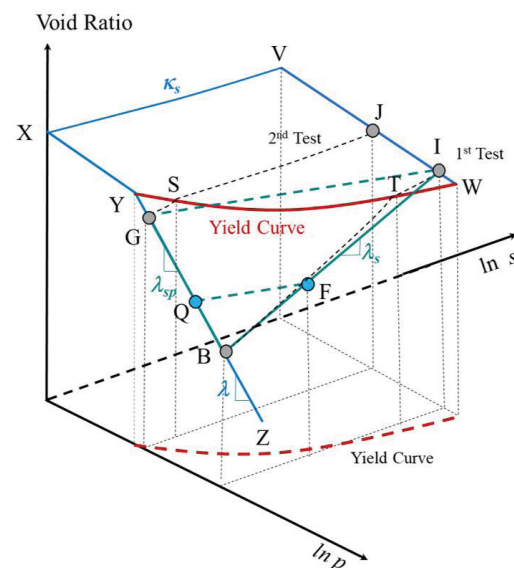


**Figure 15.** MSSA representation of the SPM for unsaturated collapsible soils: example Case C.



of the soil is in the elastic zone, and the soil remains in the elastic zone during the entire wetting process. As shown in Figure 13, the Case A stress paths, IFB and GQB, are both in the elastic zone. The slope of IFB in Figure 13 is  $m_2^s$  as defined by Fredlund & Rahardjo (1993), corresponding to  $\kappa_s$  in Alonso et al. (1990) where a natural logarithmic scale of suction is used. Using the definitions of Fredlund & Rahardjo (1993), the slope of the surrogate path BQG in Figure 13 is  $(m_1^s)_{sp}$ , corresponding to  $\kappa$  for the natural logarithmic scale of suction used in the Alonso et al. (1990).

In the SPM, if the final soil suction at point F the field is known, then the volume of the soil due to partial wetting can be mapped from point F on the stress path IFB to point Q on the surrogate path GQB using Equations 29, 30, and 31. For case A, where the soil remains in the elastic range during performance of both the ASTM D4546 swell test and for constant volume swell (ASTM, 2014), the SPM gives the correct volume at point Q on the surrogate path. The actual path (IF) follows along the slope  $m_2^s$ , and the surrogate path, QG, follows the correct corresponding state surface (with slope  $m_1^s$ ) in the  $s = 0$  plane.

Figure 14 shows Case B, an example application of the SPM for unsaturated expansive soils wherein the soil remains in the elastic range during the ASTM D4546 swell test (ASTM, 2014), but enters the plastic state during constant volume swell. As shown in Figure 14, surfaces RSU and SGVU represent the elastic and virgin (plastic) state surface of an expansive soil, respectively. The intersection of the elastic and plastic surfaces, SU, represents the initial location of the yield curve. Point I represents the soil conditions at the initial in-situ suction and at the in-situ net total stress, placing the field specimen on the initial yield curve, for Case B. The soil is fully wetted to zero suction along the stress path of IFB under a constant net total stress corresponding to field overburden conditions (ASTM D4546, Method B test). For Case B, this process is fully elastic and the final point B remains in the elastic zone. However, as shown in Figure 14, point G, which has the same void ratio as that of point I, falls on the virgin loading (plastic) surface when the specimen at point I is subjected to a constant volume swell to  $s = 0$ . Point G can be estimated by the load-back method by fully wetting (to  $s = 0$ ) a companion specimen, at net total stress significantly higher than that of point I, to obtain the slope of BQG, assumed linear with slope  $C_H$ , on the log  $p$ ,  $s = 0$  plane. Of course, point G could also be obtained by running a constant volume swell test. Regardless of the testing method used to obtain point G, yielding of the soil occurs in arriving at point G, and the yield curve expands to the position of the second yield curve, GV, depicted in Figure 14. Regardless of the different possible stress paths followed in arriving at point G, the obtained point G will be the same in that it is on the virgin surface.

When the SPM is used for the situation of Case B, the volume of the soil at partial wetting to point F is obtained by mapping from the stress path IF to point Q on the surrogate

path BQG using Equations 29, 30, and 31. As shown in Figure 14,  $\lambda_{sp}$  (the slope of the surrogate path) is not exactly  $\lambda$  nor  $\kappa$  in the elastoplastic framework. Instead,  $\lambda_{sp}$  represents a mixed effect, given the changes from elastic to elastoplastic zones. However, the SPM still gives the correct volume at point Q on the surrogate path for Case B, because path IFB remains in the elastic range while only the surrogate path crosses from an elastic to a plastic condition. Provided the actual path, IFB, is modeled correctly, the surrogate path does not have to exactly match the actual state surface in the  $s = 0$  plane to obtain the correct void ratio at point Q.

Figure 15 shows Case C, an example application of the SPM for an unsaturated collapsible soil. As shown in Figure 15, surfaces XYWV and YZW represent the elastic and virgin state surfaces, respectively, of a collapsible soil, and YW represents the initial location of the yield curve. Different from the surfaces shown in Figure 14, the state surface for the unsaturated collapsible soil is warped, and the yield stress  $p$  increases with suction along the yield curves, as can be seen by the projection of the yield curve in Figure 15. Point I represents the soil conditions at the original in-situ suction and a relatively high in-situ net total stress, which positions the soil just inside the elastic zone. The soil is fully wetted, under constant field net total stress conditions, along the stress path of IFB to point B at zero suction. This process involves a very small elastic swelling from point I to T, followed by significant wetting-induced collapse caused by plastic yielding of the soil from point T to B.

When the SPM is used for collapsible soil, normally a second wetting test at a stress level lower than that at the field conditions will be performed to obtain the surrogate path GQB. The second specimen has an initial condition of point J, different from the initial condition of point I (in general, the suction level can be different from that of point I as well). The second specimen is wetted under a constant net total stress to point S in the elastic zone, followed by a wetting collapse from point S to G at zero suction. The surrogate path GQB, with slope  $\lambda_{sp}$  is obtained by connecting points G and B.

For known final suction at point F, the SPM can be used to obtain an estimate of the field partial wetting volume change response at point F, corresponding to point Q on the surrogate path. As shown in Figure 15,  $\lambda_{sp}$  is the same as  $\lambda$  in the elastoplastic framework, because points B and G both fall on the virgin surface. When the initial point I is in the elastic zone, as for Case C, IFB is at least somewhat different from the actual stress path of ITB, which can lead to slight overestimate (conservative) estimation of the soil collapse. This overestimate is, however, very small, because the elastic swelling for unsaturated collapsible soil is normally quite small and the soil is typically very close to the yield curve (point W) under normal field conditions. If the collapsible soil is initially on the yield curve, such as having an initial state of point W (Figure 15), then the stress path ITB becomes exactly IFB. Under this situation of an initial state at point W,

the slope of the IFB is the  $\lambda_e$  in the elastoplastic framework, and the estimated partial wetting strain at point Q is correct and not even slightly overestimated.

Cases A, B, and C above demonstrate that the SPM provides good estimates, from the MSSA perspective, of volume change of unsaturated soils under conditions of wetting under constant net stress, whether the soil response is expansion or collapse, and whether the soil has elastic or elastoplastic response, or both. This is a result of the anchoring of the SPM to the correct void ratio response at the endpoints of the surrogate path, points G and B (corresponding, respectively, to the void ratio for no suction change, point I, and the void ratio for suction decrease to  $s = 0$ , point B, along the actual field stress path. Further, the SPM is consistent with, and is easily-visualized within, the elastoplastic framework of the MSSA. As can be seen through the above discussions of cases A, B, and C, point B (Figures 13 to 15) can be guaranteed to fall of the actual  $s = 0$  state surface because the exact field stress path (IFB) is followed in arrival at point B. Point G (or the corresponding G' for the case of collapse), is simply used as a part of the mapping process in going from the actual stress path (IFB) to the  $s = 0$  plane. Therefore, volume change estimates that are adequate for routine engineering foundation design are assured through use of the SPM, provided relatively undisturbed representative specimens are used in performance of the ASTM D4546, Method B test (ASTM, 2014). The soil response modeled using the SPM is consistent with known unsaturated soil volume-change behavior, and the SPM accounts for effects of net total stress in the suction-induced volume change response of unsaturated soil.

#### 4.6 Lytton Method: method of analysis of 1-D heave

The Lytton Method is used extensively in the USA for expansive soil foundation and pavement design purposes. The method has been adopted by the Post-Tensioning Institute (PTI, 2008). The method proposed by Lytton (1977) considers the influence of both net total stress and soil suction in the computation of volumetric strain.

$$\frac{\Delta V}{V_0} = -\gamma_h \log_{10} \left( \frac{h_f}{h_i} \right) - \gamma_\sigma \log_{10} \left( \frac{\sigma_f}{\sigma_i} \right) \quad (35)$$

where  $\gamma_h$  is the slope of the void ratio versus log suction curve when  $p$  is essentially zero, and  $\gamma_\sigma$  is the slope of the void ratio versus log net total stress curve when  $s$  is essentially zero. The net total stress term is only considered until the strains become zero, and soil collapse is not taken into account.

The soil volume change is assumed to be linearly related to the log of soil suction and the log of net total stress. Although Lytton offers oedometer-based methods for determination of the suction index,  $\gamma_h$ , and the compression index,  $\gamma_\sigma$ , emphasis has been placed on empirically-based

approaches to estimation of these suction and compression index values using commonly available soil parameters (PTI, 2008). As with the Fredlund Method, the Lytton approach allows for use of the slope of unload curve from a saturated consolidation test (however, multiplied by 0.7) in determining  $C_s$ , which can lead to underestimates of void ratio where the soil exhibits elastoplastic response during expansion (see Figure 10 and associated discussions). The Lytton Method (PTI, 2008) provides multiple options for estimation of the suction index, and consistency across options cannot be assured, resulting in the potential for differing heave estimates across engineering professionals.

The suction index used by Lytton is conceptualized as the suction index for zero to very light confinement. The effects of suction change and net total stress change are completely decoupled in the Lytton Method. Although the Lytton Method does not directly consider the combined effect of the two unsaturated soil stress state variables, the volume change that occurs in response to change in soil suction is reduced to account for the influence of confining stress (e.g., overburden stress). In the context of the MSSA, because of the decoupling of the suction and net total stress effects, the Lytton Method can be shown to consider only the state surface bounding curves of Figure 8 (i.e., the net total stress plane where  $s$  is essentially zero and the suction plane where  $p$  is essentially zero). Solutions based on the Lytton Method (PTI, 2008) would, in general, be expected to deviate from the MSSA because the path dependency of expansive soil volume change response is not directly addressed, and because the actual field stress path is not required to be followed in the determination of the suction index and the compression index. However, the Lytton Method (PTI, 2008) provides for use of empirically-based (field-calibrated) approaches in the determination of the suction index and compression index, which when used appropriately represent one way to mitigate (reduce) errors in void ratio estimate when using the PTI-based analyses.

## 5. Conclusions

The traditional state surface approach emerged from the recognition that unsaturated soil volume change response is complex and requires the simultaneous consideration of two stress state variables, net total stress and matric suction. One major advantage of the SSA is that the soil model is based upon observed (measured) laboratory unsaturated soil response. If a soil exhibits either expansion or collapse, or both, upon wetting under the range of total net stress conditions of interest, the surface can simply be modified to accommodate. A disadvantage of the traditional state surface approach is that there is no direct way to separate elastic soil response from elastoplastic soil response. This disadvantage becomes more severe when the tested soil specimens do not have the same stress history. In principle, incremental elastic formulations of the state surface, such as that detailed by

Fredlund & Rahardjo (1993), can handle some aspects of elastoplastic behavior, such as accommodating unload/reload via change of elastic modulus. However, the traditional state surface still suffers some difficulties in proportioning elastic and plastic soil components of volume change. Elastoplastic models, starting with the BBM (Alonso et al., 1990), emerged to address some of the challenges posed in using the SSA for unsaturated soils that are known to exhibit elastoplastic behavior. However, in the development of elastoplastic models for unsaturated soils, some of the valuable aspects of the SSA were lost. In particular, as revealed through consideration of the MSSA, the addition of multiple yield surfaces to accommodate elastoplastic expansion and collapse within the same model can result in a void ratio state surface that is inconsistent with available laboratory data when it is viewed in whole. The primary modification that can lead to simplification of most elastoplastic unsaturated soil models is the introduction of greater flexibility in defining the yield surface (i.e. the virgin state surface). Added flexibility in the establishment of the yield curve avoids the need for the introduction of multiple yield surfaces and reduces the number of required soil parameters, in general.

By adopting the relatively simple elastoplastic framework of the MSSA, practice-based oedometer methods can be evaluated for consistency with known unsaturated soil volume change response. In this way, better approaches for estimating volume change consistent with measured field stress-path dependent response can be identified. Further, because of the heavy use of oedometer testing methods for expansive and collapsible soils, it is helpful to explain common test procedures within the unsaturated soil elastoplastic framework. The MSSA was used to demonstrate, through consideration of general elastoplastic soil behavior, the importance of anchoring practice-based solutions to problems of collapse or expansion to field stress-path appropriate laboratory tests. For 1-D,  $K_0$ , constant net total stress field conditions under a path of soil wetting, the ASTM D4546 (ASTM, 2014), Method B, swell test provides the most important anchor point for volume change computation. Another important anchor point is the no-wetting (no suction change) soil response, wherein the soil specimen remains at the initial in-situ void ratio. The SPM (Houston & Houston, 2018) is an oedometer test/suction-based method, requiring: (1) initial and final soil suction values, (2) ASTM D4546, Method B, test results, and (3) a measurement or estimate of the net total stress level that, when applied to the soil specimen, results in zero volume change when suction is brought to zero. The SPM uses a suction value-based mapping to estimate volume change when field wetting is intermediate between no wetting and full wetting corresponding to the ASTM D4546 test. The SPM is based on a two-stress state variable approach to unsaturated soil mechanics, is consistent with known elastoplastic unsaturated soil volume change response, and applies to both expansive and collapsible soils. Major advantages of the SPM include simplicity and bounding of

the problem solution for consistency with path-appropriate measured soil response, which results in consistency of volume change estimates across different users of the method.

Appropriate constitutive models for volume change of unsaturated soil, whether for advanced research or practice-based foundation design, require consistency with observed soil behavior across a full spectrum of stress path conditions. The MSSA is a relatively simple elastoplastic framework that is useful in the evaluation of unsaturated soil volume change constitutive models. The MSSA makes use of the traditional state surface approach (SSA), which was based on laboratory-observed unsaturated soil behavior, requiring the use of two independent stress state variables, net total stress, and suction. Retention of these important features of the SSA in the development of unsaturated soil constitutive models is required to ensure consistency of approaches that geotechnical engineers use, regardless of level of sophistication of model required for the problem at hand.

## Acknowledgements

The authors would like to acknowledge Professor William N. Houston for his valuable review and discussions on this paper, and for his contributions and insight relative to the SPM method. The authors also acknowledge the contributions of graduate students Beshoy Riad and Javad Galinmoghdam for assistance with preparation of figures and formatting of the final manuscript.

## Declaration of interest

The authors have not conflict of interests regarding the material included in this paper.

## Authors' contributions

Sandra L. Houston: writing, reviewing, editing, investigation, methodology. Xiong Zhang: writing, reviewing, editing, investigation, methodology.

## List of symbols

$C_1, C_2, C_3,$ and $C_4$	constants
$a, b, c,$ and $d$	constants
$C_s K_0$	loading coefficient corresponding suction;
$C_m K_0$	loading coefficient corresponding net total stress;
$C_H$	swelling index;
$C_{col}$	collapsing index;
$(C_{col})_{sp}$	collapsing index for surrogate path;
$(C_H)_{sp}$	swelling index for surrogate path;
$m_{1-1D}^s$	coefficient of total volume change with respect to mechanical stress under 1D constrained loading;

$m_{2-1D}^s$	coefficient of total volume change with respect to changes in the matric suction under 1D constrained loading;	$\kappa$	slope of the unloading-reloading line associated with the mean net stress;
$e$	voids ratio;	$\kappa_s$	slope of the unloading-reloading line associated with soil suction;
$e_0$	initial voids ratio;	$\lambda_s$	slope of the virgin compression line associated with soil suction;
$e_f$	final voids ratio;	$\lambda(s)$	slope of the virgin compression line associated with the mean net stress for $s \neq 0$ ;
$\Delta e$	change in void ratio between the initial and final stress states ( $= e_f - e_0$ );	$\lambda(0)$	slope of the virgin compression line associated with the mean net stress for $s = 0$ ;
$R_w$	ratio of the final suction to the initial matric suction values;	$\lambda_{sp}$	slope of surrogate path;
$\Delta V$	volume change;	$m_1^{se}$	coefficient of volume change with respect to mechanical stress in the elastic zone, or bulk modulus of the soil in the elastic zone;
$V_0$	initial volume;	$m_2^{se}$	coefficient of volume change with respect to changes in matric suction or coefficient of expansion due to matric suction change;
$h_i$	initial sample height;	$m_1^s$	coefficient of total volume change with respect to mechanical stress in the elastoplastic zone;
$h_f$	final sample height;	$(m_1^s)_{sp}$	coefficient of total volume change with respect to mechanical stress in the elastoplastic zone for surrogate path;
$\bar{K}_0$	at-rest earth pressure coefficient;	$m_2^s$	coefficient of total volume change with respect to changes in the matric suction.
$k$	parameter that relates cohesion and suction;		
$M$	slope of theoretical critical state line;		
$N(s)$	specific volume for $p p^C$ ;		
$p$	net mean stress ( $\sigma_m - u_a$ );		
$p_{at}$	atmospheric pressure;		
$p^C$	reference stress;		
$\sigma_v$	net vertical stress;		
$\sigma_{ob}$	overburden stress;		
$\sigma_{ocv}$	constant volume swell pressure;		
$\sigma_i$	initial net stress;		
$\sigma_f$	final net stress;		
$p_0$	apparent preconsolidation pressure at a certain suction;		
$p_0^*$	preconsolidation pressure in saturated conditions;		
$P_0$	initial stress state;		
$P_f$	final stress state;		
$q$	deviatoric stress ( $\sigma_1 - \sigma_2$ );		
$r$	parameter controlling the slope of the virgin compression line;		
$s$	soil suction ( $u_a - u_w$ );		
$s_0$	maximum historical suction applied to the soil;		
$s_i$	initial suction value;		
$s_f$	final suction value;		
$u_a$	air pressure;		
$u_w$	water pressure;		
$u_{wf}$	final pre-water pressure;		
$v$	specific volume;		
$\gamma_h$	slope of the void ratio versus log suction curve when $p$ zero;		
$\gamma_\sigma$	slope of the void ratio versus log net total stress curve when $s$ zero;		
$\beta$	parameter that controls the slope of the virgin compression line for $s \neq 0$ ;		
$\varepsilon_v$	volumetric strain;		
$d\varepsilon_v$	volumetric strain increment;		
$\varepsilon_{ob}$	full wetting swell strain;		
$\varepsilon_{pw}$	partial wetting strain;		
$\varepsilon_v^e$	elastic volumetric strains;		
$\varepsilon_v^p$	plastic volumetric strain;		

## References

- Adem, H.H., & Vanapalli, S.K. (2013). Constitutive modeling approach for estimating 1-D heave with respect to time for expansive soils. *International Journal of Geotechnical Engineering*, 7(2), 199-204. <http://dx.doi.org/10.1179/1938636213Z.000000000024>.
- Adem, H.H., & Vanapalli, S.K. (2015). Review of methods for predicting in situ volume change movement of expansive soil over time. *Journal of Rock Mechanics and Geotechnical Engineering*, 7(1), 73-86. <http://dx.doi.org/10.1016/j.jrmge.2014.11.002>.
- Alonso, E.E, Gens, A., & Gehling, W.Y.Y. (1994). Elastoplastic model for unsaturated expansive soils. In *Proceedings of the 3rd European Conference on Numerical Models in Geotechnical Engineering* (pp. 11-18), Rotterdam.
- Alonso, E.E. (1987). Special problem soils: general report. In *Proceedings of the 9th European Conference on Soil Mechanics and Foundation Engineering* (Vol. 3, pp. 1087-1146). Dublin: CRC Press.
- Alonso, E.E., Gens, A., & Josa, A. (1990). A constitutive model for partially saturated soils. *Geotechnique*, 40(3), 405-430. <http://dx.doi.org/10.1680/geot.1990.40.3.405>.
- Alonso, E.E., Vaunat, J., & Gens, A. (1999). Modelling the mechanical behaviour of expansive clays. *Engineering Geology*, 54(1-2), 173-183. [http://dx.doi.org/10.1016/S0013-7952\(99\)00079-4](http://dx.doi.org/10.1016/S0013-7952(99)00079-4).
- Alonso, E.E. (August 27–30, 1998). Modelling expansive soil behaviour. In *Proceedings of the 2nd International*



- Conference on Unsaturated Soils* (Vol. 2, pp. 37–70). Beijing: International Academic Publishers.
- ASTM D4546. (2014). *Standard test methods for one-dimensional swell or collapse of soils*. ASTM International, West Conshohocken, PA. <https://doi.org/10.1520/D4546-14E01>.
- ASTM D4943. (2018). *Standard test method for shrinkage factors of cohesive soils by the water submersion method*. ASTM International, West Conshohocken, PA. <https://doi.org/10.1520/D4943-18>.
- Barden, L., McGown, A., & Collins, K. (1973). The collapse mechanism in partly saturated soil. *Engineering Geology*, 7(1), 49–60. [http://dx.doi.org/10.1016/0013-7952\(73\)90006-9](http://dx.doi.org/10.1016/0013-7952(73)90006-9).
- Bellil, S., Abbeche, K., & Bahloul, O. (2018). Treatment of a collapsible soil using a bentonite-cement mixture. *Studia Geotechnica et Mechanica*, 40(4), 233–243. <http://dx.doi.org/10.2478/sgem-2018-0042>.
- Blatz, J.A., & Graham, J. (2003). Elastic-plastic modelling of unsaturated soil using results from a new triaxial test with controlled suction. *Geotechnique*, 53(1), 113–122. <http://dx.doi.org/10.1680/geot.2003.53.1.113>.
- Bolzon, G., Schrefler, B.A., & Zienkiewicz, O.C. (1996). Elastoplastic soil constitutive laws generalized to partially saturated states. *Geotechnique*, 46(2), 279–289. <http://dx.doi.org/10.1680/geot.1996.46.2.279>.
- Brackley, I.J.A. (1973). *Swell pressure and free swell in compacted clay*. Pretoria, South Africa: National Building Research Institute, Council for Scientific and Industrial Research.
- Brackley, I.J.A. (1975). Swell under load. In *Proceedings of the 6th Regional Conference for Africa Soil Mechanics and Foundation Engineering* (Vol. 1, pp. 65–70). Durban: National Building Research Institute/CSIR.
- Briaud, J.L., Zhang, X., & Moon, S. (2003). Shrink test-water content method for shrink and swell predictions. *Journal of Geotechnical and Geoenvironmental Engineering*, 129(7), 590–600. [http://dx.doi.org/10.1061/\(ASCE\)1090-0241\(2003\)129:7\(590\)](http://dx.doi.org/10.1061/(ASCE)1090-0241(2003)129:7(590)).
- Casagrande, A. (1936). The determination of preconsolidation load and its practical significance. In *Proceedings of the 1st International Conference on Soil Mechanics and Foundation Engineering* (Vol. 3, pp. 60–64). Cambridge, MA: Graduate School of Engineering, Harvard University.
- Chao, K.C. (2007). *Design principles for foundations on expansive soils* [Doctoral dissertation, Colorado State University Fort Collins]. Colorado State University Fort Collins' repository.
- Costa, L.M., & Alonso, E.E. (2009). Predicting the behavior of an earth and rockfill dam under construction. *Journal of Geotechnical and Geoenvironmental Engineering*, 135(7), 851–862. [http://dx.doi.org/10.1061/\(ASCE\)GT.1943-5606.0000058](http://dx.doi.org/10.1061/(ASCE)GT.1943-5606.0000058).
- Cui, Y.J., & Delage, P. (1996). Yeilding and plastic behaviour of an unsaturated compacted silt. *Geotechnique*, 46(2), 291–311. <http://dx.doi.org/10.1680/geot.1996.46.2.291>.
- D'Onza, F., Wheeler, S.J., Gallipoli, D., Barrera Bucio, M., Hofmann, M., Lloret-Cabot, M., Lloret Morancho, A., Mancuso, C., Pereira, J.-M., Romero Morales, E., Sánchez, M., Sołowski, W., Tarantino, A., Toll, D.G., & Vassallo, R. (2015). Benchmarking selection of parameter values for the Barcelona basic model. *Engineering Geology*, 196, 99–118. <http://dx.doi.org/10.1016/j.enggeo.2015.06.022>.
- Dafalias, Y.F., & Herrmann, L.R. (1982). Bounding surface formulation of soil plasticity. In G.N. Pande & O.C. Zienkiewicz (Eds.), *Soil mechanics: transient and cyclic loads* (pp. 253–282). New York: John Wiley & Sons.
- Dangla, P., Malinsky, L., & Coussy, O. (1997). Plasticity and imbibition-drainage curves for unsaturated soils: a unified approach. In *Proceedings of the Numerical Models in Geomechanics: NUMOG VI* (pp. 141–146). Montreal: CRC Press.
- Delage, P., & Graham, J. (1996). Mechanical behaviour of unsaturated soils: understanding the behaviour of unsaturated soils requires reliable conceptual models. In *Proceedings of the 1st International Conference on Unsaturated Soils (UNSAT)* (Vol. 3, pp. 1223–1256). Paris: Balkema.
- Dessouky, S., Oh, J.H., Yang, M., Ilias, M., Lee, S.I., & Jao, M. (2012). *Pavement repair strategies for selected distresses in FM roadways*. Texas: Texas Transportation Institute.
- Dif, A.E., & Bluemel, W.F. (1991). Expansive soils under cyclic drying and wetting. *Geotechnical Testing Journal*, 14(1), 96–102. <http://dx.doi.org/10.1520/GTJ10196J>.
- Driscoll, R.M.C., & Crilly, M.S. (2000). *Subsidence damage to domestic buildings: lessons learned and questions remaining*. Watford, UK: Foundation for the Built Environment (FBE).
- Fityus, S., & Buzzi, O. (2009). The place of expansive clays in the framework of unsaturated soil mechanics. *Applied Clay Science*, 43(2), 150–155. <http://dx.doi.org/10.1016/j.clay.2008.08.005>.
- Fonte, N.L., de Carvalho, D., & Kassouf, R. (2017). Improvement of collapsible soil conditions for industrial floors. In *Proceedings of the International Congress and Exhibition "Sustainable Civil Infrastructures: Innovative Infrastructure Geotechnology"* (pp. 177–193). Switzerland: Springer. [https://doi.org/10.1007/978-3-319-61902-6\\_15](https://doi.org/10.1007/978-3-319-61902-6_15).
- Fredlund, D.G. (1979). Second Canadian Geotechnical Colloquium: appropriate concepts and technology for unsaturated soils. *Canadian Geotechnical Journal*, 16(1), 121–139. <http://dx.doi.org/10.1139/t79-011>.
- Fredlund, D.G., & Morgenstern, N.R. (1976). Constitutive relations for volume change in unsaturated soils. *Canadian Geotechnical Journal*, 13(3), 261–276. <http://dx.doi.org/10.1139/t76-029>.
- Fredlund, D.G., & Morgenstern, N.R. (1977). Stress state variables for unsaturated soils. *Journal of Geotechnical and Geoenvironmental Engineering*, 103(5). <http://dx.doi.org/10.1061/ajgeb6.0000423>.

- Fredlund, D.G., & Rahardjo, H. (1993). *Soil mechanics for unsaturated soils*. New York: John Wiley & Sons. <http://dx.doi.org/10.1002/9780470172759>.
- Fredlund, D.G., Hasan, J.U., & Filson, H. (1980). The prediction of total heave. In *Proceedings of the 4th International Conference on Expansive Soils* (pp. 1-11). Denver: ASCE.
- Fredlund, D.G., Rahardjo, H., & Fredlund, M.D. (2012). *Unsaturated soil mechanics in engineering practice*. Hoboken: John Wiley & Sons. <http://dx.doi.org/10.1002/9781118280492>.
- Gallipoli, D., Gens, A., Sharma, R., & Vaunat, J. (2003a). An elastoplastic model for unsaturated soil incorporating the effects of suction and degree of saturation on mechanical behaviour. *Geotechnique*, 53(1), 123-136. <http://dx.doi.org/10.1680/geot.2003.53.1.123>.
- Gallipoli, D., Wheeler, S.J., & Karstunen, M. (2003b). Modelling the variation of degree of saturation in a deformable unsaturated soil. *Geotechnique*, 53(1), 105-112. <http://dx.doi.org/10.1680/geot.2003.53.1.105>.
- Geiser, F., Laloui, L., & Vulliet, L. (2000). Modelling the behaviour of unsaturated silt. In A. Tarantino & C. Mancuso (Eds.), *Experimental evidence and theoretical approaches in unsaturated soils* (pp. 155-175). London: CRC Press. <https://doi.org/10.1201/9781482283761-15>.
- Gens, A., & Alonso, E.E. (1992). A framework for the behaviour of unsaturated expansive clays. *Canadian Geotechnical Journal*, 29(6), 1013-1032. <http://dx.doi.org/10.1139/t92-120>.
- Gens, A., & Olivella, S. (2001). THM phenomena in saturated and unsaturated porous media: fundamentals and formulation. *Revue Française de Génie Civil*, 5(6), 693-717. <http://dx.doi.org/10.1080/12795119.2001.9692323>.
- Gens, A., Alonso, E.E., & Delage, A. (1996). Constitutive modelling: application to compacted soils. In *Proceedings of the 1st International Conference on Unsaturated Soils (UNSAT)* (Vol. 3, pp. 1179-1200). Paris: Balkema.
- Houston, S.L. (2014). Characterization of unsaturated soils: the importance of response to wetting. In *Proceedings of the Geo-Congress 2014 Keynote Lectures* (pp. 77-96). Atlanta: ASCE. <https://doi.org/10.1061/9780784413289.004>.
- Houston, S.L. (2019). It is time to use unsaturated soil mechanics in routine geotechnical engineering practice. *Journal of Geotechnical and Geoenvironmental Engineering*, 145(5), 2519001. [http://dx.doi.org/10.1061/\(ASCE\)GT.1943-5606.0002044](http://dx.doi.org/10.1061/(ASCE)GT.1943-5606.0002044).
- Houston, S.L., & Houston, W.N. (1997). Collapsible soils engineering. In D. G. Fredlund & S. L. Houston (Eds.), *Unsaturated soil engineering practice geotechnical* (Special Publication, No. 68, pp. 199-232). New York: ASCE.
- Houston, S.L., & Houston, W.N. (2018). Suction-oedometer method for computation of heave and remaining heave. In *Proceedings of the 2nd Pan-American Conference on Unsaturated Soils* (pp. 93-116). Dallas: ASCE. <http://dx.doi.org/10.1061/9780784481677.005>.
- Houston, S.L., Houston, W.N., & Spadola, D.J. (1988). Prediction of field collapse of soils due to wetting. *Journal of Geotechnical Engineering*, 114(1), 40-58. [http://dx.doi.org/10.1061/\(ASCE\)0733-9410\(1988\)114:1\(40\)](http://dx.doi.org/10.1061/(ASCE)0733-9410(1988)114:1(40)).
- Houston, W.N., & Nelson, J.D. (2012). The state of the practice in foundation engineering on expansive and collapsible soils. In *Proceedings of the Geo-Congress 2014 Keynote Lectures* (pp. 608-642). Oakland: ASCE. <https://doi.org/10.1061/9780784412138.0023>.
- Jennings, J.E.B., & Burland, J.B. (1962). Limitations to the use of effective stresses in partly saturated soils. *Geotechnique*, 12(2), 125-144. <http://dx.doi.org/10.1680/geot.1962.12.2.125>.
- Jennings, J.E.B., & Knight, K. (1957). The additional settlement of foundations due to collapse of sandy soils on wetting. In *Proceedings of the 4th international conference on soil mechanics and foundation engineering* (pp. 316-319). London.
- Jones, L. (2018). Expansive soils. In P. Bobrowsky & B. Marker (Eds.), *Encyclopedia of engineering geology* (Encyclopedia of Earth Sciences Series). Cham: Springer. [http://dx.doi.org/10.1007/978-3-319-73568-9\\_118](http://dx.doi.org/10.1007/978-3-319-73568-9_118).
- Jones, L.D., & Jefferson, I. (2012). Expansive soils. In J. Burland, T. Chapman, H. Skinner & M. Brown (Eds.), *ICE manual of geotechnical engineering: geotechnical engineering principles, problematic soils and site investigation* (Vol. 1, pp. 413-441). London: ICE Publishing. <https://doi.org/10.1680/moge.57074>.
- Justo, J.L., Delgado, A., & Ruiz, J. (1984). The influence of stress-path in the collapse-swelling of soils at the laboratory. In *Proceedings of the 5th International Conference on Expansive Soils* (pp. 67-71). Adelaide: Institution of Engineers.
- Khalili, N., & Loret, B. (2001). An elastoplastic model for non-isothermal analysis of flow and deformation in unsaturated porous media: formulation. *International Journal of Solids and Structures*, 38(46-47), 8305-8330. [http://dx.doi.org/10.1016/S0020-7683\(01\)00081-6](http://dx.doi.org/10.1016/S0020-7683(01)00081-6).
- Knodel, P.C. (1992). *Characteristics and problems of collapsible soils*. Denver, CO: US Department of the Interior, Bureau of Reclamation, Research and Laboratory Services Division, Materials Engineering Branch.
- Karube, D. (1986). New concept of effective stress in unsaturated soil and its proving tests. In *Advanced triaxial testing of soil and rock*. ST 977. American Society for Testing and Materials, Philadelphia, Pa. pp. 539-552.
- Lambe, W. (1967). Stress path method. *Journal of the Soil Mechanics and Foundations Division*, 93(6), 309-331. <http://dx.doi.org/10.1061/JSFEAQ.0001058>.
- Li, P., Vanapalli, S., & Li, T. (2016). Review of collapse triggering mechanism of collapsible soils due to wetting. *Journal of Rock Mechanics and Geotechnical Engineering*, 8(2), 256-274. <http://dx.doi.org/10.1016/j.jrmge.2015.12.002>.

- Lin, B., & Cerato, A.B. (2014). Applications of SEM and ESEM in microstructural investigation of shale-weathered expansive soils along swelling-shrinkage cycles. *Engineering Geology*, 177, 66-74. <http://dx.doi.org/10.1016/j.enggeo.2014.05.006>.
- Lin, B., Cerato, A.B., Madden, A.S., & Elwood Madden, M.E. (2013). Effect of fly ash on the behavior of expansive soils: microscopic analysis. *Environmental & Engineering Geoscience*, 19(1), 85-94. <http://dx.doi.org/10.2113/gsegeosci.19.1.85>.
- Liu, X., Buzzzi, O., Yuan, S., Mendes, J., & Fityus, S. (2016). Multi-scale characterization of retention and shrinkage behaviour of four Australian clayey soils. *Canadian Geotechnical Journal*, 53(5), 854-870. <http://dx.doi.org/10.1139/cgj-2015-0145>.
- Lloret, A., & Alonso, E.E. (1985). State surfaces for partially saturated soils. In *Proceedings of the 11th International Conference on Soil Mechanics and Foundation Engineering* (Vol. 2, pp. 557-562). San Francisco: CRC Press.
- Lloret, A., & Alonso, E.E., (1980). Consolidation of unsaturated soils including swelling and collapse behaviour. *Geotechnique*, 30(4), 449-477. <http://dx.doi.org/10.1680/geot.1980.30.4.449>.
- Lloret, A., Villar, M.V., Sanchez, M., Gens, A., Pintado, X., & Alonso, E.E. (2003). Mechanical behaviour of heavily compacted bentonite under high suction changes. *Geotechnique*, 53(1), 27-40. <http://dx.doi.org/10.1680/geot.2003.53.1.27>.
- Lytton, R.L. (1977). Foundations on expansive soils. *Geofísica Internacional*, 17(3), 262. [http://dx.doi.org/10.1016/0016-7061\(77\)90058-1](http://dx.doi.org/10.1016/0016-7061(77)90058-1).
- Lytton, R. L. (1977). Foundations in expansive soils. In C. S. Desai and J. T. Christian (Eds.), *Numerical Methods in Geotechnical Engineering* (pp. 427-458). New York: McGraw-Hill.
- Lytton, R.L. (1994). *Prediction of movement in expansive clays* (Geotechnical Special Publication, Vol. 2, No. 40, pp. 1827-1845). Reston: ASCE.
- Marinho, F.A.M., & Teixeira, P.F. (2009). The use of a high capacity tensiometer for determining the soil water retention curve. *Soils and Rocks*, 32(2), 91-96.
- Matyas, E.L., & Radhakrishna, H.S. (1968). Volume change characteristics of partially saturated soils. *Geotechnique*, 18(4), 432-448. <http://dx.doi.org/10.1680/geot.1968.18.4.432>.
- Nelson, J.D., & Miller, D.J. (1992). *Expansive soils, problems and practice in foundation and pavement engineering*. New York: Wiley Press.
- Nelson, J.D., Chao, K.C., Overton, D.D., & Nelson, E.J. (2015). *Foundation engineering for expansive soils*. New York: Wiley Press. <http://dx.doi.org/10.1002/9781118996096>.
- Nelson, J.D., Durkee, D.B., & Bonner, J.P. (1998). Prediction of free field heave using oedometer test data. In *Proceedings of the 46th Annual Geotechnical Engineering Conference*. Lawrence, KS: University of Minnesota.
- Nelson, J.D., Reichler, D.K., & Cumbers, J.M. (2006). Parameters for heave prediction by oedometer tests. In *Proceedings of the 4th International Conference on Unsaturated Soils* (pp. 951-961). Carefree: ASCE. [http://dx.doi.org/10.1061/40802\(189\)76](http://dx.doi.org/10.1061/40802(189)76).
- Noorany, I. (2017). Soil tests for prediction of one-dimensional heave and settlement of compacted fills. In *Proceedings of the 2nd Pan-American Conference on Unsaturated Soils* (pp. 90-99). Dallas: ASCE. <https://doi.org/10.1061/9780784481707.010>.
- Noorany, I., & Houston, S. (1995). Effect of oversize particles on swell and compression of compacted unsaturated soils. In *Proceedings of the Conference of the Geotechnical Engineering Division of the ASCE in Conjunction with the ASCE Convention* (pp. 107-121). San Diego: ASCE.
- Noorany, I., & Stanley, J.V. (1994). Settlement of compacted fills caused by wetting. In *Proceedings of the Vertical and Horizontal Deformations of Foundations and Embankments* (pp. 1516-1530). San Diego: ASCE.
- Olaiz, A.H. (2017). *Evaluation of testing methods for suction-volume change of natural clay soils* [Doctoral dissertation, Arizona State University]. Arizona State University's repository. Retrieved in March 11, 2021, from <http://hdl.handle.net/2286/R.I.46336>.
- Overton, D.D., Chao, K.C., & Nelson, J.D. (2006). Time rate of heave prediction for expansive soils. In *GeoCongress 2006: Geotechnical Engineering in the Information Technology Age* (pp. 1-6). Atlanta: ASCE. [http://dx.doi.org/10.1061/40803\(187\)162](http://dx.doi.org/10.1061/40803(187)162).
- Pastor, M., Zienkiewicz, O.C., & Chan, A.C. (1990). Generalized plasticity and the modelling of soil behavior. *International Journal for Numerical and Analytical Methods in Geomechanics*, 14(3), 151-190. <http://dx.doi.org/10.1002/nag.1610140302>.
- Pereira, J.H.F., & Fredlund, D.G. (1997). Constitutive modeling of a meta-stable-structured compacted soil. In *Proceedings of the Symposium on Recent Developments in Soil and Pavement Mechanics* (pp. 317-326). Rio de Janeiro: Balkema.
- Picornell, M., & Lytton, R.L. (1984). Modelling the heave of a heavily loaded foundation. In *Proceedings of the 5th International Conference on Expansive Soils* (pp. 104-108). Adelaide: Institution of Engineers.
- Post Tensioning Institute – PTI. (2008). *Design and construction of post-tensioned slabs-on-ground* (3rd ed.). Phoenix: PTI.
- Pousada Presa, E. (1984). *Deformabilidad de las arcillas expansivas bajo succión controlada* [Doctoral thesis, Universidad Politécnica de Madrid]. Universidad Politécnica de Madrid's repository. Retrieved in March 11, 2021, from <http://oa.upm.es/508/>.
- Rampino, C., Mancuso, C., & Vinale, F. (2000). Experimental behaviour and modelling of an unsaturated compacted soil. *Canadian Geotechnical Journal*, 37(4), 748-763. <http://dx.doi.org/10.1139/t00-004>.

- Riad, B., & Zhang, X. (2019). A close-form formulation for continuous prediction of at-rest coefficient for saturated soils. *International Journal of Geomechanics*, 19(10), 04019110. [http://dx.doi.org/10.1061/\(ASCE\)GM.1943-5622.0001491](http://dx.doi.org/10.1061/(ASCE)GM.1943-5622.0001491).
- Riad, B., & Zhang, X. (2020). Modified state surface approach to study unsaturated soil hysteresis behavior. *Transportation Research Record: Journal of the Transportation Research Board*, 2674(10), 484-498. <http://dx.doi.org/10.1177/0361198120937014>.
- Riad, B., & Zhang, X. (2021). A consistent three-dimensional elastoplastic constitutive model to study the hydro-mechanical behavior of unsaturated soils. *Transportation Research Record: Journal of the Transportation Research Board*. In press. <http://dx.doi.org/10.1177/03611981211002217>.
- Robles, J., & Elorza, F.J. (2002). A triaxial constitutive model for unsaturated soils. In L. Vulliet, L. Laloui & B. Schrefler (Eds.), *Environmental geomechanics* (pp. 207-213). Lausanne: Presses Polytechniques et Universitaires Romandes.
- Sánchez, M., Gens, A., Nascimento Guimarães, L., & Olivella, S. (2005). A double structure generalized plasticity model for expansive materials. *International Journal for Numerical and Analytical Methods in Geomechanics*, 29(8), 751-787. <http://dx.doi.org/10.1002/nag.434>.
- Sheng, D., Fredlund, D.G., & Gens, A. (2008a). A new modelling approach for unsaturated soils using independent stress variables. *Canadian Geotechnical Journal*, 45(4), 511-534. <http://dx.doi.org/10.1139/T07-112>.
- Sheng, D., Gens, A., Fredlund, D.G., & Sloan, S.W. (2008b). Unsaturated soils: from constitutive modelling to numerical algorithms. *Computers and Geotechnics*, 35(6), 810-824. <http://dx.doi.org/10.1016/j.compgeo.2008.08.011>.
- Sheng, D., Sloan, S.W., & Gens, A. (2004). A constitutive model for unsaturated soils: thermomechanical and computational aspects. *Computational Mechanics*, 33(6), 453-465. <http://dx.doi.org/10.1007/s00466-003-0545-x>.
- Sheng, D., Sloan, S.W., Gens, A., & Smith, D.W. (2003a). Finite element formulation and algorithms for unsaturated soils. Part I: theory. *International Journal for Numerical and Analytical Methods in Geomechanics*, 27(9), 745-765. <http://dx.doi.org/10.1002/nag.295>.
- Sheng, D., Smith, D.W., Sloan, S., & Gens, A. (2003b). Finite element formulation and algorithms for unsaturated soils. Part II: verification and application. *International Journal for Numerical and Analytical Methods in Geomechanics*, 27(9), 767-790. <http://dx.doi.org/10.1002/nag.296>.
- Singhal, S. (2010). *Expansive soil behavior: property measurement techniques and heave prediction methods* [Doctoral dissertation, Arizona State University]. Arizona State University's repository.
- Tamagnini, R. (2004). An extended Cam-clay model for unsaturated soils with hydraulic hysteresis. *Geotechnique*, 54(3), 223-228. <http://dx.doi.org/10.1680/geot.2004.54.3.223>.
- Thu, T.M., Rahardjo, H., & Leong, E.C. (2007). Soil-water characteristic curve and consolidation behavior for a compacted silt. *Canadian Geotechnical Journal*, 44(3), 266-275. <http://dx.doi.org/10.1139/t06-114>.
- Vanapalli, S., & Lu, L. (2012). A state-of-the art review of 1-D heave prediction methods for expansive soils. *International Journal of Geotechnical Engineering*, 6(1), 15-41. <http://dx.doi.org/10.3328/IJGE.2012.06.01.15-41>.
- Vassallo, R., Mancuso, C., & Vinale, F. (2007). Modelling the influence of stress-strain history on the initial shear stiffness of an unsaturated compacted silt. *Canadian Geotechnical Journal*, 44(4), 447-462. <https://doi.org/10.1139/t06-130>.
- Vaunat, J., Romero, E., & Jommi, C. (2000). An elastoplastic hydromechanical model for unsaturated soils. In A. Tarantino & C. Mancuso (Eds.), *Experimental evidence and theoretical approaches in unsaturated soils* (pp. 121-139). Boca Raton: CRC Press. <https://doi.org/10.1201/9781482283761-13>.
- Vilarrasa, V., Rutqvist, J., Blanco Martin, L., & Birkholzer, J. (2016). Use of a dual-structure constitutive model for predicting the long-term behavior of an expansive clay buffer in a nuclear waste repository. *International Journal of Geomechanics*, 16(6), D4015005. [http://dx.doi.org/10.1061/\(ASCE\)GM.1943-5622.0000603](http://dx.doi.org/10.1061/(ASCE)GM.1943-5622.0000603).
- Vu, H.Q., & Fredlund, D.G. (2004). The prediction of one-, two-, and three-dimensional heave in expansive soils. *Canadian Geotechnical Journal*, 41(4), 713-737. <http://dx.doi.org/10.1139/t04-023>.
- Vu, H.Q., & Fredlund, D.G. (2006). Challenges to modelling heave in expansive soils. *Canadian Geotechnical Journal*, 43(12), 1249-1272. <http://dx.doi.org/10.1139/t06-073>.
- Washington. Department of Army. (1983). *Technical manual TM5-818-7: foundations in expansive soils*. US Army.
- Washington. Department of Navy. (1971). *Soil mechanics, foundations, and earth structures - NAVFAC Design Manual DM-7*. US Navy.
- Wheeler, S.J. (1996). Inclusion of specific water volume within an elastoplastic model for unsaturated soil. *Canadian Geotechnical Journal*, 33(1), 42-57. <http://dx.doi.org/10.1139/t96-023>.
- Wheeler, S.J., & Karube, D. (1996). Constitutive modelling. In *Proceedings of the 1st International Conference on Unsaturated Soils (UNSAT)* (Vol. 3, pp. 1323-1356). Paris: Balkema.
- Wheeler, S.J., & Sivakumar, V. (1995). An elastoplastic critical state framework for unsaturated soil. *Geotechnique*, 45(1), 35-53. <http://dx.doi.org/10.1680/geot.1995.45.1.35>.
- Wheeler, S.J., Sharma, R.S., & Buisson, M.S.R. (2003). Coupling of hydraulic hysteresis and stress-strain behaviour in unsaturated soils. *Geotechnique*, 53(1), 41-54. <http://dx.doi.org/10.1680/geot.2003.53.1.41>.
- Wheeler, S.J., Gallipoli, D., & Karstunen, M. (2002). Comments on use of the Barcelona Basic Model for unsaturated



- soils. *International Journal for Numerical and Analytical Methods in Geomechanics*, 26(15), 1561–1571.
- White, J.L. (2007). Characteristics and susceptibility of collapsible soils in Colorado: results of a Statewide study. In *Proceedings of the 2006 Biennial Geotechnical Seminar (GEO-Volution)* (pp. 86-98). Denver: ASCE. [https://doi.org/10.1061/40890\(219\)6](https://doi.org/10.1061/40890(219)6).
- Wray, W.K., El-Garhy, B.M., & Youssef, A.A. (2005). Three-dimensional model for moisture and volume changes prediction in expansive soils. *Journal of Geotechnical and Geoenvironmental Engineering*, 131(3), 311-324. [http://dx.doi.org/10.1061/\(ASCE\)1090-0241\(2005\)131:3\(311\)](http://dx.doi.org/10.1061/(ASCE)1090-0241(2005)131:3(311)).
- Wray, W.K. (1995). *So your home is built on expansive soils: a discussion of how expansive soils affect buildings*. Reston, Va: Shallow Foundation Committee of the Geotechnical Division of ASCE/ American Society of Civil Engineers (ASCE).
- Zhang, X. (2005). *Consolidation theories for saturated-unsaturated soils and numerical simulation of residential buildings on expansive soils* [Doctoral thesis, Texas A&M University]. Texas A&M University's repository. Retrieved in March 11, 2021, from <https://hdl.handle.net/1969.1/2747>
- Zhang, X. (2010). Analytical solution of the barcelona basic model. In L. R. Hoyos, X. Zhang & A. J. Puppala (Eds.), *Experimental and applied modeling of unsaturated soils* (pp. 96-103). Shanghai: ASCE. [http://dx.doi.org/10.1061/41103\(376\)13](http://dx.doi.org/10.1061/41103(376)13).
- Zhang, X. (2016). Limitations of the suction controlled tests in the characterization of constitutive behavior of unsaturated soils. *International Journal for Numerical and Analytical Methods in Geomechanics*, 40(2), 269-296. <http://dx.doi.org/10.1002/nag.2401>.
- Zhang, X., & Briaud, J. (2015). Three dimensional numerical simulation of residential building on shrink–swell soils in response to climatic conditions. *International Journal for Numerical and Analytical Methods in Geomechanics*, 39(13), 1369-1409. <http://dx.doi.org/10.1002/nag.2360>.
- Zhang, X., & Lytton, R.L. (2008). Discussion of “A new modeling approach for unsaturated soils using independent stress variables”. *Canadian Geotechnical Journal*, 45(12), 1784-1787. <http://dx.doi.org/10.1139/T08-096>.
- Zhang, X., & Lytton, R.L. (2009a). Modified state-surface approach to the study of unsaturated soil behavior. Part I: basic concept. *Canadian Geotechnical Journal*, 46(5), 536-552. <http://dx.doi.org/10.1139/T08-136>.
- Zhang, X., & Lytton, R.L. (2009b). Modified state-surface approach to the study of unsaturated soil behavior. Part II: general formulation. *Canadian Geotechnical Journal*, 46(5), 553-570. <http://dx.doi.org/10.1139/T08-137>.
- Zhang, X., & Lytton, R.L. (2012). Modified state-surface approach to the study of unsaturated soil behavior. Part III: modeling of coupled hydromechanical effect. *Canadian Geotechnical Journal*, 49(1), 98-120. <http://dx.doi.org/10.1139/t11-089>.
- Zhang, X., Liu, J., & Li, P. (2010). A new method to determine the shapes of yield curves for unsaturated soils. *Journal of Geotechnical and Geoenvironmental Engineering*, 136(1), 239-247. [http://dx.doi.org/10.1061/\(ASCE\)GT.1943-5606.0000196](http://dx.doi.org/10.1061/(ASCE)GT.1943-5606.0000196).
- Zhang, X., Alonso, E.E., & Casini, F. (2016a). Explicit formulation of at-rest coefficient and its role to calibrate elasto-plastic models for unsaturated soils. *Computers and Geotechnics*, 71, 56-68. <http://dx.doi.org/10.1016/j.compgeo.2015.08.012>.
- Zhang, X., Lu, H., & Li, L. (2016b). Characterizing unsaturated soil using an oedometer equipped with a high capacity tensiometer. *Transportation Research Record: Journal of the Transportation Research Board*, 2578(1), 58-71. <http://dx.doi.org/10.3141/2578-07>.

## Analytical and numerical methods for prediction of the bearing capacity of shallow foundations in unsaturated soils

Sai K. Vanapalli<sup>1#</sup> , Won-Taek Oh<sup>2</sup> 

Review Article

### Keywords

Unsaturated soils  
Shear strength  
Suction  
Modified effective stress approach  
Modified total stress approach  
Bearing capacity

### Abstract

Bearing capacity of saturated soils can be estimated using effective or total stress approaches extending the concepts proposed by Terzaghi (1943) and Skempton (1948), respectively. Recent studies have shown that similar approaches (i.e., Modified Effective Stress Approach, MESA and Modified Total Stress Approach, MTSA) can be used for interpretation and prediction of the bearing capacity of unsaturated soils by considering the influence of matric suction. However, comprehensive discussion for the application of the MESA and the MTSA in geotechnical engineering practice applications is lacking in the literature. For this reason, in this state-of-the-art paper, the background associated with the MESA and MTSA is first introduced. The analytical and numerical methods available for the prediction of the bearing capacity of unsaturated soils from the literature are revisited. The various available methods are explained by categorizing them into two groups: MESA and MTSA along with their applications using examples. The focus of this state-of-the-art paper is directed towards not only for providing tools for rational understanding but also for better prediction of the bearing capacity of unsaturated soils for extending them in geotechnical engineering practice applications.

## 1. Introduction

The soil bearing capacity is key information required in the design of shallow and deep foundations. In conventional engineering practice, bearing capacity of soils in many scenarios is estimated using either analytical or numerical methods. Both these methods require saturated shear strength parameters of soil taking account of their rate of loading and drainage conditions. For example, the bearing capacity equation originally proposed by Terzaghi (1943) requires the effective shear strength parameters,  $c'$  and  $\phi'$  (i.e., Effective Stress Approach, ESA) assuming drained condition in terms of pore-water. On the other hand, Skempton (1948) suggested that  $\phi_u = 0$  be used in calculating the bearing capacity of saturated soils under undrained condition (i.e., Total Stress Approach, TSA). In other words, the saturated shear strength parameters must be reliably determined taking account of rate of loading and drainage conditions to minimize the uncertainties associated with the calculation or prediction of the bearing capacity.

Research studies related to the bearing capacity of unsaturated soils highlight that it is significantly different from

saturated soils (Steensen-Bach et al., 1987; Oloo et al., 1997; Costa et al., 2003; Mohamed & Vanapalli, 2006; Rojas et al., 2007; Oh & Vanapalli, 2013; Tan et al., 2021). These studies also suggest that it is not reliable to use conventional approaches for estimating the bearing capacity of unsaturated soils. A third of the earth's surface constitutes of arid or semi-arid regions (Fredlund & Rahardjo, 1993). The natural ground water table is relatively at a greater depth from the natural ground surface in these regions. Due to this reason, the base of shallow foundation or major portion of a deep foundation is typically located in the vadose zone where soils are in a state of unsaturated condition. The influence of matric suction (or negative pore-water pressure) should be taken into account for the determination of the bearing capacity of unsaturated soils. Several researchers have developed analytical (e.g., Oloo et al., 1997; Vanapalli & Mohamed, 2007; Oh & Vanapalli, 2013; Vahedifard & Robison, 2016; Vo & Russel, 2016; Ghasemzadeh & Akbari, 2019; Garakani et al., 2020; Yan et al., 2020) & numerical (e.g., Abed & Vermeer, 2004; Ghorbani et al., 2016) methods for prediction or estimation of the bearing capacity of unsaturated soils. These studies clearly show that the bearing capacity of unsaturated soils

<sup>#</sup>Corresponding author. E-mail: vanapalli@eng.uottawa.ca

<sup>1</sup>University of Ottawa, Department of Civil Engineering, Ottawa, Ontario, Canada.

<sup>2</sup>University of New Brunswick, Department of Civil Engineering, Fredericton, New Brunswick, Canada.

Submitted on April 22, 2021; Final Acceptance on June 8, 2021; Discussion open until November 30, 2021.

<https://doi.org/10.28927/SR.2021.066521>



This is an Open Access article distributed under the terms of the Creative Commons Attribution License, which permits unrestricted use, distribution, and reproduction in any medium, provided the original work is properly cited.

can be estimated by extending the conventional ESA and TSA considering the influence of matric suction, which are referred to as the Modified Effective Stress Approach (i.e., MESA) and the Modified Total Stress Approach (i.e., MTSA).

In this state-of-the-art paper, the background of MESA and MTSA is first discussed in relation to the shear strength of unsaturated soils. The authors then revisit the analytical and numerical methods that are available in the literature to predict the bearing capacity of unsaturated soils. These methods are succinctly explained by categorizing them into two groups; namely, MESA and MTSA highlighting them with examples. In addition, the MESA proposed by Vanapalli & Mohamed (2007) is improved to provide better prediction of the bearing capacity of unsaturated coarse-grained soils for all the three zones; namely boundary effect, transition and residual zones that can be derived from the Soil-Water Characteristic Curve (SWCC). The summarized information in this state-of-the-art paper is useful for the practicing engineers for estimating the bearing capacity of unsaturated soils using limited information, which include the saturated shear strength properties and the SWCC.

### 1.1 Shear strength of unsaturated soils

The engineering behavior of saturated soils has been successfully interpreted and implemented in practice using the effective stress,  $\sigma'$  as a tool. Effective stress is an independent stress state variable that is defined as the difference between total stress,  $\sigma$  and pore-water pressure,  $u_w$  (i.e.,  $\sigma' = \sigma - u_w$ ; Terzaghi, 1936). The shear strength parameters in terms of effective stress can be determined by combining the effective stress with the Mohr-Coulomb failure criteria. The effective shear strength parameters have been widely used in conventional geotechnical engineering practice such as the design of foundations/retaining walls and stability analysis of slope/excavation by ignoring the influence of matric suction. Such an approach has been used in practice based on the assumption that ignoring the influence of matric suction leads to a conservative design. However, various case studies showed that stability analysis of natural soil slopes (Hong Kong Government, 1972) or unsupported cuts (Richard et al., 2021) conducted by ignoring the failure mechanism attributed to the influence of matric suction can result in life losses.

Bishop (1959) extended effective stress equation for saturated soils proposed by Terzaghi (1943) to unsaturated soils by introducing a parameter,  $\chi$  along with two stress state variables. The shear strength of unsaturated soils can be estimated extending Bishop (1959) equation, which is summarized in Equation 1.

$$\begin{aligned}\tau_{us} &= c' + \sigma'_{us} \tan \phi' \\ &= c' + [(\sigma_n - u_a) + \chi(u_a - u_w)] \tan \phi'\end{aligned}\quad (1)$$

where  $\tau_{us}$  is shear strength of unsaturated soil,  $c'$  is effective cohesion,  $\phi'$  is effective internal friction angle,  $\sigma'_{us}$  is

effective stress of unsaturated soil,  $(\sigma - u_a)$  is net normal stress,  $(u_a - u_w)$  is matric suction,  $u_a$  is pore-air pressure,  $u_w$  is pore-water pressure, and  $\chi$  is parameter that is a function of degree of saturation

Research studies that followed after the pioneering work of Bishop (1959) suggested that the net normal stress,  $(\sigma - u_a)$  and matric suction,  $(u_a - u_w)$  should be considered as independent stress state variables for rational interpretation of the engineering behavior of unsaturated soils. In saturated soils, there are identical changes in water content and void ratio associated with changes in  $(\sigma - u_w)$  because they are uniquely related; however, the mechanical behavior of unsaturated soils associated with similar changes in the  $(\sigma - u_a)$  and  $(u_a - u_w)$  are not identical and hence their influence cannot be rationally interpreted using a single state effective stress equation for unsaturated soils (Bishop & Blight, 1963).

Fredlund et al. (1978) analyzed the measured shear strength of unsaturated soils available in the literature and validated the 'two independent stress state variables' approach using Equation 2.

$$\tau_{us} = c' + (\sigma_n - u_a) \tan \phi' + (u_a - u_w) \tan \phi^b \quad (2)$$

where  $\phi^b$  is angle indicating the rate of increase in shear strength relative to the matric suction

For the suction values less than the air-entry value, shear strength contribution due to matric suction,  $\phi^b = \phi'$ ; therefore, shear strength increases linearly with increasing matric suction. Beyond the air-entry value,  $\phi^b$  contribution gradually decreases with an increase in matric suction; due to this reason,  $\phi^b$  is less than  $\phi'$ ; therefore, shear strength of unsaturated soils varies nonlinearly with respect to suction (Escario & Sáez, 1986, Gan et al., 1988). The typical shear strength behavior of unsaturated soils for conventional soils such as the sand, silt, glacial till and low plastic clays is illustrated in Figure 1. As can be seen, the shear strength can be either overestimated or underestimated when a constant  $\phi^b$  is used depending on the range of suction and soil type.

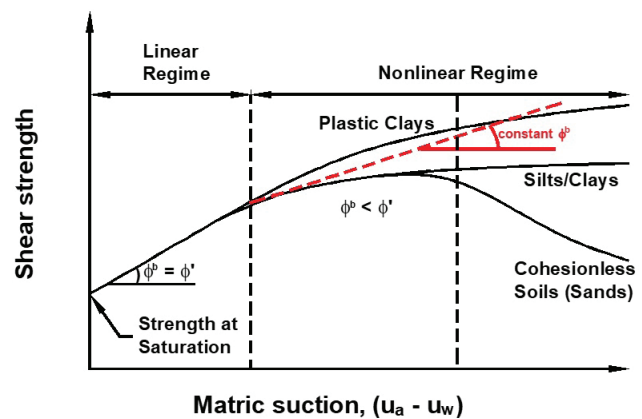


**Figure 1.** Variation of the shear strength with respect to matric suction for conventional soils.

Vanapalli (2009) provides a comprehensive summary of various models that are available in the literature to estimate or predict the nonlinear variation of shear strength of unsaturated soils. Many of the shear strength models that were proposed in the literature use the Soil-Water Characteristic Curve (SWCC), which is the relationship between degree of saturation (alternatively volumetric water content or water content) and soil suction. The matric suction in a soil specimen at failure, however, can be different from the initial matric suction due to the influence of various parameters such as volume change, stress history, shearing rate and drainage condition of pore-air and pore-water. This discrepancy of matric suction can contribute to some differences between the measured and estimated or predicted shear strength of unsaturated soils.

Lu et al. (2010) suggested a different approach which is consistent with conventional soil mechanics principles. Their approach is based on single stress state variable (i.e., effective stress) supporting the use of Equation 3 that takes the same form as Terzaghi's effective stress by using the suction stress,  $\sigma^s$ .

$$\begin{aligned}\sigma'_{us} &= (\sigma - u_a) - [-S_e(u_a - u_w)] \\ &= (\sigma - u_a) - \left[ -\left( \frac{S - S_r}{1 - S_r} \right) (u_a - u_w) \right] \\ &= (\sigma - u_a) - \sigma^s\end{aligned}\quad (3)$$

where  $S$  is degree of saturation,  $S_e = [(S - S_r)/(1 - S_r)]$  is effective degree of saturation,  $S_r$  is residual degree of saturation

A closed-form expression for suction stress,  $\sigma^s$  is shown in Equation 4 by eliminating the degree of saturation using van Genuchten (1980) SWCC model.

$$\begin{cases} \sigma^s = -(u_a - u_w) & (u_a - u_w) \leq 0 \\ \sigma^s = \frac{(u_a - u_w)}{\left(1 + [\alpha(u_a - u_w)]^n\right)^{(n-1)/n}} & (u_a - u_w) \geq 0 \end{cases} \quad (4)$$

where  $n$  and  $\alpha$  are van Genuchten (1980) empirical fitting parameters of unsaturated soil properties.

## 2. Estimation of ultimate bearing capacity of unsaturated soils

### 2.1 Modified effective stress approach

Various models have been proposed to estimate the bearing capacity of unsaturated soils (see Table 1). Oloo et al. (1997) proposed a model that can be used to estimate the bearing capacity of a shallow foundation in unsaturated soils considering the influence of matric suction (Equation 5). The model was developed extending the Terzaghi (1943)'s effective stress approach assuming both pore-air and pore-water are in drained condition during the loading stage. This approach was referred to as the Modified Effective Stress

Approach (MESA) by Oh & Vanapalli (2013). Oloo et al. (1997)'s model uses a constant  $\phi^b$  for the suction values greater than the air-entry value. However, this approach can either over- or underestimate bearing capacity depending on the range of suction. Such a behavior is consistent with the reason explained using Figure 1 for the shear strength of unsaturated soils.

Vanapalli & Mohamed (2007) improved the Oloo et al. (1997)'s model by adopting the nonlinear shear strength models proposed by Vanapalli et al. (1996) and Fredlund et al. (1996) (Equation 6) (hereafter referred to as VM model). Terzaghi (1943)'s original bearing capacity equation was developed based on a plane strain condition for continuous footings. Several research studies suggest that  $\phi'$  obtained for plane strain condition is 1.1 times greater than that obtained from a conventional triaxial test under axisymmetric condition. The same approach was also used by Danish code of practice DS 415 (DSCE 1984) and Steensen-Bach et al. (1987). Vanapalli & Mohamed (2007) also suggested that  $1.1\phi'$  can provide better prediction of bearing capacity for both saturated and unsaturated conditions. Table 2 summarizes the bearing capacity and shape factors used by Vanapalli & Mohamed (2007) and other researchers (Terzaghi, 1943; Meyerhof, 1963; Vesić, 1973). The comparison between the measured and predicted bearing capacity values using the model footing test results for saturated condition (Steensen-Bach et al., 1987; Mohamed & Vanapalli, 2006) showed better agreement when predicted using the bearing capacity and shape factors proposed by Vanapalli & Mohamed (2007), as shown in Figure 2.

Vahedifard & Robinson (2016) proposed a unified method for estimating the bearing capacity of unsaturated soils considering the variation of degree of saturation associated with steady state flow conditions (Equation 7). The contribution of matric suction on the bearing capacity was taken into account by introducing the average suction stress, which is the matric suction at the centroid of matric suction profile in a certain depth (i.e., from the base of shallow foundation to the depth of  $1.5B$  or  $2B$ , Oh & Vanapalli, 2013). The effective degree of saturation under constant infiltration and evaporation rate,  $q$  is calculated using Equation 8 (Yeh, 1989; Lu & Likos, 2004). Vo & Russel (2016) proposed charts that can be used to estimate the bearing capacity of smooth and rough footings in unsaturated soils (Equation 9) extending the research by Martin (2004). Soil suction at the depth,  $z$  under constant surface infiltration,  $q$  is estimated using Equation 10. Ghasemzadeh & Akbari (2019) proposed a method to predict the bearing capacity of footings placed on unsaturated soil extending the limit equilibrium method. The bearing capacity equation consists of two terms; bearing capacity for saturated condition and contribution of matric suction towards the bearing capacity due to uniform and nonlinear matric suction distribution. Garakani et al. (2020) proposed an analytical solution for the bearing capacity of shallow foundation in unsaturated soil (Equation 14). The influence of suction was taken into account by adopting a correction factor  $C_f$  that depends on the soil



**Table 1.** Bearing capacity models for unsaturated soil extending the Modified Effective Stress Approach.

Authors	Bearing capacity equation	Remarks
Oloo et al. (1997)	$q_{ult} = \left[ \frac{c' + (u_a - u_w)_b (\tan \phi' - \tan \phi^b)}{(u_a - u_w)_s \tan \phi^b} \right] N_c + 0.5B \left( \gamma - \lambda_m \frac{\tan \phi^b}{\tan \phi'} \right) N_\gamma \quad (5)$	$q_{ult}$ : ultimate bearing capacity
Vanapalli & Mohamed (2007)	$q_{ult} = \left\{ \frac{[c' + (u_a - u_w)_b \tan \phi' - S^w \tan \phi']}{+(u_a - u_w)_{AVE} S^w \tan \phi'} \right\} N_c \xi_c + 0.5B \gamma N_\gamma \xi_\gamma \quad (6)$	$c'$ : effective cohesion
	$q_{ult} = \left\{ \frac{c' + (u_a - u_w)_b (1 - S_{e, AVE}) \tan \phi'}{+[(u_a - u_w) S_e]_{AVE} \tan \phi'} \right\} N_c \xi_c + q_s N_q \xi_q + 0.5B \gamma_m N_\gamma \xi_\gamma \quad (7)$	
Vahedifard & Robinson (2016)	$S_e = \left( \frac{1}{1 + \left\{ -\ln \left( 1 + \frac{q}{k_s} \right) e^{-\gamma_w \alpha z} - \frac{q}{k_s} \right\}^n} \right)^{(n-1)/n} \quad (8)$	
	$\begin{cases} V = \frac{q_u}{c'_0 + (\chi s)_0 \tan \phi' + q_s \tan \phi'} \\ F = \frac{(K_c + K_{\chi s} \tan \phi') B + \gamma_t B \tan \phi'_u}{c'_0 + (\chi s)_0 + q_s \tan \phi'} \end{cases} \quad (9)$	$c'_t$ : unified effective cohesion of matric suction
Vo & Russel (2016)	$s = (u_a - u_w)_b - \frac{(u_a - u_w)_b}{A_1} \ln \left[ \left( 1 + q/k_s \right) e^{A_1 \left( 1 - \frac{\gamma_w \alpha z}{(u_a - u_w)_e} \right)} - q/k_s \right] \quad (10)$	
Ghasemzadeh & Akbari (2019)	Constant suction distribution	$(u_a - u_w)_{AVE}$ : average matric suction
Garakani et al. (2020)	$q_{ult} = [c' + c_{AVE}] N_c \xi_c + q N_q \xi_q + 0.5B \gamma N_\gamma + s (N_s)_{cst} \tan \phi^b \xi_s \quad (11)$	$(u_a - u_w)_b$ : air-entry value
Yan et al. (2020)	Linear suction distribution	$(u_a - u_w)_s$ : matric suction at soil surface
	$q_{ult} = [c' + c_{AVE}] N_c \xi_c + q N_q \xi_q + 0.5B \gamma N_\gamma + s (N_s)_l \tan \phi^b \xi_s \quad (12)$	$(u_a - u_w)_m$ : representative matric suction
	Residual zone of unsaturation	$A_f$ : fitting parameter
	$q_{ult} = [c' + c_{AVE} + c_{res}] N_c \xi_c + q N_q \xi_q + 0.5B \gamma N_\gamma + s N_s \tan \phi^r \xi_s \geq q_{sat} \quad (13)$	$B$ : width of shallow foundation
	$q_{ult} = [c' + \chi (u_a - u_w) \tan \phi'] C_f N_c \xi_c + q N_q \xi_q + 0.5B \gamma N_\gamma \xi_\gamma \quad (14)$	$c_{AEV}$ : cohesion for air-entry value
	Uniform suction distribution	$c_{res}$ : constant cohesion due to the residual suction
	$q_{ult} = \frac{1}{2} \gamma B N_{\gamma t} + q N_{qt} + [c' + (u_a - u_w) \tan \phi^b] N_{ct} \quad (15)$	$k_s$ : saturated hydraulic conductivity
	Linear suction distribution	$N_c, N_q, N_\gamma$ : bearing capacity factors

**Table 1.** Continued...

Authors	Bearing capacity equation	Remarks
	$q_{ult} = \left[ c' + (u_a - u_w)_s (u_a - u_w)_m \tan \phi_t^b \right] N_{ct} + q N_{qt} + \frac{1}{2} \gamma B N_{\gamma t} \quad (16)$	$N_{ct}, N_{qt}, N_{\gamma t}$ : bearing capacity factors based on the unified strength theory $(N_s)_{cst}, (N_s)_l$ : bearing capacity factor in terms of suction for constant and linear suction distribution, respectively $q$ : constant infiltration at the ground surface $q_s$ : surface surcharge $s$ : soil suction $F, V$ : dimensionless ratios $z'$ : height above a horizontal ground water table $\alpha$ and $n$ : van Genuchten (1980) fitting parameters $\lambda_m$ : rate of decrease of matric suction with depth $\gamma$ : unit weight of soil $\gamma_m$ : modified average unit weight $\psi$ : fitting parameter for bearing capacity $\xi_c, \xi_q, \xi_\gamma$ : shape factors $\xi_s$ : shape factor for suction ( $=\xi_c$ ) $\phi'$ : effective internal friction angle $\phi'_t$ : unified internal friction angle $\phi_t^B$ : unified internal friction angle due to the contribution of suction $\phi^B$ : internal friction angle due to the contribution of suction $\phi^R$ : internal friction angle due to the contribution of suction in residual zone

**Table 2.** Summary of the bearing capacity and shape factors used by Vanapalli & Mohamed (2007) and other researchers.

Author	$q_{ult} = cN_c\xi_c + B\gamma N_\gamma\xi_\gamma$				
	$N_c$	$N_q$	$N_\gamma$	$\xi_c$	$\xi_\gamma$
Terzaghi (1943)	$(N_q - 1) \cot \phi'$	$\frac{e^{2(3\pi/4 - \phi'/2) \tan \phi'}}{2 \cos^2 (45 + \phi'/2)}$	$\frac{\tan \phi'}{2} \left( \frac{K_{py}}{\cos^2 \phi} - 1 \right)$	1.3 (square)	0.8 (square)
Meyerhof (1963)	Terzaghi (1943)	$e^{\pi \tan \phi} \tan^2 (45 + \phi/2)$	$(N_q - 1) \tan (1.4\phi')$	$1 + 0.2K_p \left( \frac{B}{L} \right)$	$1 + 0.1K_p \left( \frac{B}{L} \right)$
Vesic (1973)	Meyerhof (1963)	Meyerhof (1963)	$2(N_q + 1) \tan \phi$	$1 + \left( \frac{N_q}{N_c} \right) \left( \frac{B}{L} \right)$	$1 - 0.4 \left( \frac{B}{L} \right)$
Vanapalli & Mohamed (2007)	Terzaghi (1943)	Terzaghi (1943)	$\frac{P_{\gamma \min}}{\gamma B^2} - \frac{\tan \phi}{2}$	Vesic (1973)	Vesic (1973)

$K_{py}$  = passive earth pressure used by Terzaghi (1943) to calculate  $N_\gamma$  (differs from the passive horizontal stress coefficient defined by Rankine's limit state);  $P_{\gamma \min}$  = minimum passive pressure used in finding the critical failure surface by Kumbhokjar (1993).

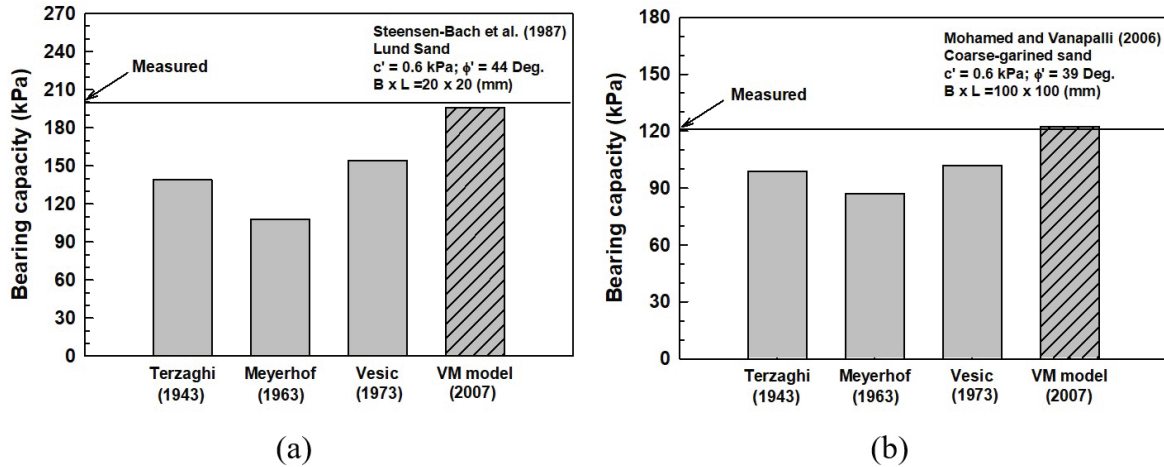


**Figure 2.** Comparison between the measured bearing capacity values (a) and those predicted (b) using four different bearing capacity models for saturated condition (modified after Oh & Vanapalli (2011)).

type, geometrical aspects and embedment of the foundation and loading conditions. More recently, Yan et al. (2020) derived the bearing capacity of a strip footing in unsaturated soil considering the influence of intermediate principal stress extending the research by Fan et al. (2005). The bearing capacity equations for uniform and linear suction profiles are shown in Equations 15 and 16, respectively.

The bearing capacity models listed in Table 1 were developed based on the failure surface under a continuous footing following the approach by Prandtl (1921) and Terzaghi (1943). The contribution of matric suction was considered as a form of total cohesion or bearing capacity factor. The change in the mechanical properties of unsaturated soils can be predominantly attributed to the environmental factors such as the rainfall. The weather-imposed conditions primarily affect the matric suction component rather than the osmotic suction. Leong & Abuel-Naga (2018) conducted unconfined compression tests on compacted soil specimens. The specimens were prepared using distilled water and sodium chloride solutions to investigate the influence of matric suction and osmotic suction on the shear strength, respectively. They concluded that the influence of osmotic suction on the shear strength of compacted specimens is negligible. According to Fredlund & Rahardjo (1993), the influence of osmotic suction on the soil behavior may be significant only when the salt content is altered by chemical contamination or chemical change. For such a scenario, it is necessary to consider the osmotic suction as part of stress state or as an independent stress state variable in estimating the bearing capacity of unsaturated soils.

In this state-of-the-art-paper, the bearing capacity model proposed by Vanapalli & Mohamed (2007, VM model) is revisited. First, the relationship between the shear strength behavior and the SWCC of sands are highlighted using Donald (1957) results, who performed direct shear tests for four different sands at different matric suction values. The variation in the bearing capacity of sands with respect to matric suction would

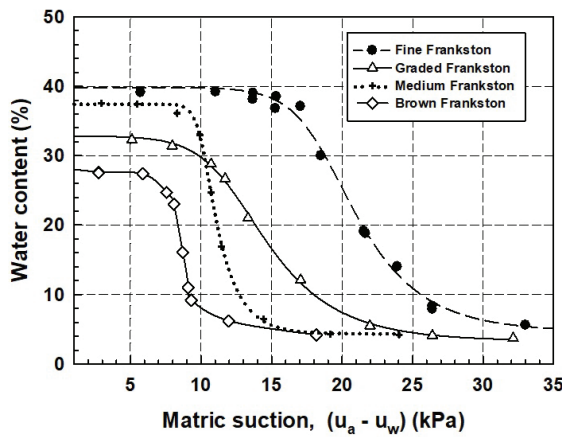
be similar to that of shear strength of the respective unsaturated sands. The results in Figure 3 highlight that the shear strength increases with an increase in the matric suction up to a certain value and then start decreasing with a further increase in matric suction. This is attributed to the reason that the contribution of matric suction towards shear strength decreases as matric suction approaches the residual suction value. This characteristic behaviour was also explained extending mathematical framework by Vanapalli et al. (1996). More comprehensive explanations related to variations in the shear strength of unsaturated soils are available in Vanapalli (2009).

Figure 4 shows the SWCC and the comparison between the measured bearing capacity values (Mohamed & Vanapalli, 2006) and those predicted using the VM model for Unimin 7030 industrial sand. The maximum average matric suction value used in the model footing tests was 6 kPa due to limitations of the tank size (i.e., height) used in the testing program; therefore, no comparisons are available beyond this suction value. However, the predicted bearing capacity clearly shows the bearing capacity starts decreasing as matric suction value approaches the residual zone of desaturation.

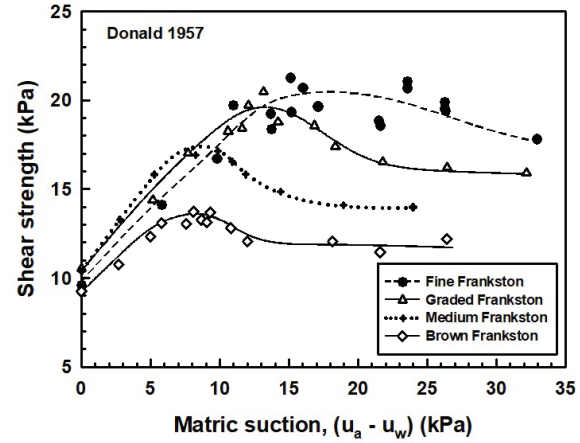
The VM model was developed by extending the approach shown in Figure 5. For a matric suction value equals to or less than air-entry value, the bearing capacity increases linearly with increasing matric suction. Hence, the bearing capacity for air-entry value can be calculated using Equation 17 assuming the soil is in a state of saturated condition.

$$\begin{aligned} q_{ult} &= BC_{sat} + BC_{AVE} \\ &= c'N_c\xi_c + (u_a - u_w)_b \tan \phi' N_c\xi_c + 0.5B\gamma N_\gamma\xi_\gamma \quad (17) \\ &= \{c' + (u_a - u_w)_b \tan \phi'\} N_c\xi_c + 0.5B\gamma N_\gamma\xi_\gamma \end{aligned}$$

where  $(u_a - u_w)_b$  is air-entry value,  $B$  is width of footing,  $\gamma$  is unit weight of soil,  $N_c$ ,  $N_\gamma$  are bearing capacity factors, and  $\xi_c$ ,  $\xi_\gamma$  are shape factors



(a)



(b)

**Figure 3.** (a) SWCCs and (b) variation of shear strength with respect to matric suction for four different sands, data from Donald (1957) (from Vanapalli & Lacasse (2009)).

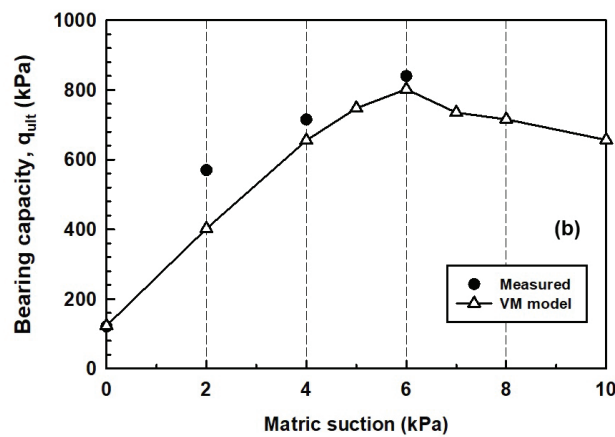
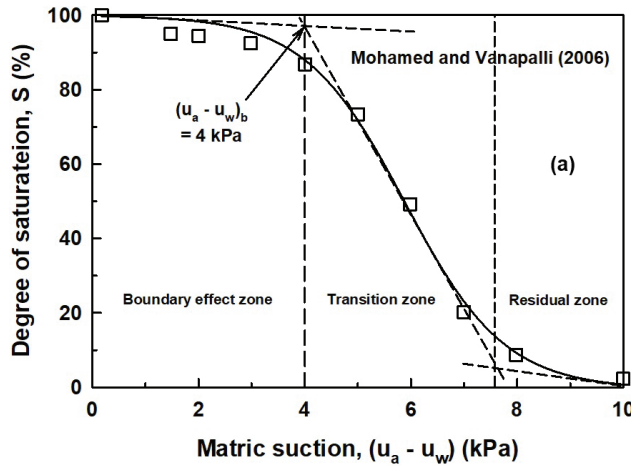


**Figure 4.** (a) SWCC and (b) comparison between the measured bearing capacity values and those predicted using the VM model (data from Mohamed & Vanapalli (2006)).

For a matric suction greater than air-entry value, the bearing capacity is represented as the sum of  $BC_{sat}$ ,  $BC_{AVE}$  and  $BC_{unsat}$  as shown in Equation 18.

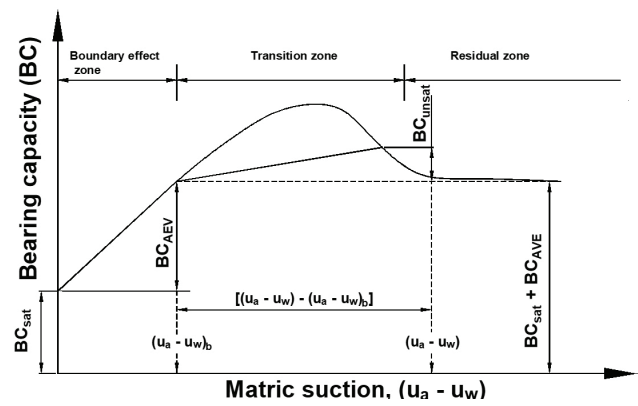


**Figure 5.** Approach used by Vanapalli & Mohamed (2007, VM model) to predict the bearing capacity of unsaturated sands.

$$\begin{aligned}
 q_{ult} &= BC_{sat} + BC_{AVE} + BC_{unsat} \\
 &= \left\{ c' + (u_a - u_w)_b \tan \phi' \right\} N_c \xi_c + \\
 &\quad \left\{ (u_a - u_w) - (u_a - u_w)_b \right\} S^w \tan \phi' N_c \xi_c + \\
 &\quad 0.5 B \gamma N_\gamma \xi_\gamma
 \end{aligned} \quad (18)$$

The degree of saturation reduces significantly and reaches a value close to zero at high suction values in the residual zone. In this zone, the contribution of matric suction towards the bearing capacity significantly reduces, which is similar to the shear strength behavior of sands. The contribution from suction which is represented by second term in Equation 18 becomes negligible. In other words, for a suction value greater than air-entry value, the predicted bearing capacity obtained VM model is equal to or greater than the one calculated with Equation 17 regardless of matric suction value. To overcome this limitation of the VM model, in this paper, the VM model is improved by adding



an additional criteria as shown in Equation 19 for the suction values in the residual zone of SWCC.

$$q_{ult} = \left\{ c' + (u_a - u_w) S^w \tan \phi' \right\} N_c \xi_c + 0.5 B \gamma N_\gamma \xi_\gamma \quad (19)$$

The model footing test results presented by Safarzadeh & Aminfar (2020) were revisited to check the validity of the revised VM model. The tests were carried out with a square footing ( $B \times L = 150 \text{ mm} \times 150 \text{ mm}$ ) in a poorly graded Goomtapeh sand. The effective cohesion, effective internal friction angle and dilatancy angle are 0 kPa,  $33.6^\circ$ , and  $6^\circ$ , respectively. Their experimental results were chosen in the study since one test was carried out at a relatively high suction value that is close to the dry condition (i.e., 30 kPa). Figure 6 shows the SWCC and the variation of bearing capacity with respect to matric suction. As shown in Figure 6b, the measured bearing capacity at 30 kPa of matric suction value (i.e., 73 kPa) is slightly higher than that of saturated condition (i.e., 48 kPa). This indicates that the bearing capacity decreases significantly as the degree of saturation approaches zero. This behavior was not captured in the original VM model due to the reason explained earlier. The revised VM model provides good agreement between the measured and predicted bearing capacity values over entire range of SWCC (i.e., with three different zones; namely, boundary, transition and residual zone). The discrepancy in the predicted bearing capacity values between the original and revised model can be noticed at the matric suction of approximately 10 kPa. This is the point where the bearing capacity starts decreasing rapidly in the residual zone of desaturation.

## 2.2 Modified total stress approach

Terzaghi (1943) bearing capacity equation was originally developed assuming general shear failure for drained conditions with respect to pore-water. There are also scenarios where shallow foundations are loaded at a relatively fast rate on/in a low permeable soils (i.e., undrained condition). The bearing capacity should be calculated extending the  $\phi_u = 0$  approach (i.e., total stress approach; Skempton, 1948) for such soils. Application of two different approaches depending on the soil type and drainage condition in saturated soils also leads to the argument to the use of MESA for calculating the bearing capacity of unsaturated fine-grained soils. Failure mode from the in-situ plate load tests on unsaturated fine-grained soils represents punching failure, rather than the general failure (Oloo 1994; Schnaid et al., 1995; Consoli et al., 1988; Costa et al., 2003; Rojas et al., 2007). For punching failure condition, i) well defined failure is not observed from the stress versus settlement behavior of model footing tests, ii) no heave is observed on the soils outside the loaded areas, and iii) the vertical displacement of a footing is caused mainly by the compression of the soil directly below the footing as well as

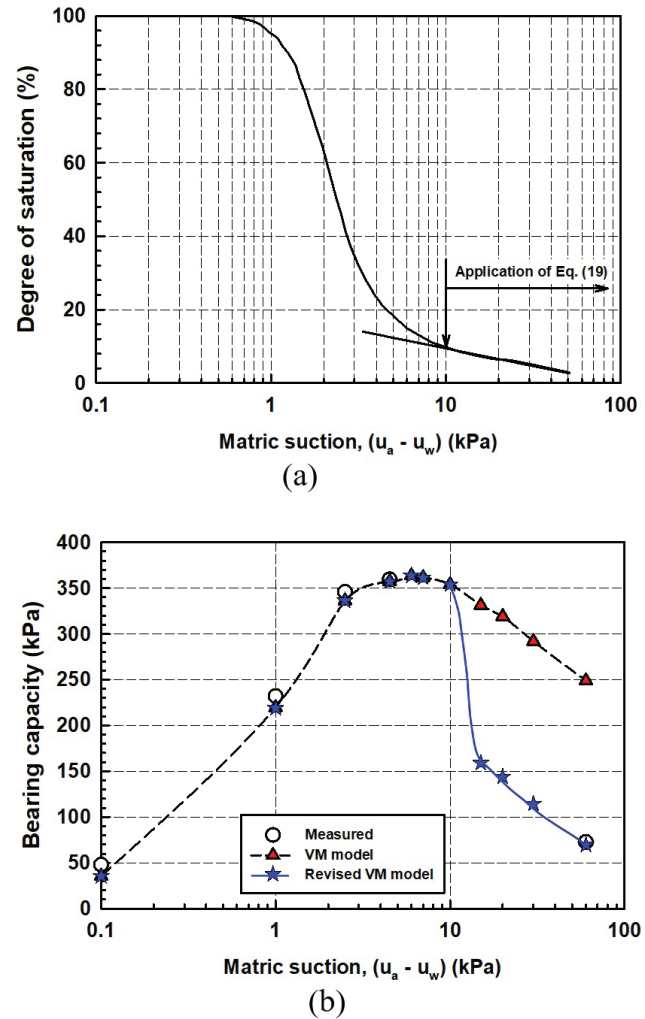


**Figure 6.** (a) SWCC and (b) the variation of bearing capacity with respect to matric suction estimated using VM and revised VM model (data from Safarzadeh & Aminfar (2020)).

the vertical shearing of the soil around the footing perimeter (Vesić, 1963, 1973; Oh & Vanapalli, 2013). Oh & Vanapalli (2013) also pointed out that the drainage conditions of pore-water and pore-air cannot be clearly defined during in-situ plate load tests on unsaturated fine-grained soils. There are no guidelines in the literature for the duration of plate loading for achieving equilibrium condition. For this reason, Oh & Vanapalli (2013) suggested that it is reasonable to assume that the pore-air is in drained condition, while pore-water is in undrained condition for plate load tests performed in unsaturated fine-grained soils. In other words, the bearing capacity of unsaturated fine-grained soils is more dependent on the compressibility of the soil below a footing (i.e., punching failure) and the constant water content (CW) test can be regarded as the most reasonable test method to simulate the loading and the drainage condition for the unsaturated fine-grained soils. However, since the CW tests are time-consuming and require elaborate equipment (Rahardjo et al., 2004), the unconfined compression test results for unsaturated soils can be used in

the MTSA to accommodate both punching failure mode and drainage conditions of pore-air and pore-water in unsaturated fine-grained soils. Oh & Vanapalli (2013) extended this background for their experimental investigations studies and interpreted the bearing capacity of unsaturated fine-grained soils using Equation 20 extending the Skempton (1948) total stress approach. This approach has been referred to as the Modified Total Stress Approach (MTSA). Oh & Vanapalli (2013) suggested using  $N_{c(unsat)} = 5.14$  for achieving good comparisons between the measured and predicted bearing capacity values in unsaturated fine-grained soils. It is interesting to note that the factor, 5.14 is the same as  $N_c$  for saturated condition with a zero internal friction angle (i.e., undrained loading).

$$\begin{aligned} q_{ult} &= (s \times \xi \times N_c)_{unsat} \\ &= \left[ \frac{q_{u(unsat)}}{2} \right] \left[ 1 + \frac{B}{L} \left( \frac{N_q}{N_c} \right) \right] N_{c(unsat)} \\ &= 5.14 \left[ \frac{q_{u(unsat)}}{2} \right] \left[ 1 + 0.2 \left( \frac{B}{L} \right) \right] \end{aligned} \quad (20)$$

where,  $s$  is shear strength based on unconfined compressive strength,  $\xi [= 1 + 0.2(B/L)]$  is shape factor ( $B$  = Breadth,  $L$  = length) proposed by Meyerhof (1963) and Vesic (1973) for undrained condition,  $N_c$  is bearing capacity factor,  $q_u$  is unconfined compressive strength and subscript unsat is unsaturated condition

Meyerhof (1974) studied the ultimate bearing capacity of a clay deposit overlain by a homogeneous thick bed of a sand (Figure 7a). For the scenario where the  $H/B$  ratio is relatively small, the sand deposit is compressed in a shape of truncated pyramid (i.e., punching failure), which typically follows after a general failure in the clay deposit. If the bearing capacity of sand bed is much greater than that of the underlying clay deposit, the net ultimate bearing capacity of a shallow foundation can be estimated using Equation 21.

$$\begin{aligned} q_{ult} &= q_b + \left( \frac{2c'_a H}{B} \right) \left( 1 + \frac{B}{L} \right) + \\ &\gamma_1 H^2 \left( 1 + \frac{B}{L} \right) \left( 1 + \frac{2D_f}{H} \right) \left( \frac{K_s \tan \phi'_1}{B} \right) - \\ &\gamma_1 H \leq q_t \end{aligned} \quad (21)$$

where,  $q_b$  is bearing capacity of the bottom soil layer,  $q_t$  is bearing capacity of the top soil layer,  $C_a$  is adhesive force ( $= c'_a H$ ),  $c'_a$  is adhesive cohesion,  $H$  is distance from the base of shallow foundation to the bottom of lower layer,  $B$  is width of the shallow foundation,  $L$  is length of the shallow foundation,  $(1 + B/L)$  is shape factor,  $D_f$  is embedded depth,  $K_s$  is punching shear coefficient,  $\phi'_1$  is effective internal friction angle of the top layer,  $\gamma_1$  is unit weight of the top layer, and  $Q_u$  is ultimate load.

Oh & Vanapalli (2013) suggested that Equation 21 can be further simplified as Equation 22, assuming that i) bearing pressure at the top of lower layer is  $q_b + \gamma_1 D_f$  and ii) bearing capacity of the upper layer is governed only by the compressibility of the soil block A-A'-B-B' without lateral deformation (i.e.,  $K_s$  in Equation 21 is zero) (Figure 7b).

$$q_{ult} = q_b + \left( \frac{2c'_a H}{B} \right) \left( 1 + \frac{B}{L} \right) + \gamma_1 D_f \quad (22)$$

The in-situ plate load tests result in an unsaturated cohesive soil by Larson (1997) showed that majority of settlements are within a depth of  $2B$  below the plate, with most of the settlements (i.e., about 87%) within the depth of  $B$ . These results justify the use of  $1.5B$  as a significant depth (Poulos & Davis, 1974). Hence, Equation 22 can be further simplified as Equation 23 with the total cohesion,  $c_a$  for a square footing on a single unsaturated fine-grained soil assuming the bearing capacity is governed by its compressibility (i.e.,  $q_b = \gamma_1 D_f = 0$ ). The total cohesion is equal to half of unconfined compressive strength,  $q_u$  of an unsaturated fine-grained soil as shown in Equation 20.

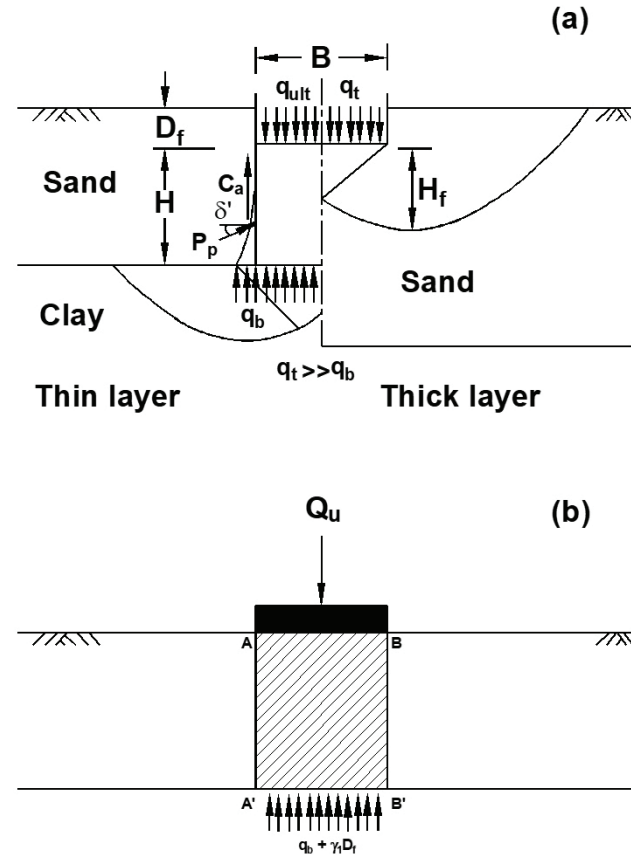


**Figure 7.** (a) Failure of soil below footing on dense layer above weak layer (modified after Meyerhof (1974) and Das (2015)) and (b) simplified failure mechanism.

$$\begin{aligned}
 q_{ult} &= \left( \frac{2c_u H}{B} \right) \left( 1 + \frac{B}{L} \right) \\
 &= 2 \left( \frac{q_{u(unsat)}}{2} \right) \left( \frac{1.5B}{B} \right) (1+1) \\
 &= 6c_{u(unsat)}
 \end{aligned} \quad (23)$$

It is interesting to note that the constant '6' in Equation 23 is close to the value calculated from Equation 20 (i.e.,  $5.14 \times 1.2 = 6.17$ ) for a square footing.

Consoli et al. (1988) conducted a series of in situ plate load tests in an unsaturated cohesive soil (lightly cemented homogeneous sandy-silt red clay,  $I_p = 20\%$ ) using three different sizes of steel circular plates (0.3, 0.45, and 0.6 m in diameter) and concrete square footings (0.4, 0.7 and 1 m). Oh & Vanapalli (2013) revisited the plate load test results and estimated bearing capacity values based on the stress versus settlement behaviours. For each of these tests, the bearing capacity was defined as a stress corresponding to the intersection of the tangents to the initial and final portion of stress versus settlement behavior within the settlement equals to 10% of width (or diameter) of a footing (or plate). The bearing capacity predicted using the MTSA (i.e., Equation 20) was 155 kPa, which was significantly lower compared to those from the plate load tests. The discrepancy gradually decreased with an increase in the plate size and becomes negligible when the plate size is of 1 m (see Figure 8). The discrepancy between the measured and predicted bearing capacity can be attributed various factors such as the disturbance of test specimen used for unconfined compression test and the scale effect (i.e., representative or average matric suction value can be different depending on the footing size). The summarized discussion validates the use of MTSA (i.e., Equation 20) for the prediction of the bearing capacity of fine-grained soils for full-size foundations used in engineering practice.

The MTSA (i.e., Equation 20) indicates that the variation of bearing capacity of unsaturated fine-grained soils with respect to matric suction can be obtained by estimating the undrained shear strength of a soil at a targeted matric suction value. Oh & Vanapalli (2018a) proposed a model to estimate the variation of undrained shear strength of unsaturated fine-grained soils with respect to matric suction using the unconfined compressive shear strength of unsaturated soil.

$$c_{u(unsat)} = c_{u(sat)} \left\{ 1 + \left[ \frac{(u_a - u_w)}{\mu} \right] \left( \frac{P_a}{101.3} \right) (S)^v \right\} \quad (24)$$

where  $c_{u(unsat)}$  and  $c_{u(sat)}$  = undrained shear strength of unsaturated and saturated soil (i.e., half of unconfined compressive strength), respectively,  $P_a$  is atmospheric pressure,  $S$  is degree of saturation, and  $\mu$ ,  $v$  are fitting parameters.

Oh & Vanapalli (2018a) analyzed seven sets of unconfined compression test results for fine-grained soils. Reasonable

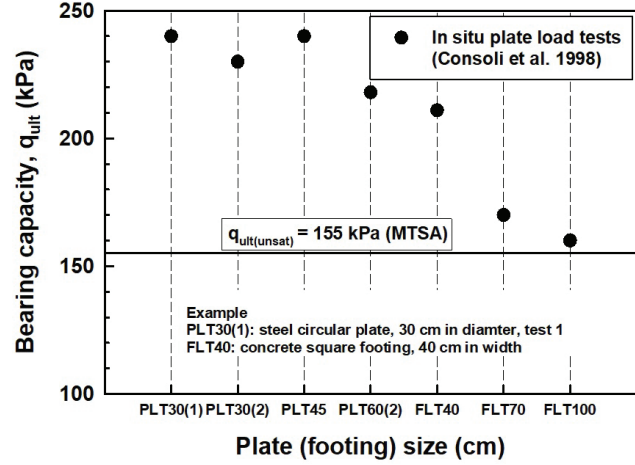


Figure 8. Comparison between the measured bearing capacity values and those predicted using the MTSA (data from Consoli et al., 1988).

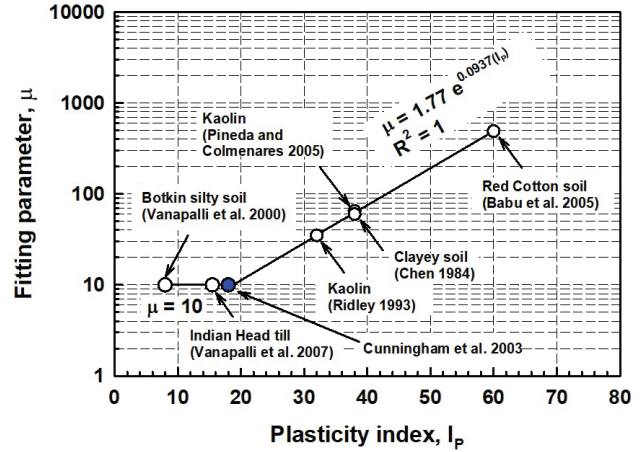


Figure 9. Relationship between plasticity index,  $I_p$ , and the fitting parameter,  $\mu$  in Equation 24 (Oh & Vanapalli, 2018a; Babu et al., 2005; Chen, 1984; Pineda & Colmenares, 2005; Ridley & Burland, 1993; Vanapalli et al., 2007, 2000).

estimates were obtained between the measured and predicted undrained shear strengths values for soils within the range of plasticity indices between 8% and 60% using the fitting parameter,  $v = 2$  ( $v = 1$  for unsaturated cohesionless soil). The fitting parameter,  $\mu$  is a function of plasticity index as shown in Figure 9.

The pore-air and pore-water pressure along the shear zone is different from those at the test specimen's boundaries. However, due to the limitations of laboratory testing techniques, the shear strength and bearing capacity models use the pore-air and pore-water pressure applied at the specimen's boundaries for initial or failure condition. The research studies by Chae et al. (2010) and Zhou et al. (2016) suggest that the unconfined compressive strength of unsaturated soils can be predicted by using the soil suction at failure condition. Oh & Vanapalli (2018a) also performed investigations along similar lines by comparing the measured undrained shear

strengths with those predicted using Equation 24 using the experimental results of Cunningham et al. (2003). Figure 10 summarizes these results highlighting the degree of saturation and soil suction for initial (subscript  $i$ ) and failure (subscript  $f$ ) condition. The undrained shear strength predicted using both  $[S_p(u_a - u_w)_i]$  and  $[S_p(u_a - u_w)_f]$  showed good agreement with the measured values when plotted against  $(u_a - u_w)_f$ . This indicates that Equation 24 can be used to estimate the variation of undrained shear strength with respect to matric suction without the information of degree of saturation and soil suction at failure. Such trends in results can be attributed to the reason that the increase in soil suction at failure leads a decrease in the degree of saturation and vice versa, which minimizes the difference in undrained shear strength obtained using  $[S_p(u_a - u_w)_i]$  and  $[S_p(u_a - u_w)_f]$ .

### 2.3 Numerical approaches

Various numerical approaches can be used for predicting the bearing capacity by simulating the vertically applied stress versus settlement behaviors. Abed & Vermeer (2006) were some of the earliest investigators who estimated bearing capacity of soils taking account of saturated and unsaturated soil conditions using the Barcelona Basic Model (BBM) and the Modified Cam Clay (MCC) model, respectively. Ghorbani et al. (2016) used an extended MCC to simulate load versus settlement behaviours of statically loaded rigid footings in both saturated and unsaturated soils. Elastic-perfectly plastic Mohr-Coulomb model was used by several researchers to estimate the behaviors of shallow foundations in unsaturated soils (Tang et al., 2016; Baker, 2004; Serrano et al., 2005; Oh & Vanapalli, 2011; Cheng et al., 2021). In this section, details of numerical methods proposed by Oh & Vanapalli (2011, MESA) and Oh & Vanapalli (2013, MTSA) to estimate the bearing capacity of unsaturated sand and fine-grained soils, respectively, are summarized.

#### 2.3.1 Estimating stress versus settlement behaviour extending MESA

Mohamed & Vanapalli (2006) performed a series of model footing ( $B \times L = 100 \text{ mm} \times 100 \text{ mm}$ ) tests on sand. The load was applied on the model footing placed on the surface of the sand housed in a specially designed tank ( $900 \text{ mm} \times 900 \text{ mm} \times 900 \text{ mm}$ ). The water table in the tank was adjusted such that the tests were carried out to achieve four different average matric suction values (i.e., 0, 2, 4, and 6 kPa). Figure 11 shows the schematic of testing set up and the matric suction distribution with depth with the water table at the depth of 600 mm from the soil surface. Matric suction values were measured using Tensiometers embedded at four different depths. The difference between the measured and assumed hydrostatic matric suction distribution was not significant. Hence, the four

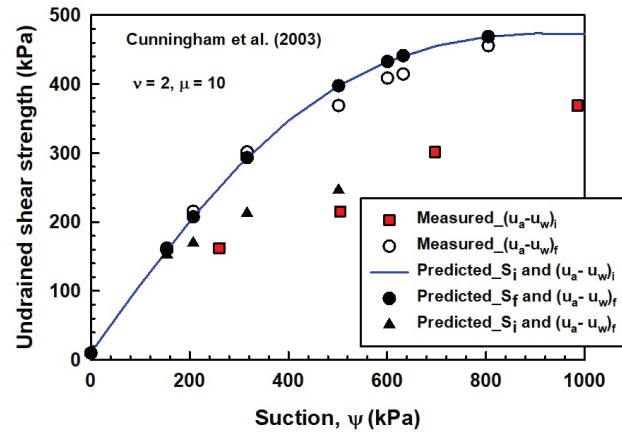


**Figure 10.** Comparison between the measured and predicted (Equation 24) undrained shear strengths using the data from Cunningham et al. (2003). Degree of saturation and soil suction for both initial and failure conditions were used in the prediction of the undrained shear strength (modified after Oh & Vanapalli (2018a)).

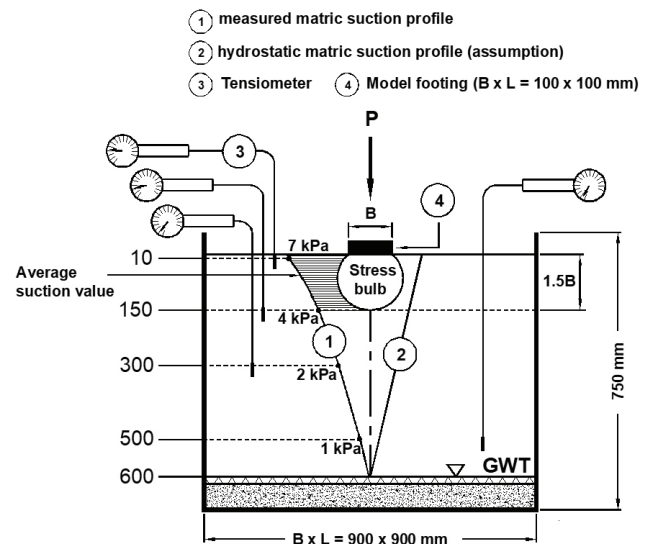


**Figure 11.** Variation of matric suction values with depth in the soil tank along with assumed hydrostatic matric suction distribution (from Oh & Vanapalli (2011)).

average matric suction values were obtained with assumed hydrostatic matric suction distributions.

Oh & Vanapalli (2011) conducted numerical analyses to estimate the bearing capacity extending the MESA using the model footing test results by Mohamed & Vanapalli (2006). Figure 12 shows the soils properties and boundary conditions used in the numerical analysis. The total cohesion was estimated using Equation 25 (Vanapalli et al., 1996). The coefficient of earth pressure at rest,  $K_0$  was calculated using Equation 26 (Jaky, 1944) and the Poisson's ratio,  $\mu_s$  was assumed equal to 0.3. The initial tangent elastic modulus,  $E_i$  for the saturated condition was obtained using Equation 27, which was used to estimate the variation of  $E_i$  with respect to matric suction (Equation 28; Oh et al., 2009).



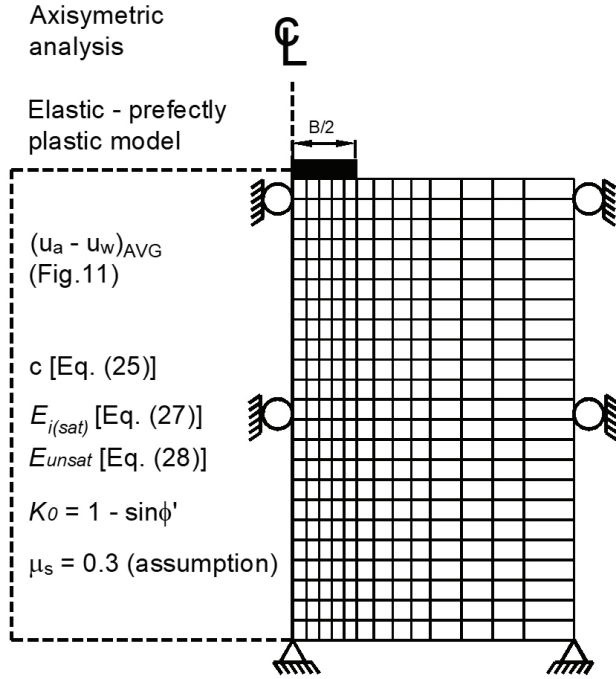


**Figure 12.** Soil properties and boundary conditions used in the numerical analysis to simulate the model footing tests from Mohamed & Vanapalli (2006) (modified after Oh & Vanapalli (2011)).

$$c = c' + (u_a - u_w) (S^\kappa) \tan \phi' \quad (25)$$

where  $S$  is degree of saturation and  $\kappa$  is fitting parameter that is a function of plasticity index (Garven & Vanapalli, 2006).

$$K_0 = 1 - \sin \phi' \quad (26)$$

$$E_{i(sat)} = \frac{1.5B}{\left(\frac{\Delta \delta}{\Delta q}\right)} \quad (27)$$

where  $K_0$  is coefficient of earth pressure at rest,  $E_{i(sat)}$  is initial tangent elastic modulus for saturated condition and  $(\Delta \delta / \Delta q)$  is the slope of the settlement versus footing pressure in elastic range.

$$E_{i(unsat)} = E_{i(sat)} \left[ 1 + \alpha' \frac{(u_a - u_w)}{(P_a / 101.3)} (S^{\beta'}) \right] \quad (28)$$

where  $E_{i(unsat)}$  is initial tangent elastic modulus for unsaturated condition,  $P_a$  is atmospheric pressure, and  $\alpha'$  and  $\beta'$  are fitting parameters.

Oh et al. (2009) studies suggest that  $\beta' = 1$  and  $2$  can be used for coarse- and fine-grained soils, respectively. Vanapalli & Oh (2010) investigated plate load and model footing test results in unsaturated soils and proposed that the fitting parameter,  $\alpha'$  is a function of plasticity index,  $I_p$  as shown in Figure 13. Although  $\alpha' = 2.5$  provided best comparison

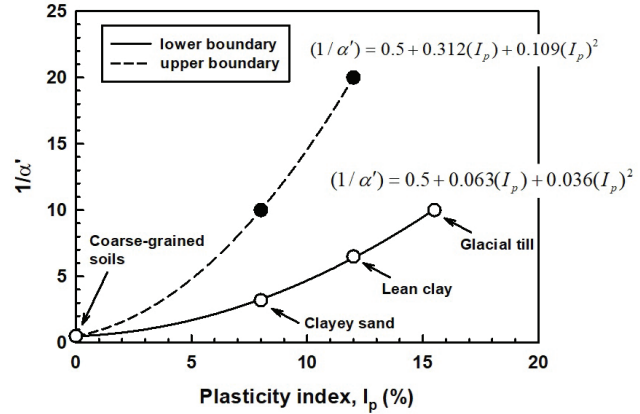


**Figure 13.** Relationship between  $(1/\alpha')$  and plasticity index,  $I_p$ , where  $\alpha'$  is fitting parameter in Equation 28 (modified after Vanapalli & Oh (2010)).

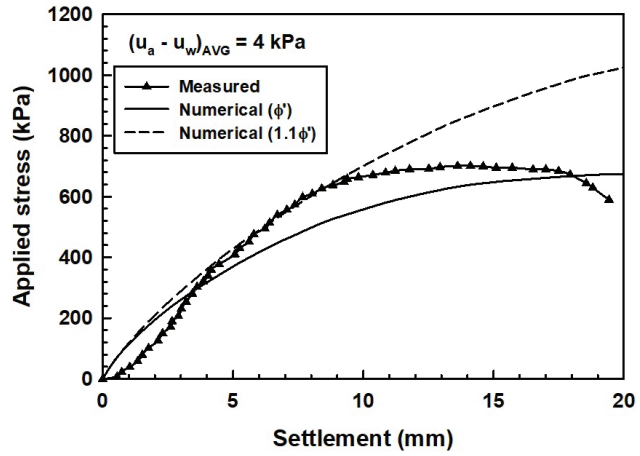


**Figure 14.** Comparison of the applied stress versus surface settlement behaviors obtained from model footing tests (Mohamed & Vanapalli, 2006) and numerical analysis for the average matric suction values of 4 kPa (modified after Oh & Vanapalli (2011)).

between the measured and estimated  $E_{i(unsat)}$  for sandy soils, Oh et al. (2009) recommended  $\alpha'$  values between 1.5 and 2 for conservative elastic settlement estimation in engineering practice applications.

Figure 14 shows the applied vertical stress versus surface settlement behaviors obtained from the model footing test and numerical analysis for an average matric suction value of 4 kPa. Figure 15 shows the comparison between the measured bearing capacity values and those predicted using the VM model (Equation 18) and numerical method. The bearing capacity values predicted using the VM model with  $\phi'$  and numerical method with  $1.1\phi'$  show better agreement when compared to the measured values. This can be attributed to the different failure mechanism between VM model (i.e., limit equilibrium method) and numeral method (i.e., Mohr-Coulomb criteria) (Oh & Vanapalli, 2011).

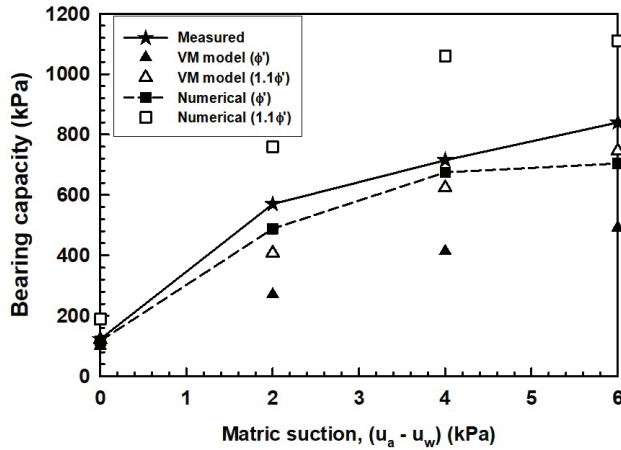


**Figure 15.** Comparison between the measured bearing capacity values (Mohamed & Vanapalli 2006) and those estimated using analytical (VM model) and numerical method for different average matric suction values (modified after Oh & Vanapalli (2011))

### 2.3.2 Estimating stress versus settlement behaviour extending MTSA

Oh & Vanapalli (2018b) proposed a modeling technique to simulate the vertical stress versus surface settlement behaviors of shallow foundations in unsaturated fine-grained soils extending the MTSA. As discussed earlier, the bearing capacity of saturated fine-grained soil is calculated extending  $\phi_u = 0$  approach. Oh & Vanapalli (2018b) suggested that the same approach can also be extended to model the vertical stress versus surface settlement behaviors of shallow foundations on unsaturated fine-grained soils. This approach is consistent with the concept used in developing Equations 20 and 23. The bearing capacity of unsaturated fine-grained soils can be predicted with Equation 20 using the unconfined compressive strength of unsaturated fine-grained soil.

The variation of elastic modulus with respect to matric suction was estimated by modifying Equation 28 for undrained condition. In other words, the elastic modulus for undrained condition was first estimated using the slope of the stress versus strain behaviour from unconfined compression test results and then Equation 28 was used to estimate the variation of elastic modulus with respect to suction for undrained condition. Figure 16 shows the mesh and boundary condition used in the numerical analysis to simulate the applied stress versus surface settlement behaviours of model footing tests from Oh & Vanapalli (2013). Figure 17 shows the comparison between the measured applied stress versus surface settlement behaviour and those predicted with numerical method. Good comparisons were obtained when the applied stress versus surface settlement behaviors were estimated with Poisson's ratio,  $\mu_s = 0.45$  and 1 for saturated and unsaturated conditions, respectively. The bender element test results by Lee & Santamarina (2005) also supports  $\mu_s = 0.1$  for unsaturated soils. The numerical analysis results also showed that the

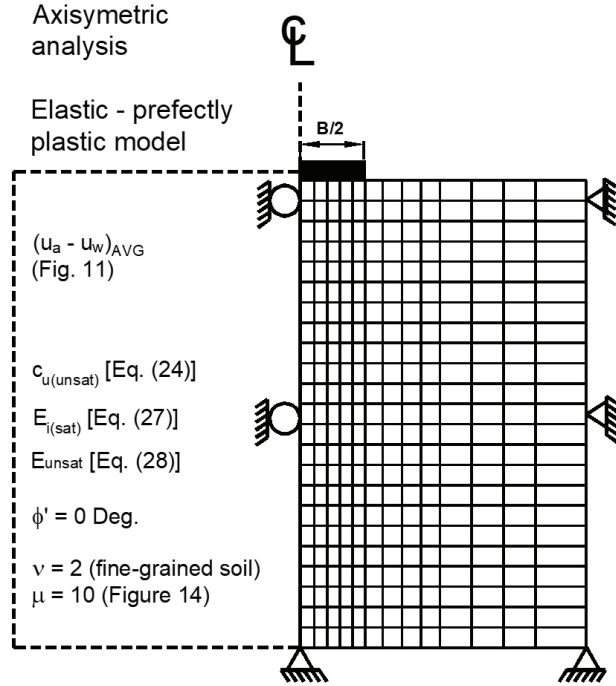


**Figure 16.** Mesh and boundary conditions used in the numerical analysis to simulate the model footing test results from Oh & Vanapalli (2013)

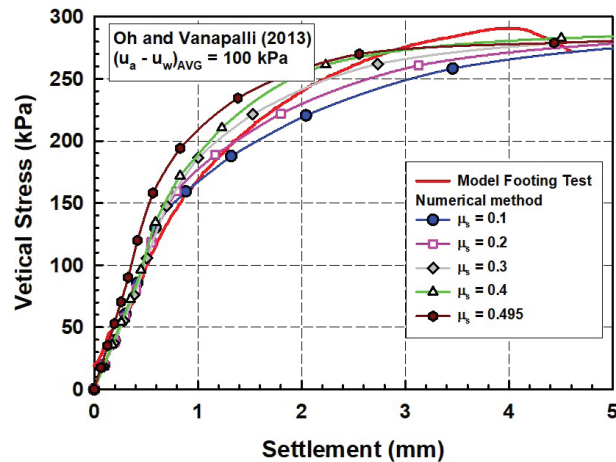


**Figure 17.** Comparison between the measured stress versus settlement behaviours (Oh & Vanapalli, 2013) and those predicted with numerical method for various Poisson's ratio (modified after Oh & Vanapalli (2018b)).

applied stress versus surface settlement behaviours is not affected by the coefficient of earth pressure at rest,  $K_0$ .

Figure 18 shows comparison between the measured bearing capacity values and those estimated from MESA (revised VM model), MTSA (Equation 20), and numerical method extending the MTSA. The bearing capacity values predicted with numerical analysis extending the MTSA provided the best agreement when compared with the measured bearing capacity values.

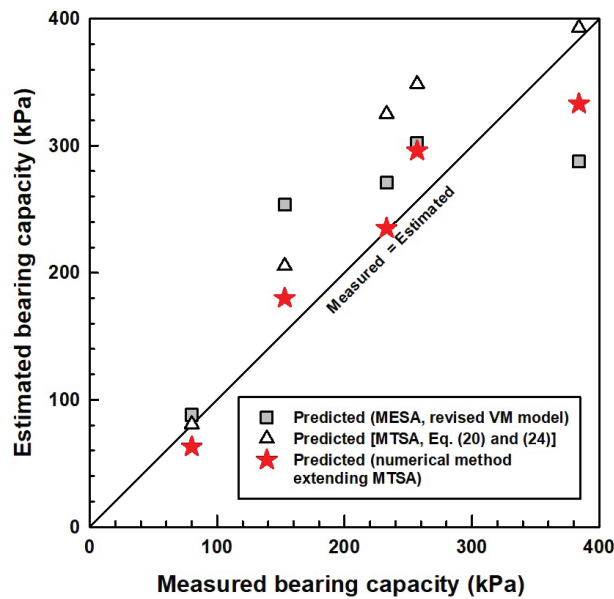


**Figure 18.** Comparison between the measured bearing capacity values (Oh & Vanapalli, 2013) and those estimated using different approaches (modified after Oh & Vanapalli (2018b)).

### 3. Summary and conclusions

Many attempts have been made to improve the Terzaghi (1943) bearing capacity model extending effective stress approach (ESA) since its development. These models are valuable for the practicing engineers to estimate the bearing capacity of saturated soils considering soil type (i.e., coarse- and fine-grained soils), drainage condition (i.e., drained and undrained condition), shape and embedment depth of footings. However, there are many scenarios where the influence of soil suction has to be taken into account for better estimation of the bearing capacity of unsaturated soils. More recently, researchers developed analytical models for this reason considering the influence of matric suction. Some of these analytical models have been successfully used in numerical analysis to simulate the applied stress versus settlement behaviours of shallow foundations in unsaturated soils. Unlike saturated soils, bearing capacity of unsaturated soils have been predicted extending the Modified Effective Stress Approach (MESA) regardless of soil type and drainage condition of pore-air and pore-water. Oh & Vanapalli (2013) provided a different approach and validated the use of Modified Total Stress Approach (MTSA) for unsaturated fine-grained soils. In this state-of-the-art paper, authors revisited the bearing capacity models for unsaturated soils and discuss the use of models by categorizing them into two groups; MESA and MTSA.

The model footing test results on unsaturated cohesionless soils show that the bearing capacity at high suction values approaches the bearing capacity values for saturated condition. This is because of the contribution of matric suction towards the bearing capacity is negligible at high suction values (i.e.,

in the residual zone of desaturation). To accommodate this behavior, the bearing capacity model proposed by Vanapalli & Mohamed (2007, VM model) extending the MESA is revised introducing additional criteria. The revised VM model reasonably captures the decrease in the bearing capacity in the residual zone of SWCC, which was verified using model footing test results for unsaturated sand.

Oh & Vanapalli (2013) showed that the bearing capacity model for saturated soils under undrained condition originally proposed by Skempton (1948) can be used for unsaturated soils by simply replacing the undrained shear strength for saturated condition with a value of half the unconfined compressive strength for unsaturated soil. The MTSA is simpler and provides better estimates when compared to those estimated with MESA based bearing capacity models. This may be attributed to the reasons that the MTSA was developed taking account of typical failure mode (i.e., punching failure) and the drainage condition that is more appropriate for unsaturated fine-grained soils beneath the shallow foundations.

Several constitutive models and modeling techniques are available in the literature that can be used to estimate deformation in unsaturated soils considering both drained and undrained conditions. However, these constitutive models require various soil parameters that require extensive laboratory test results. Typically, laboratory tests for unsaturated soils are time consuming and cumbersome since the pore-air and pore-water should be controlled separately. On the other hand, the numerical modelling techniques proposed by Oh & Vanapalli (2011) and Oh & Vanapalli (2018b) extending the MESA and MTSA, respectively are simple and requires only the laboratory test results for saturated conditions. These numerical techniques are validated by comparing measured bearing capacity values with those obtained with numerical methods.

This study focuses on the prediction of ultimate bearing capacity (i.e., ultimate limit state) considering the influence of matric suction. The bearing capacity models for unsaturated soils use soil suction as a state variable, which suggests, the estimated bearing capacity values are governed by soil suction. Hence, it is important to use appropriate climate models to predict the variation of bearing capacity of unsaturated soils with respect to soil suction in geotechnical engineering practice. However, in several scenarios, settlement behaviour (i.e., serviceability limit state) is the governing parameter in the design of shallow foundations. Therefore, both bearing capacity and settlement should be taken into account in the rational design of shallow foundations since foundation settlement can exceed the allowable settlement prior to the bearing capacity reaching its ultimate value. According to Tidlund (2021), uncertainty in geotechnical engineering is much more common in comparison to other civil engineering fields. Uncertainty in the estimation of foundation settlement in many scenarios is more likely compared to that of bearing capacity. The estimated foundation settlement using an idealized settlement calculation model without sufficient data can be 'nothing more than an educated guess based on

experience and the judgements of the engineer (Tidlund, 2021). For this reason, Szavits-Nossan (2006) suggested that the observational method is a more reliable tool in the design of shallow foundations, when it is governed by serviceability.

Sufficient site investigation and laboratory tests are required to determine mechanical properties (e.g., effective shear strength parameters, unconfined compressive strength and hydraulic conductivity for saturated condition), active zone based on seasonal base, and the SWCC for reliable use of the MESA or MTSA. More importantly, reliable climate data of the construction site is required for implementing the MESA or MTSA.

The bearing capacity of unsaturated soils can be predicted using either the MESA or MTSA depending on the soil type and drainage conditions of pore-air and pore-water. As per discussions in this paper, the MESA is recommended for unsaturated coarse-grained soils since both pore-air and pore-water are under drained conditions during loading stages. However, in many scenarios of engineering practice for unsaturated fine-grained soils, there are uncertainties with the drainage conditions of pore-air and pore-water during loading stages due to the low coefficient of permeability of the soil. Except for the scenarios, where load is applied at a significantly slow rate, it is reasonable to assume that the drained conditions of both pore-air and pore-water are somewhere between drained and undrained condition. Hence, authors suggest that the bearing capacity of unsaturated fine-grained soils should be estimated using both the MESA and MTSA; however, the final decision be made by engineers based on their engineering judgement.

## Acknowledgements

The authors thank the support from NSERC for their research programs.

## Declaration of interest

The authors declare that they have no known competing financial interests or personal relationships that could influence the work reported in this paper.

## Authors' contributions

Sai Vanapalli: supervision, funding acquisition, resources, conceptualization, methodology, writing - review & editing, formal analysis, investigation. Won Taek Oh: conceptualization, methodology, data curation, writing, formal analysis, investigation.

## List of symbols

$B, L$	width and length of foundation
$c'$	effective cohesion

$c'_a$	adhesive cohesion
$c_u$	undrained shear strength
$C_a$	adhesive force
$D_f$	embedment depth of shallow foundation
$E_i$	initial tangent elastic modulus
$I_p$	plasticity index
$K_0$	coefficient of earth pressure at rest
$K_s$	punching shear coefficient
$n, \alpha$	fitting parameters for unsaturated soil properties (van Genuchten 1980)
$N_c, N_q, N_\gamma$	bearing capacity factors
$q_t, q_b$	bearing capacity of top and bottom layer
$q_{ult}$	ultimate bearing capacity
$q_{u(unsat)}$	unconfined compressive strength of unsaturated soil
$Q_u$	ultimate load
$P_a$	atmospheric pressure
$s$	shear strength based on unconfined compressive strength
$S$	degree of saturation
$S_e$	effective degree of saturation
$S_r$	residual degree of saturation
$(u_a - u_w)$	matric suction
$(u_a - u_w)_b$	air-entry value
$(u_a - u_w)_{AVG}$	average matric suction value
$u_a$	pore-air pressure
$u_w$	pore-water pressure
$\tau_{us}$	shear strength of unsaturated soil
$\alpha', \beta'$	fitting parameters for initial tangent elastic modulus of unsaturated soil
$\phi'$	effective internal friction angle
$\phi^B$	angle indicating the rate of increase in shear strength relative to the matric suction
$\sigma_s$	suction stress
$\sigma'_{us}$	effective stress of unsaturated soil
$(\sigma - u_a)$	net normal stress
$\sigma$	normal stress
$\chi$	parameter that is a function of degree of saturation (Bishop, 1959)
$\xi_c, \xi_s, \xi_\gamma$	shape factors
$\psi$	fitting parameter for bearing capacity of unsaturated soil
$\gamma$	unit weight of soil
$\kappa$	fitting parameter for shear strength of unsaturated soil
$\alpha', \beta'$	fitting parameters for initial tangent elastic modulus of unsaturated soil
$\mu, \nu$	fitting parameters for undrained shear strength of unsaturated soil
$\mu_s$	Poisson's ratio

## References

- Abed, A., & Vermeer, P.A. (September 6-8, 2006). Foundation analyses with unsaturated soil model for



- different suction profiles. In *Proceedings 6th European Conference on Numerical Methods in Geotechnical Engineering* (pp. 547-554). Graz, Austria. <https://doi.org/10.1201/9781439833766.ch79>.
- Babu, G.L.S., Rao, R.S., & Peter, J. (2005). Evaluation of shear strength functions based on soil water characteristic curves. *Journal of Testing and Evaluation*, 33(6), 461-465. <http://dx.doi.org/10.1520/JTE12665>.
- Baker, R. (2004). Nonlinear Mohr envelopes based on triaxial data. *Journal of Geotechnical and Geoenvironmental Engineering*, 130(5), 498-506. [http://dx.doi.org/10.1061/\(ASCE\)1090-0241\(2004\)130:5\(498\)](http://dx.doi.org/10.1061/(ASCE)1090-0241(2004)130:5(498)).
- Bishop, A.W. (1959). The principle of effective stress. *Teknisk Ukeblad*, 106(39), 859-863.
- Bishop, A.W., & Blight, G.E. (1963). Some aspects of effective stress in saturated and partly saturated soils. *Geotechnique*, 13(3), 177-197. <http://dx.doi.org/10.1680/geot.1963.13.3.177>.
- Chae, J., B. Kim, B., Park, S.-W., and Kato, S. (2010). Effect of suction on unconfined compressive strength in partly saturated soils. *KSCE Journal of Civil Engineering*, 14, 281-290. <http://dx.doi.org/10.1007/s12205-010-0281-7>.
- Chen, J.C. (1984). *Evaluation of strength parameters of partially saturated soils on the basis of initial suction and unconfined compression strength*. Asian Institute of Technology Report.
- Cheng, X., Tan, M., & Vanapalli, S.K. (2021). Simple approaches for the design of shallow and deep foundations for unsaturated soils II: numerical Techniques. *Indian Geotechnical Journal*, 51(1), 115-126. <http://dx.doi.org/10.1007/s40098-021-00500-3>.
- Consoli, N.C., Schnaid, F., & Milititsky, J. (1988). Interpretation of plate load tests on residual soil site. *Journal of Geotechnical and Geoenvironmental Engineering*, 124(9), 857-867. [http://dx.doi.org/10.1061/\(ASCE\)1090-0241\(1998\)124:9\(857\)](http://dx.doi.org/10.1061/(ASCE)1090-0241(1998)124:9(857)).
- Costa, Y.D., Cintra, J.C., & Zornberg, J.C. (2003). Influence of matric suction on the results of plate load tests performed on a lateritic soil deposit. *Geotechnical Testing Journal*, 2(2), 219-226. <http://dx.doi.org/10.1520/GTJ11326J>.
- Cunningham, M.R., Ridley, A.M., Dineen, K., & Burland, J.B. (2003). The mechanical behavior of a reconstituted unsaturated silty clay. *Geotechnique*, 53(2), 183-194. <http://dx.doi.org/10.1680/geot.2003.53.2.183>.
- Das, B.M. (2015). *Principles of foundation engineering* (8th ed.). Cengage Learning.
- Danish Society of Civil Engineering DS 415. (1984). *The Danish code of practice for foundation engineering*. Danish Society of Civil Engineering.
- Donald, I.B. (1957). *Effective stresses in unsaturated non-cohesive soils with controlled negative pore pressure* [M.Sc. Thesis]. University of Melbourne.
- Escario, V., & Sáez, J. (1986). The shear strength of partly saturated soils. *Geotechnique*, 36(3), 453-456. <http://dx.doi.org/10.1680/geot.1986.36.3.453>.
- Fan, W., Bai, X., & Mao, H. (2005). Formula of ultimate bearing capacity of shallow foundation based on unified strength theory. *Yantu Lixue*, 26(10), 1617-1622.
- Fredlund, D.G., & Rahardjo, H. (1993). *Soil mechanics for unsaturated soils*. John Wiley and Sons.
- Fredlund, D.G., Morgenstern, N.R., & Widger, R.A. (1978). The shear strength of unsaturated soils. *Canadian Geotechnical Journal*, 15(3), 313-321. <http://dx.doi.org/10.1139/t78-029>.
- Fredlund, D.G., Xing, A., Fredlund, M.D., & Barbour, S.L. (1996). The relationship of the unsaturated soil shear strength to the soil-water characteristic curve. *Canadian Geotechnical Journal*, 33(3), 440-448. <http://dx.doi.org/10.1139/t96-065>.
- Gan, J.K.M., Fredlund, D.G., & Rahardjo, H. (1988). Determination of the shear strength parameters of an unsaturated soil using the direct shear test. *Canadian Geotechnical Journal*, 25(3), 500-510. <http://dx.doi.org/10.1139/t88-055>.
- Garakani, A.A., Sadeghi, H., Saheb, S., & Lamei, A. (2020). Bearing capacity of shallow foundations on unsaturated soils: analytical approach with 3D numerical simulations and experimental validations. *International Journal of Geomechanics*, 20(3), 04019181. [http://dx.doi.org/10.1061/\(ASCE\)GM.1943-5622.0001589](http://dx.doi.org/10.1061/(ASCE)GM.1943-5622.0001589).
- Garven, E., & Vanapalli, S.K. (April 2-6, 2006). Evaluation of empirical procedures for predicting the shear strength of unsaturated soils. In *Proceedings 4th International Conference on Unsaturated Soils* (pp. 2570-2581, vol. 2). Carefree, Arizona.
- Ghasemzadeh, H., & Akbari, F. (2019). Determining the bearing capacity factor due to nonlinear matric suction distribution in the soil. *Canadian Journal of Soil Science*, 99(4), 434-446. <http://dx.doi.org/10.1139/cjss-2019-0071>.
- Ghorbani, J., Nazem, M., & Carter, J.P. (2016). Numerical modelling of multiphase flow in unsaturated deforming porous media. *Computers and Geotechnics*, 71, 195-206. <http://dx.doi.org/10.1016/j.compgeo.2015.09.011>.
- Hong Kong Government (1972). *Interim Report of the Commission of Inquiry into the Rainstorm Disasters, 1972*. Government Printer.
- Jaky, J. (1944). The coefficient of earth pressure at rest. In Hungarian (A nyugalmi nyomás tenyezője). *Journal of the Society of Hungarian Architects and Engineering*, 78(22), 355-358.
- Kumbhokjar, A.S. (1993). Numerical evaluation of Terzaghi's  $N_q$ . *Journal of Geotechnical Engineering*, 119(3), 598-607.
- Larson, R. (1997). *Investigation and load tests in silty soils – Results from a series of investigations in silty soils in Sweden* (Report 54). Swedish Geotechnical Institute.
- Lee, J.-S., & Santamarina, J.C. (2005). Bender elements: performance and signal interpretation. *Journal of Geotechnical and Geoenvironmental Engineering*, 131(9), 1063-1070. [http://dx.doi.org/10.1061/\(ASCE\)1090-0241\(2005\)131:9\(1063\)](http://dx.doi.org/10.1061/(ASCE)1090-0241(2005)131:9(1063)).

- Leong, E.-C., & Abuel-Naga, H. (2018). Contribution of osmotic suction to shear strength of unsaturated high plasticity silty soil. *Geomechanics for Energy and the Environment*, 15, 65-73. <http://dx.doi.org/10.1016/j.gete.2017.11.002>.
- Lu, N., Godt, J.W., & Wu, D.T. (2010). A closed-form equation for effective stress in unsaturated soil. *Water Resources Research*, 46, W05515. <http://dx.doi.org/10.1029/2009WR008646>.
- Lu, N., & Likos, W.J. (2004). *Unsaturated soil mechanics*. Wiley.
- Martin, C.M. (2004). *User guide for ABC – Analysis of Bearing Capacity, Ver. 1.0*. University of Oxford.
- Meyerhof, G.G. (1963). Some recent research on the bearing capacity of foundations. *Canadian Geotechnical Journal*, 1(1), 16-26. <http://dx.doi.org/10.1139/t63-003>.
- Meyerhof, G.G. (1974). Ultimate bearing capacity of footings on sand layer overlying clay. *Canadian Geotechnical Journal*, 11(2), 223-229. <http://dx.doi.org/10.1139/t74-018>.
- Mohamed, F.M.O., & Vanapalli, S.K. (October, 2006). Laboratory investigations for the measurement of the bearing capacity of an unsaturated coarse-grained soil. In *Proceedings 59th Canadian Geotechnical Conference* (pp. 219-216). Vancouver.
- Oloo, S.Y. (1994). *A bearing capacity approach to the design of low-volume traffic roads* [Ph.D. thesis]. University of Saskatchewan.
- Oloo, S.Y., Fredlund, D.G., & Gan, J.K.-M. (1997). Bearing capacity of unpaved roads. *Canadian Geotechnical Journal*, 34(3), 398-407. <http://dx.doi.org/10.1139/t96-084>.
- Oh, W.T., & Vanapalli, S.K. (2011). Modelling the applied vertical stress and settlement relationship of shallow foundations in saturated and unsaturated sands. *Canadian Geotechnical Journal*, 48(3), 425-438. <https://doi.org/10.1139/T10-079>.
- Oh, W.T., & Vanapalli, S.K. (2013). Interpretation of the bearing capacity of unsaturated fine-grained soil using the modified effective and the modified total stress approaches. *International Journal of Geomechanics*, 13(6), 769-778. [http://dx.doi.org/10.1061/\(ASCE\)GM.1943-5622.0000263](http://dx.doi.org/10.1061/(ASCE)GM.1943-5622.0000263).
- Oh, W.T., & Vanapalli, S.K. (2018a). Undrained shear strength of unsaturated soils under zero or low confining pressures in the vadose zone. *Vadose Zone Journal*, <http://dx.doi.org/10.2136/vzj2018.01.0024>.
- Oh, W.T., & Vanapalli, S.K. (2018b). Modeling the stress versus settlement behavior of shallow foundations in unsaturated cohesive soils extending the modified total stress approach. *Soil and Foundation*, 58(2), 382-398. <http://dx.doi.org/10.1016/j.sandf.2018.02.008>.
- Oh, W.T., Vanapalli, S.K., & Puppala, A.J. (2009). Semi-empirical model for the prediction of modulus of elasticity for unsaturated soils. *Canadian Geotechnical Journal*, 46(8), 903-914. <http://dx.doi.org/10.1139/T09-030>.
- Pineda, J.A., & Colmenares, J.E. (June, 2005). Influence of matric suction on the shear strength of compacted Kaolin under unconfined conditions: Experimental results (Part 1). In *Proceedings International Symposium on Advanced Experimental Unsaturated Soil Mechanics* (pp. 221-226). Trento.
- Poulos, H.D., & Davis, E.H. (1974). *Elastic solutions for soil and rock mechanics*. John Wiley and Sons.
- Prandtl, L. (1921). Über die Eindringungsfestigkeit (Härte) plastischer Baustoffe und die Festigkeit von Schneiden. *Zeitschrift für Angewandte Mathematik und Mechanik*, 1(1), 15-20.
- Rahardjo, H., Heng, O.B., & Leong, E.C. (2004). Shear strength of a compacted residual soil from consolidated drained and the constant water content tests. *Canadian Geotechnical Journal*, 41(3), 1-16. <http://dx.doi.org/10.1139/t03-093>.
- Richard, A., Oh, W.T., & Brennan, G. (2021). Estimating critical height of unsupported trenches in vadose zone. *Canadian Geotechnical Journal*, 58(1), 66-82. <http://dx.doi.org/10.1139/cgj-2019-0069>.
- Ridley, A.M., & Burland, J.B. (1993). A new instrument for the measurement of soil moisture suction. *Geotechnique*, 43(2), 321-324.
- Rojas, J. C., Salinas, L. M., & Seja, C. (2007). Plate-load tests on an unsaturated lean clay. *Experimental Unsaturated Soil Mechanics*, 112, 445-452. <https://doi.org/10.1680/geot.1993.43.2.321>.
- Safarzadeh, Z., & Aminfar, M.H. (2020). Experimental study on bearing capacity of shallow footings based on sand in saturated and unsaturated conditions. *Journal of Civil and Environmental Engineering*, 50(2), 23-32. <http://dx.doi.org/10.22034/jcee.2019.9100>.
- Schnaid, F., Consoli, N.C., Cudmani, R., & Milititsky, J. (September 5-6, 1995). Load-settlement response of shallow foundations in structured unsaturated soils. In *Proceedings 1st International Conference on Unsaturated Soils* (pp. 999-1004). Rotterdam.
- Serrano, A., Olalla, C., & Jimenez, R. (2005). Analytical bearing capacity of strip footings in weightless materials with powder-law failure criteria. *International Journal of Geomechanics*, 16(1), 85-96. [http://dx.doi.org/10.1061/\(ASCE\)GM.1943-5622.0000465](http://dx.doi.org/10.1061/(ASCE)GM.1943-5622.0000465).
- Skempton, A.W. (1948). The  $\phi_u = 0$  analysis for stability and its theoretical basis. In *Proceedings 2nd International Conference of Soil Mechanics and Foundation Engineering* (pp. 72-77, vol. 1).
- Steenen-Bach, J.O., Foged, N., & Steenfelt, J.S. (1987). Capillary Induced Stresses – Fact or Fiction? In *Proceedings 9th European Conference on Soil Mechanics and Foundation Engineering* (pp. 83-89). Budapest.
- Szavits-Nossan, A. (2006). Observations on the Observational Method. In *Proceedings Active Geotechnical Design in Infrastructure Development* (pp. 171-178). Ljubljana, Slovenian Geotechnical Soc.

- Tan, M., Cheng, X., & Vanapalli, S.K. (2021). Simple approaches for the design of shallow and deep foundations for unsaturated soils I: Theoretical and Experimental Studies. *Indian Geotechnical Journal*, 51(1), 97-114. <http://dx.doi.org/10.1007/s40098-021-00501-2>.
- Tang, Y., Taiebat, H.A., & Russell, A.R. (2016). Bearing capacity of shallow foundations in unsaturated soil considering hydraulic hysteresis and three drainage conditions. *International Journal of Geomechanics*, 17(6), 1-13.
- Terzaghi, K. (1936). Relation between soil mechanics and foundation engineering: presidential address. In *Proceedings 1st International Conference on Soil Mechanics and Foundation Engineering* (vol. 3, pp. 13-18). Boston.
- Terzaghi, K. (1943). *Theoretical Soil Mechanics*. John Wiley and Sons.
- Tidlund, M. (2021). *Geotechnical risk management using the observational method* [Doctoral thesis] KTH Royal Institute of Technology.
- Vahedifard, F., & Robinson, J.D. (2016). Unified method for estimating the ultimate bearing capacity of shallow foundations in variably saturated soils under steady flow. *Journal of Geotechnical and Geoenvironmental Engineering*, 142(4), 04015095. [http://dx.doi.org/10.1061/\(ASCE\)GT.1943-5606.0001445](http://dx.doi.org/10.1061/(ASCE)GT.1943-5606.0001445).
- Vanapalli, S.K. (November 2009). Shear strength of unsaturated soils and its applications in geotechnical engineering practice. In *Proceedings 4th Asia Pacific Conference on Unsaturated Soils* (pp. 579-598). Newcastle.
- Vanapalli, S.K., Fredlund, D.G., Pufahl, D.E., & Clifton, A.W. (1996). Model for the prediction of shear strength with respect to soil suction. *Canadian Geotechnical Journal*, 33(3), 379-392. <http://dx.doi.org/10.1139/t96-060>.
- Vanapalli, S.K., & Lacasse, F. (2009). Comparison between the measured and predicted shear strength behaviour of four unsaturated sands. In O. Buzzi, S. Fityus & D. Sheng. *Unsaturated Soils - Experimental studies in unsaturated soils and expansive soils* (pp. 121-127). CRC Press.
- Vanapalli, S.K., & Mohamed, F.M.O. (2007). Bearing capacity of model footings in unsaturated soils. *Springer Proceedings in Physics*, 112, 483-493. [http://dx.doi.org/10.1007/3-540-69873-6\\_48](http://dx.doi.org/10.1007/3-540-69873-6_48).
- Vanapalli, S.K., & Oh, W.T. (2010). A model for predicting the modulus of elasticity of unsaturated soils using the soil-water characteristic curve. *International Journal of Geotechnical Engineering*, 4(4), 425-433. <http://dx.doi.org/10.3328/IJGE.2010.04.04.425-433>.
- Vanapalli, S.K., Oh, W.T., & Puppala, A.J. (October 21-24, 2007). Determination of the bearing capacity of unsaturated soils under undrained loading conditions. In *Proceedings 60th Canadian Geotechnical Conference* (pp. 1002-1009). Ottawa.
- Vanapalli, S.K., Wright, A., & Fredlund, D.G. (October, 2000). Shear strength of two unsaturated silty soils over the suction range from 0 to 1,000,000 kPa. In *Proceedings 53rd Canadian Geotechnical Conference* (pp. 1161-1168). Montreal.
- van Genuchten, M.T. (1980). A closed-form equation for predicting the hydraulic conductivity of unsaturated soils. *Soil Science Society of America Journal*, 44, 892-898. <http://dx.doi.org/10.2136/sssaj1980.03615995004400050002x>.
- Vesić, A.B. (1963). *Bearing capacity of deep foundations in sand*. *Highway Research Record* 39 (pp. 112-153). National Academy of Sciences.
- Vesić, A.B. (1973). Analysis of ultimate loads of shallow foundations. *Journal of the Soil Mechanics and Foundations Division*, 99(1), 45-73. <http://dx.doi.org/10.1061/AJGEB6.0000078>.
- Vo, T., & Russel, A.R. (2016). Bearing capacity of strip footings on unsaturated soils by the slip line theory. *Computers and Geotechnics*, 74, 122-131.
- Yan, Q., Zhao, J., Zhang, C., & Wang, J. (2020). Ultimate bearing capacity of strip foundations in unsaturated soils considering the intermediate principal stress effect. *Advances in Civil Engineering*, 2020, 1-14. <http://dx.doi.org/10.1155/2020/8854552>.
- Yeh, T.-C. (1989). One-dimensional steady state infiltration in heterogeneous soils. *Water Resources Research*, 25(10), 2149-2158. <http://dx.doi.org/10.1029/WR025i010p02149>.
- Zhou, W.-H., Xu, X., & Garg, A. (2016). Measurement of unsaturated shear strength parameters of silty sand and its correlation with unconfined compressive strength. *Measurement*, 93, 351-358. <http://dx.doi.org/10.1016/j.measurement.2016.07.049>.



# BELGO GABION. THE BEST CHOICE TO INCREASE YOUR CONSTRUCTION QUALITY.



**Belgo Geotech** provides steel solutions, for geotechnical applications, to the market. Our products include **gabions**, **rockfall mesh**, **Dramix®** steel fibers, **galvanized pannels** and **meshes for rock support** and **reinforcement systems**, **PC Strand for cable bolts** and **thread bars**. We also offer qualified technical support to meet all of your project's needs. **Our geotechnics feature the strength of steel.**



Learn more at: [belgogeotech.com.br](http://belgogeotech.com.br)

**BELGO**  
GeoTech

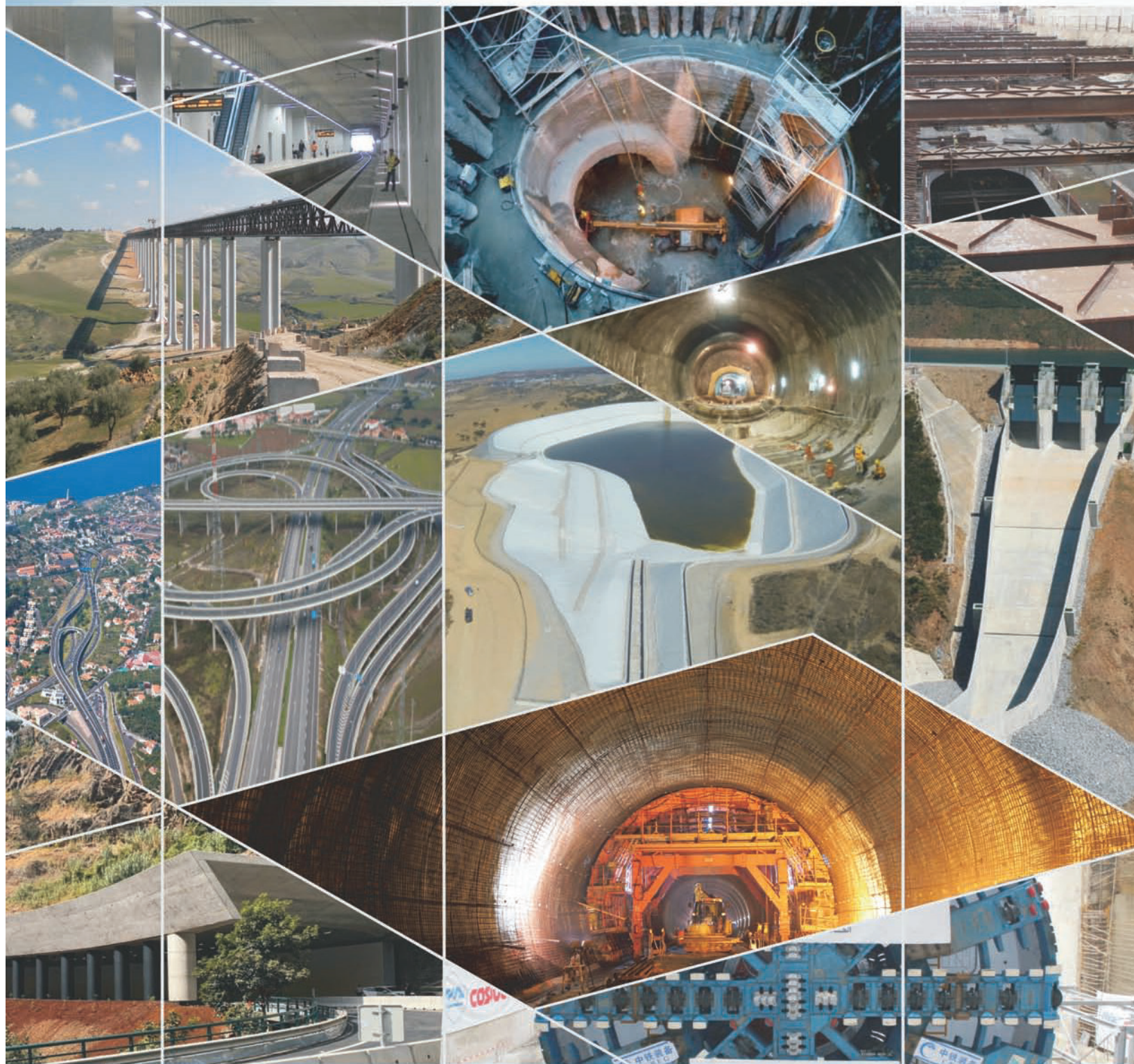
Belgo Bekaert Arames

ArcelorMittal

**BEKAERT**  
better together



BUILDING THE WORLD, BETTER



## Engineering and Architectural Consultancy

Geology, Geotechnics, Supervision of Geotechnical Works  
Embankment Dams, Underground Works, Retaining Structures  
Special Foundations, Soil Improvement, Geomaterials



MEMBER OF

TPF - CONSULTORES DE ENGENHARIA E ARQUITETURA, S.A.

[www.tpf.pt](http://www.tpf.pt)

40  
years



# DF+, YOUR TRUST FIRST

GEOLOGICAL, GEOTECHNICAL  
ENGINEERING AND WATER  
RESOURCES SOLUTIONS FOR THE  
MINING SECTOR AND OTHERS.



DF+ IS A COMPANY WITH A FOCUS ON THE MINERAL SECTOR AND MORE THAN 15 YEARS OF EXPERIENCE. WE OPERATE IN ALL PHASES OF A PROJECT, FROM FEASIBILITY STUDIES AND PROJECT DEVELOPMENT TO TECHNICAL MONITORING OF CONSTRUCTION AND MINE CLOSURE.

JOIN OUR SOCIAL NETWORKS TO  
KNOW MORE ABOUT OUR SERVICES.



AVE BARÃO HOMEM DE MELO, 4554 - 5th floor  
ESTORIL, BELO HORIZONTE/MG

+55 31 2519-1001

comercial@dfmais.eng.br



DF+ GEOTECHNICAL ENGINEERING  
AND WATER RESOURCES



# PIONEERING AND INNOVATION

SINCE 1921

 **TEIXEIRA DUARTE**  
ENGENHARIA E CONSTRUÇÕES, S.A.

PORT FACILITY CONSTRUCTION  
NACALA - MOZAMBIQUE



Building a better world.  
[teixiraduarteconstruction.com](http://teixiraduarteconstruction.com)





Safety is our nature

# SISTEMAS DE ALERTA E MONITORAMENTO

## Sistemas de Alerta e Alarme

Ideal para identificação de agentes  
deflagradores e monitoramento de  
eventos

Rua Visconde de Pirajá, 82 | Ipanema  
22410-003 | Rio de Janeiro | RJ | Brasil.  
Tel.: + 55 21 3624.1449  
[www.geobrugg.com](http://www.geobrugg.com)



Parceria:





# The Best Solution!

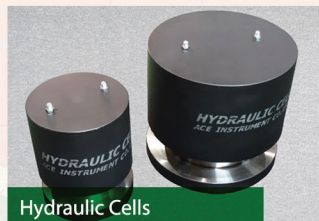
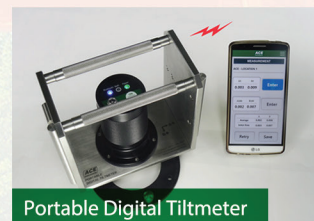
**Tecnilab Portugal, S.A.** will provide you with answers to your Geotechnical engineering needs.

**Tecnilab Portugal, S.A.** is a professional Geotechnical engineering company and has a lot of experience as a professional group that mainly engages in measurement engineering in dam, subway(Metro), harbor, power plant, soft ground and structure construction.

**WE ARE THE DISTRIBUTOR OF PORTUGAL OF ACE INSTRUMENT CO., LTD. IN KOREA.**

**ACE INSTRUMENT CO., LTD.** is a company that obtains worldwide reputation for supplying high precision, high reliability products in all Geotechnical instruments, data logger and in-situ test equipments. Independently developed automatic monitoring system can be used anywhere in the world, including buildings, bridges, ground and any constructions.

## Data Acquisition System & Web Monitoring Program



Sales company



**Tecnilab Portugal, S.A.**

A: Rua Gregorio Lopes, Lote 1512B 1449-041 Lisboa Portugal  
T: +351 217 220 870 F: +351 217 264 550  
www.tecnilab.pt

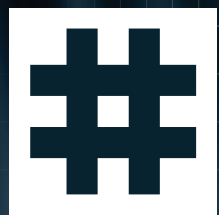
Manufacturer



**ACE INSTRUMENT CO., LTD.**

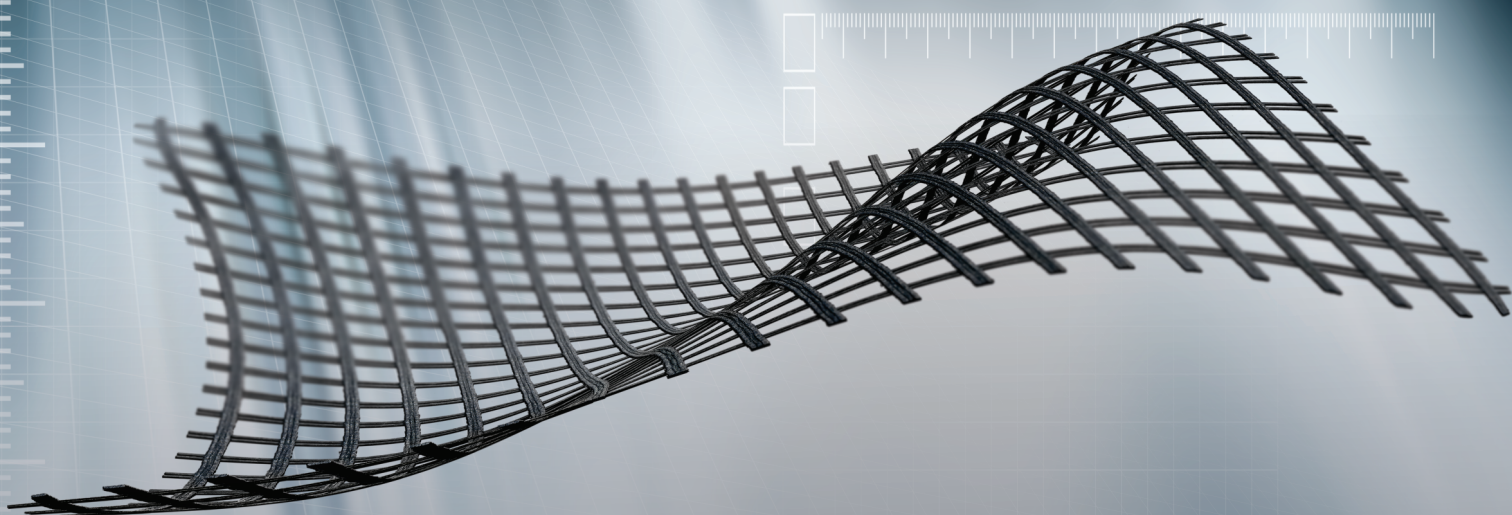
The first value in Geotechnical & Structural Instrumentation  
A: 9, Dangjung-ro 27 beon-gil, Gunpo-si, Gyeonggi-do, Korea  
T: +82 31 459 8753-7 F: +82 31 459 8758 E: acens@naver.com  
www.aceinstrument.com





# HUESKER

Ideen. Ingenieure. Innovationen.



## LEADER IN GEOSYNTHETICS

Experience HUESKER's geosynthetic building materials, systems and services now.



[www.HUESKER.com](http://www.HUESKER.com)

Find HUESKER in Social Media:





# ENGINEERING AND ENVIRONMENTAL CONSULTANTS



## COBA



## GEOLOGY AND GEOTECHNICS

Hydrogeology • Engineering Geology • Rock Mechanics • Soil Mechanics • Foundations and Retaining Structures • Underground Works • Embankments and Slope Stability  
Environmental Geotechnics • Geotechnical Mapping



- Water Resources Planning and Management
- Hydraulic Undertakings
- Electrical Power Generation and Transmission
- Water Supply Systems and Pluvial and Wastewater Systems
- Agriculture and Rural Development
- Road, Railway and Airway Infrastructures
- Environment
- Geotechnical Structures
- Cartography and Cadastre
- Safety Control and Work Rehabilitation
- Project Management and Construction Supervision



### PORTUGAL

CENTER AND SOUTH REGION  
Av. 5 de Outubro, 323  
1649-011 LISBOA  
Tel.: (351) 210125000, (351) 217925000  
Fax: (351) 217970348  
E-mail: [coba@coba.pt](mailto:coba@coba.pt)  
[www.coba.pt](http://www.coba.pt)

Av. Marquês de Tomar, 9, 6º.  
1050-152 LISBOA  
Tel.: (351) 217925000  
Fax: (351) 213537492

### NORTH REGION

Rua Mouzinho de Albuquerque, 744, 1º.  
4450-203 MATOSINHOS  
Tel.: (351) 229380421  
Fax: (351) 229373648  
E-mail: [engico@engico.pt](mailto:engico@engico.pt)

### ANGOLA

Praceta Farinha Leitão, edifício nº 27, 27-A - 2º Dto  
Bairro do Maculusso, LUANDA  
Tel./Fax: (244) 222338 513  
Cell: (244) 923317541  
E-mail: [coba-angola@netcabo.co.ao](mailto:coba-angola@netcabo.co.ao)

### MOZAMBIQUE

Pestana Rovuma Hotel. Centro de Escritórios.  
Rua da Sé nº114. Piso 3, MAPUTO  
Tel./Fax: (258) 21 328 813  
Cell: (258) 82 409 9605  
E-mail: [coba.mz@tdm.co.mz](mailto:coba.mz@tdm.co.mz)

### ALGERIA

09, Rue des Frères Hocine  
El Biar - 16606, ARGEL  
Tel.: (213) 21 922802  
Fax: (213) 21 922802  
E-mail: [coba.alger@gmail.com](mailto:coba.alger@gmail.com)

### BRAZIL

Rio de Janeiro  
COBA Ltd. - Rua Bela 1128  
São Cristóvão  
20930-380 Rio de Janeiro RJ  
Tel.: (55 21) 351 50 101  
Fax: (55 21) 258 01 026

### Fortaleza

Av. Senador Virgílio Távora 1701, Sala 403  
Aldeota - Fortaleza CEP 60170 - 251  
Tel.: (55 85) 3261 17 38  
Fax: (55 85) 3261 50 83  
E-mail: [coba@esc-te.com.br](mailto:coba@esc-te.com.br)

### UNITED ARAB EMIRATES

Corniche Road - Corniche Tower - 5th Floor - 5B  
P.O. Box 38360 ABU DHABI  
Tel.: (971) 2 627 0088  
Fax: (971) 2 627 0087





The Ground is our Challenge

## MAIN ACTIVITY AREAS

Consultancy, Supervision and Training

- Earth Retaining Structures
- Special Foundations
- Ground Improvement
- Foundations Strengthening and Underpinning
- Façades Retention
- Tunnels and Underground Structures
- Slope Stability
- Geological and Geotechnical Investigation
- Demolition

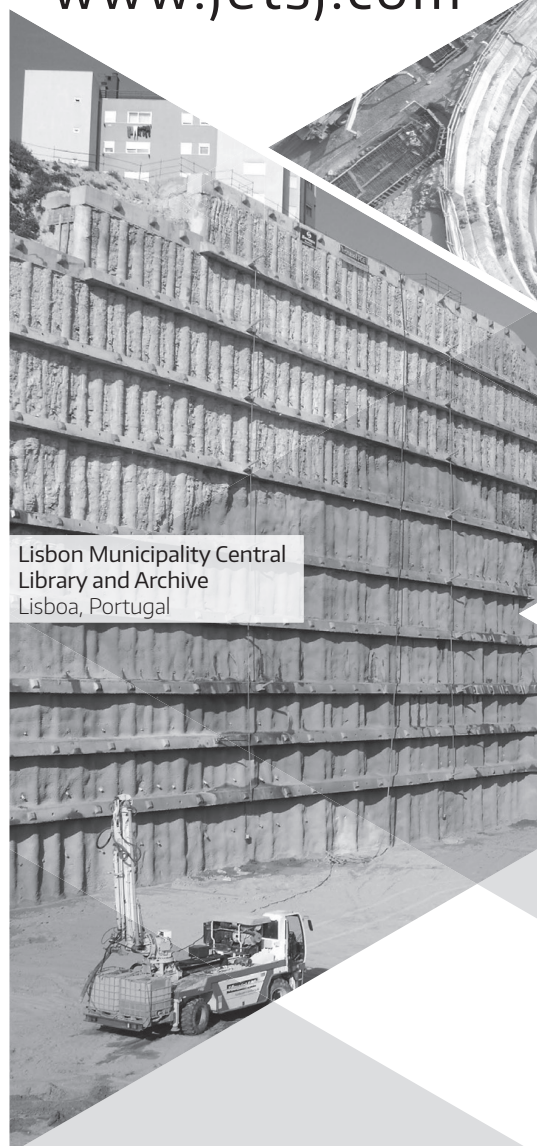
[www.jetsj.com](http://www.jetsj.com)



Tool Plazas P2 and P3  
Santa Catarina, Brazil



Mining Shaft  
Kamsar, Guiné



Lisbon Municipality Central  
Library and Archive  
Lisboa, Portugal



Solar Santana Building  
Lisboa, Portugal

## Main Office

Rua Julieta Ferrão, 12 - Office 1501

1600-131 LISBOA, Portugal

Phone.: [+351] 210 505 150 / 51

Email: [info@jetsj.com](mailto:info@jetsj.com)

[www.linkedin.com/company/jetsj-geotecnia-lda/](http://www.linkedin.com/company/jetsj-geotecnia-lda/)



# MACCAFERRI

## Learn more about GAWAC® 3.0 software

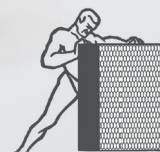
*Developed to support engineers, designers and students in a fast and reliable way to perform the analyzes of gabion retaining wall.*

The great advantage of **GAWAC® 3.0** is the inclusion of the stability analysis in serviceability conditions, through the GSC (Gabion Serviceability Coefficient). This type of analysis allows the user to evaluate the cross sections of the gabion walls in the most suitable conditions through the best performance and optimization of the gabion materials. The software allows the user to choose the type of gabion with the coating and mesh technologically appropriate to the work environment, in addition to allowing the use of international standards, various calculation analyzes with a detailed printable report.



## NEW SOFTWARE FEATURES

- **New user-friendly** interface;
- Consider the **influence of the mesh**;
- **Service Limit State (SLS) and Ultimate Limit State (ULS)** are considered in the stability analysis;
- Consider the **long-term performance of the gabion** based on the type of mesh and coating;
- **Serviceability conditions** performed by layer;
- Optimized design with the use of **Strong Face Gabion**.



**GABION  
STRONG  
FACE**



Visit our website to **learn more**  
about **Strong Face Gabion** and  
download **GAWAC® 3.0**.



/maccaferri /maccaferrimatrix



@Maccaferri\_BR



/MaccaferriWorld



/maccaferriworld





- > **Prospecção Geotécnica**  
*Site Investigation*
- > **Consultoria Geotécnica**  
*Geotechnical Consultancy*
- > **Obras Geotécnicas**  
*Ground Treatment-Construction Services*
- > **Controlo e Observação**  
*Field Instrumentation Services and Monitoring Services*
- > **Laboratório de Mecânica de Solos**  
*Soil and Rock Mechanics Laboratory*

Certificada ISO 9001 por



# Geocontrole



Parque Oriente, Bloco 4, EN10  
2699-501 Bobadela LRS  
Tel. 21 995 80 00  
Fax. 21 995 80 01  
e.mail: [mail@geocontrole.pt](mailto:mail@geocontrole.pt)  
[www.geocontrole.pt](http://www.geocontrole.pt)

  
**Geocontrole**  
Geotecnia e Estruturas de Fundação SA

## Guide for Authors

Soils and Rocks is an international scientific journal published by the Brazilian Association for Soil Mechanics and Geotechnical Engineering (ABMS) and by the Portuguese Geotechnical Society (SPG). The aim of the journal is to publish original papers on all branches of Geotechnical Engineering. Each manuscript is subjected to a single-blind peer-review process. The journal's policy of screening for plagiarism includes the use of a plagiarism checker on all submitted manuscripts.

Soils and Rocks embraces the international Open Science program and is striving to meet all the recommendations. However, at this moment, the journal is not yet accepting preprints and open data, and has not adopted open peer reviews.

Soils and Rocks provides a manuscript template available at the journal's website.

### 1. Category of papers

Submissions are classified into one of the following categories:

**Article** – an extensive and conclusive dissertation about a geotechnical topic, presenting original findings.

**Technical Note** – presents a study of smaller scope or results of ongoing studies, comprising partial results and/or particular aspects of the investigation.

**Case Study** – report innovative ways to solve problems associated with design and construction of geotechnical projects. It also presents studies of the performance of existing structures.

**Review Article** – a summary of the State-of-the-Art or State-of-the-Practice on a particular subject or issue and represents an overview of recent developments.

**Discussion** – specific discussions about published papers.

Authors are responsible for selecting the correct category when submitting their manuscript. However, the manuscript category may be altered based on the recommendation of the Editorial Board. Authors are also requested to state the category of paper in their Cover Letter.

When submitting a manuscript for review, the authors should indicate the category of the manuscript, and is also understood that they:

- a) assume full responsibility for the contents and accuracy of the information in the paper;
- b) assure that the paper has not been previously published, and is not being submitted to any other journal for publication.

### 2. Paper length

Full-length manuscripts (Article, Case Study) should be between 4,000 and 8,000 words. Review articles should have up to 10,000 words. Technical Notes have a word count limit of 3,500 words. Discussions have a word count limit of 1,000 words. These word count limits exclude the title page, notation list (e.g., symbols, abbreviations), captions of tables and figures, acknowledgments and references. Each single column and double column figure or table is considered as equivalent to 150 and 300 words, respectively.

### 3. Scientific style

The manuscripts should be written in UK or US English, in the third person and all spelling should be checked in accordance with

a major English Dictionary. The manuscript should be able to be readily understood by a Civil Engineer and avoid colloquialisms. Unless essential to the comprehension of the manuscript, direct reference to the names of persons, organizations, products or services is not allowed. Flattery or derogatory remarks about any person or organization should not be included.

The author(s) of Discussion Papers should refer to himself (herself/themselves) as the reader(s) and to the author(s) of the paper as the author(s).

The International System (SI) units must be used. The symbols are recommended to be in accordance with Lexicon in 14 Languages, ISSMFE (2013) and the ISRM List of Symbols. Use italics for single letters that denote mathematical constants, variables, and unknown quantities, either in tables or in the text.

### 4. Submission requirements and contents

A submission implies that the following conditions are met:

- the authors assume full responsibility for the contents and accuracy of the information presented in the paper;
- the manuscript contents have not been published previously, except as a lecture or academic thesis;
- the manuscript is not under consideration for publication elsewhere;
- the manuscript is approved by all authors;
- the manuscript is approved by the necessary authorities, when applicable, such as ethics committees and institutions that may hold intellectual property on contents presented in the manuscript;
- the authors have obtained authorization from the copyright holder for any reproduced material;
- the authors are aware that the manuscript will be subjected to plagiarism check.

The author(s) must upload two digital files of the manuscript to the Soils and Rocks submission system. The size limit for each submission file is 20 MB. The manuscript should be submitted in docx format (Word 2007 or higher) or doc format (for older Word versions). An additional PDF format file of the manuscript is also required upon submission. Currently, the journal is not accepting manuscripts prepared using LaTeX.

The following documents are required as minimum for submission:

- cover letter;
- manuscript with figures and tables embedded in the text (doc or docx format);



manuscript with figures and tables embedded in the text for revision (PDF format);

- permission for re-use of previously published material when applicable, unless the author/owner has made explicit that the image is freely available.

#### 4.1 Cover letter

The cover letter should include: manuscript title, submission type, authorship information, statement of key findings and work novelty, and related previous publications if applicable.

#### 4.2 Title page

The title page is the first page of the manuscript and must include:

- A concise and informative title of the paper. Avoid abbreviations, acronyms or formulae. Discussion Papers should contain the title of the paper under discussion. Only the first letter of the first word should be capitalized.
- Full name(s) of the author(s). The first name(s) should not be abbreviated. The authors are allowed to abbreviate middle name(s).
- The corresponding author should be identified by a pound sign # beside his/her and in a footnote.
- The affiliation(s) of the author(s), should follow the format: Institution, (Department), City, (State), Country.
- Affiliation address and e-mail must appear below each author's name.
- The 16-digit ORCID of the author(s) – mandatory
- Main text word count (excluding abstract and references) and the number of figures and tables

#### 4.3 Permissions

Figures, tables or text passages previously published elsewhere may be reproduced under permission from the copyright owner(s) for both the print and online format. The authors are required to provide evidence that such permission has been granted at the moment of paper submission.

#### 4.4 Declaration of interest

Authors are required to disclose conflicting interests that could inappropriately bias their work. For that end, a section entitled “Declaration of interest” should be included following any acknowledgments and prior to the “Authors’ contributions” section. In case of the absence of conflicting interests, the authors should still include a declaration of interest.

#### 4.5 Authors’ contributions

Authors are required to include an author statement outlining their individual contributions to the paper according to the CASRAI CRediT roles (as per <https://casrai.org/credit>). The minimum requirements of contribution to the work for recognition of authorship are: a) Participate actively in the discussion of results; b) Review and approval of the final version of the manuscript. A section entitled “Authors’ contributions” should be included after the declaration of interest section, and should be formatted with author's name and CRediT role(s), according to the example:

**Samuel Zheng:** conceptualization, methodology, validation. **Olivia Prakash:** data curation, writing - original draft preparation. **Fatima Wang:** investigation, validation. **Kwame Bankole:** supervision. **Sun Qi:** writing - reviewing and editing.

Do not include credit items that do not follow the Taxonomy established by CASRAI CRediT roles.

The authors’ contributions section should be omitted in manuscripts that have a single author.

#### 5. Plagiarism checking

Submitted papers are expected to contain at least 50 % new content and the remaining 50 % should not be verbatim to previously published work.

All manuscripts are screened for similarities. Currently, the Editorial Board uses the plagiarism checker Plagius ([www.plagius.com](http://www.plagius.com)) to compare submitted papers to already published works. Manuscripts will be rejected if more than 20 % of content matches previously published work, including self-plagiarism. The decision to reject will be under the Editors’ discretion if the percentage is between 10 % and 20 %.

**IMPORTANT OBSERVATION:** Mendeley software plug-in (suggested in this guide) for MS-Word can be used to include the references in the manuscript. This plug-in uses a field code that sometimes includes automatically both title and abstract of the reference. Unfortunately, the similarity software adopted by the Journal (Plagius) recognizes the title and abstract as an actual written text by the field code of the reference and consequently increases considerably the percentage of similarity. Please do make sure to remove the abstract (if existing) inside Mendeley section where the adopted reference is included. This issue has mistakenly caused biased results in the past. The Editorial Board of the journal is now aware of this tendentious feature.

#### 6. Formatting instructions

The text must be presented in a single column, using ISO A4 page size, left, right, top, and bottom margins of 25 mm, Times New Roman 12 font, and line spacing of 1.5. All lines and pages should be numbered.

The text should avoid unnecessary italic and bold words and letters, as well as too many acronyms. Authors should avoid to capitalize words and whenever possible to use tables with distinct font size and style of the regular text.

Figures, tables and equations should be numbered in the sequence that they are mentioned in the text.

##### *Abstract*

Please provide an abstract between 150 and 250 words in length. Abbreviations or acronyms should be avoided. The abstract should state briefly the purpose of the work, the main results and major conclusions or key findings.

##### *Keywords*

A minimum of three and a maximum of six keywords must be included after the abstract. The keywords must represent the



content of the paper. Keywords offer an opportunity to include synonyms for terms that are frequently referred to in the literature using more than one term. Adequate keywords maximize the visibility of your published paper.

Examples:

Poor keywords – piles; dams; numerical modeling; laboratory testing

Better keywords – friction piles; concrete-faced rockfill dams; material point method; bender element test

#### List of symbols

A list of symbols and definitions used in the text must be included before the References section. Any mathematical constant, variable or unknown quantity should appear in italics.

### 6.1 Citations

References to other published sources must be made in the text by the last name(s) of the author(s), followed by the year of publication. Examples:

- Narrative citation: [...] while Silva & Pereira (1987) observed that resistance depended on soil density
- Parenthetical citation: It was observed that resistance depended on soil density (Silva & Pereira, 1987).

In the case of three or more authors, the reduced format must be used, e.g.: Silva et al. (1982) or (Silva et al., 1982). Do not italicize “et al.”

Two or more citations belonging to the same author(s) and published in the same year are to be distinguished with small letters, e.g.: (Silva, 1975a, b, c.).

Standards must be cited in the text by the initials of the entity and the year of publication, e.g.: ABNT (1996), ASTM (2003).

### 6.2 References

A customized style for the Mendeley software is available and may be downloaded from this link.

Full references must be listed alphabetically at the end of the text by the first author's last name. Several references belonging to the same author must be cited chronologically.

Some formatting examples are presented here:

#### Journal Article

Bishop, A.W., & Blight, G.E. (1963). Some aspects of effective stress in saturated and partly saturated soils. *Géotechnique*, 13(2), 177-197. <https://doi.org/10.1680/geot.1963.13.3.177>

Castellanza, R., & Nova, R. (2004). Oedometric tests on artificially weathered carbonatic soft rocks. *Journal of Geotechnical and Geoenvironmental Engineering*, 130(7), 728-739. [https://doi.org/10.1061/\(ASCE\)1090-0241\(2004\)130:7\(728\)](https://doi.org/10.1061/(ASCE)1090-0241(2004)130:7(728))

Fletcher, G. (1965). Standard penetration test: its uses and abuses. *Journal of the Soil Mechanics Foundation Division*, 91, 67-75.

Indraratna, B., Kumara, C., Zhu S-P., Sloan, S. (2015). Mathematical modeling and experimental verification of fluid flow through deformable rough rock joints. *International Journal of Geomechanics*, 15(4): 04014065-1-04014065-11. [https://doi.org/10.1061/\(ASCE\)GM.1943-5622.0000413](https://doi.org/10.1061/(ASCE)GM.1943-5622.0000413)

Garnier, J., Gaudin, C., Springman, S.M., Culligan, P.J., Goodings, D., König, D., ... & Thorel, L. (2007). Catalogue of scaling laws and similitude questions in geotechnical centrifuge modelling. *International Journal of Physical Modelling in Geotechnics*, 7(3), 01-23. <https://doi.org/10.1680/ijpmg.2007.070301>

Bicalho, K.V., Gramelich, J.C., & Santos, C.L.C. (2014). Comparação entre os valores de limite de liquidez obtidos pelo método de Casagrande e cone para solos argilosos brasileiros. *Comunicações Geológicas*, 101(3), 1097-1099 (in Portuguese).

#### Book

Lambe, T.W., & Whitman, R.V. (1979). *Soil Mechanics, SI version*. John Wiley & Sons.

Das, B.M. (2012). *Fundamentos de Engenharia Geotécnica*. Cengage Learning (in Portuguese).

Head, K.H. (2006). *Manual of Soil Laboratory Testing - Volume 1: Soil Classification and Compaction Tests*. Whittles Publishing.

Bhering, S.B., Santos, H.G., Manzatto, C.V., Bognola, I., Fasolo, P.J., Carvalho, A.P., ... & Curcio, G.R. (2007). *Mapa de solos do estado do Paraná*. Embrapa (in Portuguese).

#### Book Section

Yerro, A., & Rohe, A. (2019). Fundamentals of the Material Point Method. In *The Material Point Method for Geotechnical Engineering* (pp. 23-55). CRC Press. <https://doi.org/10.1201/9780429028090>

Sharma, H.D., Dukes, M.T., & Olsen, D.M. (1990). Field measurements of dynamic moduli and Poisson's ratios of refuse and underlying soils at a landfill site. In *Geotechnics of Waste Fills - Theory and Practice* (pp. 57-70). ASTM International. <https://doi.org/10.1520/STP1070-EB>

Cavalcante, A.L.B., Borges, L.P.F., & Camapum de Carvalho, J. (2015). Tomografias computadorizadas e análises numéricas aplicadas à caracterização da estrutura porosa de solos não saturados. In *Solos Não Saturados no Contexto Geotécnico* (pp. 531-553). ABMS (in Portuguese).

#### Proceedings

Jamiolkowski, M.; Ladd, C.C.; Germaine, J.T., & Lancellotta, R. (1985). New developments in field and laboratory testing of soils. *Proc. 11th International Conference on Soil Mechanics and Foundation Engineering*, San Francisco, August 1985. Vol. 1, Balkema, 57-153.

Massey, J.B., Irfan, T.Y. & Cipullo, A. (1989). The characterization of granitic saprolitic soils. *Proc. 12th International Conference on Soil Mechanics and Foundation Engineering*, Rio de Janeiro. Vol. 6, Publications Committee of XII ICSMFE, 533-542.

Indraratna, B., Oliveira D.A.F., & Jayanathan, M. (2008b). Revised shear strength model for infilled rock joints considering overconsolidation effect. *Proc. 1st Southern Hemisphere International Rock Mechanics Symposium*, Perth. ACG, 16-19.

Barreto, T.M., Repsold, L.L., & Casagrande, M.D.T. (2018). Melhoria de solos arenosos com polímeros. *Proc. 19º Congresso Brasileiro de Mecânica dos Solos e Engenharia Geotécnica*, Salvador. Vol. 2, ABMS, CBMR, ISRM & SPG, 1-11 (in Portuguese).

#### Thesis

Lee, K.L. (1965). *Triaxial compressive strength of saturated sands under seismic loading conditions* [Unpublished doctoral dissertation]. University of California at Berkeley.

Chow, F.C. (1997). *Investigations into the behaviour of displacement pile for offshore foundations* [Doctoral thesis, Imperial College London]. Imperial College London's repository. <https://spiral.imperial.ac.uk/handle/10044/1/7894>

Araki, M.S. (1997). *Aspectos relativos às propriedades dos solos porosos colapsíveis do Distrito Federal* [Unpublished master's dissertation]. University of Brasília (in Portuguese).

Sotomayor, J.M.G. (2018). *Evaluation of drained and non-drained mechanical behavior of iron and gold mine tailings reinforced with polypropylene fibers* [Doctoral thesis, Pontifical Catholic University of Rio de Janeiro]. Pontifical Catholic University of Rio de Janeiro's repository (in Portuguese). <https://doi.org/10.17771/PUCRio.acad.36102>\*

\* official title in English should be used when available in the document.

#### Report

ASTM D7928-17. (2017). Standard Test Method for Particle-Size Distribution (Gradation) of Fine-Grained Soils Using the Sedimentation (Hydrometer) Analysis. *ASTM International*, West Conshohocken, PA. <https://doi.org/10.1520/D7928-17>

ABNT NBR 10005. (2004). Procedure for obtention leaching extract of solid wastes. *ABNT - Associação Brasileira de Normas Técnicas*, Rio de Janeiro, RJ (in Portuguese).

DNIT. (2010). Pavimentação - Base de solo-cimento - Especificação de serviço DNIT 143. *DNIT -Departamento Nacional de Infraestrutura de Transportes*, Rio de Janeiro, RJ (in Portuguese).

USACE (1970). Engineering and Design: Stability of Earth and Rock-Fill Dams, Engineering Manual 1110-2-1902. Corps of Engineers, Washington, D.C.

#### Web Page

Soils and Rocks. (2020). *Guide for Authors*. Soils and Rocks. Retrieved in September 16, 2020, from <http://www.soilsandrocks.com/>

### 6.3 Artworks and illustrations

Each figure should be submitted as a high-resolution image, according to the following mandatory requirements:

- Figures must be created as a TIFF file format using LZW compression with minimum resolution of 500 dpi.
- Size the figures according to their final intended size. Single-column figures should have a width of up to 82 mm. Double-column figures should have a maximum width of 170 mm.
- Use Times New Roman for figure lettering. Use lettering sized 8-10 pt. for the final figure size.
- Lines should have 0.5 pt. minimum width in drawings.
- Titles or captions should not be included inside the figure itself.

Figures must be embedded in the text near the position where they are first cited. Cite figures in the manuscript in consecutive numerical order. Denote figure parts by lowercase letters (a, b, c, etc.). Please include a reference citation at the end of the figure caption for previously published material. Authorization from the copyright holder must be provided upon submission for any reproduced material.

Figure captions must be placed below the figure and start with the term "Figure" followed by the figure number and a period. Example:

Figure 1. Shear strength envelope.

Do not abbreviate "Figure" when making cross-references to figures.

All figures are published in color for the electronic version of the journal; however, the print version uses grayscale. Please format figures so that they are adequate even when printed in grayscale.

**Accessibility:** Please make sure that all figures have descriptive captions (text-to-speech software or a text-to-Braille hardware could be used by blind users). Prefer using patterns (e.g., different symbols for dispersion plot) rather than (or in addition to) colors for conveying information (then the visual elements can be distinguished by colorblind users). Any figure lettering should have a contrast ratio of at least 4.5:1

**Improving the color accessibility for the printed version and for colorblind readers:** Authors are encouraged to use color figures because they will be published in their original form in the online version. However, authors must consider the need to make their color figures accessible for reviewers and readers that are colorblind. As a general rule of thumb, authors should avoid using red and green simultaneously. Red should be replaced by magenta, vermillion, or orange. Green should be replaced by an off-green color, such as blue-green. Authors should prioritize the use of black, gray, and varying tones of blue and yellow.

These rules of thumb serve as general orientations, but authors must consider that there are multiple types of color blindness, affecting the perception of different colors. Ideally, authors should make use of the following resources: 1) for more information on how to prepare color figures, visit <https://jfly.uni-koeln.de/>; 2) a freeware software available at <http://www.vischeck.com/> is offered by Vischeck, to show how your figures would be perceived by the colorblind.

## 6.4 Tables

Tables should be presented as a MS Word table with data inserted consistently in separate cells. Place tables in the text near the position where they are first cited. Tables should be numbered consecutively using Arabic numerals and have a caption consisting of the table number and a brief title. Tables should always be cited in the text. Any previously published material should be identified by giving the original source as a reference at the end of the table caption. Additional comments can be placed as footnotes, indicated by superscript lower-case letters.

When applicable, the units should come right below the corresponding column heading. Horizontal lines should be used at the top and bottom of the table and to separate the headings row. Vertical lines should not be used.

Table captions must be placed above the table and start with the term “Table” followed by the table number and a period. Example:

Table 1. Soil properties.

Do not abbreviate “Table” when making cross-references to tables. Sample:

Table 1. Soil properties

Parameter	Symbol	Value
Specific gravity of the sand particles	$G_s$	2.64
Maximum dry density (Mg/m <sup>3</sup> )	$\rho_{d(max)}$	1.554
Minimum dry density (Mg/m <sup>3</sup> )	$\rho_{d(min)}$	1.186
Average grain-size (mm)	$d_{50}$	0.17
Coefficient of uniformity	$C_u$	1.97

## 6.5 Mathematical equations

Equations must be submitted as editable text, created using MathType or the built-in equation editor in MS Word. All variables must be presented in italics.

Equations must appear isolated in a single line of the text. Numbers identifying equations must be flushed with the right margin. International System (SI) units must be used. The definitions of the symbols used in the equations must appear in the List of Symbols.

Do not abbreviate “Equation” when making cross-references to an equation.



# BELGO GABION. THE BEST CHOICE TO INCREASE YOUR CONSTRUCTION QUALITY.



**Belgo Geotech** provides steel solutions, for geotechnical applications, to the market. Our products include **gabions**, **rockfall mesh**, **Dramix®** steel fibers, **galvanized pannels** and **meshes for rock support** and **reinforcement systems**, **PC Strand for cable bolts** and **thread bars**. We also offer qualified technical support to meet all of your project's needs. **Our geotechnics feature the strength of steel.**



Learn more at: [belgogeotech.com.br](http://belgogeotech.com.br)

**BELGO**  
GeoTech

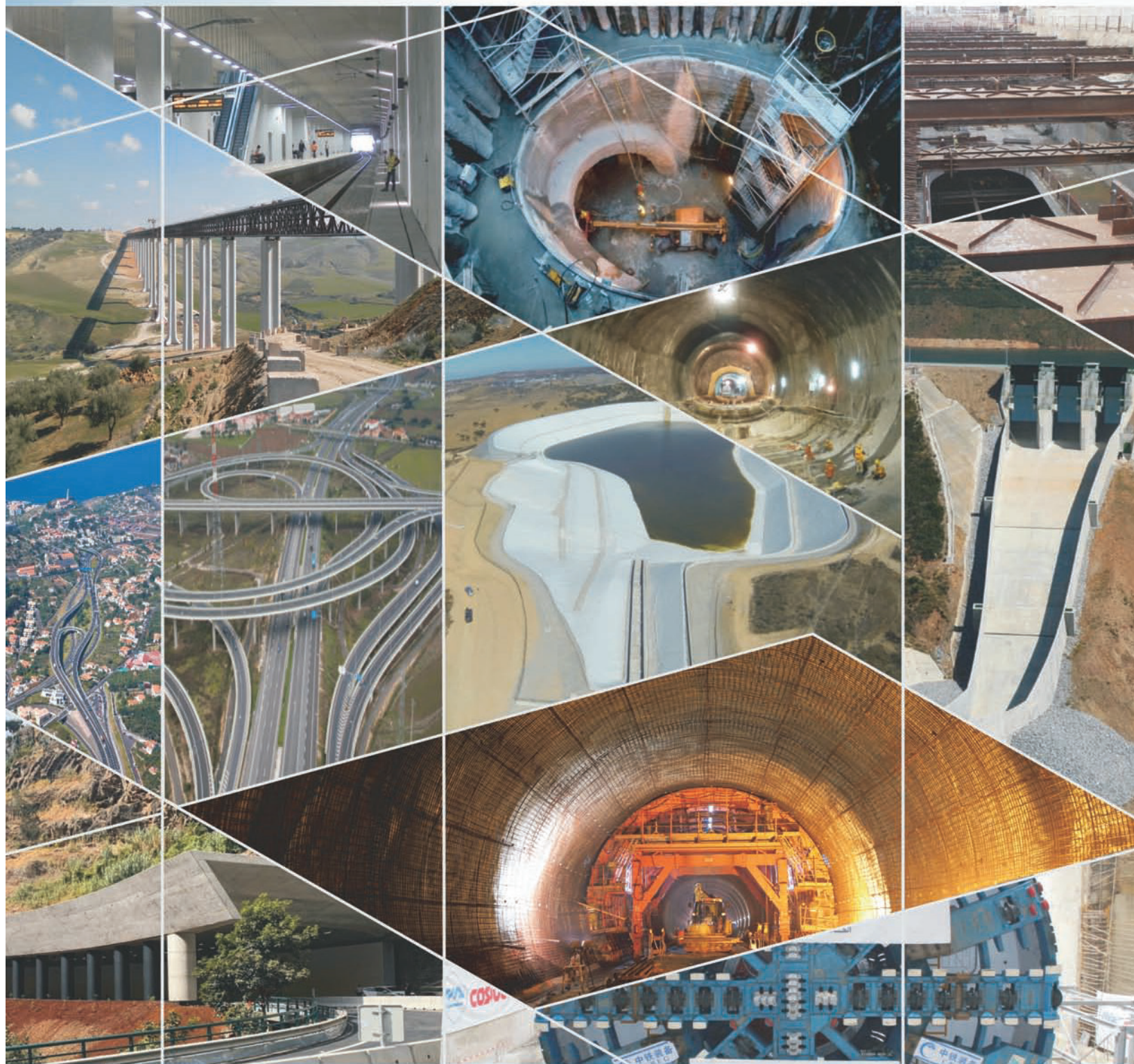
Belgo Bekaert Arames

ArcelorMittal

BEKAERT  
better together



BUILDING THE WORLD, BETTER



## Engineering and Architectural Consultancy

Geology, Geotechnics, Supervision of Geotechnical Works  
Embankment Dams, Underground Works, Retaining Structures  
Special Foundations, Soil Improvement, Geomaterials



MEMBER OF

TPF - CONSULTORES DE ENGENHARIA E ARQUITETURA, S.A.

[www.tpf.pt](http://www.tpf.pt)

40  
years



# DF+, YOUR TRUST FIRST

GEOLOGICAL, GEOTECHNICAL  
ENGINEERING AND WATER  
RESOURCES SOLUTIONS FOR THE  
MINING SECTOR AND OTHERS.



DF+ IS A COMPANY WITH A FOCUS ON THE MINERAL SECTOR AND MORE THAN 15 YEARS OF EXPERIENCE. WE OPERATE IN ALL PHASES OF A PROJECT, FROM FEASIBILITY STUDIES AND PROJECT DEVELOPMENT TO TECHNICAL MONITORING OF CONSTRUCTION AND MINE CLOSURE.

JOIN OUR SOCIAL NETWORKS TO  
KNOW MORE ABOUT OUR SERVICES.



AVE BARÃO HOMEM DE MELO, 4554 - 5th floor  
ESTORIL, BELO HORIZONTE/MG

+55 31 2519-1001

comercial@dfmais.eng.br



DF+ GEOTECHNICAL ENGINEERING  
AND WATER RESOURCES



# PIONEERING AND INNOVATION

SINCE 1921

 **TEIXEIRA DUARTE**  
ENGENHARIA E CONSTRUÇÕES, S.A.

PORT FACILITY CONSTRUCTION  
NACALA - MOZAMBIQUE



Building a better world.  
[teixiraduarteconstruction.com](http://teixiraduarteconstruction.com)





Safety is our nature

# SISTEMAS DE ALERTA E MONITORAMENTO

## Sistemas de Alerta e Alarme

Ideal para identificação de agentes  
deflagradores e monitoramento de  
eventos

Rua Visconde de Pirajá, 82 | Ipanema  
22410-003 | Rio de Janeiro | RJ | Brasil.  
Tel.: + 55 21 3624.1449  
[www.geobrugg.com](http://www.geobrugg.com)



Parceria:





# The Best Solution!

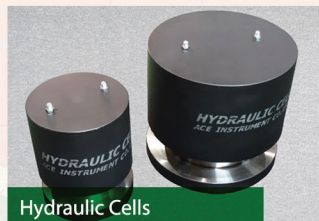
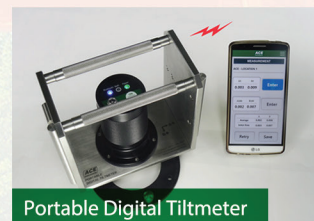
**Tecnilab Portugal, S.A.** will provide you with answers to your Geotechnical engineering needs.

**Tecnilab Portugal, S.A.** is a professional Geotechnical engineering company and has a lot of experience as a professional group that mainly engages in measurement engineering in dam, subway(Metro), harbor, power plant, soft ground and structure construction.

**WE ARE THE DISTRIBUTOR OF PORTUGAL OF ACE INSTRUMENT CO., LTD. IN KOREA.**

**ACE INSTRUMENT CO., LTD.** is a company that obtains worldwide reputation for supplying high precision, high reliability products in all Geotechnical instruments, data logger and in-situ test equipments. Independently developed automatic monitoring system can be used anywhere in the world, including buildings, bridges, ground and any constructions.

## Data Acquisition System & Web Monitoring Program



Sales company



**Tecnilab Portugal, S.A.**

A: Rua Gregorio Lopes, Lote 1512B 1449-041 Lisboa Portugal  
T: +351 217 220 870 F: +351 217 264 550  
www.tecnilab.pt

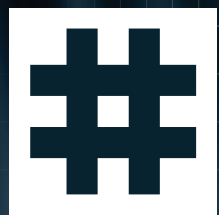
Manufacturer



**ACE INSTRUMENT CO., LTD.**

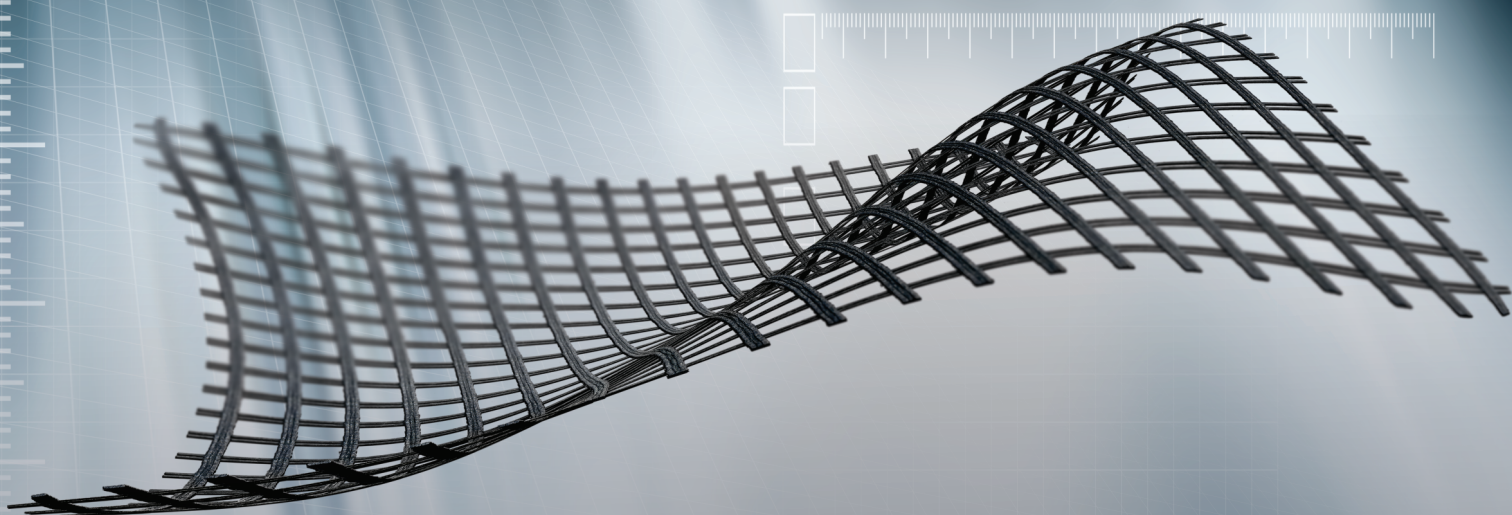
The first value in Geotechnical & Structural Instrumentation  
A: 9, Dangjung-ro 27 beon-gil, Gunpo-si, Gyeonggi-do, Korea  
T: +82 31 459 8753-7 F: +82 31 459 8758 E: acens@naver.com  
www.aceinstrument.com





# HUESKER

Ideen. Ingenieure. Innovationen.



## LEADER IN GEOSYNTHETICS

Experience HUESKER's geosynthetic building materials, systems and services now.



[www.HUESKER.com](http://www.HUESKER.com)

Find HUESKER in Social Media:





# ENGINEERING AND ENVIRONMENTAL CONSULTANTS



## COBA



## GEOLOGY AND GEOTECHNICS

Hydrogeology • Engineering Geology • Rock Mechanics • Soil Mechanics • Foundations and Retaining Structures • Underground Works • Embankments and Slope Stability  
Environmental Geotechnics • Geotechnical Mapping



- Water Resources Planning and Management
- Hydraulic Undertakings
- Electrical Power Generation and Transmission
- Water Supply Systems and Pluvial and Wastewater Systems
- Agriculture and Rural Development
- Road, Railway and Airway Infrastructures
- Environment
- Geotechnical Structures
- Cartography and Cadastre
- Safety Control and Work Rehabilitation
- Project Management and Construction Supervision



### PORTUGAL

CENTER AND SOUTH REGION  
Av. 5 de Outubro, 323  
1649-011 LISBOA  
Tel.: (351) 210125000, (351) 217925000  
Fax: (351) 217970348  
E-mail: [coba@coba.pt](mailto:coba@coba.pt)  
[www.coba.pt](http://www.coba.pt)

Av. Marquês de Tomar, 9, 6º.  
1050-152 LISBOA  
Tel.: (351) 217925000  
Fax: (351) 213537492

### NORTH REGION

Rua Mouzinho de Albuquerque, 744, 1º.  
4450-203 MATOSINHOS  
Tel.: (351) 229380421  
Fax: (351) 229373648  
E-mail: [engico@engico.pt](mailto:engico@engico.pt)

### ANGOLA

Praceta Farinha Leitão, edifício nº 27, 27-A - 2º Dto  
Bairro do Maculusso, LUANDA  
Tel./Fax: (244) 222338 513  
Cell: (244) 923317541  
E-mail: [coba-angola@netcabo.co.ao](mailto:coba-angola@netcabo.co.ao)

### MOZAMBIQUE

Pestana Rovuma Hotel. Centro de Escritórios.  
Rua da Sé nº114. Piso 3, MAPUTO  
Tel./Fax: (258) 21 328 813  
Cell: (258) 82 409 9605  
E-mail: [coba.mz@tdm.co.mz](mailto:coba.mz@tdm.co.mz)

### ALGERIA

09, Rue des Frères Hocine  
El Biar - 16606, ARGEL  
Tel.: (213) 21 922802  
Fax: (213) 21 922802  
E-mail: [coba.alger@gmail.com](mailto:coba.alger@gmail.com)

### BRAZIL

Rio de Janeiro  
COBA Ltd. - Rua Bela 1128  
São Cristóvão  
20930-380 Rio de Janeiro RJ  
Tel.: (55 21) 351 50 101  
Fax: (55 21) 258 01 026

### Fortaleza

Av. Senador Virgílio Távora 1701, Sala 403  
Aldeota - Fortaleza CEP 60170 - 251  
Tel.: (55 85) 3261 17 38  
Fax: (55 85) 3261 50 83  
E-mail: [coba@esc-te.com.br](mailto:coba@esc-te.com.br)

### UNITED ARAB EMIRATES

Corniche Road - Corniche Tower - 5th Floor - 5B  
P.O. Box 38360 ABU DHABI  
Tel.: (971) 2 627 0088  
Fax: (971) 2 627 0087





The Ground is our Challenge

## MAIN ACTIVITY AREAS

Consultancy, Supervision and Training

- Earth Retaining Structures
- Special Foundations
- Ground Improvement
- Foundations Strengthening and Underpinning
- Façades Retention
- Tunnels and Underground Structures
- Slope Stability
- Geological and Geotechnical Investigation
- Demolition

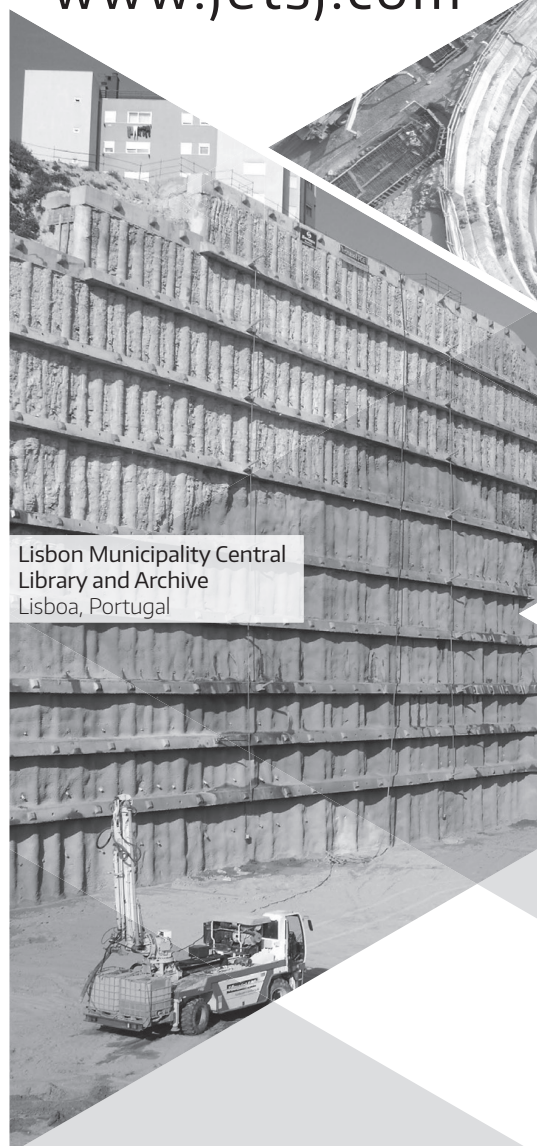
[www.jetsj.com](http://www.jetsj.com)



Tool Plazas P2 and P3  
Santa Catarina, Brazil



Mining Shaft  
Kamsar, Guiné



Lisbon Municipality Central  
Library and Archive  
Lisboa, Portugal



Solar Santana Building  
Lisboa, Portugal

## Main Office

Rua Julieta Ferrão, 12 - Office 1501

1600-131 LISBOA, Portugal

Phone.: [+351] 210 505 150 / 51

Email: [info@jetsj.com](mailto:info@jetsj.com)

[www.linkedin.com/company/jetsj-geotecnia-lda/](http://www.linkedin.com/company/jetsj-geotecnia-lda/)



# MACCAFERRI

## Learn more about **GAWAC® 3.0** software

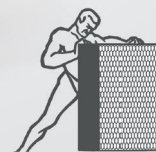
*Developed to support engineers, designers and students in a fast and reliable way to perform the analyzes of gabion retaining wall.*

The great advantage of **GAWAC® 3.0** is the inclusion of the stability analysis in serviceability conditions, through the GSC (Gabion Serviceability Coefficient). This type of analysis allows the user to evaluate the cross sections of the gabion walls in the most suitable conditions through the best performance and optimization of the gabion materials. The software allows the user to choose the type of gabion with the coating and mesh technologically appropriate to the work environment, in addition to allowing the use of international standards, various calculation analyzes with a detailed printable report.



## NEW SOFTWARE FEATURES

- **New user-friendly** interface;
- Consider the **influence of the mesh**;
- **Service Limit State (SLS) and Ultimate Limit State (ULS)** are considered in the stability analysis;
- Consider the **long-term performance of the gabion** based on the type of mesh and coating;
- **Serviceability conditions** performed by layer;
- Optimized design with the use of **Strong Face Gabion**.



GABION  
STRONG  
FACE



Visit our website to **learn more**  
about **Strong Face Gabion** and  
download **GAWAC® 3.0**.



/maccaferri /maccaferrimatrix



@Maccaferri\_BR



/MaccaferriWorld



/maccaferriworld





- > **Prospecção Geotécnica**  
*Site Investigation*
- > **Consultoria Geotécnica**  
*Geotechnical Consultancy*
- > **Obras Geotécnicas**  
*Ground Treatment-Construction Services*
- > **Controlo e Observação**  
*Field Instrumentation Services and Monitoring Services*
- > **Laboratório de Mecânica de Solos**  
*Soil and Rock Mechanics Laboratory*

Certificada ISO 9001 por



# Geocontrole



Parque Oriente, Bloco 4, EN10  
2699-501 Bobadela LRS  
Tel. 21 995 80 00  
Fax. 21 995 80 01  
e.mail: mail@geocontrole.pt  
www.geocontrole.pt

  
**Geocontrole**  
Geotecnia e Estruturas de Fundação SA

## Guide for Authors

Soils and Rocks is an international scientific journal published by the Brazilian Association for Soil Mechanics and Geotechnical Engineering (ABMS) and by the Portuguese Geotechnical Society (SPG). The aim of the journal is to publish original papers on all branches of Geotechnical Engineering. Each manuscript is subjected to a single-blind peer-review process. The journal's policy of screening for plagiarism includes the use of a plagiarism checker on all submitted manuscripts.

Soils and Rocks embraces the international Open Science program and is striving to meet all the recommendations. However, at this moment, the journal is not yet accepting preprints and open data, and has not adopted open peer reviews.

Soils and Rocks provides a manuscript template available at the journal's website.

### 1. Category of papers

Submissions are classified into one of the following categories:

**Article** – an extensive and conclusive dissertation about a geotechnical topic, presenting original findings.

**Technical Note** – presents a study of smaller scope or results of ongoing studies, comprising partial results and/or particular aspects of the investigation.

**Case Study** – report innovative ways to solve problems associated with design and construction of geotechnical projects. It also presents studies of the performance of existing structures.

**Review Article** – a summary of the State-of-the-Art or State-of-the-Practice on a particular subject or issue and represents an overview of recent developments.

**Discussion** – specific discussions about published papers.

Authors are responsible for selecting the correct category when submitting their manuscript. However, the manuscript category may be altered based on the recommendation of the Editorial Board. Authors are also requested to state the category of paper in their Cover Letter.

When submitting a manuscript for review, the authors should indicate the category of the manuscript, and is also understood that they:

- a) assume full responsibility for the contents and accuracy of the information in the paper;
- b) assure that the paper has not been previously published, and is not being submitted to any other journal for publication.

### 2. Paper length

Full-length manuscripts (Article, Case Study) should be between 4,000 and 8,000 words. Review articles should have up to 10,000 words. Technical Notes have a word count limit of 3,500 words. Discussions have a word count limit of 1,000 words. These word count limits exclude the title page, notation list (e.g., symbols, abbreviations), captions of tables and figures, acknowledgments and references. Each single column and double column figure or table is considered as equivalent to 150 and 300 words, respectively.

### 3. Scientific style

The manuscripts should be written in UK or US English, in the third person and all spelling should be checked in accordance with

a major English Dictionary. The manuscript should be able to be readily understood by a Civil Engineer and avoid colloquialisms. Unless essential to the comprehension of the manuscript, direct reference to the names of persons, organizations, products or services is not allowed. Flattery or derogatory remarks about any person or organization should not be included.

The author(s) of Discussion Papers should refer to himself (herself/themselves) as the reader(s) and to the author(s) of the paper as the author(s).

The International System (SI) units must be used. The symbols are recommended to be in accordance with Lexicon in 14 Languages, ISSMFE (2013) and the ISRM List of Symbols. Use italics for single letters that denote mathematical constants, variables, and unknown quantities, either in tables or in the text.

### 4. Submission requirements and contents

A submission implies that the following conditions are met:

- the authors assume full responsibility for the contents and accuracy of the information presented in the paper;
- the manuscript contents have not been published previously, except as a lecture or academic thesis;
- the manuscript is not under consideration for publication elsewhere;
- the manuscript is approved by all authors;
- the manuscript is approved by the necessary authorities, when applicable, such as ethics committees and institutions that may hold intellectual property on contents presented in the manuscript;
- the authors have obtained authorization from the copyright holder for any reproduced material;
- the authors are aware that the manuscript will be subjected to plagiarism check.

The author(s) must upload two digital files of the manuscript to the Soils and Rocks submission system. The size limit for each submission file is 20 MB. The manuscript should be submitted in docx format (Word 2007 or higher) or doc format (for older Word versions). An additional PDF format file of the manuscript is also required upon submission. Currently, the journal is not accepting manuscripts prepared using LaTeX.

The following documents are required as minimum for submission:

- cover letter;
- manuscript with figures and tables embedded in the text (doc or docx format);



manuscript with figures and tables embedded in the text for revision (PDF format);

- permission for re-use of previously published material when applicable, unless the author/owner has made explicit that the image is freely available.

#### 4.1 Cover letter

The cover letter should include: manuscript title, submission type, authorship information, statement of key findings and work novelty, and related previous publications if applicable.

#### 4.2 Title page

The title page is the first page of the manuscript and must include:

- A concise and informative title of the paper. Avoid abbreviations, acronyms or formulae. Discussion Papers should contain the title of the paper under discussion. Only the first letter of the first word should be capitalized.
- Full name(s) of the author(s). The first name(s) should not be abbreviated. The authors are allowed to abbreviate middle name(s).
- The corresponding author should be identified by a pound sign # beside his/her and in a footnote.
- The affiliation(s) of the author(s), should follow the format: Institution, (Department), City, (State), Country.
- Affiliation address and e-mail must appear below each author's name.
- The 16-digit ORCID of the author(s) – mandatory
- Main text word count (excluding abstract and references) and the number of figures and tables

#### 4.3 Permissions

Figures, tables or text passages previously published elsewhere may be reproduced under permission from the copyright owner(s) for both the print and online format. The authors are required to provide evidence that such permission has been granted at the moment of paper submission.

#### 4.4 Declaration of interest

Authors are required to disclose conflicting interests that could inappropriately bias their work. For that end, a section entitled “Declaration of interest” should be included following any acknowledgments and prior to the “Authors’ contributions” section. In case of the absence of conflicting interests, the authors should still include a declaration of interest.

#### 4.5 Authors’ contributions

Authors are required to include an author statement outlining their individual contributions to the paper according to the CASRAI CRediT roles (as per <https://casrai.org/credit>). The minimum requirements of contribution to the work for recognition of authorship are: a) Participate actively in the discussion of results; b) Review and approval of the final version of the manuscript. A section entitled “Authors’ contributions” should be included after the declaration of interest section, and should be formatted with author's name and CRediT role(s), according to the example:

**Samuel Zheng:** conceptualization, methodology, validation. **Olivia Prakash:** data curation, writing - original draft preparation. **Fatima Wang:** investigation, validation. **Kwame Bankole:** supervision. **Sun Qi:** writing - reviewing and editing.

Do not include credit items that do not follow the Taxonomy established by CASRAI CRediT roles.

The authors’ contributions section should be omitted in manuscripts that have a single author.

#### 5. Plagiarism checking

Submitted papers are expected to contain at least 50 % new content and the remaining 50 % should not be verbatim to previously published work.

All manuscripts are screened for similarities. Currently, the Editorial Board uses the plagiarism checker Plagius ([www.plagius.com](http://www.plagius.com)) to compare submitted papers to already published works. Manuscripts will be rejected if more than 20 % of content matches previously published work, including self-plagiarism. The decision to reject will be under the Editors’ discretion if the percentage is between 10 % and 20 %.

**IMPORTANT OBSERVATION:** Mendeley software plug-in (suggested in this guide) for MS-Word can be used to include the references in the manuscript. This plug-in uses a field code that sometimes includes automatically both title and abstract of the reference. Unfortunately, the similarity software adopted by the Journal (Plagius) recognizes the title and abstract as an actual written text by the field code of the reference and consequently increases considerably the percentage of similarity. Please do make sure to remove the abstract (if existing) inside Mendeley section where the adopted reference is included. This issue has mistakenly caused biased results in the past. The Editorial Board of the journal is now aware of this tendentious feature.

#### 6. Formatting instructions

The text must be presented in a single column, using ISO A4 page size, left, right, top, and bottom margins of 25 mm, Times New Roman 12 font, and line spacing of 1.5. All lines and pages should be numbered.

The text should avoid unnecessary italic and bold words and letters, as well as too many acronyms. Authors should avoid to capitalize words and whenever possible to use tables with distinct font size and style of the regular text.

Figures, tables and equations should be numbered in the sequence that they are mentioned in the text.

##### *Abstract*

Please provide an abstract between 150 and 250 words in length. Abbreviations or acronyms should be avoided. The abstract should state briefly the purpose of the work, the main results and major conclusions or key findings.

##### *Keywords*

A minimum of three and a maximum of six keywords must be included after the abstract. The keywords must represent the

content of the paper. Keywords offer an opportunity to include synonyms for terms that are frequently referred to in the literature using more than one term. Adequate keywords maximize the visibility of your published paper.

Examples:

Poor keywords – piles; dams; numerical modeling; laboratory testing

Better keywords – friction piles; concrete-faced rockfill dams; material point method; bender element test

#### List of symbols

A list of symbols and definitions used in the text must be included before the References section. Any mathematical constant, variable or unknown quantity should appear in italics.

### 6.1 Citations

References to other published sources must be made in the text by the last name(s) of the author(s), followed by the year of publication. Examples:

- Narrative citation: [...] while Silva & Pereira (1987) observed that resistance depended on soil density
- Parenthetical citation: It was observed that resistance depended on soil density (Silva & Pereira, 1987).

In the case of three or more authors, the reduced format must be used, e.g.: Silva et al. (1982) or (Silva et al., 1982). Do not italicize “et al.”

Two or more citations belonging to the same author(s) and published in the same year are to be distinguished with small letters, e.g.: (Silva, 1975a, b, c.).

Standards must be cited in the text by the initials of the entity and the year of publication, e.g.: ABNT (1996), ASTM (2003).

### 6.2 References

A customized style for the Mendeley software is available and may be downloaded from this link.

Full references must be listed alphabetically at the end of the text by the first author's last name. Several references belonging to the same author must be cited chronologically.

Some formatting examples are presented here:

#### Journal Article

Bishop, A.W., & Blight, G.E. (1963). Some aspects of effective stress in saturated and partly saturated soils. *Géotechnique*, 13(2), 177-197. <https://doi.org/10.1680/geot.1963.13.3.177>

Castellanza, R., & Nova, R. (2004). Oedometric tests on artificially weathered carbonatic soft rocks. *Journal of Geotechnical and Geoenvironmental Engineering*, 130(7), 728-739. [https://doi.org/10.1061/\(ASCE\)1090-0241\(2004\)130:7\(728\)](https://doi.org/10.1061/(ASCE)1090-0241(2004)130:7(728))

Fletcher, G. (1965). Standard penetration test: its uses and abuses. *Journal of the Soil Mechanics Foundation Division*, 91, 67-75.

Indraratna, B., Kumara, C., Zhu S-P., Sloan, S. (2015). Mathematical modeling and experimental verification of fluid flow through deformable rough rock joints. *International Journal of Geomechanics*, 15(4): 04014065-1-04014065-11. [https://doi.org/10.1061/\(ASCE\)GM.1943-5622.0000413](https://doi.org/10.1061/(ASCE)GM.1943-5622.0000413)

Garnier, J., Gaudin, C., Springman, S.M., Culligan, P.J., Goodings, D., König, D., ... & Thorel, L. (2007). Catalogue of scaling laws and similitude questions in geotechnical centrifuge modelling. *International Journal of Physical Modelling in Geotechnics*, 7(3), 01-23. <https://doi.org/10.1680/ijpmg.2007.070301>

Bicalho, K.V., Gramelich, J.C., & Santos, C.L.C. (2014). Comparação entre os valores de limite de liquidez obtidos pelo método de Casagrande e cone para solos argilosos brasileiros. *Comunicações Geológicas*, 101(3), 1097-1099 (in Portuguese).

#### Book

Lambe, T.W., & Whitman, R.V. (1979). *Soil Mechanics, SI version*. John Wiley & Sons.

Das, B.M. (2012). *Fundamentos de Engenharia Geotécnica*. Cengage Learning (in Portuguese).

Head, K.H. (2006). *Manual of Soil Laboratory Testing - Volume 1: Soil Classification and Compaction Tests*. Whittles Publishing.

Bhering, S.B., Santos, H.G., Manzatto, C.V., Bognola, I., Fasolo, P.J., Carvalho, A.P., ... & Curcio, G.R. (2007). *Mapa de solos do estado do Paraná*. Embrapa (in Portuguese).

#### Book Section

Yerro, A., & Rohe, A. (2019). Fundamentals of the Material Point Method. In *The Material Point Method for Geotechnical Engineering* (pp. 23-55). CRC Press. <https://doi.org/10.1201/9780429028090>

Sharma, H.D., Dukes, M.T., & Olsen, D.M. (1990). Field measurements of dynamic moduli and Poisson's ratios of refuse and underlying soils at a landfill site. In *Geotechnics of Waste Fills - Theory and Practice* (pp. 57-70). ASTM International. <https://doi.org/10.1520/STP1070-EB>

Cavalcante, A.L.B., Borges, L.P.F., & Camapum de Carvalho, J. (2015). Tomografias computadorizadas e análises numéricas aplicadas à caracterização da estrutura porosa de solos não saturados. In *Solos Não Saturados no Contexto Geotécnico* (pp. 531-553). ABMS (in Portuguese).

#### Proceedings

Jamiolkowski, M.; Ladd, C.C.; Germaine, J.T., & Lancellotta, R. (1985). New developments in field and laboratory testing of soils. *Proc. 11th International Conference on Soil Mechanics and Foundation Engineering*, San Francisco, August 1985. Vol. 1, Balkema, 57-153.

Massey, J.B., Irfan, T.Y. & Cipullo, A. (1989). The characterization of granitic saprolitic soils. *Proc. 12th International Conference on Soil Mechanics and Foundation Engineering*, Rio de Janeiro. Vol. 6, Publications Committee of XII ICSMFE, 533-542.

Indraratna, B., Oliveira D.A.F., & Jayanathan, M. (2008b). Revised shear strength model for infilled rock joints considering overconsolidation effect. *Proc. 1st Southern Hemisphere International Rock Mechanics Symposium*, Perth. ACG, 16-19.

Barreto, T.M., Repsold, L.L., & Casagrande, M.D.T. (2018). Melhoria de solos arenosos com polímeros. *Proc. 19º Congresso Brasileiro de Mecânica dos Solos e Engenharia Geotécnica*, Salvador. Vol. 2, ABMS, CBMR, ISRM & SPG, 1-11 (in Portuguese).

#### Thesis

Lee, K.L. (1965). *Triaxial compressive strength of saturated sands under seismic loading conditions* [Unpublished doctoral dissertation]. University of California at Berkeley.

Chow, F.C. (1997). *Investigations into the behaviour of displacement pile for offshore foundations* [Doctoral thesis, Imperial College London]. Imperial College London's repository. <https://spiral.imperial.ac.uk/handle/10044/1/7894>

Araki, M.S. (1997). *Aspectos relativos às propriedades dos solos porosos colapsíveis do Distrito Federal* [Unpublished master's dissertation]. University of Brasília (in Portuguese).

Sotomayor, J.M.G. (2018). *Evaluation of drained and non-drained mechanical behavior of iron and gold mine tailings reinforced with polypropylene fibers* [Doctoral thesis, Pontifical Catholic University of Rio de Janeiro]. Pontifical Catholic University of Rio de Janeiro's repository (in Portuguese). <https://doi.org/10.17771/PUCRio.acad.36102>\*

\* official title in English should be used when available in the document.

#### Report

ASTM D7928-17. (2017). Standard Test Method for Particle-Size Distribution (Gradation) of Fine-Grained Soils Using the Sedimentation (Hydrometer) Analysis. *ASTM International*, West Conshohocken, PA. <https://doi.org/10.1520/D7928-17>

ABNT NBR 10005. (2004). Procedure for obtention leaching extract of solid wastes. *ABNT - Associação Brasileira de Normas Técnicas*, Rio de Janeiro, RJ (in Portuguese).

DNIT. (2010). Pavimentação - Base de solo-cimento - Especificação de serviço DNIT 143. *DNIT -Departamento Nacional de Infraestrutura de Transportes*, Rio de Janeiro, RJ (in Portuguese).

USACE (1970). Engineering and Design: Stability of Earth and Rock-Fill Dams, Engineering Manual 1110-2-1902. Corps of Engineers, Washington, D.C.

#### Web Page

Soils and Rocks. (2020). *Guide for Authors*. Soils and Rocks. Retrieved in September 16, 2020, from <http://www.soilsandrocks.com/>

### 6.3 Artworks and illustrations

Each figure should be submitted as a high-resolution image, according to the following mandatory requirements:

- Figures must be created as a TIFF file format using LZW compression with minimum resolution of 500 dpi.
- Size the figures according to their final intended size. Single-column figures should have a width of up to 82 mm. Double-column figures should have a maximum width of 170 mm.
- Use Times New Roman for figure lettering. Use lettering sized 8-10 pt. for the final figure size.
- Lines should have 0.5 pt. minimum width in drawings.
- Titles or captions should not be included inside the figure itself.

Figures must be embedded in the text near the position where they are first cited. Cite figures in the manuscript in consecutive numerical order. Denote figure parts by lowercase letters (a, b, c, etc.). Please include a reference citation at the end of the figure caption for previously published material. Authorization from the copyright holder must be provided upon submission for any reproduced material.

Figure captions must be placed below the figure and start with the term "Figure" followed by the figure number and a period. Example:

Figure 1. Shear strength envelope.

Do not abbreviate "Figure" when making cross-references to figures.

All figures are published in color for the electronic version of the journal; however, the print version uses grayscale. Please format figures so that they are adequate even when printed in grayscale.

**Accessibility:** Please make sure that all figures have descriptive captions (text-to-speech software or a text-to-Braille hardware could be used by blind users). Prefer using patterns (e.g., different symbols for dispersion plot) rather than (or in addition to) colors for conveying information (then the visual elements can be distinguished by colorblind users). Any figure lettering should have a contrast ratio of at least 4.5:1

**Improving the color accessibility for the printed version and for colorblind readers:** Authors are encouraged to use color figures because they will be published in their original form in the online version. However, authors must consider the need to make their color figures accessible for reviewers and readers that are colorblind. As a general rule of thumb, authors should avoid using red and green simultaneously. Red should be replaced by magenta, vermillion, or orange. Green should be replaced by an off-green color, such as blue-green. Authors should prioritize the use of black, gray, and varying tones of blue and yellow.

These rules of thumb serve as general orientations, but authors must consider that there are multiple types of color blindness, affecting the perception of different colors. Ideally, authors should make use of the following resources: 1) for more information on how to prepare color figures, visit <https://jfly.uni-koeln.de/>; 2) a freeware software available at <http://www.vischeck.com/> is offered by Vischeck, to show how your figures would be perceived by the colorblind.



## 6.4 Tables

Tables should be presented as a MS Word table with data inserted consistently in separate cells. Place tables in the text near the position where they are first cited. Tables should be numbered consecutively using Arabic numerals and have a caption consisting of the table number and a brief title. Tables should always be cited in the text. Any previously published material should be identified by giving the original source as a reference at the end of the table caption. Additional comments can be placed as footnotes, indicated by superscript lower-case letters.

When applicable, the units should come right below the corresponding column heading. Horizontal lines should be used at the top and bottom of the table and to separate the headings row. Vertical lines should not be used.

Table captions must be placed above the table and start with the term “Table” followed by the table number and a period. Example:

Table 1. Soil properties.

Do not abbreviate “Table” when making cross-references to tables. Sample:

Table 1. Soil properties

Parameter	Symbol	Value
Specific gravity of the sand particles	$G_s$	2.64
Maximum dry density (Mg/m <sup>3</sup> )	$\rho_{d(max)}$	1.554
Minimum dry density (Mg/m <sup>3</sup> )	$\rho_{d(min)}$	1.186
Average grain-size (mm)	$d_{50}$	0.17
Coefficient of uniformity	$C_u$	1.97

## 6.5 Mathematical equations

Equations must be submitted as editable text, created using MathType or the built-in equation editor in MS Word. All variables must be presented in italics.

Equations must appear isolated in a single line of the text. Numbers identifying equations must be flushed with the right margin. International System (SI) units must be used. The definitions of the symbols used in the equations must appear in the List of Symbols.

Do not abbreviate “Equation” when making cross-references to an equation.